Polycyclic- and Sulfurcontaining-Compounds: From Polycyclic Hydrocarbons to Thiaspherophane

Inauguraldissertation

zur
Erlangung der Würde eines Doktors der Philosophie

vorgelegt der

Philosophisch-Naturwissenschaftlichen Fakultät der Universität Basel

Von

Lorenzo Delarue Bizzini

Aus

Basel-Stadt (CH), Schweiz

Basel 2019

Genehmigt von der Philosophisch-Naturwissenschaftlichen Fakultät
auf Antrag von

Prof. Dr. Marcel Mayor

Prof. Dr. Konrad Tiefenbacher

Basel, den 19. November 2019

Prof. Dr. Martin Spiess
Dekan

Dedicated to my Father

Err
and err
and err again
but less
and less
and less.

Piet Hien

Acknowledgement

This thesis would not have been possible without the support provided by Professor Marcel Mayor. Thank you for motivating me with these, in many aspects, challenging pojects. I feel honoured and gratefull for the time we had and for being a member of your group.

Thank you Professor Konrad Tiefenbacher for the commitment of co-refereeing my thesis.

I would like to thank Linda and Patrick for being the awesome people they are. Further, I would like to thanks all the members of the Mayor Group for all the good and bad moments we had. Thanks to all the great researchers I had the pleasure to meet and work during this time: Yves, Viktor, Tomaš, Thomas M., Thomas B, Rajesh, Michal, Michel, Markus, Manuel, Lukas, Laurent, Kevin, Juraj, Henrik, Erik and David.

To all the students I had the privilege to teach, Fabian, Martin, Ksenia, Simon, Tim, Viviane and Zlatko. I wish you all the best on your way and I am gratefull for all your engagement.

I would like to thank PD Daniel Häussinger and his group for the unmeasurable help and effort they provided. No work I did here would have been possible without the commitment of Silvie, Oliver, Michael, Brigitte, Markus A., Markus H., Hisni, Adreas and Andres. Thank you!

To my father, mother and brother without whom I would not be who I am, thank you for everything you did for me.

For my love and dearest friend, Martina.

This thesis contains the examination of four, in first glance, unrelated topics. However, the overarching motivation behind these subjects are the same: The Art and Challenge of Organic Chemistry.

I. The first chapter deals with the design, based on theoretical principles, and preparation of unsaturated spirocyclic compounds bearing sulfur functionalities with the aim of elucidating the charge-transport properties of such molecules on the level of single molecules. In collaboration with the Group of Professor Herre van der Zant from the Delft University of Technology preliminary conductance measurements of such spirocyclic structures could be gathered. The motivation for this joint endeavor is the prospect of using such spirocyclic structures as a molecular switch for the construction of molecular electronic devices.

II. The second part shows our engagement in the long tradition among organic chemist to challenge our abilities to synthesize inspiring, complex and aesthetical pleasing structures. One such structure was identified by employing predictive computational methods by the group of Professor Jean-Louis Reymond. The structure of interest was recognized as one of the last three remaining and not yet synthesized fully-cyclic C_{11} isomers without strain. Encouraged by this finding, we accepted the challenge to synthesize this tetracyclic saturated hydrocarbon with the molecular formula $C_{11}H_{16}$ with the proposed trivial name of trinorbornane.

III. Thirdly, Thiaspherophane: A highly symmetrical structure consisting of eight benzene rings bridged over twelve sulfur atoms describing a cuboctahedron: one of the 13 Archimedean solids. This elusive molecule, predicted over 25 years ago, bears the potential of being transformed into a cryptatium. Our efforts and progress on the synthesis of thiaspherophane will be discussed.

IV. Unsymmetrical disulfides are ubiquitous in the field of chemistry and at the interface with physics, where nanotechnology emerges. In this chapter, our investigation of an efficient method for the preparation of unsymmetrical disulfides will be presented Whereby the potential of this method for the formation of functional units bearing multiple unsymmetrical disulfides was assessed with the aim of using these compounds for functionalization of gold surfaces.

1 Spiroconjugated Compounds for Single Molecule Experiments

1.1 Introduction

The concept of spiroconjugation, first introduced in 1967,[1,2] describes the through space interaction (homoconjugation) of two perpendicularly arranged π-systems connected *via* a common tetrahedral carbon.[1–4] Spiroconjugation has been extensively investigated[3–9] and in principle spiroconjugated compounds can be divided in two larger classes: class A and class B. In compounds belonging to class A only endocyclic double bonds are present while in class B also exocyclic unsaturations are present (Figure 1 shows one example of each class, **1** belonging to class A and **2** to B).[3,4]

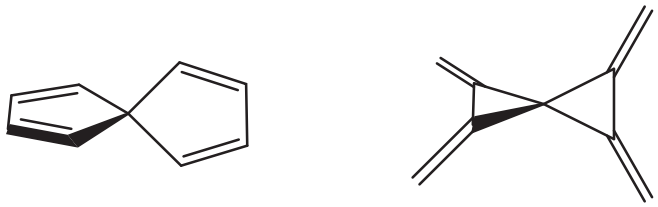

Figure 1: Two example of spiroconjugated compounds belonging to class A and B.

The phenomenon of spiroconjugation can be qualitatively described with the aid of interaction diagrams.[3,4] Let us first consider the case of spiro[4.4.]nonatetraene (**1**), where the molecule can be dissected into two perpendicular butadiene fragments (shown on the left and right side of Figure 2) and characterized with respect to the two symmetry planes σ^1 and σ^2. The denomination A (antisymmetric) and S (symmetric) stand in respect to the planes of symmetry σ^1 and σ^2. In respect to symmetry principles, only the orbitals which are antisymmetric to both planes can interact and thus lead to two linear combinations since only orbitals with the same symmetry can interact constructively. In the case of molecule **1** one occupied (π_2) and one unoccupied (π_4) orbital have the same symmetry (AA) leading each to two linear combinations with the irreducible representation b_1 and a_2 in the D_{2d} point group.[1,2] The orbitals with mismatched symmetry (AS, SA) do not interact destructively and form degenerate levels with the irreducible representation e.[1,2]

As illustrated in Figure 2, the splitting of the AA levels arises from the interaction of the 2p AOs of the carbons C1 and C2 with C6 and C9 giving rise to a bonding and an antibonding interaction which is further illustrated as a Newman projection in Figure 3 which also shows the corresponding symmetry of the orbitals states.

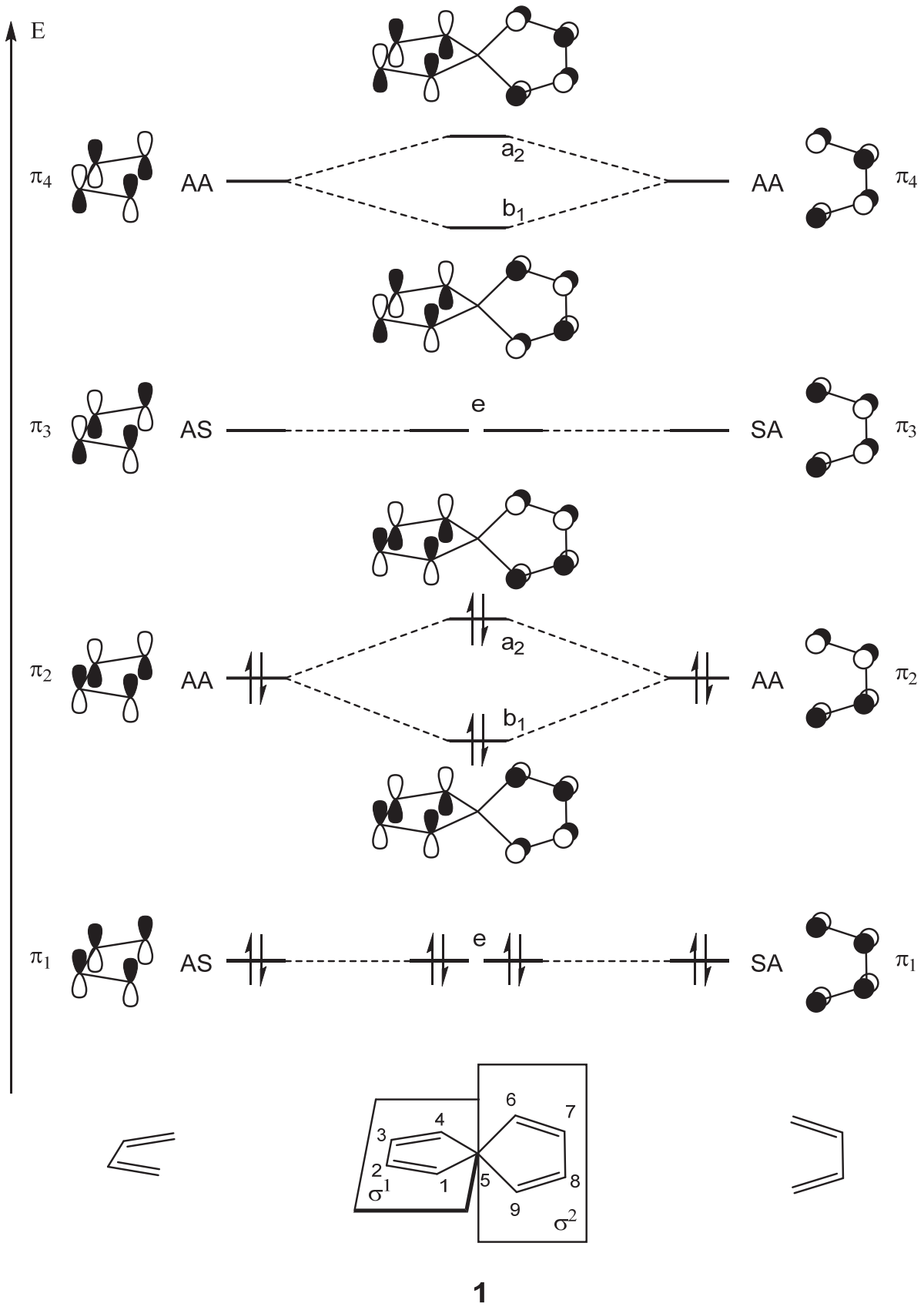

1

Figure 2: Qualitative interaction diagram of spiro[2.2]nonatetraene **1** with two perpendicularly arranged butadiene moieties, where A means antisymmetric and S symmetric in respect to the symmetry planes σ_1 and σ_2. Reproduced from [3].

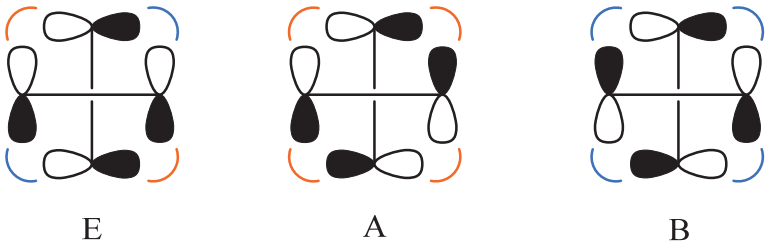

Figure 3: Newman projection showing the spatial interactions of the 2p orbitals of a spiroconjugated molecule and the correspondig symmetry of the states (E, A and B) in a D_{2d} symmetric molecule.

Performing the same analysis for compound **2** reveals a very similar picture compared to the previously discussed compound **1** (Figure 4a), the difference being the magnitude of the splitting of the interacting orbitals. While the splitting of the occupied AA orbitals in **1** is larger the opposite is true for **2** where the larger splitting is found on the unoccupied AA orbitals. This difference arises from the change in connectivity which affects the coefficients of the wave function and therefore the magnitude of the overlap.[3,4] As presented in the interaction diagrams of **1** and **2** spiroconjugation leads in both case to a destabilization of the HOMO. In the case of spirocompound **3** (Figure 4b) the interaction diagram reveals that both frontier orbitals (HOMO and LUMO) are degenerated therefore, spiroconjugation has neither a destabilizing nor stabilizing effect.

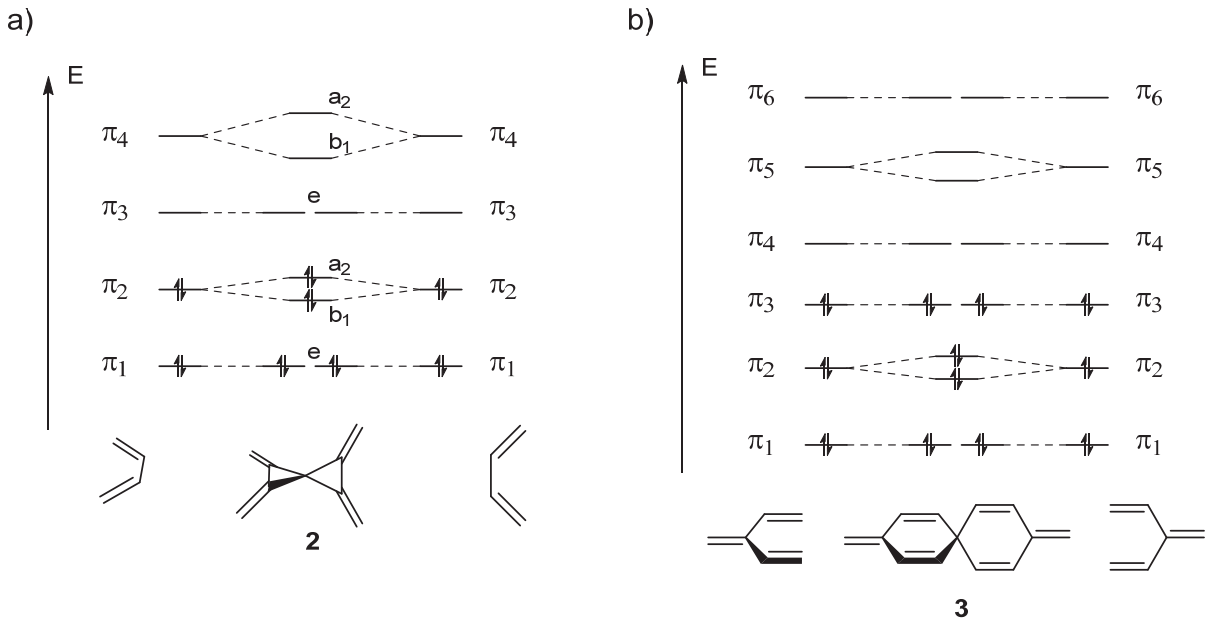

Figure 4: Qualitative interaction diagram for compounds **2** and **3**.Reproduced from [3].

1.1.1 Spectroscopic Measurements of Spiroconjugated Compounds

As discussed in the previous section spiroconjugation leads to a change in the energy of certain molecular orbitals due to spatial interactions between the π orbitals. Therefore, one method to observe the effect of spirocojungation is by comparing the electronic spectra of the spirocompound of interest with a reference compound lacking the spiroconjugation feature. Spiroconjugation could be demonstrated by comparing the UV-vis of spiro[2.2]nonatetraene (**1**) and spiro[2.2]nonadiene (**4**),[10,11] 1,1'-spirobiinden (**5**) and 2,3-dihydro-1,1'-spirobiinden (**6**),[12,13] spiro[5.5]undeca-1,4,6,9-tetraene-3,8-dione (**7**) and spiro[5.5]undeca-1,4-dien-3-one (**8**)[9] and more recently 2,2'-spirobiindantetraone (**9**) and 2,2-dimethylindan-1,3-dione (**10**).[5] In all these cases a bathochromic shift of the p-p* transition was observed by going from the reference compound to the spiroconjugated molecules.

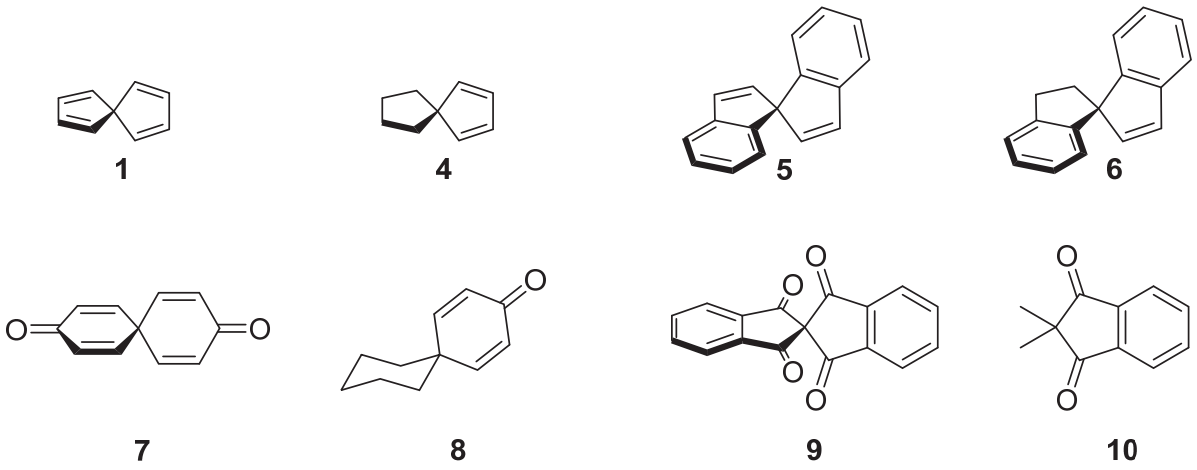

Figure 5: Spiroconjugated compounds and corresponding reference compounds used to observe spiroconjugation by UV-vis spectroscopy.

1.1.2 Spiroconjugated Molecular Junctions

Recently, the electronic transport behavior of spiroconjugated compounds in single-molecule junctions were examined from a theoretical point of view.[14] It has been shown that the unusual geometry of spiroconjugated molecules such as **1**, when incorporated into molecular junctions, display destructive quantum interference. This quantum interference effect would result in a current blockade distinct from meta-connected benzene,[14] which is the one of the best investigated form of quantum interference in single-molecule junctions.

The destructive quantum interference (DQI) in spiroconjugated systems is a result of the degenerate e-states.[14] As shown in Figure 3, DQI occurs for states with *E* symmetry (antisymmetric with respect to the C_2(z) rotation) as the perpendicular fragments are antisymmetric to each other and therefore cancel out.[1,2,14] This leads to a picture where the *E* states are localized on each moiety corresponding to a complete destructive quantum interference. For positive gate voltage and increasing bias, the e-states become populated (reduction of the molecule) leading to a current blockade as the propagating charge is localized on either moiety (Figure 6c).[14]

However, populating degenerate electronic states, typically results in Jahn-Teller distortion.[14,15] In the case of **1**, charging the molecule may lower the symmetry from D_{2d} to D_2 as the two ring planes twist away from a 90° angle (Figure 6a and c). This would in theory lift the DQI as the two spiro fragments are not antisymmetric anymore and therefore giving rise to bonding and antibonding states (overall stabilization of the system) thus removing the current blockade as depictured in Figure 6b.[14]

It has been predicted that the lift of the current bloackade caused by Jahn-Teller distortion depends on the hopping rate of the electron from and to the electrodes (γ) and the frequency of the twisting mode of vibration (ω). In case where $\omega << \gamma$, the current blockade will not be lifted as the Jahn-Teller distortion is a result of the coupling of vibrational mode to electronic states.[14]

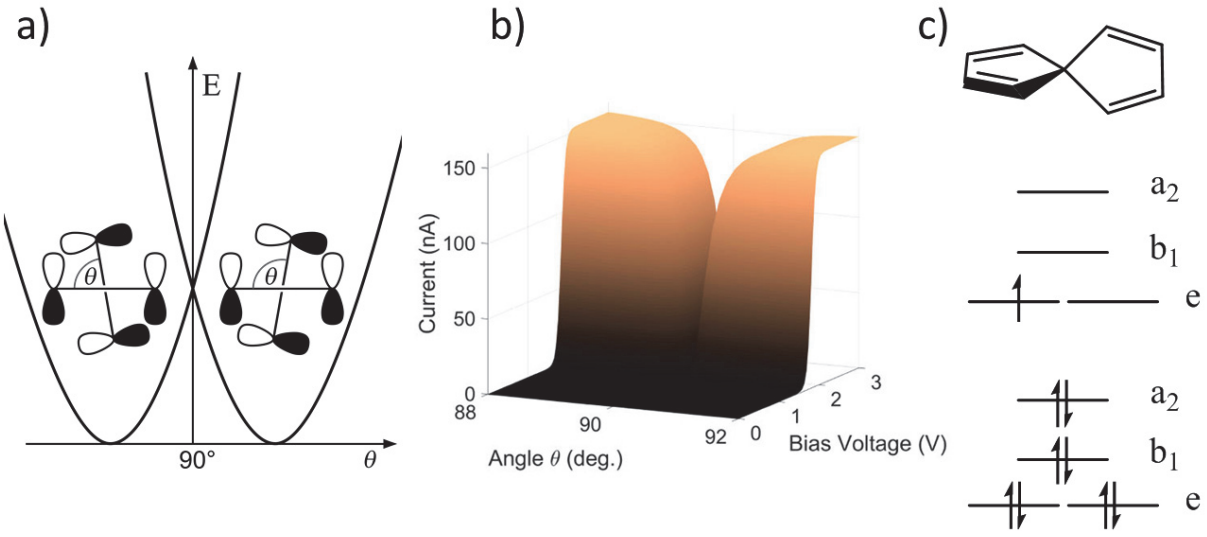

Figure 6: Destructive Quantum Interference and Jahn-Teller distortion effects on electronic transport in spiroconjugated molecular junctions. a) Schematic stability diagram of the radical anion **1**$^{\bullet-}$ in dependence of the angle θ. b) IV characteristic of **1** with V_g=+4V and γ=0.01 eV for different varying angle θ. c) Schematic MO diagramm of undistorted **1**$^{\bullet-}$. Adapted with permission from ref. [14] Copyright 2018 American Chemical Society.

The possibility of controlling quantum interference in spiroconjugated molecules in single-molecule junctions is of great interest for possible future implementations in the design of functional molecular circuits.

To the best of our knowledge, there is no previous work on the design and implementation of spiroconjugated compounds in single-molecule junction experiments. Thus, based on the herein discussed theoretical analysis and predictions we began to investigate the synthesis of suitable model compounds for the study of quantum interference phenomena in spiroconjugated molecular junctions.

1.2 Results and Discussion

In the following chapter, design considerations based on DFT calculations and literature reports as well as the synthesis of compounds for the measurement of spiroconjugated molecular junctions will be discussed. The work presented below consists of three iterative attempts to synthesize spiroconjugated compounds bearing thioacetyl functionalities serving as gold anchor groups to ensure connection to the gold electrodes included in the experimental setup.

1.2.1 First Generation Molecular Design

From the leading theoretical work outlined in the section 1.1 several key design features must be fulfilled in order to obtain a structure capable of displaying the desired quantum interference behavior leading to current blockade: i) symmetry considerations around the spirocenter, ii) suitable orbital interactions across the spirocenter leading to degenerated levels on either one of the frontier orbitals and iii) two sulfur anchor groups in direct conjugation to the π-system on each side of the structure. Following this guideline, structural candidates were sought using DFT calculation methods to provide insight into the energy levels of the structures.

Since the sulfur substituted analog of **1** treated in the theoretical work[14] was deemed chemically not accessible other reported spiroconjugated compounds (Figure 5) were considered as a functional core. As a starting point the sulfur-functionalized derivative of **9,** where spiroconjugation has been experimentally observed, was investigated. DFT calculation at the B3LYP/6-31G* level of this first synthetic target (**11**, Figure 7) revealed that the carbonyl groups lower the energy of the degenerate molecular orbitals to an extent that they do not

represent the frontier molecular orbitals in contrast to **2** (see Figure 4). This structure therefore does not fulfill all the requirements necessary for current blockade to arise. However, exchanging the oxygen atoms for methylene groups lifts the e-states such that they become the LUMO.

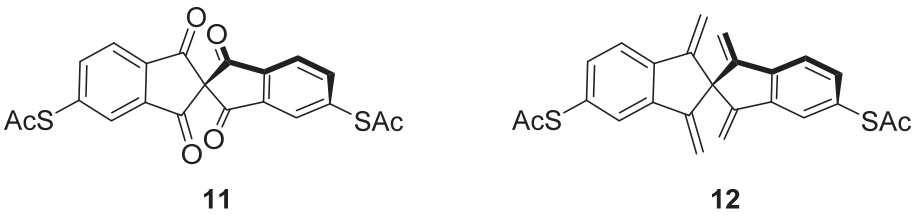

11 **12**

Figure 7: Structure of a **11** as a first molecular target.

As a result, compound **12** fulfils the structural and orbital symmetry requirements needed for the experimental investigation of current blockade induced by destructive quantum interference. Having identified the desired synthetic target, the elaboration of a synthetic route was necessary.

1.2.1.1 First Generation Synthesis

The approach to construct the first candidate, spiroconjugated tetraene **13**, bearing two perpendicular π planes as well as two gold anchor groups needed for the single molecule experiments is displayed in Scheme 1. We envisioned tetraene **13** to be accessible by a twofold Wittig reaction from the diketodiene **14**, which in turn should be obtained by benzylic bromination of the dione **15** followed by double elimination. Nucleophilic aromatic substitution by a sulfur nucleophile on the activated position *para* to the ketones of the intermediate **16** would allow the introduction of the needed sulfur functionality. The key step of this sequence, namely the spiroannelation, relies on a “double thermal cyclization” of the dienedione **17** *via* thermolysis.[16] This key precursor **17** should be reachable by a twofold Suzuki reaction of the dibromo derivative **18**, which in turn should be obtainable from the commercially available precursors **19** and **20** *via* Aldol condensation followed by formal oxidation.

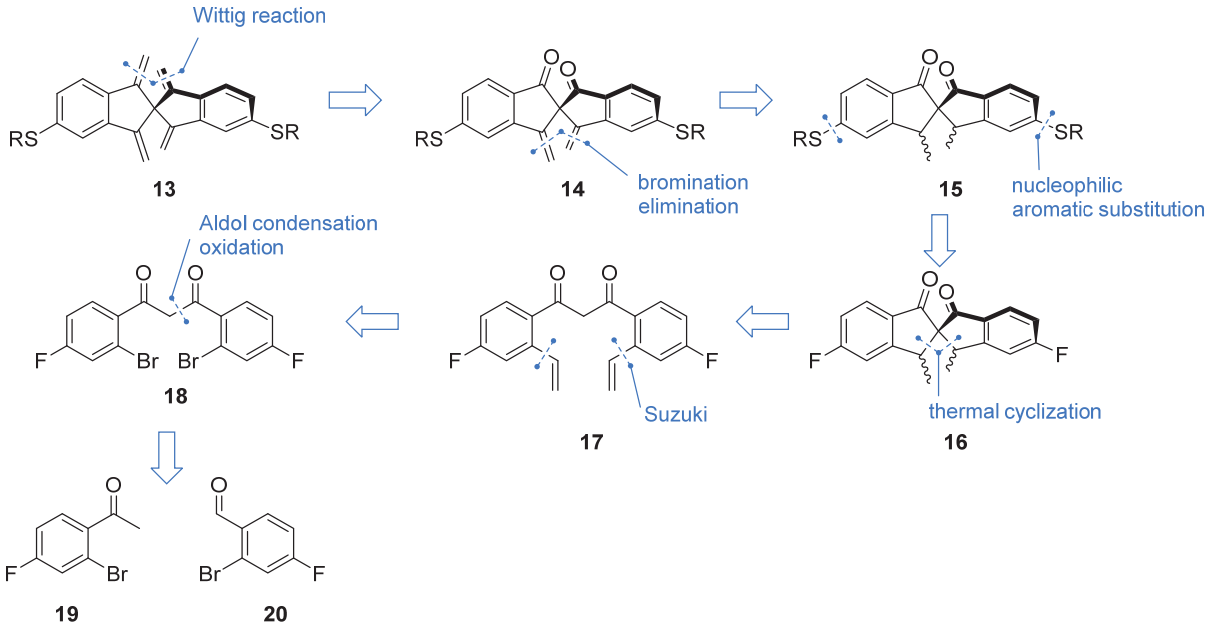

Scheme 1: Retrosynthetic analysis of spirotetraene **13**. For clarity only one enantiomer of each structure is drawn.

Following this approach, we started our synthetic efforts towards the spiroconjugated tetraene **13** (Scheme 2a) by carrying out an Aldol condensation with 1-(2-bromo-4-fluorophenyl) ethane-1-one (**19**) and 2-bromo-4-fluorobenzaldehyde (**20**) in ethanol at room temperature using catalytic amounts of sodium hydroxide giving the enone **21** as a white powder after recrystallization from ethanol in excellent 96% yield.[17] The enone **22** was subsequently brominated using elemental bromine in chloroform whereby the precipitate was collected and further purified by recrystallization from ethanol affording the tetrabromo compound **21** in 97% yield.[18,19] The hydrolysis to the diketone **18** was achieved by first refluxing **21** in a solution of potassium hydroxide in methanol followed by acid hydrolysis of the intermediate methyl enolether at reflux yielding the dione **18** in 80% after recrystallization from acetic acid.[18,19] Having compound **18** in hands we could address the strategically placed bromides of dione **18** by palladium catalyzed Suzuki reaction using vinyl trifluoroborate.[20] After initial ligand screening (PPh_3, XantPhos, RuPhos, DPPF, and SPhos) we found that using $PdCl_2$(DPPF) gave the highest isolated yield of **17** with 46%.

After having accomplished the synthesis of this key intermediate **17** we proceeded with the thermally induced spiroannelation reaction by sealing the substance under argon in a glass tube followed by heating it at 300°C for 16 h. The crude material was then purified by column chromatography and yielded a colorless solid.

However, analysis of the obtained product by NMR-spectrometry clearly revealed that 6,6'-difluoro-2,2'-spirobi-1-tetralon (**23**) comprising a spiro[5,5]undecane scaffold was formed

in the reaction instead of the desired spiro[4,4]none framework **16** (Scheme 1). This discrepancy of the formed ring size to the previously reported thermally induced spiroannelation reaction (Scheme 2b) might be related to a different transition state conformation due to decreased degrees of freedom of molecule **17** compared to **24**.

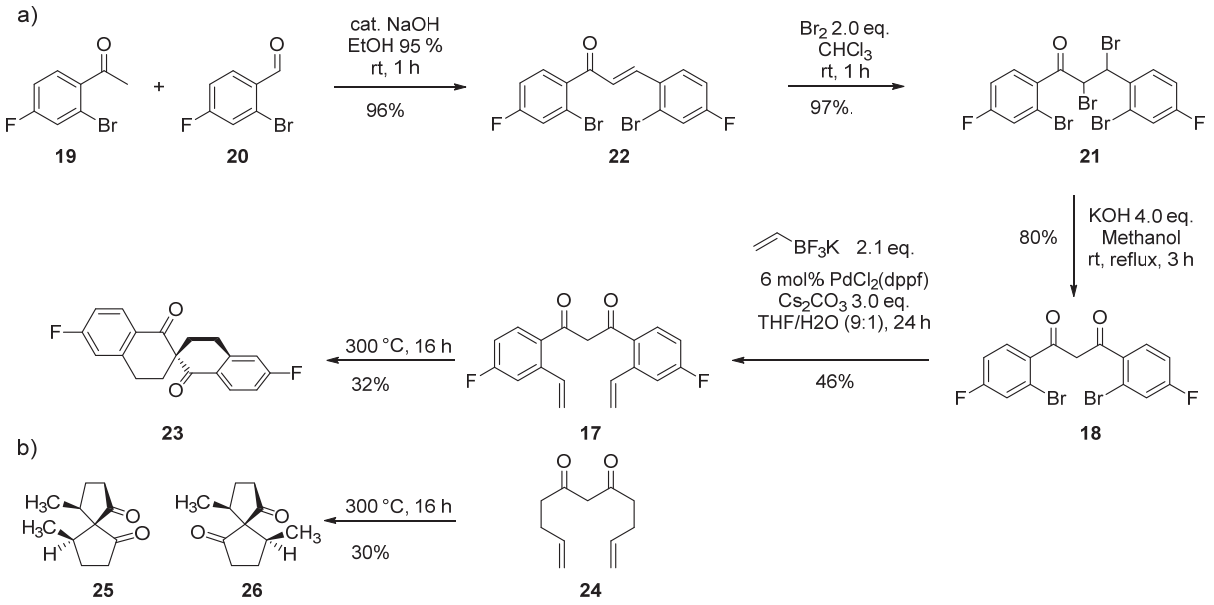

Scheme 2: Synthetic plan with used conditions and previously described "double thermal cyclization". a) Synthesis of unexpected spiroannelation product **23** as a racemate. b) Products 4*S*,9*S*-dimethyl-Spiro [4,4] nonane-1,6-dione (**25**) and 4*R*,9*S*-dimethyl-spiro [4,4]nonane-1,6-dione (**26**) of the previously reported thermally induced spiroannelation of undeca-1,10-diene-5,7-dione (**24**). For reasons of clarity only one enantiomer of each product (**26** and **25**) is displayed.

In the case of the spiroannelation of undeca-1,10-diene-5,7-dione (**24**) it is proposed[16] that the mechanism proceeds over a concerted six-membered transition state **27** (Scheme 3a), whereby the proton of the enol tautomer shifts to the terminal position of the alkene while a new bond is formed between the internal carbon of the alkene and the alpha carbon of the diketone. The same reaction can occur again with the mono-annelated intermediate **28** (only one transition state (**29)** to one of the two diastereomers **26** and **25** is depicted in Scheme 3a) giving rise to the spiro [4,4] nonane scaffold of **26** and **25** in a 1:2 ratio and in a total yield of 30 % (Scheme 2b).

However, as we could observe from the spiroannelation reaction of the thermolysis of compound **17,** another transitions state is possible, leading to a spiro [5,5,]undecane framework. In Scheme 3b a plausible mechanism explaining this observation is shown which also proceeds over a six-membered transition state **30**. Yet, the hydrogen of the enol is transferred to the internal position of the alkene while the terminal carbon forms a new bond to the enolizable carbon of the diketone forming a six-membered ring (**31**). The same reaction occurs a second time (**32**), thus forming the spirocyclic compound **23**.

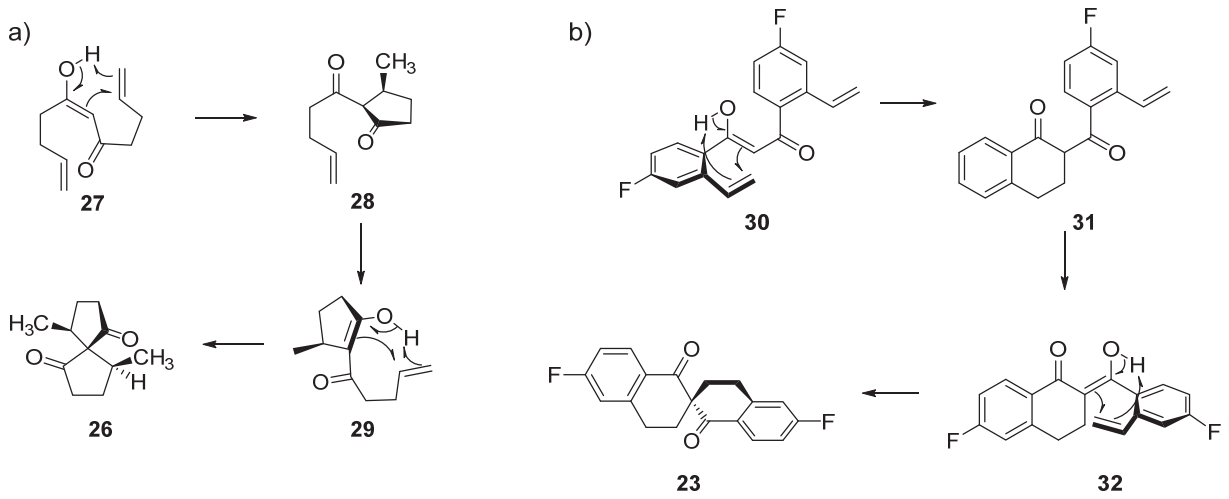

Scheme 3: Proposed mechanism thermally induced spiroannelation reactions. a) Mechanism of flexible, alkylchain spaced molecule. b) Mechanism of constrained, aryl spaced molecule. For clarity only the diastereomer **26** and one enantiomer of **23** is shown.

One possible explanation for the distinctness of the reaction mechanism is the difference in flexibility of the connecting units between the alkene and the diketone. In contrast to the flexible ethylene connected compound **24** the aryl spacer of compound **17** (Scheme 2a and b) seems to be constraining the geometry accessible to the transition states **30** and **33**, thus leading to the observed reaction product.

Even though we were not able to achieve the synthesis of the desired spiroconjugated compound **13** for single molecule experiments using this strategy, it is worth noting that, only one other method for the preparation of such 2,2'-spirobi-1-tetralon scaffold as present in molecule **23** has been reported.[21]

1.2.1.2 Second Generation Synthesis

Following our goal of preparing a suitable spiroconjugated compound suitable for single molecule experiments we decided to change our approach to construct the spirocycle **13**. Our modified approach is elucidated in Scheme 4. We focused our efforts on the synthesis of an 5,5’ sulfenyl substituted 2,2’-spirobiindantetraone (**34**) based on the reports that the 2,2’-spirobiindantetraone motif shows clear spiroconjugation effects.[5,6]

The required sulfur functionality, serving as anchor group for the single molecule measurements, might be installed either by nucleophilic aromatic substitution on the activated aryl halide **35** or *via* Buchwald-Hartwig reaction. Sulfenylation as the final step is appealing, since the transformation of 2,2'-spirobiindan-1,1'-dione scaffold **36** to the 2,2’-

spirobiindantetraone derivative **37** requires harsh oxidative conditions, which is incompatible with sulfides. The key step of this strategy, namely the formation of the spirocenter of the dione **37**, was envisioned *via* Claisen condensation after decarboxylation of compound **38**.[22] This key 2-ethoxycarbonyl-2-benzyl-1-indanone intermediate **38** should be obtainable by benzylation from 2-ethoxycarbonyl-1-indanone precursor **39** and methyl 2-(bromomethyl)benzoate derivative **40**. The halogenated 2-ethoxycarbonyl-1-indanone product **39** should be accessible via ethoxycabonylation of indanone **41**.

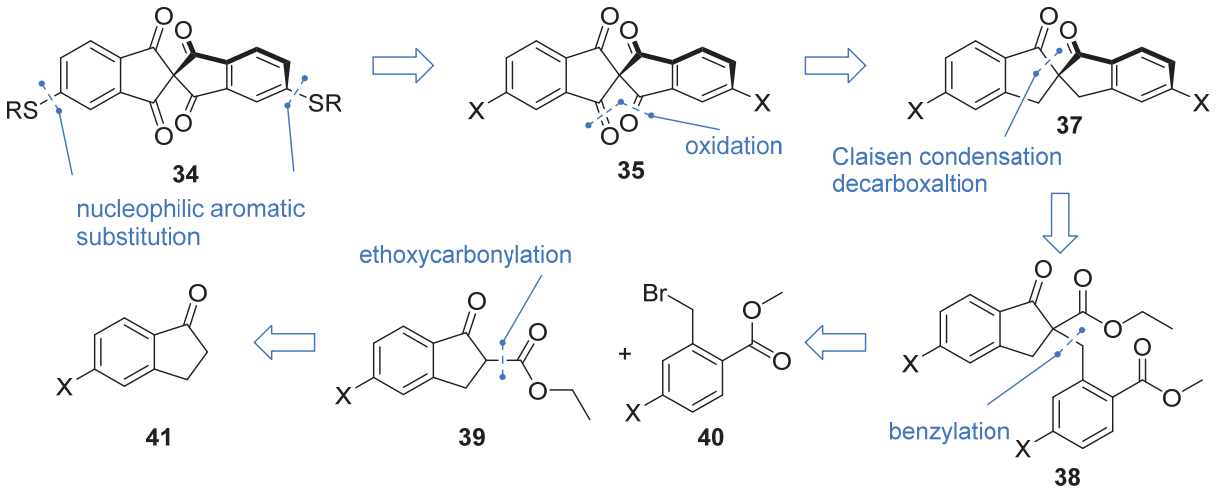

Scheme 4: Retrosynthetic analysis of spirobiindantetraone **34**. For clarity only one enantiomer of each structure (**34, 35, 37**) is drawn.

Having recognized suitable starting materials, 5-chloro -1-indanone **42** was refluxed with diethoxy carbonate **43** and sodium hydride in toluene for 5 h providing 5-chloro-2-ethoxycarbonyl 1-indanone **44**[22] in 90% yield (Scheme *5*). Using chloride as the halide for the synthesis enables the sulfide functionality to be later introduced either by nucleophilic aromatic substitution or Buchwald-Hartwig reaction. By reacting the ketoester **44** with the commercially available methyl 2-bromomethyl-4-chloro benzoate **45** and sodium hydride in dimethyl formamide at 60°C for 24 h the 2-ethoxycarbonyl-2-benzyl-1-indanone[22] derivative **46** could be obtained. Refluxing a solution of **46** in hydro bromic acid and acetic acid for 2 h[22] lead to a reaction cascade, whereby compound **46** initially decarboxylates and the newly generated enol undergoes an intramolecular mixed Claisen condensation forming 5,5'-dichloro-2,2'-spirobiindan-1,1'-dione **47** in good yield.

The efficient synthetic route to this spirobiindandione precursor **47** enabled the synthesis of the model compound **48** which lacks the symmetry required to observe the theorized quantum interference phenomena caused by spiroconjugation. However, model compound **48** allowed

us to search for suitable conditions to install the required sulfur functionality required for the single molecule experiments of **34**. It was found that treating the spirobiindandione **47** with 2-(trimethylsilyl)ethane-1-thiol and sodium hydride in deoxygenated dimethylformamide at 0°C followed by additional 24 h at room temperature gave the desired substitution product **49** in acceptable yield of 59%. To our delight transprotection of compound **49** to the dithioacetate **48** could be achieved albeit in low yield.

Encouraged by the successful installment of the sulfur anchor functionality we started searching for conditions for the double oxidation of spirobiindandione **47.** Although this transformation was already described in previous work[5] the procedure was challenged by several drawbacks. The reported synthesis of spirobiinadantetraone from spirobiindandione proceeds over several steps, one of which is a fourfold bromination step with long reaction time (>100h) requiring the use of carbon tetrachloride which is nowadays scarcely available. Substitution of the solvent for chloroform was reported to not form the required product[23] Therefore, alternative conditions for the formation of spirobiindanetetraone **50** from spirobiindanedione **47** were needed. After initial reaction screening, we could identify that a photooxidation reaction using a combination of potassium bromide/Oxone® in a biphasic dichloromethane/water system indeed formed the desired spirobiindanetetraone derivative **50** in one step.

Having found suitable conditions for the synthesis of tetraone **50** and motivated by the successful functionalization of the intermediate dione **47** the same sulfenylation conditions were applied for the synthesis of spirobiindantetraone **50.** The addition of a deoxygenated solution of substrate **50** in dimethylformamide to a deoxygenated mixture of sodium hydride and 2-(trimethylsilyl)ethane-1-thiol in dimethylformamide at 0°C led to an immediate color change of the solution to dark orange. This observation was distinct from the previous sulfenylation reaction of **47** where no color change was observed and therefore indicated a different reaction outcome. Indeed, TLC analysis revealed full conversion of the starting material **50** accompanied by a complex mixture of products. From this complex mixture no product **51** could be isolated or observed by means of mass spectroscopy. Presumably a nucleophilic promoted rearrangement[5] took place followed by subsequent reactions leading to an inseparable mixture.

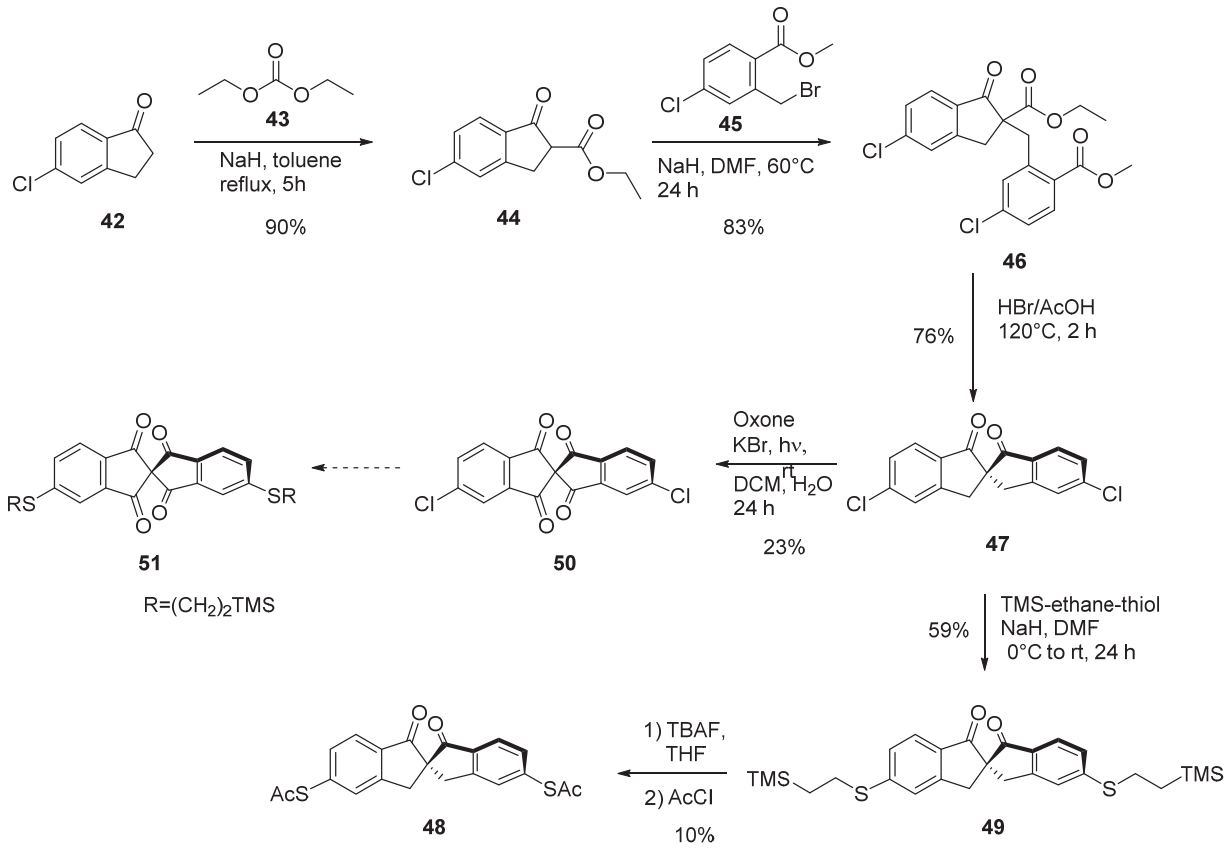

Scheme 5: Synthetisis of spirobiindandione **48** and spirobiindantetraone **50** with used conditions. Only one enatiomere is shown due to visibility.

1.2.2 Second Generation Molecular Design

Due to the instability of spirobiindantetraone **50** towards nucleophiles the synthesis of **51** was not realizable. Therefore, other spiroconjugated units were investigated. An interesting compound where spiroconjugation effects have been demonstrated[24] is spiro[5.5]undeca-1,4,7,10-tetraene-3,9-dione **7** (Figure 8). This spirotetraene **7** was first prepared by Dreiding *et. al.* in 1966 in 7 steps from 1,2,5,6-tetrahydrobenzaldehyde[24] and more recently utilized for the preparation of electroactive systems.[25]

7

Figure 8: Structure of spiro[5.5]undeca-1,4,7,10-tetraene-3,9-dione **7.**

Computer assisted DFT calculations at the B3LYP/631-G* level of theory indeed showed that **7** exhibits degenerate e-states at the frontier orbitals, therefore further emphasizing the suitability of this spiroconjugated building block to act as a current blockade. However, the need for a gold anchor functionality conjugated to this spirotetraene represents a conceptual challenge. S-Phenyl thioacetate, as most well-established anchor groups for gold has a mismatch in valency to **7** and therefore an alternative anchor motif was needed. In Figure *9* an alternative anchor group is shown which has previously been found to form molecular junctions with gold.[26,27]

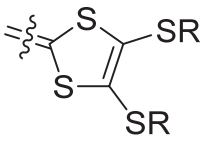

Figure 9: "Dithiafulvalene" motive as possible gold anchor functionality.

Building on these works we concluded that the unprecedent compound **52** (Figure *10*) could be a promising structure for the observation of quantum interference effects in spiroconjugated molecules by single molecular junction experiments. This molecule fulfills the requirements laid out by the theoretical work,[14] as it is highly symmetrical (D_{2d}), contains an spiroconjugated core and has conjugated gold anchor groups (RSAc). Furthermore, DFT calculations at the B3lyp/631-G* level of theory indicated that the relative placement of the frontier orbitals is not changed by the functionalization, and **52** still comprises degenerate frontier orbitals.

52

Figure 10: Target molecule **52** for the observation of quantum interference effects of spiroconjugation in single molecule experiments

Having found a promising molecular structure for the experimental observation of destructive quantum interference, the synthetic route needed to be laid out.

1.2.2.1 Synthesis

For this, the literature known compound **53** (Scheme 6) needed to be prepared. However, we recognized that the synthesis of spiro[5.5]undeca-1,4,7,10-tetraene-3,9-dione (**7**) could be significantly shortened. The original route[24] to **7** (Scheme *6*) starts from compound **53** involving a Birch reduction, acetylation, epoxidation, reductive epoxide opening, followed by Jones-Oxidation and a final oxidation to the tetraene **7** with 2,3-dichloro-5,6-dicyano-1,4-benzoquinone (DDQ). Yet, performing a Tsuji-Wacker Oxidation on **53** followed by oxidation with DDQ would allow spirotetraene **7** to be synthesized in two steps.

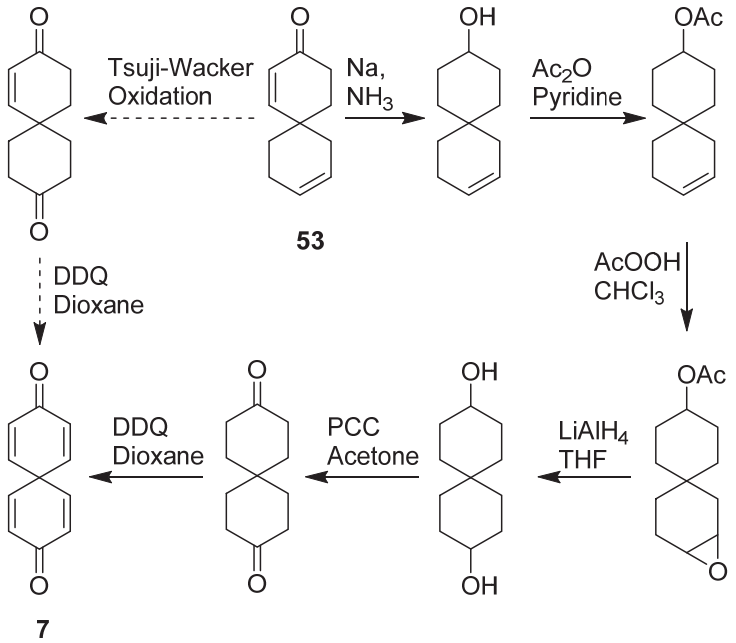

Scheme 6*:* Original route to spiro[5.5]undeca-1,4,7,10-tetraene-3,9-dione **7** (right, plain arrows) and proposed improved two step route to **7** (left, dashed arrows).

Therefore, the above described spirodienone **53** was synthesized (Scheme *7*) from methyl vinyl ketone (**54**) and 1,2,5,6-tetrahydrobenzaldehyde (**55**) *via* acid catalyzed Robinson annulation according to literature.[24] With compound **53** in hands, the original Tsuji-Wacker Oxidation[28] condition using palladium (II) chloride, copper (II) chloride in dimethylformamide (DMF)/water (7:1) and molecular oxygen as oxidant were initially employed for the conversion to spiro compound **56**. However, under these reaction conditions only minor conversion was observed. The low reactivity of internal and cyclic olefins towards the applied reaction conditions has already been previously reported.[29] Still, using palladium (II) acetate in acetonitrile (MeCN)/water 9:1 and *p*-benzoquinone as the oxidant with perchloric acid as an additive,[30] gave full conversion after refluxing for 16 h and yielded the desired compound **56** in good yield and regio selectivity (10:1). The observed regio selectivity presumably arises due to sterically shielding by the perpendicular ring attached to the spirocarbon on **7**. The inseparable mixture of isomers was then further oxidized using, as previously reported,[24] DDQ in refluxing dioxane for 48 h. The isolation of spirotetraenedione **7** by column chromatography using activated basic aluminium oxide followed by sublimation was achieved in 27% yield, which is comparable to the original report.

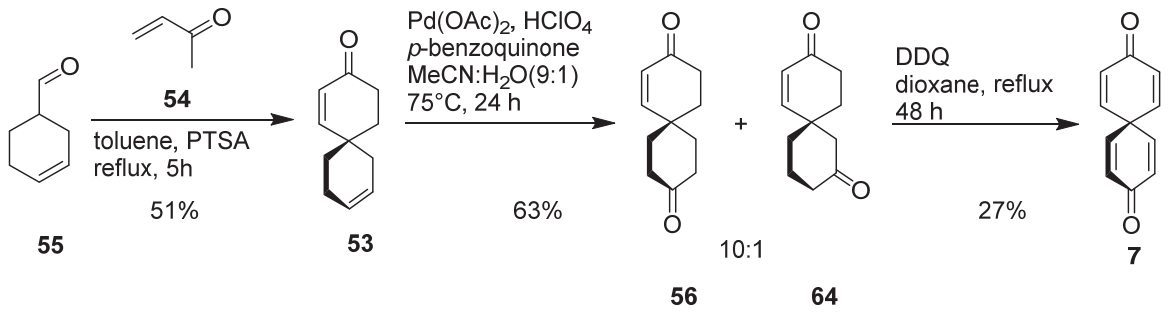

Scheme 7: Optimized synthesis of spirotetraenedione **7**.

Having successfully synthesized spirotetraenedione **7,** which will serve as the core of structure **52** displaying spiroconjugation, the synthesis of the interconnecting unit and assembly thereof was performed (Scheme *8*). The literature known[31] thion **57** bearing cyanoethyl protection groups could be converted in one step to the phosphonate **58** by refluxing a solution of **57** in xylene with triethylphosphite ($POEt_3$) for 5 h.[32] Phosphonate **58** and spirotetraenedione **7** were reacted together in a Horner-Wadsworth-Emmons reaction[25] yielding the double addition product **59** in 33% yield. This spiroconjugated compound **59** bearing four cyanoethyl groups was then transprotected[26] by adding a solution of 4 equivalents of caesium hydroxide

monohydrate ($CsOH{\cdot}H_2O$) in dry methanol to a solution of **59** in dry THF at room temperature. The formed tetrathiolate intermediate was then trapped by the addition of acetyl chloride (AcCl) at 0°C, allowing the mixture to warm up to room temperature over the course of 16 h. Isolation by column chromatography yielded the desired target structure **52** in 42% as an orange oil.

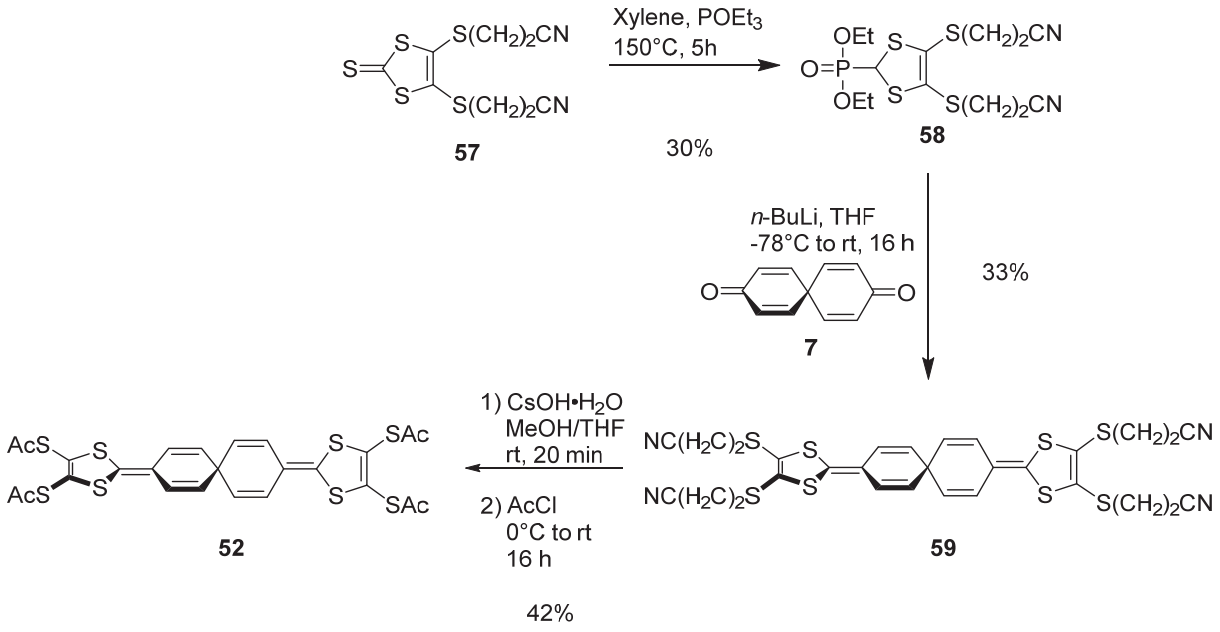

Scheme 8: Synthesis of target spiroconjugation extended tetrathiafulvalene **52** bearing four thioacetate functionalities as gold anchor groups.

1.2.3 Transport measurements

In order to validate the theory that spiroconjugated compounds with suitable anchor functionalities, geometry, symmetry and frontier orbital levels show quantum interference phenomena in molecular junctions, conductance experiments on single molecules are necessary. Several methods for the measurement of the electronic transport through single molecules have been developed such as scanning tunneling microscopy (STM),[33–35] current probe atomic force microscopy (CP-AFM),[36–38] STM break-junction (STM-BJ),[39–44] crossed wire geometry,[45] mechanically controllable break junctions (MCBJ),[46–51] electro migration setups[52,53] and liquid metal junction setups.[54,55] Whereby MCBJ and STM-BJ have been recognized as a widely applicable and reliable approach to investigate the electronic transport through single molecules.[56] The conceptual working principle of MCBJ is shown in Figure 11. The setup consists of a thin gold wire on top of a flexible phosphorous bronze substrate coated with a polyimide layer for insulation. Mounting the sample on a three-point bending contraption with a central piezoelectric actuator and two lateral clamps allows the gold wire to be stretched until rupture occurs. This leaves two atomically sharp electrodes whose separation can be mechanically controlled. By reducing the displacement, the gold wire fuses again, whereby this breaking-making process can be repeated thousands of time while recording the conductance of the junction. This manipulation of the electrode displacement with subnanometer precision permits observation of the formation and breaking of a molecular junction with increasing gap size and thus providing characteristic molecular conductance features.

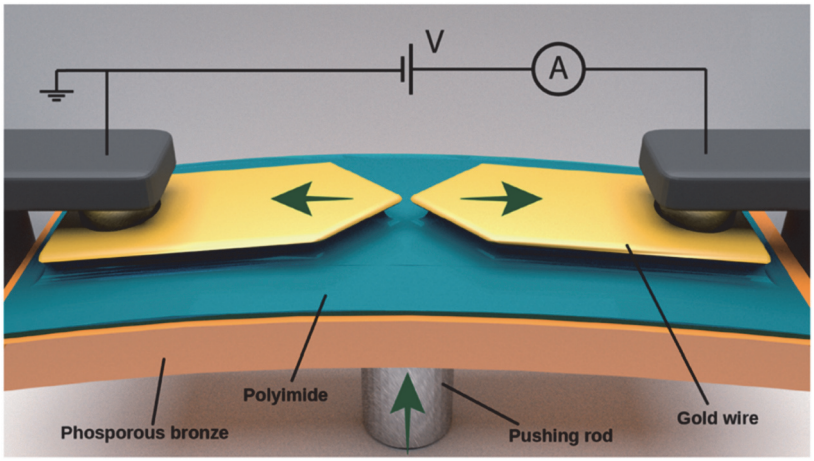

Figure 11: Schematic representation of a mechanically controllable break-junction (MCBJ). Adapted with permission from ref. [57]- Published by The Royal Society of Chemistry.

A well-studied molecular junction by MCBJ is based on functionalized oligophenyleneethylene (OPE-3, Figure 12b).[58] Measurements showing the superimposed collection of conductance *vs* displacement (two-dimensional histogram) of such a molecular junctions showing the influence of the anchor functionality is shown in Figure 12. The conductance values are displayed relative to the conductance of one single gold atom (G_0) and is for organic molecules usually several orders of magnitude lower. As outlined in Figure 12a the conductance property of the molecular junction is dependent on the anchoring group (Figure 12b) and from the investigated functionalities thioacetate A has the best electronic coupling to the gold electrodes.[58]

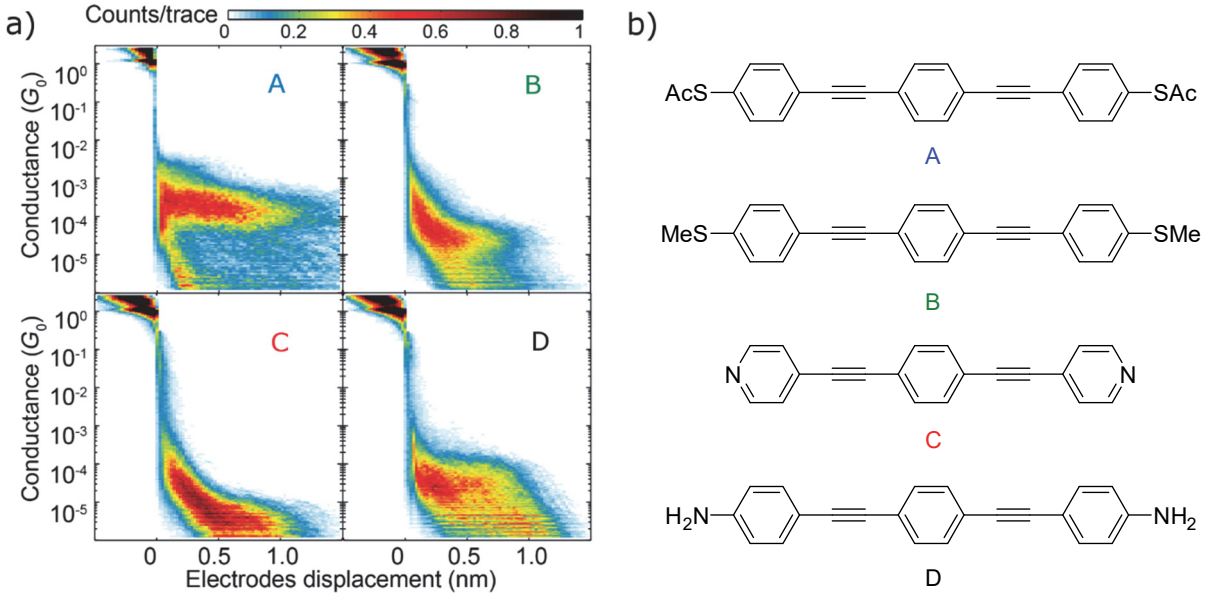

Figure 12: Anchoring group effect on conductance through single molecules. a) Conductance–distance histograms built from the breaking traces of b) molecules A–D. Adapted from ref. [58] – Published by Beilstein Journal of Nanotechnology.

Upon breaking of the gold molecule junction, a sharp decrease of the conductance is observed. In cases where a molecule is bridging the gap a conductance plateau arises with increasing electrode displacement. This plateau is usually of the same length as the molecule spanning the cleft and with further displacement of the electrodes the gold-molecule bond breaks leading again to a sharp decrease in conductivity. Typically, several thousand traces are collected by consecutively closing and breaking of the junction in order to obtain statistically representative distribution.

In cooperation with the group of Professor Herre van der Zant from the Technical University of Delft the electronic transport properties of spiroconjugated molecular junctions were investigated. Transport experiments with model compound **48** indeed showed signatures of a molecular junction. A two-dimensional (2D) histogram consisting of 10 000 individual conductance traces of molecule **48** is shown in Figure 13a. The observed conductance of the

fully stretched molecule is ~10^{-5} G_0, which is one order of magnitude lower than OPE-3. However, this indicates that spiroconjugation is indeed present in compound **48** leading to electronic transport though the molecule. Furthermore, the probability of junction formation for this compound is unusually high with a yield close to 100%. To our knowledge these are the first transport measurements of a spiroconjugated molecular junction.

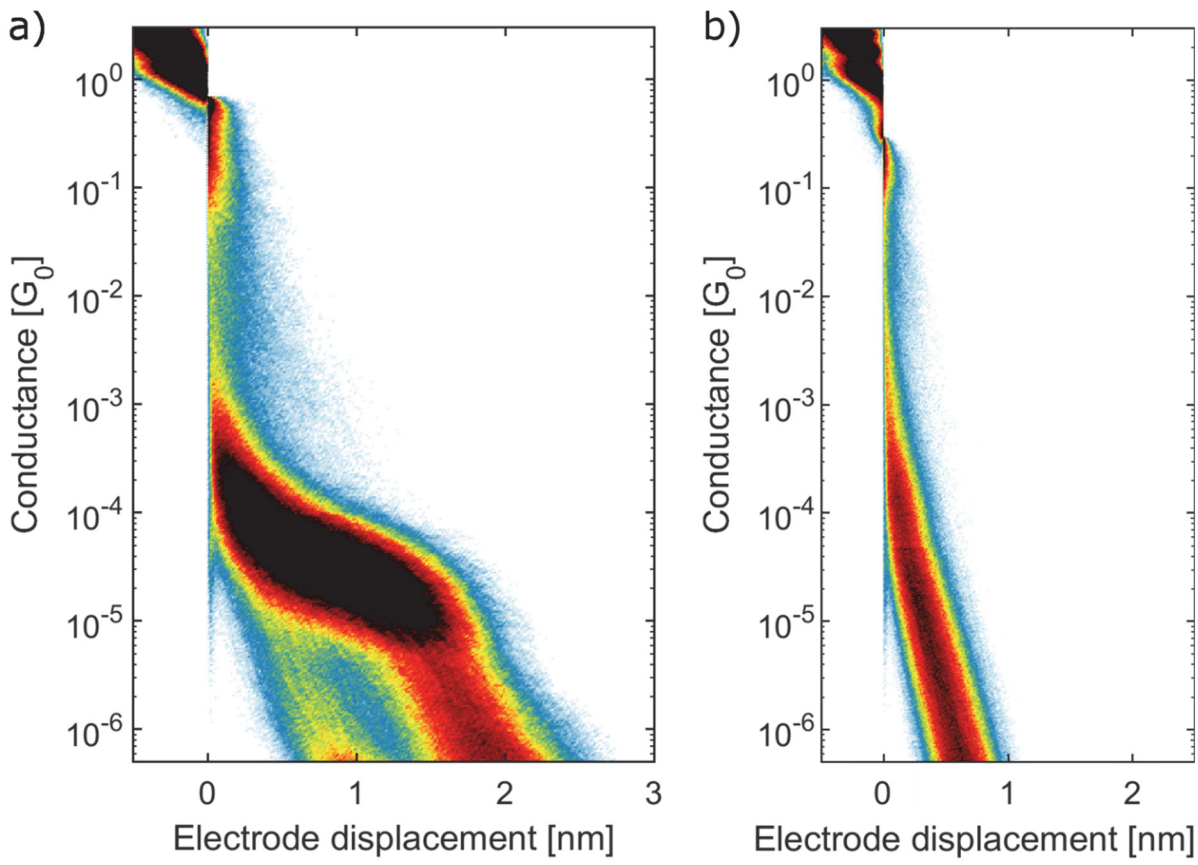

Figure 13: Two-dimensional conductance *vs.* displacement histograms built from 10 000 consecutive breaking traces of a) **48** and b) **52**.

In contrast to these strong evidences for the formation of a well-behaved molecular junction stands the results of the measurements of the higher symmetrical spiroconjugated compound **52** where quantum interference effects leading to current blockade are expected. For **52** a representable 2D histogram of 10 000 consecutive traces is shown in Figure 13. It is clearly visible that no molecular features are present in the accessible conductance window of $G_0 > G > 10^{-7} \times G_0$. This leaves room to two possible explanations: i) the yield of junction formation is close to zero or ii) the conductance of **52** is lower than $10^{-7} \times G_0$. Therefore, either the anchor groups of **52** are not suitable for the formation of a molecular junction or the quantum interference effects predicted to be present in this molecule leads to an almost complete current blockade.

1.3 Summary and Outlook

In this work a new synthetic strategy for the synthesis of a 2,2'-spirobi-1-tetralon scaffold (**23**) by thermolysis was developed. Further, two spiroconjugated compounds bearing thioacetates as gold anchor groups were successfully synthesized. The reference compound 5,5'-di(acetylsulfenyl)-2,2'-spirobiindan-1,1'-dione **48,** which was expected not to show current blockade due the presence of only two interacting moieties, is to our knowledge, the first spiroconjugated compound measured in a mechanically controlled break-junction experiment. Indeed, first evidence for the formation of spiroconjugated molecular junctions could be observed. However, the synthesis of the derivative **51** which should display DQI induced current blockade was not achieved due to chemoselectivity issues, as the spiroconjugated core of compound **50** turned out to be more reactive towards thiolate nucleophiles than the desired reaction site. Despite that, the synthesis of **50** showcases the first successful synthesis of a dihalogenated spirobiindantetraone.[23] Yet, a third attempt of synthesizing a spiroconjugated compound meeting the orbital and molecular symmetry requirements for the observation of DQI was achieved with the synthesis of the tetrathioacetyl functionalized compound **52**. Preliminary experiments employing spirocompound **52** were not conclusive, as the conductance traces lack any molecular features. However, this observation may be attributed to DQI effects leading to complete current blockade.[14] Further experiments where the current blockade is lifted by gating the junction are needed in order to obtain conclusive results.

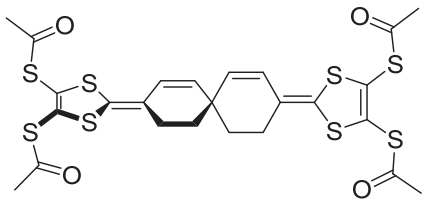

60

Figure 14: Proposed structure of refence compound **57** in order to gain insight to the molecular junction formation in MCBJ experiments.

It is also desirable to synthesize and measure a corresponding reference compound where no current blockade can be expected, in order to exclude that the lack of molecular features in the conductance traces is a result of not well behaving junction formation. In Figure 14 a proposed structure (**60**) of such a reference compound is shown. If compound **60** forms a molecular junction in MCBJ experiments conductance features should be observed similar to reference compound **48**. This would provide concise evidence that **52** indeed shows DQI leading to a current blockade.

A further possibility would be to probe the angle dependency of DQI on the twisting angle around the spirocenter. According to theory an increased conductance should be observed by deviation from a 90° angle between the π-systems upon application of a gating voltage. Therefore, one may consider the structure of spirotetraenedione **61** where an angle deviating from 90° can be expected due to steric repulsion between the appended tert-butyl substituents. This structure may be accessible *via* the reported procedure for the efficient one-pot synthesis of β-alkyl substitude enones, which has been shown to be suitable even for the introduction of the *tert*-butyl functionality in beta-position in good yields.[59] Conducting the following reactions according to the strategy employed in this work may deliver the twisted molecule **62**, which could provide further insight on the DQI as the extend of the current blockade should decrease allowing for molecular features to be observable by MCBJ experiments.

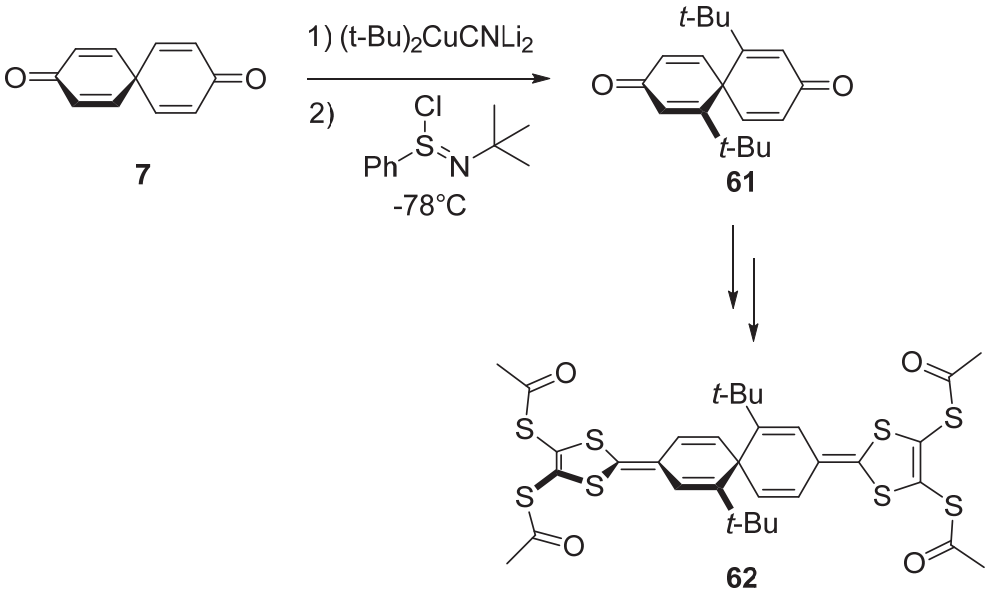

Scheme 9: Proposed derivatisation of spirotetraenedione **7** by introduction of two tert-butyl units *via* double β-addition followed by oxidation for the assembly of a twisted spiroconjugated molecule for single molecule measurements.

Further, the synthesis of a four-fold β-substituted compound by subjecting the disubstituted compound to the same conditions may be attainable. This strategy can be useful for tuning of the frequency of the twisting mode vibration (ω) to the resonant charge transport (γ) by increasing the reduced mass of the vibrational mode and therefore reducing the frequency. Since, matching of the frequency of the electron hopping to the nuclear dynamics associated with the twisting vibrational mode around the spirocentes is required for lifting the current bloacked caused by DQI. [14]

1.4 Experimental Part

General Information

All commercially available compounds were purchased and used as received unless explicitly stated otherwise. All NMR experiments were performed on Bruker Avance III or III HD, two or four-channel NMR spectrometer operating at 400.13 or 500.13 MHz proton frequency. The instruments were equipped with direct observe BBFO, indirect BBI or cryogenic four-channel QCI (H/C/N/F) 5 mm probes all with self-shielded z-gradient. The experiments were performed at 298 K and the temperature was calibrated using a methanol standard showing accuracy within +/- 0.2 K. GC-MS was performed on a Shimadzu GCMS-2020 SE equipped with a Zebron 5 MS Infernocolumn which allowed to achieve temperatures up to 350 °C. High-resolution mass spectra (HRMS) were measured as HR-ESI-ToF- MS with a Maxis 4G instrument from Bruker and were measured on a Bruker solariX spectrometer with a MALDI source for HR-MALDI-ToF MS. For column chromatography silica gel Siliaflash® p60 (40–63 µm) from Silicycle was used, and TLC was performed on silica gel 60 F254 glass plates with a thickness of 0.25 mm purchased from Merck Melting point were measured with a Stuart SMP3 with a slope of 5°C/min.

(E)-1,3-bis(2-bromo-4-fluorophenyl)prop-2-en-1-one (22):

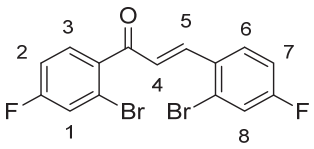

A procedure from literature[17] was modified as followed: A mixture of 1-(2-bromo-4-fluorophenyl) ethane-1-one **19** (8.68 g, 40.0 mmol, 2.0 eq.), 2-bromo-4-fluorobenzaldehyde **20** (4.06 g, 20.0 mmol, 1.0 eq.) and NaOH pellets (200 mg, 5 mmol, 0.25 eq.) in absolute EtOH (40 mL) was stirred for 0.5 h and then allowed to stand for 1 h. The precipitated product was collected by filtration and purified by recrystallization from EtOH yielding enone **22** as a white powder (7.7 g, 19.2 mmol, 96 %).$^{1}H\{^{19}F\}$ NMR (500 MHz, CD_2Cl_2): δ [ppm]= 7.74 (d, $^{3}J_{HH}$ = 16.0 Hz, 1H, CH^{5}), 7.73 (d, $^{3}J_{HH}$ = 8,8 Hz, 1 H, ArH^{3}), 7.50 (d, $^{3}J_{HH}$ = 8.5 Hz, 1H, ArH^{6}), 7.44 (d, $^{4}J_{HH}$ = 2.5 Hz, 1H, ArH^{1}), 7.40 (d, $^{3}J_{HH}$ = 2.6 Hz, 1H, ArH^{8}), 7.18 (dd, $^{3}J_{HH}$ = 8.8 Hz, $^{4}J_{HH}$ = 2.5 Hz, 1H, ArH^{2}), 7.13 (dd, $^{3}J_{HH}$ = 8.5 Hz, $^{3}J_{HH}$ =2.6 Hz, , 1H, ArH^{7}), 6.99 (d, $^{3}J_{HH}$ = 16.0 Hz, 1H, CH^{4}). ^{13}C NMR (151 MHz, CD_2Cl_2): δ [ppm]= 193.09 (CO), 164.75 (d, $^{1}J_{CF}$ = 23 Hz, CF), 162,72 (d, $^{1}J_{CF}$ = 23 Hz, CF), 143.69 (CH^{5}), 137.44 (d, $^{4}J_{CF}$ = 3.7 Hz, C), 131.51 (d, $^{3}J_{CF}$ = 9.1 Hz, CH), 131.27 (d, $^{4}J_{CF}$ = 3.7 Hz, C), 129.74 (d, $^{3}J_{CF}$ = 9.0 Hz, CH), 128.55 (CH), 126.61 (d, $^{3}J_{CF}$ = 9.8 Hz, CBr), 121.30 (d, $^{2}J_{CF}$ = 24.6 Hz, CH), 121.10 (d, $^{2}J_{CF}$ = 24.6 Hz, CH), 120.80 (d, $^{3}J_{CF}$ = 9.8 Hz, CBr), 115.90 (d, $^{2}J_{CF}$ = 21.8 Hz, CH), 115.24 (d, $^{2}J_{CF}$ = 21.5 Hz, CH). GC-MS (EI): *m/z* (%) = 320.9, (100); 120.0, (97.4); 322.9, (96.7); 94.0, (69.8); 107.0, (38.5); 99.0, (32.4); 213.9, (30.3); 200.8, (24.8); 119.0, (21.2); 73.95, (20.49); 172.9, (19.6); 93.0, (19.2); 202.8, (18.7); 174.9, (18.1); 321.9, (16.6); 148.0, (16.3); 50.0, (16.3); 75.0, (15.3); 323.9, (15.2); 240.9, (14.3); 241.9, (13.9); 95.0, (13.5); 100.0, (11.0); 106, (10.3); 68.0, (9.9).

2,3-dibromo-1,3-bis(2-bromo-4-fluorophenyl) propan-1-one (21):

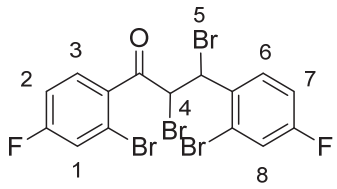

A procedure from literature[18] was modified as followed: To a vigorously stirred solution of enone **22** (4.02 g, 10.0 mmol 1.0 eq.) in $CHCl_3$ (10 mL) was added bromine (800 mg, 10.0 mmol, 1.0 eq.) in a dropwise manner over the course of 0.5 h. After complete addition the reaction mixture was stirred for 1 h and let stand for 1h. The precipitate was filtered, washed with MTBE (3x 20 mL) and recrystallized from EtOH yielding the desired 2,3-dibromo-1,3-bis(2-bromo-4-fluorophenyl) propan-1-one **21** (5.45g, 9.7 mmol, 97%). $^1H\{^{19}F\}$ NMR (400 MHz, $CDCl_3$): δ [ppm]= 7.81 (d, $^3J_{HH}$ = 8.8 Hz, 1H, ArH^3), 7.59 (d $^3J_{HH}$ = 8.8 Hz, 1H, ArH^2), 7.47 (d, $^4J_{HH}$ = 2.1 Hz, 1H, ArH^1), 7.37 (d, $^4J_{HH}$ = 3.2 Hz, 1H, ArH^8), 7.22 – 7.11 (m, 2H, ArH^6, ArH^7), 6.17 (d, $^3J_{HH}$ = 11.6 Hz, 1H, H^5), 5.74 (d, $^3J_{HH}$ = 11.6 Hz, 1H, H^5).

1,3-bis(2-bromo-4-fluorophenyl)propane-1,3-dione (18):

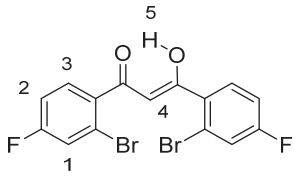

A procedure from literature[18] was modified as followed: To a solution of 2,3-dibromo-1,3-bis(2-bromo-4-fluorophenyl) propan-1-one **21** (2.81 g, 5.00 mmol, 1.0 eq.) in MeOH (100 mL) was added a solution of KOH (2.5 g) in MeOH (13 mL) and the reaction mixture was refluxed for 3 h. The precipitated salt was removed by filtration and the filtrate was acidified with HCl (aq., 37%), diluted with water (30 mL) and refluxed for 2 h. The reaction mixture was cooled down and the precipitate was filtered, washed with water and recrystallized from acetic acid yielding 1,3-bis(4-fluoro-2-vinylphenyl) propane-1,3-dione **63** (1.69 g, 4.04 mmol, 80%) $^1H\{^{19}F\}$ NMR (250 MHz, $CDCl_3$): δ [ppm]= 15.83 (s, 1H, OH^5), 7.65 (d, $^3J_{HH}$ = 8.7 Hz, 2H, ArH^3), 7.42 (d, $^4J_{HH}$ = 2.5 Hz, 2H, ArH^1), 7.13 (dd, $^3J_{HH}$ = 8.7 Hz, $^4J_{HH}$ = 2.5 Hz, 2H, ArH^2), 6.50 (s, 1H, CH^4). GC-MS (EI): *m/z* (%) = 138, (100); 110, (77); 256.9, (53.5); 335.8, (46.2); 337.8, (45.3); 82, (34.6); 100.5, (25.4); 119, (21.8); 99, (21.3); 201, (16.8); 81, (14.6); 307.8, (13.7); 309.8, (13.3); 94, (11.4); 63, (11.1); 199.9, (10.7); 154.9, (10.7); 154, (9.6).

1,3-bis(4-fluoro-2-vinylphenyl) propane-1,3-dione (17):

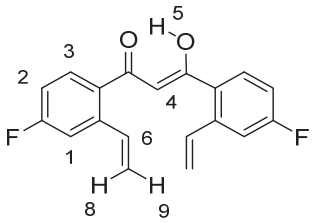

A 5 mL Schlenk flask was charged with 1,3-bis(2-bromo-4-fluorophenyl)propane-1,3-dione **18** (79,8 mg, 0,191 mmol, 1.0 eq.), potassium vinyltrifluoroborate (102 mg, 0,764 mmol, 4 eq.), $CsCO_3$ (747 mg, 2,29 mmol, 12 eq.) and PdCl2(dppf) (14 mg, 19,1 mmol, 0,1 eq.). Under argon a deoxygenated 9:1 solution of THF and water was added. The reaction mixture was heated to 85°C fo16 h. THF was removed under reduced pressure and the residue was extracted with EtOAc, the combined organic layers were dried over anhydrous Na_2SO_4 and filtered. The solvent was removed under reduced pressure and the crude product was purified by column chromatography (SiO_2, CH_2Cl_2/cyclohexane; 2:1) yielding 1,3-bis(4-fluoro-2-vinylphenyl) propane-1,3-dione **17** (29.1 mg, 9.3 μmol, 49%).$^1H\{^{19}F\}$ NMR (400 MHz, CD_2Cl_2) : δ [ppm]= 16.38 (s, 1H, OH^5), 7.64 (d, $^3J_{HH}$ = 8.5 Hz, 2H,H^3), 7.32 (d, $^4J_{HH}$ = 2.5 Hz, 2H, H^1), 7.18 (dd, $^4J_{HH}$ = 17.4 Hz, $^4J_{HH}$ = 10.9 Hz, 2H,H^6), 7.07 (dd, *J* = 8.7, 2.7 Hz, 2H, H^2), 6.19 (s, 1H, H^4), 5.75 (dd, *J* = 17.4 Hz, 2H, H^8), 5.43 (d, $^4J_{HH}$ = 10.9Hz, 2H,H^9). GC-MS (EI): *m/z* (%) = 78, (100); 77.1, (82.8); 125, (52.9); 51, (36.4); 109, (33.2); 64, (31.1); 250, (23.8); 141, (21.9); 50, (19.8); 65, (18.5); 52.1, (15.6); 110, (11.4).

6,6'-difluoro-2,2'-spirobi-1-tetralon (23):

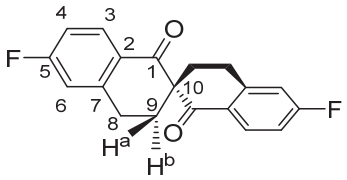

A test tube was charged with 1,3-bis(4-fluoro-2-vinylphenyl) propane-1,3-dione **17** (29.1 mg, 9.3 mmol) under argon atmosphere and sealed. The tube was heated to 300°C for 16h. The black residue was purified by column chromatography (SiO_2, CH_2Cl_2/cyclohexane; 1:1) yielding spirodione **23** as a white solid (9.3 mg, 3.0 mmol, 32%). $^1H\{^{19}F\}$ NMR (500 MHz, $CDCl_3$): δ [ppm]= 8.08 (d, $^3J_{HH}$ = 8.7 Hz, 2H, ArH), 7.02 (dd, $^3J_{HH}$ = 8.7 Hz, $^4J_{HH}$ = 2.5 Hz, 2H, ArH), 6.94 (d, $^4J_{HH}$ = 2.5 Hz, 2H, ArH), 3.01 (dd, $^3J_{HH}$ = 7.4 Hz, $^3J_{HH}$ = 5.0 Hz, 4H,CH_2), 2.81 (ddd, *J* = $^2J_{HH}$ 13.5, $^3J_{HH}$ 7.1, $^3J_{HH}$ 6.0 Hz, 2H,H^a), 2.07 (ddd, $^3J_{HH}$ = 14.0 Hz, $^3J_{HH}$ = 6.7 Hz, $^3J_{HH}$ = 5.5 Hz, 2H, H^b). ^{13}C NMR (151 MHz, $CDCl_3$): δ [ppm]= 196.31 (C-1), 166.92(C-5), 146.17 (C-7), 130.99 (C-3), 128.50 (C-2), 114.92 (C-

6) 114.73 (C-4), 56.02 (C-10), 29.60 (C-9), 25.07 (C-8). GC-MS (EI): *m/z* (%) = 149, (100) ; 101, (18.1) ; 121, (17.3) ; 150, (16.2) ; 312, (15.7) ; 162, (15.6) ; 163, (12.4) ; 133, (10.6).

2-ethoxycarbonyl 5-chloro 2-(2-methoxycarbonyl 5-chloro benzyl)-1-indanone (46):

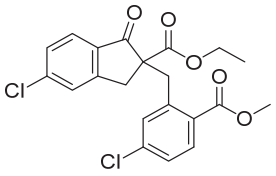

A procedure from literature[22] was modified as followed: A mixture of indanone **44** (823 mg, 3,45 mmol, 1.0 eq.), NaH (60%, 152 mg, 3,80 mmol, 1,1 eq.) in DMF (2 mL) was stirred at room temperature for 30 minutes. A solution of 2-bromomethyl-4-chloro-benzoic acid methyl ester (1.00 g, 3,79 mmol, 1.1 eq.) in DMF (2 mL) was added and the solution was heated to 60°C for 24 h. The reaction was quenched by addition of water and extracted with MTBE. The combined organic layers were washed with brine, dried over anhydrous Na_2SO_4 and filtered. The solvent was removed under reduced pressure. The crude product was purified by column chromatography (SiO_2, CH_2Cl_2/cyclohexane; 3:1) yielding **46** as an colorless oil (1.05 g, 3.45 mmol, 73%). ^{1}H NMR (400 MHz, $CDCl_3$): δ [ppm]= 7.68 – 7.58 (m, 2H, ArH), 7.51 – 7.42 (m, 1H), 6.91 (dd, $^3J_{HH}$ = 8.4 Hz, $^4J_{HH}$ =2.2 Hz, 1H, ArH), 6.81 (m, 2H, ArH), 4.37 (d, $^2J_{HH}$ = 14.0 Hz, 1H), 4.03 – 3.78 (m, 3H), 3.53 (d, $^2J_{HH}$ = 17.6, 1H), 3.44 (s, 3H), 2.98 (d, $^2J_{HH}$ = 17.6 Hz, 1H), 0.87 (t, $^3J_{HH}$ = 7.1 Hz, 3H). GC-MS (EI): *m/z* (%) = 73.1, (100); 386.1, (21.3); 388.1, (9.4).

5,5'-dichloro-2,2'-spirobiindan-1,1'-dione (47):

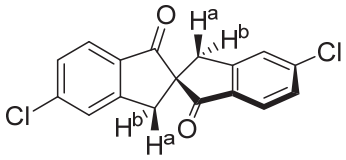

A procedure from literature[22] was modified as followed: A mixture of indano **46** (1.20 g, 2.85 mmol) in AcOH (2 mL) and HBr (48% , aq.) was heated to 120°C for 2.5 h. After cooling to room temperature, the mixture was filtered, washed with ice cold methanol and dried under vacuum yielding spirobiindandione **47** as white crystals (689 mg, 2.17 mmol, 76% yield). ^{1}H NMR (250 MHz, $CDCl_3$): δ [ppm]= 7.68 (d, $^3J_{HH}$ = 8.2 Hz, 2H, ArH), 7.59-7.53 (m, 2H, ArH), 7.45 – 7.34 (m, 2H, ArH), 3.69 (d, $^2J_{HH}$ = 17.1 Hz, 2H, H^a), 3.17 (d, $^2J_{HH}$ = 17.2 Hz, 2H, H^b). ^{13}C NMR (63 MHz, $CDCl_3$): δ [ppm]= 200.43 (CO), 155.18 (C), 142.29 (C), 133.78 (C), 128.94 (CH), 126.78 (CH), 126.16 (CH), 65.82 (C), 37.3 (CH_2). GC-MS (EI): *m/z* (%) = 316, (100) ; 94.5, (66.7) ; 318, (65.5) ; 189.1, (50.8) ; 288, (48.8) ; 218.1, (43.2) ; 253, (35.8) ; 225, (33.2) ; 290, (32.1) ; 152.1, (30.2) ; 89.1, (26.3) ; 317, (24.2) ; 93.5, (24.1) ; 287, (23.9) ; 289, (23) ; 75.1, (17.9) ; 126, (17.7) ; 63.1,

(17.1) ; 190.05, (16.21) ; 124.05, (14.71) ; 252.05, (14.41) ; 319, (13.5) ; 281.05, (13.26) ; 255.05, (12.42) ; 253.95, (11.51) ; 95.35, (11.33) ; 187.1, (11.03) ; 319.95, (10.91) ; 299, (10.37) ; 188.1, (10.31).

5,5'-di(2-trimethylsilylethylsulfenyl)-2,2'-spirobiindan-1,1'-dione (49):

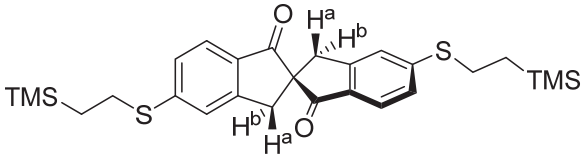

To dry and deoxygenated DMF (2 mL) was added at 0°C 2-trimethylsilylthiol (0,10 mL, 0,662 mmol, 2,1 eq.) followed by NaH (16,6 mg, 0,693 mmol, 2.2 eq.). After gas evolution ended a deoxygenated solution of spirobiindanone **47** (100 mg, 0,315 mmol, 1.0 eq.) was added. The ice bath was removed and the reaction stirred for 24h. The reaction was quenched by the addition of a few drops of 1M HCl (aq.) diluted with MTBE and washed with water followed by 1M HCl (aq.) and brine. The organic layer was dried over anhydrous Na_2SO_4, filtered and the solvent was removed under reduced pressure. The residue was submitted to column chromatography (SiO_2, DCM/cyclohexane; 2:1) yielding spirobiindandione **49** as a white solid (95,2 mg, 0,185 mmol, 59%). ^{1}H NMR (500 MHz, $CDCl_3$): δ [ppm]= 7.62 (d, $^3J_{HH}$ = 8.2 Hz, 2H, ArH), 7.36-7.30 (m, 2H, ArH), 7.22 (dd, $^3J_{HH}$ = 8.2 Hz, $^4J_{HH}$ = 1.6 Hz 2H, ArH), 3.65 (d, $^2J_{HH}$ = 17.1 Hz, 2H, H^a), 3.11 (d, $^2J_{HH}$ = 17.1 Hz, 2H, H^b), 3.09 - 3.03 (m, 2H, CH_2), 1.14 – 0.91 (m, 2H, CH_2), 0.10 (s, 18H; CH_3). ^{13}C NMR (126 MHz, $CDCl_3$): δ [ppm]= 201.65 (CO), 154.54 (C), 148.90 (C), 132.32 (C), 126.06 (CH), 124.97 (CH), 122.90 (CH), 65.50 (C), 38.00 (CH_2), 28.08 (CH_2), 16.39 (CH_2), -1.59 (CH_3).

5,5'-di(acetylsulfenyl)-2,2'-spirobiindan-1,1'-dione (48):

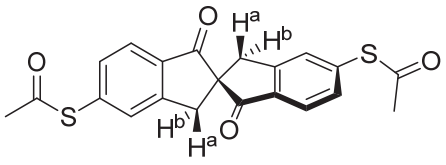

To a deoxygenated solution of spirobiindandione **49** (32.0 mg, 62.3 μmol, 1.0 eq) in THF (2 mL) was added a solution of TBAF in THF (1 M, 0.37 mL, 0.37 mmol, 6 eq.) at room temperature. After 1 h the reaction mixture was cooled to 0°C and AcCl (0.1 mL, 1.40 mmol, 22.5 eq.) was added dropwise. After 2h the reaction was poured on ice and extracted with EtOAc. The combined organic layers were washed with water, brine, dried over anhydrous Na_2SO_4 and filtered. The solvent was removed under reduced pressure and the obtained residue was purified by column chromatography (SiO_2, EtOAc/cyclohexane; 2:1) yielding spirobiindandione **48** as a white waxy solid (2.5 mg, 6.0 μmol, 10%). ^{1}H NMR (250 MHz, $CDCl_3$): δ [ppm]= 7.77 (d, $^3J_{HH}$ = 8.0 Hz, 2H, ArH), 7.66 (s, 2H, ArH), 7.46 (d, $^3J_{HH}$ = 8.0 Hz, 2H, ArH), 3.73 (d, $^2J_{HH}$ = 17.2 Hz, 2H, H^a), 3.23 (d, $^2J_{HH}$ = 17.2 Hz, 2H, H^b), 2.49 (s, 6H, CH_3).

5,5'-dichloro-2,2'-spirobiindantetraone (50):

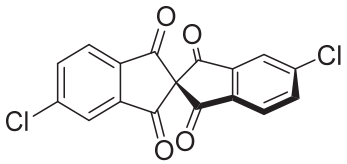

A mixture containing spirobiindandione **48** (50.1 mg, 158 μmol, 1.0 eq.), KBr (45.1 mg, 379 μmol, 2.4 eq.) and Oxone® (233 mg, 379 μmol, 2.4 eq.) in 2 mL of a 9:1 mixture of DCM and water was sealed in a microwave vial and irradiated with a XXX watt halogen lamp for 24 h while being cooled in a water bath. The reaction mixture was diluted with DCM and the organic layer was washed with water. The combined organic layers were dried over anhydrous $MgSO_4$, filtered and the solvent was removed under reduced pressure. Purification by column chromatography (SiO_2, DCM/cyclohexane; 1:1) yielded spirobiindantetraone **50** as a white solid (12.4 mg, 36 μmol, 23%). ^{1}H NMR (600 MHz, $CDCl_3$): δ [ppm]= 8.04 (d, $^3J_{HH}$ = 1.8 Hz, 2H, ArH), 8.03 (d, $^3J_{HH}$ = 8.2 Hz, 1H, ArH), 7.89 (dd, $^3J_{HH}$ = 8.2, $^4J_{HH}$ = 1.9 Hz, 1H, ArH). ^{13}C NMR (151 MHz, $CDCl_3$): δ [ppm]= 189.92 (CO), 189.72 (CO), 145.82 (C), 143.95 (C), 142.73 (C), 136.82 (CH), 125.72 (CH), 124.58 (CH). GC-MS (EI): *m/z* (%) = 138, (100); 110, (92.7); 343.9, (89.2); 75, (73.4); 345.9, (59.9); 315.9, (42.2); 140, (32.5); 112, (31.2); 74.1, (28.8); 317.9, (27.8); 344.9, (21); 264.9,

(20.9); 98.5, (20.6); 287.9, (20.4); 196.9, (17); 87, (15.5); 289.9, (12.3); 130, (12.2); 346.8, (12.03); 347.9, (11.06); 316.9, (10.6); 50, (10.6).

Spiro[5.5]undeca-1,8-dien-3-one (53):

A procedure from literature[24] was modified as followed: A solution of 1,2,3,6-tetrahydrobenzaldehyde (8.5 mL, 73 mmol, 1.0 eq.), methylvinylketone (6.1 mL, 73 mmol, 1.0 eq.) and added *p*-toluenesulfonic acid (50 mg, 0.29 mmol, 0.4 mol%) in toluene (30 mL) was refluxed for 4 hours. After cooling to room temperature, the mixture was washed with saturated aqueous $NaHCO_3$ solution followed by water. The aqueous layer was extracted with Et_2O (2x) and the combined organic layers were dried over $MgSO_4$, filtered and the solvent was removed under reduced pressure. The product was further purified by vacuum distillation (boiling point: 66 – 69°C, 3×10^{-10}mbar) yielding **53** a colorless, viscous oil (6.05 g, 37.3 mmol, 51%). ^{1}H NMR (250 MHz, $CDCl_3$): δ [ppm]= 6.80 (d, $^3J_{HH}$ = 10.2, 1H, CH), 5.92 (d, $^3J_{HH}$ = 10.2 Hz, 1H, CH), 5.82 – 5.60 (m, 2H, CH), 2.59 – 2.31 (m, 2H, CH_2), 2.16 – 1.89 (m, 5H, CH_2), 1.88 – 1.74 (m, 2H, CH_2), 1.64-1.51 (m, 1H, CH_2).

Spiro[5.5]undeca-1-ene-3,9-dione (56):

To a 500 mL flask containing a mixture of spiro[5.5]undeca-1,8-dien-3-one **53** (6.05 g, 37.3 mmol, 1.0 eq.), palladium (II) acetate (420 mg, 1.87 mmol 4.9 mol%) and p-benzoquinone (4.30g, 37.3 mmol, 1.0 eq.) in MeCN (110 mL) and water (15 mL), was added perchloric acid (3 mL, 70% aq., 22.4 mmol, 0,60 eq.) and refluxed for 16 h. After cooling down 100 mL saturated aqueous sodium hydroxide solution was added, and the mixture was extracted with MTBE (3x 200 mL). The combined organic layers were washed with brine, dried over MgSO4 and the solvent evaporated under reduced pressure. The product was further purified by column chromatography (SiO_2, EtOAc/cyclohexane, 2:1) yielding a brown oil (4.335 g, 65%) containing a 10:1 of isomers **56** and **64** which was used in the subsequent reaction step without further purification. Major Compound **56:** ^{1}H NMR (250 MHz, $CDCl_3$): δ [ppm]= 6.00 (d, $^3J_{HH}$ = 9.8 Hz, 1H, CH), 5.35 (d, $^3J_{HH}$ = 9.8 Hz, 1H, CH), 4.14 (d, $^3J_{HH}$ = 7.1 Hz, 1H, CH_2), 4.09 (d, $^3J_{HH}$ = 7.1 Hz, 1H, CH_2), 2.86 (d, $^3J_{HH}$ = 7.4 Hz, 2H, CH_2), 2.81 (d, J = 7.4 Hz, 2H, CH_2), 1.37 – 1.19 (m, 6H, CH_2).

GC-MS (EI): *m/z* (%) = (100); (60.5); (51.7); (42.6); (37); (34.8); (31.7); (29.5); (27.7); (26.9); (26); (24.4); (24.2); (21.1); (20.8); (20.6); (18.2); (17.7); (17.62); (16.13); (14.3); (14.29); (14.19); (13.4); (12.77); (10.1)

Spiro[5.5]undeca-1,4,7,10-tetraene-3,9-dione (7):

To a solution of the obtained mixture containing spiroenedione **56** and **64** (4,34 g, 24.3 mmol, 1.0 eq) in 400 mL dioxane was added DDQ (33,1 g, 146 mmol, 6.0 eq) and the mixture was refluxed for 48 hours. After cooling down to room temperature the mixture was filtered, and the filtrate concentrated under reduced pressure. The residue was suspended in MTBE and filtered. The solvent was removed under reduced pressure and the crude product was purified by column chromatography (activated basic aluminium oxide, EtOAc). Further purification by sublimation yielded spiro[5.5]undeca-1,4,7,10-tetraene-3,9-dione **7** as a white solid (1.13 g, 6.57 mmol, 27%). ^{1}H NMR (400 MHz, $CDCl_3$): δ [ppm]= 6.51 (s, 8H).

4,5-bis-(2-cyanoethylthio)-1,3-dithiole-2-thione (57):

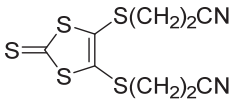

A procedure from literature[31] was modified as followed: Di(tetraethylammonium)bis(1,3-dithiol-2-thione-4,5-dithiol)-zincate (**65**)(2.00 g, 2.78 mmol, 1.0 eq.) was dissolved in MeCN (35 mL) under an argon atmosphere. To the solution 3-bromoporpionitrile (1.15 mL, 13.9 mmol, 5.0 eq.) was added and the mixture was refluxed for 1 hour. The resulting solution was cooled down to room temperature and the precipitated solid was filtered. The filtrate was evaporated *in vacuo*. The crude product was dissolved in CH_2Cl_2 and washed four times with water. The organic layer was dried over anhydrous $MgSO_4$, filtered and the solvent evaporated under reduced pressure. The crude product was further purified by recrystallization from toluene yielding 4,5-bis-(2-cyanoethylthio)-1,3-dithiole-2-thione **57** as orange needles (0.754 g, 2.48 mmol 45%). ^{1}H NMR (250 MHz, $CDCl_3$): δ [ppm]= 3.16 (t, $^{3}J_{HH}$ = 6.9 Hz, 4H), 2.81 (t, $^{3}J_{HH}$ = 6.9 Hz, 4H).

Diethyl(4,5-bis((2-cyanoethyl)thio)-1,3-dithiol-2-yl)phosphonate (58):

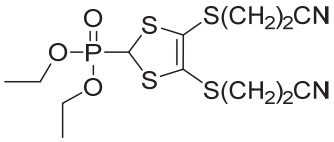

A solution of 4,5-bis-(2-cyanoethylthio)-1,3-dithiole-2-thione **57** (0.754 g, 2.48 mmol) in xylene (50 mL) and triethylphosphite (4.32 mL, 25.1 mmol, 10.1 eq.) mixture was refluxed for 5 hours at 150°C. The volatile materials were removed by vacuum distillation. The product was further purified by column chromatography (SiO_2, EtOAc/cyclohexane, 2:1) yielding diethyl(4,5-bis((2-cyanoethyl)thio)-1,3-dithiol-2-yl)phosphonate **58** as an orange solid (300 mg, 0.730 mmol, 30%).^{1}H NMR (250 MHz, $CDCl_3$): δ [ppm]= 4.55 (d, $^2J_{HP}$ = 7.3 Hz, 1H, CH), 4.25 (dq, $^3J_{HP}$ = 8.5 Hz, $^3J_{HH}$ = 7.1 Hz, 4H, CH_2), 3.42 – 3.27 (m, 2H), 3.17 – 3.01 (m, 2H), 2.99 – 2.78 (m, 4H), 1.38 (t, *J* = 7.1 Hz, 6H, CH_3).

3,9-di(4,5-bis(2-cyanoethylthio)-1,3-dithiol-2-ylidene)spiro[5.5]undeca-1,4,7,10-tetraene (59):

To a deoxygenated solution of spiro[5.5]undeca-1,4,7,10-tetraene-3,9-dione **7** (30.1 mg, 0.175 mmol, 1.0 eq) and diethyl(4,5-bis((2-cyanoethyl)thio)-1,3-dithiol-2-yl)phosphonate **58** (180 mg, 0.438 mmol, 2.5 eq.) in dry THF (2 mL) at -78°C was added *n*-BuLi (1.6 M, 0.30 mL, 0.481 mmol, 2.75 eq.) The reaction was stirred for 15 min. at -78°C and 1h at room temperature. The reaction was quenched by addition of a few drops of saturated aqueous $NaHCO_3$ solution and the solvent was removed under reduced pressure. The residue was partitioned between water and DCM. The aqueous layer was extracted with DCM and the combined organic layers were dried over anhydrous $MgSO_4$, filtered and the solvent removed under reduced pressure. The crude product was further purified by column chromatography (SiO_2, EtOAc/Cyclohexane, 2:1) yield the spiro compound **59** as an orange oil (39.0 mg, 57.0 μmol, 33%). ^{1}H NMR (250 MHz, $CDCl_3$): δ [ppm]= 6.00 (d, $^3J_{HH}$ = 9.8 Hz, 4H), 5.41 (d, $^3J_{HH}$ = 9.8 Hz, 4H, CH), 3.09 (t, $^3J_{HH}$ = 7.1 Hz, 8H, CH_2), 2.76 (t, $^3J_{HH}$ = 7.1 Hz, 8H, CH_2).

3,9-di(4,5-bis(acetylthio)-1,3-dithiol-2-ylidene)spiro[5.5]undeca-1,4,7,10-tetraene (52):

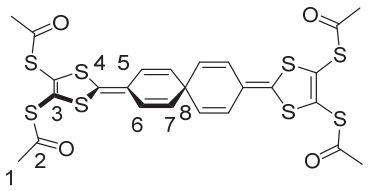

To a deoxygenated solution of compound **59** (19 mg, 27.7 μmol, 1.0 eq.) in dry THF (1mL) was added a solution of $CsOH{\cdot}H_2O$ (38.1 mg, 227 μmol, 8.2 eq.) in dry methanol (1 mL). The mixture was stirred for 30 min at room temperature the cooled down to 0°C. At 0°C AcCl (60.0 μL, 831 μmol, 30 eq.) was added and the reaction mixture was allowed to warm up to room temperature. The volatiles were removed under reduced pressure and the residue was partitioned between water and DCM. The aqueous phase was extracted with DCM and the combined organic layers were dried with anhydrous $MgSO_4$, filtered and the solvent removed under reduced pressure. The crude product was purified by column chromatography (SiO_2, EtOAc/cyclohexane, 3:1) yielding tetrathioacetate **52** as an orange oil (7.5 mg, 12 μmol, 42%). ^{1}H NMR (400 MHz, $CDCl_3$): δ [ppm]= 5.95 (d, $^3J_{HH}$ = 9.8 Hz, 4H, H^6), 5.35 (d, $^3J_{HH}$ = 9.8 Hz, 4H, H^7), 2.42 (s, 12H, H^1). ^{13}C NMR (101 MHz, $CDCl_3$): δ [ppm]= 190.82 (C-2), 128.50 (C-4), 128.34 (C-7), 126.34 (C-3), 121.51 (C-6), 117.33(C-5), 44.06 (C-8), 30.09 (C-1). HRMS (ESI, +): m/z calcd. for $C_{25}H_{20}NaO_4S_8$ $[M+Na]^+$ 662.9019; found: 642.9013.

2 Synthesis of Trinorbornane

The following chapter was reproduced from the following publication:
L. D. Bizzini, T. Müntener, D. Häussinger, M. Neuburger, M. Mayor, *Chem. Commun.* **2017**, *53*, 11399–11402.

2.1 Introduction

The Chemical Universe Database GDB which was introduced by the group of Reymond is in its first iteration an exhaustive enumeration of all possible molecules up to a eleven atoms (C, N, O and F) considering chemical stability and synthetic feasibility.[60] Through employing the molecular quantum number (MQN) classification method, which is an equivalent of the periodic system of the elements for molecules, the interactive search of the chemical space was rendered possible.[61]

Analysis of the enumerated database for structures with up to 11 carbon atoms revealed 124 polycyclic hydrocarbons without 3- and 4-membered rings. From these structures only three have no real world counterpart, neither as pure hydrocarbons nor as substructures containing heteroatoms or unsaturations.[61] One of these structures is tetracyclo[5.2.2.$0^{1,6}$.$0^{4,9}$]undecane (**66**) a particularly appealing and eye catching example of a new structural type.[60,61]

Its scaffold consists of two norbornanes that share a pair of neighboring edges (red and blue in Figure 1 left). Interestingly this arrangement results in a third norbornane subunit (highlighted in yellow in Figure 1 left). Furthermore, the structure is an example of axial chirality and Figure 1 shows the two enantiomers (1*S*$_a$,4*S*,6*R*, 7*S*,9*R*)-tetracyclo-[5.2.2.$0^{1,6}$.$0^{4,9}$]undecane (left) and (1*R*$_a$,4*R*,6*S*, 7*R*,9*S*)-tetracyclo[5.2.2.$0^{1,6}$.$0^{4,9}$]undecane (right), to which we will refer to as **66**-*S*$_a$ and **66**-*R*$_a$ for convenience. We suggest for the scaffold of **66** consisting of three superposed norbornane units the trivial name trinorbornane. Figure 1 also shows the mirror plane between both enantiomers and for **66**-*R*$_a$ the molecule's C_2-axis. The numbering of the carbon atoms resulting in the IUPAC name is indicated for **66**-*S*$_a$.

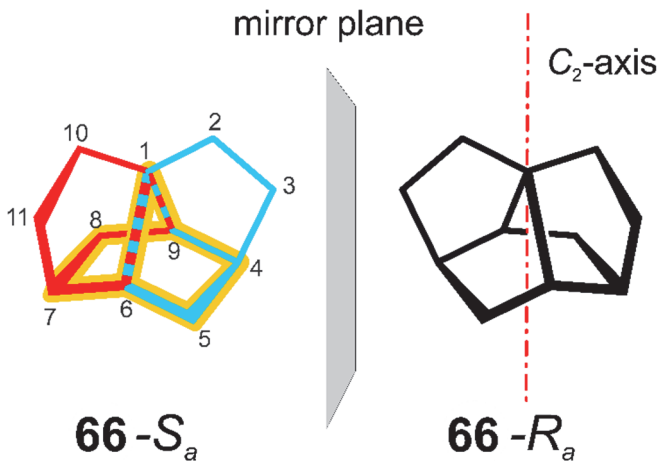

Figure 15: The two enantiomers (1*S*$_a$,4*S*,6*R*,7*S*,9*R*)tetracyclo[5.2.2. $0^{1,6}.0^{4,9}$]undecane (**66**-*S*$_a$) and (1*R*$_a$,4*R*,6*S*,7R,9*S*)-tetracyclo[5.2.2. $0^{1,6}.0^{4,9}$]undecane (**66**-*R*$_a$) displaying axial chirality. For **66**-*S*$_a$ on the left side the three norbornane subunits of the structure are displayed in red, blue, and yellow together with the numbering of the eleven carbon atoms corresponding to the IUPAC name. The enantiomer **66**-*R*$_a$ is displayed together with the molecules C_2-axis.

There is a long tradition in organic chemistry to explore the chemical space for complex, symmetrical and aesthetical appealing hydrocarbons by synthetic means.[62] One paramount example, dodecahedrane (Figure 16), has been called "the Mount Everest of hydrocarbon chemistry"[63] and was first synthesised by Paquette in 1982.[64] It is composed of twelve fused cyclopentane rings and possesses the highest known point group symmetry (I_h).[63]

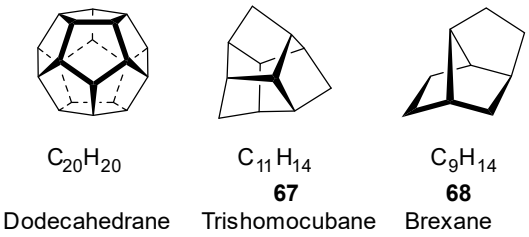

Figure 16: Examples of already known polycyclic hydrocarbons with rigid scaffolds: Dodecahedrane, Trishomocubane (**67**) and Brexane (**68**).

Our search for compounds resembling the unstrained but highly rigid carbon framework of **66** guided us to the pentacyclic, chiral, and D_3-symmetric trishomocubane **67** (pentacyclo-[6.3.0.$0^{2,6}.0^{3,10}.0^{5,9}$]undecane). It is also composed of three partially superposed norbornyl units (Figure 16) and was first synthesized by Underwood in 1970 in a sequence of brominations and eliminations from pentacyclo-[5.4.0.$0^{2,6}.0^{3,10}.0^{5,9}$]undecane-8,11-diol.[65] Since then, several routes to **67** and derivatives thereof have been developed.[66]

Probably the structurally most similar known compound is brexane **68** (tricyclo[4.3.0.$0^{3,7}$]nonane), which lacks only one interconnecting ethylene bridge compared to **66** and was synthesized by Nickon in 1964 in 9 steps (Figure 16).[67] Later its synthesis has been

improved by Brieger profiting from an intramolecular *Diels-Alder* reaction as the key step.[68] In similarity to **66**, this tricyclic structure is also C_2-symmetric but is composed of two superposed norbonyl units instead of three. Interestingly, the tricyclic scaffold has been found in the natural products Pallambin A and B, whose total syntheses were recently achieved.[69]

2.2 Results and Discussion

Our approach to construct the tetracyclic scaffold of **66** (Scheme 10) was based on the tricyclic brexene derivative **69**, which might form the desired target structure **66** in a *6-endo-trig/5-exo-trig* radical cyclization mechanism. The compound **69** should be formed in an intramolecular *Diels-Alder* reaction[68] from the cyclopentadiene **70,** which is envisioned to be accessible from the literature known compound **71** *via Michael* addition to phenyl vinyl sulfone and a series of reduction and elimination reactions.

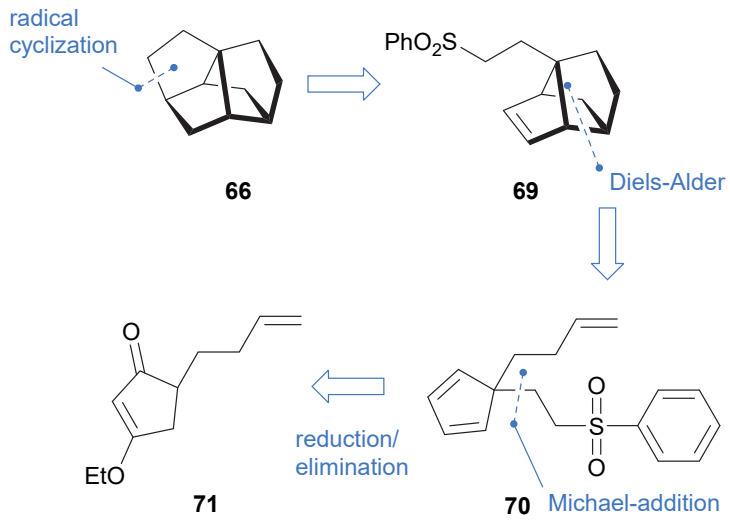

Scheme 10: Retrosynthetic analysis for racemic trinorbornane **66** (to improve the visibility only the **66**-R_a enantiomer is displayed).

The synthesis of the target structure trinorbornane **66** as a racemate is displayed in Scheme 11 and starts with the assembly of the 3-ethyloxycyclopent-2-enone derivative **71**. The assembly of **72** starting from methyl (*E*)-4-chloro-3-methoxy-2-butenoate (**73**) is straightforward and even suitable for industrial production.[70] The addition of **73** to a solution of dimethyl malonate (**74**) in DMF under basic conditions at room temperature resulted in trimethyl (*E*)-3-methoxy-3-butene-1,1,4-tricarboxylate (**72**) in very good yield of 85%. The triester **72** was subsequently cyclized in a solution of sodium methoxide in methanol at 60 °C providing methyl 4-methoxy-2-oxo-3-cyclopentenecarboxylate (**75**) in 86% isolated yield.

The 5-membered ring of **75** is already a subunit of the tetracyclic structure **66** and in order to form the next two rings in similarity of the strategy reported for brexane[68] *via* an intramolecular *Diels-Alder* reaction, a but-3-ene chain had to be introduced. Following a reported procedure,[71] compound **75** was deprotonated with potassium hydride in DMF at room temperature and alkylated by addition of 4-bromo-1-butene providing the 1-(but-3-enyl)-4-methoxy-2-oxo-cyclopent-3-enecarboxylic acid methyl ester (**76**) in 76% isolated yield. In order to form the quaternary center decarboxylation of **76** was required. Following a reported protocol,[71] **76** was treated in refluxing ethanol with potassium hydroxide for 16 hours. The applied reaction conditions not only decarboxylated the compound, but also the complete substitution of the methoxy group by an ethoxy group was observed, which does not handicap the further proceeding along the reaction sequence. Thus 5-(but-3-enyl)-3-ethoxycyclopent-2-enone (**71**) was obtained in 76% isolated yield.

A key step of the synthesis was the formation of the quaternary center, which was achieved by modifying the procedure reported by Cory and Reeneboog[72] using phenyl vinyl sulfone as *Michael*-acceptor. After formation of the kinetic enolate of **71** with LDA in dry THF under cryogenic conditions, the solution was allowed to warm up to 0 °C and 1,3-dimethyl-2-imidazolidinone (DMI) was added. A solution of phenyl vinyl sulfone in dry THF was added at 0 °C and allowed to warm up to room temperature. After about 1 hour the reaction mixture was worked up and 5-(but-3-enyl)-3-ethoxy-5-(2-(phenylsulfonyl)ethyl)cyclopent-2-enone (**77**) was isolated in good yields of 74-82% by column chromatography (CC). Water exclusion turned out to be crucial for the success of this reaction as in the presence of traces of water mainly polymeric material was formed.

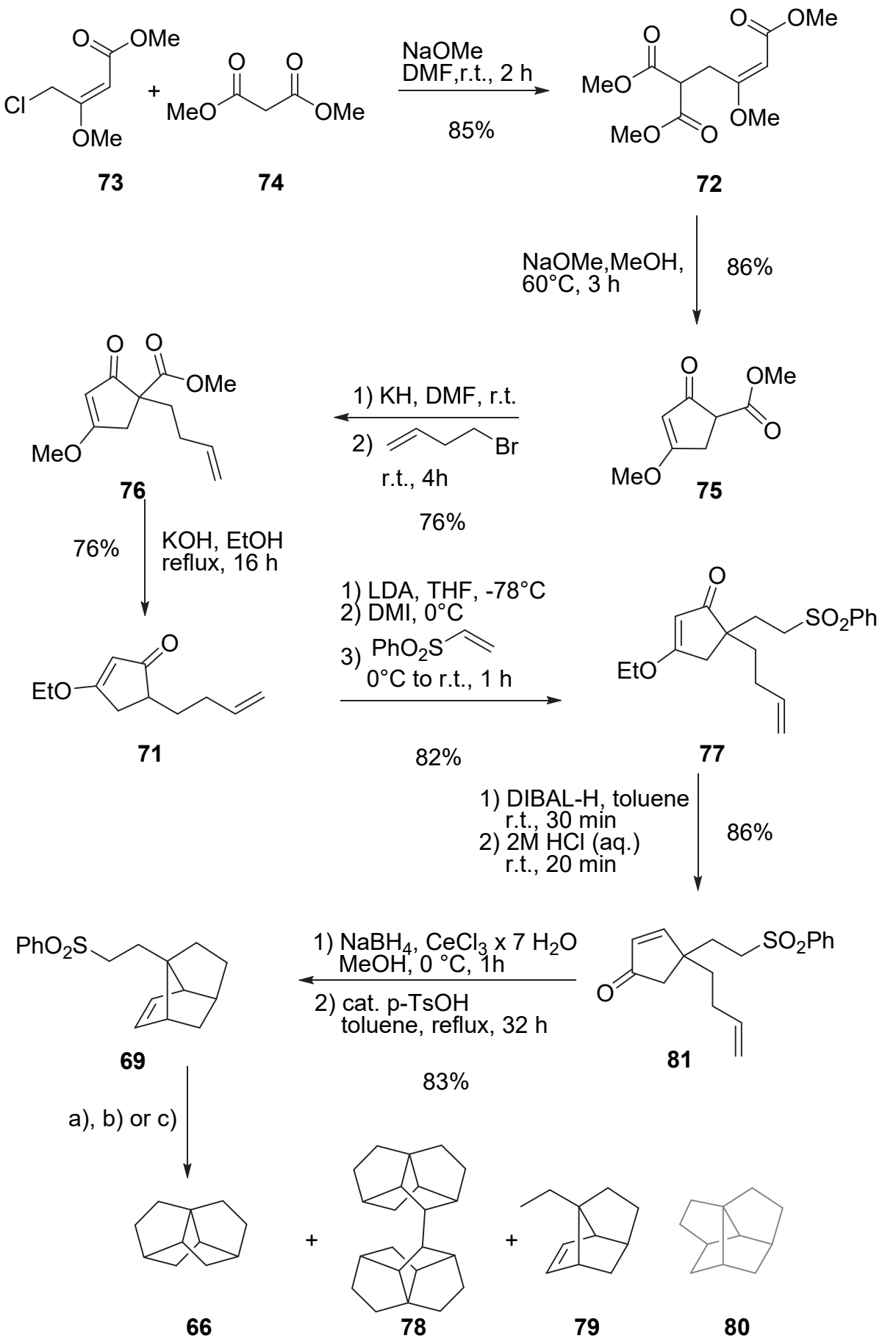

Scheme 11: Syntheses of the polycyclic hydrocarbons **66** (for clarity only the **66**-S_a enantiomer is displayed), **78**, **79,** and **80** as the not (yet) synthesized constitutional isomer of **66**.

First attempts to reduce **77** with either DIBAL-H or $LiAlH_4$ in THF and subsequent treatment with hydrochloric acid gave in agreement with the literature[73] mixtures of 1,2-, 1,4- and over-reduced species. Changing the solvent to toluene and using DIBAL-H as the reducing agent provided selectively 4-(but-3-en-1-yl)-4-(2-(phenylsulfonyl)ethyl)cyclopent-2-enone (**81**), which was, after stirring in 2M aqueous hydrochloric acid for 20 minutes, isolated in excellent 86% yield. The cyclopent-2-enone fragment of **81** was reduced to the cyclopent-2-enol with the typical conditions for a *Luche* reduction.[74] Thus **81** was treated with cerium (III) chloride and sodium borohydride in 0 °C cold methanol. The crude reaction product comprising 4-(but-3-en-1-yl)-4-(2-(phenylsulfonyl)ethyl)cyclopent-2-enol as mixture of stereoisomers was not purified but instead directly dehydrated in toluene with catalytic amounts of *p*-TsOH at 110 °C. Under these conditions the *in situ* formed cyclopentadienyl derivative **70** reacts with the but-3-ene chain in an intramolecular *Diels-Alder* reaction[68] providing 1-(2-(phenylsulfonyl)-ethyl)tricyclo[4.3.0.$0^{4,9}$]non-7-ene (**69**), which was isolated as a racemate in very good 83% yield over the three steps.

The second key step of the synthesis was the reduction of the sulfone moiety of **69** with single-electron reducing agents in order to form the 2-ethyl radical which was expected to cyclize to the target structure **66** by reacting intramolecularily with the olefin of the brexene scaffold. In first attempts **66** was treated with large excesses of lithium 1-*N*,*N*-dimethylaminonaphthalenide (LDMAN)[75] as the single-electron reducing agent at -78 °C in THF. To our delight we were able to observe up to 30% conversion and further analysis of the reaction mixture by GC-MS unravelled a 5:1 ratio in favor of the reduced brexene derivative **79** compared to the cyclized target structure **66**. In addition, also the formation of radical dimerization product **78** was observed. The mixture of compounds was subjected to CC using silica gel as solid phase and pentane as eluent at -20°C. The target structure **66** was isolated together with the dimer **78** in a combined yield of about 3%, while the open brexene derivative **79** was isolated in 13% yield. The dimer **78** was separated from the mixed fraction by crystallization in a mixture of diethyl ether and acetonitrile and was isolated in 1% yield.

While the reaction sequence with its poor conversion, low yield of the desired compound, and complex product mixture was not particular appealing, it shows that the target structure **66** can indeed be formed by a radical cyclisation reaction. Furthermore, the dimeric side product **78** was crystalline in the solid state and indeed, single crystals suitable for X-ray analysis were obtained by sublimation in a sealed capillary at 130°C. While the dimer was formed as mixture

of diastereomers, the single crystal consisted exclusively of the meso-form combining a **66**-R_a with a **66**-S_a subunit (top and bottom part respectively in Figure 17). The solid-state structure of **78** is displayed in Figure 17. **78** crystallizes in the monoclinic space group $P2_1/n$ with two formula units per unit cell. Only one half of the dimeric molecule is present in the asymmetric unit. The complete molecule is generated by an inversion center of the space group $P2_1/n$.

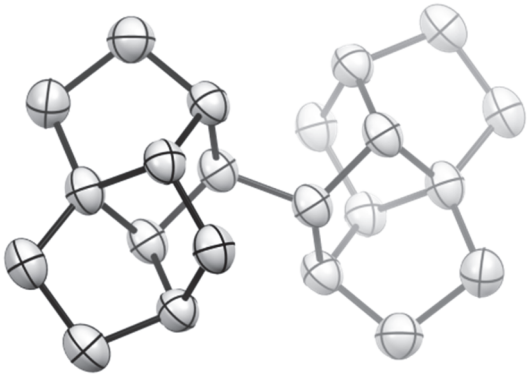

Figure 17: Solid state structure of the dimer **78** corroborating the existence of the tetracyclo[5.2.2.$0^{1,6}$.$0^{4,9}$]undecane system as it consists of an interlinked **66**-R_a subunit (top) and a **66**-S_a subunit (bottom). Hydrogen atoms are omitted for clarity and rotational ellipsoids are displayed at a 50% probability level.

As alternative SmI_2 in THF with 1,3-dimethyltetrahydropyrimidin-2(1*H*)-one (DMPU) as cosolvent is reported to be a strong enough single-electron reducing agent for sulfones.[76] To our delight, employing 10 equivalents of SmI_2 in THF with 8 equivalents of DMPU in respect to SmI_2 at 80 °C for 2 h resulted exclusively in cyclized **66** with 67% conversion determined by GC-MS. After the usual work up the desired tetracyclic target structure **66** was isolated in 28% yield as colorless crystalline solid by filtering off the remaining starting material and polar residues through a silica pad using pentane as the eluent. The low isolated yield compared to the conversion determined by GC-MS is due to the high volatility of the compound resulting in losses during solvent evaporation. Pentane was distilled off through a vigreux column and the residual solvent was removed under vacuum while the flask was placed in an ice bath. It is noteworthy that the ring closing radical reaction seems to occur in a regioselective manner, as exclusively the formation of the trinorbornane scaffold is observed and the also not yet known C_{11}-analogue (**80** in Scheme 11), which should be obtained when the other olefinic carbon atom would be attacked as well, could not be detected with any of the investigated reaction conditions.

The racemic mixture of **66** was fully characterized by ^{1}H- and ^{13}C-NMR, and high-resolution mass spectrometry. Despite the apparent simplicity of the molecular architecture of **66** with only six carbon and eight proton resonances, it turned out exceedingly difficult to unambiguously confirm the suggested structure by standard HSQC / HMBC / NOESY NMR experiments due to the high order nature of the ^{1}H NMR spectrum and multiple pathways for long-range H-C couplings in the rigid tetracyclic framework. We therefore resorted to the very sensitive 1,1-ADEQUATE experiment[77] using chirp pulses[78] that selectively delivers correlations between protons and carbon atoms that are separated by two bonds and thus allowed to assign the topology of **66** without any doubt (Figure 18). With the proton and carbon assignment at hand it was possible to distinguish the diastereotopic protons in the CH_2-groups by 2D-NOESY NMR using an unusually long mixing time of 3 seconds (Figure S1 shows key NOE contacts). The crucial NOE contact between symmetry related protons 5b and 8b could be obtained from a pseudo 3D HSQC-NOESY experiment without carbon decoupling during the ^{1}H acquisition which splits the diagonal peak into a 130 Hz doublet allowing for the detection of a weak but significant NOE between protons 5b and 8b (data not shown).

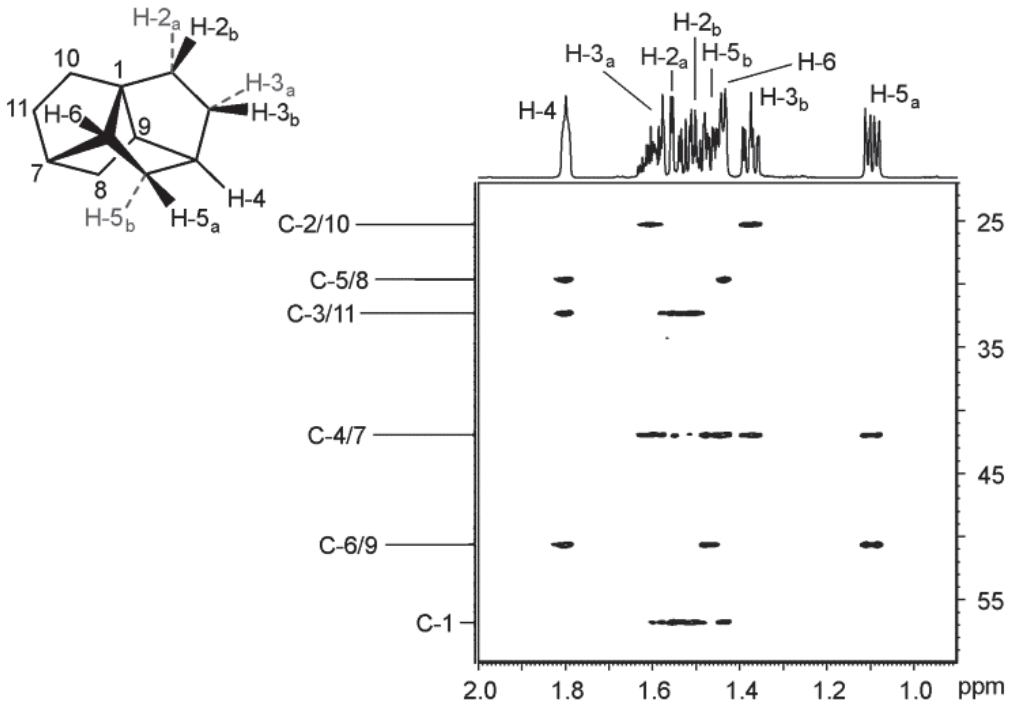

Figure 18: *1,1 ADEQUATE spectrum of trinorbonane **66** recorded in C_6D_6 with assignment.*

While all spectra unambiguously prove the identity of **66**, all attempts to analyze its solid-state structure by X-ray analysis failed. In spite the fact that **66** is a crystalline solid at room temperature, the compound crystallizes by sublimation in thin needles, which are notoriously too thin to allow for analyzing the solid-state structure with the available X-ray sources.

2.3 Summary and Outlook

In conclusion we report the first synthesis of trinorbornane, a tetracyclic saturated hydrocarbon with the elemental formula $C_{11}H_{16}$. While theoretical considerations predicted the stability and accessibility of the trinorbornane scaffold, it has neither be synthesized nor been found in nature so far. The tetracyclic scaffold has been assembled in a linear sequence of 9 steps and a total isolated yield of 7%. The key steps of the synthesis are the introduction of quaternary carbon atom in an early stage providing the precursor **77** already comprising not only the first 5-membered ring of the target structure, but also all the required eleven carbon atoms. An intramolecular *Diels-Alder* reaction resulted in the next two ring structures of the framework and the last cyclization was achieved by an intramolecular radical reaction. The preparation of functionalized derivatives as well as enantiomerically pure trinorbornane are currently under investigation.

2.4 Experimental Part

General Information

All commercially available compounds were purchased and used as received unless explicitly stated otherwise. 1,3-dimethyl-2-imidazolidinone (DMI) was dried over 4Å molecular sieves and THF was dried over sodium and benzophenone. All NMR experiments were performed on Bruker Avance III or III HD, two or four-channel NMR spectrometer operating at 400.13, 500.13 or 600.27 MHz proton frequency. The instruments were equipped with direct observe BBFO, indirect BBI or cryogenic four-channel QCI (H/C/N/F) 5 mm probes all with self-shielded z-gradient. The experiments were performed at 298 K and the temperature was calibrated using a methanol standard showing accuracy within +/- 0.2 K. The 1,1-ADEQUATE experiment was performed on a ca. 140 mM sample of **66** using 1344 and 512 increments in F2 and F1 resulting in acquisition times of 139.8 and 17 ms, respectively. The delays were set to corresponding coupling constants of 135 Hz for $^{1}J_{H,C}$ and 35 Hz $^{1}J_{C,C}$. Each increment in F1 was recorded with 16 scans resulting in a total experiment time of 3 h and 52 min. The spectra were processed with 2048 $\times$ 1024 data points using a $\pi/2$ shifted square sine-bell function in both dimensions. The NOESY spectrum was acquired with a mixing time of 3.0 s, for the HSQC-NOESY 0.85 s were used. GC-MS was performed on a Shimadzu GCMS-2020 SE equipped with a Zebron 5 MS Infernocolumn which allowed to achieve temperatures up to 350 °C. High-resolution mass spectra (HRMS) were measured as HR-ESI-ToF- MS with a Maxis 4G instrument from Bruker and HR-EI spectra were measured on a Waters Micromass AutoSpec Ultima (EI-Sector). For column chromatography silica gel Siliaflash® p60 (40–63 µm) from Silicycle was used, and TLC was performed on silica gel 60 F254 glass plates with a thickness of 0.25 mm purchased from Merck. The diffraction data were collected on a Stoe StadiVari diffractometer attached to a Ga Metaljet X-ray source at low temperature. The structure was solved with the program Superflip [1] using the charge flipping method and refined with CRYSTALS [2] using Least Squares minimisation. All carbon atoms were refined anisotropically. Molecular drawings were generated using Mercury [3].

Trimethyl (*E*)-3-methoxy-3-butene-1.1.4-tricarboxylate (72)[70]**:**

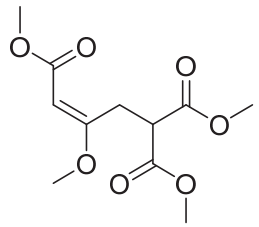

NaOMe (11.3 g, 210 mmol) was added to a stirred solution of dimethyl malonate (27.7 g, 210 mmol) in DMF (100 mL) at 20 °C. After 10 min methyl (E)-4-chloro-3-methoxy-2-butenoate (17.3 g, 105 mmol) was added dropwise over 5 min. The reaction mixture was stirred for 2 h. All the volatiles were removed under vacuum. The residue was partitioned between CH_2Cl_2 and H_2O. The aqueous layer was neutralized with HCl (32%, aq.). The organic layer was separated, dried over $MgSO_4$ and the solvent was removed under reduced pressure. The residue was purified by column chromatography (SiO_2, cyclohexane/EtOAc 2:1) yielding trimethyl (*E*)-3-methoxy-3-butene-1.1.4-tricarboxylate **72** (19.9 g, 76.5 mmol, 73%) as a colorless oil. ^{1}H NMR (400 MHz, $CDCl_3$): δ = 3.40 (d, $^3J_{H,H}$ = 7.7 Hz, 1H), 3.60 (s, 3H), 3.68 (s, 3H) 3.73 (s, 6H), 3.74 (d, $^3J_{H,H}$ = 7.7 Hz, 2H).

Methyl 4-methoxy-2-oxo-3-cyclopentenecarboxylate (75)[70]**:**

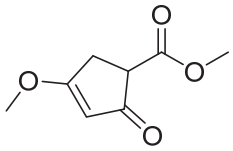

Na (157 mmol, 3.61 g) was added under an Ar atmosphere to MeOH (180 mL) over 30 min. The mixture was heated to 60 °C for 30 minutes. Trimethyl (E)-3-methoxy-3-butene-1,1,4-tricarboxylate **72** (76.6 mmol, 19.9 g) was added dropwise during 10 min. The mixture was stirred for 2 h at 60 °C then AcOH (10 mL) was added. The solvent was removed under reduced pressure and the residue was partitioned between CH_2Cl_2 and H_2O. The aqueous phase was further extracted with CH_2Cl_2 (2x). The combined organic layers were dried over $MgSO_4$ and the solvent was removed under reduced pressure. The residue was purified by column chromatography (SiO_2, cyclohexane/EtOAc 1:1) yielding methyl 4-methoxy-2-oxo-3-cycloppentenecarboxylate **75** (9.33 g, 54.8 mmol, 72%) as a yellow oil. ^{1}H NMR (250 MHz, $CDCl_3$): δ = 2.78 (ddd, $^2J_{H,H}$ = 17.7 Hz, $^3J_{H,H}$ = 7.6, $^4J_{H,H}$ =1.2 Hz, 1H), 3.06 (ddd, $^2J_{H,H}$ = 17.7 Hz, $^3J_{H,H}$ = 3.1, $^4J_{H,H}$ =1.2 Hz, 1H), 3.54 (dd, $^3J_{H,H}$ = 7.6, $^3J_{H,H}$ = 3.1 Hz, 1H), 3.78 (s, 3H), 3.88 (s, 3H), 5.29

(dd, $^4J_{H,H}$ =1.2 Hz, 1H). GC-MS (EI): m/z (%) = 170.0 (100.0), 142.0 (15.7), 138.0 (25.5), 127.0 (25.3), 123.0 (32.5), 110.0 (26.2), 95.0 (31.4), 69.0 (27.2).

1-(But-3-enyl)-4-methoxy-2-oxo-cyclopent-3-enecarboxylic acid methyl ester (76)[71]:

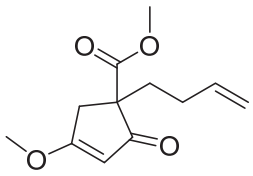

Methyl 4-methoxy-2-oxo-3-cyclopentenecarboxylate **75** (58.8 mmol, 10.0 g) in DMF (50 mL) was added dropwise to a suspension of KH (61.2 mmol, 2.45 g) in DMF (350 mL). The mixture was stirred for 10 min and 4-bromo-1-butene (68.2 mmol, 9.49 g) was added dropwise. The reaction mixture was stirred at room temperature for 3 h then quenched by addition of saturated aqueous NH_4Cl. The mixture was extracted with diethyl ether (3x) and washed with brine. The solvent was removed under reduced pressure. The residue was purified by column chromatography (cyclohexane/EtOAC 1:1) yielding 1-but-3-enyl-4-methoxy-2-oxo-cyclopent-3-enecarboxylic acid methyl ester **76** (40.7 mmol, 9.13 g, 69%) as a brown oil. ^{1}H NMR (400 MHz, $CDCl_3$): δ = 1.85 (ddd, $^2J_{H,H}$ = 13.2, $^3J_{H,H}$ = 10.0, $^3J_{H,\ H}$ = 6.0 Hz, 1H), 2.05 - 1.95(m, 2H), 2.16 (ddd, $^2J_{H,H}$ = 13.2, $^3J_{H,H}$ = 10.1, $^3J_{H,H}$ =6.1 Hz, 1H), 2.54 (dd, $^2J_{H,H}$ = 17.8, $^4J_{H,H}$ = 1.1 Hz, 1H), 3.24 (dd, $^2J_{H,H}$ = 17.8, $^4J_{H,H}$ = 1.2 Hz, 1H), 3.72 (s, 3H), 3.88 (s, 3H), 4.94 - 5.04 (m, 2H), 5.26 (dd, $^4J_{H,H}$ = 1.1 Hz, 1H), 5.78 (ddt, $^3J_{H,H}$ = 16.8, $^3J_{H,H}$ = 10.1, $^3J_{H,H}$ = 6.4 Hz, 1H). GC-MS (EI): *m/z* (%) = 126.0 (51.1), 98.0 (100.0), 80.0 (12.8), 69.0 (55.5).

5-(But-3-enyl)-3-ethoxycyclopent-2-enone (71)[71]:

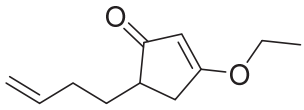

The β-ketoester **76** (40.7 mmol, 9.13 g) was dissolved in EtOH (100 mL) and KOH (48.8 mmol, 2.74 g) was added. The reaction mixture was heated to reflux for 16 h. After cooling to room temperature the solution was diluted with saturated aqueous NH_4Cl and concentrated under reduced pressure. The residue was portioned between EtOAc and H_2O. The aqueous layer was further extracted with EtOAc (3x) The combined organic layers were washed with brine, dried over $MgSO_4$ and the solvent was removed under reduced pressure. The residue was purified by column chromatography (SiO_2, EtOAc/cyclohexane, 4:1) to yield 5-But-3-enyl-3-ethoxy-

cyclopent-2-enone **71** (31.8 mmol, 5.74 g, 86%) as a yellow oil. ^{1}H NMR (400 MHz, $CDCl_3$, 25°C):δ = 5.81 (ddt, $^{3}J_{H,H}$ = 17.0, $^{3}J_{H,H}$ = 10.2, $^{3}J_{H,H}$ = 6.6 Hz, 1H), 5.24 (t, $^{4}J_{H,H}$ = 1.1 Hz, 1H), 5.07 – 4.94 (m, 2H), 4.04 (q, *J* = 7.1 Hz, 2H), 2.75 (ddd, $^{2}J_{H,H}$ = 17.6, $^{3}J_{H,H}$ = 7.3, $^{4}J_{H,H}$ = 1.1 Hz, 1H), 2.48 (m, 1H), 2.30 (ddd, $^{2}J_{H,H}$ = 17.6, $^{3}J_{H,H}$ = 2.9, $^{4}J_{H,H}$ = 1.1 Hz, 1H), 2.22 – 2.06 (m, 2H), 1.97 (m, 1H), 1.50 – 1.39 (m, 1H), 1.41 (t, *J* = 7.1 Hz, 3H). GC-MS (EI): *m/z* (%) = 126.0 (51.1), 98.0 (100.0), 80.0 (12.8), 69.0 (55.5).

5-(But-3-enyl)-3-ethoxy-5-(2-(phenylsulfonyl)ethyl)cyclopent-2-enone (77):

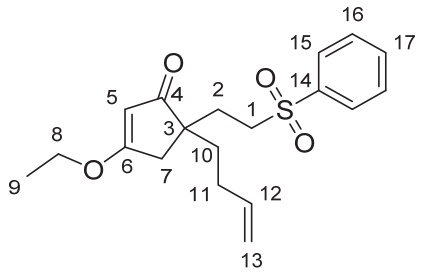

To a solution of diisopropylamine (47.7 mmol, 6.74 mL) in 32 mL dry THF was added at 0 °C a solution of *n*-BuLi in hexane (1.6 M, 38.2 mmol, 23.8 mL). After 30 minutes the solution was cooled to -78 °C and a solution of the cyclopentenone **71** (31.8 mmol, 5.73 g) in 32 mL dry THF was added drop wise. The solution was stirred for 30 min at -78 °C and then warmed up to 0°C. After addition of 22 mL of dry 1,3-dimethyl-2-imidazolidinone (DMI) the solution turned red. Then a solution of phenyl vinyl sulfone (38.2 mmol, 6.42 g) in THF (80 mL) was added dropwise. After complete addition the solution was allowed to reach room temperature. After 1 h the reaction was quenched by the addition of NH_4Cl and the aqueous phase was extracted with EtOAc (3x). The combined organic layers were washed with brine, dried over $MgSO_4$ and the solvent was removed under reduced pressure. The crude residue was purified by column chromatography (SiO2, EtOAc/cyclohexane, 4:1) to yield **77** (20.2 mmol, 7.03 g, 64%) as a yellow oil. ^{1}H NMR (400 MHz, $CDCl_3$, 25°C):δ = 7.89 – 7.83 (m, 2H, H-16), 7.70–7.62 (m, 1H, H-17), 7.60–7.54 (m, 2H, H-15), 5.71 (ddt, $^{3}J_{H,H}$ = 16.8, $^{3}J_{H,H}$ = 10.2, $^{3}J_{H,H}$ = 6.5 Hz, 1H, H-12), 5.19 (t, $^{4}J_{H,H}$ = 1.1 Hz, 1H, H-5), 5.02–4.83 (m, 2H, H-13), 4.03 (q, $^{3}J_{H,H}$ = 7.1 Hz, 2H, H-8), 3.18 – 2.90 (m, 2H, H-1), 2.56 (dd, $^{2}J_{H,H}$ = 18.1, $^{4}J_{H,H}$ = 1.1 Hz, 1H, H-7), 2.36 (dd, $^{2}J_{H,H}$ = 18.1, $^{4}J_{H,H}$ = 1.1 Hz, 1H, H-7), 2.01 – 1.81 (m, 4H, H-2, H-11), 1.64 – 1.45 (m, 2H, H-10), 1.41 (t, $^{3}J_{H,H}$ = 7.1 Hz, 3H, H-9). ^{13}C NMR (101 MHz, $CDCl_3$): δ = 207.80 (C-4), 187.99 (C-6), 138.95 (C-14), 137.63 (C-12), 133.96 (C 17), 129.49 (C-15), 128.18 (C-16), 115.28 (C-13), 104.07 (C-5), 68.07 (C-8), 51.96 (C-1), 49.19 (C-3), 39.57 (C-7), 35.40 (C-10), 29.57 (C-2), 28.45 (C-11), 14.24 (C-9). HRMS (ESI, +): *m/z* calcd. for $C_{19}H_{24}O_4S$ $[M+H]^+$ 349.1468; found: 349.1468.

4-(But-3-en-1-yl)-4-(2-(phenylsulfonyl)ethyl)cyclopent-2-enone (81):

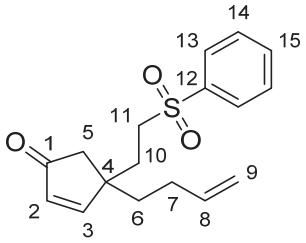

Cyclopentenone **77** (8.61 mmol, 3.00 g) was dissolved in toluene (50 mL) and DIBAL-H (1 M in hexane, 9.47 mmol, 9.47 mL) was added dropwise while cooling with a water bath. After complete addition of the reagent the reaction stirred for 1 h at room temperature. The solution was quenched with 2 M aq. HCl (30 mL) and stirred for 20 min at room temperature. The aqueous phase was extracted with DCM (2x) and the combined organic phase was washed with water (2x) and dried over $MgSO_4$. The solvent was removed under reduced pressure. The crude product was purified by column chromatography (SiO_2, EtOAc/cyclohexane 1:1) yielding cyclopentenone **81** (7.41 mmol, 2.26 g, 86%) as a colorless oil. ^{1}H NMR (400 MHz, $CDCl_3$, 25°C): δ = 7.91 – 7.88 (m, 2H, H-14), 7.71 – 7.67 (m, 1H, H-15), 7.62 – 7.57 (m, 2H, H-13), 7.32 (d, $^3J_{H,H}$ = 5.7 Hz, 1H, H-2), 6.13 (d, $^3J_{H,H}$ = 5.7 Hz, 1H, H-3), 5.72 (ddt, $^3J_{H,H}$ = 16.8, $^3J_{H,H}$ = 10.2, $^3J_{H,H}$ = 6.5 Hz, 1H, H-8), 5.01 – 4.95 (m, 2H, H-9), 3.01 – 2.86 (m, 2H, H-11), 2.25 (d, $^2J_{H,H}$ = 18.8 Hz, 1H, H-5), 2.07 (d, $^2J_{H,H}$ = 18.8 Hz, 1H, H-5), 2.07 – 1.87 (m, 4H, H-10, H-7), 1.68 – 1.54 (m, 2H, H-6). ^{13}C NMR (126 MHz, $CDCl_3$): δ = 207.77 (C-1), 168.94 (C-2), 138.92 (C-12), 137.29 (C8), 134.33 (C-3), 134.16 (C-15), 129.62 (C-13), 128.10 (C-14), 115.65 (C-9), 52.32 (C-11), 47.34 (C-4), 44.83 (C-5), 37.98 (C-6), 30.58 (C-10), 28.81 (C-7).

1-(2-(phenylsulfonyl)ethyl)tricyclo[4.3.0.0^{4,9}]non-7-en (69):

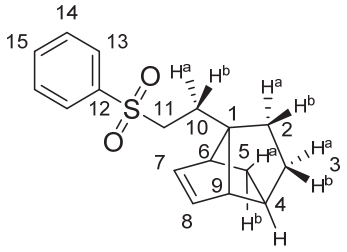

Cyclopentenone **81** (7.56 mmol, 2.30 g) was dissolved in MeOH (70 mL) and $CeCl_3 \cdot 7H_2O$ (9.07 mmol, 3.38 g) was added. The reaction mixture was cooled to 0 °C and $NaBH_4$ was slowly added. The mixture was stirred for 1 h. Upon completion, the mixture was quenched with saturated aqueous NH_4Cl and extracted with DCM (3x). The organic phase was washed with water (1x), brine (1x) and dried over $MgSO_4$. The solvent was removed under reduced pressure.

The crude product was passed through a silica plug (*t*BME) and the solvent was removed. The oil was dissolved in toluene (600 mL) and a catalytic amount of *p*-TsOH was added. The solution was heated to reflux under *Dean-Stark* conditions for 32h. After cooling to room temperature, the solution was washed with saturated aqueous Na_2CO_3 (1x), water (1x) and brine (1x). The solvent was removed under reduced pressure and the crude product was purified by column-chromatography (SiO_2, EtOAc/cyclohexane, 1:2) to yield **69** (5.38 mmol, 1.55 g, 71%) as a colorless oil. ^{1}H NMR (500 MHz, $CDCl_3$, 25°C): δ = 7.90-7.87 (m, 2H, H-14), 7.66-7.63 (m, 1H, H-15), 7.58-7.54 (m, 2H, H-13), 5.98-5.96 (m, 1H, H-7), 5.72-5.70 (m, 1H, H-8), 2.99-2.88 (m, 2H, H-11), 2.30-2.28 (m, 1H, H-9), 2.16-2.14 (m, 1H, H-6), 1.87-1.81 (m, 1H, H$^{a\text{ or }b}$-10), 1.71-1.65 (m, 3H, H$^{a\text{ or }b}$-10, H-4, H^a-2), 1.62-1.55 (m 1H, H^b-3), 1.36-1.24 (m, 3H, H^b-5, H^a-2, H^b-2), 0.91 (ddd, $^2J_{H,H}$ = 11.4, $^3J_{H,H}$ = 6.3, $^4J_{H,H}$ = 2.3 Hz, 1H, H^b-5). ^{13}C NMR (126 MHz, $CDCl_3$): δ = 139.27 (C-12), 136.92 (C-7), 133.65 (C-15), 129.34 (C-13), 129.26 (C-8), 128.18 (C-14), 67.83 (C-1), 55.97 (C-9), 54.63 (C-11), 49.30 (C-6), 35.40 (C-4), 34.14 (C-5), 32.89 (C-3), 27.11 (C-2), 23.69 (C-10).

Tetracyclo[5.2.2.0^{1,6}.0^{4,9}]undecane (66):

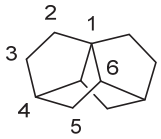

According to the literature known procedure[75], a freshly prepared solution of LDMAN (0.5 M in THF, 20.0 mmol) was cooled to -78 °C and added dropwise to a stirring solution of sulfone **69** (5.38 mmol, 1.55 g) in THF at -78 °C. After complete addition the reaction mixture was stirred for 20 min and quenched by the addition of 1 M aq. HCl. The mixture was allowed to warm up to room temperature and the organic layer was diluted with pentane and washed consecutively with 1 M aqueous HCl (2x), 32% aq. NaOH (2x) and brine (1x). The solvent was evaporated under reduced pressure and the residue was purified by column chromatography (SiO_2, pentane) to yield **1** (0.135 mmol, 21.0 mg, 3%) as a colorless solid.

To an oven-dried 50 mL Schlenk filled with argon a 0.1 M solution of SmI_2 in THF (2.58 mmol, 25.8 mL, 10.0 eq) and 1,3-dimethyl-3,4,5,6-tetrahydro-2(1*H*)-pyrimidinone (20.6 mmol, 2.50 mL, 80.0 eq.) were added. Under stirring a solution of **69** (74.4 mg, 0.258 mmol, 1.00 eq) in THF (1 mL) was added. The mixture was stirred for 2 h at 80°C. The mixture was cooled to 0°C and quenched with water (20 mL). The solution was extracted with pentane (3x) and the organic

phase was washed with 2 M auqueous HCl (3x), 1 M aqueous NaOH (3x) and water (2x). The solvent was removed by distillation with a Vigreux column. The crude mixture was passed through a silica plug (pentane). The solvent was removed by distillation with a Vigreux column and the remaining pentane was allowed to evaporate at room temperature yielding **66** (0.0723 mmol, 10.7 mg, 28%) as a colorless solid. ^{1}H NMR (600 MHz, C_6D_6 25°C): δ = 1.80 (m_c, 1H, H-4), 1.61 (m_c, 1H, H^a-3), 1.56 (m_c, 1H, H^a-2), 1.51 (m_c, 1H, H^b-2), 1.46 (m_c, 1H, H^b-5), 1.44 (m_c, 1H, H-6), 1.38 (m_c, 1H, H^b-3), 1.10 (m_c, 1H, H^a-5). ^{13}C NMR (151 MHz, C_6D_6): δ = 57.11 (C-1), 50.97 (C-6), 42.28 (C-4), 32.62 (C-3), 29.96 (C-5). 25.60 (C-2). GC-MS (EI, 70 eV): *m/z* (%) = 148.2 (54), 120.2 (41), 119.2 (100), 106.2 (22), 105.1 (24), 93.1 (20.22), 92.1 (47), 91.1 (67), 80.1 (33), 79.1 (87), 77.1 (35). HRMS (EI, +): *m/z* calcd. for $C_{11}H_{16}$ $[M]^+$ 148.1252; found: 148.1249. Melting point: 49°C

3 Chemical Synthesis Towards Thiaspherophane

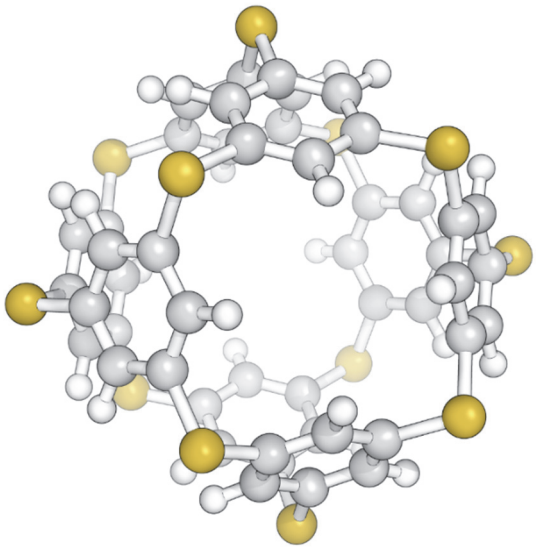

3.1 Introduction

Spherical container molecules, especially fullerenes and its inclusion complexes also known as endohedral fullerenes,[79] have been studied for a wide variety of applications such as switching units in molecular electronics,[80] electron acceptors for organic solar cell,[81] X-ray contrast agents,[82] superconductors[83] and ferroelectric materials.[84] Another type of material conceptually linked to endohedral fullerenes is represented by cryptates.[85] Cryptates are described by a positively charged inclusion complex between cation and cryptand.[86,87] Reduction of this large and charge-diffuse cationic complex to its neutral form yields what is known as cryptatium, where a negatively charged ligand balances the positive charge of the bound cation. From this context, the analogy with endohedral fullerenes becomes evident. Both classes can be regarded as “expanded atoms” since a positively charged “nucleus” is shielded by its surrounding negatively charged “shell” and thus properties similar to those found in metals can be expected.[85] In 1991, Lehn *et. al.* achieved the X-ray characterization of the first cryptatium single crystal (Figure 19), obtained by reductive electrocrystallization, showing that the electron added during reduction of the complex is mainly localized on one bipyridyl unit.[88]

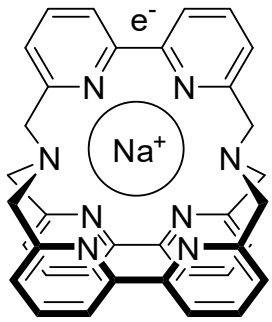

Figure 19: Structure of the first prepared cryptatium by eletrochemical reduction of one of the bipyridyl ligands.

An interesting compound class closely related to cryptatia and endohedral fullerenes complexes has been reported by Ross *et al.*[89] based on the theoretical calculation of the polarizabilities of hollow spherical molecules with encapsulated cations, the so called heterospherophanes (Figure 20). These heterospherophanes consists of eight benzene rings linked to each other by 12 single heteroatoms. In particular the sulfur heterospherophane derivative called thiaspherophane (**82**) is expected to allow the electrons which compensate the charge of the cationic guest to be delocalized over the entire molecule due to the higher polarizability of sulfur and matching of the orbital energies.[89]

In contrast to the closed-cage fullerene, the highly symmetrical thiaspherophane **82**, which is topologically identical to a cuboctahedron[90] has an open-cage structure which could allow endohedral host-guest interactions similar to cryptands. Therefore, thiaspherophane may be regarded as an intermediary structure between fullerenes and cryptands. However, these heterospherophanes have yet to be synthesized.

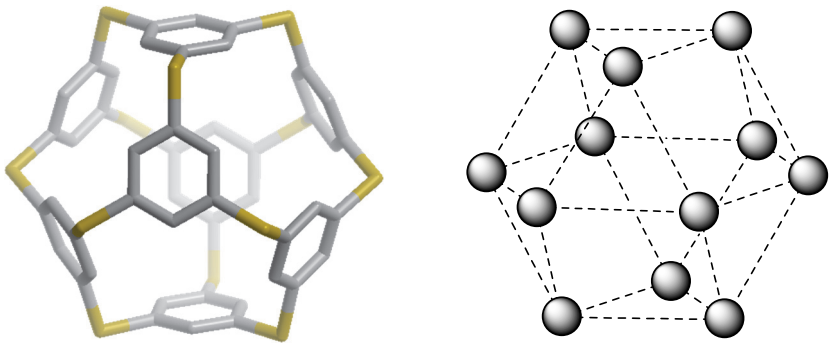

Figure 20: Molecular structure of thiaspherophane **82** (left) and graphical representation of its cuboctahedral shape (right).

Probably, the closest related structure to thiaspherophane **82** has been reported by Pascal *et. al.*[91], whereby a molecular bowl (**83**) consisting of seven benzene rings bridged with in total

nine single sulfur atoms has been synthesized in two steps *via* nucleophilic aromatic substitution (Scheme 12). The solid-state structure of **83** was obtained from X-ray diffraction analysis of single crystals (Scheme 12) and shows that the benzene units at the rim are rotated outwards.

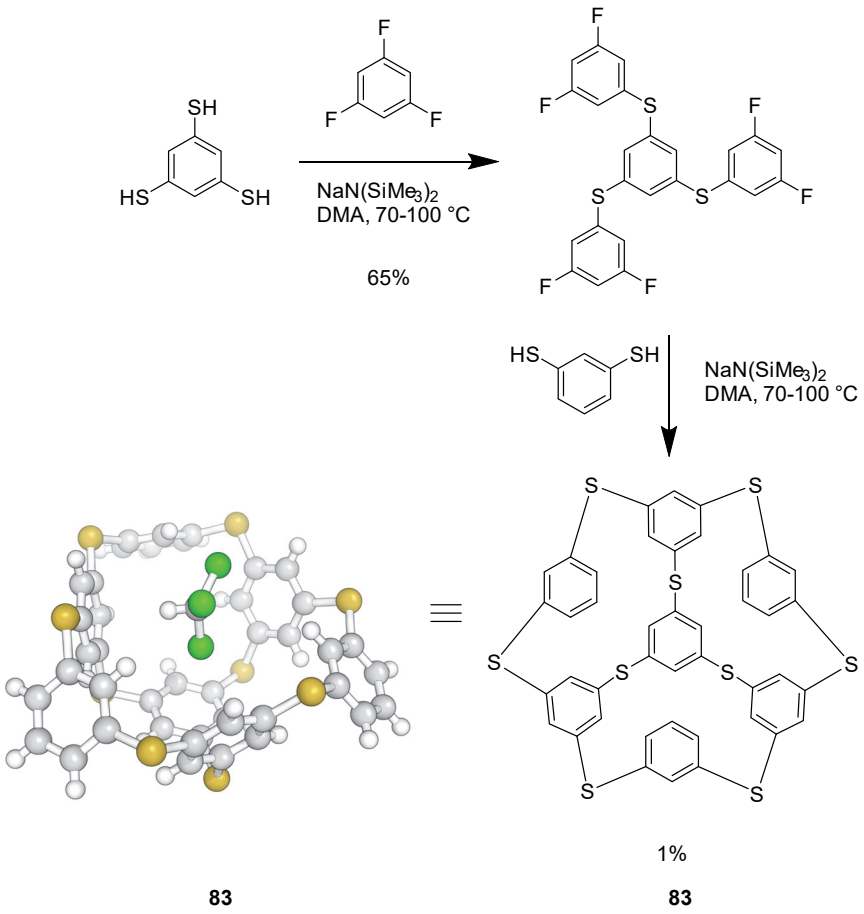

Scheme 12: Synthesis of molecular bowl **\cmpd{bowl}** and its crystal structure with an chloroform solvent molecule present in the cavity.

Other reported compounds related to the structural motifs present in thiaspherophane **82** are cyclotris(meta-phenylene sulfide)[92] and are achieved by nucleophilic aromatic substitution of 1,3-dibromobenzene with sodium sulfide in dimethyl acetamide and thiacalix[4]arene.[93–95] Inspired by these works, the goal was design a suitable synthesis route towards thiaspherophane.

3.2 Results and Discussion

In this chapter two different approaches will be presented where the key step of the synthesis, the reaction which leads to the closure of the spherical scaffold, was performed under

conditions promoting either an electrophilic or a nucleophilic aromatic substitution. Both investigated strategies envisaged intramolecular reactions of a preorganized cyclic compound for the assembly of the scaffold present in thiaspherophane **82**.

Thiacalix[4]arene was recognized as a promising cyclic building-block for the assembly of the thiaspherophane scaffold since thiacalix[4]arene comprises already one cyclotetrakis(m-phenylenesulfide) core which is a structural motif also present in thiaspherophane. Furthermore, the commercial availability of thiacalix[4]arene and the preceding work on its derivatization paves the road for the synthesis of highly preorganized precursors needed for the assembly of the yet to be synthesized thiaspherophane **82**.

3.2.1 Electrophilic Spherification Approach

Electrophilic aromatic substitution has been utilized for the synthesis of a variety of diaryl sulfides,[93–104] diaryl sulfoxides[105,106] and diaryl sulfones[107,108]. One prominent example being the synthesis of 5,11,17,23-tetra-tert-butyl-25,26,27,28-tetrahydroxy-thiacalix[4]arene (**84**).[93–95] Its first synthesis has been achieved by reaction of *p*-tert-butyl phenol (**85**)with sulfur dichloride in DCM yielding the sulfur bridged *tert*-butyl-phenol (**86**) (Scheme 15). Treatment of an excess of compound **86** with sulfur dichloride in DCM at 0°C yielded thiaclix[4]arene **84** in 24**%** yield.[94] Later a more facile and high yielding synthesis of thiaclix[4]arene **84** has been discovered, where *p-tert*-butyl phenol, elemental sulfur and sodium hydroxide in tetraethylene glycol was reacted under elevated temperature forming thiacalix[4]arene **84** in 54% yield.[95]

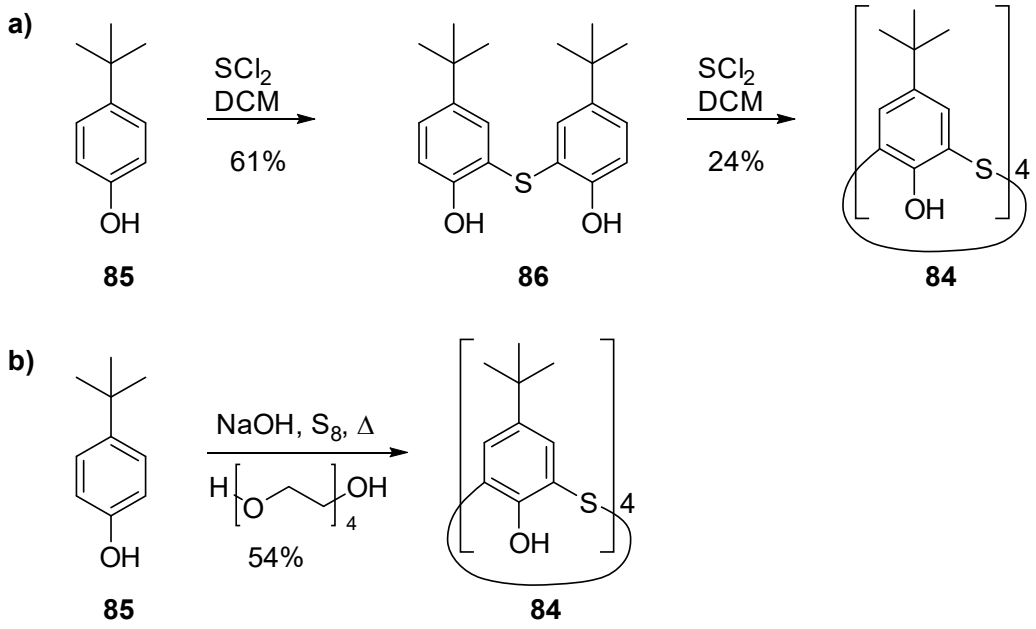

Scheme 13: Reported synthetisis of thiacalix[4]arene **84**: a) first synthetic route to **84** using sulfur dichloride as the electrophile;[94] b) improved one-step synthesis of **84** using elemental sulfur as the electrophile.[95]

Inspired by this work, the assembly of the thiaspherophane scaffold of **82** using sulfur, sulfur dichloride and other electrophilic sulfur reagents for the spherification reaction was investigated.

An appealing approach to assemble the scaffold of thiaspherophane **82** consists of bridging two thiacalix[4]arene units by four sulfur atoms (Scheme 14), thus forming compound **87** *via* conditions promoting an electrophilic aromatic substitution mechanism.

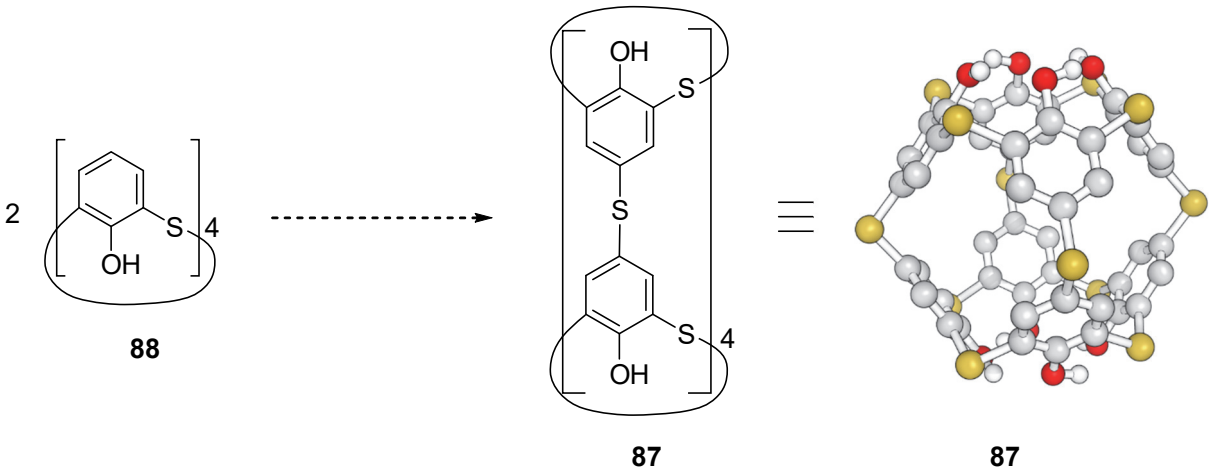

Scheme 14: Investigated reaction for the assembly of **87** from two thiacylix[4]arene **88**. Conditions are shown in Table 1.

The conditions attempted to synthesize the octahydroxy thiaspherophane derivative **87** from the reaction of two tetrahydroxy thiacalix[4]arene **88** and electrophilic sulfur reagents are summarized in Table 1.

Table 1: Tested condition for the synthsis of spherophane **87**.

Entry	Solvent	Temperature [°C]/Time [h]	Reagent	Product
1	TEG	140-170/	$NaOH/S_8$	-
2	TEG	140-170/	KOH/S_8	-
3	$CHCl_3$	r.t./	$AlCl_3/S_2Cl_2$	-
4	CH_2Cl_2	-10/	$AlCl_3/S_2Cl_2$	-

Both reactions performed under basic conditions[95] (Table 1, entry 1 and 2) led to the exclusive formation of insoluble polymeric material and no dimeric or monomeric species could be observed neither by means of mass spectroscopy nor by NMR. The same reaction outcome was observed in the Lewis acid promoted reaction[97,104] (Table 1 entry 3 and 4) with exclusive formation of insoluble polymeric material. However, using the methylated compound **89** under the same conditions as entry 4 led to the formation of dithianthrene derivatives **90** and **91** Scheme 15 in a 1:1 mixture of stereomers in low yield (1%).

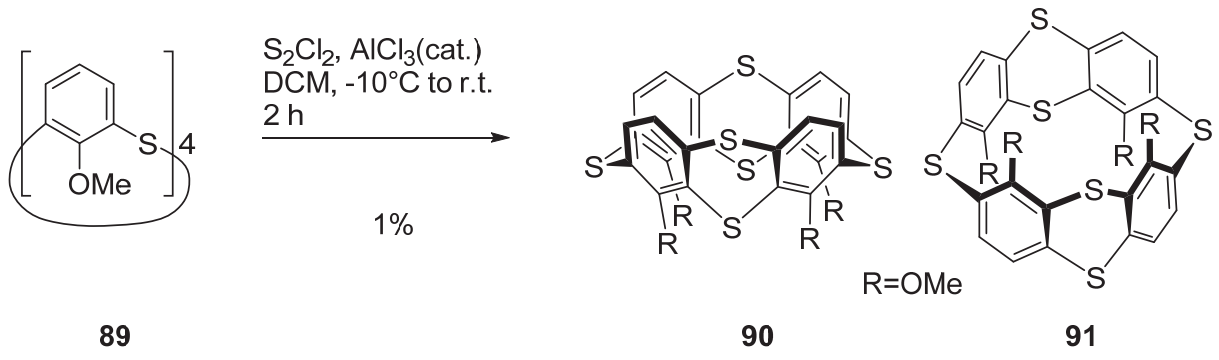

Scheme 15: Sideproducts from the attempted spherification with 4 eq. S_2Cl_2 and 2.8 eq. $AlCl_3$ as a 1:1 mixture as determined by ^{1}H-NMR.

From these experiments, it was concluded that the dimerization of two thiacalix[4]arene **88,** stabilized in the cone conformation by circular intramolecular hydrogen bonding,[93,94] or its methylated derivative **89**, which is known to rapidly interconvert between its conformation in solution at room temperature[109], is not suitable for the synthesis of **87**. The employed reaction

conditions did not allow for a controlled reactivity of the substrate thus the initially formed statistical distribution of intermediates gave rise to a complex mixture of polymeric products. Therefore, a more preorganized substrate was envisaged which would permit a more controlled reactivity in order to reduce the extent of polymer formation. An intramolecular spherification was recognized as possible alternative, since high-dilution reaction conditions should favor the desired reactivity over intermolecular polymerization.

It was identified that functionalization of thiacalix[4]arene with four *p*-hydroxy phenyl sulfanes (**92**, Scheme 16) would provide a preorganized structure , which can be closed using the same synthetic methodology used for the synthesis of thiacalix[4]arene **84** (see Scheme 13). The *p*-hydroxy phenyl functionality is appealing since it directs the required ortho positions and may as well stabilize the forming spherical structure with a second intramolecular hydrogen bonding system.

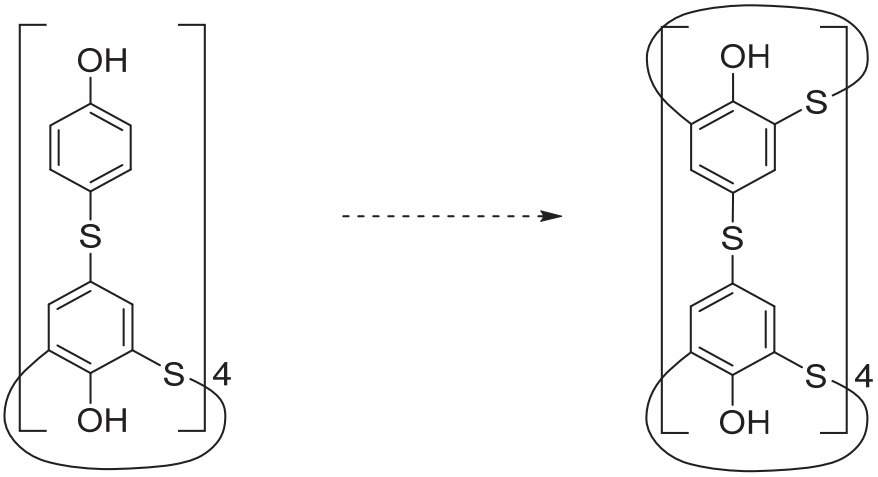

92 **87**

Scheme 16: Intramolecular electrophilic spherification approach for the synthesis of spherophane **87** from the preorganized thiacalixarene **92**.

The synthetic approach to the preorganized precursor **92** is shown in Scheme 17. The four-fold bromo substituted intermediate **93**[110,111] could be prepared from the commercially available *tert*-butyl-thiacalixa[4]arene with 66% yield in three steps.

The ease of purification by precipitation enabled multigramm qunatities of **93** to be accessible. However, the tranformation of **88** to the tetrabromo derivative **94** with N-bromo succinimide in acetone was found to provide significantly higher yields if performed in small scales up to 1 gram. A possible explanation for this observation can be attributed to the low solubility of both

starting material and product in acetone leading to a dependency on the mixing of the reaction mixture.

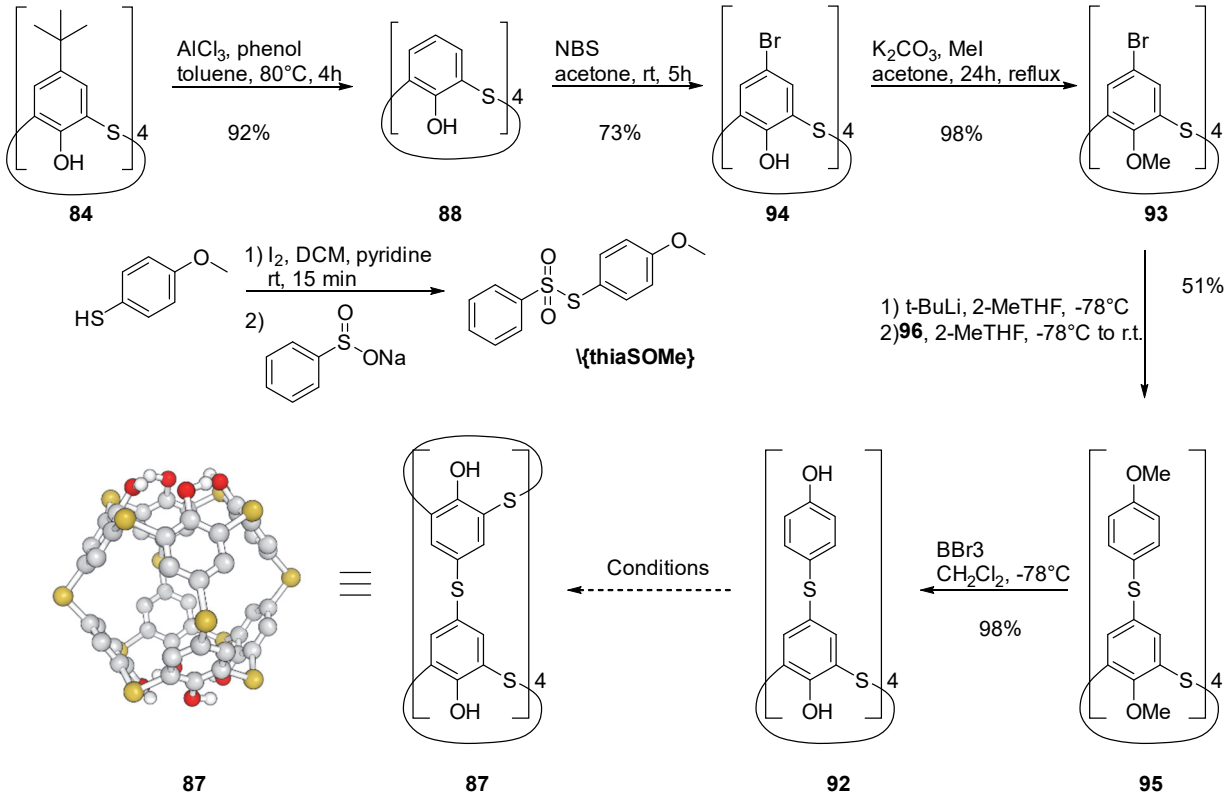

Scheme 17: Synthetic route to **92** and following key step for the synthesis of spherophane **87.**

Attempts of introducing the *p*-methoxy thiophenol *via* palladium catalyzed Buchwald-Hartwig reaction using Josiphos[112] or DPPF[113] as a ligand with Pd_2dba_3 or $Pd(OAc)_2$ yielded the desired product **95** only in low yield (<15%) due to incomplete conversion. However, four-fold lithium-halogen exchange of **93** at -78°and subsequent addition of the thiosulfonate **96** provided the desired product **95** in satisfactory 51% yield after precipitation from TBME with methanol. Deprotection of the eight methoxy groups of **95** with BBr_3 in DCM afforded the key intermediate **92** in excellent 98% yield after precipitation from THF with methanol. To our delight, the envisaged preorganization of **92,** arising from stabilization of the cone conformation by the intramolecular hydrogen bond network, could be clearly observed by ^{1}H NMR. This was apparent from the high symmetry of the spectrum and the characteristic shift of the phenolic protons participating in circular intramolecular hydrogen bonding present in thiacalix[4]arenes in the cone conformation.[93,114] Furthermore, in contrast to the ^{1}H NMR spectrum of **95** which features broad signals implying conformational exchanges on the NMR timescale, the signal in the spectra of **92** are sharp due to either fast or the absence of conformational exchange. However, a peculiar conformational effect was observed in the ^{13}C NMR spectrum of **92** where

the two carbons in 1 and 4 position of the pendant phenols each split into two signals. This indicates a deviation from the C_{4v} to a C_{2v} symmetry which can be attributed either to a slow pinched cone-pinched-cone interconversion[109] or to a C_{2v} symmetric conformation of the pendant phenols.

For the ensuing key step, the reaction of **92** (Scheme 17) with sodium hydroxy and elemental sulfur in high boiling solvents[95] was investigated. At lower temperatures (<120°C) only low conversion of the starting material was observed and with increasing temperature decomposition of **92** was observed. The decomposition of 4,4' thiodiphenol, a motif present in **92,** under alkaline conditions and high temperature (>150°C) has been reported to yield a mixture of 2,2'-, 2,4- and 4,4'-thiodiphenol and lies in close agreement to the observed decomposition products. This unwanted reactivity is prohibitive for the synthesis of **92** using the condition known to yield thiacalix[4]arens in good yield.

Therefore, conditions were chosen where stronger electrophilic sulfur reagents are used in order to avoid base-induced rearrangement and fragmentation. It has been reported that thiacalixarenes can be casted in high yields from the corresponding calixarenes by tethering *p-tert*-butyl phenols with alkyl chains to the lower rim and performing the cyclization step with sulfur dichloride (SCl_2).[100] The analogous reaction with **92**, where thiophenols are connected to the upper rim *via* an sulfur atom displays a promising approach for the synthesis of spherophane **87**. However, the octa hydroxy thicalix[4]arene derivative was found to be insoluble in dichloromethane or chloroform, which are solvents commonly used in reactions with SCl_2. This observed low solubility is probably a consequence of intermolecular hydrogen bonding networks present in the solid state therefore limiting its solubility in less polar solvents. Indeed, reacting **92** using similar condition found to form a casted thiacalixarene,[100] using either dichloromethane or chloroform with addition of freshly prepared SCl_2 led to the formation of polymeric material and no product formation could be observed by mass spectroscopic means. Therefore, solvents able to interrupt the intermolecular hydrogen bonding network and with tolerance to SCl_2 were needed. First attempts with THF providing the required solubility of **92** indeed showed the formation of trace amounts of **87** as determined from LC-MS and MALDI-TOF analysis. Yet, isolation of the desired octahydroxy spherophane derivate **87** from the complex mixture of products was not possible. Further screening for alternative solvents was not successful as with increasing polarity of the solvent decomposition of reactants was observed. The decomposition was most prominent in the reaction of **92** with

SCl_2 in nitrobenzene which afforded substantial amounts of 1,3,5 trichlorophenol after 24 h. Presumably, this highly polar solvents promote the reaction of the phenylenesulfides with chlorine gas arising from the disproportion of SCl_2.

Despite the evidences for the formation of **87,** representing an eight-fold hydroxy functionalized thiaspherophane, the investigated reaction conditions suffer from low specificity and decomposition of the starting material and the intermediates. Having recognized the limitations of the electrophilic approach for the synthesis of spherophane **87,** alternative reaction conditions for the spherification reaction were needed.

3.2.2 Nucleophilic Spherification Approach

Another reaction class which has been shown to form cyclopoly(m-phenylenesulfides) is the nucleophilic aromatic substitution reaction (S_NAr). The developed conditions for the preparation of 5,11,17,23-thioaryl substituted thiacalix[4]arene shown in the previous chapter enables the access to derivatives with the required functionalities for an S_NAr mechanism.

Therefore a direct approach was considered where a thiacalix[4]arene decorated with four 3,5-difluorophenyl (**97**) would provide the substitution pattern and reactivity towards sulfur nucleophiles necessary for the spherification reaction. Analogous to the preparation of **95**, the *in situ* formed tetralithium thiacalix[4]arene derived from **93** was intercepted by addition of thiosulfonate **98** (Scheme 18) providing the octafluorinated calixarene **99** after recrystallization from dichloromethane and methanol in moderate yield of 32%. Single crystals of compound **99** suitable for X-ray crystallography could be obtained by slow evaporation from acetone. The solid-state structure of **99** is shown in Figure 21 and adopts an 1,3-alternate conformation. Deprotection of **99** using BBr_3 in DCM afforded the tetrahydroxy compound **97** in good yield.

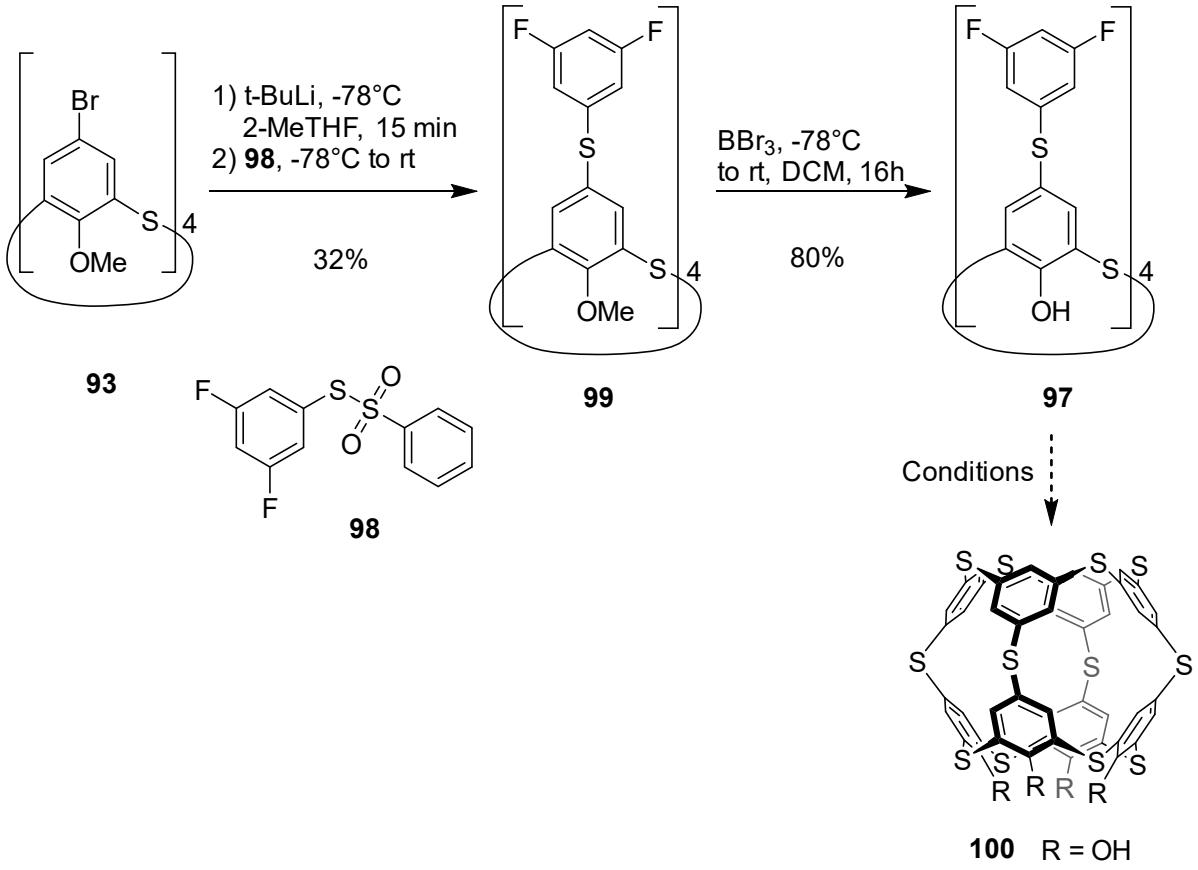

Scheme 18: Synthetis of **97** from **93** and the following key step for the synthesis of spherophane **100.**

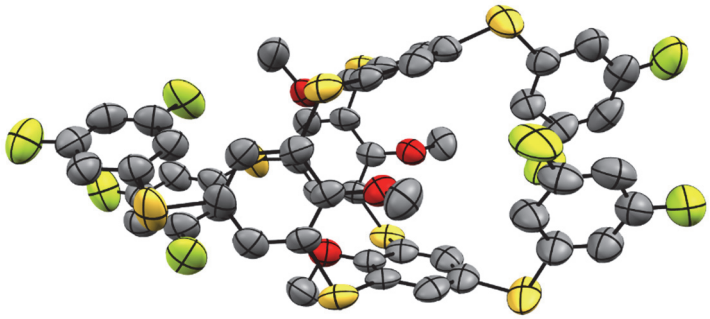

Figure 21: Solid state structure of compound **99**. Hydrogens and solvent molecules are omitted for clarity and rotational ellipsoids are displayed at a 50% probability level.

Treating of the octafluoro compound **97** (Scheme 18) with sodium sulfide in N-Methyl-2-pyrrolidon (NMP) at 100°C afforded a mixture of products with different degrees of substitution, however, no evidences for the formation of **100** could be obtained by MALDI-TOF or ESI-MS spectroscopy. Similar behavior was observed by reacting compound **97** with 2-trimethylsilyl ethyl thiol with cesium carbonate as a base, which upon substitution liberates fluoride ions leading to deprotection of the trimethyl silyl ethyl fragment.

In order to circumvent this unspecific substitution of **97** by thiolates leading to a mixture of regioisomers the asymmetric intermediate **101** (Figure 22) was envisioned where each of the pendant phenyl rings on the thiacalix[4]arene is substituted with a protected thiol and a fluoride. This compound already bears all carbon and sulfur atoms found in **100** with the required substitution pattern suitable for an intramolecular spherification reaction. Moreover, the choice of trimethyl silyl ethyl protecting group would allow the thiolate species to be formed *in situ* in the presence of fluoride ions which is appealing for two reasons: i) using the protected species as a precursor allows easier purification and handling of the starting material in comparison to thiols and ii) the intramolecular substitution reaction would release a fluoride ion essentially rendering the spherification reaction catalytic to fluoride ions.

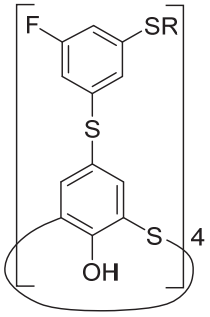

101 $R=CH_2CH_2Si(CH_3)_3$

Figure 22: Asymmetrically substituted thiacalix[4]arene **101** fir the intramolecular cyclization.

Thus the required precursor **102** for the synthesis of **103** was prepared (Scheme 19) from 3-bromo-5-fluorophenyl *tert*-butyl sulfide (**104**) by trans *tert*-butylation with aluminum chloride in toluene providing the thiol after work up **105**. Protection of **105** with vinyl trimethylsilane yielded compound **106** in excellent yield. The disubstituted thiophenol **107** was obtained in 85% yield after performing a lithium-halogen exchange reaction with **106** followed by addition of elemental sulfur. The subsequent transformation to the thiosulfonate **102** was accessible by *in situ* formation of the corresponding disulfide followed by the addition of sodium benzene sulfinate in presence of iodine in DCM yielding intermediate **102**.

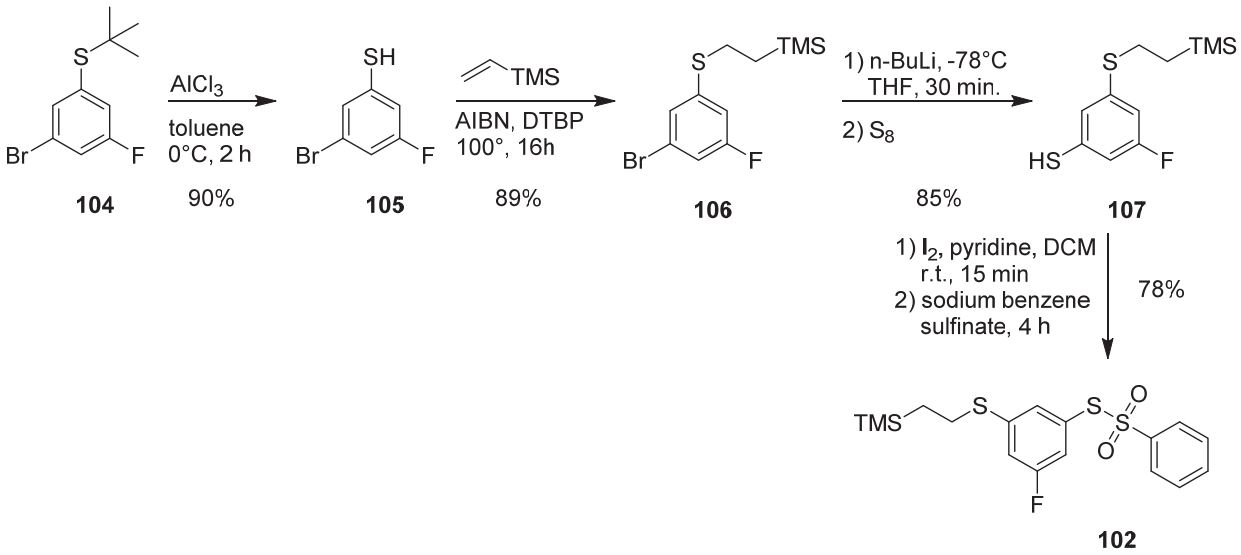

Scheme 19: Synthesis of thiosulfonate **102** bering an protected.

With compound **102** in hands, the synthesis of thiacalix[4]arene derivative **108** was achieved in analogous fashion to the previously described method for the tetrasubstitution of **93** in low yield of 24% (Scheme 20). Attempts on the spherification of compound **108** under high dilution using 1,3-dimethyl-2-imidazolidinonled (DMI) as a solvent and stoichiometric amounts of cesium fluoride gave rise to the unexpected formation of **109** by transmethylation from the oxygen to the sulfur atoms. The near quantitative formation of **109** without scrambling of the methyl substitution as judged from ^{1}H NMR and MALDI-TOF spectroscopy indicate an intramolecular process. Therefore, the interfering methyl groups were cleaved by reaction of **108** with BBr_3 yielding **101** in excellent yield and, most importantly, without deprotection of the trimethylsilyl ethyl functionalities.

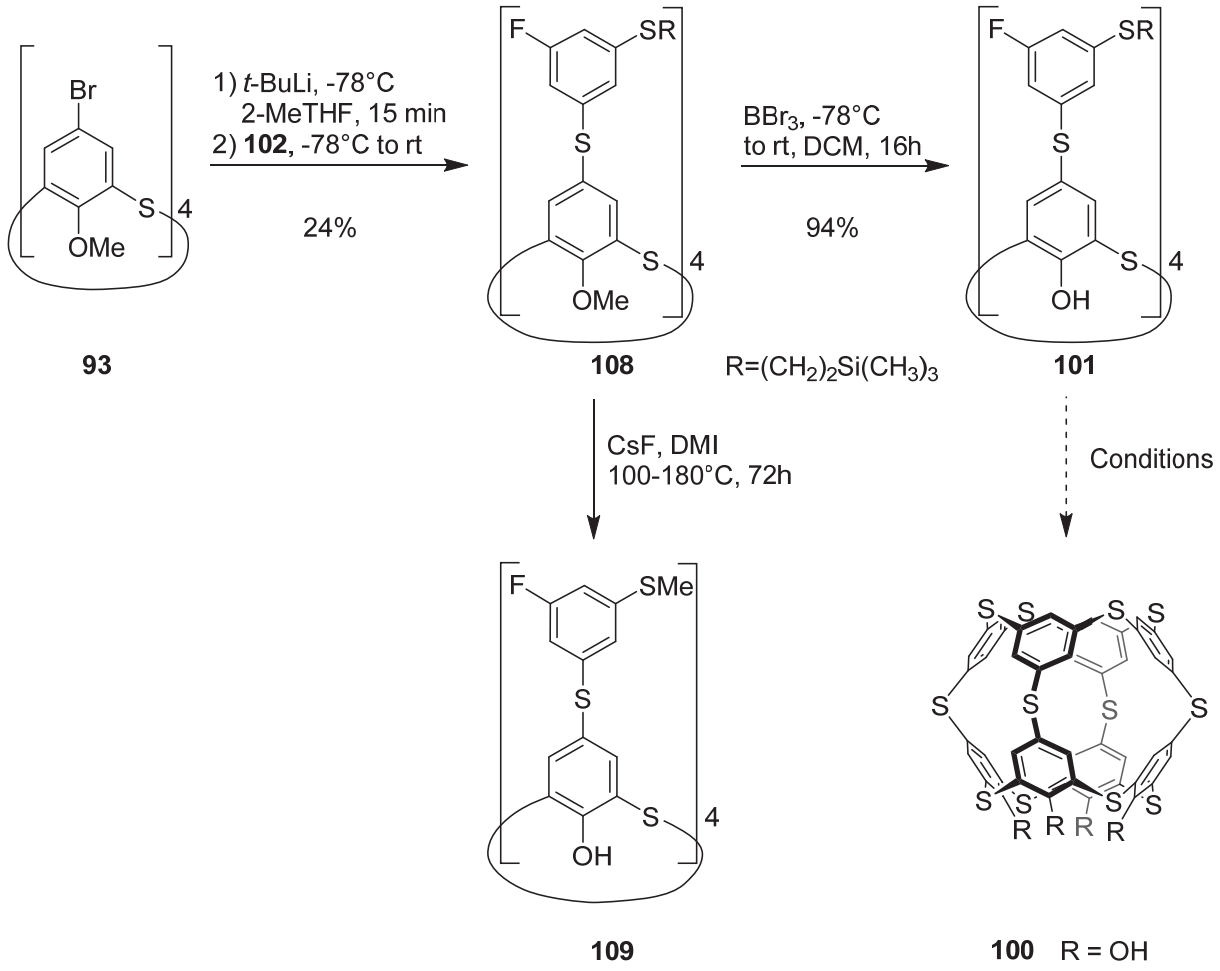

Scheme 20: Synthetis of **101** from **93** and the following key step for the synthesis of spherophane **100**. Transmethylation reaction of the in situ formed thiolate derived from **110** yielding **109.**

Despite of the efficient *in situ* deprotection of **101** in the presence of cesium fluoride (CsF) in either DMF, DMA or DMI, no catalytic activity was observed. Even with increasing temperatures from 100°C up to 170°C no evidences of the formation of **100** could be observed by spectroscopic means. Even stoichiometric amounts of CsF leading to a complete deprotection of starting material did not provide any signs of product formation under the applied reaction conditions. One reason for this observation might be due to a decrease in the nucleophilicity of the deprotected thiolate due to the strong electronegativity of the fluoride substituent. In order to test this hypothesis the chloride derivate **111** (Scheme 21) was envisioned to be less deactivating but still able to engage in a nucleophilic substitution reaction.[115] Yet the low yield of the four-fold substitution reaction by lithium halogen exchange was not satisfactory and the screening for palladium catalyzed reaction conditions was resumed. It was found that Xantphos[116] together with Pd_2dba_3 in toluene and using sodium *tert*-butoxide as a base was a highly active system for the four-fold substitution of **93**. Indeed, the thiol **112** (Scheme 21), obtained in a similar fashion to **107** (Scheme 20), and **93** reacted under the found conditions

affording the tetrasubstituted compound **113** in excellent 79% yield after isolation by column chromatography. Deprotection of the methoxy groups with BBr_3 afforded the precursor **111** in 98% yield after work up. The preorganization of the system into the cone conformation was confirmed by ^{1}H-NMR due to the characteristic shift of the phenolic protons and the high symmetry of the spectrum.

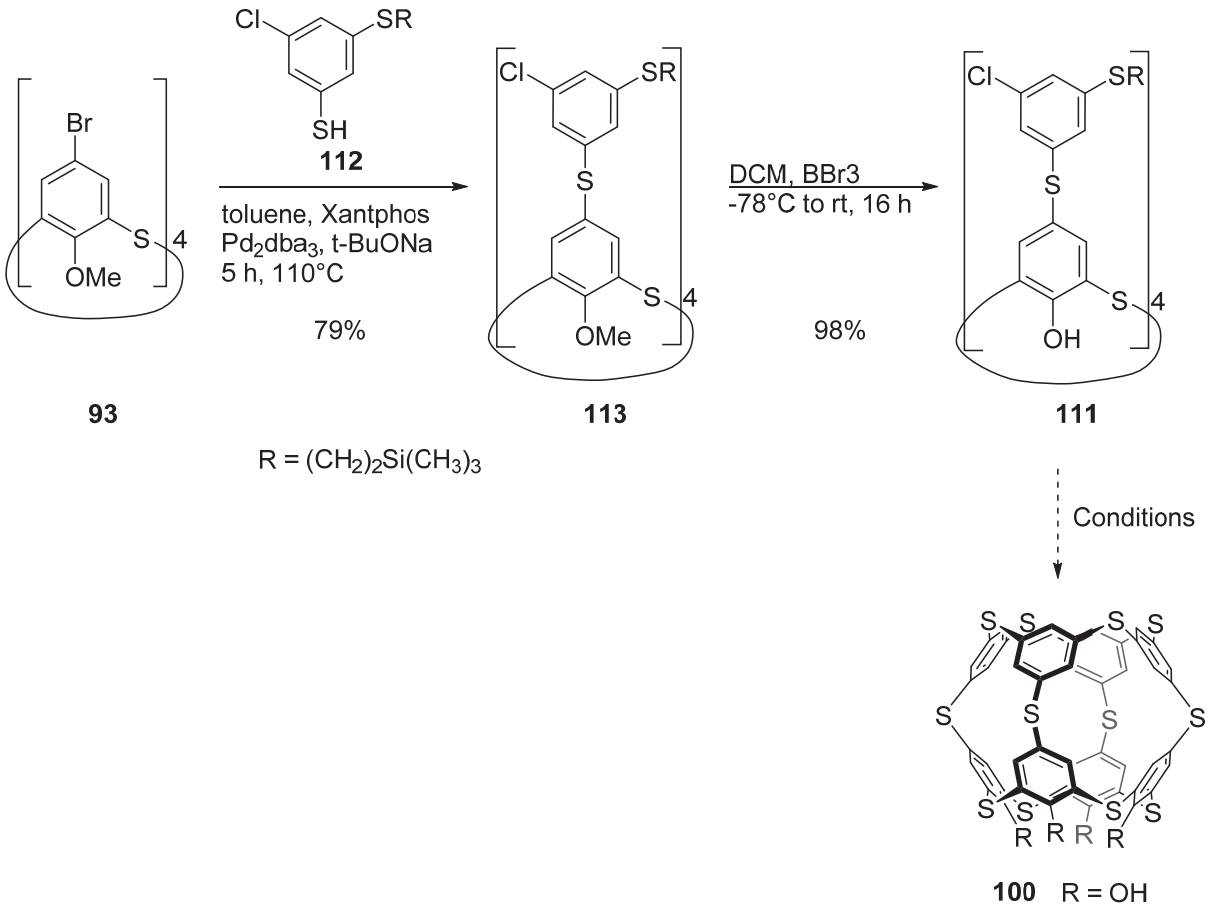

Scheme 21: Synthetis of **100** from **93** and **112** with the following key step for the synthesis of spherophane **100**.

To our delight, heating thiacalix[4]arene **111** in the presence of stoichiometric amounts of CsF in DMA at 170-200°C for 2 h under high dilution in a microwave reactor led to the formation of trace amounts of **100** as observed by MALDI-TOF and HR-MS ESI. Under these harsch reaction conditions significant amounts of hydrodehalogenated species could be observed, however the major component of the reaction mixture appeared to be the in situ formed tetra deprotected thiolate derived from **111**. Attempts to isolate **100** *via* column chromatography, preparative thin layer chromatography (TLC) or cyclic gel permeation chromatography were not successful in isolating the desired product. Yet, the high-resolution mass ESI spectrum measured from the enriched mixture indeed showed the presence of a species matching the monoisotopic mass of the spherophane **100** together with the hydrodehalogenated compound **114** as depictured in

Figure 23. Varying the reaction times and temperatures did not improve the reaction outcome and prolonged reaction times led only to decomposition of the mixture. Nonetheless, these findings represent the most concise evidence obtained during this work for the existence of a thiaspherophane derivative.

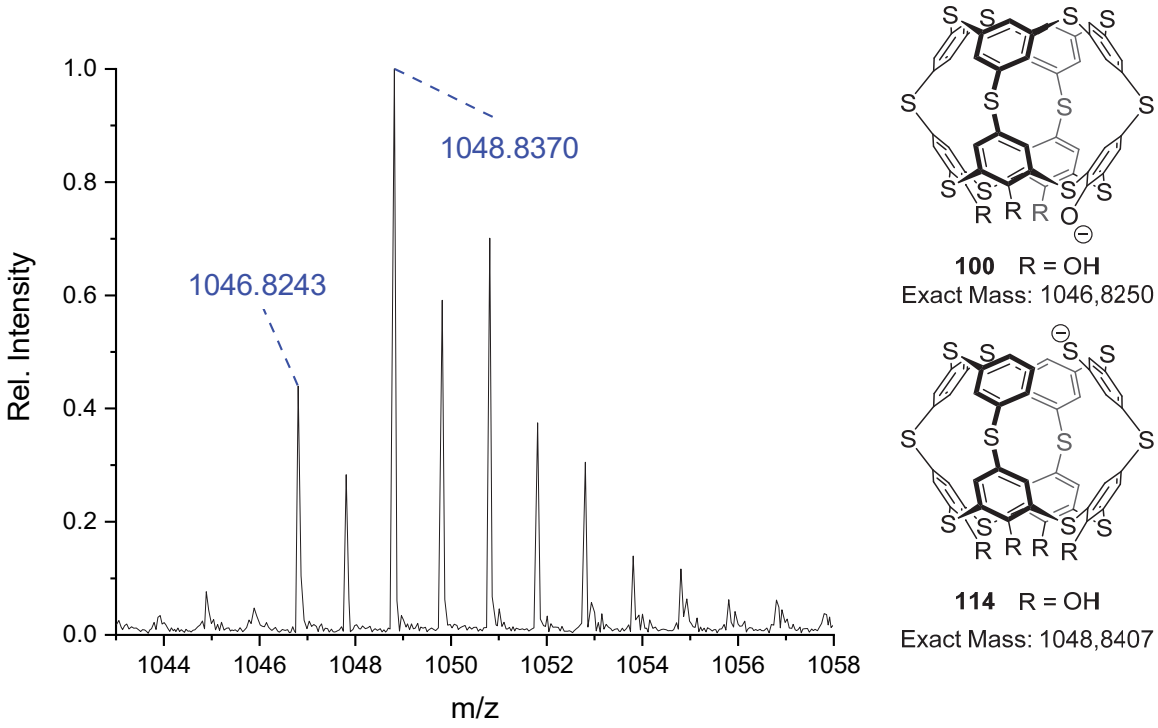

Figure 23: Measured High-resolution ESI spectrum of the reaction mixture after purification by column chromatography showing a superimposed isotopic distribution of **100** and its dehydrogenated form.

The observation of hydrodehalogenation was surprising and indicates that the governing reaction mechanism may proceed over a single electron transfer (SET) mechanism. Indeed, a control experiment with addition of dibutylhydroxytoluene (BHT) as a radical scavenger to the found reaction conditions suppressed the hydrodehalogenation as well as formation of the product. From these observations and from literature reports[117–126], it is reasonable to assume that the observed spherification reaction proceeds via a radical nucleophilic aromatic substitution ($S_{RN}1$) mechanism. However, for this type of reaction the reactivity decreases through the series ArI>ArBr>ArCl>ArF and only few examples exist where it has been demonstrated that chlorobenzenes undergo $S_{RN}1$ substitutions.[117,118] Yet, the observation that in contrast to **111** the fluoro derivative **101** did not undergo substitution, indicates that the predominant mechanism for the spherification reaction is *via* a $S_{RN}1$ mechanism.

The identity of the initiator has not been determined yet, however, a possible explanation for the observed reactivity is a thermally induced SET[117] from the thiolate to the aryl halide, therefore forming an thiyl radical and an aryl radical anion. By elimination of the halide anion the formed aryl radical may subsequently recombine with the thiyl radical forming a C-S bond(Scheme 22).

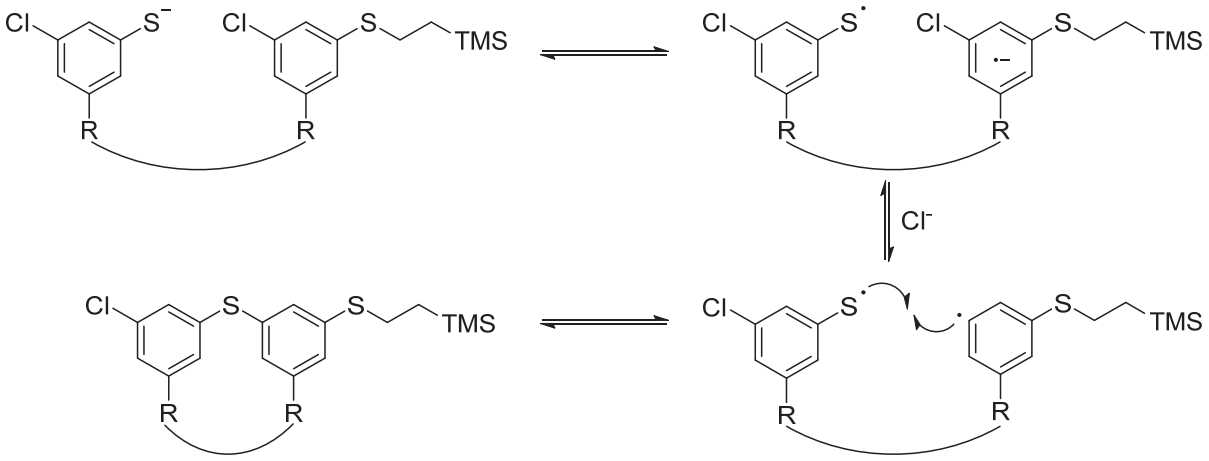

Scheme 22: Proposed $S_{RN}1$ mechanism for the spherification reaction. Only one step of the four required steps is shown.

Yet, the implication of this proposed mechanism is that the deprotection rate of **115** may have great influence on the conversion of the reaction. Since due to Coulomb repulsion, SET should only occur between a deprotected thiolate and a still protected aryl sulfide. Hence, it can be expected that with a slow deprotection the conversion to **100** may be increased. However, slow addition of a CsF solution in methanol to a vigorously stirring solution of **115** in DMI at 200°C showed similar low conversion as in the “one-pot” method. This contradicting observation may be attributed to the low nucleofugality of the chloride in comparison to the bromide or iodide.

Having identified a possible reaction mechanism leading to the desired spherophane **100**, it would be highly desirable to exchange the aryl chloride **115**, which reacts only sluggishly, with an aryl bromide. This may lead to an higher conversion as has been reported in literature.[119] Therefore, a synthetic route towards the tetrabromo derivative **116** was developed (Scheme 23a). The tetrabromo thiacalix[4]arene derivative **93** was converted to **117** by four-fold palladium catalyzed substitution with 2-trimethyl silyl ethyl thiol (**118**) in 90% yield after column chromatography. Subsequent transformation to compound **119** by *in situ* deprotection of **116** with tetrabutyl ammonium fluoride in the presence of the dihalide **120**, palladium catalyst and cesium carbonate was achieved in satisfactory 59% yield. Deprotection of **119** using an excess BBr_3 afforded **121** quantitavely. Yet, the standard protection procedure

using neat starting material and a initiator failed to provide the tetra protected compound **122**, probably due to insolubility of **121** in vinyl trimethyl silane and only polymeric material could be obtained. Adding benzene as cosolvent indeed provided an homogeneous reaction mixture, however, only partially protected intermediates together with starting material could be observed. Therefore, an alternative protection procedure was developed using benzophenone as a photoredox catalyst[127] under iradiation (366 nm). Despite excellent protection of the test substrate **123** to **124** under these conditions the analogous reaction with **121** showed only low conversion to partially protected species. Suitable protection conditions have yet to be found in order to perform the spherification reaction under the previously found conditions. Still, the obtained tetra thiol **121** represents a valuable precursor for the synthesis of **100**.

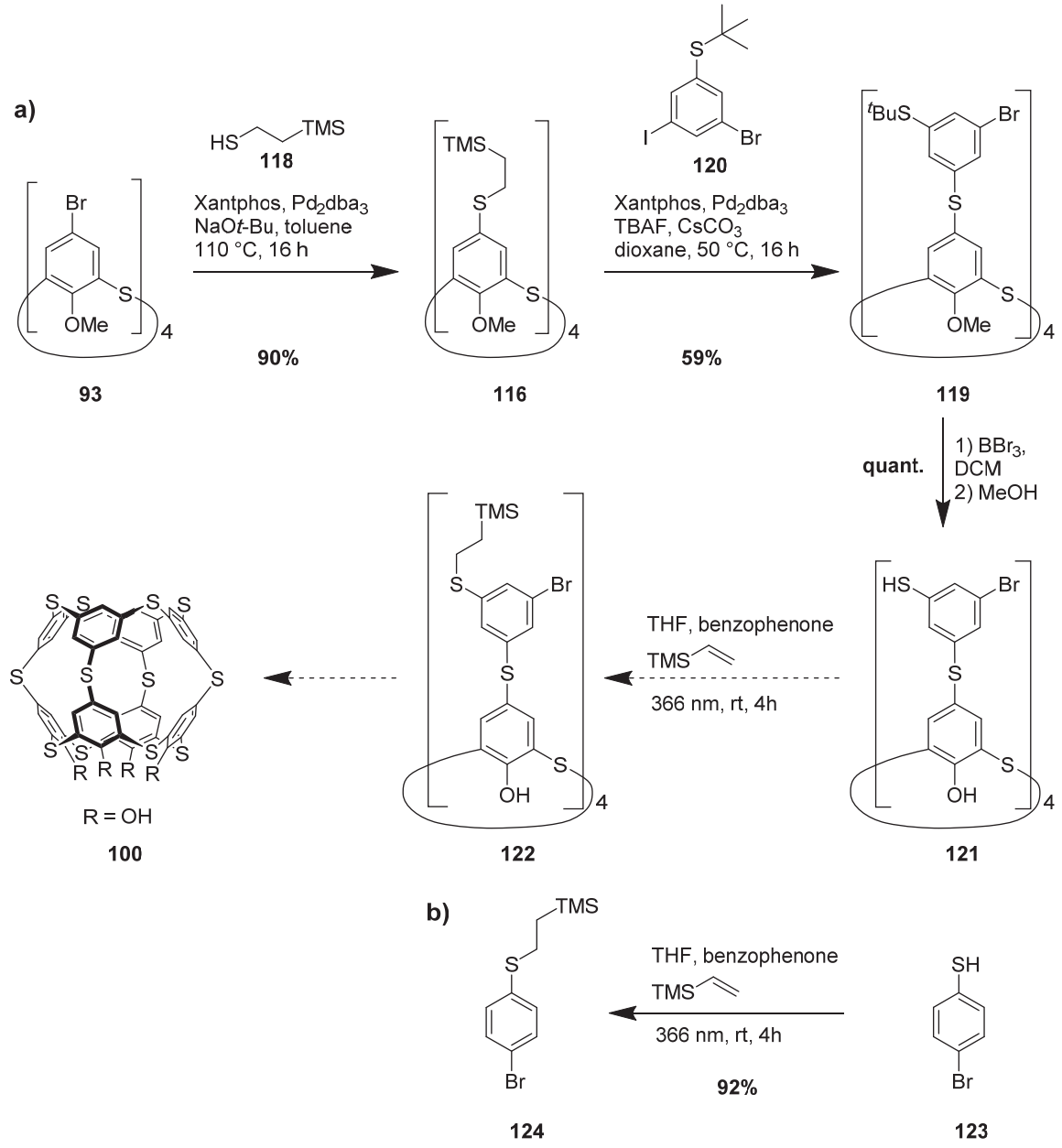

Scheme 23: Synthesic route towards spherophane **100** and photcatalyzed thiol protection with vinyl trimethyl silane. a) Synthesis of **121** and attempted protection to **122**. b) Photocatalyzed test reaction for the protection of **123** to **124**.

As a result, reactions condition shown to proceed over an aryl radical intermediate derived from the reduction of aryl bromides in presence of thiols[128,129] were chosen for the spherification of **121** to **100** (Scheme 24). It has been reported[129] that irradiating a mixture of a thiophenol and an aryl halide in DMSO with visible light at room temperature allows the preparation of diaryl sulfides in good to excellent yields. The proposed mechanism for this reaction is similar to the mechanism discussed in Scheme 22 whereby a visible light mediated charge transfer step occurs thus forming a thiyl radical and an aryl halide radical anion. Elimination of the halide allows the thiyl and aryl radicals to recombine leading to the formation of a new carbon sulfur bond. Indeed, the reaction of the **121** under the described reaction conditions showed higher conversions, however, no formation of thiaspherophane **100** could be observed and hydrodehalogenation was the main reaction outcome. Also using $Ir(ppy)_3$ a highly reducing photoredox catalyst known to catalyse $S_{RN}1$ reactions forming diarylsulfides[128] led to a complex mixture of compounds probably due to scrambling of the sulphide bonds.

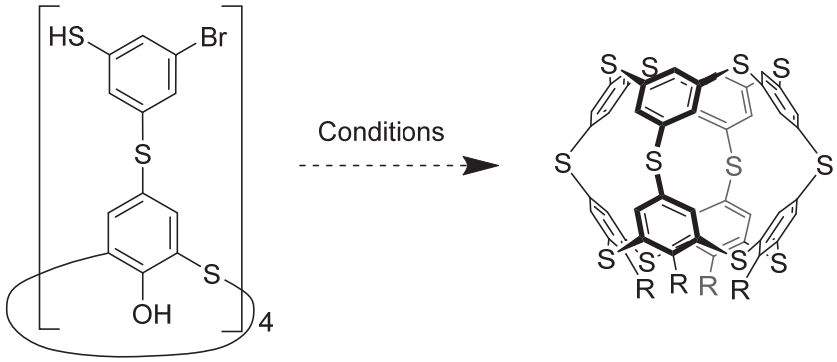

121 **100** R = OH

Scheme 24: Attempted spherication of **121** to thiaspherophane **100.**

3.3 Summary and Outlook

In this work the use of thiacalix[4]arene precursors has been identified as a promising synthetic platform for the assembly of thiaspherophanes. The investigation of intramolecular reactions required for the spherification step using sulfur reactants, either as an electrophile or as nucleophile, was discussed. This was enabled by the development of two distinct approaches for the decoration of four-fold brominated thiacalix[4]arene **93** with functionalized sulfanyl phenyl units required for the spherification reactions: i) nucleophilic addition of a tetralithiated calixarene to four thiosulfonates and ii) palladium catalyzed substitution with functionalized thiols.

The electrophilic spherification approach, which has been successfully used for the synthesis of thiacalixarenes,[93,94,100] was hampered by formation of complex mixtures with varying degrees of sulfanylation accompanied by decomposition of the substrate in polar solvents. Therefore, the approach was changed by synthesizing substrates favoring a nucleophilic aromatic substitution reaction for the spherification step. Similar approaches have been used to prepare macrocyclic oligo *meta*-phenylene sulfides.[92] Also, the $S_{RN}1$ reaction appears to be a promising reaction mechanism for the spherification step as the analysis of the formed products delivered spectroscopic evidences for the existence of a thispherophane. However, reactions using **111** in DMA at high temperature showed only minor conversion. Yet, it appears that elevated temperatures are required for the closing of the cuboctahedral scaffold since the reaction of the bromide substituted analog **121** at room temperature and under visible-light promoted charge-transfer provided mostly hydrodehalogenated products.

It seems that having the nucleophile and electrophile on the same aryl unit is detrimental for the conversion of the reaction as the formation of negatives charge upon deprotection results in a four-fold charged molecule. Therefore, it is reasonable to assume that Coulomb repulsion prohibits the intramolecular reaction between the negatively charged subunits to proceed and only a low percentage of molecules happen to be sequentially deprotected and engage into a bond forming reaction.

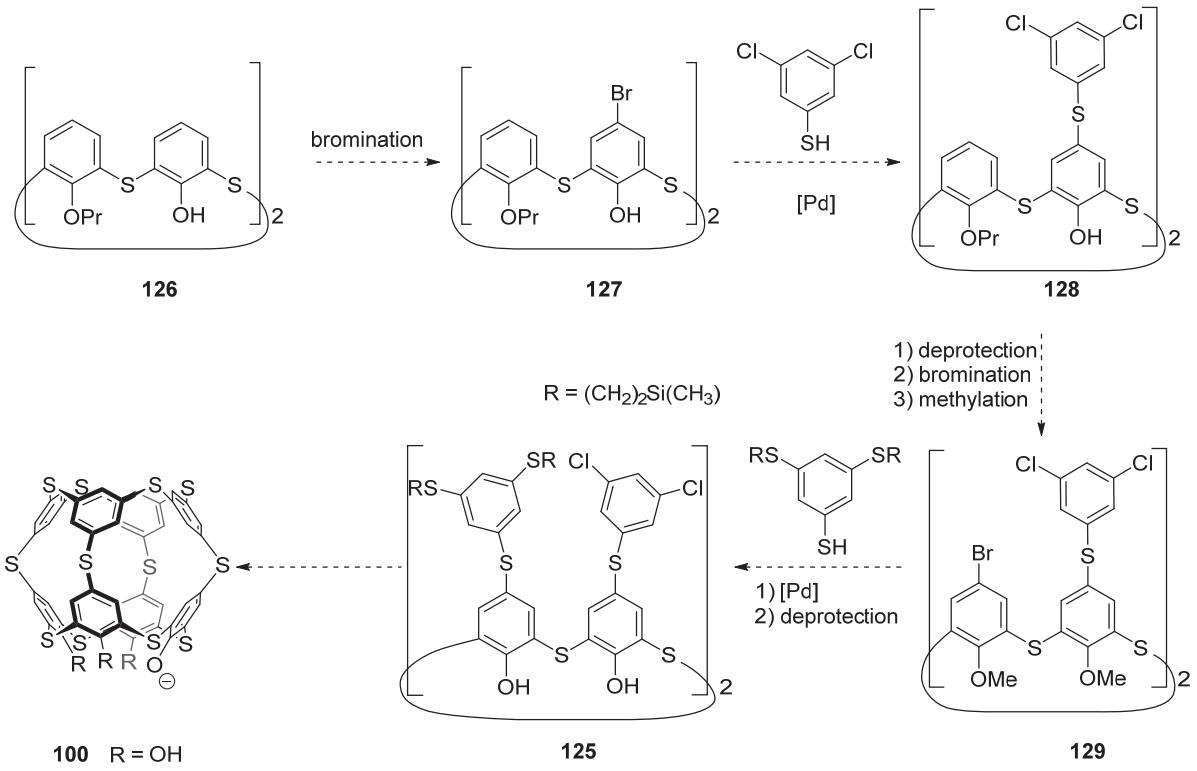

Scheme 25: Proposed synthesis of the distally functionalized thiacalix[4]arene **125** as an improved substrate for the synthesis of thiaspherophane **100**.

Consequently, having a thiacalix[4]arene substituted with two phenyls bearing the halides and two bearing the sulfur functionalities each distally arranged may allow the fully deprotected compound to react intramolecularly with minor degree of deactivation. This approach would be highly similar to previous methods for the assembly of cyclic oligo(meta-phenylene sulfides)[91,92] by nucleophilic aromatic substitution in the sense of having the electrophilic and nucleophilic atoms on separate subunits. A proposed synthesis of such an highly preorganized and distally functionalized thiacalix[4]arene **125** is shown in Scheme 25. The reported regioselective alkylation[130] of 25,26,27,28-tetrahydroxy[4]arene **88** with n-propyl iodide enabled the distal bromination of **126** forming the dibromo thiacalix[4]arene compound **127** by selective bromination of the phenolic units.[131] Building on these findings, we expect the disubstituted derivative **128** to be accessible from the literature known compound **127** and 3,5-dichloro thiophenol *via* the palladium catalyzed procedure developed during this work. However, interference of the hydroxy groups with the applied reaction conditions may occur requiring prior methylation (not displayed in Scheme 25). Deprotection of the alkoxy moieties should then provide the required activation of the liberated phenolic units, allowing selective bromination of the remaining positions of the thiacalix[4]arene core. Subsequent methylation of the hydroxy groups providing **129** should allow its substitution with 3,5-di(2-

trimethylsilylethyl sulfanyl) thiophenol providing the key intermediate **125** under palladium catalysis. Following deprotection of the four methoxy groups should provide compound **125**, allowing beneficial preorganization of the system due to the expected formation of circular hydrogen bonding contributing to the stabilization of the cone conformation. Therefore, subjection of this compound to similar conditions where evidences for the formation of thiaspherophane **100** could be obtained may allow the formation **100** in higher yield.

3.4 Experimental Part

General Information

All commercially available compounds were purchased and used as received unless explicitly stated otherwise. All NMR experiments were performed on Bruker Avance III or III HD, two or four-channel NMR spectrometer operating at 400.13 or 500.13 MHz proton frequency. The instruments were equipped with direct observe BBFO, indirect BBI or cryogenic four-channel QCI (H/C/N/F) 5 mm probes all with self-shielded z-gradient. The experiments were performed at 298 K and the temperature was calibrated using a methanol standard showing accuracy within +/- 0.2 K. GC-MS was performed on a Shimadzu GCMS-2020 SE equipped with a Zebron 5 MS Infernocolumn which allowed to achieve temperatures up to 350 °C. High-resolution mass spectra (HRMS) were measured as HR-ESI-ToF- MS with a Maxis 4G instrument from Bruker and were measured on a Bruker solariX spectrometer with a MALDI source for HR-MALDI-ToF MS. For column chromatography silica gel Siliaflash® p60 (40–63 μm) from Silicycle was used, and TLC was performed on silica gel 60 F254 glass plates with a thickness of 0.25 mm purchased from Merck Melting point were measured with a Stuart SMP3 with a slope of 5°C/min. Elementary analyses were measured by W. Kirsch on a Perkin-Elmer Analysator 240.

25,26,27,28-Tetrahydroxy[4]arene (88):

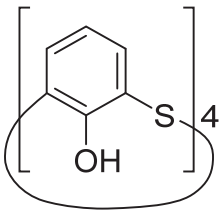

A procedure from literature[110] was modified as followed: A 1 L flask equipped with a reflux condenser was loaded with an mixture of toluene (300 mL) and 4-tertbutyl-thiacalix[4]arene **84** (10.5 g, 14.6 mmol, 1.0 eq). This mixture was heated up to 80 °C until completely dissolved. To the solution at room temperature was added phenol (7.19 g, 76.4 mmol, 5.23 eq.) followed by $AlCl_3$ (23.9 g, 180 mmol, 12.3 eq). The mixture was heated to 80°C under a constant stream of nitrogen. After 2h further 150 mL of toluene was added. After 4h the mixture was cooled to rt and poured into 1 L of ice cold 2 M HCl (aq.) and left stirring for 16 h. The precipitate was filtered and washed with chloroform (30 mL) and acetone (30 mL) The solid was dried under argon until weight remained constant yielding thiacalix[4]arene **88** as a white powder (6.65 g, 13.4 mmol, 92% yield).^{1}H NMR (250 MHz, $CDCl_3$): δ [ppm]= 9.46 (s, 4H), 7.61 (d, *J* = 7.6 Hz, 8H), 6.75 (t, *J* = 7.7 Hz, 4H). Spectrum was found to be identical to the one previously reported.[110]

5,11,17,23-Tetrabromothiacalix-25,26,27,28-tetrahydroxy[4]arene (94):

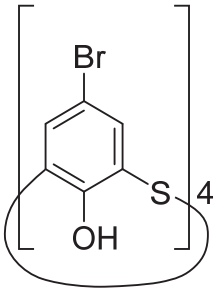

A procedure from literature[110] was modified as followed: NBS (1.79 g, 10.0 mmol, 5.0 eq) was added to a suspension of **88** (993 mg, 2.00 mmol, 1.0 eq.) in anhydrous acetone (200 mL). The mixture was stired for 4h at room temperature. The solid material was filtered, washed with acetone and dried under vacuum until constant weight. Compound **94** was isolated as a white powder (1.21 g, 1.49 mmol, 74%). ^{1}H NMR (250 MHz, DMSO-d_6): δ [ppm]= 7.77 (s, 8H). Spectrum was found to be identical to the one previously reported.[110]

5,11,17,23-Tetrabromo-25,26,27,28-tetramethoxy-thiacalix[4]arene (93):

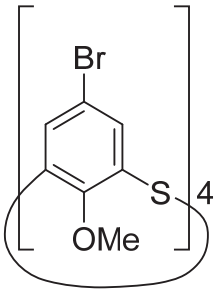

A procedure from literature[111] was modified as followed: To a suspension of compound **94** (4.42 g, 5.44 mmol, 1.0 eq.) and anhydrous K_2CO_3 (15.0 g, 109 mmol, 20.0 eq.) in anhydrous acetone (650 mL) was added methyl iodide (6.77 mL, 109 mmol, 20.0 eq.). The mixture was refluxed for 24 h. After cooling to room temperature, the reaction was quenched with saturated NH_4OH (aq.). The solvent removed under reduced pressure. The residue was portioned in DCM and 1M HCl (aq.). The organic phase was separated and washed with water and dried with anhydrous Na_2SO_4. The solvent was removed under reduced pressure and the residue was precipitated from DCM with methanol yielding **93** as a white solid (4,42 g, 5,10 mmol, 94 %). ^{1}H NMR (250 MHz, $CDCl_3$): δ [ppm] = 7.55 (s, 8H), 3.69 (s, 12H). Spectrum was found to be identical to the one previously reported.[111]

_S_-_p_-Methoxyphenyl bezenethiosulfonate(96):

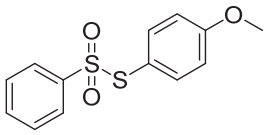

To a solution of 4-methoxythiophenol (250mg, 1.78mmol, 1.00 eq.) in DCM (3 mL) was added iodine (904mg, 3.56mmol, 2.00 eq.) followed by pyridine (0.151 mL, 1.87mmol, 1.05 eq.). After 15 minutes sodium benzene sulfinate (497mg, 3.03mmol, 1.70 eq.) was added and reacted 30 minutes at room temperature. The mixture was diluted with ethyl acetate and washed with water and sat. aq. $Na_2S_2O_3$, dried over anhydrous Na_2SO_4, filtered and the solvent was removed under reduced pressure. The crude product was purified by column chromatography (cyclohexane/ethyl acetate 5:1) yielding S-p-methoxyphenyl bezenesulfonate as a colorless oil (487mg, 1.737 mmol, 98%). ^{1}H NMR (500 MHz, CD_2Cl_2): δ [ppm] = 7.63-7.59 (m, 1H), 7.57-7.54 (m, 2H), 7.48-7.44 (m, 2H), 7.26-7.23 (m, 2H), 6.87-6.84 (m, 2H), 3.82 (s, 3H). ^{13}CNMR (126 MHz, CD_2Cl_2): δ= 163.1 (q), 143.5 (q), 138.8 (t), 134.2 (t), 129.5 (t), 128.1 (t), 119.0 (q), 115.5 (t), 56.1 (p). HRMS (ESI, +): m/zcalcd. for $C_{13}H_{12}NaO_3S_2[M+Na]^+$ 303.0119; found:303.0120.

5,11,17,23-Tetra-_S_-4-methoxyphenyl-sulfanyl-25,26,27,28-tetramethoxythiacalix[4]arene (95):

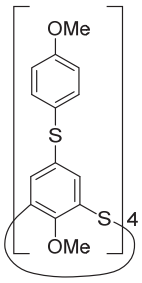

To a solution of **93** (4.00 g, 4.61 mmol, 1,0 eq.) in dry 2-MeTHF (200 mL) at -78°C was added *t*-BuLi (1,9M in pentane, 20,4 mL, 38,7 mmol, 8,4 eq.) whereby the addition rate was adjusted such that the temperature of the mixture does not exceed -70°C. After complete addition the reaction was stirred for 5 min at -78°C followed by slow addition of **96** (6,62 g, 23,6 mmol, 5,12 eq.). After complete addition the cooling bath was removed, and the reaction mixture allowed to warm up to room temperature. The mixture was quenched by the addition of water and the organic layer was washed with water, dried over anhydrous Na_2SO_4, filtered and concentrated under reduced pressure. The crude product was recrystallized from TBME/methanol yielding

95 a white solid. ^{1}H NMR (250 MHz, CD_2Cl_2): δ [ppm] = 7.40 – 7.29 (m, 8H), 7.26 (br s, 8H), 7.01 – 6.84 (m, 8H), 3.83 (s, 12H), 3.53 (br s, 12H). Elemental Analysis: Anal. Calcd for $C_{56}H_{48}O_8S_8$: C, 60.84; H, 4.38. Found: C, 60.53; H, 4.49.

5,11,17,23-Tetra-*S*-4-hydroxyphenyl-sulfanyl-25,26,27,28-tetrahydroxythiacalix[4]arene (92):

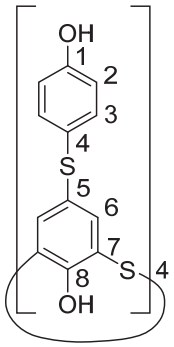

To a solution of **95** (2,58 g, 2,33 mmol, 1.0 eq.) in anhydrous DCM (25 mL) at -78°C was added BBr_3 (2 mL, 21 mmol, 9,0 eq) and the reaction was stirred for 16 h. The mixture was cooled to 0°C and was quenched by slow addition of dry methanol and the volatiles were removed under vacuum. The crude product was further purified by recrystallization from THF/methanol yielding **92** as a white solid (1,91 g, 1,92 mmol, 83%). ^{1}H NMR (500 MHz, Acetone d_6): δ= [ppm] 9.24 (s, 1H, OH-8), 8.82 (s, 1H, OH-1), 7.47 (s, 4H,H-6), 7.35 – 7.18 (m, 4H, H-3), 7.04 – 6.80 (m, 4H, H-2). ^{13}CNMR (126 MHz, Acetone d_6): δ= 159.17 (C1), 159.05 (C1'), 156.93 (C8), 140.03 (C6), 136.18 (C3), 132.42 (C5), 123.30 (C4), 123.28 (C4'), 122.15 (C7), 117.68 (C2), 117.59 (C2').

***S*-3,5-Difluorophenyl benzenethiosulfonate (98):**

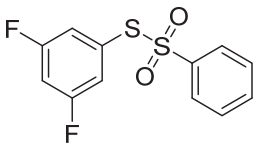

To a solution of 3,5 difluoro thiophenol (1.00 g, 6.84 mmol, 1.00 eq.) in DCM (20 mL) was added iodine (3,47 g, 13.7 mmol, 2.00 eq.) followed by pyridine (0.58 mL, 7.18 mmol, 1.05 eq.). After 15 minutes sodium benzene sulfinate (1.91 g, 11.6 mmol, 1.70 eq.) was added and the mixture was stirred for 3h at room temperature. The mixture was diluted with ethyl acetate and washed with water and sat. aq. $Na_2S_2O_3$, dried over anhydrous $Na2SO_4$, filtered and the solvent was

removed under reduced pressure. The crude product was purified by column chromatography (cyclohexane/ethyl acetate 5:1) yielding S-3,5-difluorophenyl bezenesulfonate **98** as a white solid (1.83 g, 6.39 mmol, 93%). ^{1}H NMR (500 MHz, $CDCl_3$): δ [ppm] = 7.72 – 7.58 (m, 3H), 7.57 – 7.43 (m, 2H), 7.01 – 6.84 (m, 3H).^{13}C NMR (126 MHz, $CDCl_3$): δ [ppm] = 162.49 (dd, $^{1}J_{C,F}$ = 253.7, $^{3}J_{C,F}$ = 12.5 Hz, CF), 142.71 (C), 134.23 (CH), 130.62 (t, $^{3}J_{C,F}$ = 10.2 Hz, C), 129.11 (CH), 127.58 (CH), 119.47 – 118.98 (m, CH), 107.25 (t, $^{2}J_{C,F}$ = 25.0 Hz). ^{19}F NMR (471 MHz, $CDCl_3$): δ = -107.31. HRMS (ESI, +): *m/z* calcd. for $C_{12}H_8NaO_2S_2$ $[M+Na]^+$ 308.9826; found: 308.9831. Melting point 78.2 °C

5,11,17,23-Tetra-*S*-3,5-difluorophenyl-sulfanyl-25,26,27,28-tetramethoxythiacalix[4]arene (99):

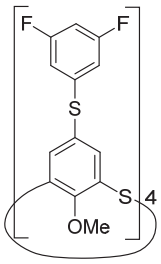

To a solution of **93** (490 mg, 0.564 mmol, 1,0 eq.) in dry 2-MeTHF (25 mL) at -78°C was added *t*-BuLi (1,7 M in pentane, 2.79 mL, 4.74 mmol, 8,4 eq.) whereby the addition rate was adjusted such that the temperature of the mixture does not exceed -70°C. After complete addition the reaction was stirred for 5 min at -78°C followed by slow addition of a solution of **98** (825 mg, 2,88 mmol, 5,12 eq.) in 2-MeTHF (7 mL). After complete addition the cooling bath was removed, and the reaction mixture allowed to warm up to room temperature. The mixture was quenched by the addition of water and the organic layer was washed with water, dried over anhydrous Na_2SO_4, filtered and concentrated under reduced pressure. The crude product was purified by column chromatography (SiO_2, cyclohexane/DCM 5:1) yielding **99** as a white solid (204 mg, 0.180 mmol, 32 %). ^{1}H NMR (250 MHz, $CDCl_3$): δ [ppm] = 7.62 (s, 8H), 6.63-6.56 (m,12H), 3.75 (s, 12H). ^{19}F NMR (235 MHz, $CDCl_3$) δ = [ppm] -108.30 (t, $^{3}J_{HF}$ = 7.9 Hz).

5,11,17,23-Tetra-*S*-3,5-difluorophenyl-sulfanyl-25,26,27,28-tetrahydroxythiacalix[4]arene (97):

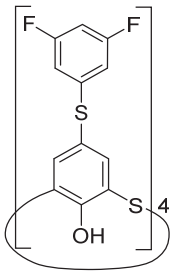

To a solution of **99** (87 mg, 77.9 μmol, 1.0 eq.) in anhydrous DCM (2.5 mL) at -78°C was added BBr_3 (0.03 mL, 308 μmol, 4,0 eq.) and the reaction was stirred for 16 h. The mixture was cooled to 0°C and was quenched by slow addition of dry methanol and the volatiles were removed under vacuum. The crude product was further purified by recrystallization from DCM/methanol yielding **97** as a white solid (66 mg, 62.0 μmol, 80%). ^{1}H NMR (250 MHz, Acetone d_6): δ = 9.38 (s, 4H) 8.01 (s, 8H), 6.99 – 6.53 (m, 12H). {^{1}H}^{19}F NMR (235 MHz, Acetone d_6): δ [ppm] = 67.42 (s).

***S*-2-Trimethylsilylethyl sulfanyl 3-bromo 5-fluoro benzene (106):**

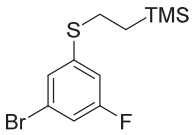

A flask equipped with a $CaCl_2$ drying tube was charged with a solution of (3-bromo-5-fluorophenyl)(tert-butyl)sulfane[132] **104** (1.93 g, 7.33 mmol, 1.0 eq.) in toluene (70 mL) at 0°C. To this solution anhydrous $AlCl_3$ (586 mg, 4,40 mmol, 0,6 eq.) was slowly added. The reaction mixture was stirred for 1h at 0°C. After all the starting material was consumed (TLC, SiO_2, cyclohexane/DCM 10:1) the reaction was poured onto ice and after vigorously stirring, the organic layer was extracted with 2 M NaOH (aq.). The aqueous layer was acidified by the addition of 37% HCl (aq.) whereby a precipitate formed. The aqueous layer was extracted with TBME, dried over Na_2SO_4, filtered and the solvent removed under reduced pressure. The thiol **105** was obtained as a white solid (1.37 g) and was used directly without further purification. The thiol **105** (1.37 g, 6.60 mmol, 1.0 eq.) and vinyltrimethylsilane (4.13 mL, 26.4 mmol, 4 eq.) was loaded into an oven dried 10 mL microwave vial. The mixture was purged with argon followd by the addition of AIBN (111 mg, 0.66 mmol, 0.1 eq.) and di-tert-butyl peroxide (0.122 mL, 0.66 mmol,

0.1 eq.). The caped vial was heated to 105°C in an oil bath for 16 h. The volatiles were removed under reduced pressure and the residue purified by column chromatography (SiO_2, cyclohexane/toluene 20:1) yielding compound **106** as an colorless oil (1.81 g, 5.89 mmol, 80% over two steps). ^{1}H NMR (250 MHz, $CDCl_3$): *δ* [ppm] = 7.16-7.15 (m, 1H), 7.03-6.99 (m, 1H), 6.92-6.86 (m, 1H), 3.06 – 2.75 (m, 2H), 1.05 – 0.75 (m, 2H), 0.07 (s, 9H). ^{19}F{^{1}H} NMR (235 MHz, $CDCl_3$): δ [ppm] = -110.59 (s).

***S*-2-Trimethylsilylethyl sulfanyl 3-fluoro 5-thiophenol (107):**

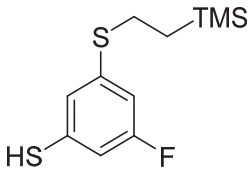

To a solution of compound **106** (1.80 g, 5.86 mmol, 1.0 eq.) in THF (20 mL) at -78°C *t*-BuLi (1.7 M in pentane, 7.58 mL, 12.9 mmol, 2.2 eq.) was added dropwise. After 30 minutes sulfur (188 mg, 5.86 mmol, 1.0 eq.) was added in one portion and the mixture was allowed to warm up to room temperature over the period of 3 h. The reaction was quenched by the addition of 1 M HCl (aq.) and diluted with ethyl acetate. The aqueous layer was extracted with ethyl acetate and the combined organic layers were washed with brine, dried over Na_2SO_4, filtered and the solvent evaporated under reduced pressure. The crude product was further purified by vacuum distillation (20 mbar, 120-126 °C) yielding **107** as a colorless oil (1.30 g, 5.00 mmol, 85%). ^{1}H NMR (250 MHz, $CDCl_3$): *δ* [ppm] = 6.93-6.91 (m, 1H), 6.77-6.74(m, 2H), 3.02 – 2.82 (m, 2H), 1.14 – 0.82 (m, 2H), 0.06 (s, 12H).

***S*-3-(2-Trimethylsilylethyl sulfanyl) 5-fluorophenyl benzenethiosulfonate (102):**

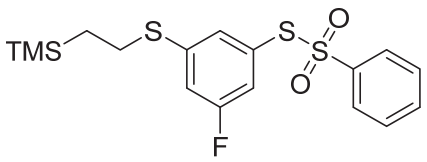

To a solution of **107** (1.30 g, 5.00 mmol, 1.00 eq.) in DCM (10 mL) was added iodine (2.80 g, 10.0 mmol, 2.00 eq.) followed by pyridine (0.42 mL, 5.25 mmol, 1.05 eq.). After 15 minutes sodium benzene sulfinate (1.40 g, 8.50 mmol, 1.70 eq.) was added and the mixture was stirred for 3h at room temperature. The mixture was diluted with ethyl acetate and washed with water

and sat. aq. $Na_2S_2O_3$, dried over anhydrous Na2SO_4, filtered and the solvent was removed under reduced pressure. The crude product was purified by column chromatography (cyclohexane/ethyl acetate 5:1) yielding **102** as a colorless oil (1.83 g, 4.58 mmol, 92%). ^{1}H NMR (400 MHz, $CDCl_3$): δ [ppm] = 7.65 – 7.58 (m, 3H), 7.52 – 7.42 (m, 2H), 7.03 (ddd, $^3J_{HF}$ = 9.0 Hz, $^4J_{HH}$ = 2.4 Hz, $^4J_{HH}$ = 1.6 Hz, 1H), 6.94 (dd, , $^4J_{HH}$ = 1.6 Hz, 1H), 6.84 (ddd, $^3J_{HF}$ = 7.9 Hz, $^4J_{HH}$ = 2.4 Hz, $^4J_{HH}$ = 1.6 Hz, 1H), 3.32 – 2.61 (m, 2H), 1.05 – 0.71 (m, 2H), 0.06 (s, 9H). ^{13}C NMR (101 MHz, $CDCl_3$): δ [ppm] = 142.92, 142.25 (d, $^3J_{CF}$ = 8.04 Hz, 134.10, 130.47 (d, $^3J_{CF}$ = 3.0 Hz), 129.10, 127.79, 119.61 (d, $^2J_{CF}$ = 22.8 Hz), 117.30 (d, $^2J_{CF}$ = 23.2 fHz), 27.07, 16.42, -1.61.

5,11,17,23-Tetra-*S*-3-(2-trimethylsilylethyl sulfanyl)-5-fluorophenyl-sulfanyl-25,26,27,28-tetramethoxythiacalix[4]arene (108):

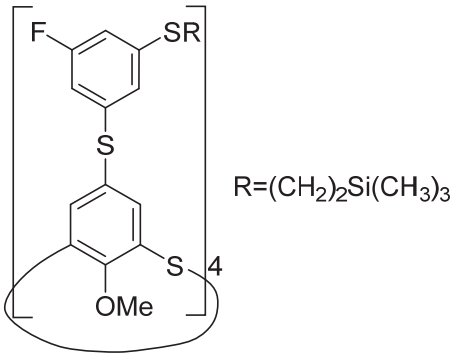

To a solution of **93** (228 mg, 0.527 mmol, 1,0 eq.) in dry 2-MeTHF (12.5 mL) at -78°C was added *t*-BuLi (1,7 M in pentane, 1.3mL, 2.21 mmol, 8,4 eq.) whereby the addition rate was adjusted such that the temperature of the mixture does not exceed -70°C. After complete addition the reaction was stirred for 15 min at -78°C followed by slow addition of a solution of **102** (527 mg, 1.32 mmol, 5,0 eq.) in 2-MeTHF (3 mL). After complete addition the cooling bath was removed, and the reaction mixture was allowed to warm up to room temperature. The mixture was quenched by the addition of water and the organic layer washed with water, dried over anhydrous Na_2SO_4, filtered and concentrated under reduced pressure. The crude product was purified by column chromatography (SiO_2, cyclohexane/DCM 5:1) yielding **108** as a colorless oil (204 mg, 0.180 mmol, 32%). ^{1}H NMR (400 MHz, $CDCl_3$) : δ [ppm] = 7.53 (s, 8H), 6.94 (s, 4H), 6.78 (ddd, $^3J_{HF}$ = 9.2 Hz, $^4J_{HH}$ = 2.3, Hz $^4J_{HH}$ = 1.6 Hz, 4H), 6.59 (d, $^3J_{HF}$ = 8.7 Hz, 4H), 3.70 (s, 12H), 3.00 – 2.88 (m, 8H), 1.05 – 0.79 (m, 8H), 0.06 (s, 36H). ^{19}F{^{1}H} NMR (376 MHz, $CDCl_3$): δ [ppm] = -110.74 (s). ^{13}C NMR (101 MHz, $CDCl_3$): δ [ppm] = 164.36 (d, $^1J_{CF}$ = 251.0 Hz), 161.86, 141.33 ($^3J_{CF}$ = d, *J* = 8.5 Hz), 139.34 (d, $^3J_{CF}$ = 8.5 Hz), 138.91, 130.71, 127.84, 123.68, 112.73 (d, $^2J_{CF}$ = 23.3 Hz), 112.68 (d, $^2J_{CF}$ = 24.0 Hz), 29.00, 16.59, -1.58.

5,11,17,23-Tetra-*S*-3-(2-trimethylsilylethyl sulfanyl)-5-fluorophenyl-sulfanyl-25,26,27,28-tetrahydroxythiacalix[4]arene (101):

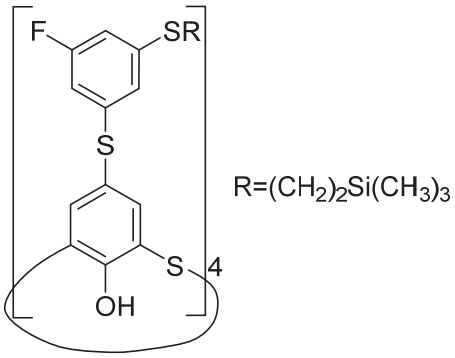

To a solution of **108** (63.9 mg, 40.3 μmol, 1.0 eq.) in anhydrous DCM (1 mL) at -78°C was added BBr_3 (1M in DCM, 0.242 mL, 242 μmol, 6,0 eq.) and the reaction was stirred for 16 h. The mixture was cooled to 0°C and was quenched by slow addition of dry methanol and the volatiles were removed under vacuum yielding **101** as a white solid (58 mg, 38.0 μmol, 94%) which was used without further purification. ^{1}H NMR (400 MHz, $CDCl_3$) : δ [ppm] = 9.41 (s, 4H), 7.75 (s, 8H), 6.85 (dd, $^3J_{HH}$ = 1.6 Hz, 4H), 6.79 (ddd, $^3J_{HF}$ = 9.1 Hz, $^4J_{HH}$ = 2.3, $^4J_{HH}$ =1.6 Hz, 4H), 6.58 (ddd, $^3J_{HF}$ = 8.8 Hz, $^4J_{HH}$ = 2.3 Hz, $^4J_{HH}$ =1.6 Hz, 4H), 3.22 – 2.32 (m, 8H), 1.17 – 0.63 (m, 8H), 0.06 (s, 36H). ^{19}F{^{1}H} NMR (376 MHz, $CDCl_3$): δ [ppm] = -111.15 (s). ^{13}C NMR (101 MHz, $CDCl_3$): δ [ppm] = 163.11 (d, $^1J_{CF}$ = 250.7 Hz), 158.38, 144.61, 141.56 (d, $^3J_{CF}$ = 8.5 Hz), 139.74 (d, $^3J_{CF}$ = 8.5 Hz), 125.53, 122.79 (d, $^4J_{CF}$ = 2.7 Hz), 121.64, 112.56 (d, $^2J_{CF}$ = 23.5 Hz), 112.17 (d, $^2J_{CF}$ = 24.0 Hz), 28.97, 16.56, -1.62.

***S*-2-Trimethylsilylethyl sulfanyl 3-bromo 5-Chloro benzene (130):**

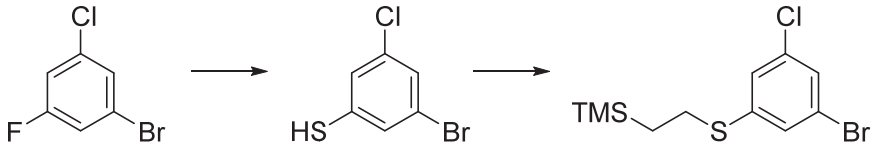

131 **130**

To a flask containing a stirring mixture of sodium 2-methyl-2-propanethiolate (2.95 g, 26.3 mmol, 1.1 eq.) in deoxygenated DMF (25 mL) 3-chloro 5-fluoro bromobenzene (5 g, 23.9 mmol, 1.0 eq.) was added at room temperature and stirred for 16 h. The mixture was diluted with water and TBME and the aqueous layer was extracted with TBME (2x). The combined organic layers were washed with 2M HCl (aq.), water and brine, dried over anhydrous Na_2SO_4, filtered and the solvent removed under reduced pressure yielding the crude product as a yellow oil. In a flask equipped with a $CaCl_2$ drying tube containing a solution of the crude product in toluene (25 mL) and cooled to 0°C anhydrous $AlCl_3$ (586 mg, 4,40 mmol, 0,6 eq.) was slowly added and the reaction mixture was stirred for 1h at 0°C. After all the starting material was consumed (TLC, SiO_2, cyclohexane/DCM 10:1) the reaction was poured onto ice and after vigorously stirring, the organic layer was extracted with 2 M NaOH (aq.). The aqueous layer was acidified by the addition of 37% HCl (aq.) and the formed precipitate was filtered off yielding the thiol **131** as a white solid (1.58 g, 7.05 mmol, 37 % over two steps) and was used directly without further purification. The obtained thiol **131** (1.57 g, 7.05 mmol, 1.0 eq.) and vinyltrimethylsilane (1.43 mL, 9.14 mmol, 1.3 eq.) was loaded into an oven dried 10 mL microwave vial. The mixture was purged with argon followed by the addition of di-tert-butyl peroxide (0.17 mL, 0.66 mmol, 0.1 eq.). The caped vial was heated to 105°C in an oil bath for 16 h. The volatiles were removed under reduced pressure and the residue purified by column chromatography (SiO_2, cyclohexane/toluene 20:1) yielding compound **130** as an colorless oil (2.09 g, 6.47 mmol, 92%). **131**: ^{1}H NMR (400 MHz, $CDCl_3$) : δ [ppm] = 7.31-7.29 (m, 2H), 7.20-7.18 (m, 1H), 3.54 (s, 1H). ^{13}C NMR (101 MHz, $CDCl_3$): δ [ppm] = 135.52, 134.95, 129.93, 128.72, 127.61, 123.05.

_S_-2-Trimethylsilylethyl sulfanyl 3-chloro 5-thiophenol (112):

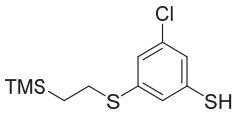

To a solution of compound **130** (5.12 g, 15.8 mmol, 1.0 eq.) in THF (50 mL) at -78°C *t*-BuLi (1.7 M in pentane, 19.5 mL, 33.2 mmol, 2.1 eq.) was added dropwise. After 15 minutes sulfur (507 mg, 15.8 mmol, 1.0 eq.) was added in one portion and the mixture was allowed to warm up to room temperature over the period of 3 h. The reaction was quenched by the addition of 1 M HCl (aq.) and diluted with ethyl acetate. The aqueous layer was extracted with ethyl acetate and the combined organic layers were washed with brine, dried over Na_2SO_4, filtered and the solvent evaporated under reduced pressure. The crude product was further purified by vacuum distillation (20 mbar, 142-146 °C) yielding **112** as a colorless oil (1.30 g, 4.96 mmol, 30%). ^{1}H NMR (400 MHz, $CDCl_3$): δ [ppm] = 7.04-7.01 (m, 3H), 3.05 – 2.79 (m, 2H), 1.04 – 0.80 (m, 2H), 0.06 (s, 9H). ^{13}C NMR (101 MHz, $CDCl_3$): δ [ppm] = 140.76, 135.00, 133.38, 126.34, 125.81, 124.86, 29.12, 16.62, -1.62.

5,11,17,23-Tetra-_S_-3-(2-trimethylsilylethyl sulfanyl)-5-chlorophenyl-sulfanyl-25,26,27,28-tetramethoxythiacalix[4]arene (113):

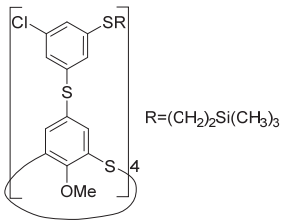

An oven dried Schlenk flask was loaded with **93** (500 mg, 0.576 mmol, 1.0 eq.), *t*-BuONa (314 mg, 3.17 mmol, 5.5 eq.), Pd_2dba_3 (13.2 mg, 2.5 mol%) and Xantphos (34 mg, 10 mol %). The flask was evacuated and backfilled with argon (3x) followed by the addition of a deoxygenated solution of **112** (798 mg, 2.88 mol, 5 eq.) in toluene (5 mL). The reaction mixture was brought to 110°C in a preheated oil bath for 5h. After cooling down the mixture was filtered over Celite. The filtrate was concentrated under reduced pressure and the residue was further purified by column chromatography (SiO_2, cyclohexane/DCM 5:1) yielding compound **113** as an amorphous solid (752 mg 0.455 mmol, 79%). ^{1}H NMR (400 MHz, CD_2Cl_2) : δ [ppm] = 7.50 (s, 8H), 7.09 (s, 8H), 6.97 (s, 4H), 3.66 (s, 12H), 2.98 – 2.92 (m, 8H0.93 – 0.88f (m, 8H), 0.05 (s, 38H).

5,11,17,23-Tetra-*S*-3-(2-trimethylsilylethyl sulfanyl)-5-chlorophenyl-sulfanyl-25,26,27,28-tetrahydroxythiacalix[4]arene (115):

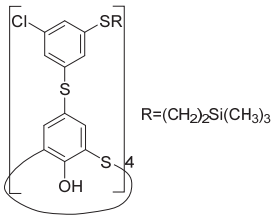

To a solution of **113** (752 mg, 0.455 mmol, 1.0 eq.) in anhydrous DCM (5 mL) at -78°C was added BBr_3 (0.3 mL, 3.18 mmol, 7 eq.). After 16 h. the solution was cooled to 0°C and quenched by slow addition of dry methanol. The volatiles were removed under vacuum (3x) yielding **115** as a white solid (714 mg, 0.447 mmol, 98%). ^{1}H NMR (500 MHz, CD_2Cl_2): δ [ppm] = 9.40 (s, 4H), 7.76 (s, 9H), 7.05 (dd, $^3J_{HH}$ = 1.7 Hz, 4H), 6.94 (dd, $^3J_{HH}$ = 1.7 Hz, 4H), 6.86 (dd, $^3J_{HH}$ = 1.7 Hz, 4H), 3.05 – 2.71 (m, 7H), 1.14 – 0.58 (m, 7H), 0.03 (s, 36H). ^{13}C NMR (126 MHz, CD_2Cl_2): δ [ppm] = 158.70, 144.81, 141.68, 139.84, 135.50, 125.80, 125.76, 125.49, 125.11, 121.93, 29.21, 16.75, -1.73. HRMS (ESI, -): m/z calcd. for $C_{68}H_{75}Cl_4O_4S_{12}Si_4$ $[M]^-$ 1591.0150; found: 1591.0125.

5,11,17,23-Tetra-*S*-2-trimethylsilylethyl sulfanyl-25,26,27,28-tetrahydroxythiacalix[4]arene (116):

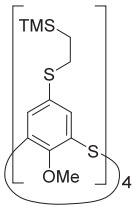

An oven dried Schlenk flask was loaded with **93** (1.00 g, 1.15 mmol, 1.0 eq.), *t*-BuONa (570 mg, 5.75 mmol, 5.0 eq.), Pd_2dba_3 (26.3 mg, 2.5 mol%) and Xantphos (67.9 mg, 10 mol %). The flask was evacuated and backfilled with argon (3x) followed by the addition of a deoxygenated solution of 2-(trimethyl)ethanethiol (0.81 mL, 5.06 mmol, 4.4 eq.) in toluene (10 mL). The reaction mixture was lowered in a preheated oil bath at 110°C for 5h. After cooling down the mixture was filtered over Celite. The filtrate was concentrated under reduced pressure and the residue was further purified by column chromatography (SiO_2, cyclohexane/DCM 7:1) yielding compound **116** as an amorphous solid (1.12g 1.036 mmol, 90%). ^{1}H NMR (500 MHz, CD_2Cl_2): δ [ppm] = 7.36 (s, 8H), 3.62 (s, 12H), 3.05 – 2.77 (m, 8H), 1.07 – 0.55 (m, 8H), 0.05 (s, 32H). ^{13}C NMR (126 MHz, CD_2Cl_2): δ [ppm] = 160.04, 135.47, 132.38, 130.48, 67.46, 30.71, 17.12, -1.63.

5,11,17,23-Tetra-*S*-3-(tert-butyl sulfanyl)-5-bromophenyl-sulfanyl-25,26,27,28-tetramethoxythiacalix[4]arene (119):

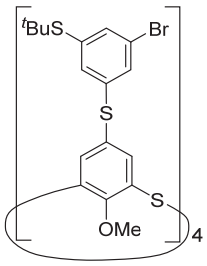

An oven dried Schlenk flask was loaded with 3-bromo-5-iodophenyl tert-butyl-sulfane **120** (771 mg, 2.08 mmol, 4.5 eq.), compound **116** (500 mg, 0.462 mmol, 1.0 eq.), Pd_2dba_3 (26.3 mg, 2.5 mol%), Xantphos (67.9 mg, 10 mol %) and $CsCO_3$ (602 mg, 1.85 mmol, 4.0 eq.). The flask was evacuated and backfilled with argon (3x) followed by the addition of a deoxygenated solution of TBAF (1M in THF, 2.31 mL, 5 eq.) in toluene (3 mL). The reaction mixture was lowered in a preheated oil bath at 50°C for 24 h. After cooling down the mixture was filtered over Celite. The filtrate was concentrated under reduced pressure and the residue was further purified by column chromatography (SiO_2, cyclohexane/DCM 5:1) yielding compound **119** as an amorphous solid (454 mg 0.274 mmol, 59%). ^{1}H NMR (500 MHz, CD_2Cl_2): δ [ppm] = 7.54 (s, 4H), 7.49 (s, 8H), 7.41 (s, 4H), 7.36 (s, 4H), 3.63 (s, 4H), 1.26 (s, 36H). ^{13}C NMR (126 MHz, CD_2Cl_2): δ [ppm] = 161.58, 139.16, 138.37, 138.12, 137.11, 136.43, 132.62, 131.11, 128.65, 122.78, 60.20, 47.16, 31.16.

5,11,17,23-Tetra-*S*-3-bromo-5-mercaptophenyl-sulfanyl-25,26,27,28-tetramethoxythiacalix[4]arene (121):

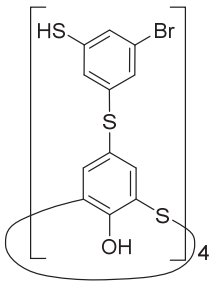

To a solution of **113** (752 mg, 0.455 mmol, 1.0 eq.) in anhydrous DCM (5 mL) at -78°C was added BBr_3 (0.3 mL, 3.18 mmol, 7 eq.). After 16 h. the solution was cooled to 0°C and quenched by slow addition of dry methanol. The volatiles were removed under vacuum (3x) yielding **121** as a white solid (714 mg, 0.447 mmol, 98%). ^{1}H NMR (500 MHz, CD_2Cl_2): δ [ppm] = 9.32 (s, 4H), 7.68 (s, 8H), 7.16 (dd, *J* = 1.7 Hz, 4H), 6.97 (dd, *J* = 1.7 Hz, 4H), 6.89 (dd, *J* = 1.7 Hz, 4H), 3.49 (s, 4H). ^{13}C NMR (126 MHz, CD_2Cl_2): δ [ppm] = 158.79, 144.82, 140.45, 135.03, 129.77, 128.38, 127.39, 125.51, 123.50, 122.00.

4 Unsymmetrical Dissulfide

The following chapter was reproduced from the following publication:
L. Delarue Bizzini, P. Zwick, M. Mayor, *Eur. J. Org. Chem.*, **2019,** *41***,** 6956-6960
DOI 10.1002/ejoc.201901283.

4.1 Introduction

The thiol (sulfhydryl) group is one of the most prominent anchor groups for the immobilization of organic molecules on noble metal surfaces, mainly due to the balanced features of the resulting metal sulfur bond. For example, the sulfur-gold bond is strong enough to retain a molecule on the surface even under ultra-high vacuum conditions, but weak enough to provide the mobility required to enable self-assembly behaviors. The anchor group is thus not only frequently used for the preparation of self-assembled monolayers (SAMs),[133–136] but also for the immobilization of functional structures in single molecule junctions.[46,48,137] In the latter case, the molecule of interest bridges the gap between two metal electrodes and thus exposes a thiolate anchor group at both ends. The tendency of free thiols to form disulfides in the presence of an oxidizing agent like oxygen makes their handling challenging. While this is a minor issue in the case of molecules with a single anchor group forming SAMs, it becomes a serious handicap for structures exposing several thiol groups due to the formation of insoluble polymers upon disulfide formation. The strategies addressing this issue are either to make disulfides on purpose, or to mask the thiol group e.g. by an acetyl group, which is hydrolyzed prior to bond formation with the noble metal surface.[134]

The disulfide approach is particular advantageous for SAM precursors, as the disulfide bond is cleaved electrochemically by the reduction potential of the noble metal surface. Consequently, a SAM formed from the corresponding homo-disulfide contains exclusively the molecule of interest.[138]

For molecules exposing several thiol anchor groups, like e.g. functional rods bridging the electrodes of a single molecule junction[139–142] or tripodal platforms controlling the spatial arrangement of molecular architectures on surfaces,[143,144] the disulfide strategy is still appealing, as the cleavage of the disulfide bond on the noble metal sample renders the presence of additional deprotection chemicals unnecessary. The approach however requires the ability of forming unsymmetrical disulfides. Ideally, the thiol anchor groups of the molecule

of interest should be engaged in the disulfide formation with a small alkylthiol, guaranteeing the differentiation of both immobilized thiolates in the experiment.

Guided by this thought, we became interested in a general method for the synthesis of unsymmetrical disulfides, which would allow the preparation of discrete molecular species bearing disulfides as sulfur anchor groups. Numerous functional model compounds for single molecule junctions are available as acetyl protected derivatives, but the required additional deprotection reagents might interfere with the transport experiments. Thus, making those derivatives available as unsymmetrical disulfides releasing the experiment form the presence of additional reagents would increase its trustworthiness. Consequently, we focused our efforts towards methods enabling the transformation of an acetyl-protected thiophenol into an unsymmetrical 1-alkyl-2-aryldisulfane.

The synthesis of unsymmetrical disulfides has been extensively investigated[145] whereby two general concepts have been employed. (i) Generation of an electrophilic sulfenyl derivative followed by reaction with a thiol or one of its derivatives[146–154] or (ii) oxidative heterocoupling.[155–157] The concept of an electrophilic reagent is appealing since it allows for a more controlled reactivity without the inherent distribution of products usually observed in oxidative heterocoupling, which relies on the electronic difference between the thiols.

In order to convert thioacetates into unsymmetrical disulfides, we investigated the suitability of thiosulfonates as a sulfenylating agent, with the aim of applying this method to compounds bearing multiple disulfide functionalities. Formation of unsymmetrical disulfides from thioacetate and thiosulfonates was already reported for the synthesis of 1,6-disulfide-bridged D-hexopyranoses[158] and ajoene analogues[159–161] containing unsymmetrical alkyl vinyl disulfides. However, these reported synthetic methods require methanol as a solvent which limits its application for larger polyaromatic structures of interest.

In comparison to other electrophilic agents used to prepare unsymmetrical disulfides such as *N*-sulfenamides,[151] sufenyl chlorides[152] or dialkoxythioxaphosphorane disulfides,[153,154] thiosulfonates[162] are both, easily prepared in one step and highly reactive towards thiolates. This is necessary in order to prevent thiolysis of the formed product and therefore giving rise to symmetrical disulfides as a side reaction.

4.2 Results and Discussion

From literature precedence[158,159] we expected that the electrophile *S*-pentyl benzenethiosulfonate **132** (prepared from pentylthiol and sodium benzene sulfinate using a modified literature procedure[162]) and thioacetate **133** should form the unsymmetrical disulfide **134** upon *in situ* formation of the thiolate of **133** (Scheme 26). To our delight, addition of sodium methoxide (NaOMe, 5.4 M in methanol) to a solution of thiosulfonate **132** and thioacetate **133** in either THF or DMF at room temperature led to fast and clean conversion to the desired unsymmetrical disulfide **134** whereby no symmetric disulfide was monitored by GC-MS.

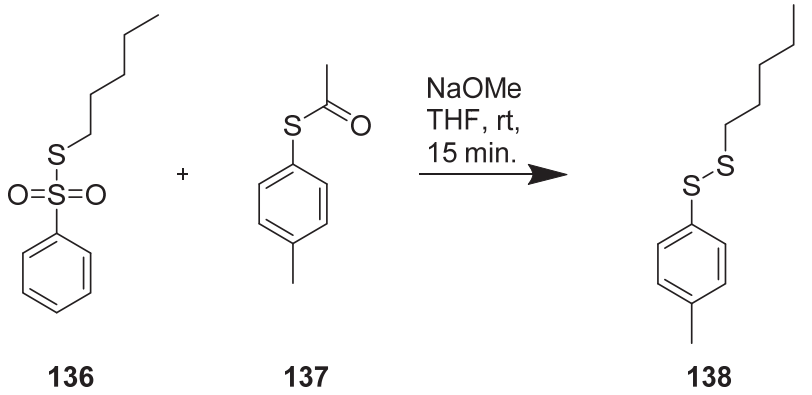

136 **137** **138**

Scheme 26: Proof-of-concept reaction using **132** (1.10 eq.), **133** (1.00 eq.) and sodium methoxide (1.20 eq.) in THF at room temperature.

To investigate the scope of the method a series of thiosulfonates were prepared from their corresponding thiols, following the modified literature protocol.[162] Using pyridine as a base allows thiosulfonates to be prepared in one-pot fashion together with sodium benzene sulfonate and iodine in dichloromethane (DCM) (Table 2). Different alkyl- and aryl- benzene thiosulfonates were prepared in good yields, but the limitations of the protocol became obvious as soon as bulky thiols were considered.

1-Adamanethiol (entry 1) showed low reactivity as after 3 hours, the desired *S*-adamantyl benzene thiosulfonate could be isolated in only 6% yield after column chromatography. Conducting the reaction in DCM at reflux for 3 hours yielded only 1-adamantyl iodide as a side product together with unreacted intermediary symmetric disulfide. Further, *S*-pentyl-, *S*-4-methoxyphenyl-, and *S*-1*H*,1*H*,2*H,2*H-perfluorodecyl benzenethiosulfonate (entries 2, 4 and 5) could be prepared in excellent yield. Electronic effects appears to have a minor role in the formation of thiosulfonates as both electron withdrawing (entries 7 and 8) and donating substituents (entry 2) could be isolated in excellent yield. However, *S*-triphenylmethyl benzenethiosulfonate (entry 6) could not be obtained using this method, as the only isolatable

product from this reaction was triphenylmethan-1-ol. The transformation of 2-(2-ethoxyethoxy) ethane-1-thiol[163] to the benzenethiosulfonate derivative (entry 3) provided only a moderate isolated yield of 36% after purification by column chromatography. Similarly, methyl thiosalicylate and 4-amino thiophenol (entries 8 and 10) could be transformed to the corresponding thiosulfonates in moderate yield. In the case of methyl thiosalicylate (entry 8) the moderate reactivity appears to arise due to steric reasons, since after 3 h the corresponding disulfide was still present in the reaction mixture. This stands in contrast to the reaction of 4-aminothiophenol where complete conversion of the disulfide was observed after 1 h, yet accompanied by oxidative side reactions resulting in a lower yield of the thiosulfonate of 40%.

Table 2: One-pot sulfonylation of thiols.[a]

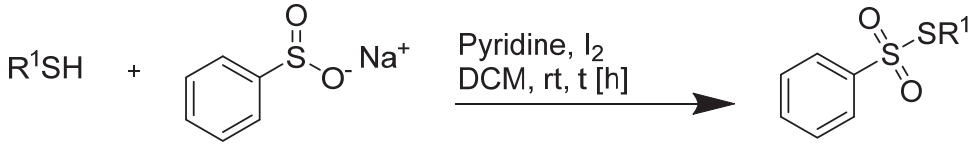

Entry	R_1SH	t [h]	Yield [%][b]
1	1-AdamantylSH	3	6
2	4-$MeOC_6H_4SH$	0.5	97
3	$CH_3CH_2(OCH_2CH_2)_2SH$	2	36
4	$CF_3(CF_2)_7CH_2CH_2SH$	3[c]	87
5	PentylSH	0.5	95
6	$(C_6H_5)_3CSH$	3	-
7	4-$NO_2C_6H_4SH$	1	81
8	2-$COOMeC_6H_4SH$	3	40
9	3,5-$F_2C_6H_3SH$	0.5	88
10	4-$NH_2C_6H_4SH$	1	52

[a] Reaction conditions: mixture of thiol (1.00 eq.), pyridine (1.05 eq.), iodine (2.00 eq.) in dichloromethane with added sodium benzene sulfinate (1.7 eq.) under ambient conditions. [b] Yield of isolated product after column chromatography. [c] Reaction at 40°C.

With these thiosulfonates derivatives in hands, the previously evaluated reaction conditions were used to synthesize unsymmetrical disulfides using *S*-4-methylphenyl

thioacetate as model substrate (Table 3, entries 1-5). With the exception of *S*-(2-(2-ethoxyethoxy)ethyl thiosulfonate (entry 3), all thiosulfonates of this first series behaved as anticipated and the corresponding unsymmetrical disulfides could be isolated in excellent yield (84-89%) after purification by column chromatography. In the case of *S*-(2-(2-ethoxyethoxy)ethyl thiosulfonate only the symmetrical tolyldisulfide was obtained. To explore the scope of the reaction sequence, hexyl thioacetate as an unactivated thioacetate (Table 3, entries 6-9) was exposed. And indeed, the reaction with electron deficient 4-nitrophenyl benzenethiosulfonate (entry 6) at room temperature provided the unsymmetrical disulfide in low yield (33% isolated) and favored the formation of symmetrical disulfides upon work up. Upon inverting the reacting groups however (entry 10), the unsymmetrical product was isolated in 75% yield. It appears that 4-nitrophenyl benzenethiosulfonate undergoes methanolysis competing with the unactivated hexyl thioacetate leading to low formation of the unsymmetrical product. Therefore, the reaction (entry 6) was repeated at 0 °C and the selectivity towards the unsymmetrical product increased considerably with 67% isolated yield.

To further investigate the functional group tolerance of the method 4-aminophenyl benzenethiosulfonate and hexyl thioacetate (entry 7) were reacted yielding the unsymmetrical product in moderate yield of 57%. Another challenging issue of the method was spotted upon reacting the methyl ester substituted phenyl benzenethiosulfonate and hexyl thioacetate (entry 9). In this case the symmetrical disulfides were formed as major product and the unsymmetrical target compound could be isolated in only 15% yield.

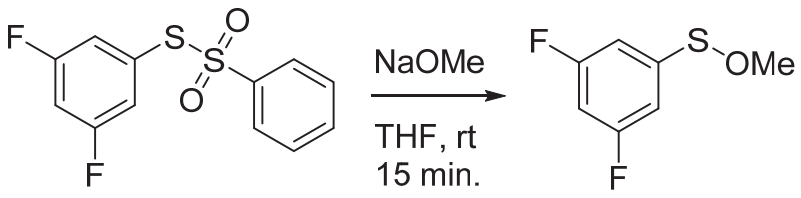

135 **136**

Scheme 27 Formation of methyl sulfonate by methanolysis of thiosulfonates.

The methanolysis of thiosulfonates seems to be the major competing side reaction decomposing the starting material. To investigate this hypothesis, 3,5 difluoro phenyl benzene thiosulfonate (**135**) was treated with 1 equivalent of sodium methoxide in THF at room temperature without any thioacetate present (Scheme 27). And indeed, the quantitative formation of methyl 3,5-difluoro sulfenate **136** after 15 minutes was observed. Sulfenates are

known to hydrolyze under basic or neutral conditions giving rise to symmetric disulfides.[164] This competing reaction path is more pronounced with thiosulfonates bearing electron withdrawing groups and thus rationalizes the observed lower yields in the formation of unsymmetrical disulfides in entries 6 and 9.

Table 3: Sulfenylation reactions.[a]

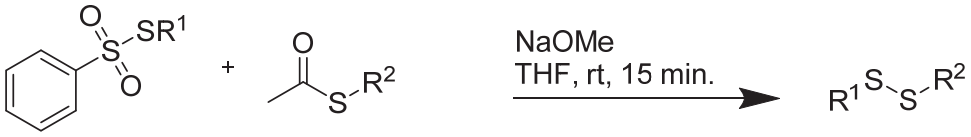

Entry	R^1	R^2	Yield [%][b]
1	1-Adamantyl	4-MeC_6H_4	88
2	4-$MeOC_6H_4$	4-MeC_6H_4	89
3	$CH_3CH_2(OCH_2CH_2)_2$	4-MeC_6H_4	-
4	$CF_3(CF_2)_7CH_2CH_2$	4-MeC_6H_4	88
5	Pentyl	4-MeC_6H_4	84
6	4-NO_2Ph	Hexyl	33 (67)[c]
7	4-NH_2Ph	Hexyl	57
8	3,5-$F_2C_6H_3$	Hexyl	81
9	2-$COOMeC_6H_4$	Hexyl	15
10	Pentyl	4-NO_2Ph	75
11	Pentyl	4-$MeOC_6H_4$	85

[a] Reaction conditions: Mixture of thioacetate (1.00 eq.), thiosulfonate (1.10 eq.), sodium methoxide (1.20 eq.) in tetrahydrofuran under argon at room temperature. [b] Yield of isolated product after column chromatography. [c] Isolated yield after reaction at 0°C.

As shown in entries 5, 10 and 11, the reported method shows only low dependency on electronic effects of the substituents on the thioacetate in the reaction with pentyl benzenethiolsulfonate.

While most of the isolated unsymmetrical disulfides were stable under ambient conditions, an interesting intrinsic structural lability of *p*-methoxyphenyl *p*-methylphenyl disulfide (Table 3, entryl 2) was observed. The unsymmetric disulfide disproportionated slowly

to the symmetric disulfides not only dissolved, but also in substance. The disproportionation reaction was followed by ^{1}H-NMR (CD_2Cl_2, 298 K, Figure 1) over the course of 280 h and is in well agreement with previously measured first order dependencies of unsymmetrical diaryl disulfides[165] The only further example of an unstable unsymmetrical disulfide observed in the series was *p*-methoxyphenyl pentyl disulfide (Table 3, entry 11) which equilibrates to an approximate 1:1 mixture of the unsymmetrical and symmetrical disulfides after 4 h at room temperature (see Appendix). We thus hypothesize that the electron rich anisole-type aryl is responsible for the degradation of the corresponding unsymmetrical disulfides.

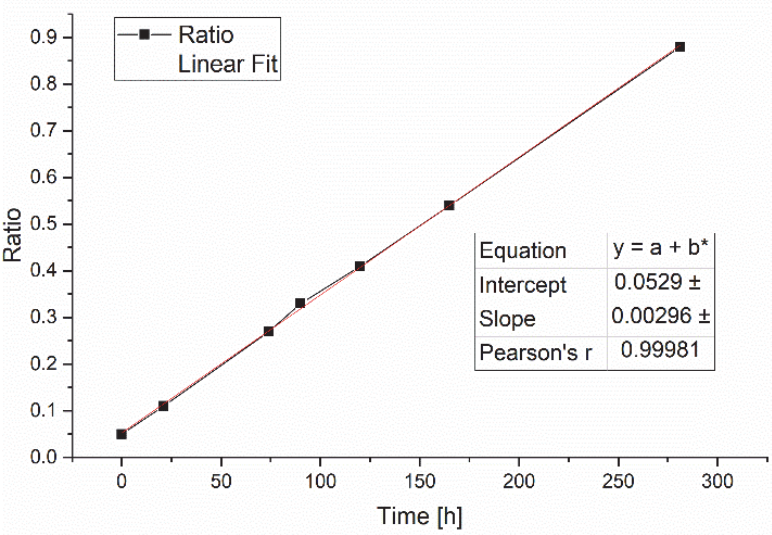

Figure 24: Ratio of unsymmetrical p-methoxyphenyl p-methylpheny disulfide to symmetrical p-methoxyphenyl disulfide.

To investigate the potential of the method to decorate the periphery of more complex molecules with unsymmetrical disulfides, the protocol was applied to the three model compounds **137-139** (Scheme 28) exposing several thioacetates. These structures were already investigated in the past either by mechanically controlled break junction experiments analyzing their transport behavior (compounds **137**[166] and **138**[137,167]), or in scanning tunneling microscopy studies as self-assembled monolayer (compound **139**[168]).

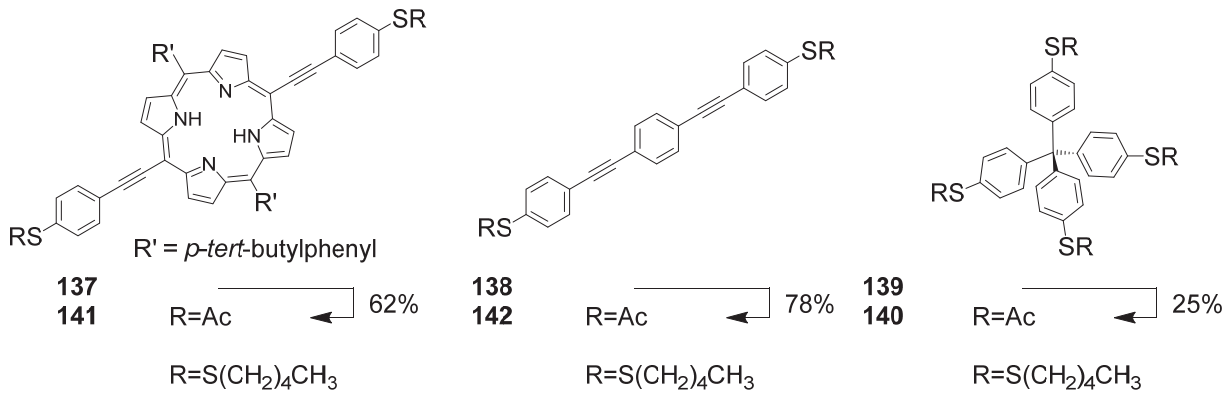

Scheme 28: Example of relevant molecules bearing multiple asymmetric disulfides synthesized from the corresponding thioacetates and S-pentyl benzene thiosulfonate using the here reported one-pot method. The displayed yields are the isolated amounts after column chromatography

Indeed, the unsymmetrical disulfides of all the three compounds could be isolated with yields varying from 25% in case of the four-fold disulfide formation (compound **140** in Scheme 3), 62% and 78% for the two-fold reaction (compounds **141** and **142**, respectively).

4.3 Summary and Outlook

In conclusion, we report a versatile and robust method to synthesize unsymmetrical disulfides. The *in situ* deprotection of thioacetates in presence of a variety of thiosulfonates gave after 15 to 30 minutes at room temperature unsymmetrical disulfides in good yields, thus enabling the synthesis of compounds bearing multiple unsymmetrical disulfide moieties. The preferential formation of unsymmetrical disulfides and the polarity difference of the starting material and the product facilitates the purification by column chromatography, as the desired product is the first eluting substance.

With this versatile and convenient synthetic access to unsymmetrical disulfides we are currently investigating their potential as anchor groups on noble metal substrates.

4.4 Experimental Part

General Informations

All commercially available compounds were purchased and used as received unless explicitly stated otherwise. All NMR experiments were performed on Bruker Avance III or III HD, two or four-channel NMR spectrometer operating at 400.13 or 500.13 MHz proton frequency. The instruments were equipped with direct observe BBFO, indirect BBI or cryogenic four-channel QCI (H/C/N/F) 5 mm probes all with self-shielded z-gradient. The experiments were performed at 298 K and the temperature was calibrated using a methanol standard showing accuracy within +/- 0.2 K. GC-MS was performed on a Shimadzu GCMS-2020 SE equipped with a Zebron 5 MS Infernocolumn which allowed to achieve temperatures up to 350 °C. High-resolution mass spectra (HRMS) were measured as HR-ESI-ToF- MS with a Maxis 4G instrument from Bruker and were measured on a Bruker solariX spectrometer with a MALDI source for HR-MALDI-ToF MS. For column chromatography silica gel Siliaflash® p60 (40–63 µm) from Silicycle was used, and TLC was performed on silica gel 60 F254 glass plates with a thickness of 0.25 mm purchased from Merck Melting point were measured with a Stuart SMP3 with a slope of 5°C/min.

Genral procedure for the preparation of thiosulfonates:

To a solution of thiol (1.00 eq.) and pyridine (1.05 eq.) in DCM (1 m in respect to the thiol) iodine (2.00 eq.) was added slowly. After 5 minutes sodium benzene sulfinate (1.7 eq.) was added to the reaction mixture under stirring (time and temperatures are given in Table 2). After all the disulfide intermediate was consumed (as monitored by TLC SiO_2, cyclohexane/EtOAc 10:1) the reaction was quenched by addition of water and diluted with EtOAc. The organic phase was separated, washed with water (2x), sat. aq. $Na_2S_2O_3$ (2x), dried over dried over Na_2SO_4, filtered and the solvent was removed und reduced pressure. The crude product was further purified by column chromatography (SiO_2, cyclohexane/EtOAc 5:1) yielding the thiosulfonate.

S-Adamantyl benzenethiosulfonate:

Following the general procedure for the preparation of thiosulfonates a mixture of 1-adamantanthiol (500 mg, 2.97 mmol, 1.00 eq.), sodium benzene sulfinate (829 mg, 5.05 mmol, 1.70 eq.), pyridine (0.252 mL, 3.12 mmol, 1.05 eq.) and iodine (1508 mg, 5.94 mmol, 2.00 eq.) in DCM (3 mL) was reacted for 3 hours at room temperature yielding S-adamantyl benzenethiosulfonate (55.0 mg, 0.178 mmol) in 6% as a white solid.

^{1}H NMR (500 MHz, CD_2Cl_2): δ = 7.96-7.93 (m, 2H), 7.64-7.61 (m, 1H), 7.57-7.53 (m, 2H), 2.03-2.02 (m, 9H), 1.68-1.67 (m, 6H). ^{13}C NMR (126 MHz, CD_2Cl_2): δ = 148.2 (q), 133.8 (t), 129.7 (t), 127.3 (t), 58.9 (q), 43.5 (s), 36.3 (s), 30.9(t). HRMS (ESI, +): *m/z* calcd. for $C_{16}H_{20}NaO_2S_2$ $[M+Na]^+$ 331.0800; found: 331.0797. Melting point: 115.7 °C

_S_-_p_-Methoxyphenyl bezenethiosulfonate:

Following the general procedure for the preparation of thiosulfonates a mixture of 4-methoxythiophenol (250 mg, 1.78 mmol, 1.00 eq.), sodium benzene sulfinate (497 mg, 3.03 mmol, 1.70 eq.), pyridine (0.151 mL, 1.87 mmol, 1.05 eq.) and iodine (904 mg, 3.56 mmol, 2.00 eq.) in DCM (3 mL) was reacted for 30 minutes at room temperature yielding S-p-methoxyphenyl bezenesulfonate (487 mg, 1.737 mmol) in 98% a colorless oil.

^{1}H NMR (500 MHz, CD_2Cl_2): δ = 7.63-7.59 (m, 1H), 7.57-7.54 (m, 2H), 7.48-7.44 (m, 2H), 7.26-7.23 (m, 2H), 3.82(s, 3H). ^{13}C NMR (126 MHz, CD_2Cl_2): δ = 163.1 (q), 143.5 (q), 138.8 (t), 134.2 (t), 129.5 (t), 128.1 (t), 119.0 (q), 115.5 (t), 56.1 (p). HRMS (ESI, +): *m/z* calcd. for $C_{13}H_{12}NaO_3S_2$ $[M+Na]^+$ 303.0119; found: 303.0120.

_S_-1_H_,1_H_,2_H_,2_H_-Perfluorodecyl bezenethiosulfonate:

Following the general procedure for the preparation of thiosulfonates a mixture of 1*H*,1*H*,2*H*,2*H*-perfluorodecanthiol (420 mg, 0.874 mmol, 1.00 eq.), sodium benzene sulfinate (245 mg, 1.49 mmol, 1.70 eq.), pyridine (75.0 µL, 0.921 mmol, 1.05 eq.) and iodine (445 mg, 1.75 mmol, 2.00 eq.) in DCM (1 mL) was refluxed for 3 hours yielding 1H,1H,2H,2H-perfluorodecyl bezenesulfonate (473 mg, 0.762 mmol) in 87% as an white amorphous solid.

^{1}H NMR (500 MHz, CD_2Cl_2): δ = 7.96-7.53 (m, 2H), 7.72-7.69 (m, 1H), 7.63-7.60 (m, 2H), 3.19-3.16 (m, 2H), 2.56-2.45(s, 3H). ^{13}C NMR (126 MHz, CD_2Cl_2): δ = 144.6 (q), 134.8 (t), 130.2 (t), 127.6 (t), 32.1 (t, $^{2}J_{C,F}$ = 22. Hz, CH_2), 27.3 (t, $^{3}J_{C,F}$ = 4.7 Hz, CH_2). HRMS (ESI, +): *m/z* calcd. for $C_{16}H_9F_{17}NaO_2S_2$ $[M+Na]^+$ 642.9669; found: 642.9665.

_S_-(2-(2-Ethoxyethoxy)ethyl) benzenethiosulfonate:

Following the general procedure for the preparation of thiosulfonates a mixture of S-(2-(2-ethoxyethoxy)ethanthiol (103 mg, 0.686 mmol, 1.00 eq.), sodium benzene sulfinate (191 mg, 1.17 mmol, 1.70 eq.), pyridine (61.0 µL, 0.755 mmol, 1.10 eq.) and iodine (348 mg, 1.37 mmol, 2.00 eq.) in DCM (1 mL) was reacted for 2 hours at room temperature yielding S-(2-(2-ethoxyethoxy)ethyl) benzenethiosulfonate (69 mg, 0.237 mmol) in 35% as a yellow oil.

^{1}H NMR (500 MHz, CD_2Cl_2): δ = 7.94-7.91 (m, 2H), 7.65-7.61 (m, 1H), 7.58-7.53 (m, 2H), 3.63 (t, $^{3}J_{H,H}$ = 6.2 Hz, 2H), 3.50-3.43 (m, 6H), 3.18 (t, $^{3}J_{H,H}$ = 6.2 Hz, 2H), 1.15 (t, $^{3}J_{H,H}$ = 7.0 Hz, 3H). ^{13}C NMR (126 MHz, CD_2Cl_2): δ = 145.4 (q), 134.3 (t), 129.9 (t), 127.5 (t), 71.2 (s), 70.2 (s), 69.4 (s), 67.02 (s), 36.5 (s), 15.6(p). HRMS (ESI, +): *m/z* calcd. for $C_{12}H_{18}NaO_4S_2$ $[M+Na]^+$ 313.0535; found: 313.0539.

_S_-Pentyl benzenethiosulfonate:

Following the general procedure for the preparation of thiosulfonates a mixture of 1-pentanthiol (420 mg, 4.03 mmol, 1.00 eq.), sodium benzene sulfinate (1125 mg, 6.85 mmol, 1.70 eq.), pyridine (0.341 mL, 4.24 mmol, 1.05 eq.) and iodine (2046 mg, 8.06 mmol, 2.00 eq.) in DCM (4 mL) was reacted for 30 minutes at room temperature yielding S-pentyl benzenethiosulfonate (938 mg, 3.84 mmol) in 95% as a colorless oil.

^{1}H NMR (400 MHz, $CDCl_3$): δ = 7.94-7.92 (m, 2H), 7.68-7.64 (m, 1H), 7.60-7.55 (m, 2H), 3.00 (t, $^{3}J_{H,H}$ = 7.5 Hz, 2H), 1.63-1.57 (m, 2H), 1.31-1.21 (m, 4H), 0.84 (t, $^{3}J_{H,H}$ = 7.0 Hz, 3H). ^{13}C NMR (101 MHz, $CDCl_3$): δ = 145.1 (q), 133.7 (t), 129.4 (t), 127.1 (t), 36.2 (s), 30.8 (s), 28.4 (s), 22.1 (s), 13.9 (s). HRMS (ESI, +): *m/z* calcd. for $C_{11}H_{16}NaO_2S_2$ $[M+Na]^+$ 267.0481; found: 267.0484.

_S-p_-Nitrophenyl benzenethiosulfonate:

Following the general procedure for the preparation of thiosulfonates a mixture of 4-nitrothiophenol (500 mg, 3.22 mmol, 1.00 eq.), sodium benzene sulfinate (899 mg, 5.47 mmol, 1.70 eq.), pyridine (0.272 mL, 3.38 mmol, 1.05 eq.) and iodine (1.64 g, 8.06 mmol, 2.00 eq.) in DCM (4 mL) was reacted for 30 minutes at room temperature yielding *S*-pentyl benzenethiosulfonate (774 mg, 2.62 mmol) in 81% as a yellow solid.

^{1}H NMR (500 MHz, $CDCl_3$): δ = 8.22 – 8.12 (m, 2H), 7.66 – 7.60 (m, 3H), 7.60 – 7.56 (m, 2H), 7.50 – 7.44 (m, 2H). ^{13}C NMR (126 MHz, $CDCl_3$): δ = 149.59(q), 143.03(q), 137.27(t), 135.67(q), 134.44(t), 129.34(t), 127.65(t), 124.32(t). Spectra found to be identical as previously reported.[169]

_S-p_-Aminophenyl benzenethiosulfonate:

Following the general procedure for the preparation of thiosulfonates a mixture of 4-aminothiophenol (500 mg, 3.99 mmol, 1.00 eq.), sodium benzene sulfinate (1.13 g, 6.78 mmol, 1.70 eq.), pyridine (0.337 mL, 4.19 mmol, 1.05 eq.) and iodine (2.03 g, 8.06 mmol, 2.00 eq.) in DCM (4 mL) was reacted for 30 minutes at room temperature yielding S-pentyl benzenethiosulfonate (555 mg, 2.09 mmol) in 52 % as a yellow oil.

^{1}H NMR (500 MHz, $CDCl_3$): δ = 7.63 – 7.54 (m, 3H), 7.45 – 7.40 (m, 2H), 7.14 – 7.08 (m, 2H), 6.64 – 6.58 (m, 2H), 4.31 (s, 2H). ^{13}C NMR (126 MHz, $CDCl_3$): δ = 148.87(q), 143.23(q), 138.44(t), 133.52(t), 128.89(t), 127.74(t), 115.90(t), 115.71(q). Spectra found to be identical as previously reported.[169]

Methyl 2-((phenylsulfonyl)thio)benzoate:

Following the general procedure for the preparation of thiosulfonates a mixture of o-mercapto benzoic acid methyl ester (500 mg, 2.97 mmol, 1.00 eq.), sodium benzene sulfinate (829 mg, 5.05 mmol, 1.70 eq.), pyridine (0.250 mL, 4.19 mmol, 1.05 eq.) and iodine (1.51 g, 5.94 mmol, 2.00 eq.) in DCM (4 mL) was reacted for 30 minutes at room temperature yielding S-pentyl benzenethiosulfonate (364 mg, 1.18 mmol) in 40% as a yellow oil.

^{1}H NMR (500 MHz, $CDCl_3$): δ = 7.77 – 7.68 (m, 2H), 7.58 -7.55 (m, 1H), 7.54 – 7.50 (m, 3H), 7.44 – 7.37 (m, 2H), 3.70 (s, 3H).^{13}C NMR (126 MHz, $CDCl_3$): δ = 166.25(q), 143.45(q), 138.63(t), 136.22(q), 133.77(t), 132.17(t), 131.15(t), 130.85(t), 129.05(t), 127.79(q), 127.47(p). Spectra found to be identical as previously reported.[169]

***S*-3,5-Difluorophenyl benzenethiosulfonate:**

Following the general procedure for the preparation of thiosulfonates a mixture of 3,5 diflurothiophenol (1.00 g, 6.84 mmol, 1.00 eq.), sodium benzene sulfinate (1.91 g, 11.6 mmol, 1.70 eq.), pyridine (0.58 mL, 7.18 mmol, 1.05 eq.) and iodine (3.47 g, 13.7 mmol, 2.00 eq.) in DCM (10 mL) was reacted for 3 h at room temperature yielding S-pentyl benzenethiosulfonate (1.83 g, 1.18 mmol) in 93% as white solid.

^{1}H NMR (500 MHz, $CDCl_3$): δ = 7.72 – 7.58 (m, 3H), 7.57 – 7.43 (m, 2H), 7.01 – 6.84 (m, 3H).^{13}C NMR (126 MHz, $CDCl_3$): δ = 162.49 (dd, $^{1}J_{F,H}$ = 253.7, $^{3}J_{F,H}$ = 12.5 Hz, q), 142.71 (q), 134.23 (t), 130.62 (t, $^{3}J_{F,H}$ = 10.2 Hz, q), 129.11 (t), 127.58 (t), 119.47 – 118.98 (m, t), 107.25 (t, $^{2}J_{F,H}$ = 25.0 Hz). ^{19}F NMR (471 MHz, $CDCl_3$): δ = -107.31. HRMS (ESI, +): *m/z* calcd. for $C_{12}H_8NaO_2S_2$ $[M+Na]^+$ 308.9826; found: 308.9831. Melting point 78.2 °C

Genral procedure for the preparation of asymmetric disulfides:

To a solution of thioacetate (1.00 eq.) and thiosulfonate (1.10 eq.) in degassed THF (0.15 m) at room temperature was added sodium methanolate (1.2 eq., 5.4 M in methanol). Directly after addition a white precipitate formed. After 15 to 30 minutes the thiosulfonate is usually consumed (as monitored by TLC SiO_2, cyclohexane/EtOAc 5:1) and the reaction is quenched by addition of water and diluted with *n*-heptane. The organic phase was separated and the aqueous phase was extracted with *n*-heptane (3x). The combined organic phase were dried over Na_2SO_4, filtered and the solvent was removed under reduced pressure affording the crude product. The mixture was further purified by column chromatography (SiO_2, pentane/DCM 10:1 or pure pentane) affording the asymmetric disulfide.

***p*-Methylphenyl pentyl disulfide:**

Following the general procedure for the preparation of asymmetric disulfides sodium methoxide (14.5 µL, 0.0787 mmol, 1.20 eq., 5.4 m in methanol) was added to a degassed solution of S-pentyl benzenethiosulfonate (17.2 mg, 0.0721 mmol, 1.10 eq.) and *S*-*p*-tolyl thioacetate (10.9 mg, 0.0656, 1.00 eq.) in THF (1 mL) under stirring. After 15 minutes, the reaction was quenched by addition of water. The crude was purified by column chromatography (SiO_2, pentane) affording *p*-methylphenyl pentyl disulfide (12.5 mg, 0.055 mmol) in 84% yield as a colorless oil.

^{1}H NMR (500 MHz, CD_2Cl_2): δ = 7.44-7.41 (m, 2H), 7.16-7.13f (m, 2H), 2.75-2.72 (m, 2H), 2.33 (s, 3H), 1.69-1.64 (m, 2H), 1.37-1.26(m, 4H), 0.87(t, $^3J_{H,H}$ = 7.2 Hz, 3H). ^{13}C NMR (126 MHz, CD_2Cl_2): δ = 137.7 (q), 134.8 (q), 130.3 (t), 128.9 (t), 39.5 (s), 31.2 (s), 29.1 (s), 22.8 (s), 21.3 (p), 14.3 (p). HRMS (ESI, +): *m/z* calcd. for $C_{12}H_{18}S_2$ $[M]^+$ 226.0842; found: 285.0844.

1*H*,1*H*,2*H*,2*H*-perfluorodecyl *p*-methylphenyl disulfide:

Following the general procedure for the preparation of asymmetric disulfides sodium methoxide (68.2 µL, 0.368 mmol, 1.20 eq., 5.4 m in methanol) was added to a degassed solution of *S*-1*H*,1*H*,2*H*,2*H*-perfluorodecyl bezenesulfonate (209 mg, 0.338 mmol, 1.10 eq.) and *S*-*p*-tolyl thioacetate (51.0 mg, 0.307, 1.00 eq.) in THF (2 mL) under stirring at room temperature. After 15 minutes, the reaction was quenched by addition of water. The crude was purified by column chromatography (SiO_2, pentane) affording 1H,1H,2H,2H-perfluorodecyl p-methylphenyl disulfide (162 mg, 0.269 mmol) in 88% yield as an amorphous solid.

^{1}H NMR (500 MHz, CD_2Cl_2): δ = 7.46-7.44 (m, 2H), 7.19-7.16 (m, 2H), 2.93-2.90 (m, 2H), 2.59-2.53 (m, 2H), 2.34 (s, 3H). ^{13}C NMR (126 MHz, CD_2Cl_2): δ = 138.9 (q), 133.5 (q), 130.6 (t), 130.0 (t), 31.95 (t, $^2J_{C,F}$ = 22.1 Hz, CH_2), 29.45 (t, $^3J_{C,F}$ = 3.4 Hz, CH_2), 21,32 (p). HRMS (MALDI-TOF, +): *m/z* calcd. for $C_{17}H_{11}F_{17}S_2$ $[M]^+$ 602.0025; found 602.0027

1-Adamantyl p-methoxyphenyl disulfide:

Following the general procedure for the preparation of asymmetric disulfides sodium methoxide (27.8 µL, 0.150 mmol, 1.20 eq., 5.4 m in methanol) was added to a degassed solution of *S*-adamantyl benzenethiosulfonate (42.4 mg, 0.138 mmol, 1.10 eq.) and *S*-*p*-tolyl thioacetate (20.8 mg, 0.125, 1.00 eq.) in THF (1 mL) under stirring at room temperature. After 15 minutes, the reaction was quenched by addition of water. The crude was purified by column chromatography (SiO_2, pentane) affording 1-adamantyl p-methoxyphenyl disulfide (32.0 mg, 0.125 mmol) in 88% yield as a colorless oil.

^{1}H NMR (500 MHz, CD_2Cl_2): δ = 7.67-7.28 (m, 2H), 7.18-7.05 (m, 2H), 2.32 (s, 3H), 2.04-2.01 (m, 3H), 1.85-1.84 (m, 6H), 1.70-1.62 (m, 6H). ^{13}C NMR (126 MHz, CD_2Cl_2): δ = 136.8 (q), 136.3 (q), 130.0 (t), 127.6 (t), 51.2 (q), 43.1 (s), 36.6 (s), 30.6 (t), 21.2 (p). HRMS (ESI, +): *m/z* calcd. for $C_{17}H_{22}S_2$ $[M]^+$ 313.1055; found: 313.1054.

***p*-Methoxyphenyl *p*-methylphenyl disulfide:**

Following the general procedure for the preparation of asymmetric disulfides sodium methoxide (73.9 µL, 0.399 mmol, 1.30 eq., 5.4 m in methanol) was added to a degassed solution of *S*-*p*-methoxyphenyl bezenesulfonate (103 mg, 0.368 mmol, 1.20 eq.) and *S*-*p*-tolyl thioacetate (51 mg, 0.307, 1.00 eq.) in THF (2 mL) under stirring at room temperature. After 15 minutes, the reaction was quenched by addition of water. The crude was purified by column chromatography (SiO_2, pentane/DCM 10:1) affording *p*-methoxyphenyl *p*-methylphenyl disulfide (72.0 mg, 0.274 mmol) in 89% yield as a yellow oil.

^{1}H NMR (500 MHz, CD_2Cl_2): δ = 7.51-7.32 (m, 4H), 7.20-7.09 (m, 2H), 6.91-6.78 (m, 2H), 3.78 (s, 3H), 2.34 (s, 3H). ^{13}C NMR (126 MHz, CD_2Cl_2): δ = 160.6 (q), 138.5 (q), 134.5 (q), 132.5 (t), 130.4 (t), 129.6 (t), 128.6 (q), 115.2 (t), 55.9 (p), 21.36 (p). HRMS (ESI, +): *m/z* calcd. for $C_{14}H_{14}NaOS_2$ $[M+Na]^+$ 285.0375; found: 285.0378.

***p*-Nitrophenyl hexyl disulfide:**

Following the general procedure for the preparation of asymmetric disulfides sodium methoxide (135 µL, 0.727 mmol, 1.20 eq., 5.4 m in methanol) was added to a degassed solution of *S*-*p*-nitrophenyl bezenesulfonate (197 mg, 0.667 mmol, 1.10 eq.) and S-hexyl ethanethioate (97.1 mg, 0.606 mmol, 1.00 eq.) in THF (4 mL) under stirring at room temperature. After 15 minutes, the reaction was quenched by addition of water. The crude was purified by column chromatography (SiO_2, cyclohexane/ethylacetate 8:1) affording *p*-nitrophenyl hexyl disulfide (110 mg, 0.407 mmol) in 67% yield as a colorless oil.

^{1}H NMR (500 MHz, $CDCl_3$): δ = 7.51-7.32 (m, 4H), 7.20-7.09 (m, 2H), 6.91-6.78 (m, 2H), 3.78 (s, 3H), 2.34 (s, 3H). ^{13}C NMR (126 MHz, $CDCl_3$): δ = 147.48 (q), 146.29 (q), 125.92 (t), 124.17 (t), 39.23 (s), 31.45 (s), 29.04 (s), 28.25 (s), 22.62 (s), 14.13 (p). Spectra found to be identical as previously reported.[170]

_p_-Nitrophenyl pentyl disulfide:

Following the general procedure for the preparation of asymmetric disulfides sodium methoxide (0.04 mL, 230 µmol, 1.20 eq., 5.4 m in methanol) was added to a degassed solution of S-pentyl benzenethiosulfonate (51.6 mg, 211 µmol, 1.10 eq.) and p-nitrophenyl thioacetate (37.9 mg, 192 µmol, 1.00 eq.) in THF (1 mL) under stirring. After 15 minutes, the reaction was quenched by addition of water. The crude was purified by column chromatography (SiO_2, cyclohexane/EtOAc 5:1) affording p-nitrophenyl hexyl disulfide (37 mg, 144 µmol) in 75% yield as a colorless oil.

^{1}H-NMR (500 MHz, $CDCl_3$): δ = 7.70 – 7.61 (m, 2H), 2.79 – 2.74 (m, 2H), 1.67 (p, $^3J_{HH}$ = 7.4 Hz, 2H), 1.43 – 1.23 (m, 5H), 0.88 (t, $^3J_{HH}$ = 7.2 Hz, 3H). ^{13}C{^{1}H}-NMR (126 MHz, $CDCl_3$, 298 K): δ = 147.47, 146.29, 125.92, 124.16, 39.19, 30.71, 28.76, 22.35, 14.02. HRMS (ESI, +): *m/z* calcd. for $C_{11}H_{15}NNaO_2S_2$ $[M+Na]^+$: 280.0436, found: 280.0440.

_p_-Aminophenyl hexyl disulfide:

Following the general procedure for the preparation of asymmetric disulfides sodium methoxide (0.12 mL, 641 µmol, 1.20 eq., 5.4 m in methanol) was added to a degassed solution of *S-p*-aminophenyl benzenethiosulfonate (156 mg, 587 µmol, 1.10 eq.) and S-hexyl thioacetate (85.6 mg, 534 µmol, 1.00 eq.) in THF (2 mL) under stirring. After 15 minutes, the reaction was quenched by addition of water. The crude was purified by column chromatography (SiO_2, cyclohexane/ethyl acetate 5:1) affording *p*-nitrophenyl pentyl disulfide (74 mg, 307 µmol) in 57% yield as a yellow oil.

^{1}H-NMR (500 MHz, $CDCl_3$): δ = 7.42 – 7.31 (m, 2H), 6.78 – 6.64 (m, 2H), 4.57 (s, 2H), 2.76 – 2.69 (m, 2H), 1.66 (p, $^3J_{HH}$ = 7.4 Hz, 2H), 1.41 – 1.19 (m, 7H), 0.87 (t, $^3J_{HH}$ = 7.0 Hz, 3H). ^{13}C{^{1}H}-NMR (126 MHz, $CDCl_3$): δ = 132.53, 129.01, 125.35, 116.43, 38.93, 31.52, 28.83, 28.33, 22.66, 14.16. HRMS (ESI, +): *m/z* calcd. for $C_{12}H_{20}NS_2$ $[M+H]^+$: 242.1032, found: 242.1034.

_p_-Methoxyphenyl pentyl disulfide:

Following the general procedure for the preparation of asymmetric disulfides sodium methoxide (0.16 mL, 857 µmol, 1.20 eq., 5.4 m in methanol) was added to a degassed solution of S-pentyl benzenethiosulfonate (192 mg, 785 µmol, 1.10 eq.) and S-(4-methoxyphenyl) thioacetate (130 mg, 713 µmol, 1.00 eq.) in THF (2 mL) under stirring. After 15 minutes, the reaction was quenched by addition of water. The crude was purified by column chromatography (SiO_2, cyclohexane/ethyl acetate 5:1) affording *p*-methoxy phenyl disulfide (147 mg, 606 µmol) in 85% yield as a colorless oil but was found to rapidly disproportionate.

^{1}H-NMR (250 MHz, $CDCl_3$): δ = 7.48 (d, $^3J_{HH}$ = 8.9 Hz, 2H [title compound]), 7.43 – 7.36 (m, 0.2H [1,2-bis(4-methoxyphenyl)disulfane]), 6.92 – 6.78 (m, 2,2H [title compound + 1,2-bis(4-methoxyphenyl)disulfane]), 2.78 – 2.64 (m, 2.3H [title compound + 1,2-dipentyldisulfane]), 1.76 – 1.58 (m, 2.3H, [title compound + 1,2-dipentyldisulfane]), 1.32 (m, 4.6H [title compound + 1,2-dipentyldisulfane]), 0.94 – 0.80 (m, 3.4H [title compound + 1,2-dipentyldisulfane]). HRMS (ESI, +): *m/z* calcd. for $C_{12}H_{18}NaOS_2$ $[M+Na]^+$: 265.0691, found: 265.0681. HRMS (ESI, +): *m/z* calcd. for $C_{14}H_{14}NaO_2S_2$ [1,2-bis(4-methoxyphenyl)disulfane+Na]$^+$: 301.0327, found: 301.0326.

Methyl 2-(hexyldisulfaneyl)benzoate:

Following the general procedure for the preparation of asymmetric disulfides sodium methoxide (135 µL, 0.727 mmol, 1.20 eq., 5.4 m in methanol) was added to a degassed solution of methyl 2-((phenylsulfonyl)thio)benzoate (218 mg, 0.707 mmol, 1.10 eq.) and S-hexyl ethanethioate (103 mg, 0.643 mmol, 1.00 eq.) in THF (4 mL) under stirring at room temperature. After 15 minutes, the reaction was quenched by addition of water. The crude was purified by column chromatography (SiO_2, cyclohexane/ethylacetate 4:1) affording *p*-nitrophenyl hexyl disulfide (27 mg, 0.095 mmol) in 15% yield as a colorless oil.

^{1}H NMR (500 MHz, $CDCl_3$): δ = 8.18 (dd, $^3J_{H,H}$ = 8.2, $^4J_{H,H}$ = 1.2 Hz, 1H), 8.01 (dd, $^3J_{H,H}$ = 7.8, $^4J_{H,H}$ = 1.6 Hz, 1H), 7.55 (ddd, $^3J_{H,H}$ = 8.2, $^3J_{H,H}$ = 7.2, $^4J_{H,H}$ = 1.6 Hz, 1H), 7.25 – 7.19 (m, 1H), 2.72 – 2.69 (t, $^3J_{H,H}$ = 7.33 Hz, 2H), 1.72 – 1.61 (m, 2H), 1.41 – 1.33 (m, 2H), 1.32 – 1.20 (m, 4H), 0.87 (t, $^3J_{H,H}$ = 7.0 Hz, 3H). ^{13}C NMR (126 MHz, $CDCl_3$): δ = 166.96 (q), 142.31 (q), 132.83 (t), 131.55 (t), 127.13 (q), 125.80 (t), 125.10 (t), 52.37 (p), 38.65 (s), 31.49 (s), 29.11 (s), 28.40 (s), 22.65 (s), 14.14 (p). HRMS (ESI, +): *m/z* calcd. for $C_{14}H_{20}NaO_2S_2$ $[M+Na]^+$ 307.0797; found: 307.0794.

3,5-difluorophenyl hexyl disulfide:

Following the general procedure for the preparation of asymmetric disulfides sodium methoxide (139 µL, 0.749 mmol, 1.20 eq., 5.4 m in methanol) was added to a degassed solution of 3,5 difluorophenyl benzenthiosulfonate (197 mg, 0.686 mmol, 1.10 eq.) and S-hexyl ethanethioate (100 mg, 0.624 mmol, 1.00 eq.) in THF (4 mL) under stirring at room temperature. After 15 minutes, the reaction was quenched by addition of water. The crude was purified by column chromatography (SiO_2, cyclohexane) affording *p*-nitrophenyl hexyl disulfide (132 mg, 0.503 mmol) in 81% yield as a colorless oil.

^{1}H NMR (500 MHz, $CDCl_3$): δ = 7.11 – 6.98 (m, 2H), 6.63 (tt, $^3J_{H,H}$ = 8.7, $^4J_{H,H}$ = 2.3 Hz, 1H), 2.81 – 2.59 (m, 2H), 1.75 – 1.61 (m, 2H), 1.41-1.35 (m, 2H), 1.32 – 1.21 (m, 4H), 0.88 (t, $^3J_{H,H}$ = 7.0 Hz, 3H). ^{13}C NMR (126 MHz, $CDCl_3$): δ = 163.33 (dd, $^1J_{F,H}$ = 250.9, $^3J_{F,H}$ = 12.8 Hz, q), 142.36 (t, $^3J_{F,H}$ = 8.82, q), 109.68 – 108.62 (m, t), 101.97 (t, $^2J_{F,H}$ = 25.7 Hz, t), 39.22 (s), 31.47 (s), 28.92 (s), 28.24 (s), 22.63 (s), 14.12 (p). ^{19}F NMR (471 MHz, $CDCl_3$): δ = -108.89. GC-MS (EI): m/z(%) =176.0 (100.0), 161.0 (100), 101.1 (93.1), 145.0 (49.9), 133.0 (33.8), 113.0 (26.0), 63.0 (22.2), 146.0 (17.5), 69.0 (11.6).

Tetrakis(4-(pentyldisulfanyl)phenyl)methane (140):

Following the general procedure for the preparation of asymmetric disulfides sodium methoxide (23.0 µL, 0.124 mmol, 4.5 eq., 5.4 m in methanol) was added to a degassed solution of pentyl bezenesulfonate (33.7 mg, 0.138 mmol, 5 eq.) and tetrakis(4-(acetylsulfanyl)phenyl)methane (17 mg, 0.0276, 1.00 eq.) in THF (1 mL) under stirring at room temperature. After 15 minutes, the reaction was quenched by addition of water. The crude was purified by column chromatography (SiO_2, pentane) affording tetrakis(4-(pentyldisulfaneyl)phenyl)methane (72.0 mg, 0.274 mmol) in 89% yield as a colorless amorphous solid.

^{1}H NMR (500 MHz, CD_2Cl_2): δ = 7.44-7.14 (m, 8H), 7.18-7.14 (m, 8H), 2.78-2.74 (m, 8H), 1.70-1.62 (m, 8H), 1.38-1.23 (s, 16H), 0.87 (t, $^3J_{H,H}$ = 7.2 Hz, 12H). ^{13}C NMR (126 MHz, CD_2Cl_2): δ = 145.5 (q), 136.4 (q), 131.9 (t), 127.1 (t), 64.3 (q), 39.8 (s), 31.1 (s), 29.1 (s), 22.8 (s), 14.3 (p). HRMS (ESI, +): *m/z* calcd. for $C_{45}H_{64}NS_8$ $[M+NH_4]^+$ 285.0375; found: 285.0378.

1,4-Bis((4-(pentyldisulfaneyl)phenyl)ethynyl)benzene (OPE-3) 142:

A solution of **OPE-3** (80.2 mg, 188 µmol, 1.00 eq.) and *S*-pentyl benzenethiosulfonate (138 mg, 564 µmol, 3.00 eq.) in THF (2.5 mL) was degassed by purging with argon for 15 min. A solution of sodium methoxide in methanol (5.4 m, 104 µL, 564 µmol, 3.00 eq) was added and the mixture was stirred for 30 min at rt. Water was added to the mixture and the aqueous phase was extracted with toluene three times. The combined organic layers were dried over anhydrous Na_2SO_4 and concentrated under reduced pressure. The crude material was subjected to column chromatography (SiO_2, CH_2Cl_2 1:10 *n*-heptane) to give the title compound (82.0 mg, 188 µmol, 78%) as a white solid.

^{1}H NMR (400 MHz, $CDCl_3$): δ = 7.54 – 7.50 (m, 4H), 7.50 (s, 4H), 7.49 – 7.46 (m, 4H), 2.80 – 2.72 (m, 4H), 1.71 - 1.64 (m, 4H), 1.39 – 1.22 (m, 8H), 0.88 (t, $^3J_{HH}$ = 7.2 Hz, 6H. ^{13}C NMR (101 MHz, $CDCl_3$): δ = 138.8 (q), 132.1 (t), 131.7 (t), 126.9 (t), 123.2 (q), 121.2 (q), 91.06 (q), 89.8 (q), 39.2 (s), 30.8 (s), 28.7 (s), 22.34 (s), 14.1 (p). HRMS (ESI, +): *m/z* calcd. for $C_{32}H_{35}S_4$ $[M+H]^+$: 547.1616, found: 547.1608.

5,15-bis(4-(tert-butyl)phenyl)-10,20-bis((4-(pentyldisulfaneyl)phenyl)ethynyl)porphyrin (P-1-ADS) (141):

A solution of P-1[y] (2.03 mg, 2.19 µmol, 1.00 eq.) and *S*-pentyl benzenethiosulfonate (1.61 mg, 6.59 µmol, 3.00 eq.) in THF (1.0 mL) was degassed by purging with argon for approximately 10 min. A solution of sodium methoxide in methanol (5.4 m, 1.224 µL, 6.59 µmol, 3.00 eq) was added and the mixture was stirred for 30 min at rt. Water was added to the mixture and the aqueous phase was extracted with toluene three times. The combined organic layers were dried over anhydrous Na_2SO_4 and concentrated under reduced pressure. The crude material was subjected to column chromatography (SiO_2, CH_2Cl_2 1:2 *n*-heptane) to give the title compound (1.42 mg, 1.36 µmol, 62%) as a purple solid.

^{1}H NMR (250 MHz, $CDCl_3$, $CDCl_3$): δ = 9.65 (d, $^3J_{HH}$ = 4.8 Hz, 4H, H_β), 8.88 (d, $^3J_{HH}$ = 4.8 Hz, 4H, H_β), 8.16 – 8.08 (m, 4H, H_{Ar}), 7.99 – 7.92 (m, 4H, H_{Ar}), 7.84 – 7.77 (m, 4H, H_{Ar}), 7.77 – 7.70 (m, 4H, H_{Ar}), 2.90 – 2.77 (m, 4H, H_{Alk}), 1.82 – 1.66 (m, 4H, , H_{Alk}), 1.46 – 1.32 (m, 8H, , H_{Alk}), 1.64(s, 18H, H_{tBu}), 0.97 – 0.88 (m, 1H, H_{Alk}), -1.92 (s, 2H, H_{NH}). HRMS (ESI, +): *m/z* calcd. for $C_{66}H_{67}N_4S_4$ $[M+H]^+$: 1043.4243, found: 1043.4229.

Synthesis of 2-(2-ethoxyethoxy)ethane-1-thiol:[163]

2-(2-ethoxyethoxy)ethane-1-thiol was synthesized following an modified version of the literature procedure[163] whereby 2-(2-ethoxyethoxy)ethyl 4-methylbenzenesulfonate (347 mg, 1.20 mmol 1.00 eq.), thiourea (92.3 mg, 1.21 mmol, 1.01 eq) in ethanol (1 mL) and H_2O (0.1 mL) was refluxed for 3 h. Then an aqueous sodium hydroxide solution (0.84 mL, 1.68 mmol, 1.4 eq., 2 m) was added and the mixture was refluxed for 4 h. The solvents were evaporated under reduced pressure and diluted with water (1 mL), acidified with aqueous HCl (2 m), extracted with dichloromethane (2x), dried over Na_2SO_4, filtered and the solvent was removed under reduced pressure. The residue was purified by kugelrohr distillation yielding the thiol (141 mg, 0.938 mmol) in 78% yield.

^{1}H NMR (400 MHz, CD_2Cl_2): δ = 3.60-3.52 (m, 6H), 3.48 (q, $^3J_{H,H}$ = 7.0 Hz, 2H), 2.67 (dt, $^3J_{H,H}$ = 8.1 Hz, $^3J_{H,H}$ = 6.4 Hz 2H), 1.61 (t, $^3J_{H,H}$ = 8.1 Hz, 1H), 1.17 (t, $^3J_{H,H}$ = 7.0 Hz, 3H). ^{13}C NMR (126 MHz, CD_2Cl_2): δ = 73.4 (s), 70.1 (s), 70.3 (s), 67.02 (s), 24.9 (s), 15.6 (s). GC-MS (EI): m/z (%) =61.0 (100.0), 91.1 (81.9), 73.1 (37.9), 72.0 (35.8), 60.0 (32.9), 59.0 (55.3).

Synthesis of 3,5-Difluorophenyl methyl sulfenate:

To a solution of 3,5-difluorophenyl benzenethiosulfonate (100 mg, 0.349 mmol, 1.00 eq.) in THF (4 mL) was added A solution of sodium methoxide in methanol (5.4 m, 65 µL, 0.349 mmol, 1.00 eq) at room temperature. A white precipitate immediately formed. After stirring for 15 minutes the mixture was diluted with cyclohexane and filtered. The filtrated was concentranted under reduced pressure yielding 3,5-difluorophenyl methyl sulfenate (61.0 mg, 0.346 mmol) in 99 % yield as an yellow liquid.

^{1}H NMR (500 MHz, $CDCl_3$): δ = 6.74 – 6.69 (m, 2H), 6.58 (tt, $^3J_{H,H}$ = 8.9, $^4J_{H,H}$ = 2.3 Hz, 1H), 3.79 (s, 3H). ^{13}C NMR (126 MHz, $CDCl_3$): δ = 163.68 (dd, $^1J_{F,H}$ = 251.0, $^3J_{F,H}$ = 12.9 Hz, q), 145.41 (t, $^3J_{F,H}$ = 9.3, q), 104.68 – 103.85 (m, t), 101.04 (t, $^2J_{F,H}$ = 25.7 Hz, t), 66.39(p). . GC-MS (EI): m/z (%)

=262.0 (100.0), 178.0 (63.7), 57.1 (58.5), 101.0 (53.3), 85.1 (51.0), 55.1 (38.2), 114.0 (34.6), 145 (26.9), 263.0 (15.2), 176.9 (14.4), 127.1 (13.9), 133.0 (13.2), 113.0 (10.4).

5 References

[1] Roald. Hoffmann, Akira. Imamura, G. D. Zeiss, *J. Am. Chem. Soc.* **1967**, *89*, 5215–5220.
[2] H. E. Simmons, Tadamichi. Fukunaga, *J. Am. Chem. Soc.* **1967**, *89*, 5208–5215.
[3] H. Dürr, R. Gleiter, *Angew. Chem.* **1978**, *90*, 591–601.
[4] H. Dürr, R. Gleiter, *Angew. Chem. Int. Ed.* **1978**, *17*, 559–569.
[5] P. Maslak, S. Varadarajan, J. D. Burkey, *J. Org. Chem.* **1999**, *64*, 8201–8209.
[6] V. Galasso, J. Bogdanov, P. Maslak, D. Jones, A. Modelli, *J. Phys. Chem. A* **2002**, *106*, 10622–10629.
[7] P. Maslak, A. Chopra, C. R. Moylan, R. Wortmann, S. Lebus, A. L. Rheingold, G. P. A. Yap, *J. Am. Chem. Soc.* **1996**, *118*, 1471–1481.
[8] P. Maslak, *Adv. Mater.* **1994**, *6*, 405–407.
[9] R. Boschi, A. S. Dreiding, E. Heilbronner, *J. Am. Chem. Soc.* **1970**, *92*, 123–128.
[10] M. F. Semmelhack, J. S. Foos, S. Katz, *J. Am. Chem. Soc.* **1972**, *94*, 8637–8638.
[11] C. Batich, E. Heilbronner, E. Rommel, M. F. Semmelhack, J. S. Foos, *J. Am. Chem. Soc.* **1974**, *96*, 7662–7668.
[12] J. H. Brewster, R. T. Prudence, *J. Am. Chem. Soc.* **1973**, *95*, 1217–1229.
[13] R. K. Hill, D. A. Cullison, *J. Am. Chem. Soc.* **1973**, *95*, 1229–1239.
[14] J. K. Sowa, J. A. Mol, G. A. D. Briggs, E. M. Gauger, *J. Phys. Chem. Lett.* **2018**, *9*, 1859–1865.
[15] I. Bersuker, "The Jahn-Teller Effect by Isaac Bersuker," DOI 10.1017/CBO9780511524769can be found under /core/books/jahnteller-effect/05766FA392314EE9022AA86A53AC52E5, **2006**.
[16] F. Leyendecker, J. Drouin, J. M. Conia, *Tetrahedron Lett.* **1974**, *15*, 2931–2934.
[17] D. H. Jadhav, C. S. Ramaa, *IJCB.* **2007**, *46B*, 2064-2067.
[18] A. H. More, C. S. Ramaa, *IJCB* **2010**, *49B*, 1681-1684.
[19] G. Markopoulos, L. Henneicke, J. Shen, Y. Okamoto, P. G. Jones, H. Hopf, *Angewandte Chemie International Edition* **2012**, *51*, 12884–12887.
[20] G. A. Molander, A. R. Brown, *J. Org. Chem.* **2006**, *71*, 9681–9686.
[21] H. Leuchs, F. Reinhart, *Ber. d. Dt. Chem. Ges.* **1924**, *57*, 1208–1214.
[22] A. Martínez, M. Fernández, J. C. Estévez, R. J. Estévez, L. Castedo, *Tetrahedron* **2005**, *61*, 1353–1362.
[23] J. Wilbuer, G. Schnakenburg, B. Esser, *Eur. J. Org. Chem.* **2016**, *2016*, 2404–2412.
[24] G. Farges, A. S. Dreiding, *Helv. Chim. Acta* **1966**, *49*, 552–561.
[25] P. Sandín, A. Martínez-Grau, L. Sánchez, C. Seoane, R. Pou-Amérigo, E. Ortí, N. Martín, *Org. Lett.* **2005**, *7*, 295–298.
[26] C. R. Parker, Z. Wei, C. R. Arroyo, K. Jennum, T. Li, M. Santella, N. Bovet, G. Zhao, W. Hu, H. S. J. van der Zant, et al., *Adv. Mater.* **2013**, *25*, 405–409.
[27] C. R. Parker, E. Leary, R. Frisenda, Z. Wei, K. S. Jennum, E. Glibstrup, P. B. Abrahamsen, M. Santella, M. A. Christensen, E. A. Della Pia, et al., *J. Am. Chem. Soc.* **2014**, *136*, 16497–16507.
[28] J. Tsuji, H. Nagashima, H. Nemoto, *Org. Synth.* **1984**, *62*, 9.
[29] J. Tsuji, *Synthesis* **1984**, *1984*, 369–384.
[30] D. G. Miller, D. D. M. Wayner, *J. Org. Chem.* **1990**, *55*, 2924–2927.
[31] N. Svenstrup, K. M. Rasmussen, T. K. Hansen, J. Becher, *Synthesis* **1994**, *1994*, 809–812.
[32] R. P. Parg, J. D. Kilburn, T. G. Ryan, *Synthesis* **1994**, *1994*, 195–198.
[33] Z. J. Donhauser, B. A. Mantooth, K. F. Kelly, L. A. Bumm, J. D. Monnell, J. J. Stapleton, D. W. Price, A. M. Rawlett, D. L. Allara, J. M. Tour, et al., *Science* **2001**, *292*, 2303–2307.
[34] R. P. Andres, T. Bein, M. Dorogi, S. Feng, J. I. Henderson, C. P. Kubiak, W. Mahoney, R. G. Osifchin, R. Reifenberger, *Science* **1996**, *272*, 1323–1325.
[35] J. Repp, G. Meyer, S. Paavilainen, F. E. Olsson, M. Persson, *Science* **2006**, *312*, 1196–1199.
[36] D. J. Wold, R. Haag, M. A. Rampi, C. D. Frisbie, *J. Phys. Chem. B* **2002**, *106*, 2813–2816.
[37] X. D. Cui, A. Primak, X. Zarate, J. Tomfohr, O. F. Sankey, A. L. Moore, T. A. Moore, D. Gust, G. Harris, S. M. Lindsay, *Science* **2001**, *294*, 571–574.
[38] F.-R. F. Fan, J. Yang, L. Cai, D. W. Price, S. M. Dirk, D. V. Kosynkin, Y. Yao, A. M. Rawlett, J. M. Tour, A. J. Bard, *J. Am. Chem. Soc.* **2002**, *124*, 5550–5560.

[39] L. Venkataraman, J. E. Klare, C. Nuckolls, M. S. Hybertsen, M. L. Steigerwald, *Nature* **2006**, *442*, 904–907.
[40] A. Mishchenko, D. Vonlanthen, V. Meded, M. Bürkle, C. Li, I. V. Pobelov, A. Bagrets, J. K. Viljas, F. Pauly, F. Evers, et al., *Nano Lett.* **2010**, *10*, 156–163.
[41] A. Mishchenko, L. A. Zotti, D. Vonlanthen, M. Bürkle, F. Pauly, J. C. Cuevas, M. Mayor, T. Wandlowski, *J. Am. Chem. Soc.* **2011**, *133*, 184–187.
[42] B. Xu, N. J. Tao, *Science* **2003**, *301*, 1221–1223.
[43] N. J. Tao, *Phys. Rev. Lett.* **1996**, *76*, 4066–4069.
[44] W. Haiss, H. van Zalinge, S. J. Higgins, D. Bethell, H. Höbenreich, D. J. Schiffrin, R. J. Nichols, *J. Am. Chem. Soc.* **2003**, *125*, 15294–15295.
[45] D. S. Seferos, S. A. Trammell, G. C. Bazan, J. G. Kushmerick, *PNAS* **2005**, *102*, 8821–8825.
[46] M. A. Reed, C. Zhou, C. J. Muller, T. P. Burgin, J. M. Tour, *Science* **1997**, *278*, 252–254.
[47] C. Kergueris, J.-P. Bourgoin, S. Palacin, D. Esteve, C. Urbina, M. Magoga, C. Joachim, *Phys. Rev. B* **1999**, *59*, 12505–12513.
[48] J. Reichert, R. Ochs, D. Beckmann, H. B. Weber, M. Mayor, H. v. Löhneysen, *Phys. Rev. Lett.* **2002**, *88*, 176804.
[49] M. L. Perrin, C. J. O. Verzijl, C. A. Martin, A. J. Shaikh, R. Eelkema, J. H. van Esch, J. M. van Ruitenbeek, J. M. Thijssen, H. S. J. van der Zant, D. Dulić, *Nat. Nanotechnol.* **2013**, *8*, 282–287.
[50] S. Wu, M. T. González, R. Huber, S. Grunder, M. Mayor, C. Schönenberger, M. Calame, *Nat. Nanotechnol.* **2008**, *3*, 569–574.
[51] E. Lörtscher, J. W. Ciszek, J. Tour, H. Riel, *Small* **2006**, *2*, 973–977.
[52] J. Park, A. N. Pasupathy, J. I. Goldsmith, C. Chang, Y. Yaish, J. R. Petta, M. Rinkoski, J. P. Sethna, H. D. Abruña, P. L. McEuen, et al., *Nature* **2002**, *417*, 722–725.
[53] E. A. Osorio, T. Bjørnholm, J.-M. Lehn, M. Ruben, H. S. J. van der Zant, *J. Phys.: Condens. Matter* **2008**, *20*, 374121.
[54] K. Slowinski, H. K. Y. Fong, M. Majda, *J. Am. Chem. Soc.* **1999**, *121*, 7257–7261.
[55] R. Haag, M. A. Rampi, R. E. Holmlin, G. M. Whitesides, *J. Am. Chem. Soc.* **1999**, *121*, 7895–7906.
[56] W. Hong, H. Valkenier, G. Mészáros, D. Manrique, A. Mishchenko, A. Putz, P. Moreno Garcia, C. Lambert, J. C. Hummelen, T. Wandlowski, *Beilstein J. Nanotechnol.* **2011**, *2*, 699–713.
[57] M. E. Abbassi, P. Zwick, A. Rates, D. Stefani, A. Prescimone, M. Mayor, H. S. J. van der Zant, D. Dulić, *Chem. Sci.* **2019**, DOI 10.1039/C9SC02497B.
[58] R. Frisenda, S. Tarkuç, E. Galán, M. L. Perrin, R. Eelkema, F. C. Grozema, H. S. J. van der Zant, *Beilstein J. Nanotechnol.* **2015**, *6*, 1558–1567.
[59] J. Matsuo, Y. Aizawa, *Chem. Commun.* **2005**, 2399–2401.
[60] T. Fink, J.-L. Reymond, *J. Chem. Inf. Model.* **2007**, *47*, 342–353.
[61] J.-L. Reymond, L. C. Blum, R. van Deursen, *CHIMIA* **2011**, *65*, 863–867.
[62] H. Hopf, *Classics in Hydrocarbon Chemistry : Syntheses, Concepts, Perspectives*, Wiley-VCH, Weinheim, **2000**.
[63] *Nachr. Chem. Tech. Lab.* **1977**, *25*, 59–70.
[64] R. J. Ternansky, D. W. Balogh, L. A. Paquette, *J. Am. Chem. Soc.* **1982**, *104*, 4503–4504.
[65] G. R. Underwood, B. Ramamoorthy, *Tetrahedron Lett.* **1970**, *11*, 4125–4127.
[66] I. A. Levandovsky, D. I. Sharapa, O. A. Cherenkova, A. V. Gaidai, T. E. Shubina, *Russ. Chem. Rev.* **2010**, *79*, 1005.
[67] A. Nickon, H. Kwasnik, T. Swartz, R. O. Williams, J. B. DiGiorgio, *J. Am. Chem. Soc.* **1965**, *87*, 1613–1615.
[68] G. Brieger, D. R. Anderson, *J. Org. Chem.* **1971**, *36*, 243–244.
[69] C. Ebner, E. M. Carreira, *Angew. Chem. Int. Ed.* **2015**, *54*, 11227–11230.
[70] R. Fuchs, J. F. Mcgarrity, *Synthesis* **1992**, *1992*, 373–374.
[71] B. Guay, P. Deslongchamps, *J. Org. Chem.* **2003**, *68*, 6140–6148.
[72] R. M. Cory, R. M. Renneboog, *J. Org. Chem.* **1984**, *49*, 3898–3904.
[73] R. L. Funk, K. P. C. Vollhardt, *Synthesis* **1980**, *1980*, 118–119.
[74] A. L. Gemal, J. L. Luche, *J. Am. Chem. Soc.* **1981**, *103*, 5454–5459.
[75] R. Ivanov, I. Marek, T. Cohen, *Tetrahedron Lett.* **2010**, *51*, 174–176.

[76] G. E. Keck, K. A. Savin, M. A. Weglarz, *J. Org. Chem.* **1995**, *60*, 3194–3204.
[77] B. Reif, M. Kock, R. Kerssebaum, J. Schleucher, C. Griesinger, *J Magn Reson B* **1996**, *112*, 295–301.
[78] M. Köck, R. Kerssebaum, W. Bermel, *Magn. Reson. Chem.* **2003**, *41*, 65–69.
[79] A. A. Popov, S. Yang, L. Dunsch, *Chem. Rev.* **2013**, *113*, 5989–6113.
[80] H. J. Chandler, M. Stefanou, E. E. B. Campbell, R. Schaub, *Nat Commun* **2019**, *10*, 1–8.
[81] R. B. Ross, C. M. Cardona, D. M. Guldi, S. G. Sankaranarayanan, M. O. Reese, N. Kopidakis, J. Peet, B. Walker, G. C. Bazan, E. V. Keuren, et al., *Nat. Mater.* **2009**, *8*, 208–212.
[82] E. B. Iezzi, J. C. Duchamp, K. R. Fletcher, T. E. Glass, H. C. Dorn, *Nano Lett.* **2002**, *2*, 1187–1190.
[83] A. Takeda, Y. Yokoyama, S. Ito, T. Miyazaki, H. Shimotani, K. Yakigaya, T. Kakiuchi, H. Sawa, H. Takagi, K. Kitazawa, et al., *Chem. Commun.* **2006**, 912–914.
[84] J. Cioslowski, A. Nanayakkara, *Phys. Rev. Lett.* **1992**, *69*, 2871–2873.
[85] P. L. Boulas, M. Gómez-Kaifer, L. Echegoyen, *Angew. Chem. Int. Ed.* **1998**, *37*, 216–247.
[86] J. M. Lehn, *Acc. Chem. Res.* **1978**, *11*, 49–57.
[87] J. M. Lehn, *Pure Appl. Chem.* **1980**, *52*, 2303–2319.
[88] L. Echegoyen, A. DeCian, J. Fischer, J.-M. Lehn, *Angew. Chem. Int. Ed.* **1991**, *30*, 838–840.
[89] R. S. Ross, P. Pincus, F. Wudl, *J. Phys. Chem.* **1992**, *96*, 6169–6172.
[90] L. R. MacGillivray, J. L. Atwood, *Angew. Chem. Int. Ed.* **1999**, *38*, 1018–1033.
[91] A. P. West, D. Van Engen, R. A. Pascal, *J. Am. Chem. Soc.* **1989**, *111*, 6846–6847.
[92] V. A. Sergeev, Y. É. Ovchinnikov, V. I. Nedel'kin, A. V. Astankov, O. B. Andrianova, V. E. Shklover, I. A. Zamaev, Y. T. Struchkov, *Russ. Chem. Bull.* **1988**, *37*, 1440–1444.
[93] T. Sone, Y. Ohba, K. Moriya, H. Kumada, K. Ito, *Tetrahedron* **1997**, *53*, 10689–10698.
[94] Y. Ohba, K. Moriya, T. Sone, *BCSJ* **1991**, *64*, 576–582.
[95] H. Kumagai, M. Hasegawa, S. Miyanari, Y. Sugawa, Y. Sato, T. Hori, S. Ueda, H. Kamiyama, S. Miyano, *Tetrahedron Lett.* **1997**, *38*, 3971–3972.
[96] H. Zimmermann, R. Poupko, Z. Luz, *Tetrahedron* **1988**, *44*, 277–279.
[97] L. Engman, J. Hellberg, C. Ishag, S. Söderholm, *J. Chem. Soc., Perkin Trans. 1* **1988**, *0*, 2095–2101.
[98] G. Dougherty, P. D. Hammond, *J. Am. Chem. Soc.* **1935**, *57*, 117–118.
[99] M. Huko, H. Dvoáková, V. Eigner, P. Lhoták, *Chem. Commun.* **2015**, *51*, 7051–7053.
[100] M. H. Patel, P. S. Shrivastav, *Chem. Commun.* **2009**, *0*, 586–588.
[101] F. Berger, M. B. Plutschack, J. Riegger, W. Yu, S. Speicher, M. Ho, N. Frank, T. Ritter, *Nature* **2019**, *567*, 223–228.
[102] A. J. Neale, P. J. S. Bain, T. J. Rawlings, *Tetrahedron* **1969**, *25*, 4593–4597.
[103] A. J. Neale, P. J. S. Bain, T. J. Rawlings, *Tetrahedron* **1969**, *25*, 4583–4591.
[104] W. W. Hartman, L. A. Smith, J. B. Dickey, *Ind. Eng. Chem.* **1932**, *24*, 1317–1318.
[105] G. A. Olah, E. R. Marinez, G. K. S. Prakash, *Synlett* **1999**, *1999*, 1397–1398.
[106] J. S. Yadav, B. V. S. Reddy, R. S. Rao, S. P. Kumar, K. Nagaiah, *Synlett* **2002**, *2002*, 0784–0786.
[107] Marquié Julien, A. Laporterie, J. Dubac, N. Roques, J.-R. Desmurs, *J. Org. Chem.* **2001**, *66*, 421–425.
[108] S. Répichet, C. Le Roux, P. Hernandez, J. Dubac, J.-R. Desmurs, *J. Org. Chem.* **1999**, *64*, 6479–6482.
[109] P. Lhoták, M. Himl, I. Stibor, J. Sýkora, H. Dvořáková, J. Lang, H. Petříčková, *Tetrahedron* **2003**, *59*, 7581–7585.
[110] O. Kasyan, D. Swierczynski, A. Drapailo, K. Suwinska, J. Lipkowski, V. Kalchenko, *Tetrahedron Lett.* **2003**, *44*, 7167–7170.
[111] M. Yamada, F. Hamada, *Cryst. Growth Des.* **2015**, *15*, 1889–1897.
[112] M. A. Fernández-Rodríguez, Q. Shen, J. F. Hartwig, *J. Am. Chem. Soc.* **2006**, *128*, 2180–2181.
[113] T. Okauchi, K. Kuramoto, M. Kitamura, *Synlett.* **2010**, *2010*, 2891–2894.
[114] P. Lhoták, T. Šmejkal, I. Stibor, J. Havlíček, M. Tkadlecová, H. Petříčková, *Tetrahedron Lett.* **2003**, *44*, 8093–8097.
[115] J. R. Campbell, *J. Org. Chem.* **1964**, *29*, 1830–1833.
[116] T. Itoh, T. Mase, *Org. Lett.* **2004**, *6*, 4587–4590.
[117] P. C. Taylor, M. D. Wall, P. R. Woodward, *Tetrahedron* **2005**, *61*, 12314–12322.
[118] R. A. Rossi, A. B. Pierini, A. B. Peñéñory, *Chem. Rev.* **2003**, *103*, 71–168.

[119] R. A. Rossi, J. F. Guastavino, M. E. Budén, in *Arene Chemistry*, John Wiley & Sons, Ltd, **2015**, pp. 243–268.
[120] C. D. Baumgarner, A. H. Malen, S. D. Pastor, M. A. NabiRahni, *Helv. Chim. Acta* **1992**, *75*, 480–486.
[121] S. Montanari, C. Paradisi, G. Scorrano, *J. Org. Chem.* **1993**, *58*, 5628–5631.
[122] J. F. Bunnett, F. J. Kearley, *J. Org. Chem.* **1971**, *36*, 184–186.
[123] J.-M. Savéant, *Tetrahedron* **1994**, *50*, 10117–10165.
[124] C. Costentin, P. Hapiot, M. Médebielle, J.-M. Savéant, *J. Am. Chem. Soc.* **1999**, *121*, 4451–4460.
[125] J. F. Bunnett, X. Creary, *J. Org. Chem.* **1974**, *39*, 3611–3612.
[126] C. Amatore, C. Combellas, J. Pinson, M. A. Oturan, S. Robvieille, J. M. Saveant, A. Thiebault, *J. Am. Chem. Soc.* **1985**, *107*, 4846–4853.
[127] M. Singh, A. K. Yadav, L. D. S. Yadav, R. K. P. Singh, *Tetrahedron Lett.* **2017**, *58*, 2206–2208.
[128] M. Jiang, H. Li, H. Yang, H. Fu, *Angew. Chem. Int. Ed.* **2017**, *56*, 874–879.
[129] B. Liu, C.-H. Lim, G. M. Miyake, *J. Am. Chem. Soc.* **2017**, *139*, 13616–13619.
[130] M. Himl, M. Pojarová, I. Stibor, J. Sýkora, P. Lhoták, *Tetrahedron Lett.* **2005**, *46*, 461–464.
[131] P. Lhoták, M. Himl, I. Stibor, J. Sykora, I. Cisarová, *Tetrahedron Lett.* **2001**, *42*, 7107–7110.
[132] E. L. Grimm, C. Brideau, N. Chauret, C.-C. Chan, D. Delorme, Y. Ducharme, D. Ethier, J.-P. Falgueyret, R. W. Friesen, J. Guay, et al., *Bioorg. Med. Chem. Lett.* **2006**, *16*, 2528–2531.
[133] H. Grönbeck, A. Curioni, W. Andreoni, *J. Am. Chem. Soc.* **2000**, *122*, 3839–3842.
[134] J. M. Tour, L. Jones, D. L. Pearson, J. J. S. Lamba, T. P. Burgin, G. M. Whitesides, D. L. Allara, A. N. Parikh, S. Atre, *J. Am. Chem. Soc.* **1995**, *117*, 9529–9534.
[135] M. I. Béthencourt, L. Srisombat, P. Chinwangso, T. R. Lee, *Langmuir* **2009**, *25*, 1265–1271.
[136] M. D. Porter, T. B. Bright, D. L. Allara, C. E. D. Chidsey, *J. Am. Chem. Soc.* **1987**, *109*, 3559–3568.
[137] R. Huber, M. T. González, S. Wu, M. Langer, S. Grunder, V. Horhoiu, M. Mayor, M. R. Bryce, C. Wang, R. Jitchati, et al., *J. Am. Chem. Soc.* **2008**, *130*, 1080–1084.
[138] H. A. Biebuyck, C. D. Bain, G. M. Whitesides, *Langmuir* **1994**, *10*, 1825–1831.
[139] T. Brandl, M. E. Abbassi, D. Stefani, R. Frisenda, G. D. Harzmann, H. S. J. van der Zant, M. Mayor, *Eur. J. Org. Chem.* **2019**, *2019*, 5334–5343.
[140] D. Stefani, K. J. Weiland, M. Skripnik, C. Hsu, M. L. Perrin, M. Mayor, F. Pauly, H. S. J. van der Zant, *Nano Lett.* **2018**, *18*, 5981–5988.
[141] G. D. Harzmann, R. Frisenda, H. S. J. van der Zant, M. Mayor, *Angew. Chem. Int. Ed.* **2015**, *54*, 13425–13430.
[142] R. Frisenda, G. D. Harzmann, J. A. Celis Gil, J. M. Thijssen, M. Mayor, H. S. J. van der Zant, *Nano Lett.* **2016**, *16*, 4733–4737.
[143] M. Valášek, M. Mayor, *Chem.: Eur. J.* **2017**, *23*, 13538–13548.
[144] M. Valášek, M. Lindner, M. Mayor, *Beilstein J. Nanotechnol.* **2016**, *7*, 374–405.
[145] M. Musiejuk, D. Witt, *OPPI* **2015**, *47*, 95–131.
[146] R. Hunter, M. Caira, N. Stellenboom, *J. Org. Chem.* **2006**, *71*, 8268–8271.
[147] E. Brzezinska, A. L. Ternay, *J. Org. Chem.* **1994**, *59*, 8239–8244.
[148] J. M. Swan, *Nature* **1957**, *180*, 643–645.
[149] P. Dubs, R. Stüssi, *Helv. Chim. Acta* **1976**, *59*, 1307–1311.
[150] T. F. Parsons, J. D. Buckman, D. E. Pearson, L. Field, *J. Org. Chem.* **1965**, *30*, 1923–1926.
[151] D. N. Harpp, D. K. Ash, T. G. Back, J. G. Gleason, B. A. Orwig, W. F. VanHorn, J. P. Snyder, *Tetrahedron Lett.* **1970**, *11*, 3551–3554.
[152] D. N. Harpp, B. T. Friedlander, C. Larsen, K. Steliou, A. Stockton, *J. Org. Chem.* **1978**, *43*, 3481–3485.
[153] J. Kowalczyk, P. Barski, D. Witt, B. A. Grzybowski, *Langmuir* **2007**, *23*, 2318–2321.
[154] S. Lach, S. Demkowicz, D. Witt, *Tetrahedron Lett.* **2013**, *54*, 7021–7023.
[155] X. Qiu, X. Yang, Y. Zhang, S. Song, N. Jiao, *Org. Chem. Front.* **2019**, *6*, 2220–2225.
[156] T. Mukaiyama, K. Takahashi, *Tetrahedron Lett.* **1968**, *9*, 5907–5908.
[157] J. K. Vandavasi, W.-P. Hu, C.-Y. Chen, J.-J. Wang, *Tetrahedron* **2011**, *67*, 8895–8901.
[158] E. D. Goddard-Borger, R. V. Stick, *Aust. J. Chem.* **2005**, *58*, 188–198.

[159] C. H. Kaschula, R. Hunter, N. Stellenboom, M. R. Caira, S. Winks, T. Ogunleye, P. Richards, J. Cotton, K. Zilbeyaz, Y. Wang, et al., *Eur. J. Med. Chem.* **2012**, *50*, 236–254.
[160] F. Silva, S. S. Khokhar, D. M. Williams, R. Saunders, G. J. S. Evans, M. Graz, T. Wirth, *Angew. Chem. Int. Ed.* **2018**, *57*, 12290–12293.
[161] R. Hunter, C. H. Kaschula, I. M. Parker, M. R. Caira, P. Richards, S. Travis, F. Taute, T. Qwebani, *Bioorg. Med. Chem. Lett.* **2008**, *18*, 5277–5279.
[162] K. Fujiki, N. Tanifuji, Y. Sasaki, T. Yokoyama, *Synthesis* **2002**, *2002*, 0343–0348.
[163] A. W. Snow, E. E. Foos, *Synthesis* **2003**, *2003*, 0509–0512.
[164] Norman. Kharasch, S. J. Potempa, H. L. Wehrmeister, *Chem. Rev.* **1946**, *39*, 269–332.
[165] L. Field, T. F. Parsons, D. E. Pearson, *J. Org. Chem.* **1966**, *31*, 3550–3555.
[166] M. E. Abbassi, P. Zwick, A. Rates, D. Stefani, A. Prescimone, M. Mayor, H. S. J. van der Zant, D. Dulić, *Chem. Sci.* **2019**, *10*, 8299–8305.
[167] X. Xiao, L. A. Nagahara, A. M. Rawlett, N. Tao, *J. Am. Chem. Soc.* **2005**, *127*, 9235–9240.
[168] M. Lindner, M. Valášek, M. Mayor, T. Frauhammer, W. Wulfhekel, L. Gerhard, *Angew. Chem. Int. Ed.* **2017**, *56*, 8290–8294.
[169] P. Mampuys, Y. Zhu, S. Sergeyev, E. Ruijter, R. V. A. Orru, S. Van Doorslaer, B. U. W. Maes, *Org. Lett.* **2016**, *18*, 2808–2811.
[170] N. Stellenboom, R. Hunter, M. R. Caira, *Tetrahedron* **2010**, *66*, 3228–3241.

6 List of Abreviations

AcCl	Acetyl chloride
AOs	Atomic Orbitals
BHT	Butylated hydroxytoluene
dba	Dibenzylideneacetone
DCM	Dichloromethane
DDQ	2,3-Dichloro-5,6-dicyano-1,4-benzoquinone
DFT	Density functional theory
DIBAL-H	Diisobutylaluminium hydride
DMF	Dimethylformamide
DMI	1,3-Dimethyl-2-imidazolidinone
DMPU	*N,N'*-Dimethylpropyleneurea
DMSO	Dimethyl sulfoxide
DPPF	1,1'-Bis(diphenylphosphino)ferrocene
DQI	Destructive quantum interference
ESI-MS	Electrospray ionization mass spectrometry
EtOAc	Ethyl acetate
GC-MS	Gas chromatography-mass spectrometry
HOMO	Highest occupied molecular orbital
Josiphos	(2*R*)-1-[(1*R*)-1-[Bis(1,1-dimethylethyl)phosphino]ethyl]-2-(dicyclohexylphosphino)ferrocene
LC-MS	Liquid chromatography-mass spectrometry
LUMO	Lowest unoccupied molecular orbital
MALDI-TOF	Matrix-assisted laser desorption/ionization time of flight mass spectrometer
MCBJ	Mechanically controllable break junction
MeCN	Acetonitrile
MeOH	Methanol
NMP	*N*-Methyl-2-pyrrolidon
NMR	Nuclear Magnetic Resonance
ppy	2-Phenylpyridin
***p*-TsOH**	*Para*-toluene sulfonic acid
RuPhos	2-Dicyclohexylphosphino-2',6'-diisopropoxybiphenyl
SET	Single electron transfer
S_NAr	Nucleophilic aromatic substitution
$S_{RN}1$	Radical-nucleophilic aromatic substitution
STM	Scanning tunneling microscope
TBME	Tert-butyl methyl ether
TEG	Tetraethyleneglycol
THF	Tetrahydrofuran
TLC	Thin-layer chromatography
Xantphos	4,5-Bis(diphenylphosphino)-9,9-dimethylxanthene

7 Appendix

$^{1}H\{^{19}F\}$ NMR (500 MHz, CD_2Cl_2) and ^{13}C NMR (151 MHz, CD_2Cl_2) of **22**

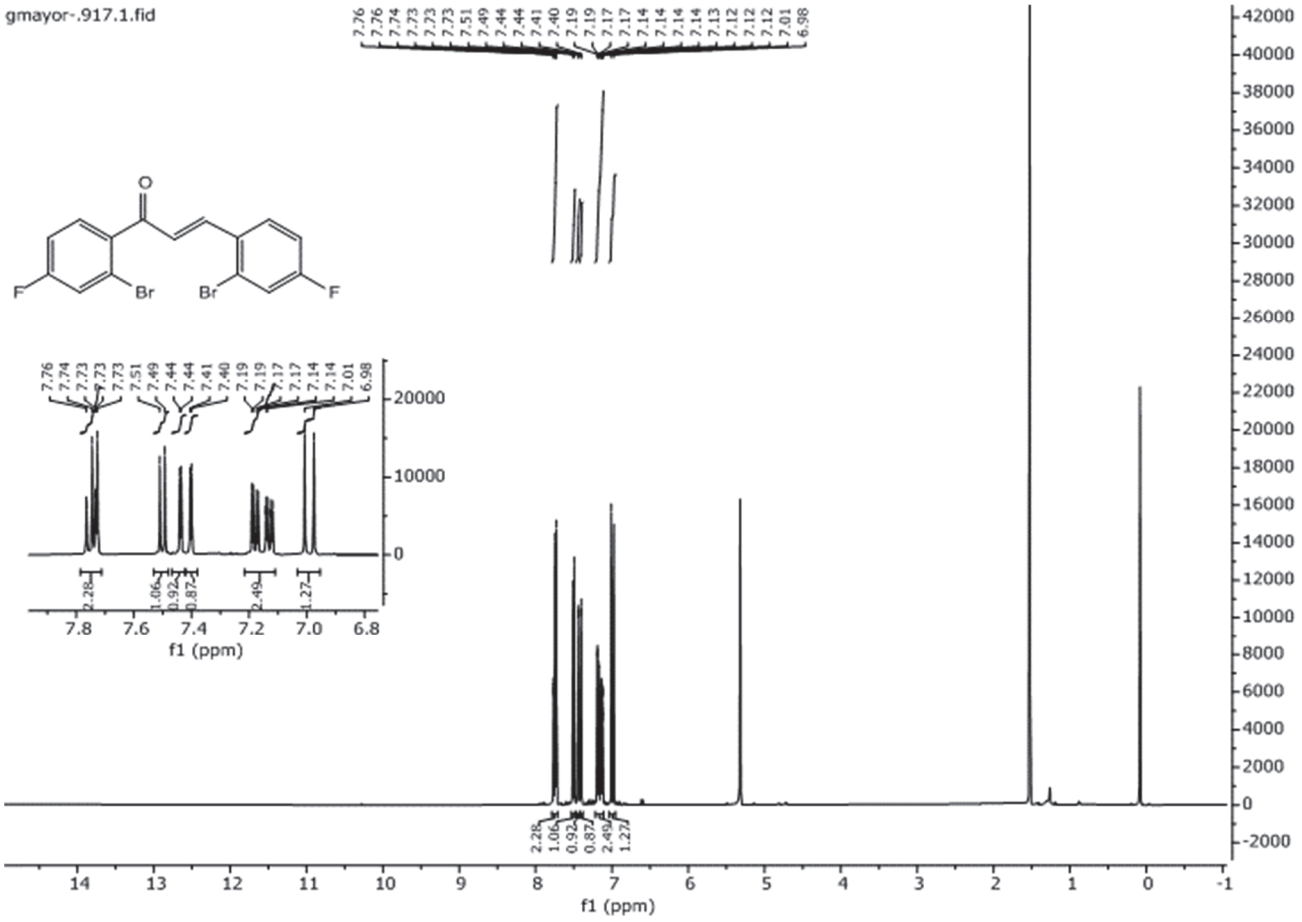

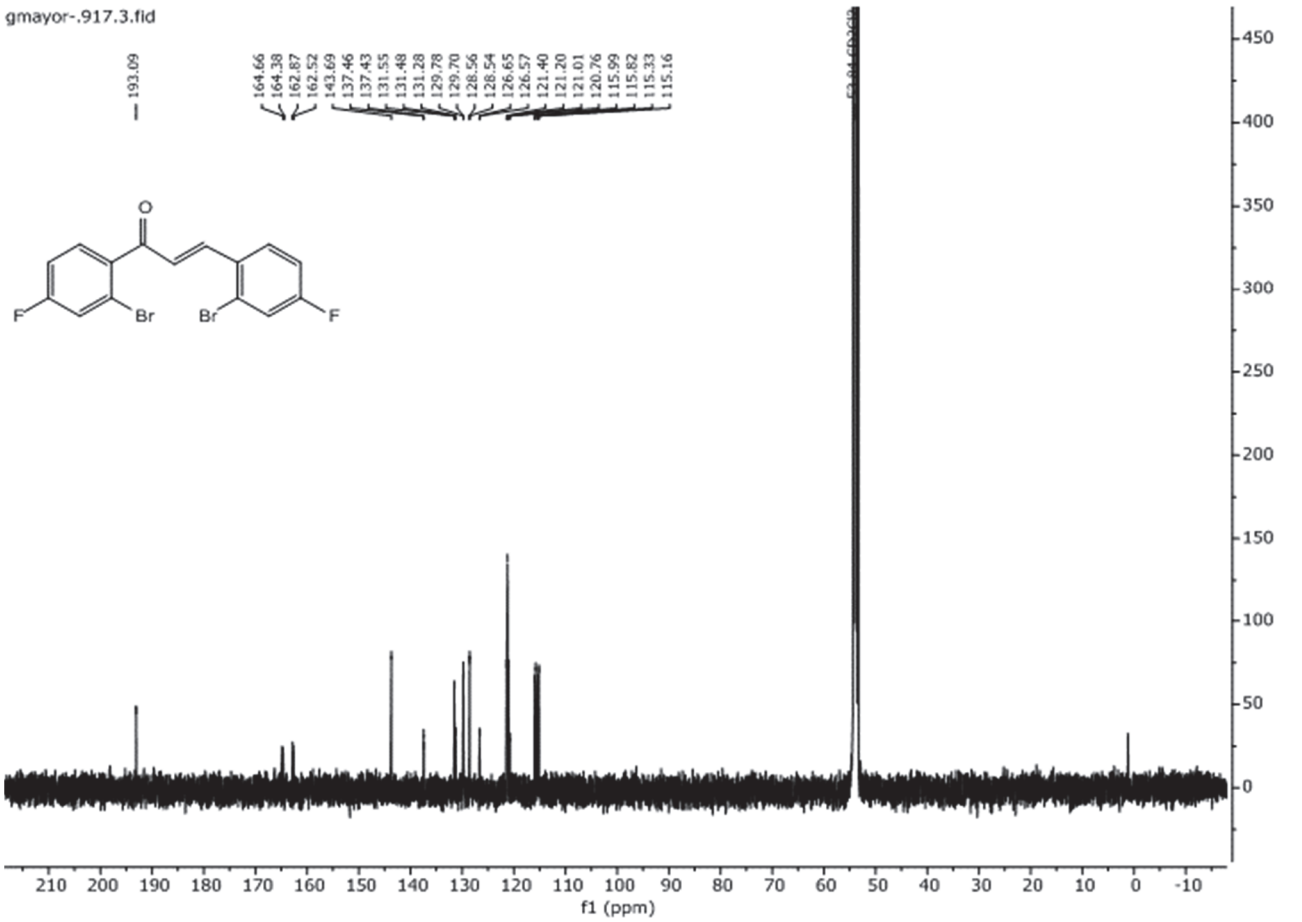

$^{1}H\{^{19}F\}$ NMR (400 MHz, $CDCl_3$) of **21** and $^{1}H\{^{19}F\}$ NMR (250 MHz, $CDCl_3$) of **18**

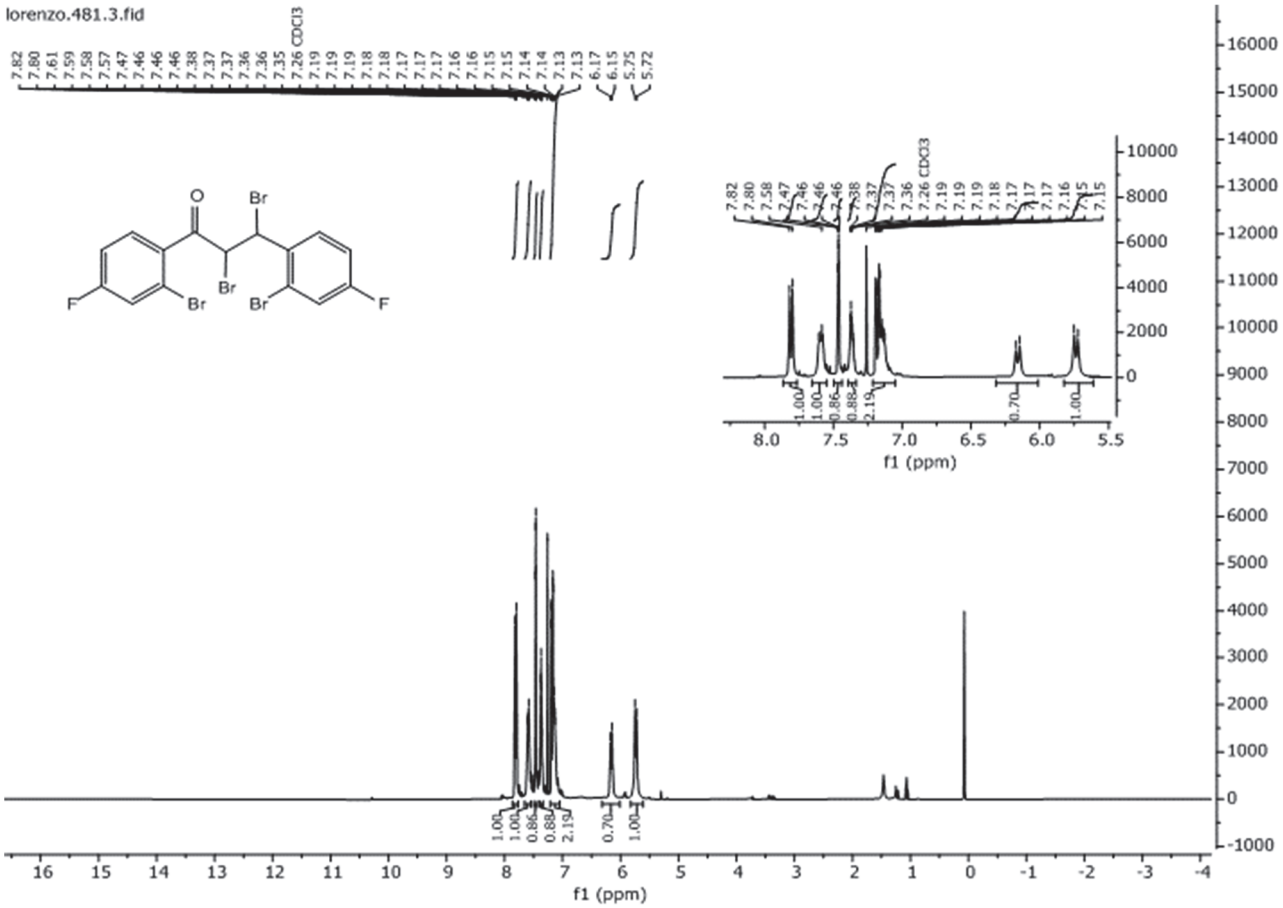

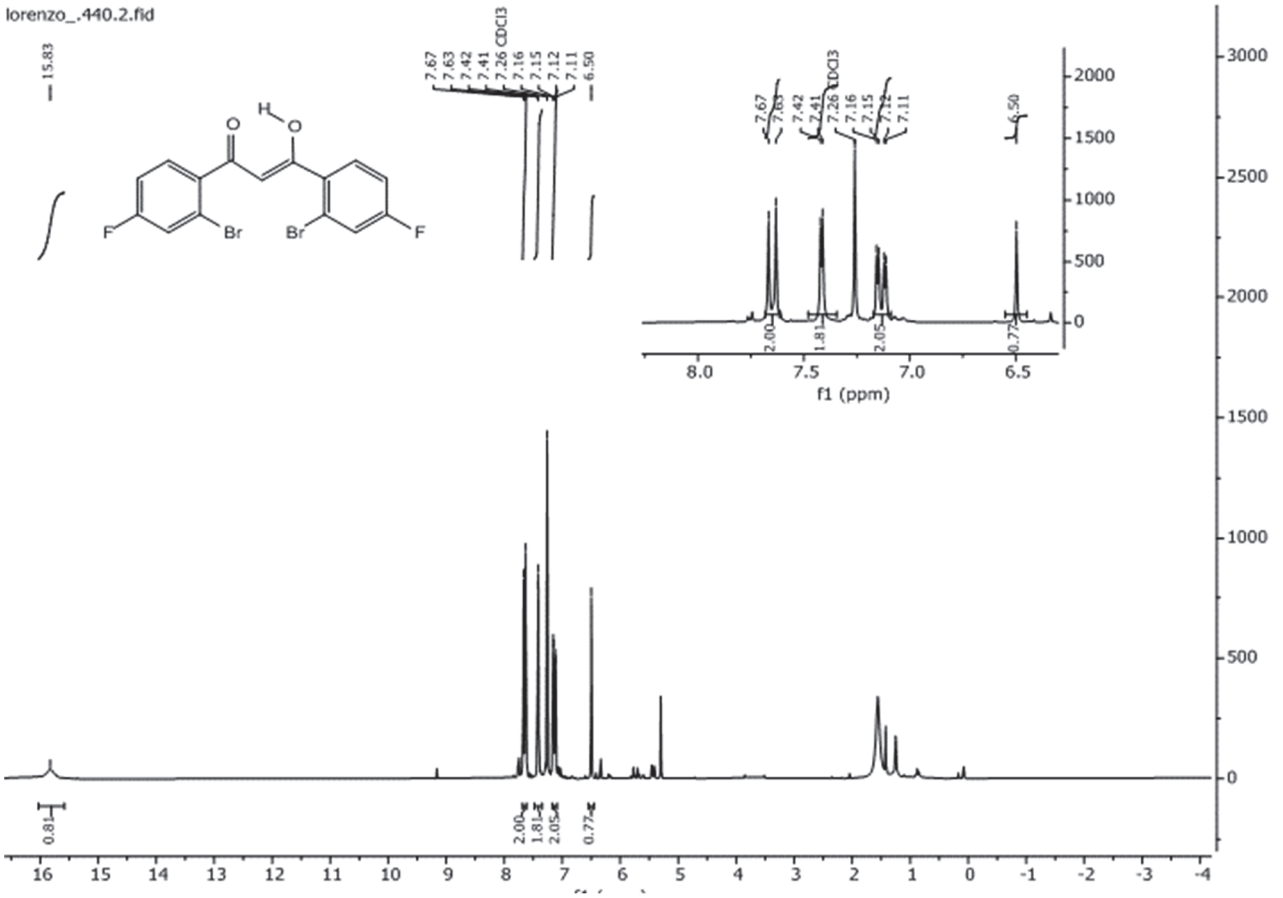

$^{1}H\{^{19}F\}$ NMR (400 MHz, CD_2Cl_2) of **17** and $^{1}H\{^{19}F\}$ NMR (500 MHz, $CDCl_3$) of **23**

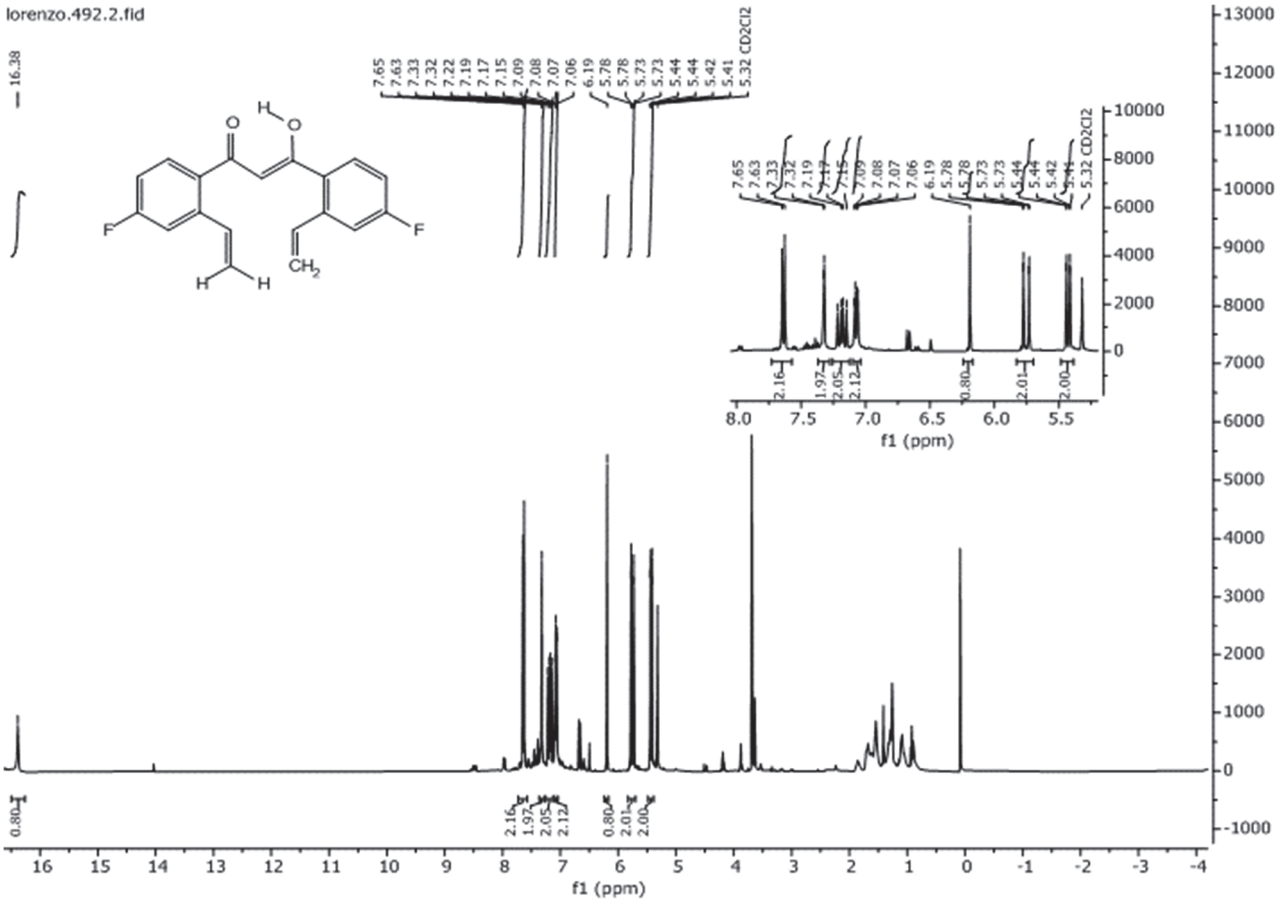

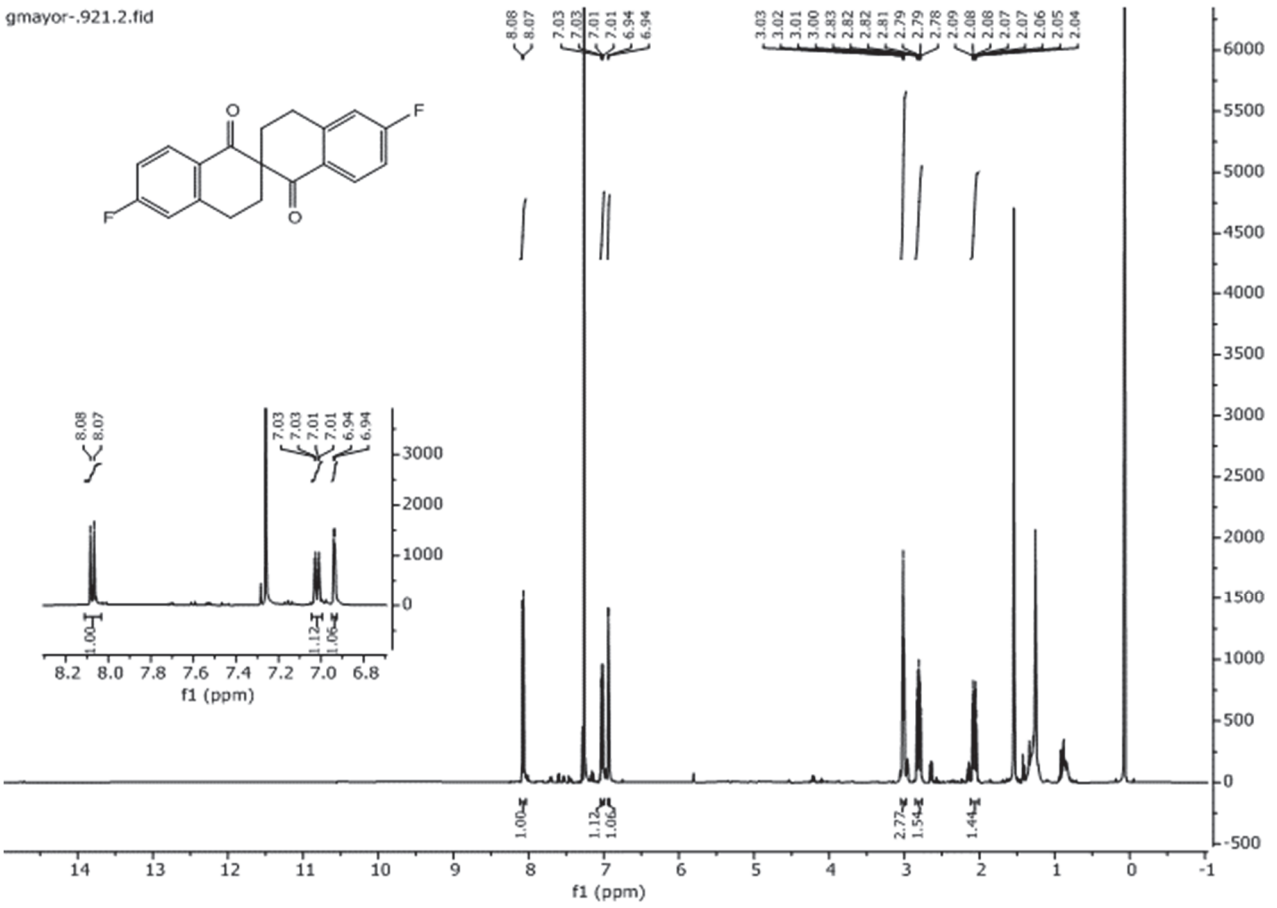

COSY NMR (500MHz, $CDCl_3$, 298K) and NOESY (500MHz, $CDCl_3$, 298K) of **23**

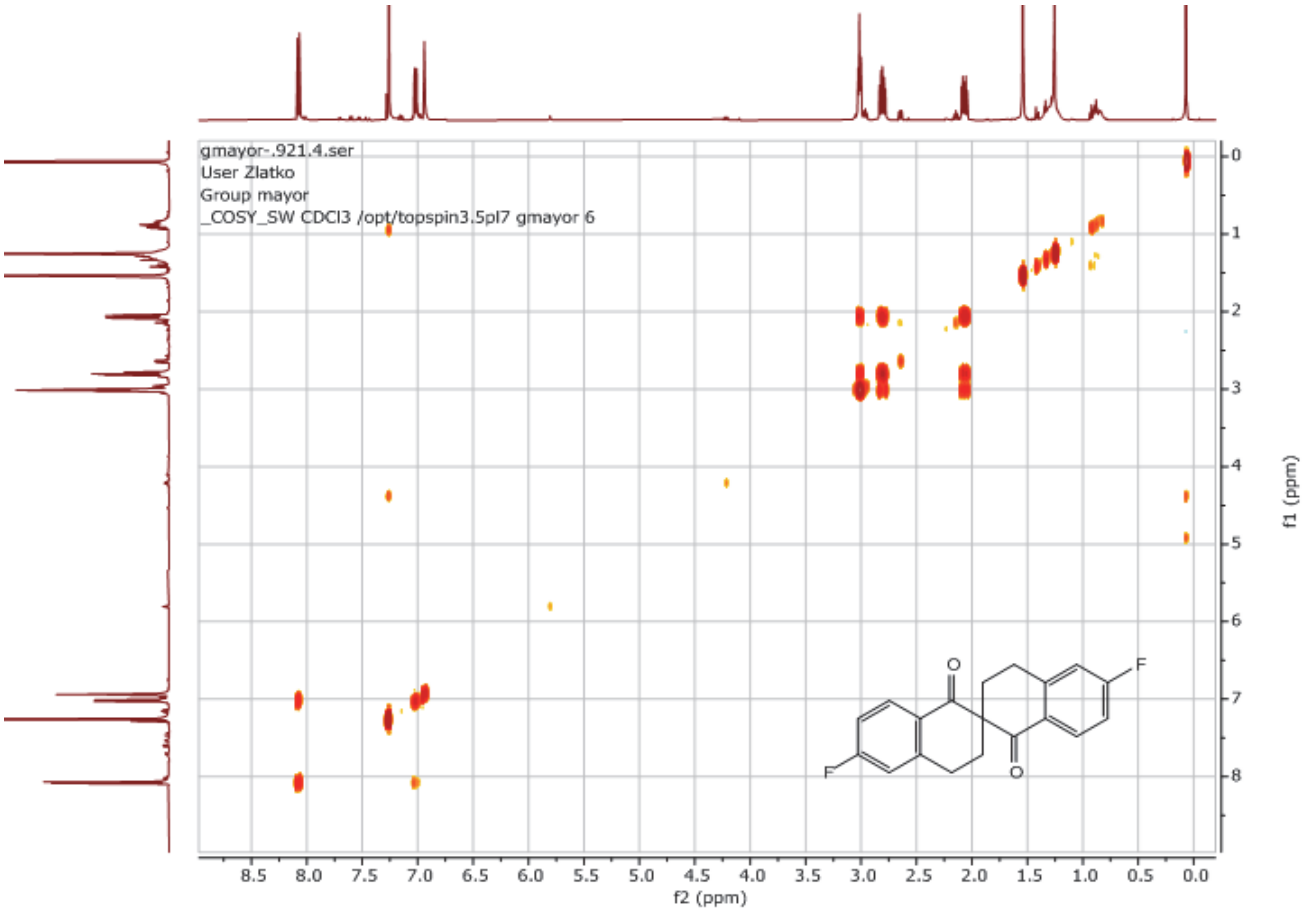

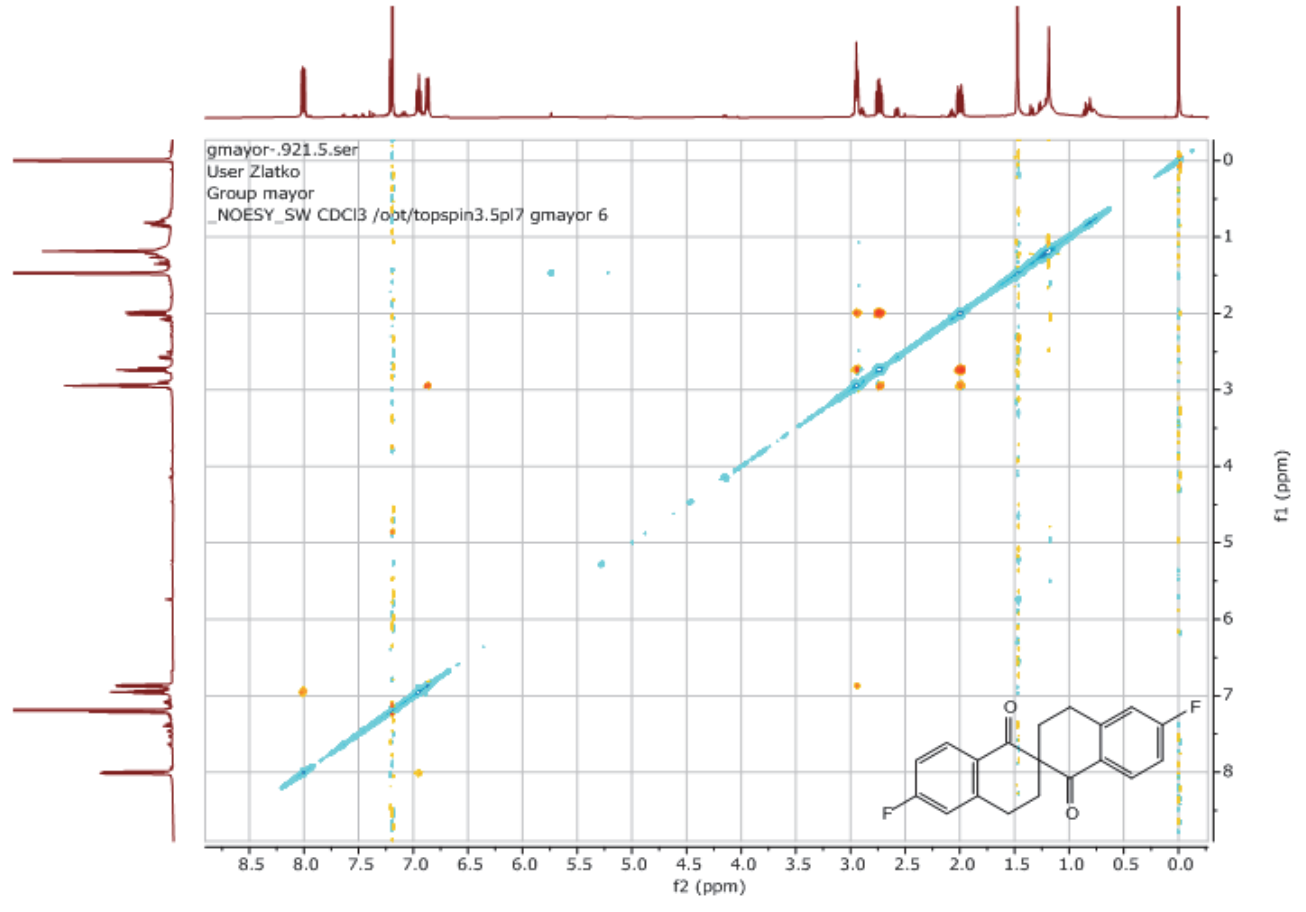

HMQC NMR (500MHz, $CDCl_3$, 298K) and HMBC (500MHz, $CDCl_3$, 298K) of **23**

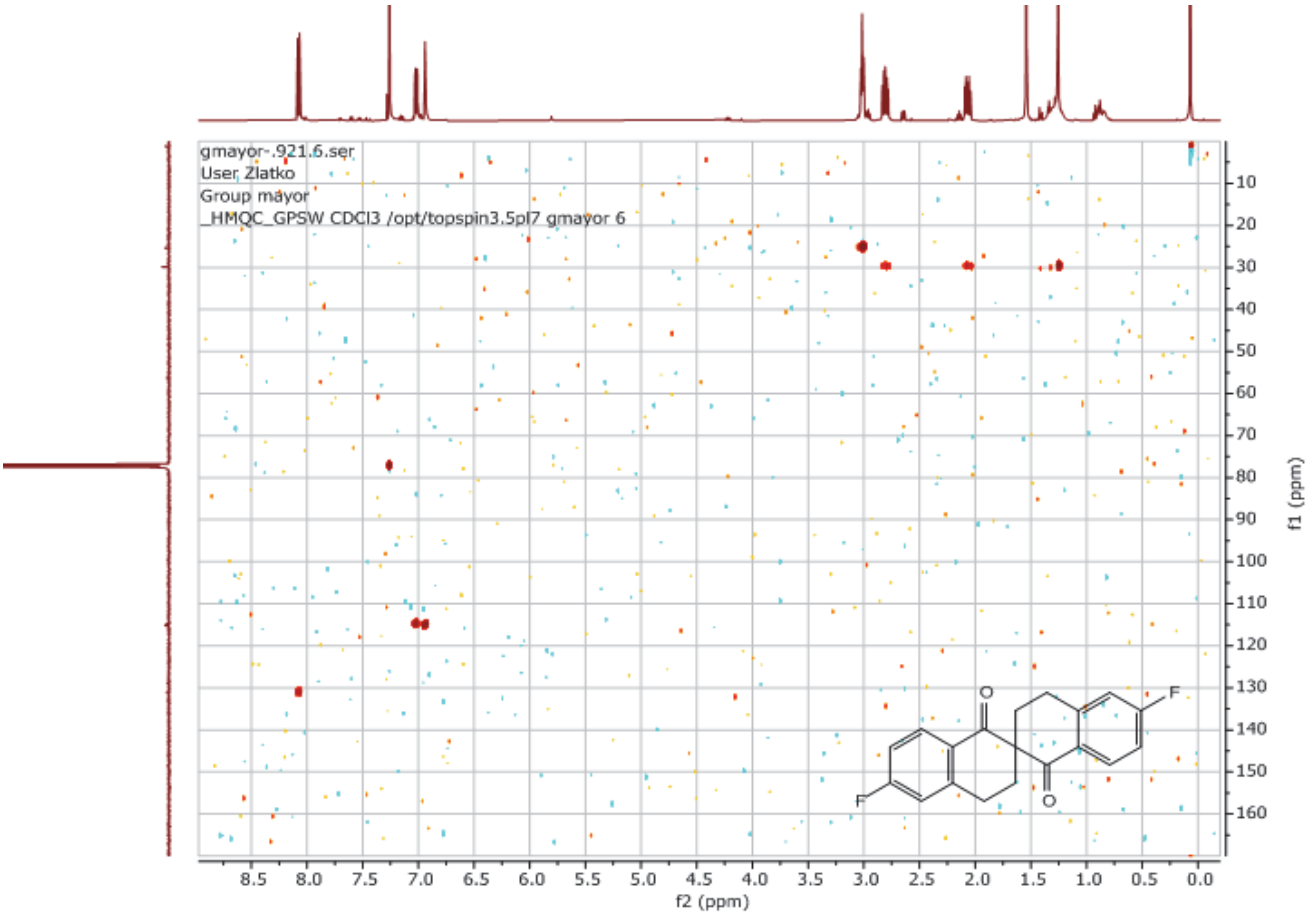

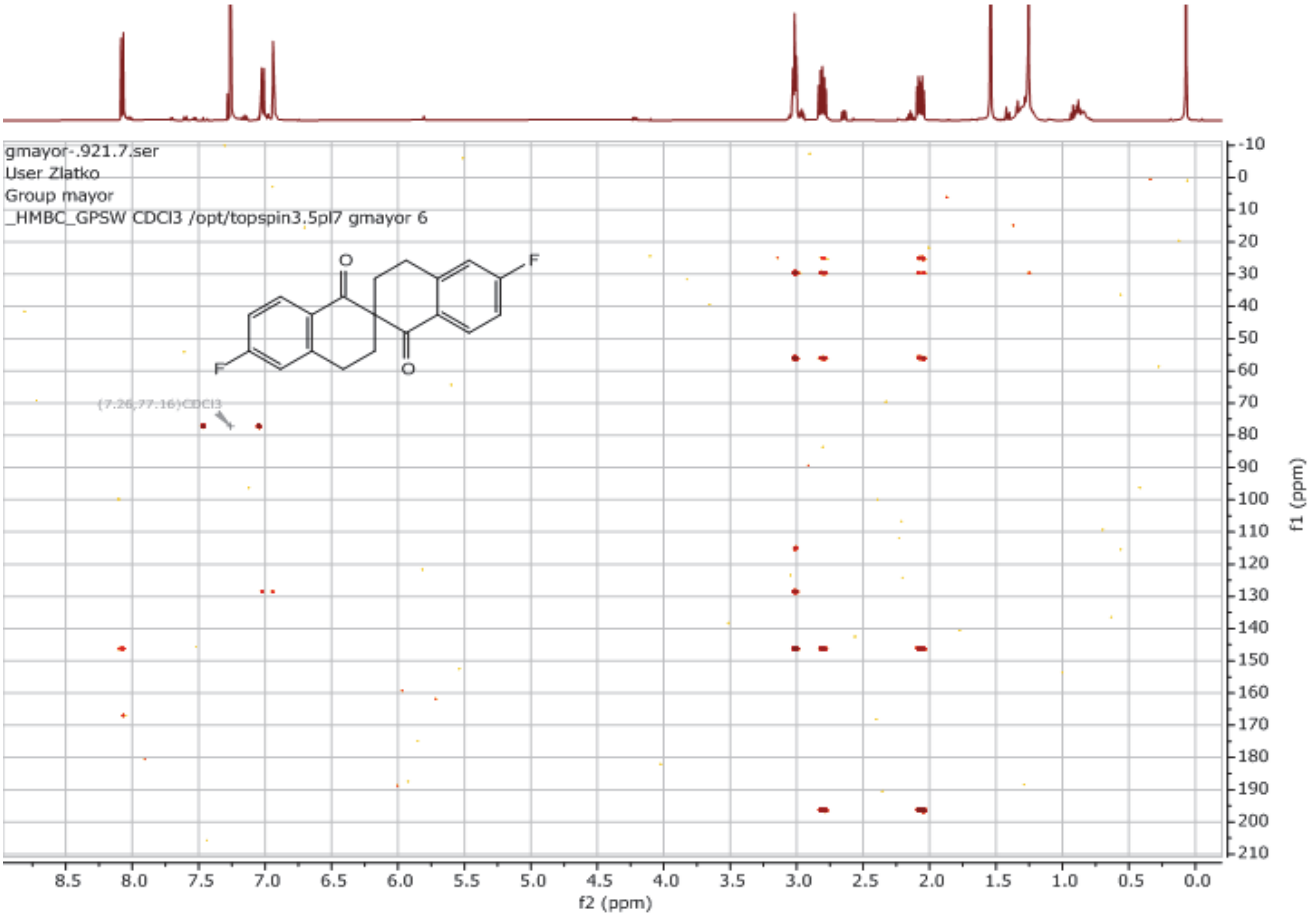

^{1}H NMR (400 MHz, $CDCl_3$) of **46**

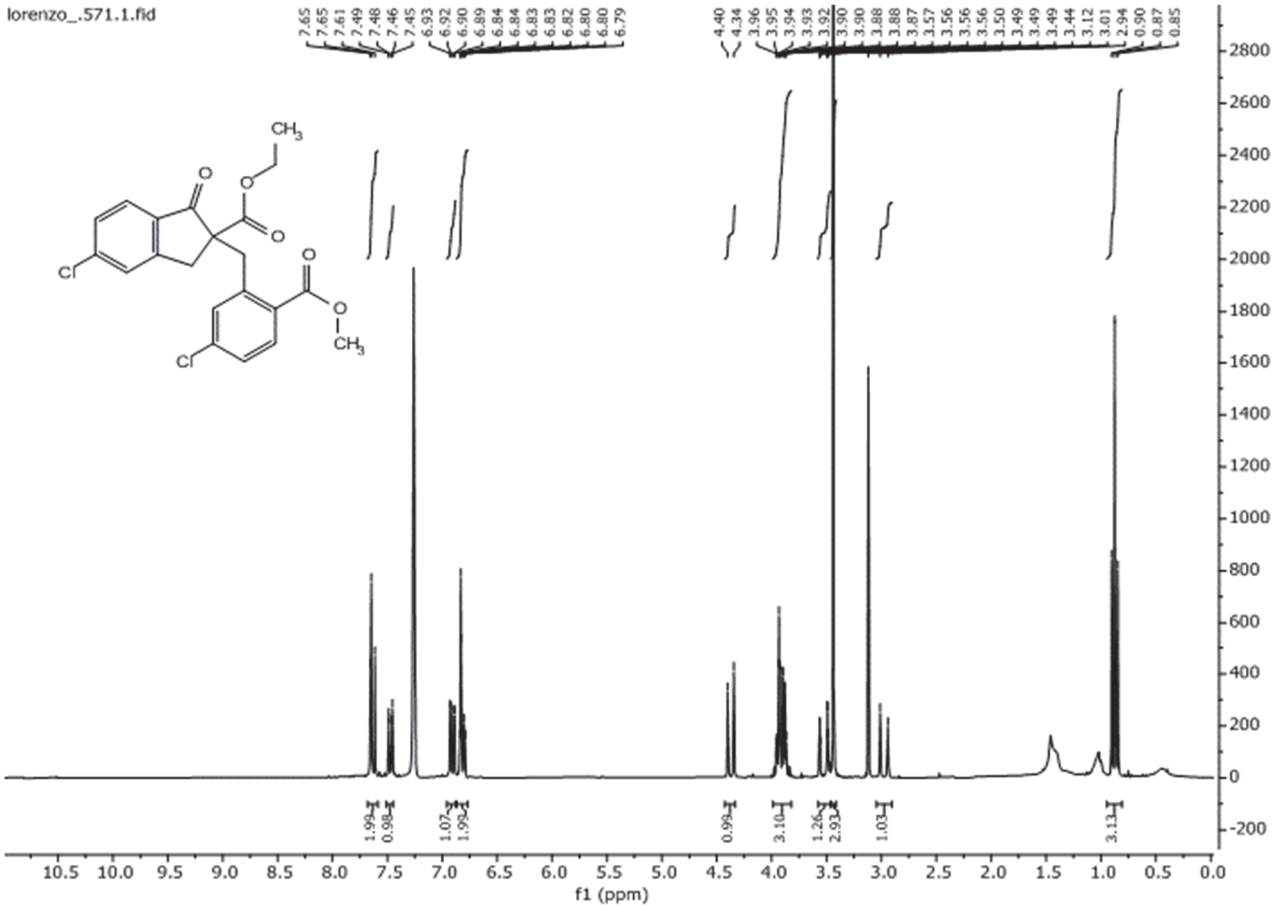

^{1}H NMR (400 MHz, $CDCl_3$) and ^{13}C NMR (151 MHz, $CDCl_3$) of **50**

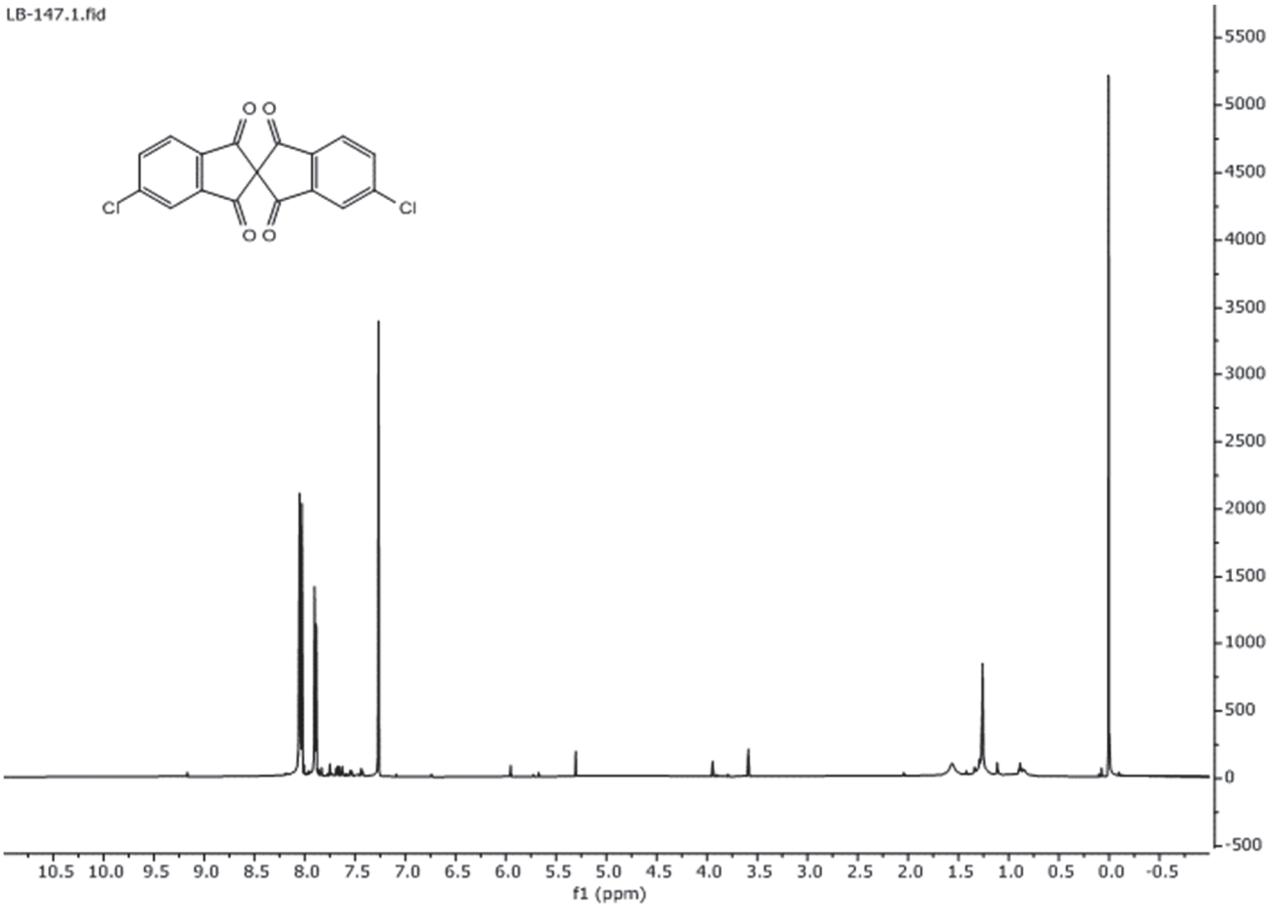

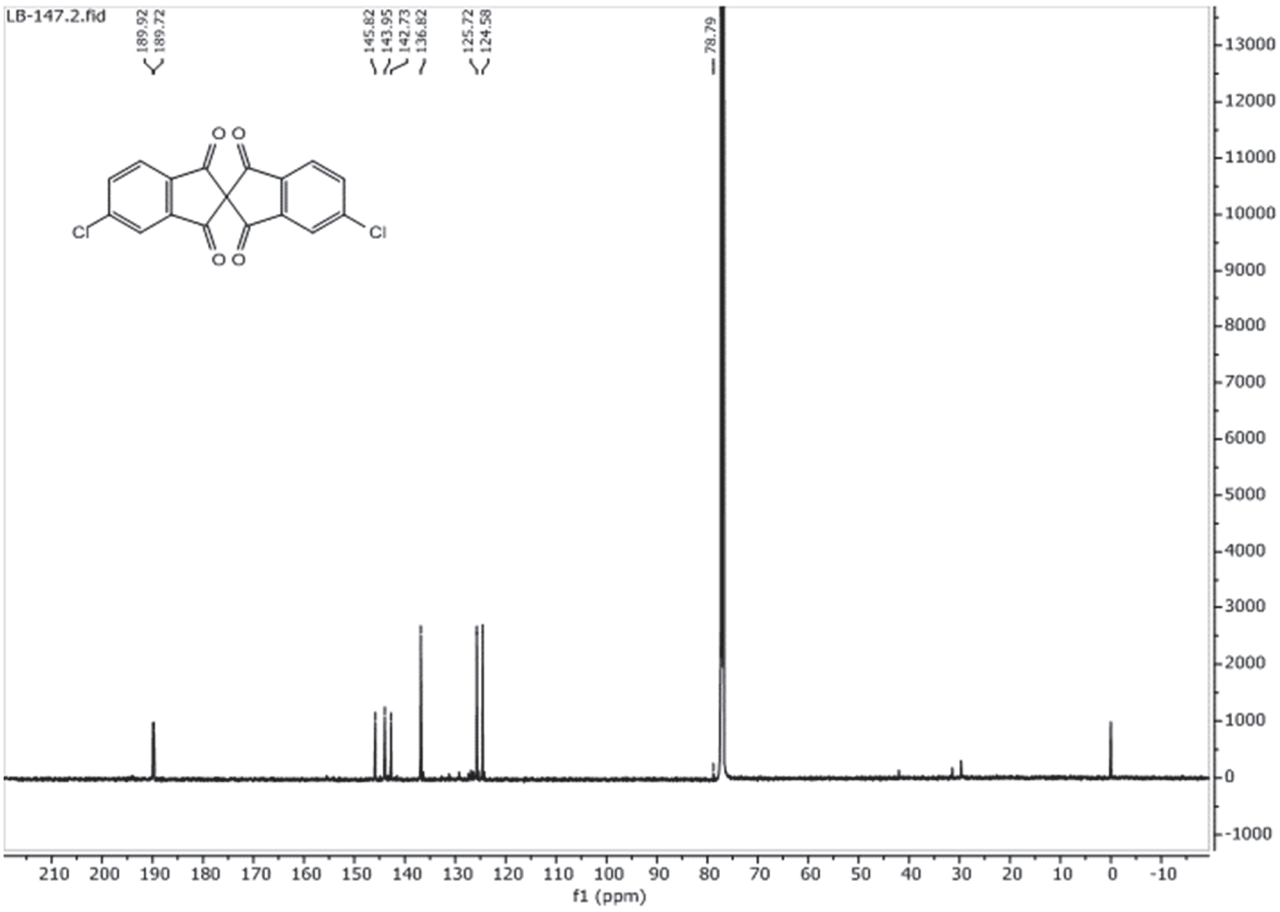

^{1}H NMR (250 MHz, $CDCl_3$) and ^{13}C NMR (63 MHz, $CDCl_3$) of **47**

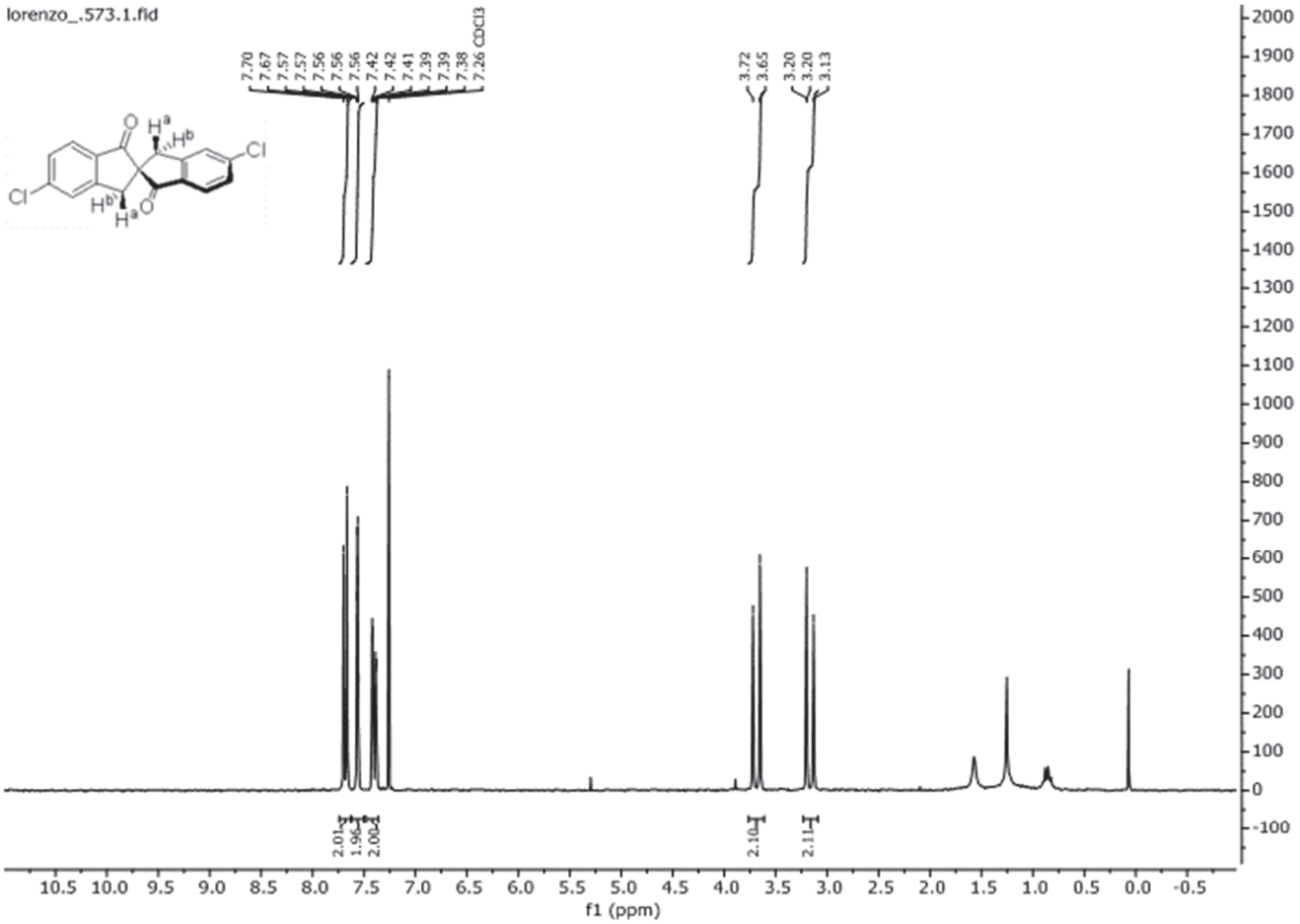

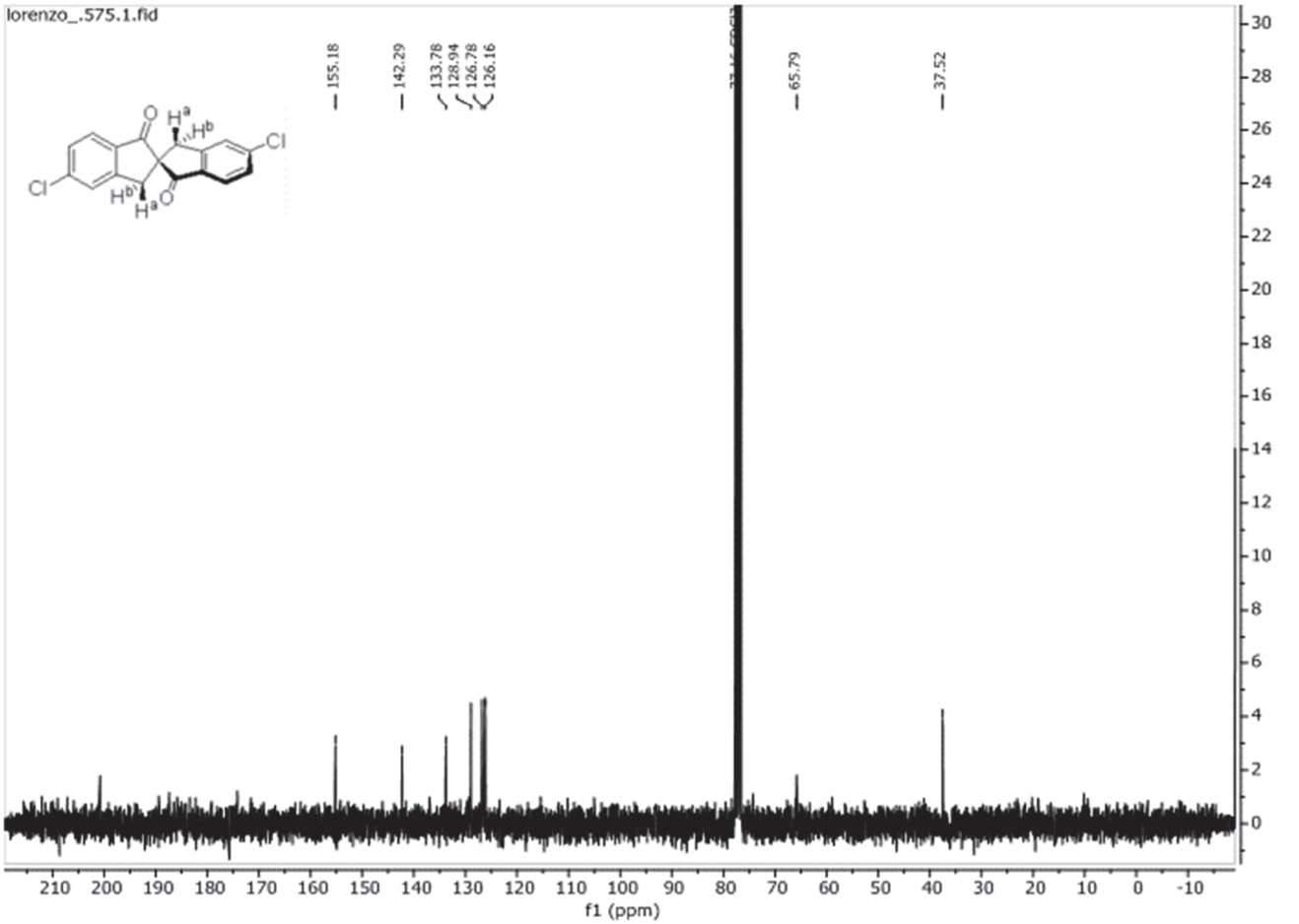

^{1}H NMR (500 MHz, $CDCl_3$) and ^{13}C NMR (126 MHz, $CDCl_3$) of **49**

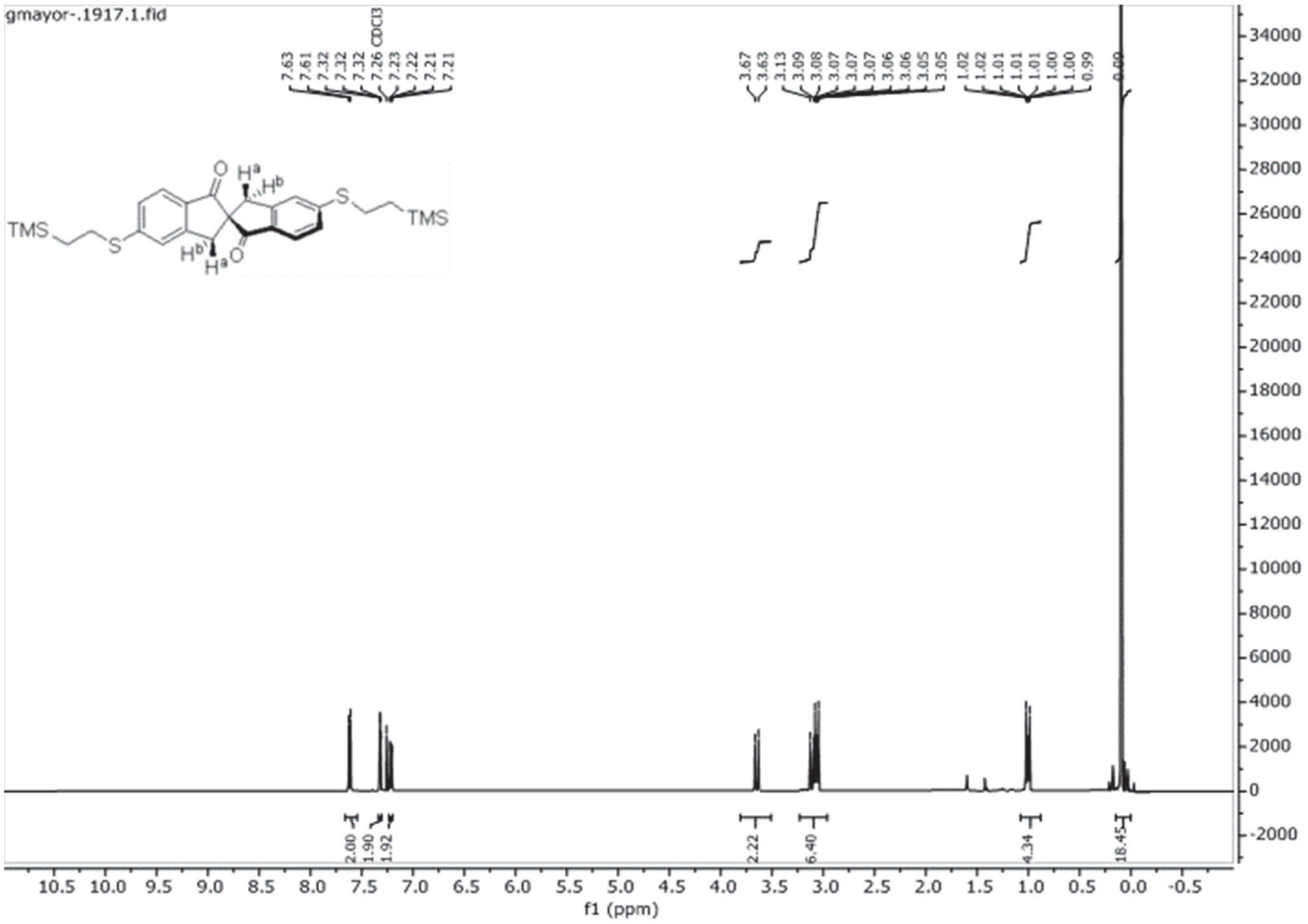

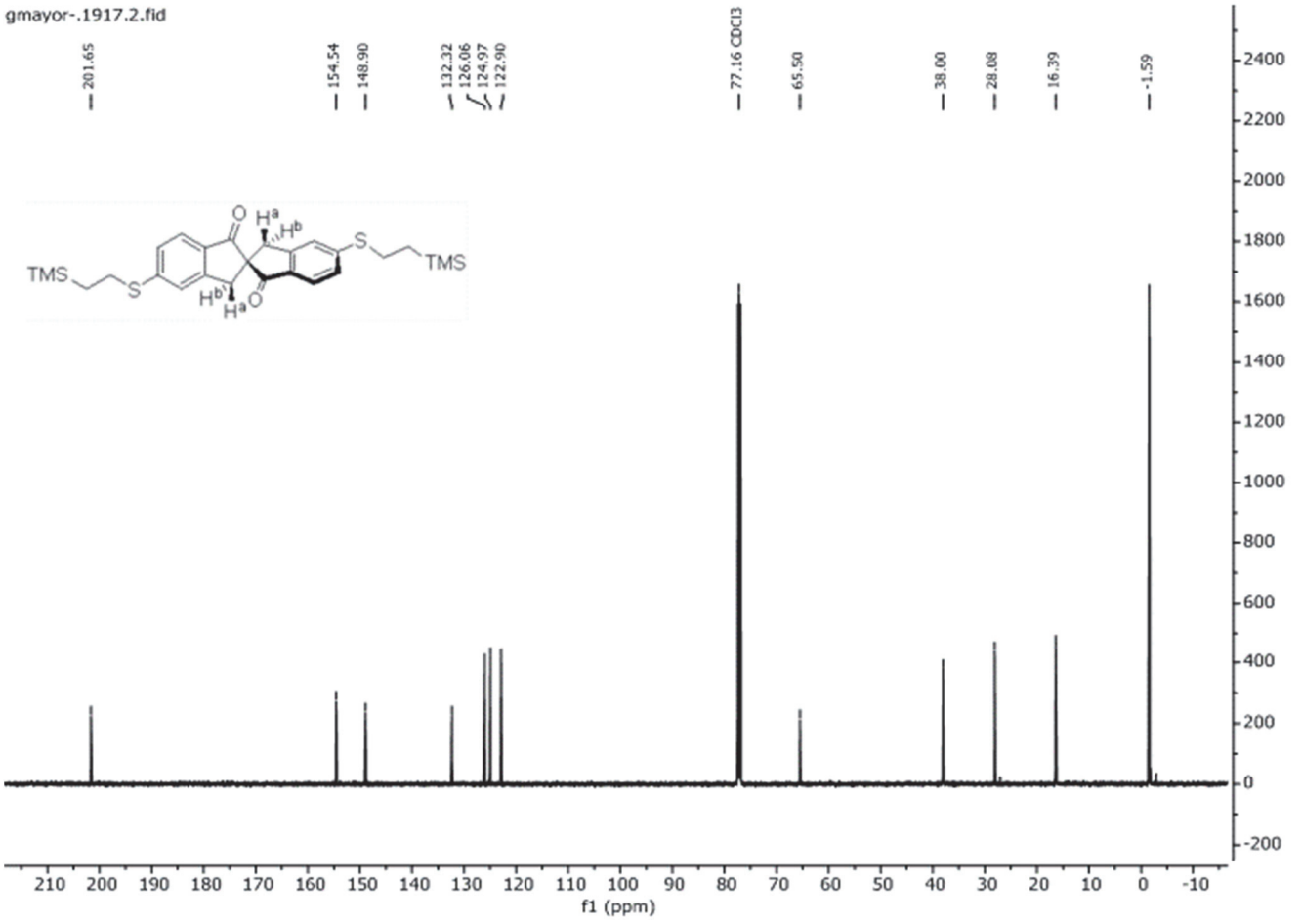

^{1}H

NMR (250 MHz, $CDCl_3$) of **48**

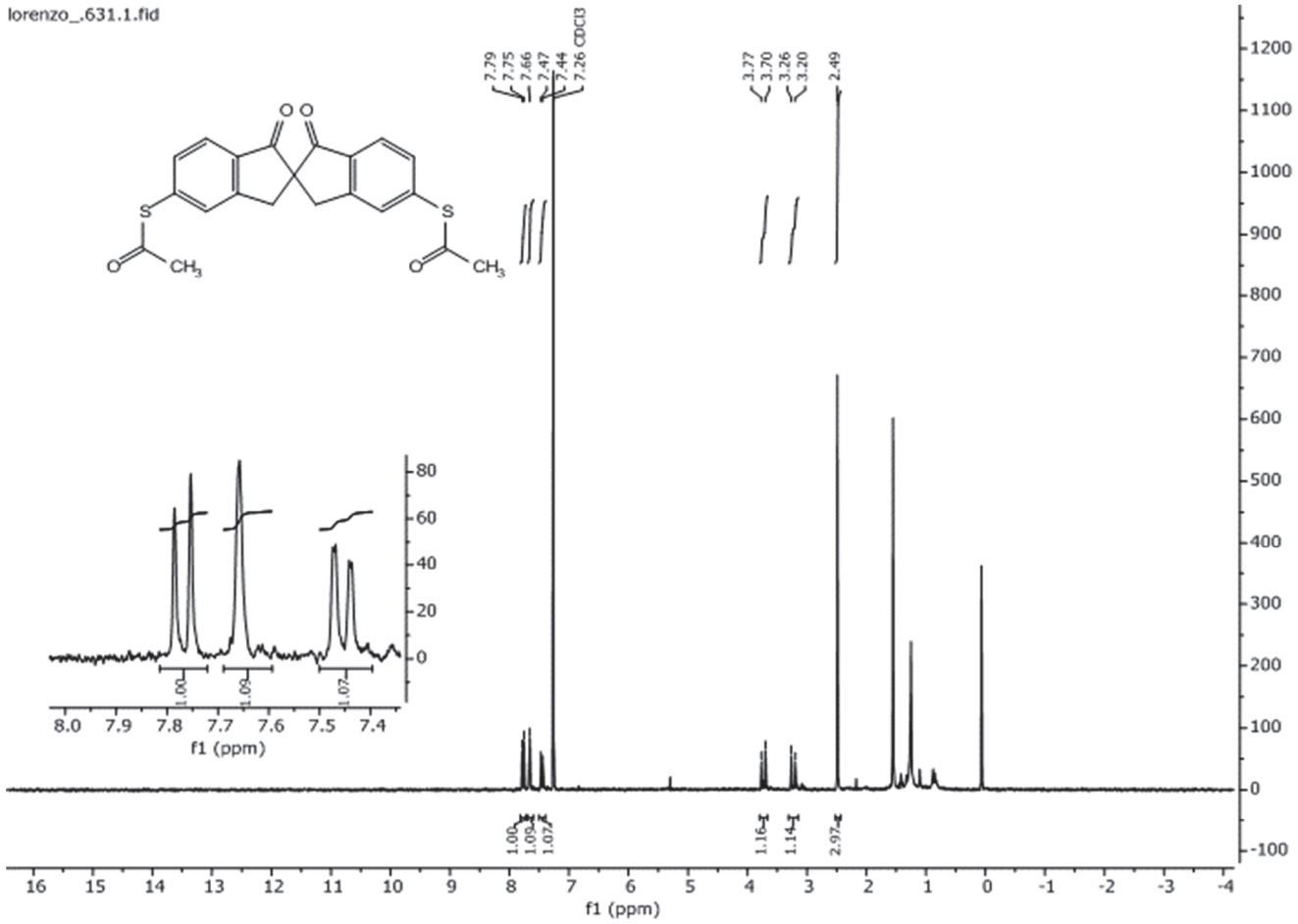

^{1}H NMR (250 MHz, $CDCl_3$) of **53** and ^{1}H NMR (250 MHz, $CDCl_3$) of **56**

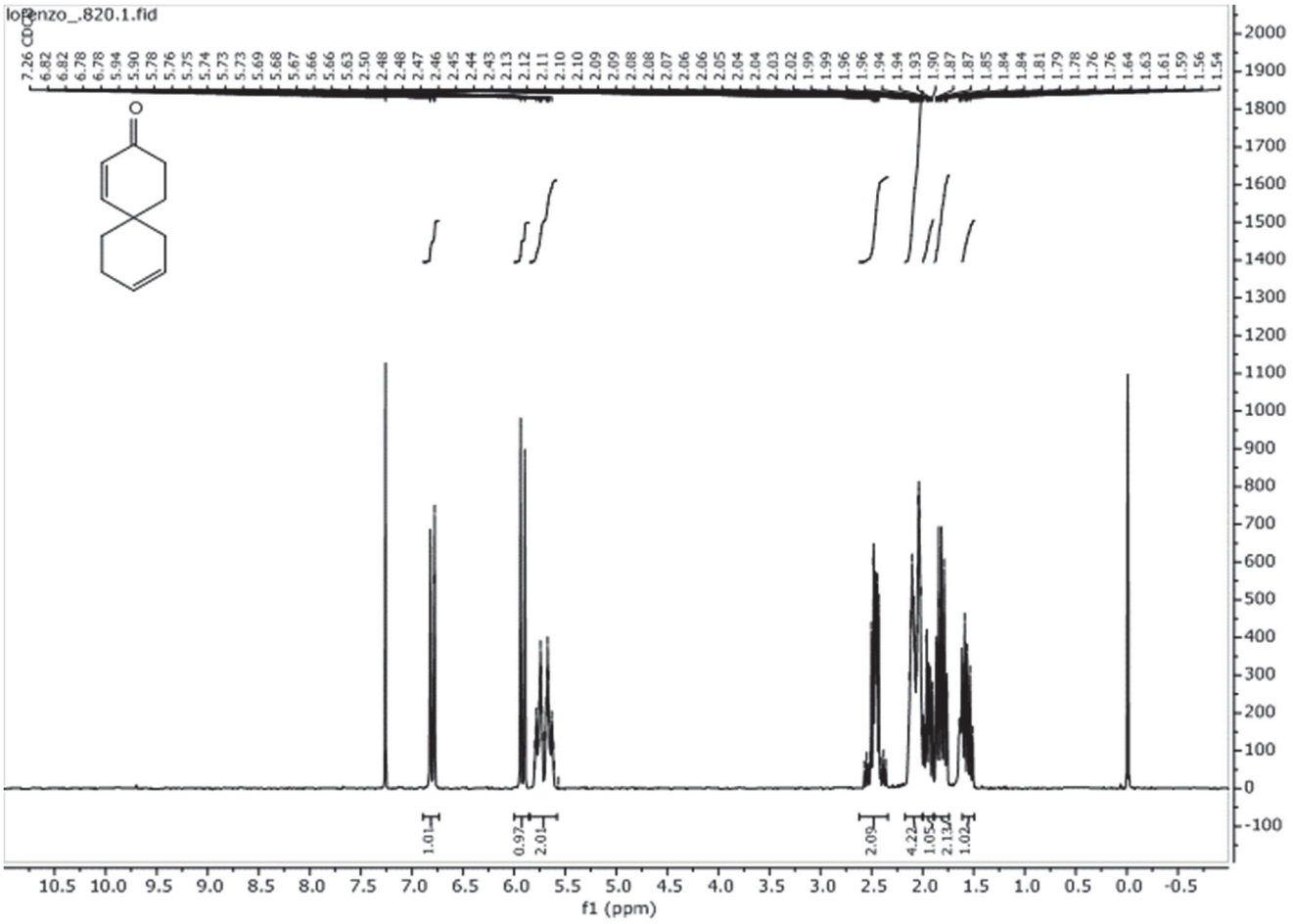

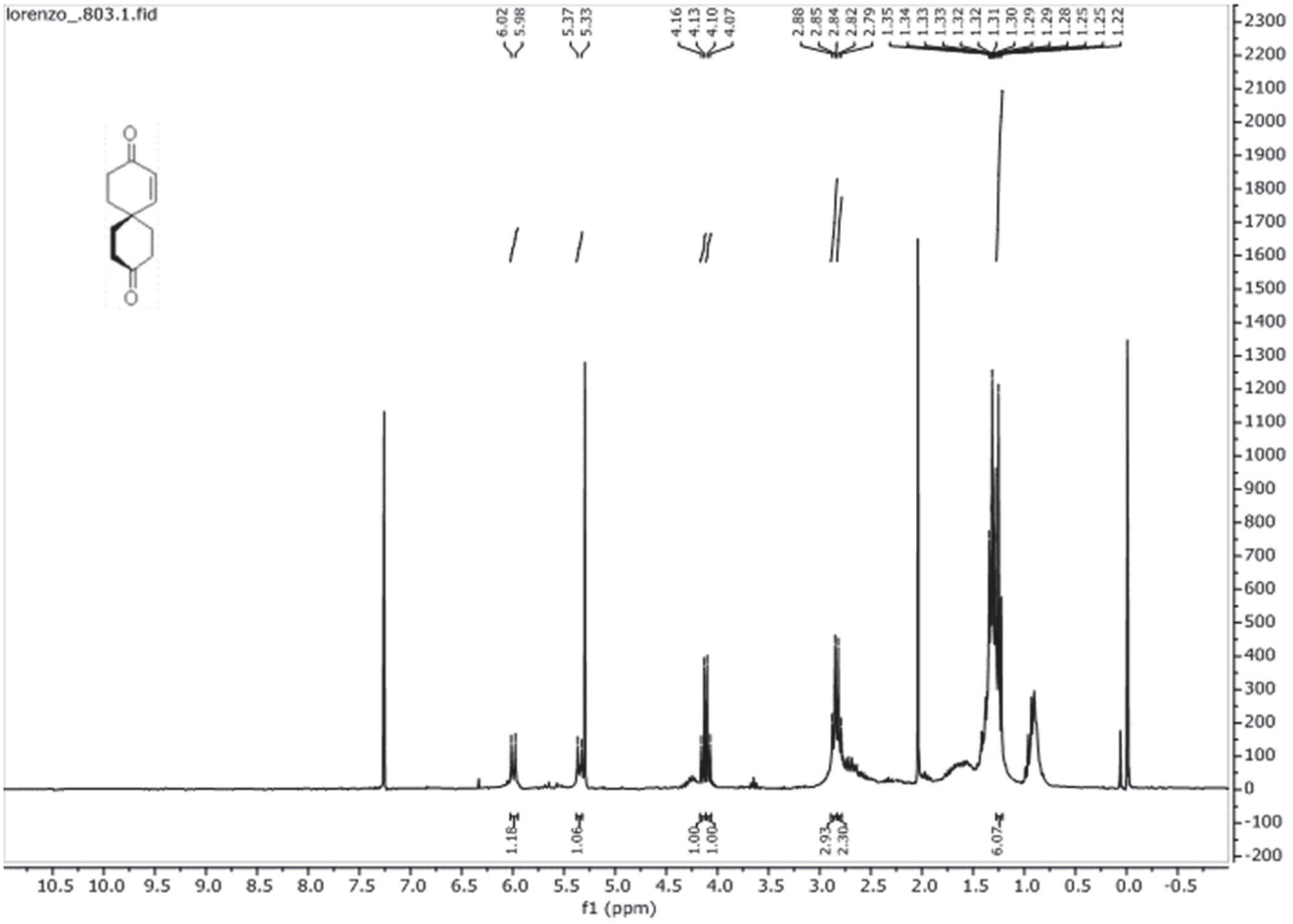

^{1}H NMR (400 MHz, $CDCl_3$) of **7** and ^{1}H NMR (250 MHz, $CDCl_3$) of **57**

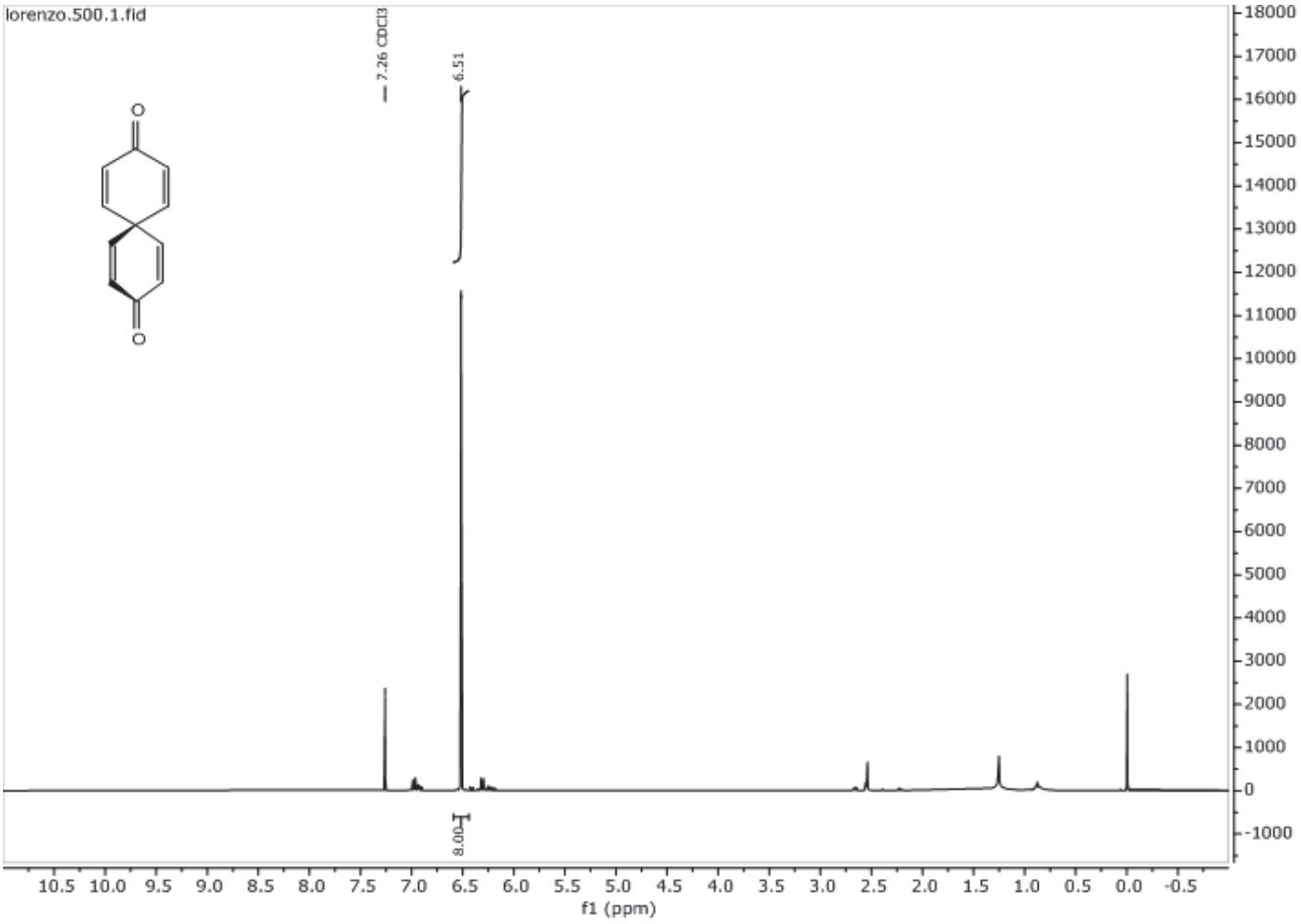

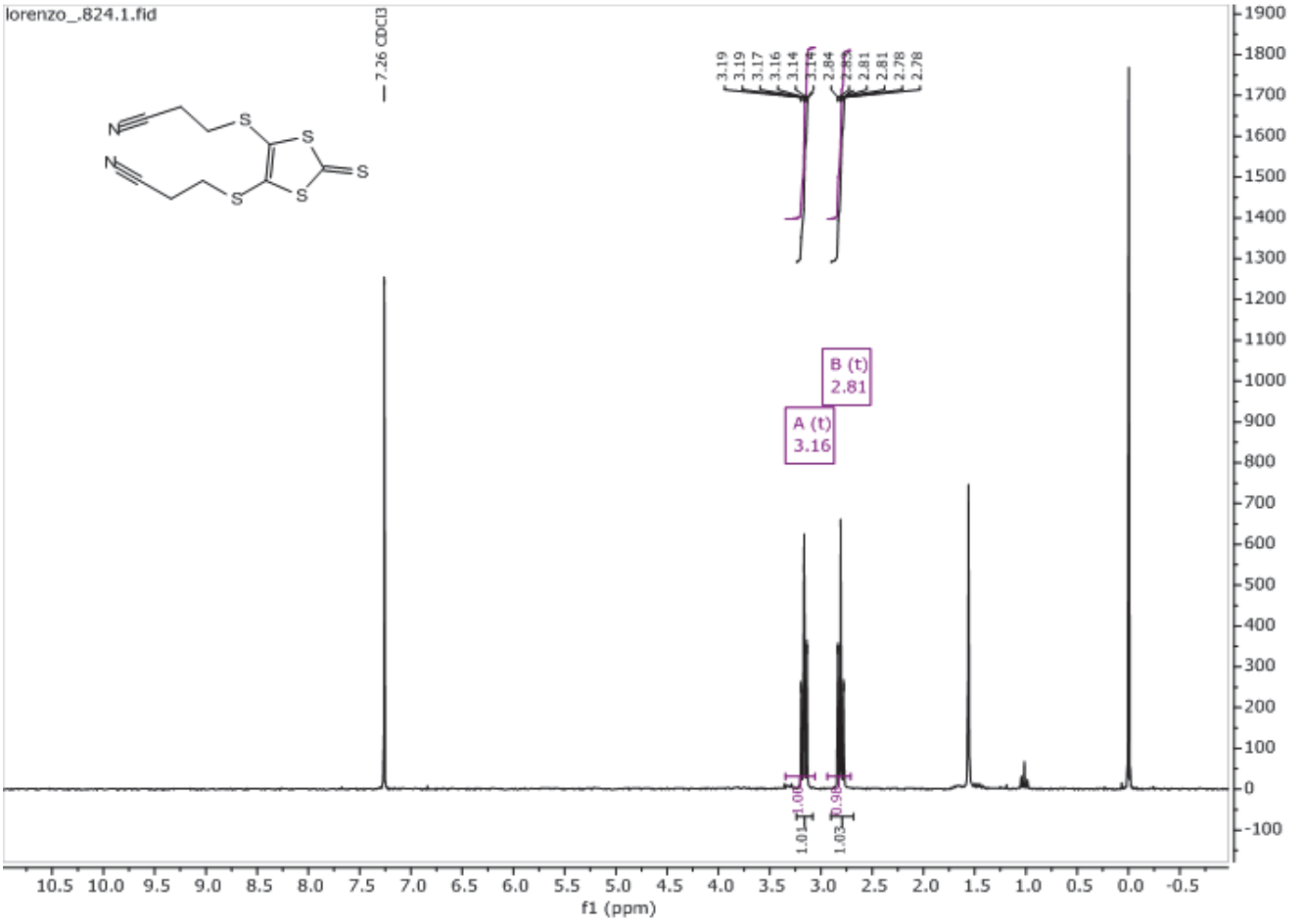

^{1}H NMR (250 MHz, $CDCl_3$) of **58** and ^{1}H NMR (250 MHz, $CDCl_3$) of **59**

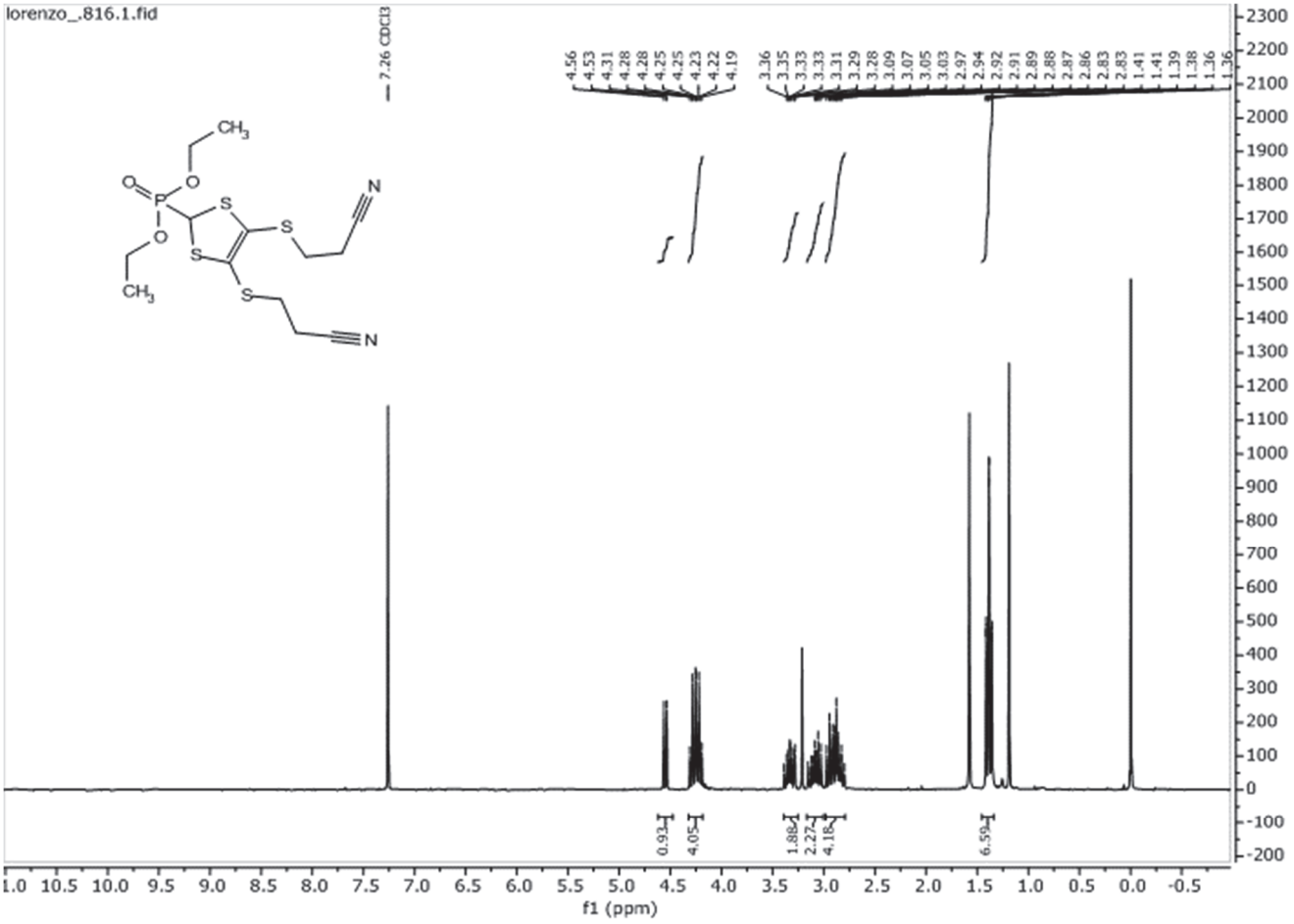

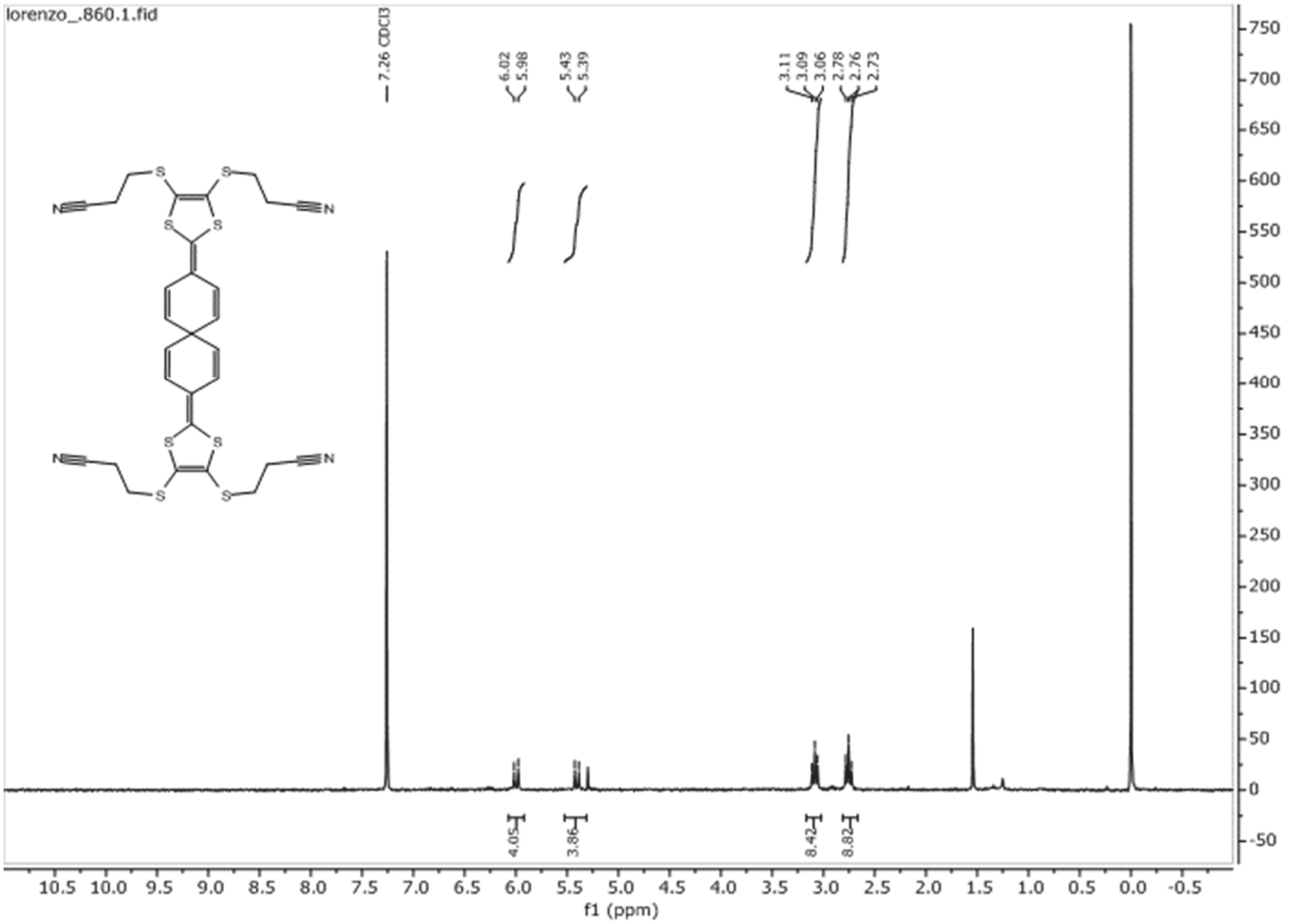

^{1}H NMR (400 MHz, $CDCl_3$) and ^{13}C NMR (101 MHz, $CDCl_3$) of **52**

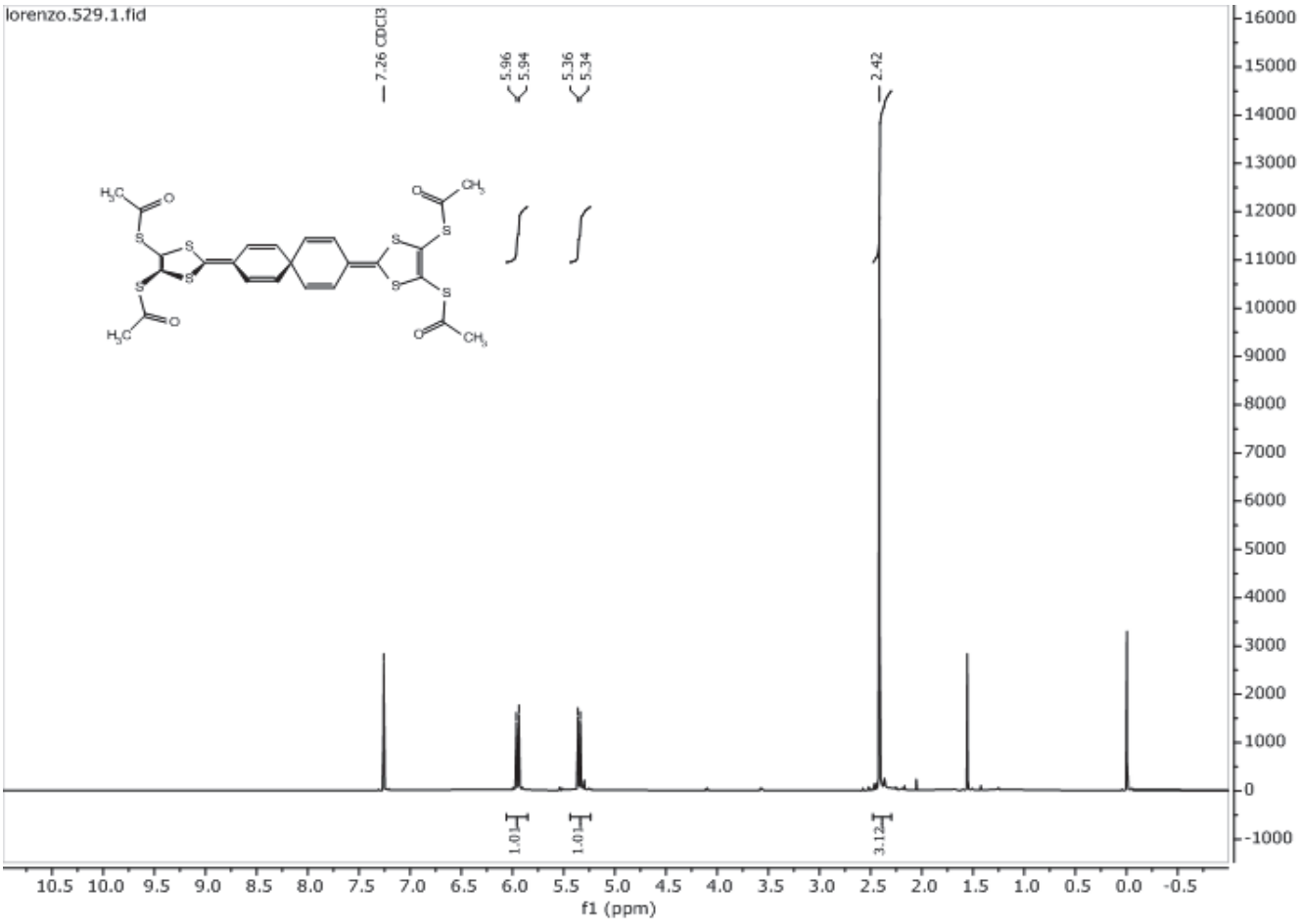

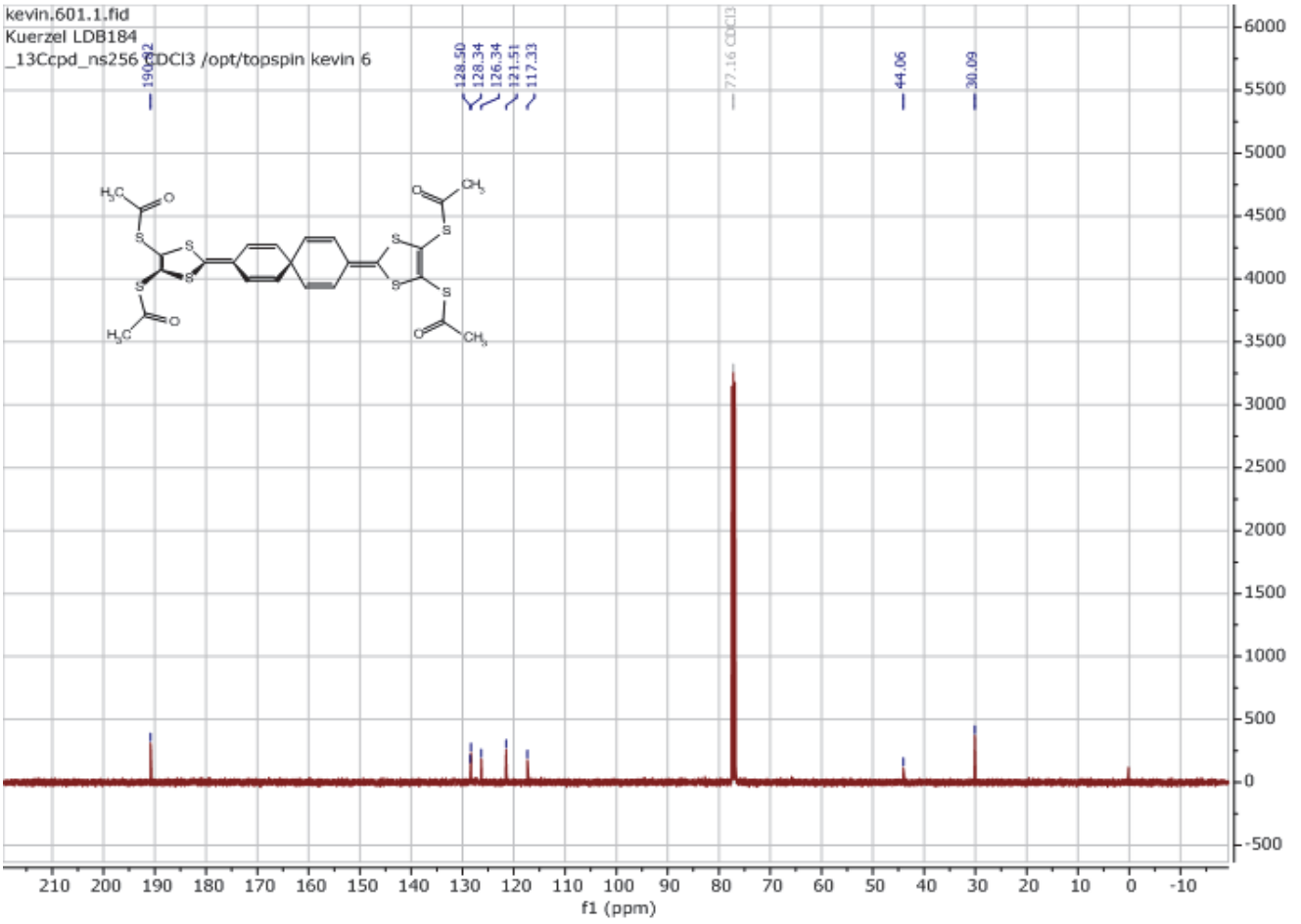

COSY (500 MHz, $CDCl_3$) and HMQC (500 MHz, $CDCl_3$) of **52**

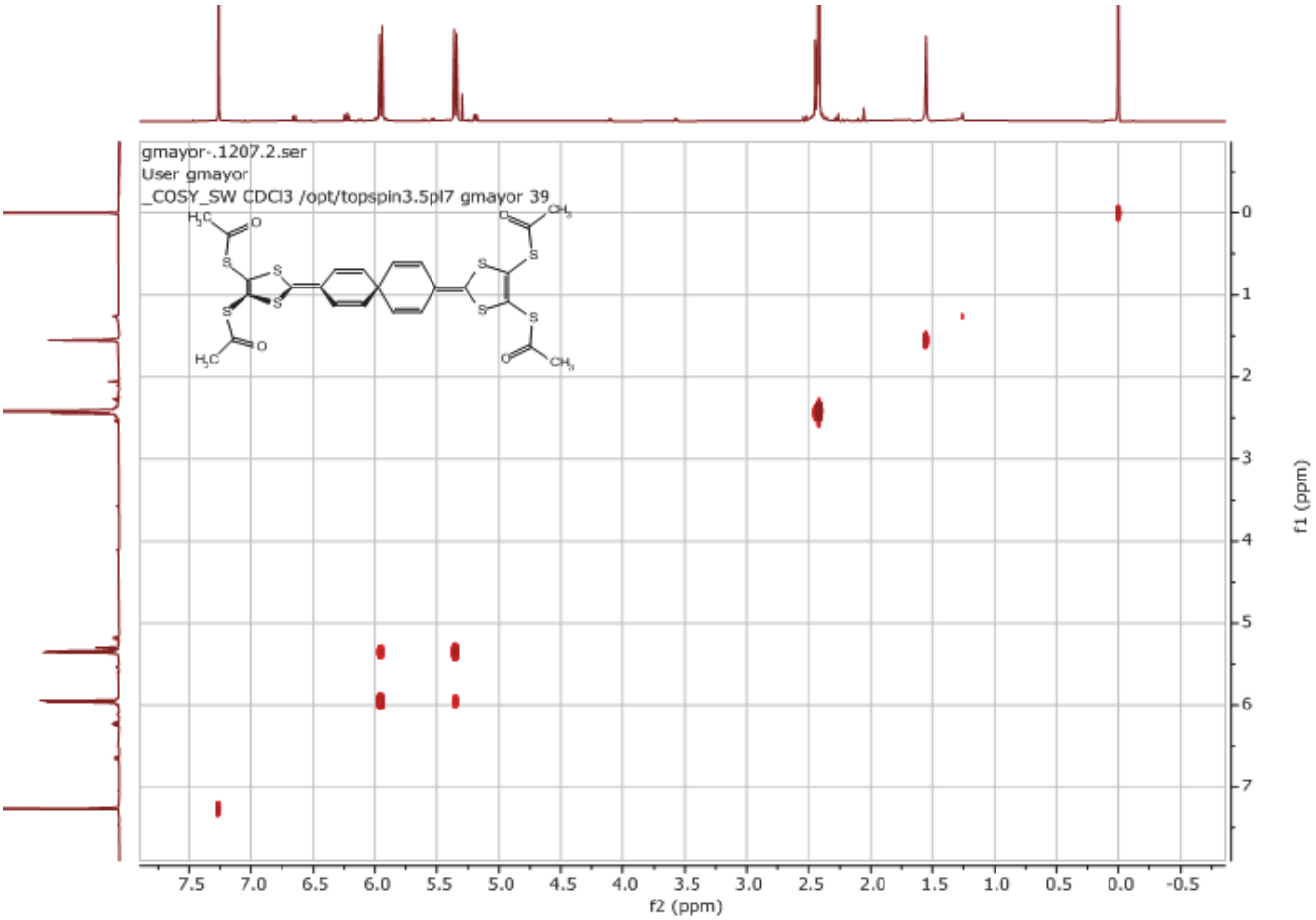

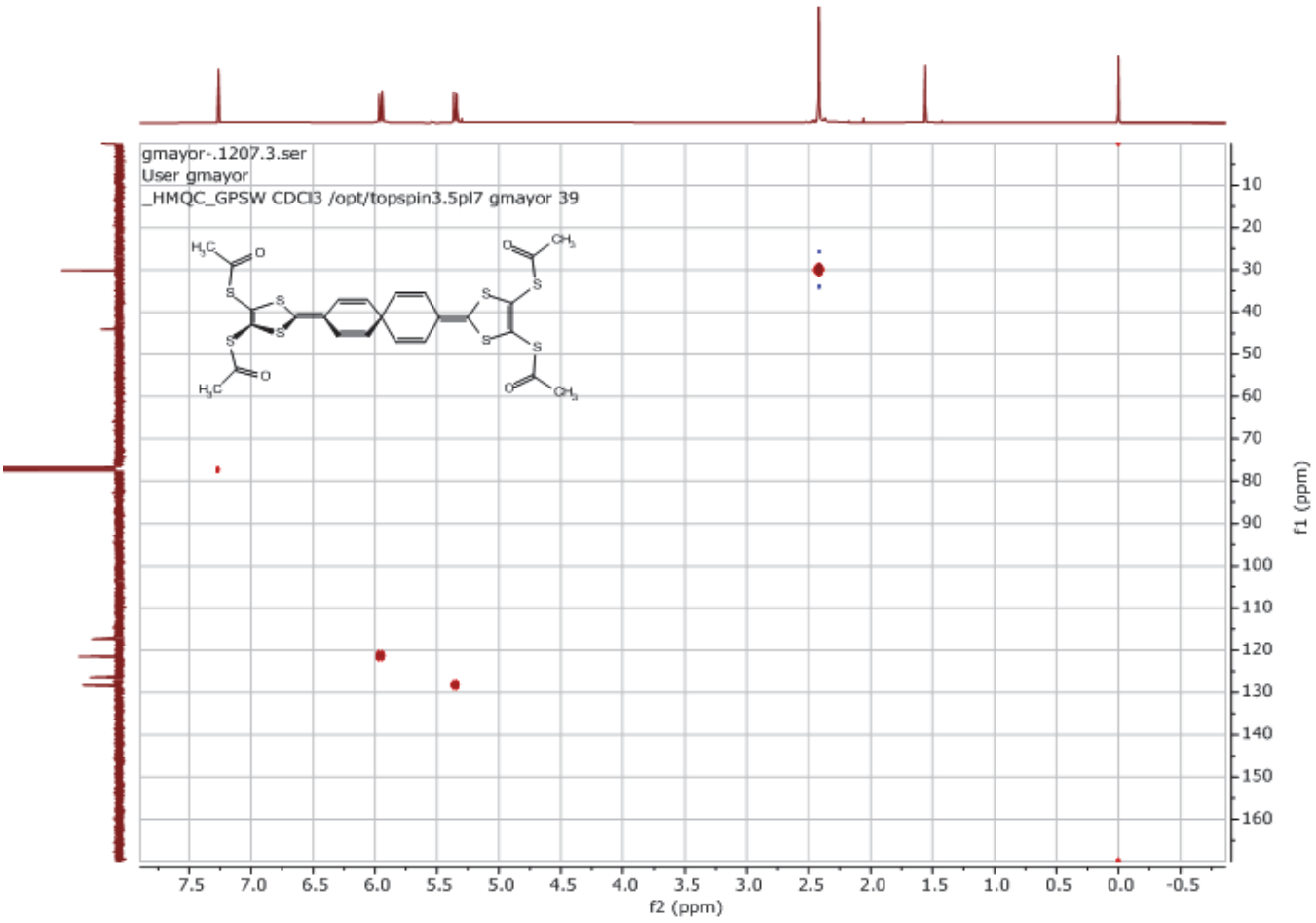

HMBC (500 MHz, $CDCl_3$) of **52**

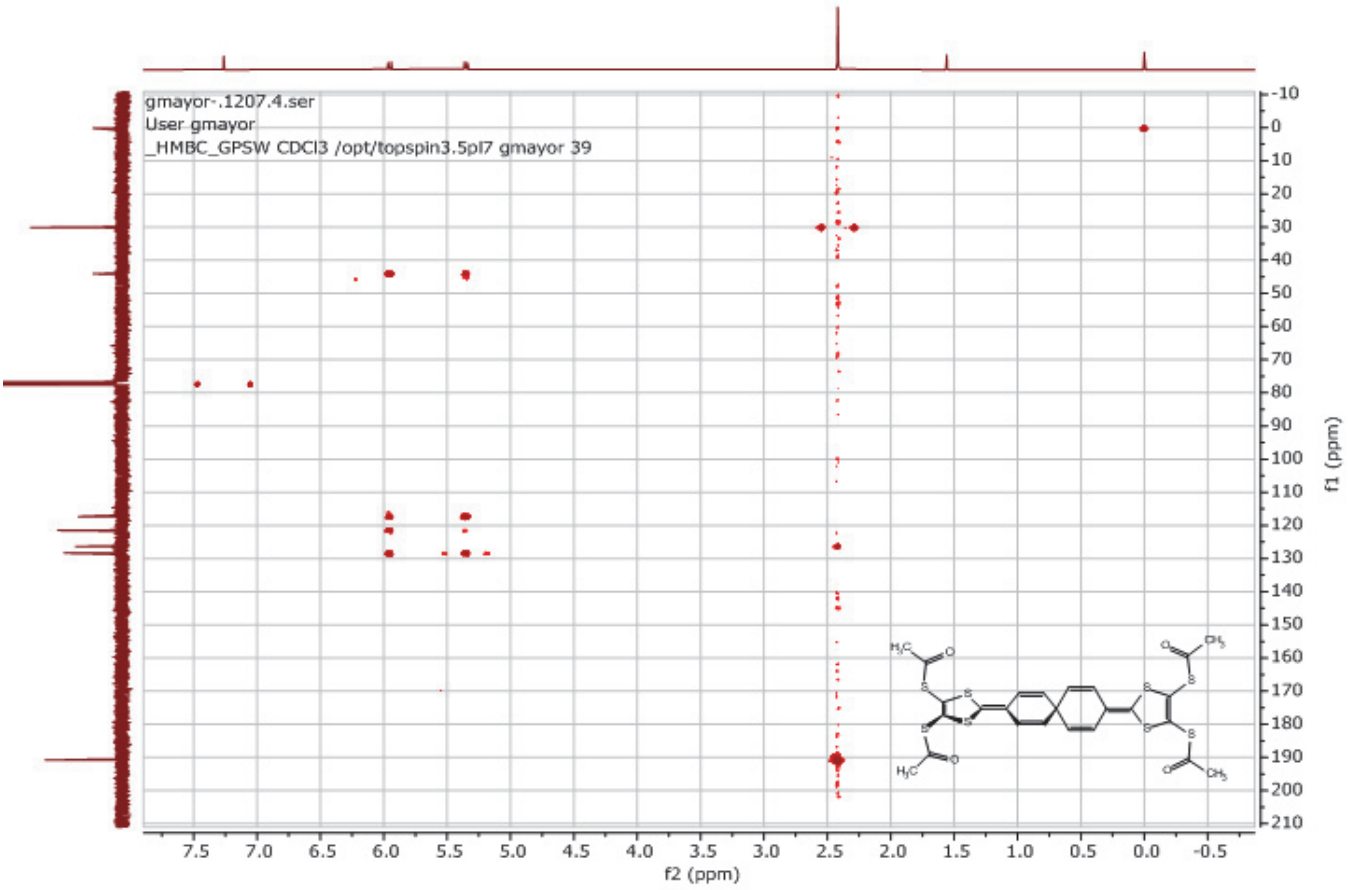

HR-ESI spectra of **76**.

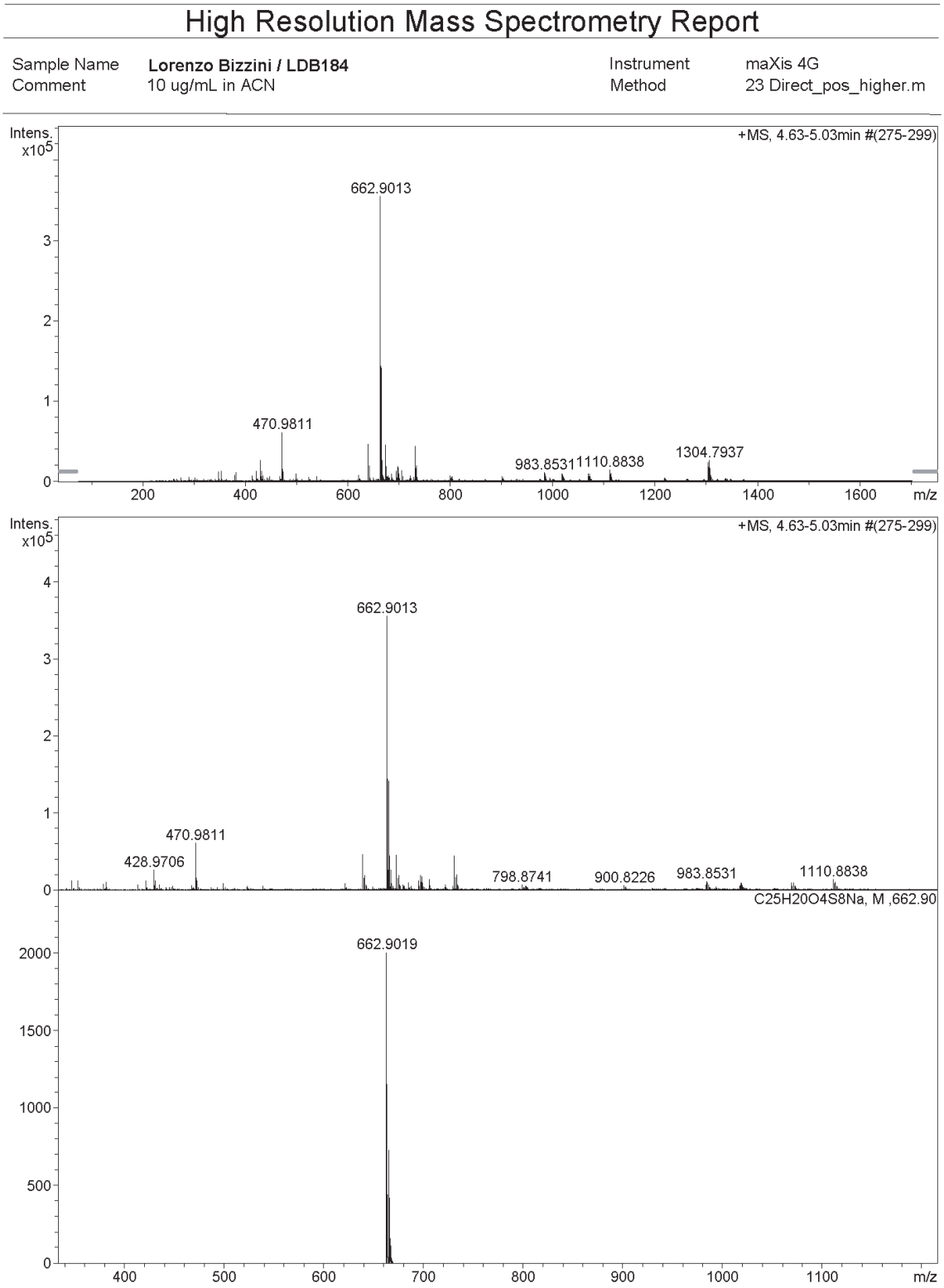

High Resolution Mass Spectrometry Report

Measured m/z vs. theoretical m/z

Meas. m/z	#	Formula	Score	m/z	err [mDa]	err [ppm]	mSigma	rdb	e⁻ Conf	z
662.9013	1	C 25 H 20 Na O 4 S 8	100.00	662.9019	0.7	1.0	28.4	15.5	even	1+

Mass list

#	m/z	I %	I
1	288.9097	1.5	5210
2	301.2114	1.2	4382
3	346.9501	3.3	11550
4	353.2653	3.4	12224
5	378.9221	2.2	7753
6	381.2965	3.0	10699
7	413.2649	1.9	6735
8	420.9147	3.5	12256
9	428.9706	7.1	25383
10	429.9733	1.7	6094
11	430.9856	3.4	12192
12	434.8940	1.8	6455
13	447.9912	1.5	5476
14	466.8661	1.6	5735
15	470.9811	17.1	60591
16	471.9838	4.2	14827
17	472.9781	3.3	11832
18	498.8378	2.5	8880
19	523.3227	1.4	4811
20	538.9683	1.5	5335
21	620.8893	2.2	7836
22	638.9028	13.0	46135
23	639.9055	4.4	15653
24	640.8999	5.5	19436
25	641.9016	1.8	6378
26	642.8977	1.3	4519
27	662.9013	100.0	355243
28	663.4021	8.0	28525
29	663.9030	40.4	143456
30	664.4020	7.1	25332
31	664.8998	39.7	141074
32	665.4018	3.3	11647
33	665.9012	12.5	44362
34	666.8998	7.3	25972
35	667.9011	2.3	8002
36	668.9087	1.3	4752
37	672.9082	12.8	45344
38	673.9107	4.4	15583
39	674.9050	5.2	18598
40	675.9071	1.7	6110
41	676.9028	1.1	4060
42	676.9375	1.4	4816
43	678.8877	1.9	6899
44	679.8876	1.2	4378
45	680.8870	1.2	4361
46	684.9074	2.7	9563
47	686.9064	1.3	4500
48	694.8761	3.5	12418
49	695.8781	1.2	4354
50	696.8925	5.2	18615
51	697.3955	2.8	10122
52	697.8941	4.8	16979
53	698.3954	2.7	9498
54	698.8940	2.6	9371
55	699.3955	1.2	4269
56	705.5803	3.8	13329
57	706.5838	1.7	5956
58	721.5750	1.8	6429
59	728.8972	1.4	4843
60	730.8876	12.3	43867
61	731.8903	4.5	16005
62	732.8877	5.5	19480

High Resolution Mass Spectrometry Report

#	m/z	I %	I
63	733.8902	1.7	6137
64	734.8929	1.3	4741
65	798.8741	1.8	6419
66	802.0095	1.4	4856
67	802.5112	1.1	4075
68	803.0108	1.5	5482
69	900.8226	1.6	5774
70	982.8520	1.8	6227
71	983.3542	1.7	6207
72	983.8531	3.1	10882
73	984.3544	2.5	8978
74	984.8534	2.7	9553
75	985.3542	1.8	6332
76	985.8543	1.5	5365
77	993.1721	1.2	4242
78	1016.8456	1.5	5484
79	1017.3474	1.6	5536
80	1017.8458	2.6	9118
81	1018.3470	2.2	7837
82	1018.8464	2.4	8452
83	1019.3475	1.6	5792
84	1019.8466	1.4	4858
85	1068.8750	2.7	9473
86	1069.8783	1.5	5302
87	1070.8808	2.7	9488
88	1071.8826	1.4	4802
89	1072.8860	1.5	5313
90	1110.8838	3.9	13924
91	1111.8867	2.3	8298
92	1112.8832	2.9	10296
93	1113.8848	1.5	5233
94	1302.7931	6.5	23182
95	1303.7955	4.8	17185
96	1304.7937	7.3	26092
97	1305.7955	4.3	15393
98	1306.7947	3.8	13358
99	1307.7962	2.0	7129
100	1308.7962	1.4	4918

Acquisition Parameter

Source Type	ESI	Ion Polarity	Positive	Set Nebulizer	0.4 Bar
Focus	Not active	Set Capillary	3600 V	Set Dry Heater	180 °C
Scan Begin	75 m/z	Set End Plate Offset	-500 V	Set Dry Gas	4.0 l/min
Scan End	1700 m/z	Set Collision Cell RF	500.0 Vpp	Set Ion Energy (MS only)	4.0 eV

^{1}H-NMR ($CDCl_3$, 400 MHz, 298 K) and ^{13}C-NMR ($CDCl_3$, 126 MHz, 298 K) of **77.**

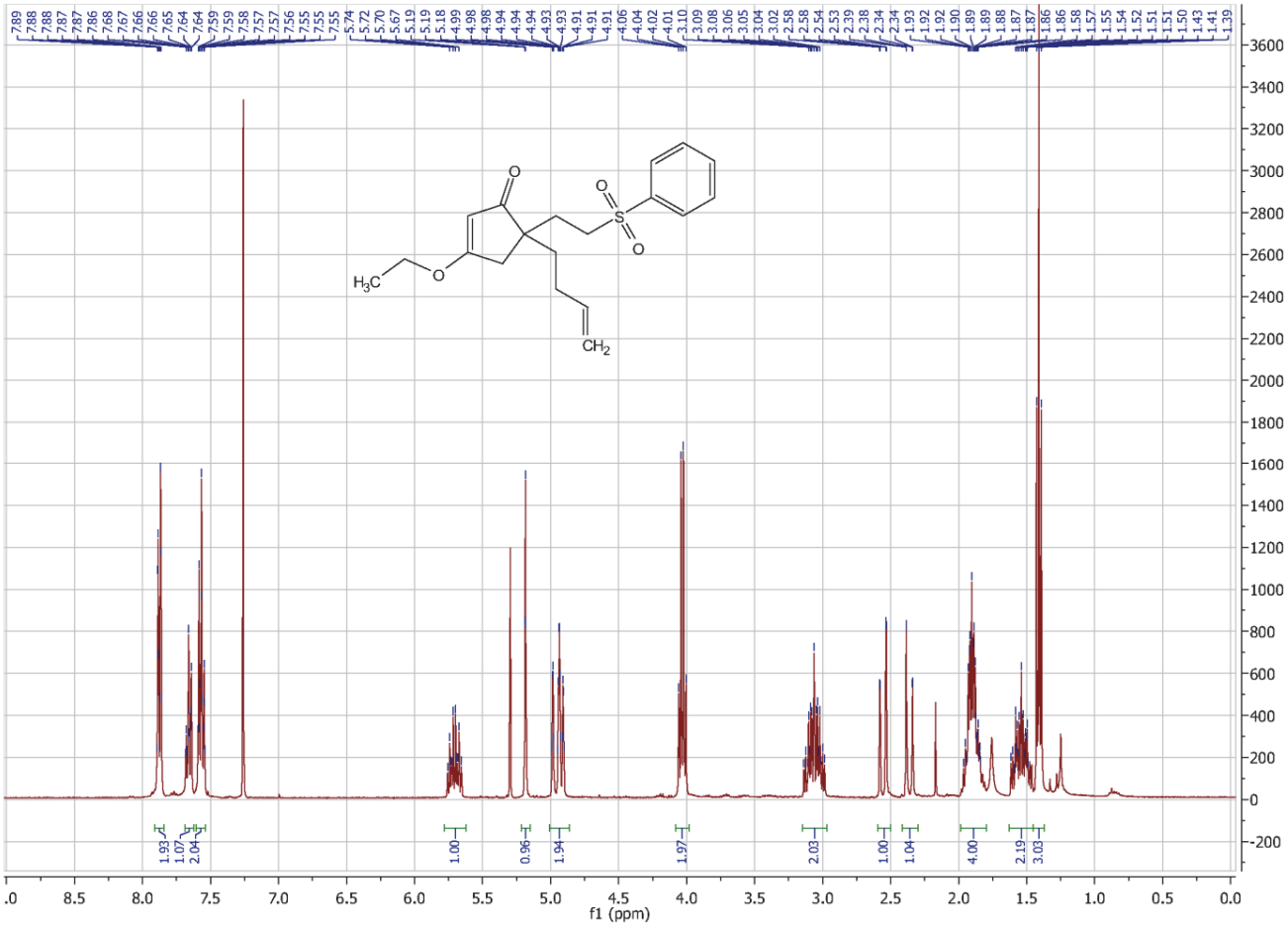

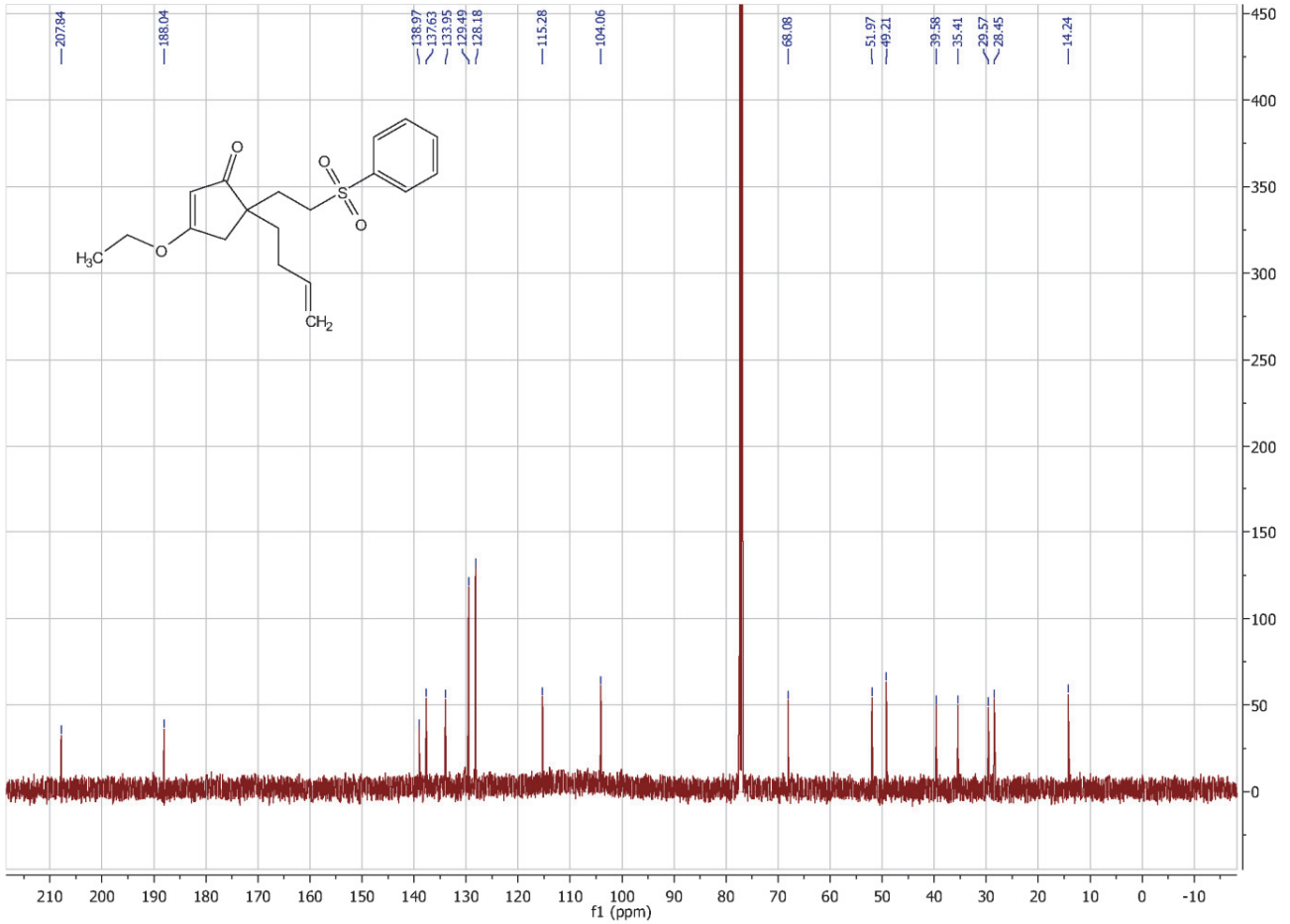

HR-ESI spectra of **77**.

Mass Spectrum SmartFormula Report

Analysis Info

Analysis Name	E:\acq data for data analysis\LDB25 002.d	Acquisition Date	16.05.2017 11:22:04
Method	hn Direct_Infusion_pos mode_75-1700 mid 4eV.m	Operator	hn
Sample Name	Lorenzo Delarue Bizzini	Instrument / Ser#	maXis 4G 21243
Comment	LDB25, ca. 10 ug/ml MeOH		

Acquisition Parameter

Source Type	ESI	Ion Polarity	Positive	Set Nebulizer	0.4 Bar
Focus	Not active	Set Capillary	3600 V	Set Dry Heater	180 °C
Scan Begin	75 m/z	Set End Plate Offset	-500 V	Set Dry Gas	4.0 l/min
Scan End	1700 m/z	Collision Energy	8.0 eV	Set Ion Energy (MS only)	4.0 eV

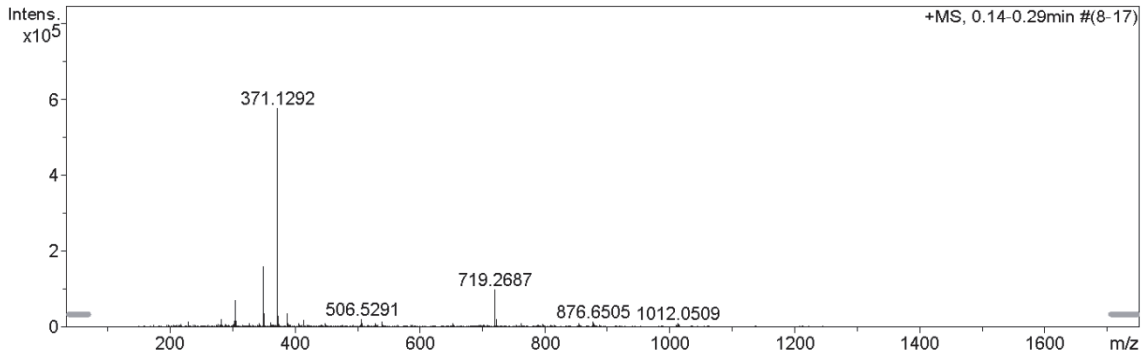

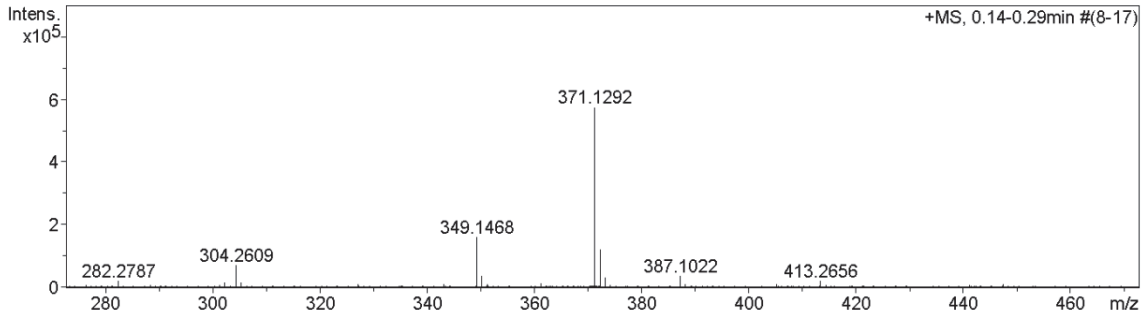

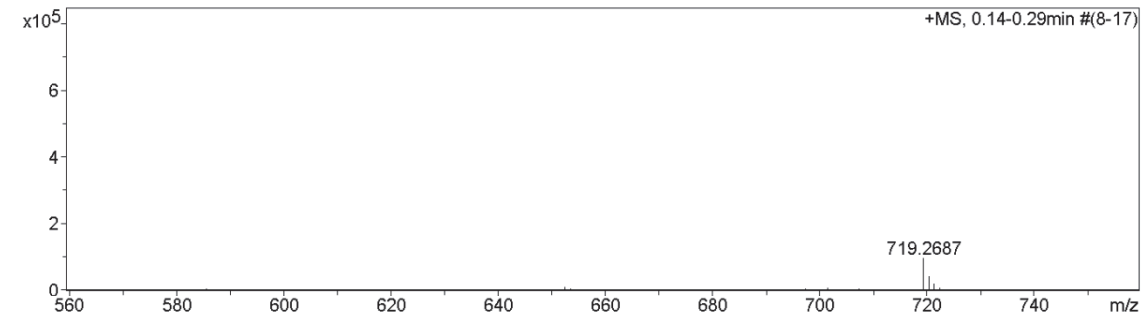

Meas. m/z	#	Formula	Score	m/z	err [mDa]	err [ppm]	mSigma	rdb	e⁻ Conf	z
349.1468	1	C 19 H 25 O 4 S	100.00	349.1468	-0.0	-0.0	12.1	7.5	even	1+
371.1292	1	C 19 H 24 Na O 4 S	100.00	371.1288	-0.5	-1.2	14.2	7.5	even	
387.1022	1	C 19 H 24 K O 4 S	100.00	387.1027	0.4	1.2	11.2	7.5	even	
697.2856	1	C 38 H 49 O 8 S 2	100.00	697.2863	0.8	1.1	98.4	14.5	even	
719.2687	1	C 38 H 48 Na O 8 S 2	100.00	719.2683	-0.4	-0.6	5.5	14.5	even	

^{1}H-NMR ($CDCl_3$, 400 MHz, 298 K) and ^{13}C-NMR ($CDCl_3$, 126 MHz, 298 K) of **81**.

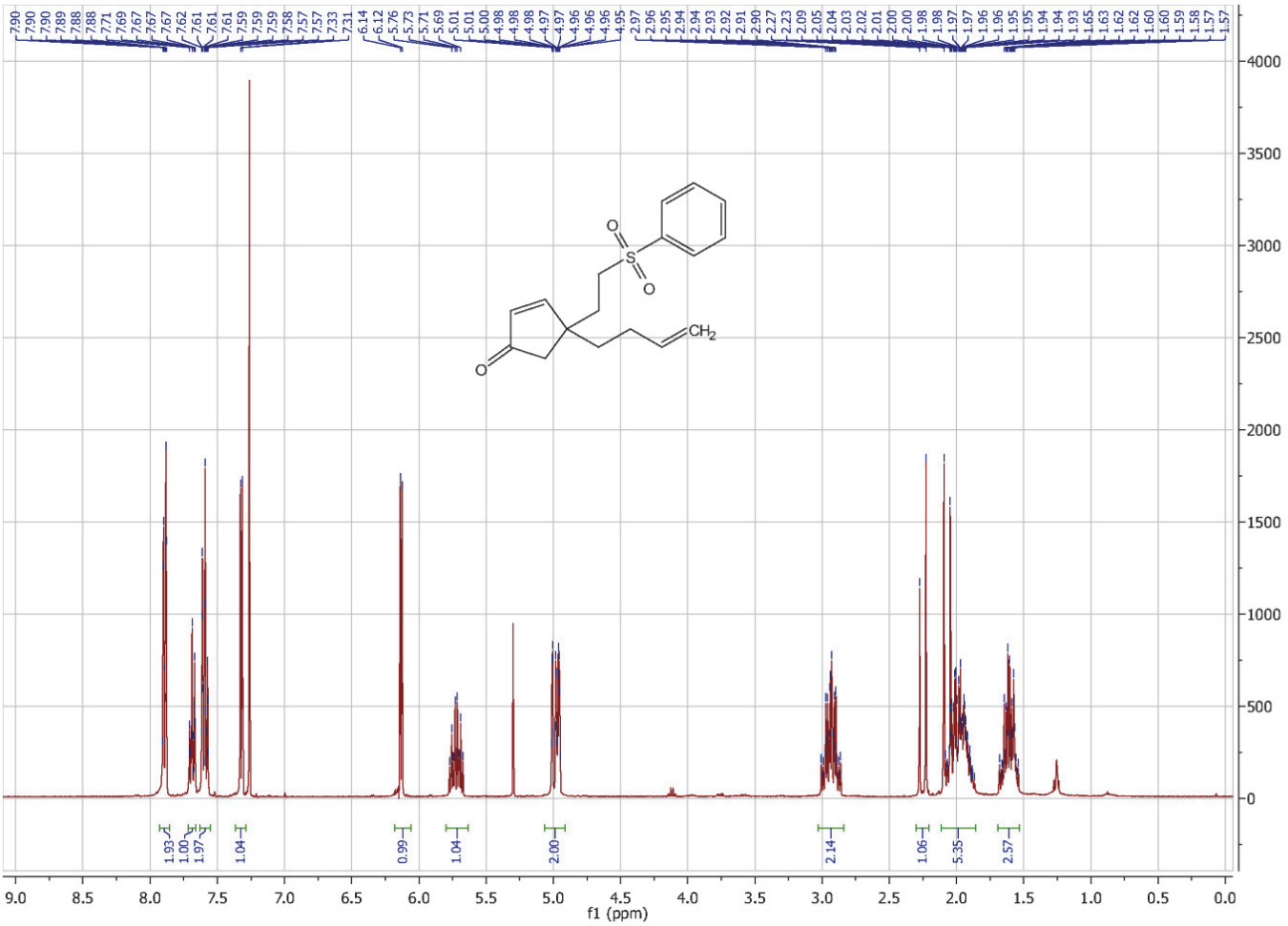

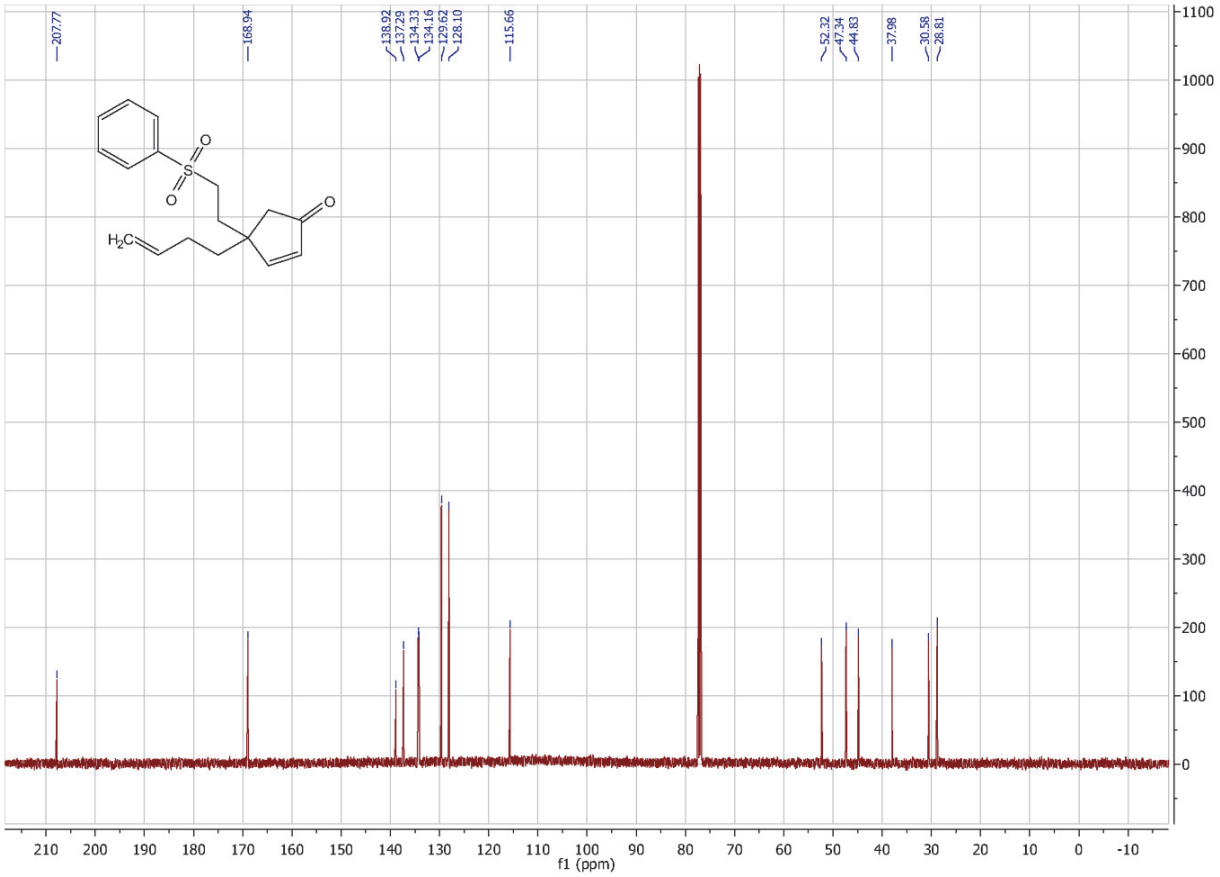

HR-ESI spectra of **81**.

Mass Spectrum SmartFormula Report

Analysis Info

Analysis Name	E:\acq data for data analysis\LDB26 001.d	Acquisition Date	16.05.2017 09:16:21
Method	hn Direct_Infusion_pos mode_75-1700 mid 4eV.m	Operator	hn
Sample Name	Lorenzo Delarue Bizzini	Instrument / Ser#	maXis 4G 21243
Comment	LDB26, ca. 10 ug/ml MeOH		

Acquisition Parameter

Source Type	ESI	Ion Polarity	Positive	Set Nebulizer	0.4 Bar
Focus	Not active	Set Capillary	3600 V	Set Dry Heater	180 °C
Scan Begin	75 m/z	Set End Plate Offset	-500 V	Set Dry Gas	4.0 l/min
Scan End	1700 m/z	Collision Energy	8.0 eV	Set Ion Energy (MS only)	4.0 eV

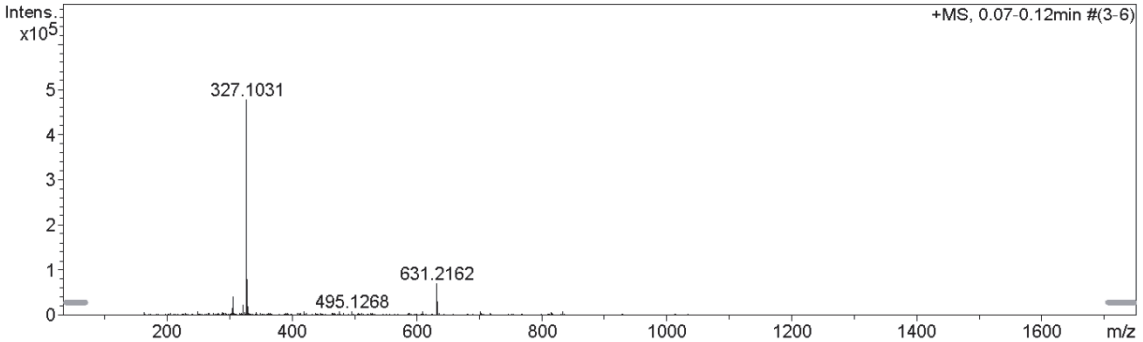

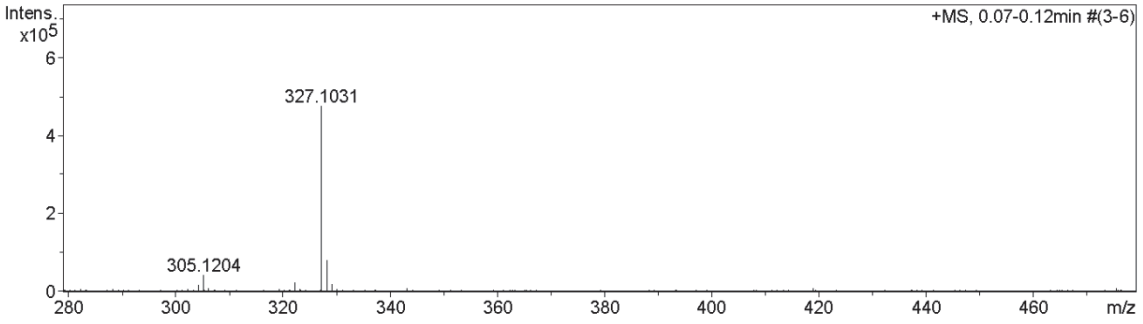

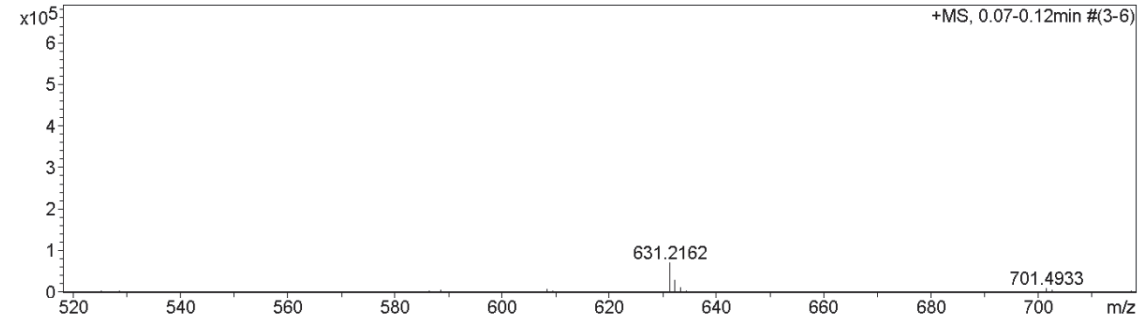

Meas. m/z	#	Formula	Score	m/z	err [mDa]	err [ppm]	mSigma	rdb	e⁻ Conf	z
305.1204	1	C 17 H 21 O 3 S	100.00	305.1206	0.2	0.7	8.0	7.5	even	1+
322.1469	1	C 17 H 24 N O 3 S	100.00	322.1471	0.2	0.7	14.8	6.5	even	
327.1031	1	C 17 H 20 Na O 3 S	100.00	327.1025	-0.5	-1.6	20.2	7.5	even	
631.2162	1	C 34 H 40 Na O 6 S 2	100.00	631.2159	-0.3	-0.5	10.7	14.5	even	

^{1}H-NMR ($CDCl_3$, 500 MHz, 298 K) and 13C-NMR (CDCl3, 126 MHz, 298 K) of **69**.

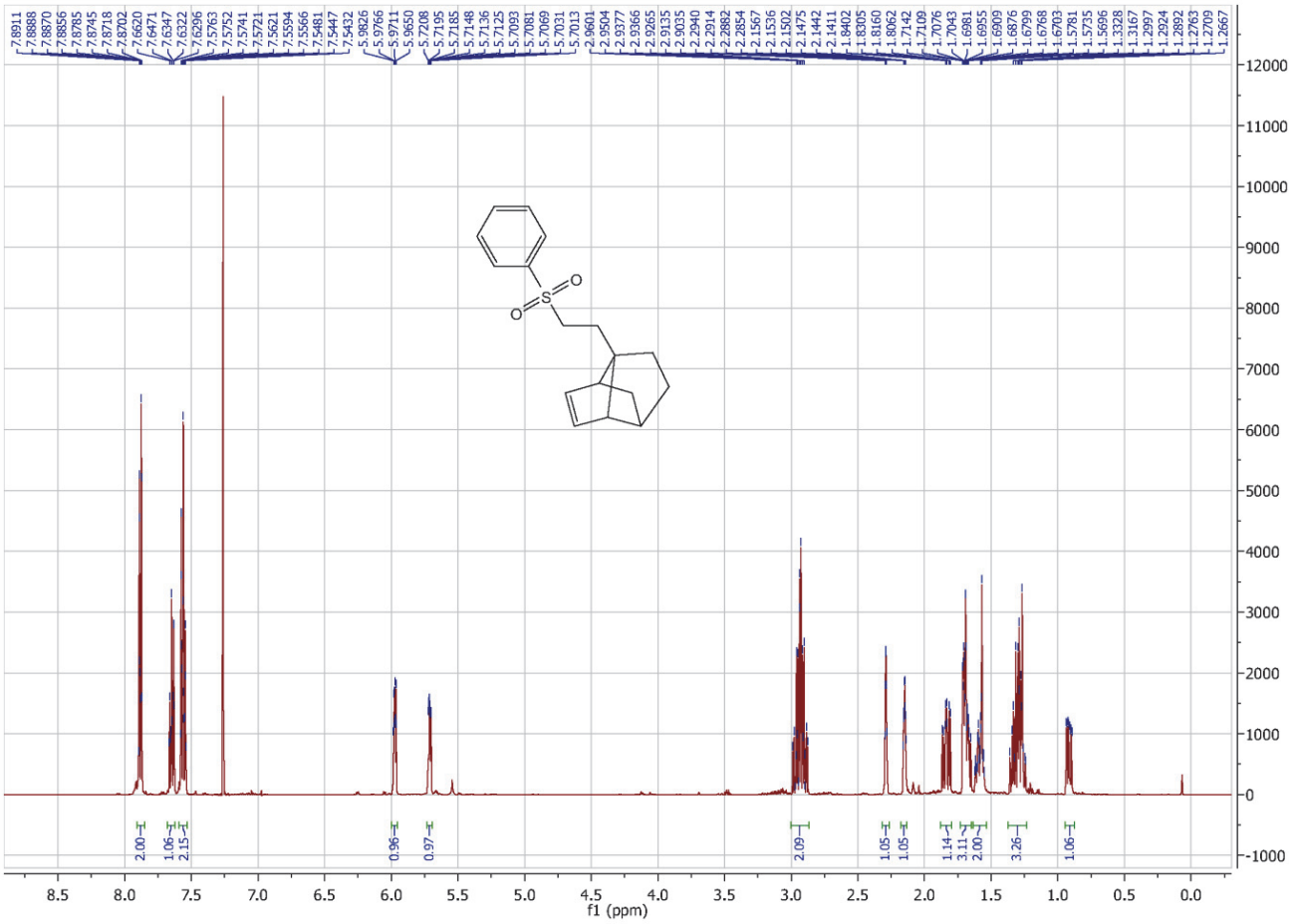

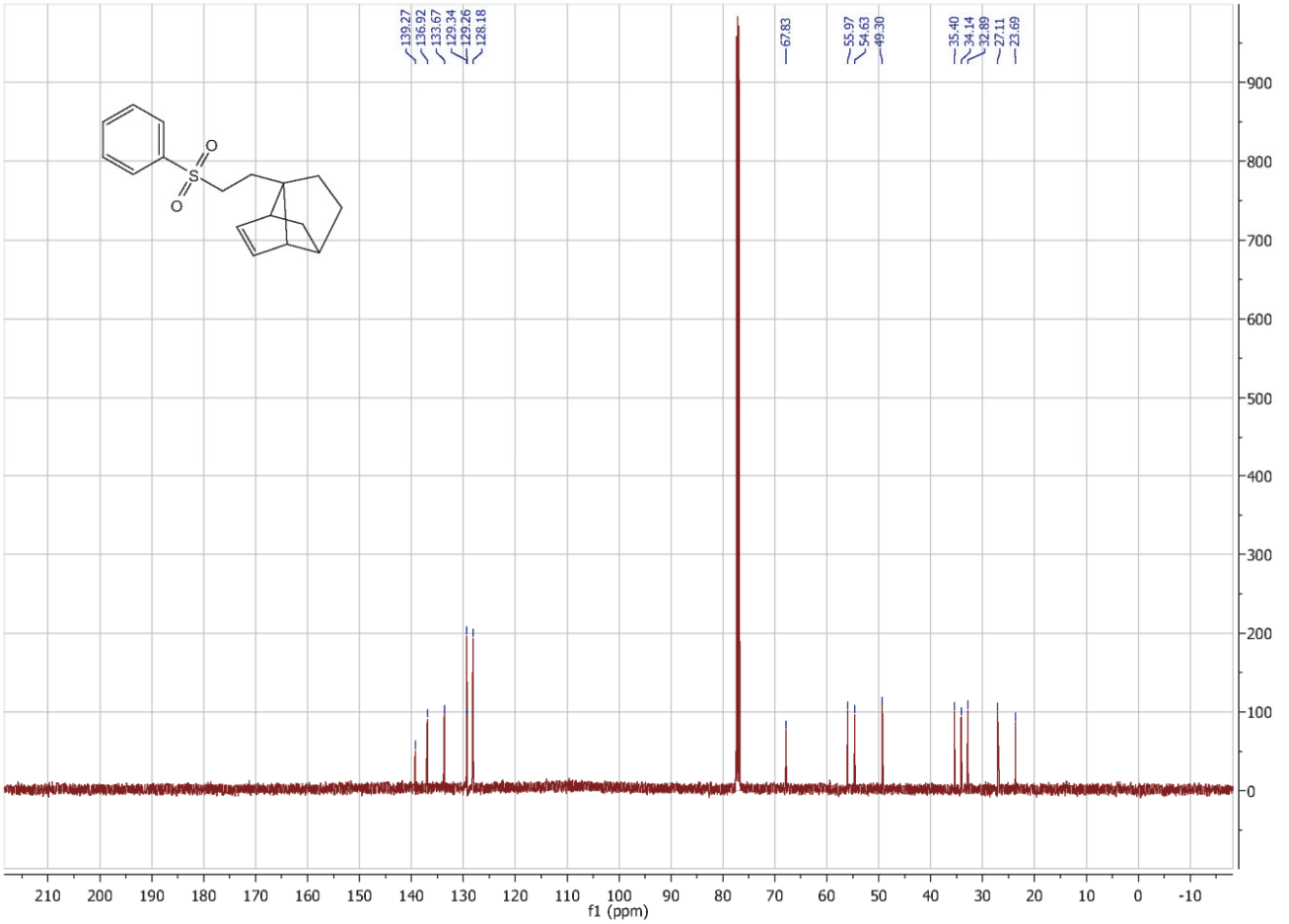

HR-ESI spectra of **69**.

Mass Spectrum SmartFormula Report

Analysis Info

Analysis Name	E:\acq data for data analysis\LDB27 001.d	Acquisition Date	06.06.2017 15:09:45
Method	hn Direct_Infusion_pos mode_75-1700 mid 4eV.m	Operator	hn
Sample Name	Lorenzo Delarue Bizzini	Instrument / Ser#	maXis 4G 21243
Comment	LDB27, ca. 10 ug/ml MeOH		

Acquisition Parameter

Source Type	ESI	Ion Polarity	Positive	Set Nebulizer	0.4 Bar
Focus	Not active	Set Capillary	3600 V	Set Dry Heater	180 °C
Scan Begin	75 m/z	Set End Plate Offset	-500 V	Set Dry Gas	4.0 l/min
Scan End	1700 m/z	Collision Energy	8.0 eV	Set Ion Energy (MS only)	4.0 eV

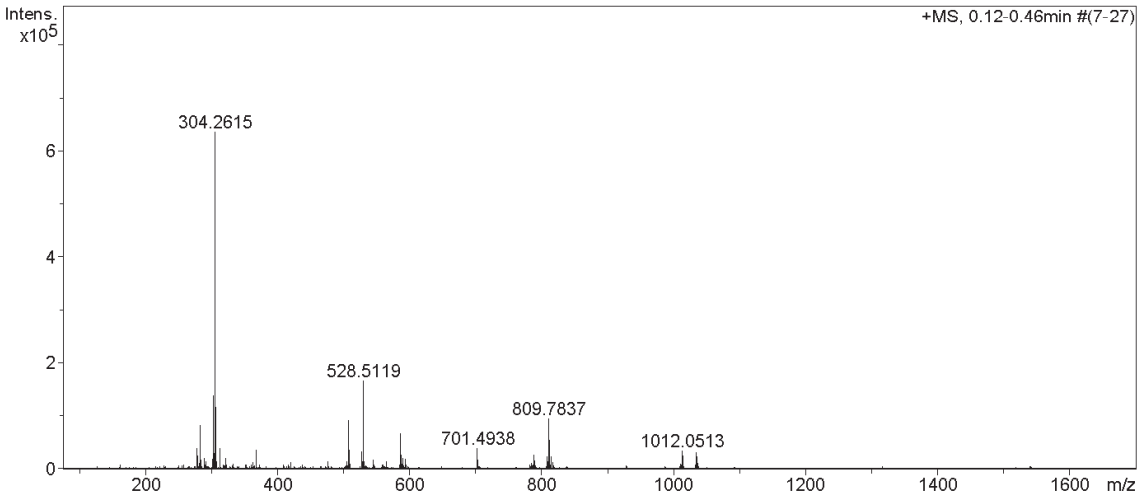

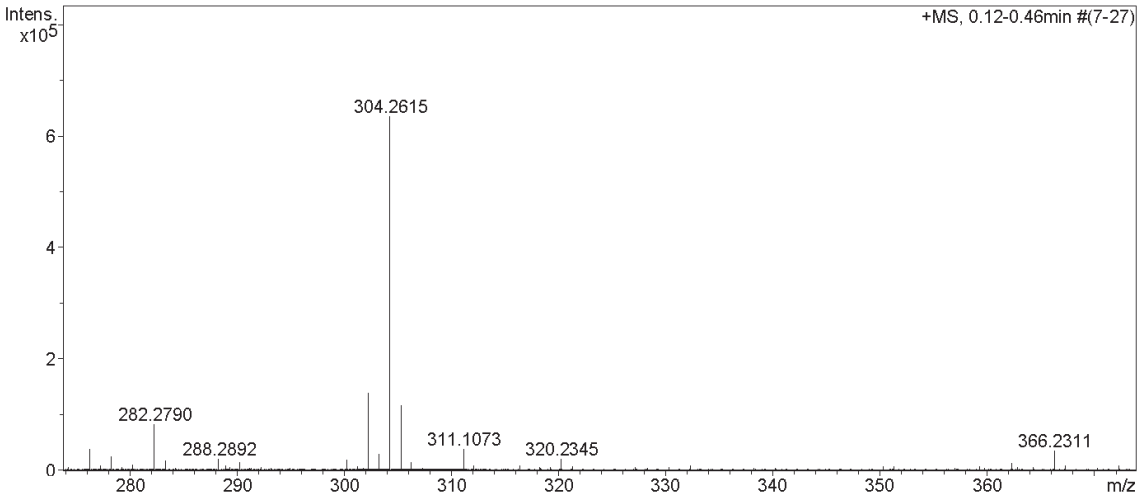

Meas. m/z	#	Formula	Score	m/z	err [mDa]	err [ppm]	mSigma	rdb	e⁻ Conf	z
311.1073	1	C 17 H 20 Na O 2 S	100.00	311.1076	0.3	0.9	14.0	7.5	even	1+

^{1}H-NMR (C_6D_6, 600 MHz, 298 K) and ^{13}C-NMR (C_6D_6, 151 MHz, 298 K) of **66**.

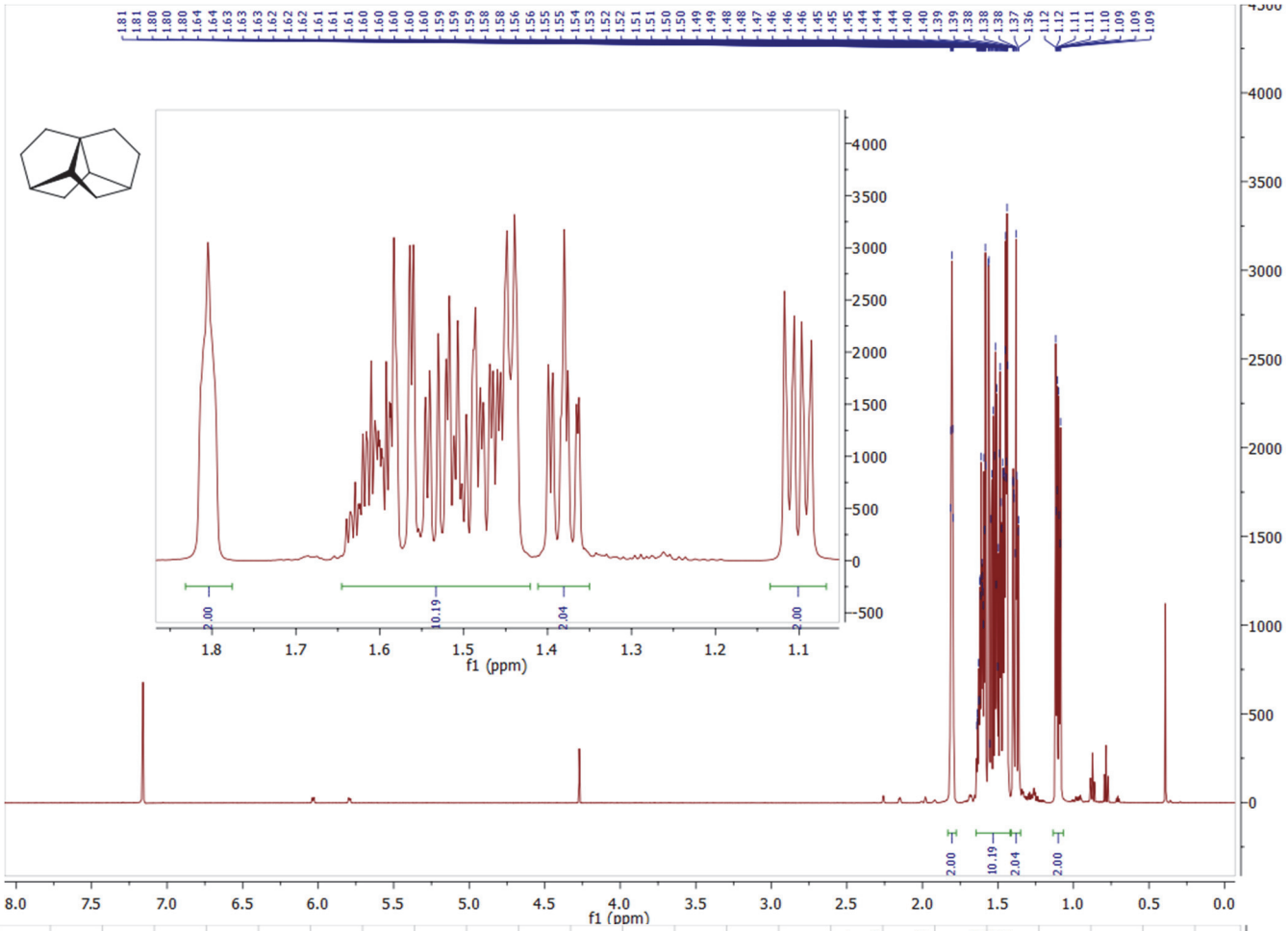

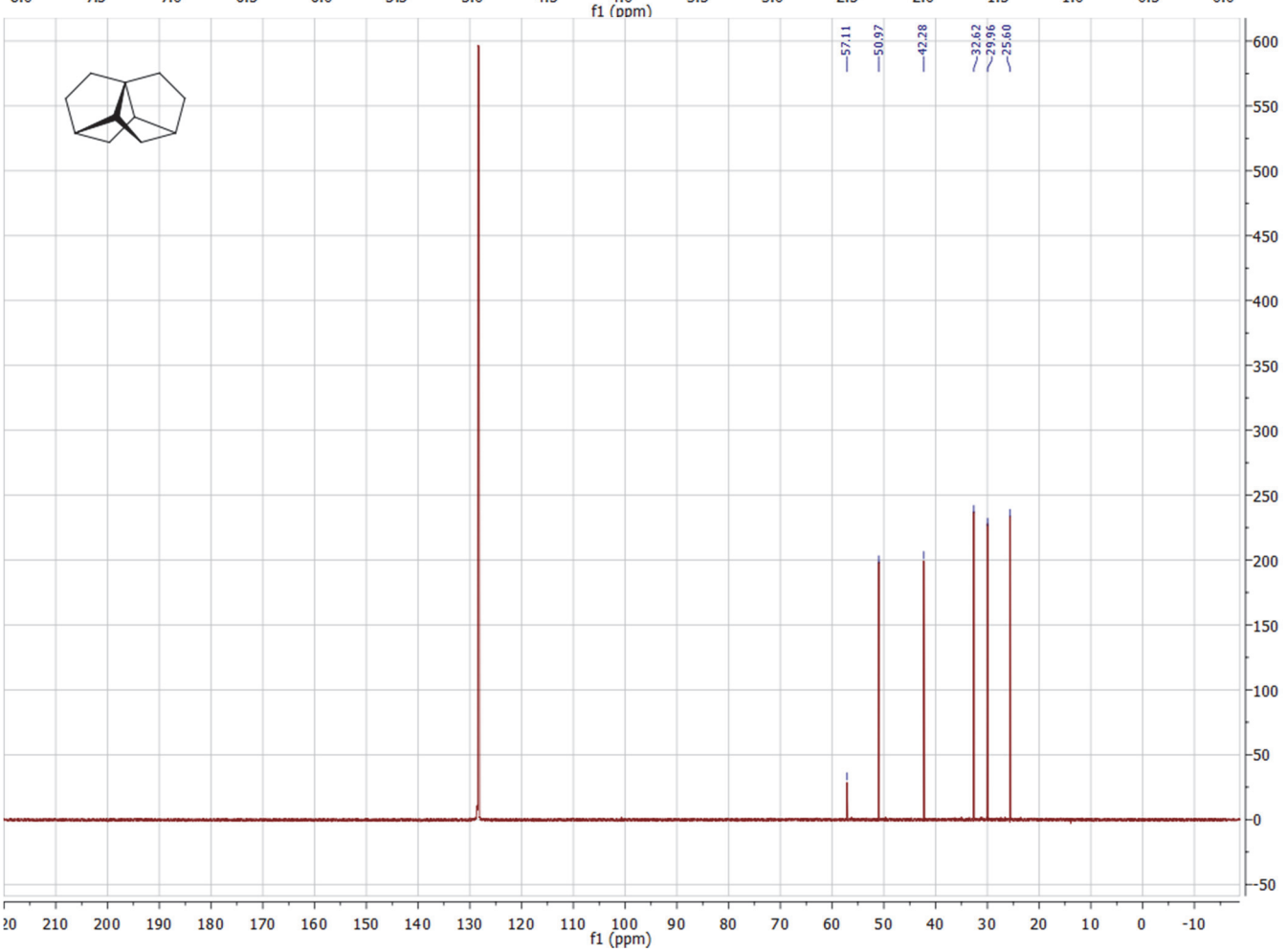

1,1 adequate and HSQC (C_6D_6, 298 K) of **66**.

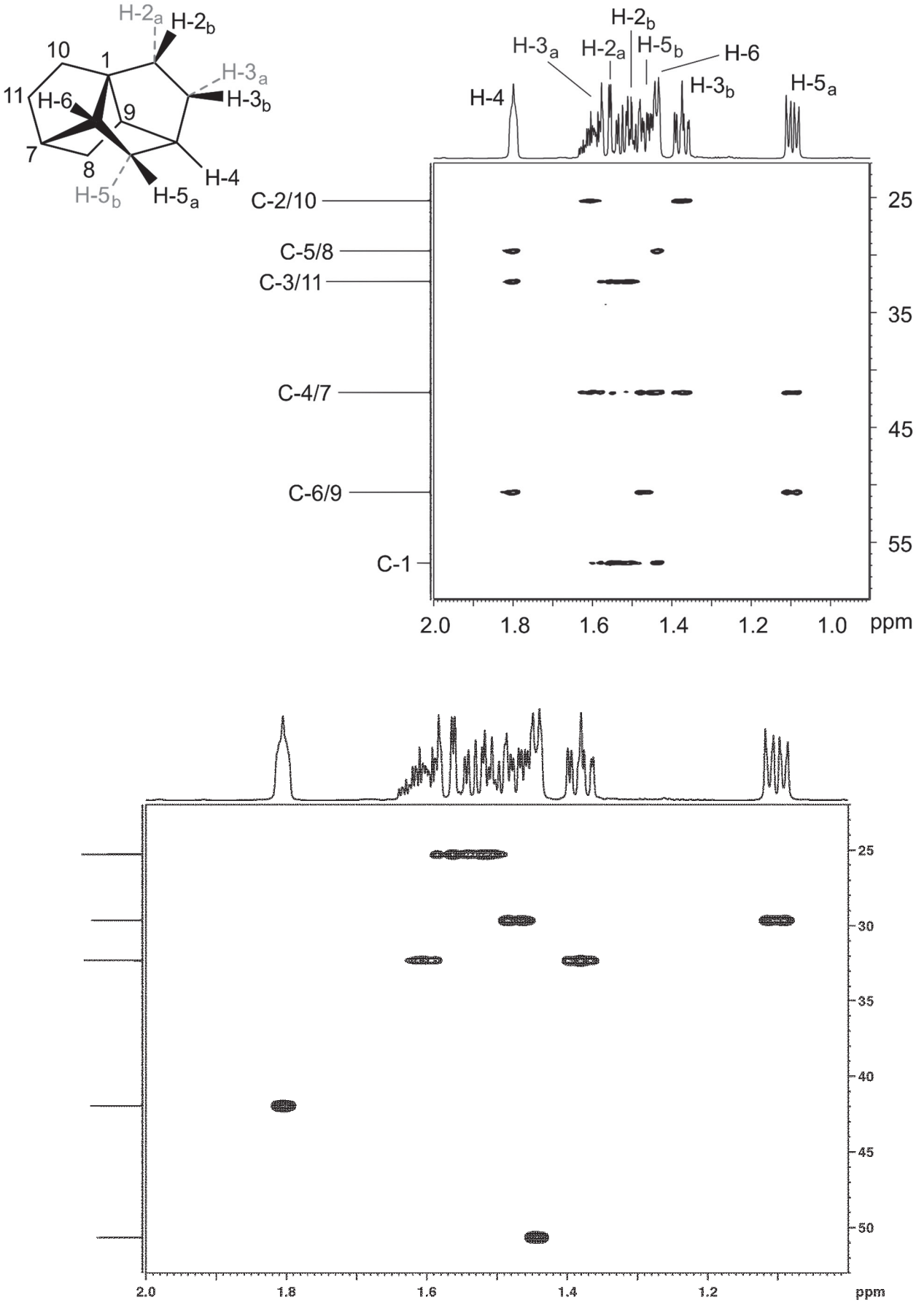

NOESY (C_6D_6 298 K) of **66**.

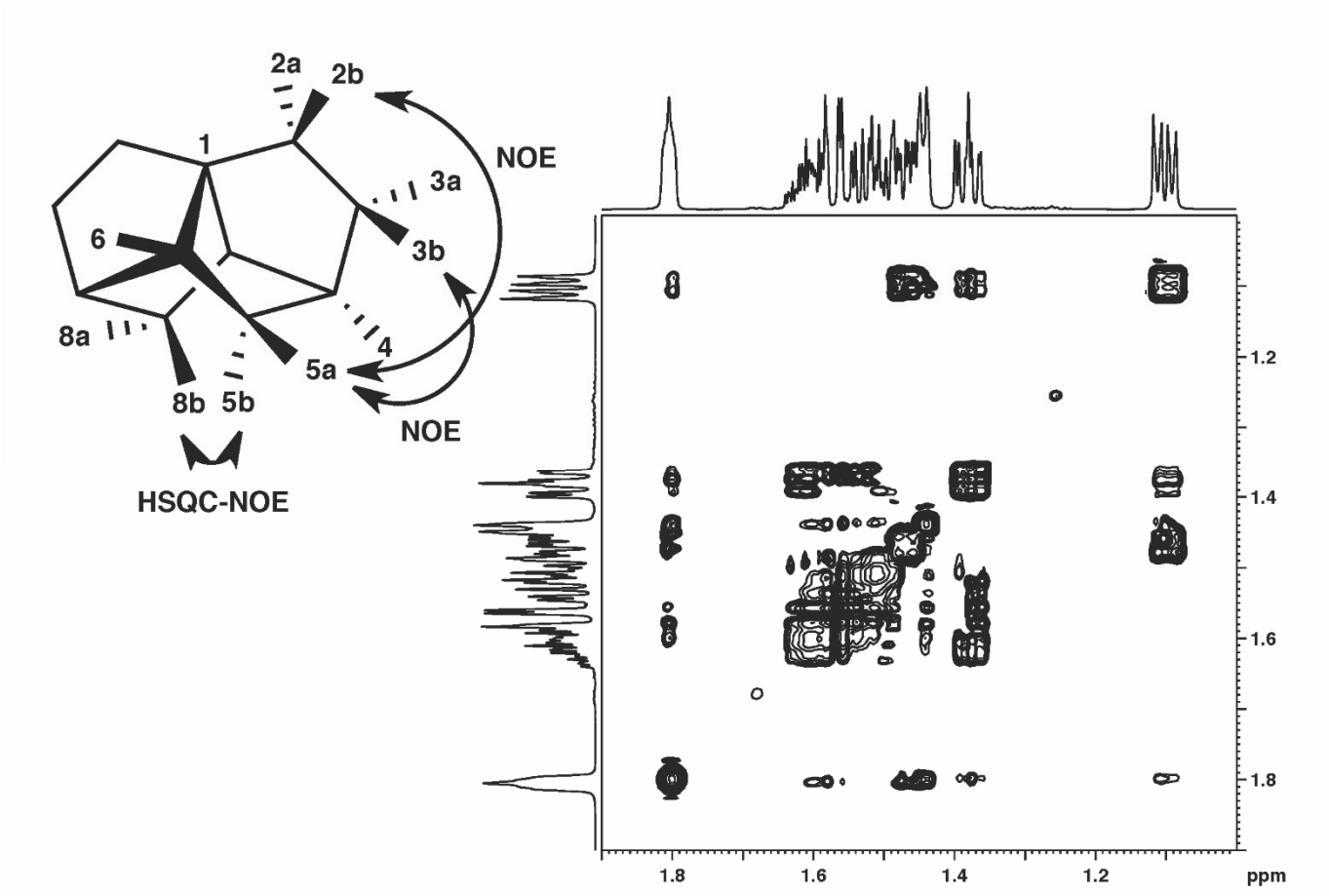

Figure S25: 2D-NOESY NMR of **66**.

HR-EI spectra of **66**.

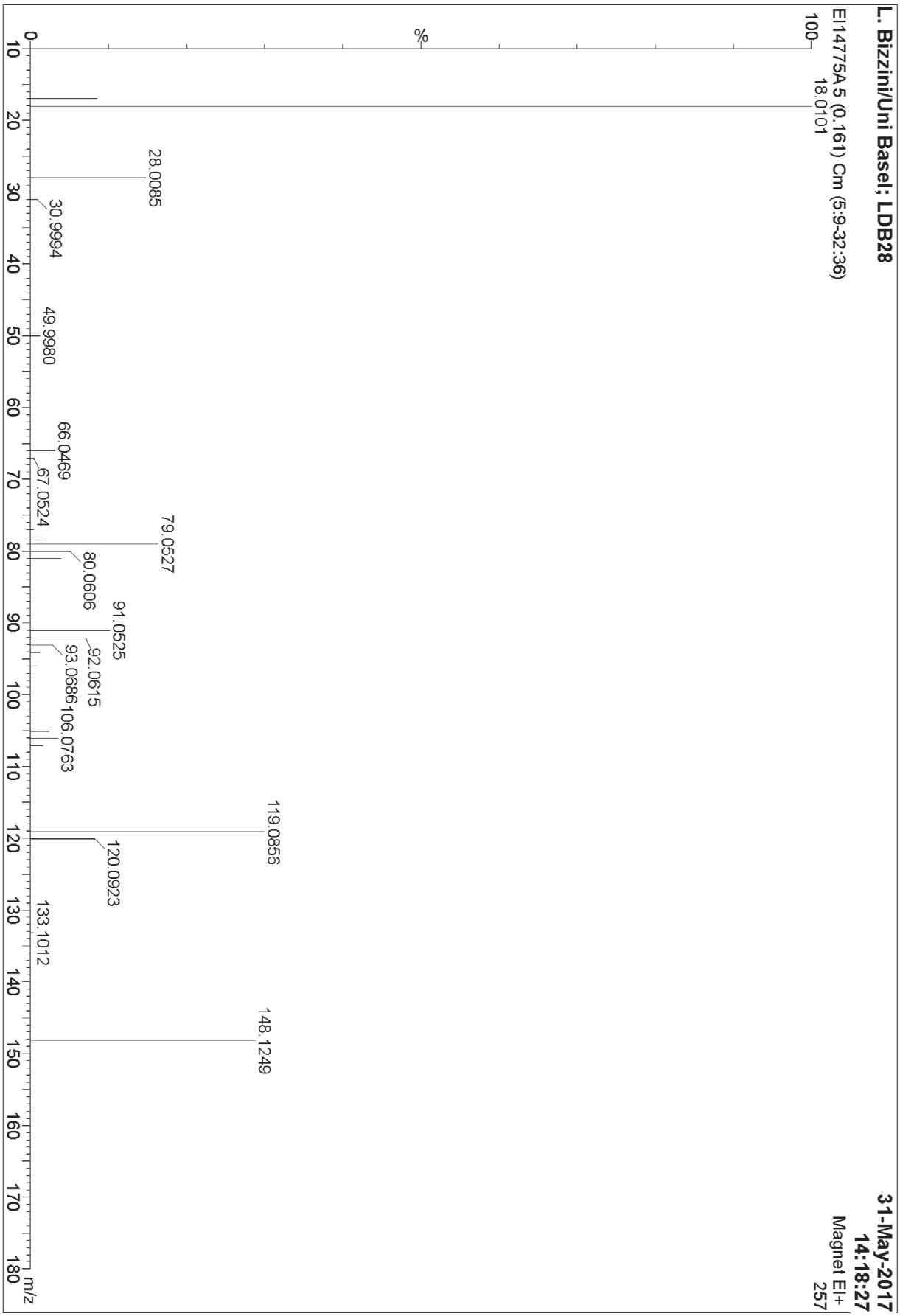

X-Ray Cristallography Data

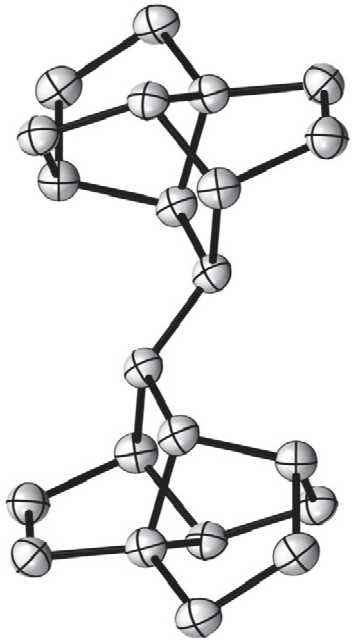

Fig. 1: Molecular structure of **78**, the ellipsoids represent the 30% probability level. Hydrogen atoms have been omitted for clarity.

Table A1: Crystal data and structure refinement for **78**.

Empirical formula	$C_{22}H_{30}$
Formula weight	294.48
Temperature/K	123
Crystal system	monoclinic
Space group	$P2_1/n$
a/Å	5.8515(4)
b/Å	11.0768(8)
c/Å	12.6463(9)
α/°	90
β/°	99.386(5)
γ/°	90
Volume/Å^3	808.71(10)
Z	2
ρ_{calc}g/cm^3	1.209
μ/mm^{-1}	0.315
F(000)	324
Crystal size/mm^3	0.06 × 0.19 × 0.25
Radiation	GaKα (λ = 1.34143)
Θ range for data collection/°	4.644 to 57.411
Index ranges	$-7 \leq h \leq 6$ $-13 \leq k \leq 12$ $-9 \leq l \leq 15$
Reflections collected	5526
Independent reflections	1626 [R_{int} = 0.078]
Observed reflections	1507 [I > 2σ(I)]
Parameters	100
Goodness-of-fit on F^2	1.074
Final R indexes [I≥2σ(I)]	R_1 = 0.0836, wR_2 = 0.0982
Final R indexes [all data]	R_1 = 0.0851, wR_2 = 0.0997
Largest diff. peak/hole / e Å-3	*0.35/–0.26*
CCDC number	*1556107*

^{1}H NMR (250 MHz, $CDCl_3$) of **88** and ^{1}H NMR (250 MHz, DMSO-d_6) of **94**

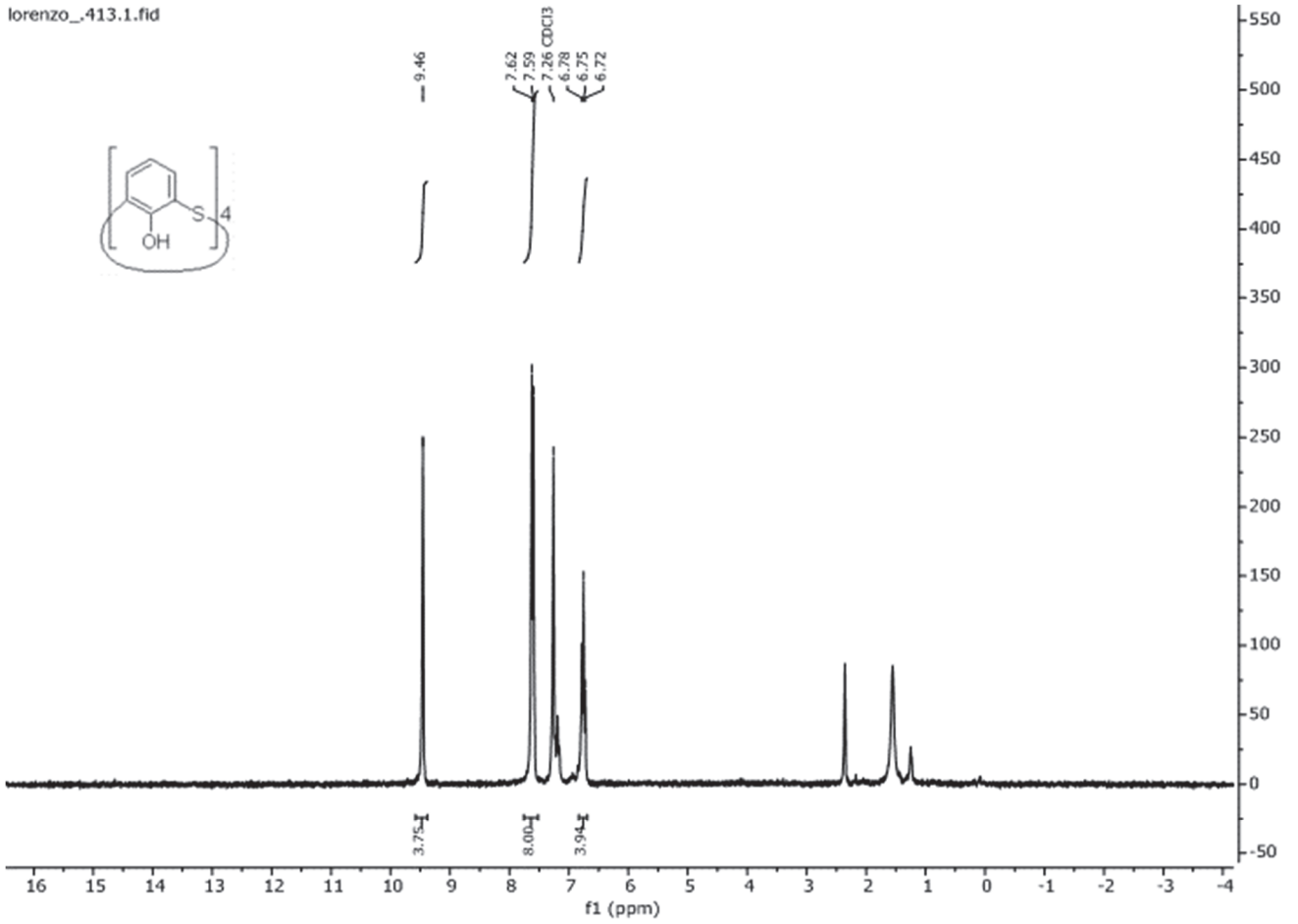

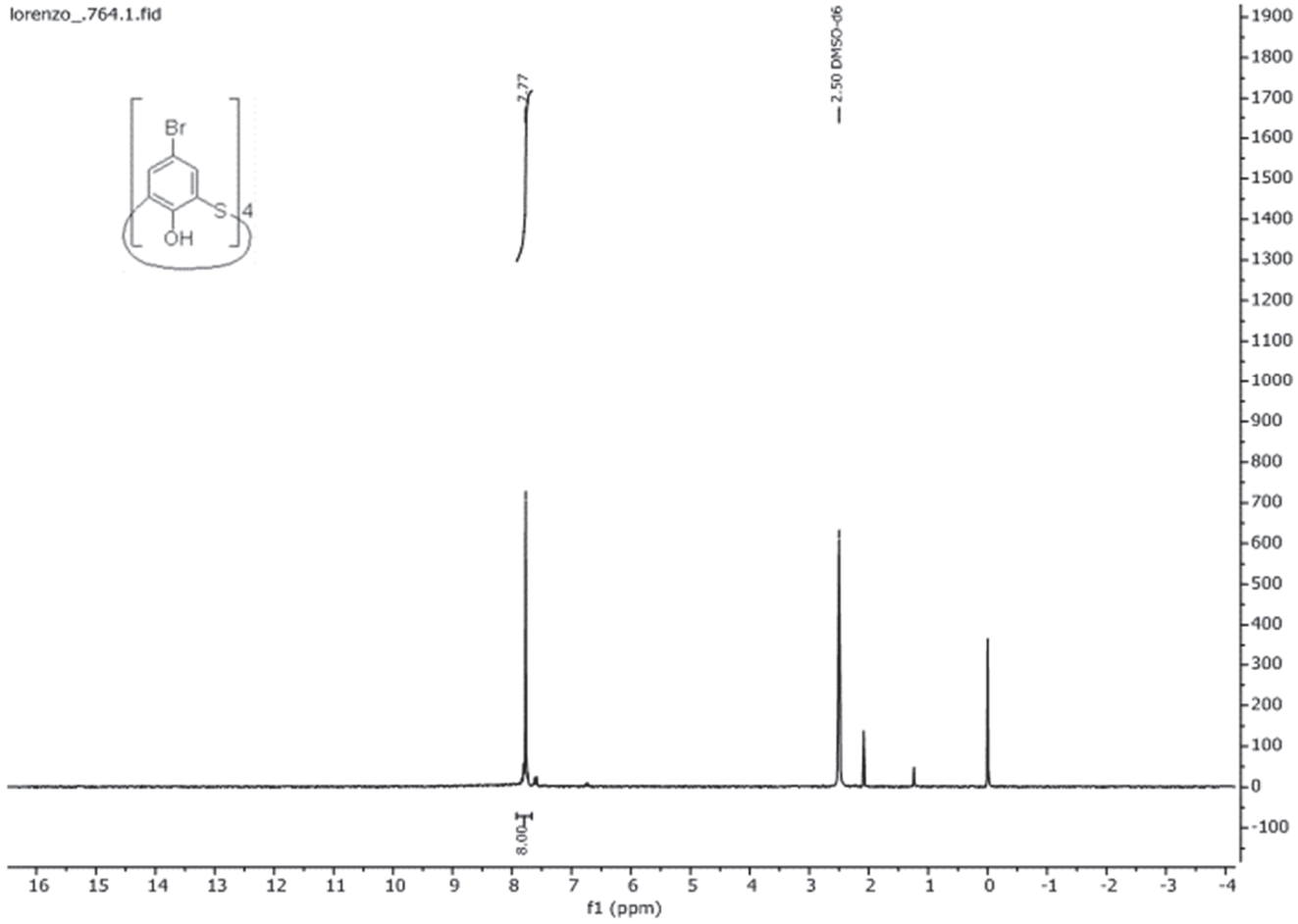

^{1}H NMR (250 MHz, CD_2Cl_2) of **95**

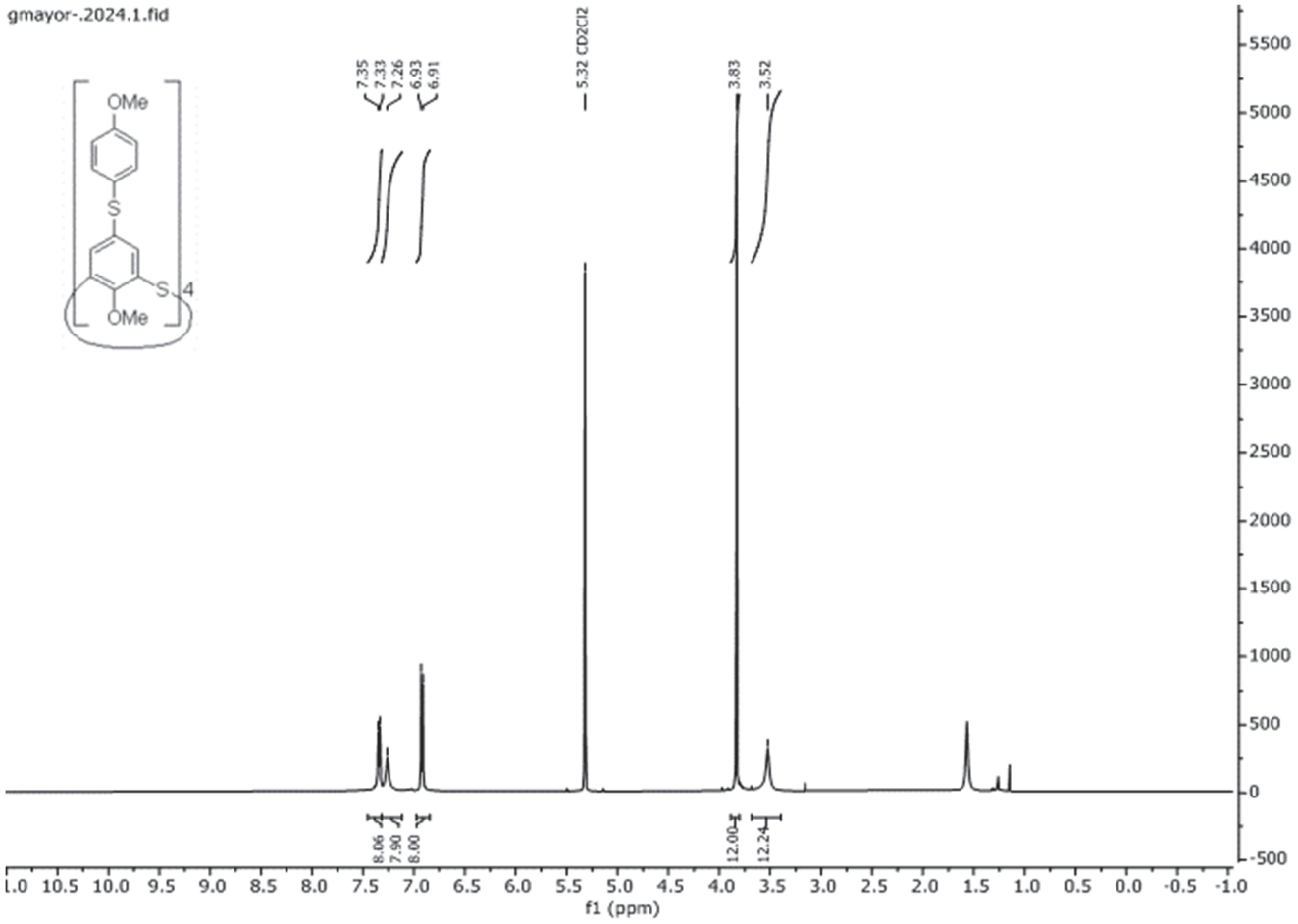

Elemental Analysis of **95**.

Sylvie Mittelheisser
Department Chemistry
Microlab 07
Tel: 7 11 19
email: sylvie.mittelheisser@unibas.ch

Elemental analysis

Sample name:LDB123

Single determination ☒ Double determination ☐

C ☒	H ☒	N ☒
Other elements: S, O		

Results

Analysis number: 2018-05			
Sample name:LDB123			
Expected values:	C 60.84 %	H 4.38 %	N 0.00 %
Results:	C 60.53 % - %	H 4.49 % - %	N 0.00 % - %
	Other elements:S, O		
Remarks:			

Date/Visa operator
18.01.2018, Sylvie Mittelheisser

^{1}H NMR (500 MHz, Acetone d_6) and ^{13}CNMR (126 MHz, Acetone d_6)of **92**

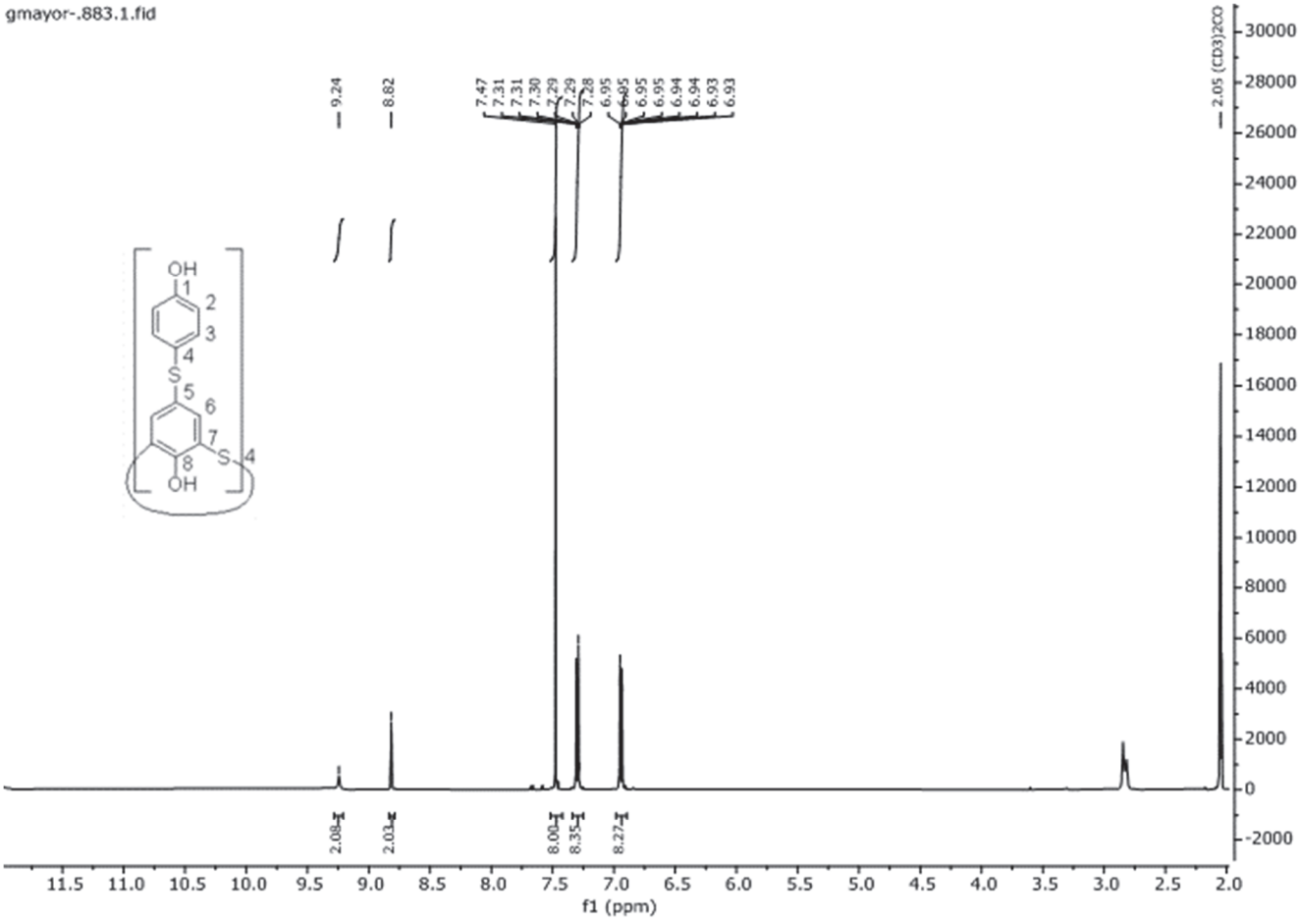

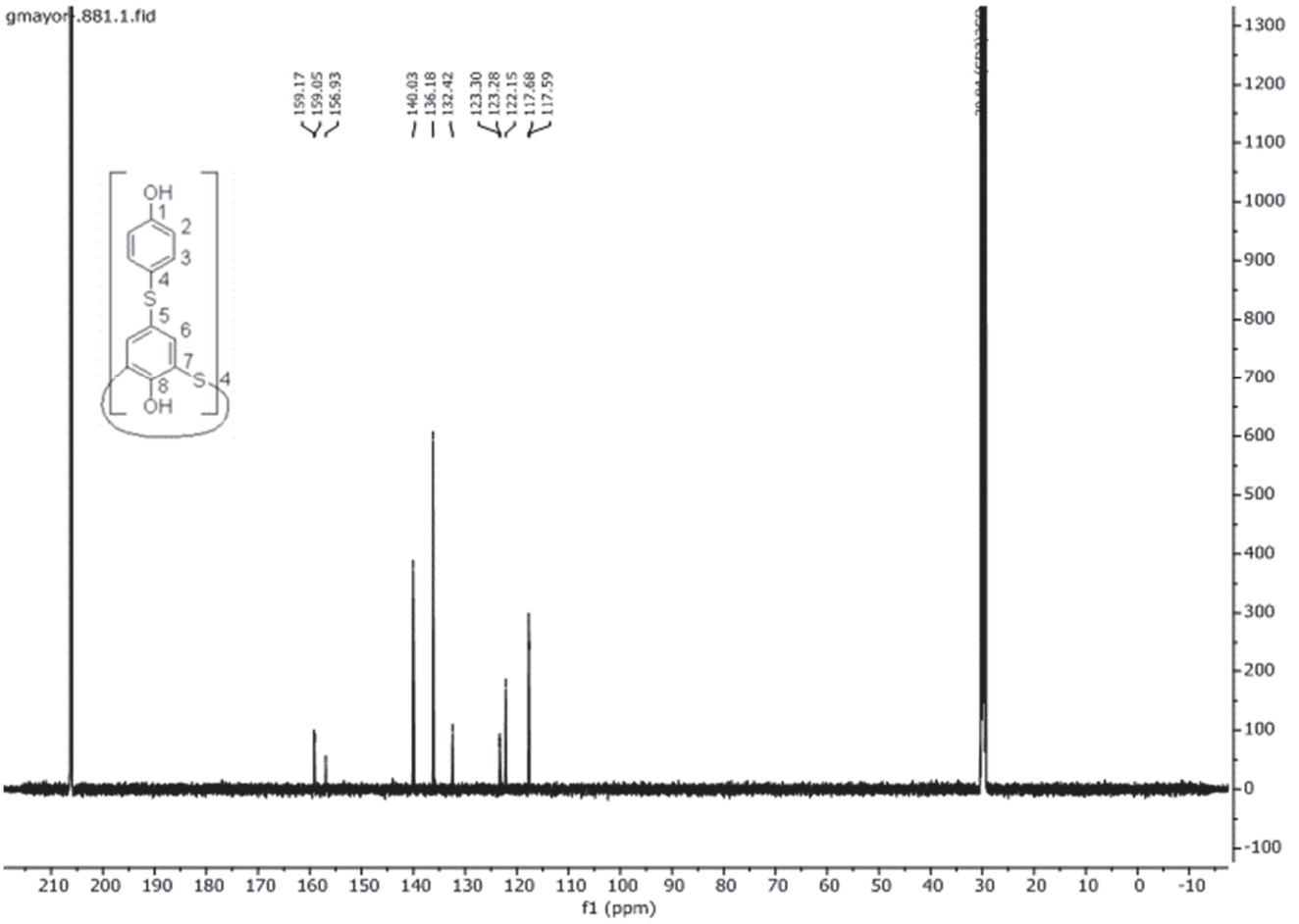

^{1}H NMR (250 MHz, $CDCl_3$) and ^{19}F NMR (235 MHz, $CDCl_3$) of **99**

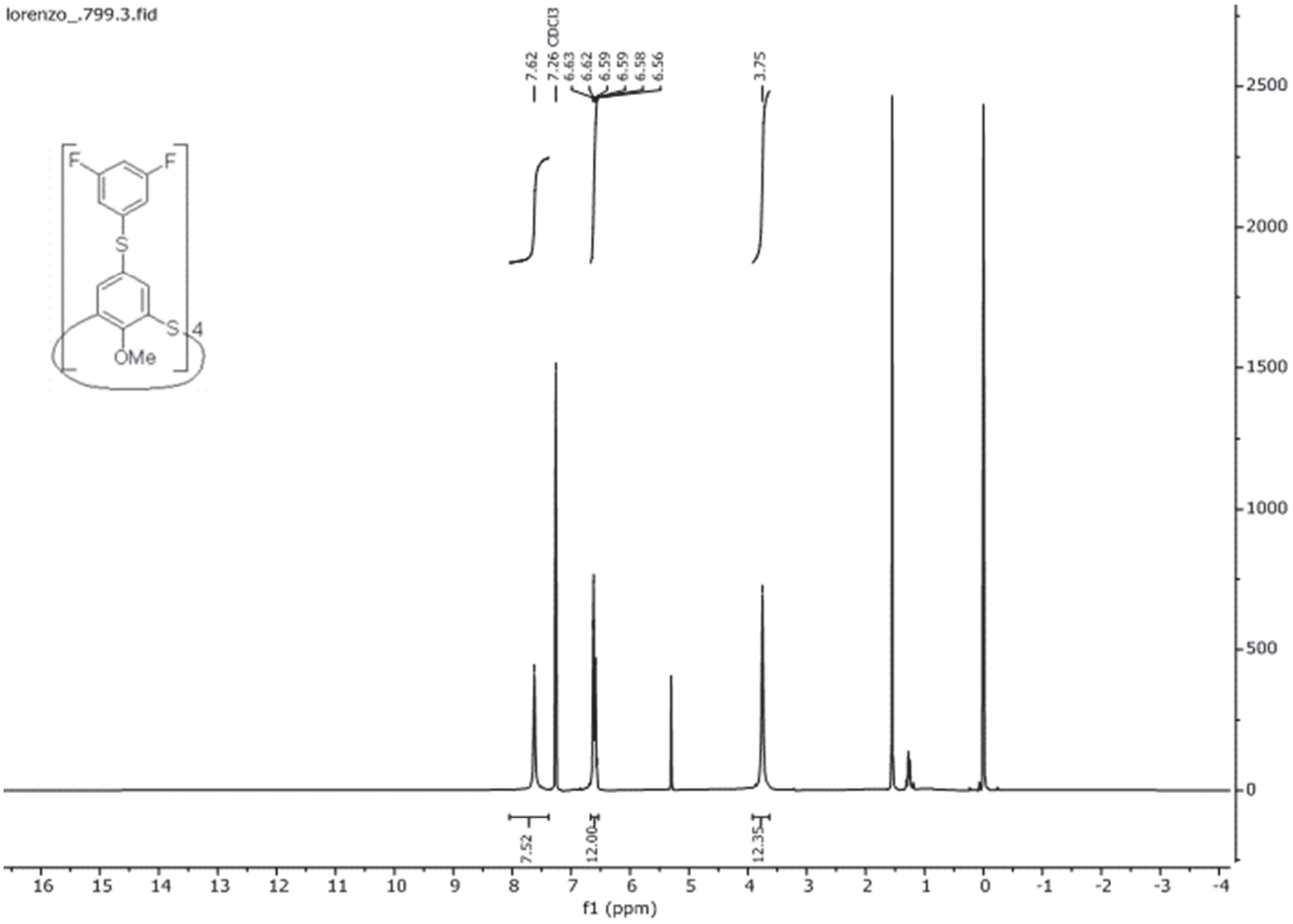

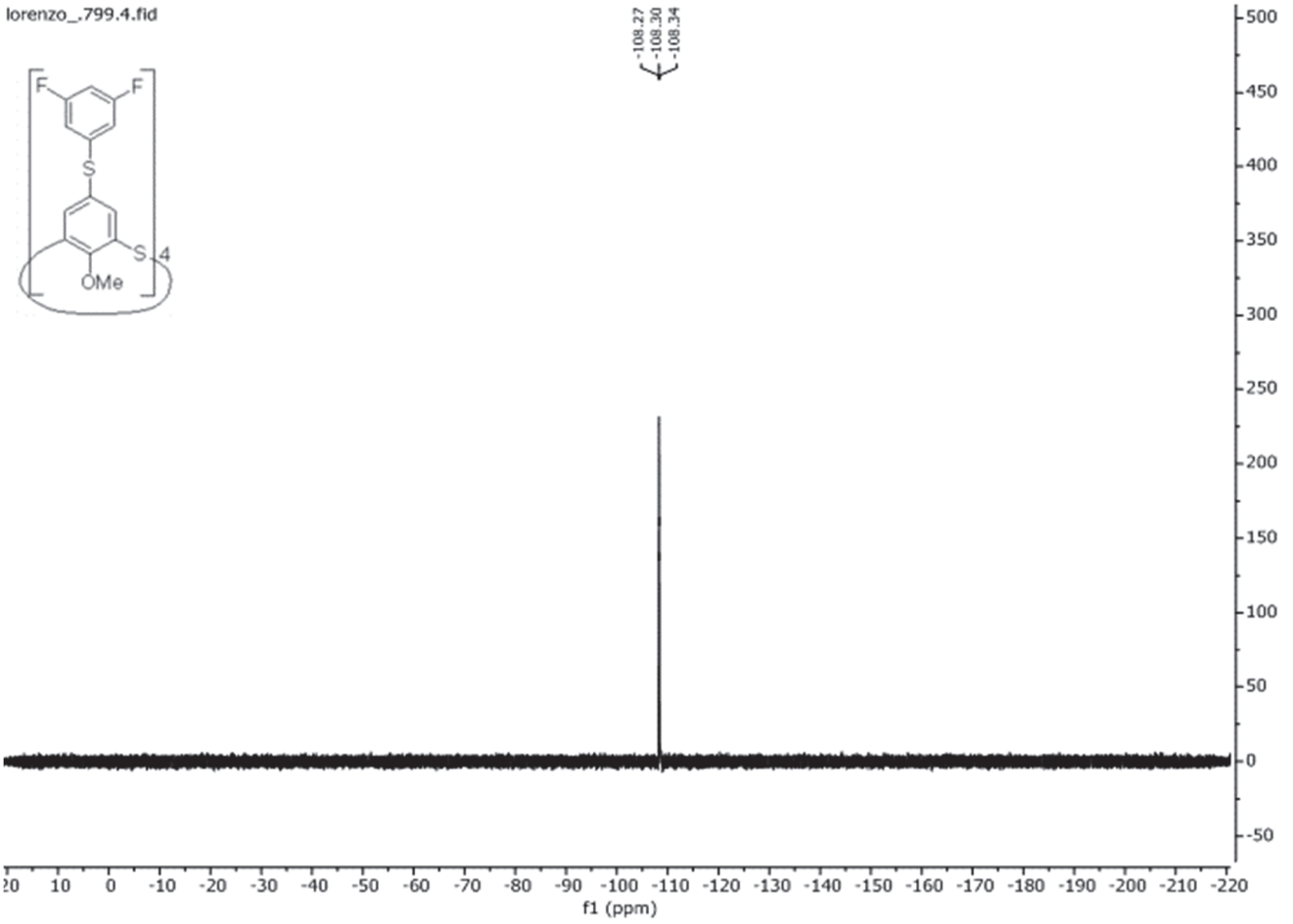

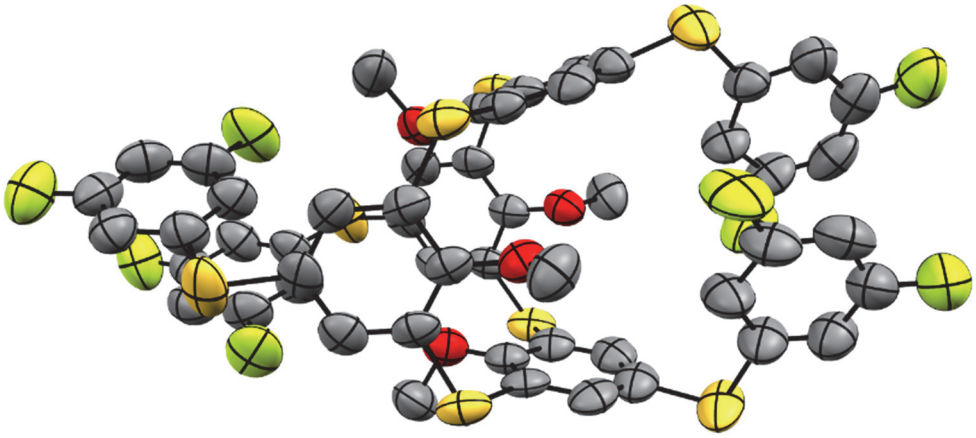

Figure 26: Solid state structure of compound **99**. Hydrogens and solvent molecules are omitted for clarity and rotational ellipsoids are displayed at a 50% probability level.

Table A2. Crystal data for **99**

formula	$C_{55}H_{38}F_8O_5S_8$
formula weight	1187.42
Z, calculated density	8, 1.467 g/cm^{-3}
F(000)	4864
description and size of crystal	colourless block, 0.030 × 0.070 × 0.120 mm^3
absorption coefficient	3.737 mm^{-1}
min/max transmission	0.74 / 0.89
temperature	130K
radiation(wavelength)	Cu K_α (λ = 1.54178 Å)
Crystal system, space group	monoclinic, C 2/c
a	20.6005(12) Å
b	20.5969(12) Å
c	26.7959(17) Å
α	90°
β	108.934(4)°
γ	90°
V	10754.5(11) Å^3
min/max Θ	3.122° / 70.569°
number of collected reflections	57412
number of independent refections	10113 (merging r = 0.000)
number of observed reflections	10090 (I>2.0σ(I))
number of refined parameters	673
r	0.1148
rW	0.3911
goodness of fit	0.9962

^{1}H NMR (250 MHz, Acetone d_6) and {^{1}H}^{19}F NMR (235 MHz, Acetone d_6) of **97**

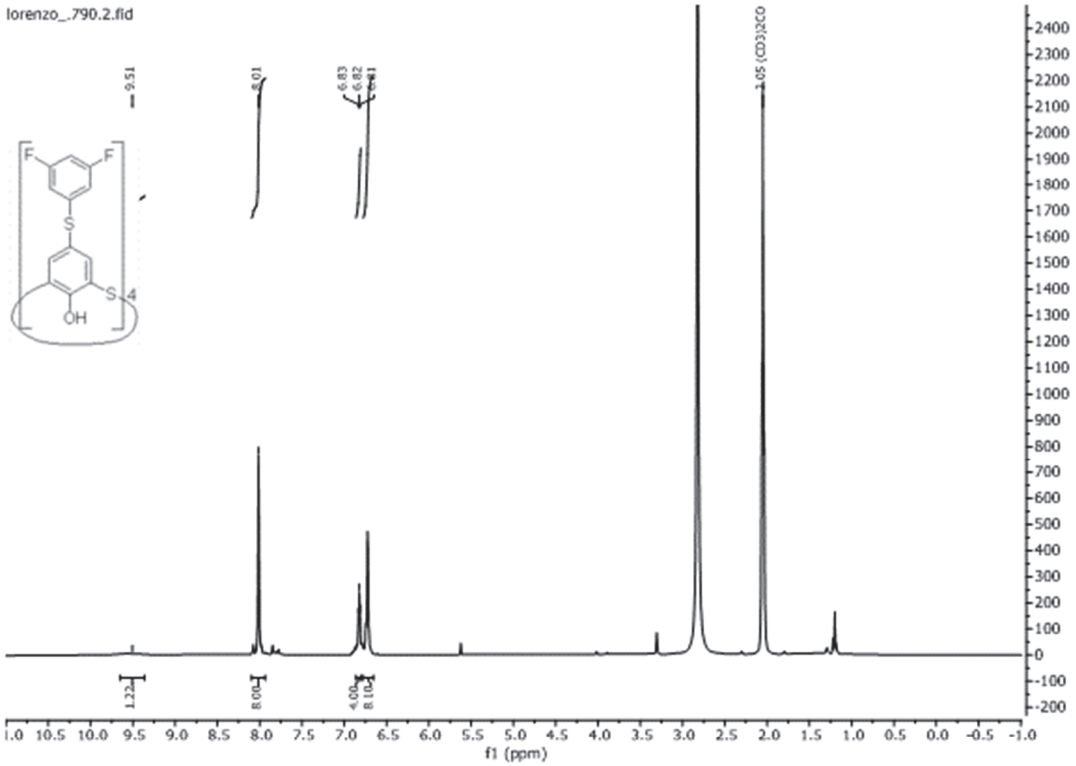

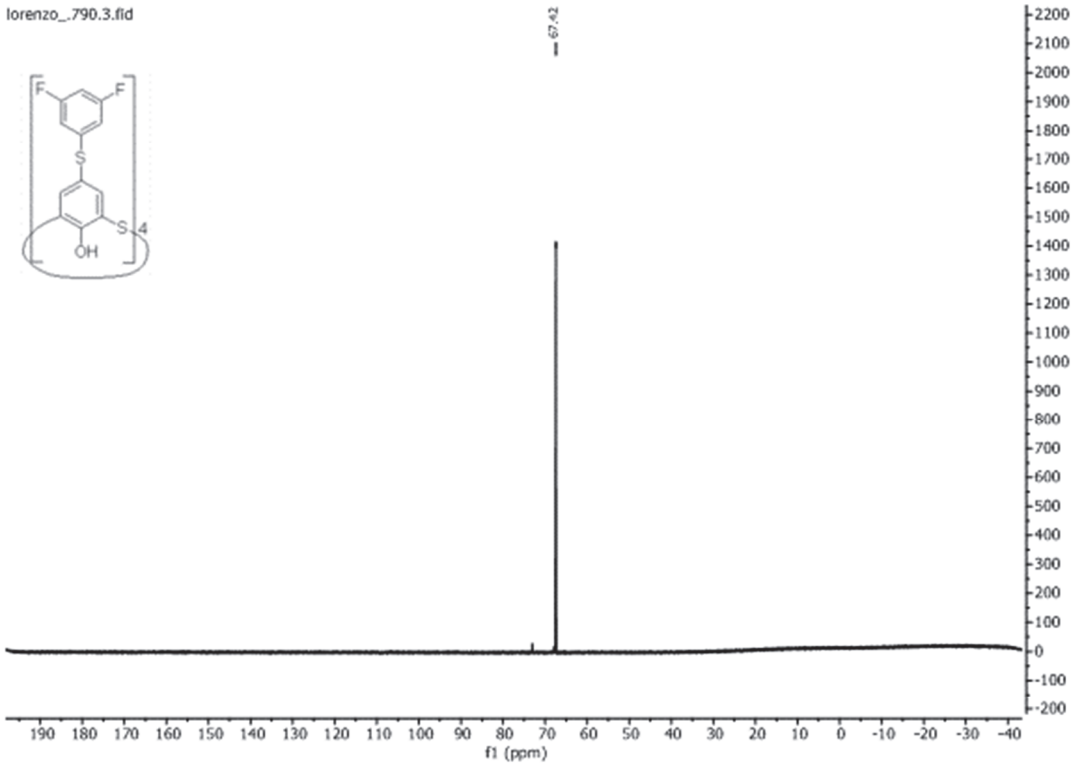

^{1}H NMR (250 MHz, $CDCl_3$) and $^{19}F\{^{1}H\}$ NMR (235 MHz, $CDCl_3$) of **106**

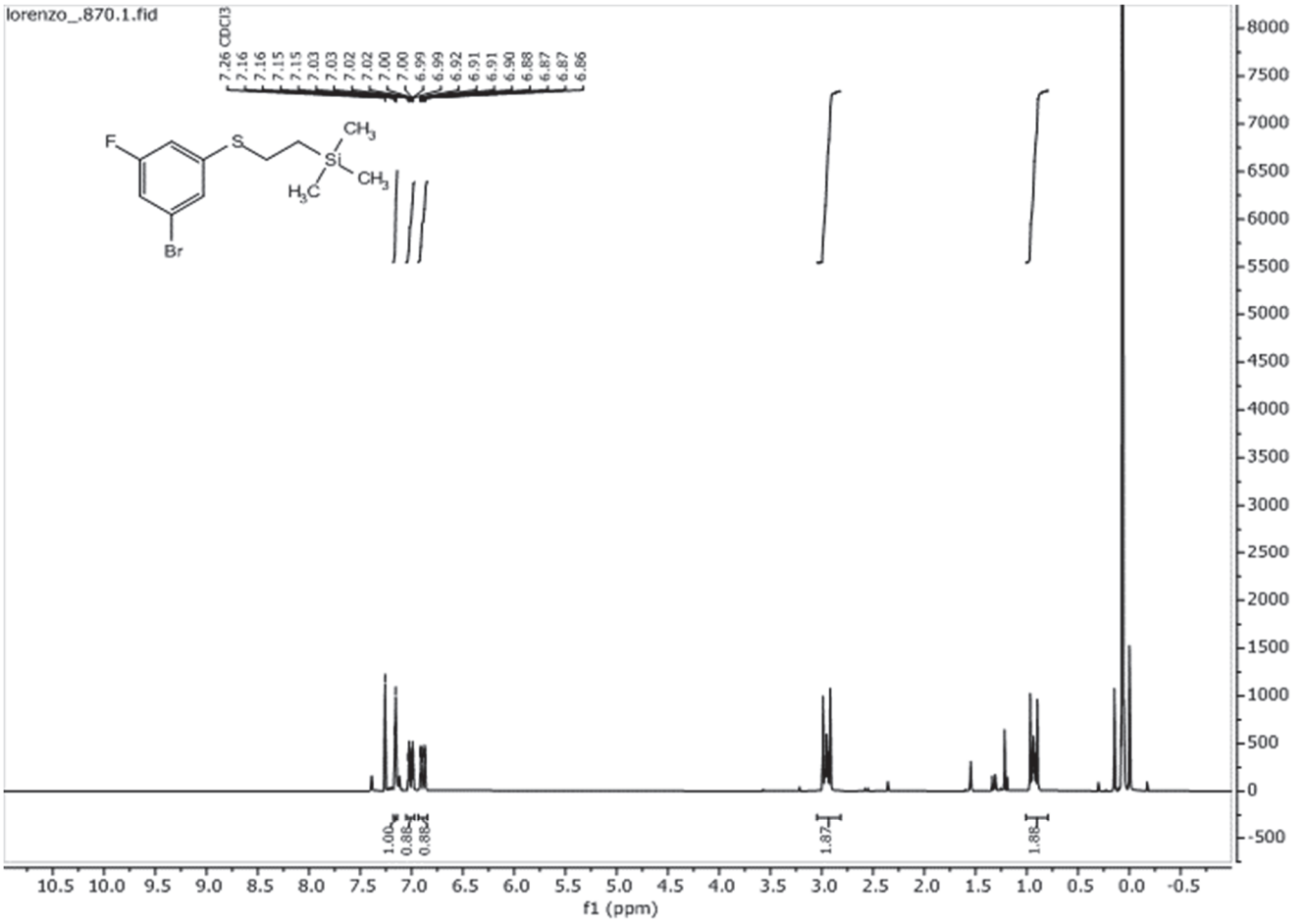

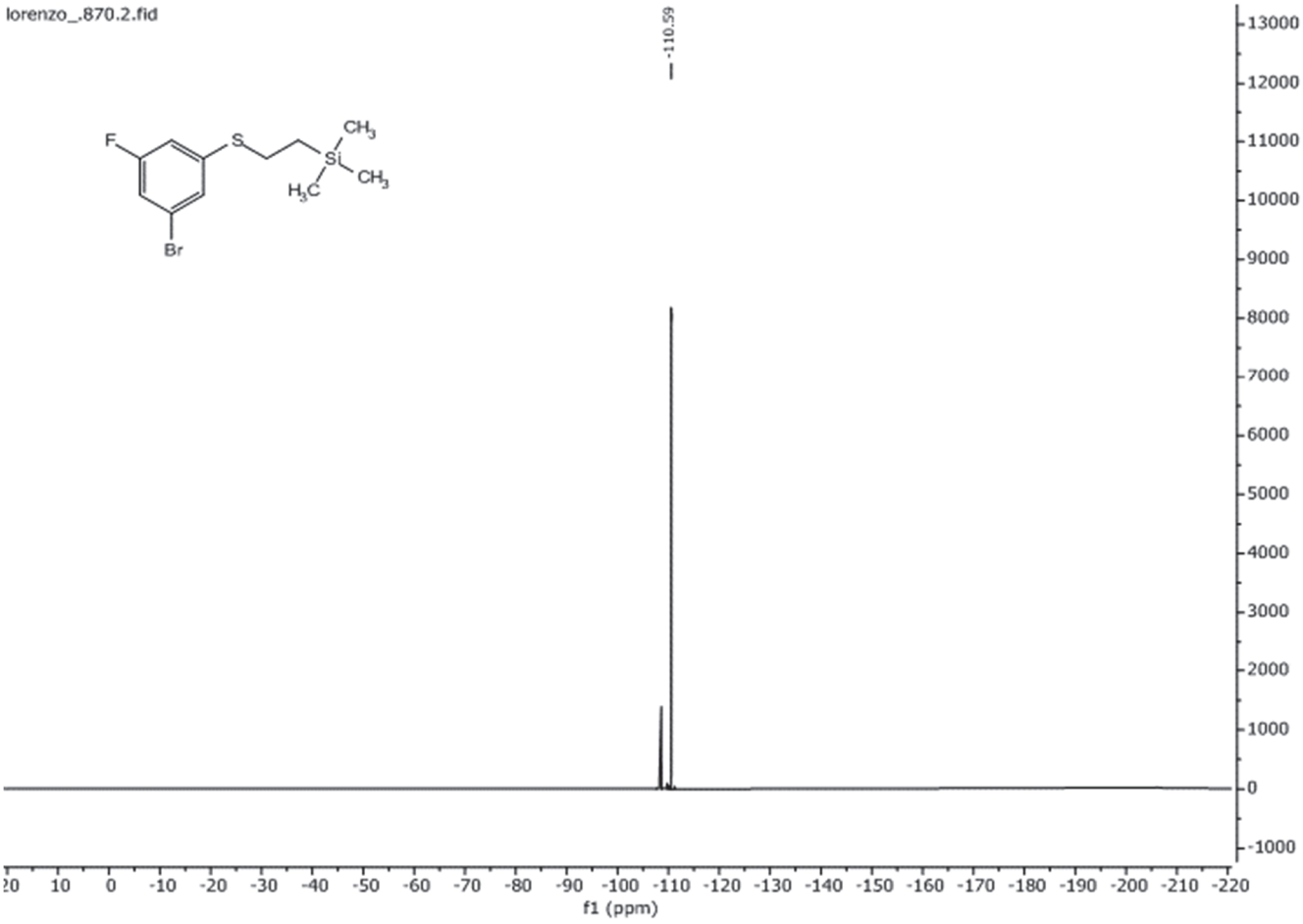

^{1}H NMR (250 MHz, $CDCl_3$) of **107**

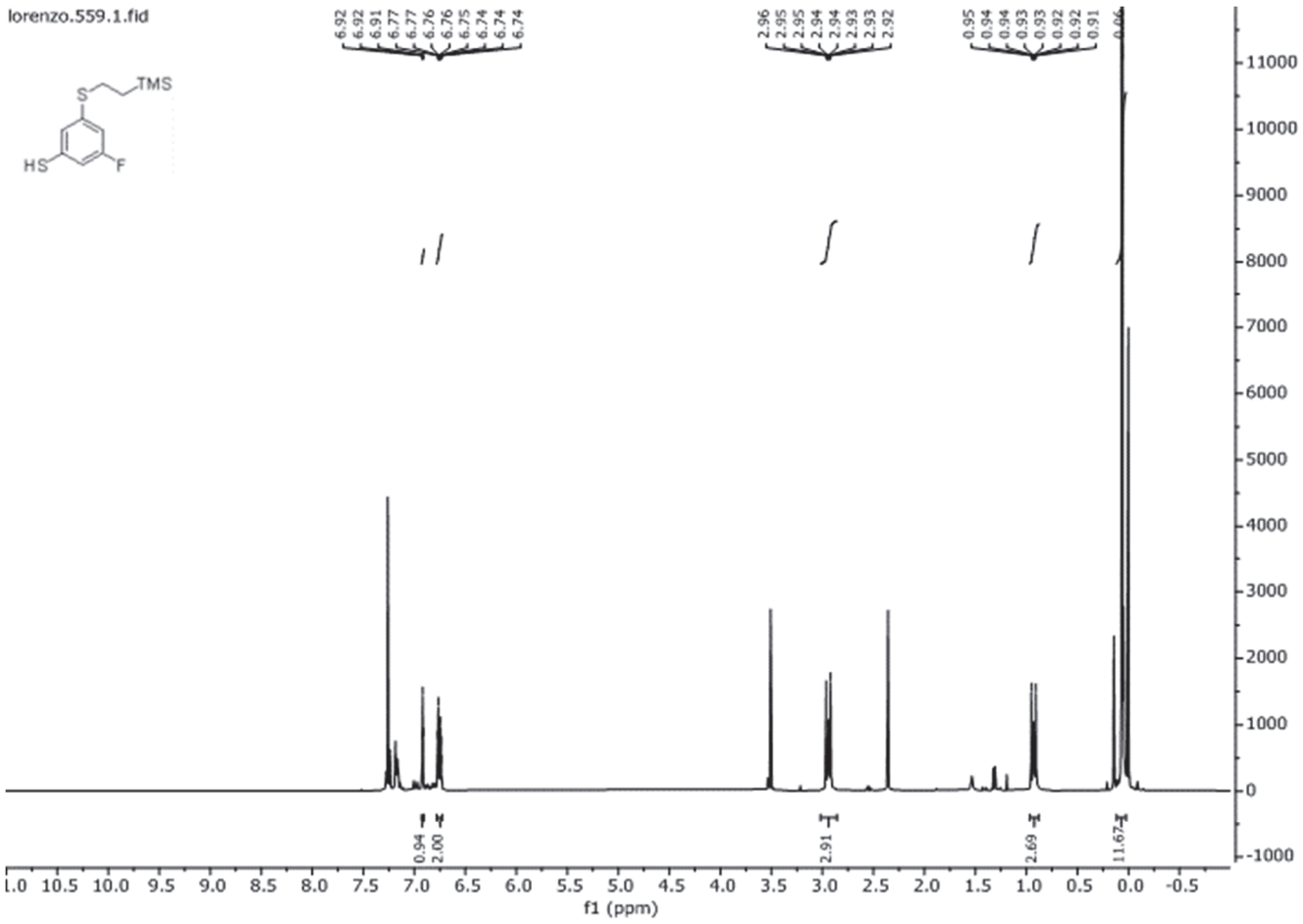

^{1}H NMR (400 MHz, $CDCl_3$) and ^{13}C NMR (101 MHz, $CDCl_3$) of **102**

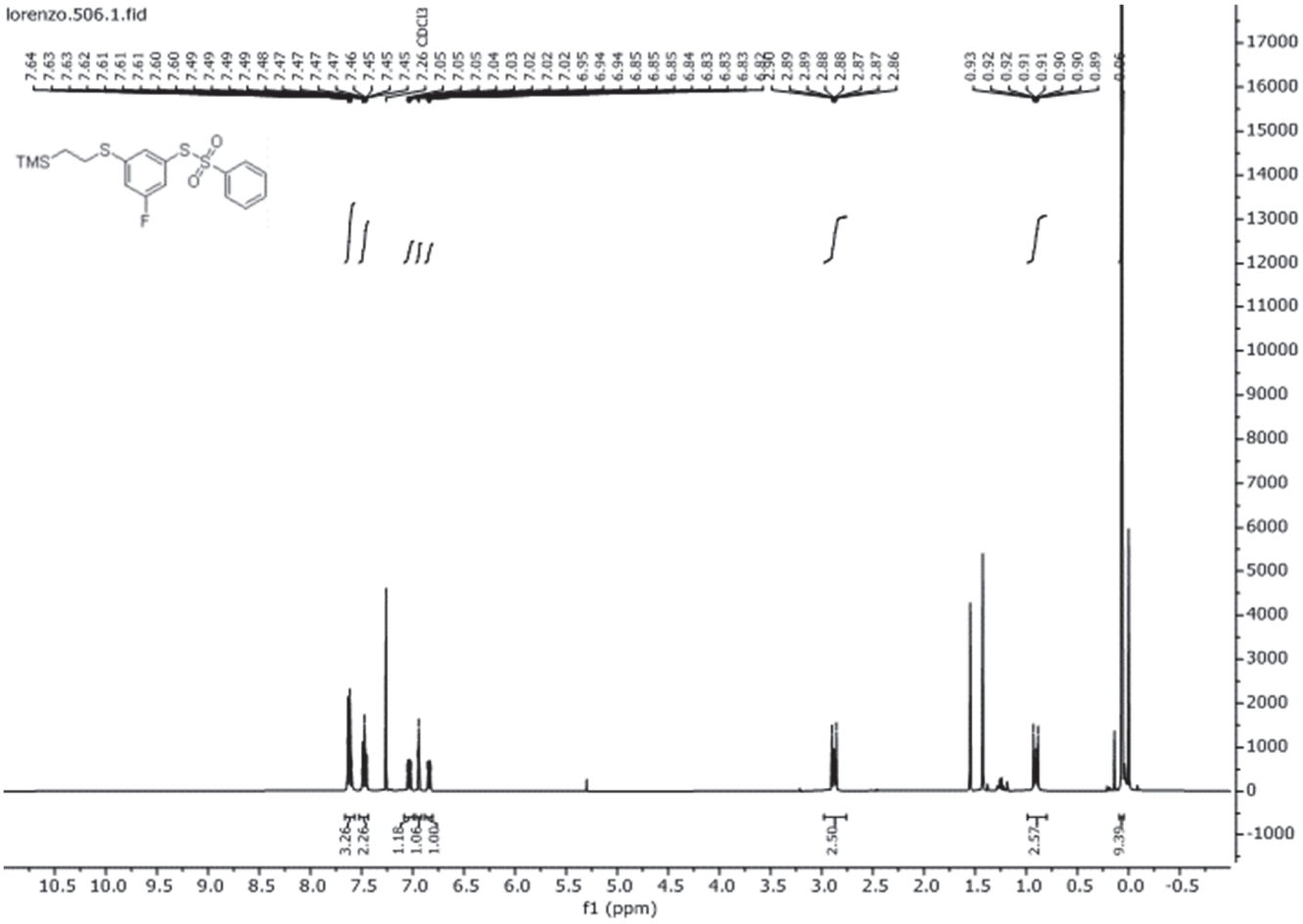

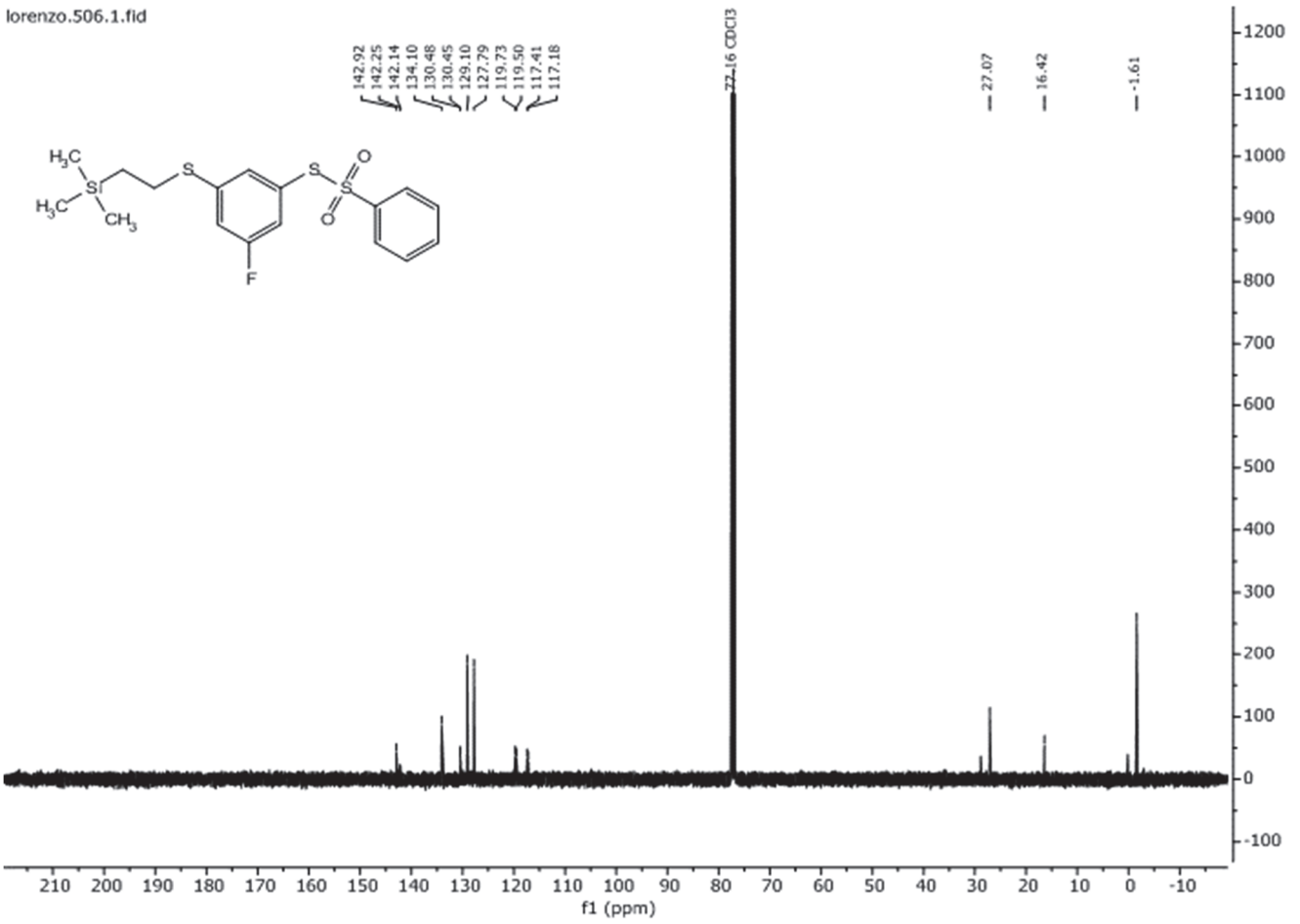

^{1}H NMR (400 MHz, $CDCl_3$) and $^{19}F\{^{1}H\}$ NMR (376 MHz, $CDCl_3$) of **108**

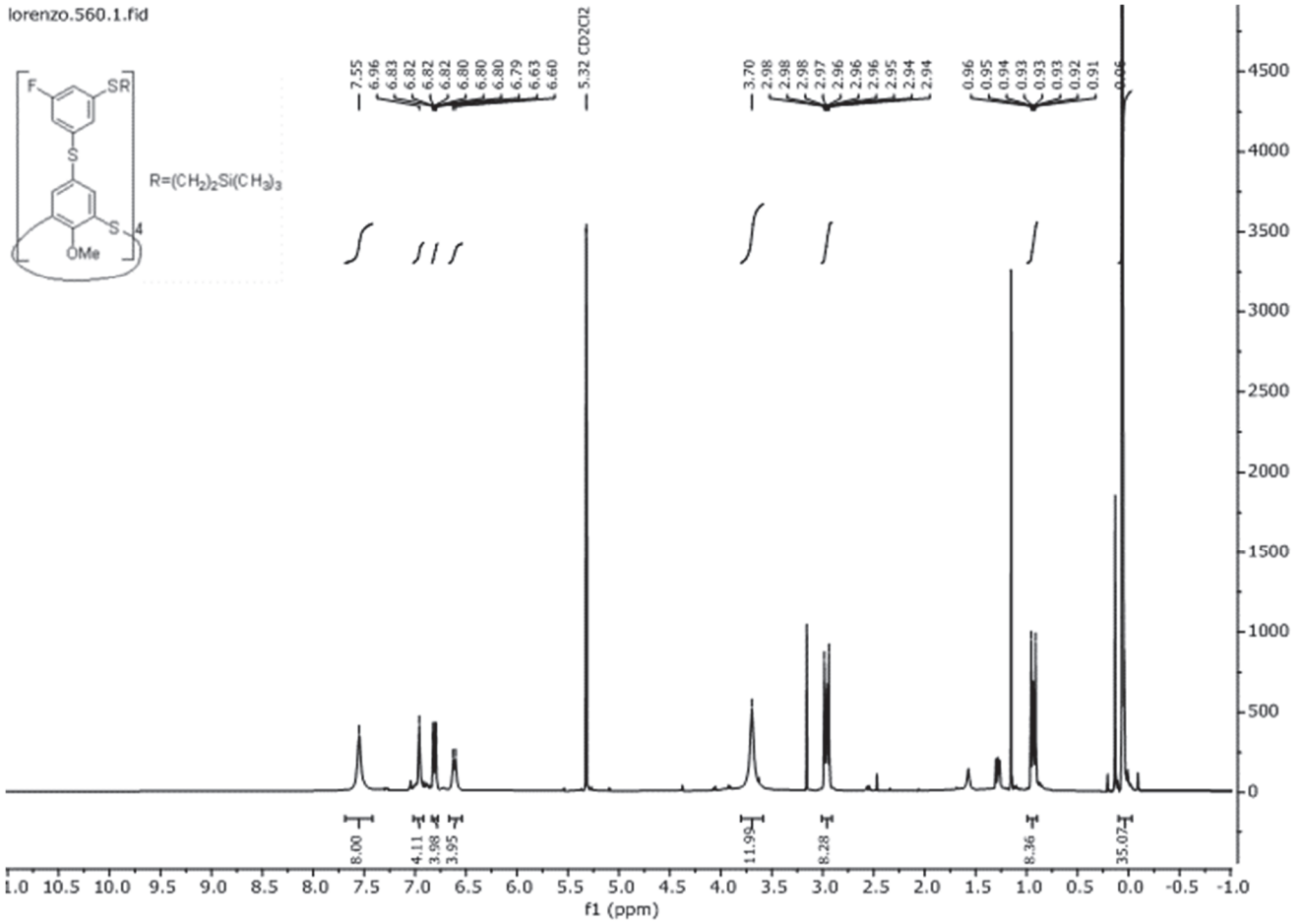

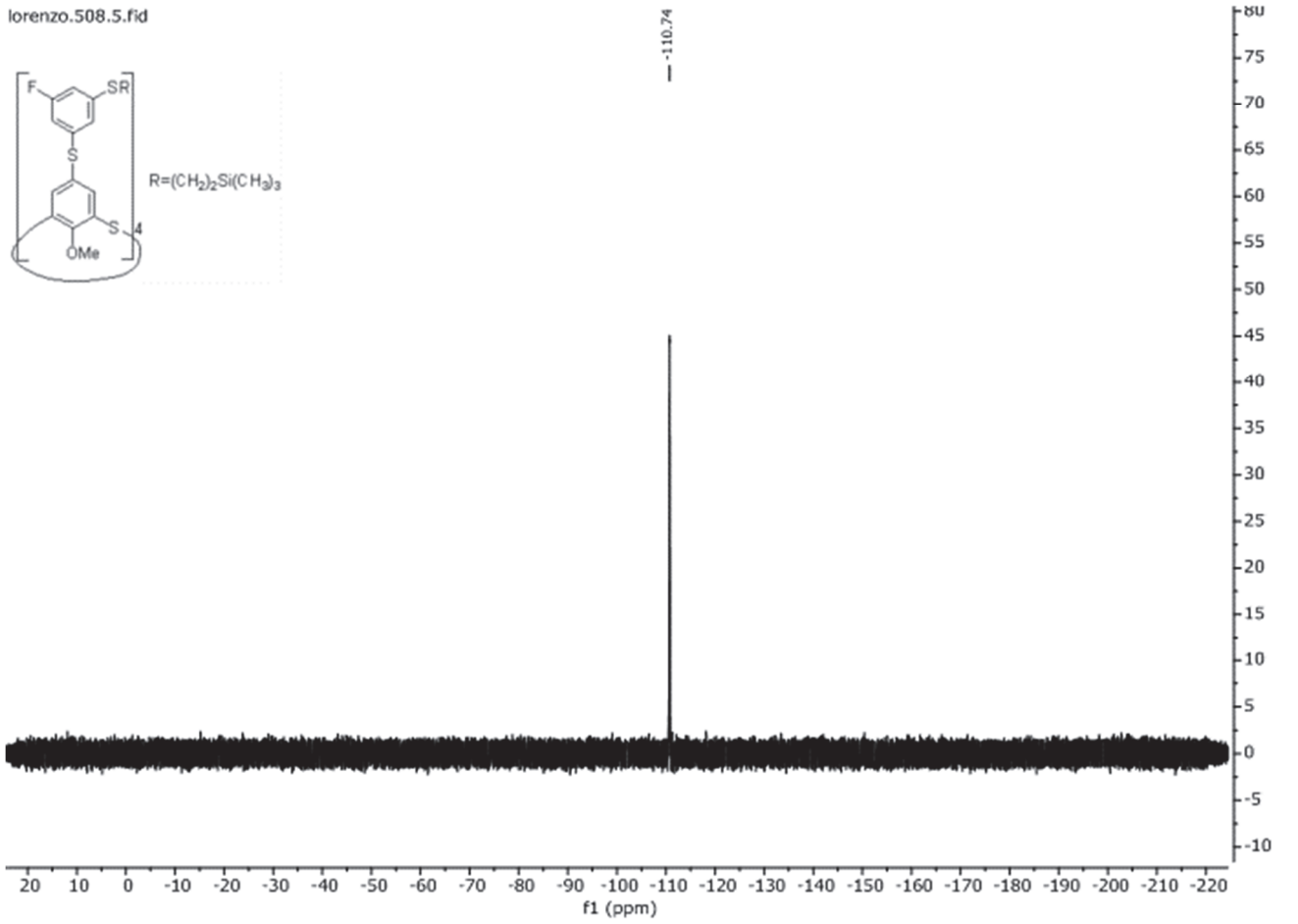

^{1}H NMR (400 MHz, $CDCl_3$) and ^{13}C NMR (101 MHz, $CDCl_3$) of **108**

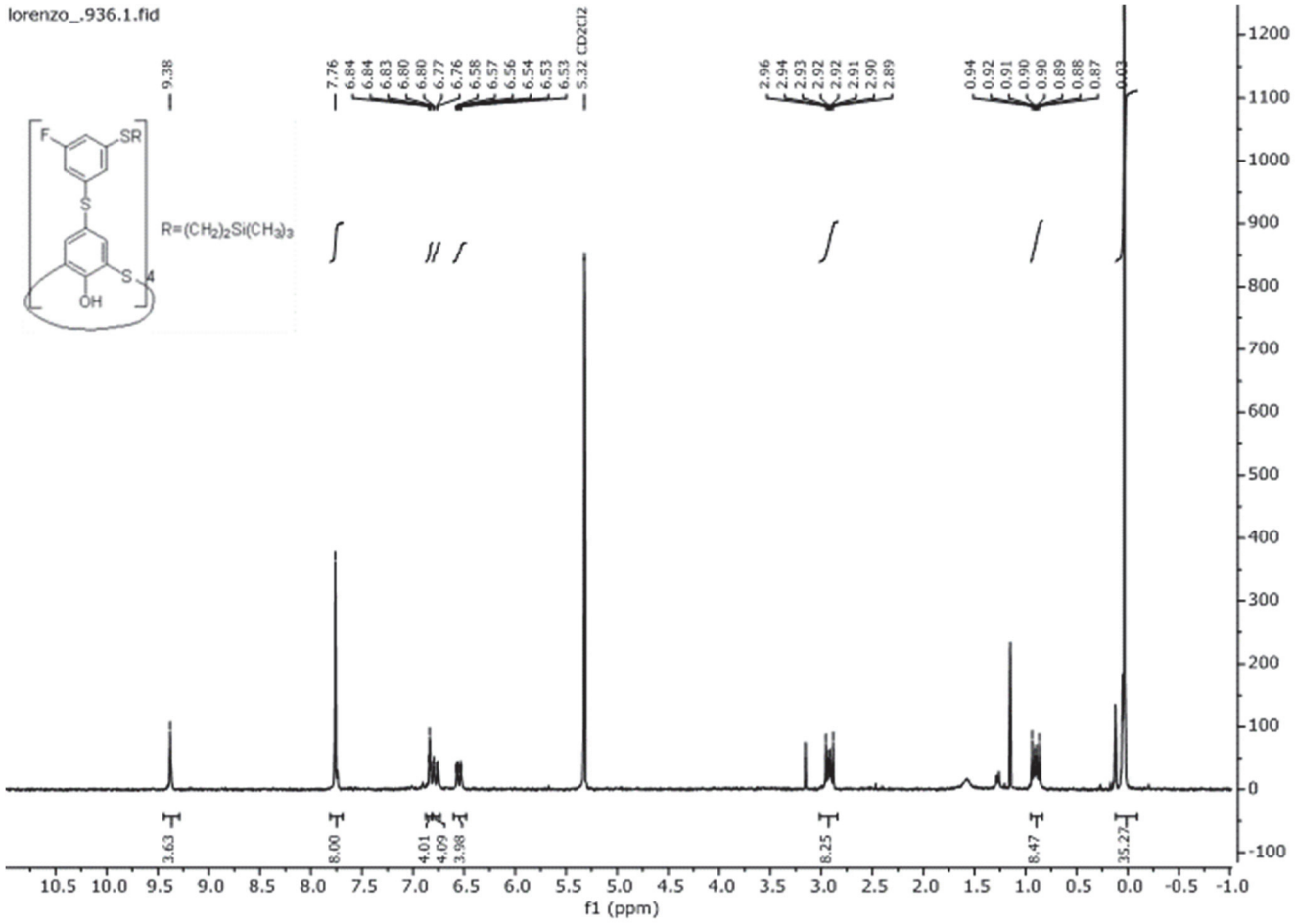

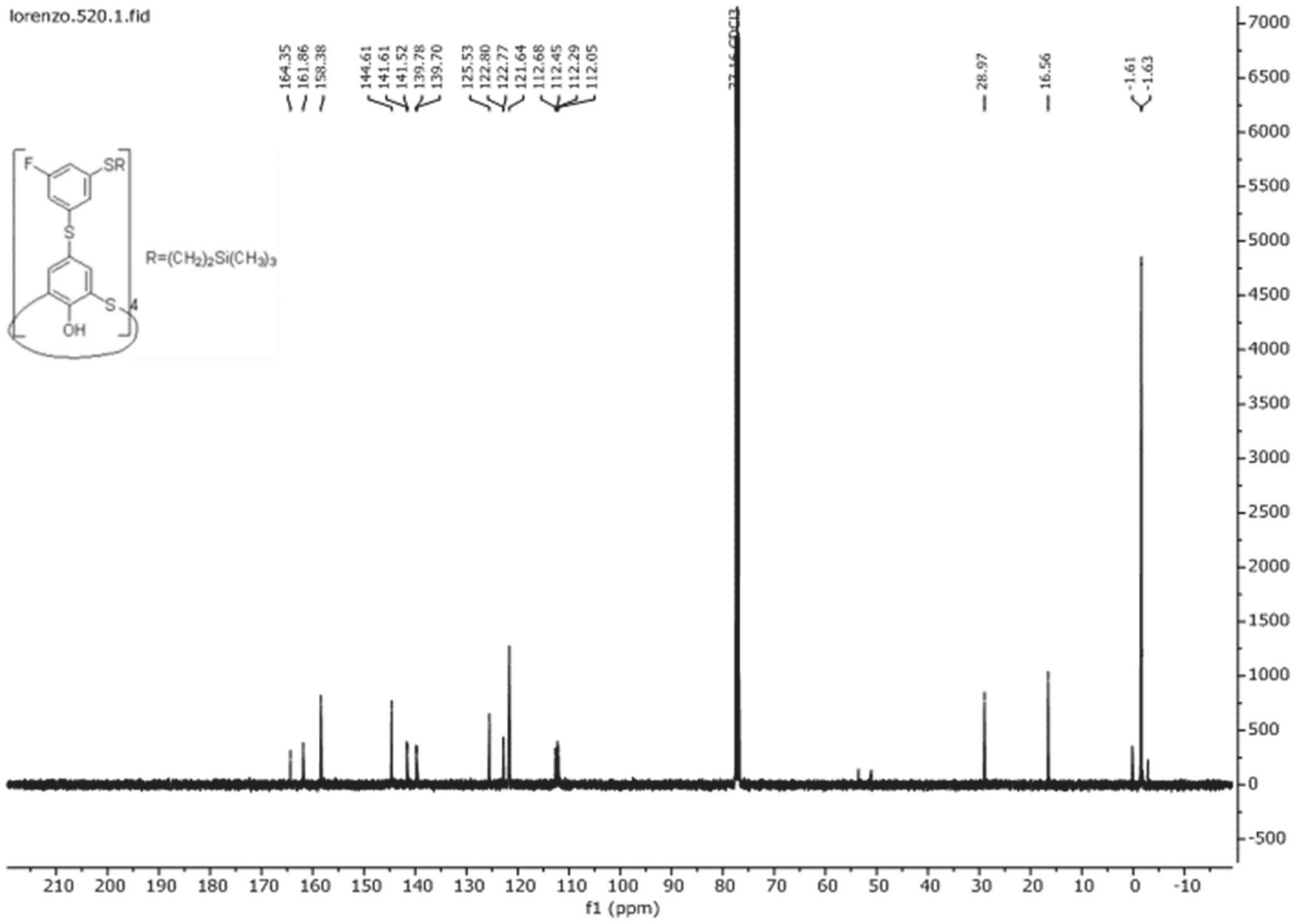

$^{19}F\{^{1}H\}$ NMR (376 MHz, $CDCl_3$) of **108**

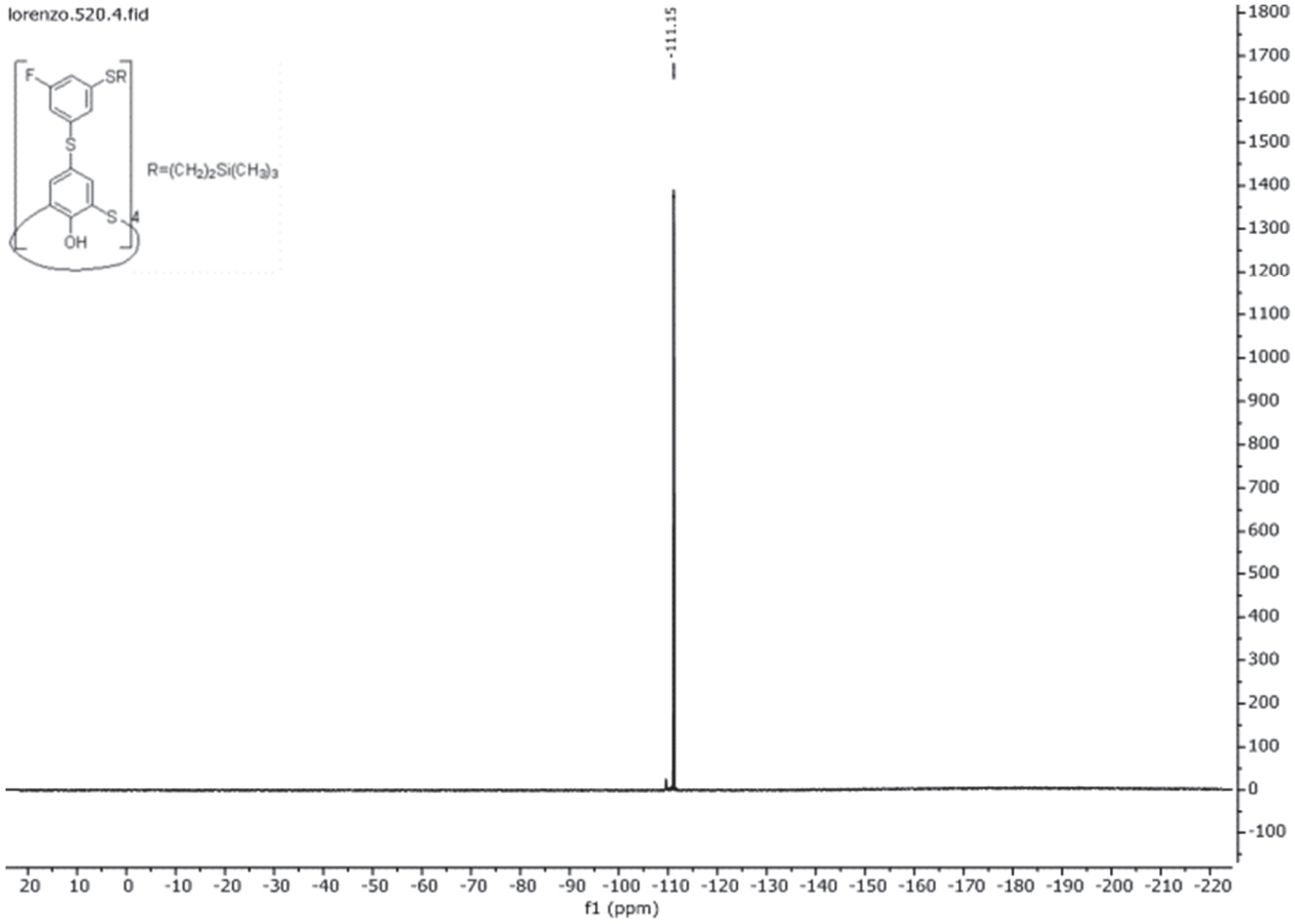

^{1}H NMR (400 MHz, $CDCl_3$) and ^{13}C NMR (101 MHz, $CDCl_3$) of **131**

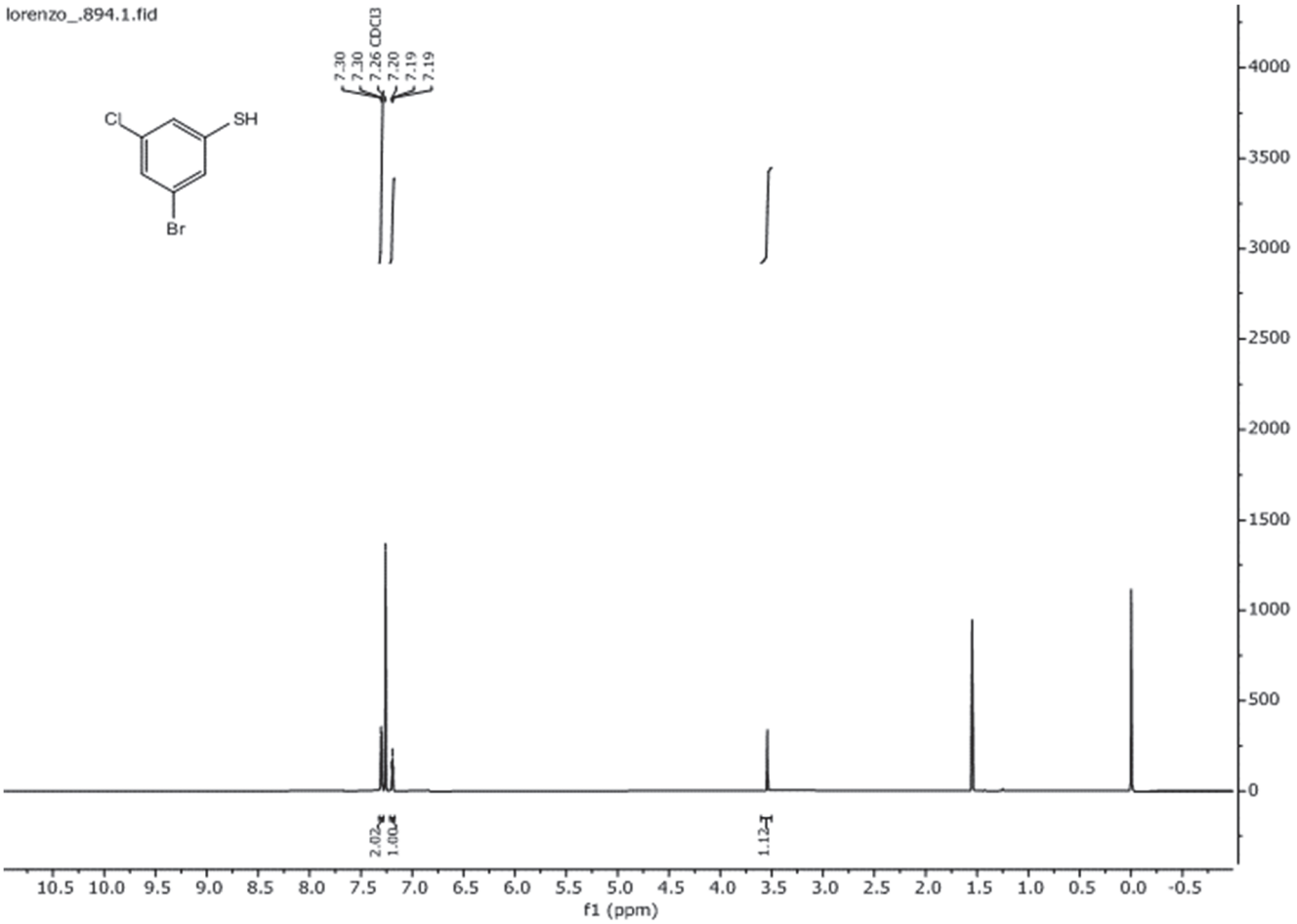

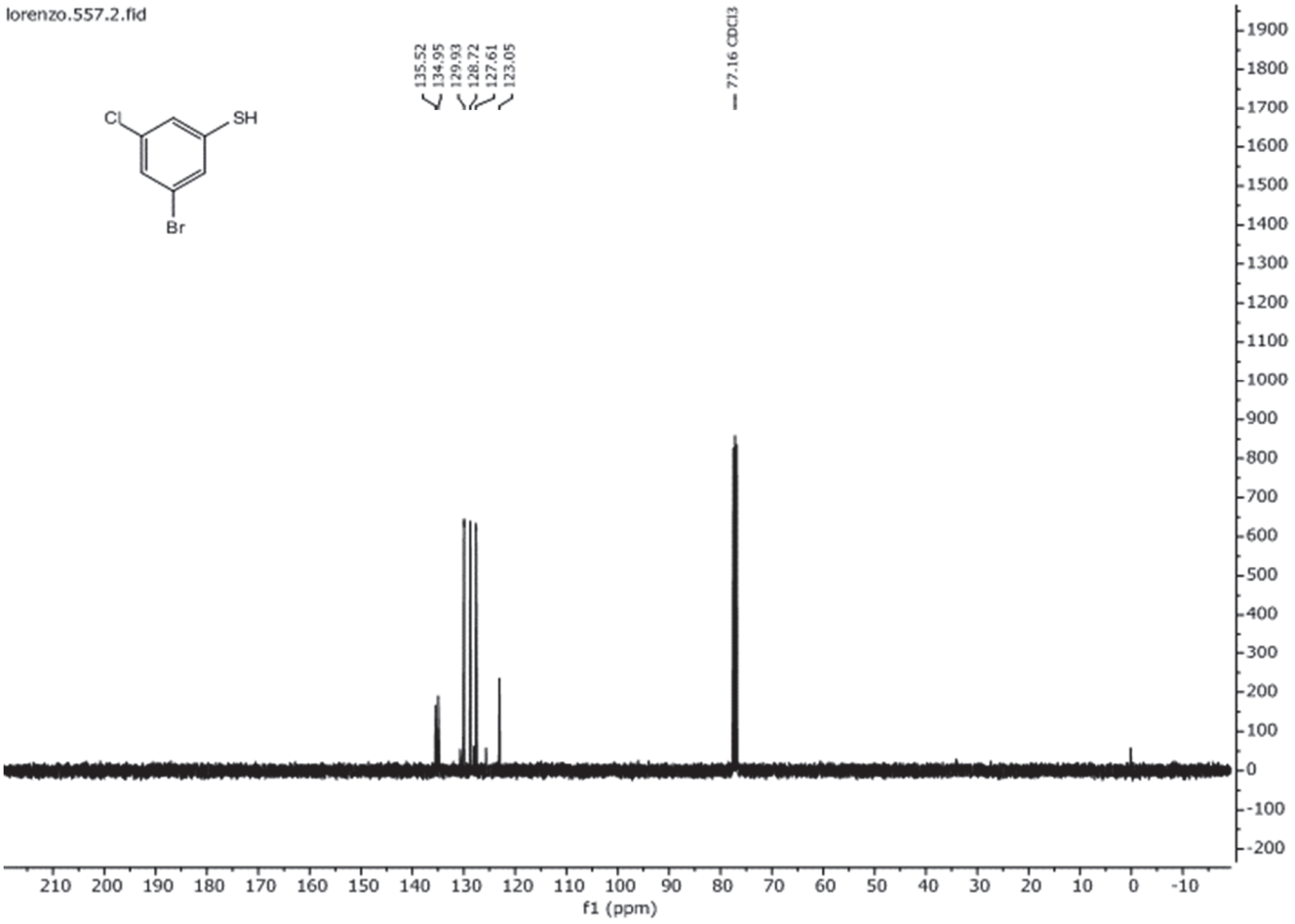

^{1}H NMR (400 MHz, $CDCl_3$) and ^{13}C NMR (101 MHz, $CDCl_3$) of **112**

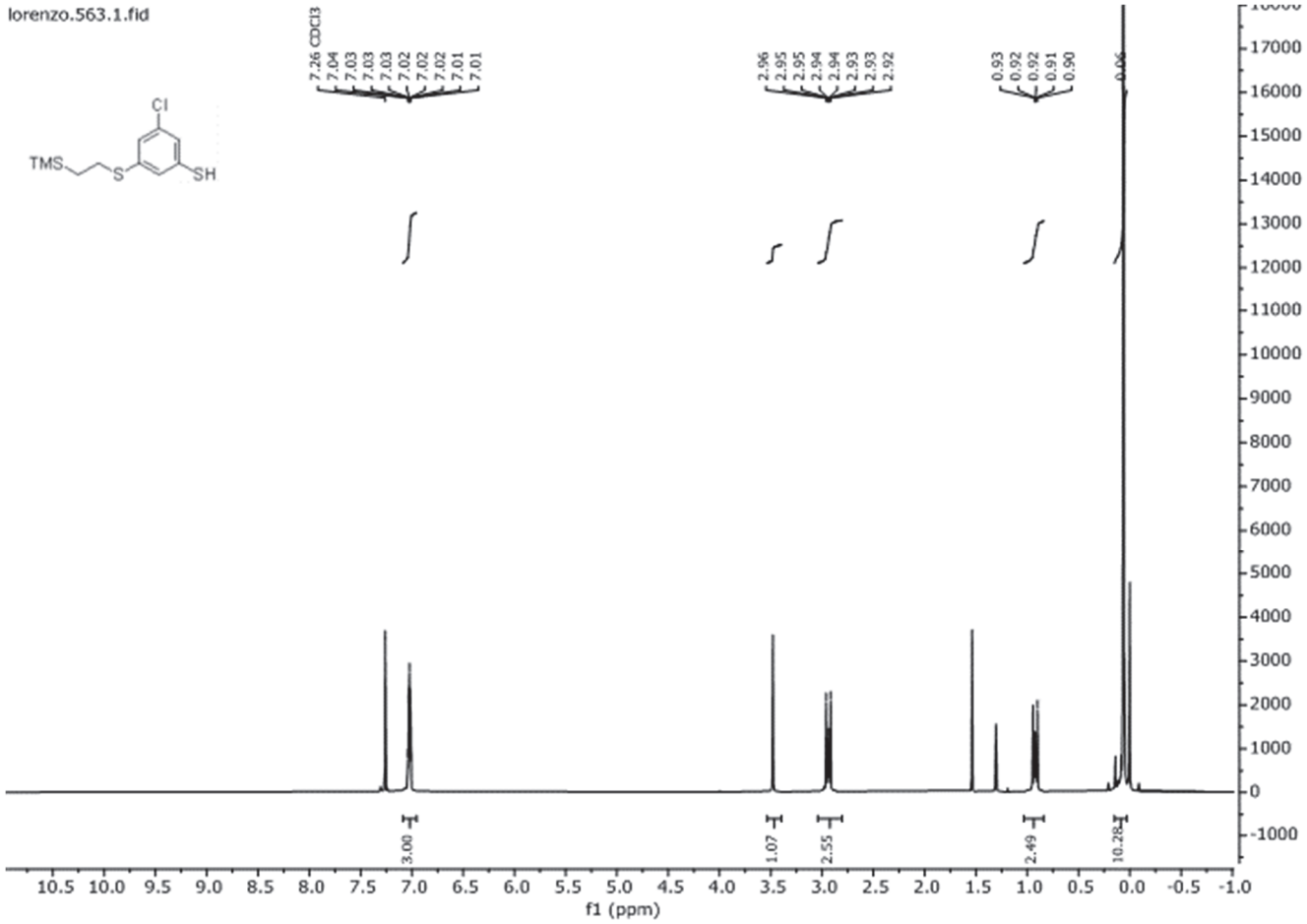

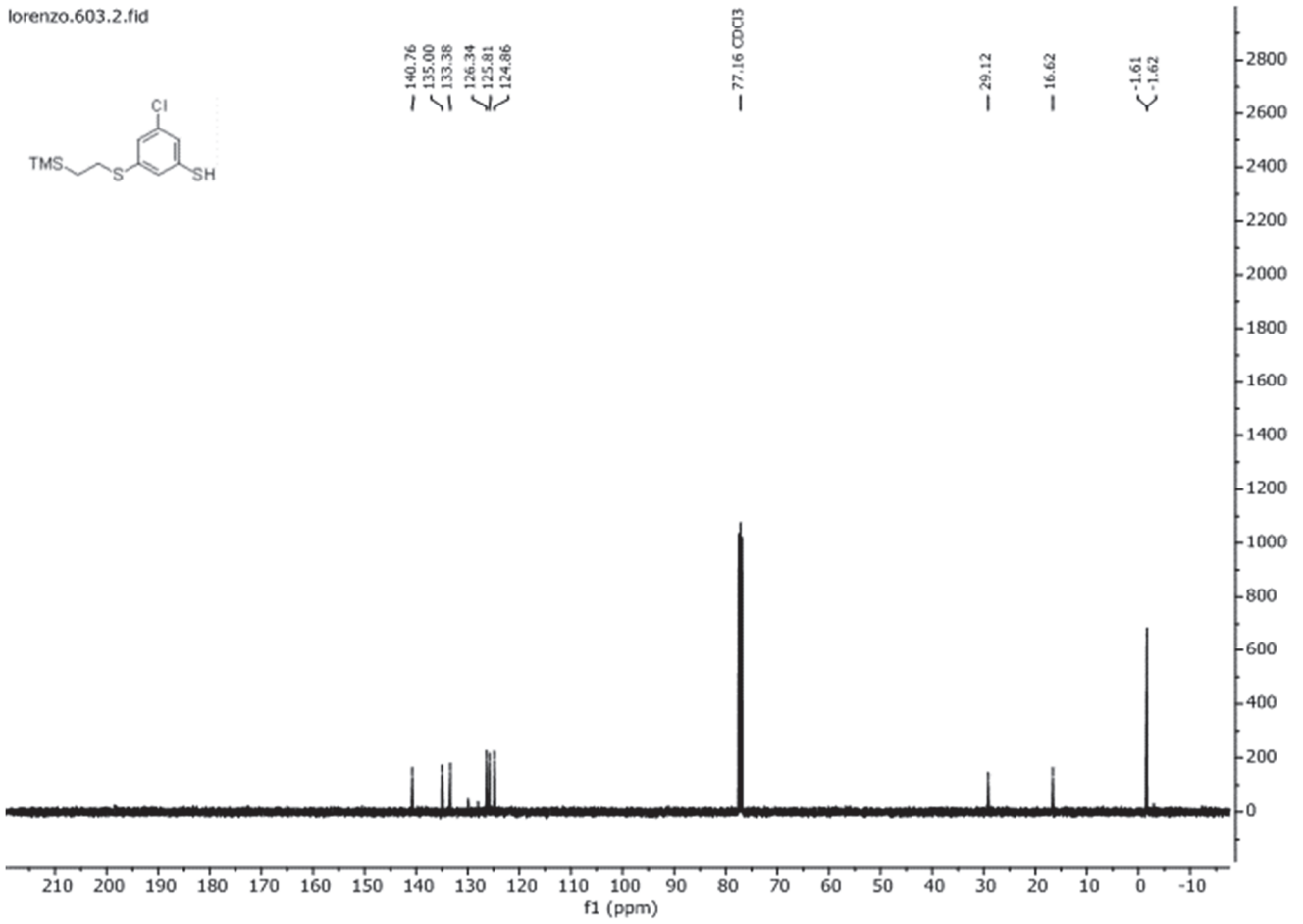

^{1}H NMR (400 MHz, CD_2Cl_2) of **113**

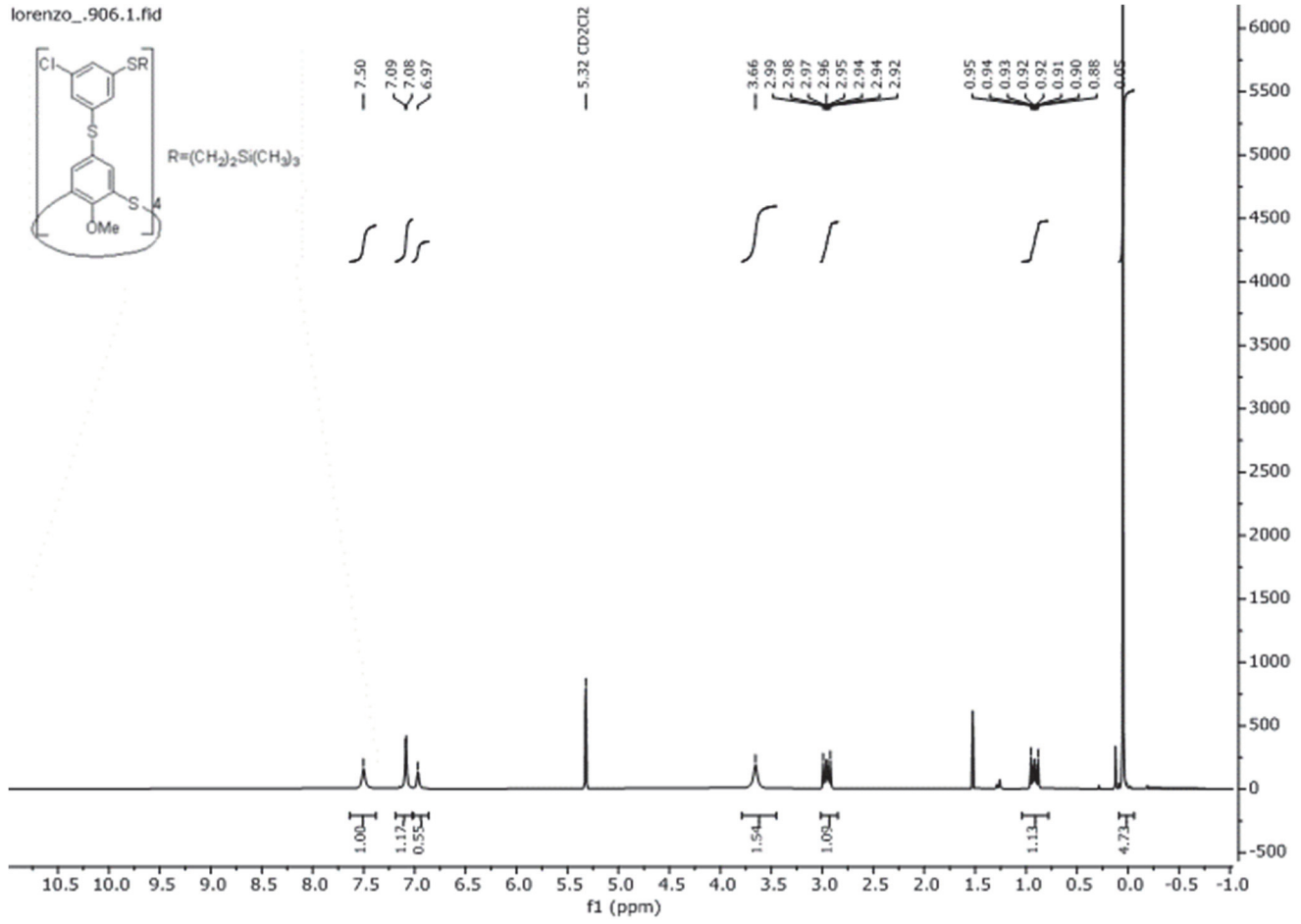

^{1}H NMR (500 MHz, CD_2Cl_2) and ^{13}C NMR (126 MHz, CD_2Cl_2) of **115**

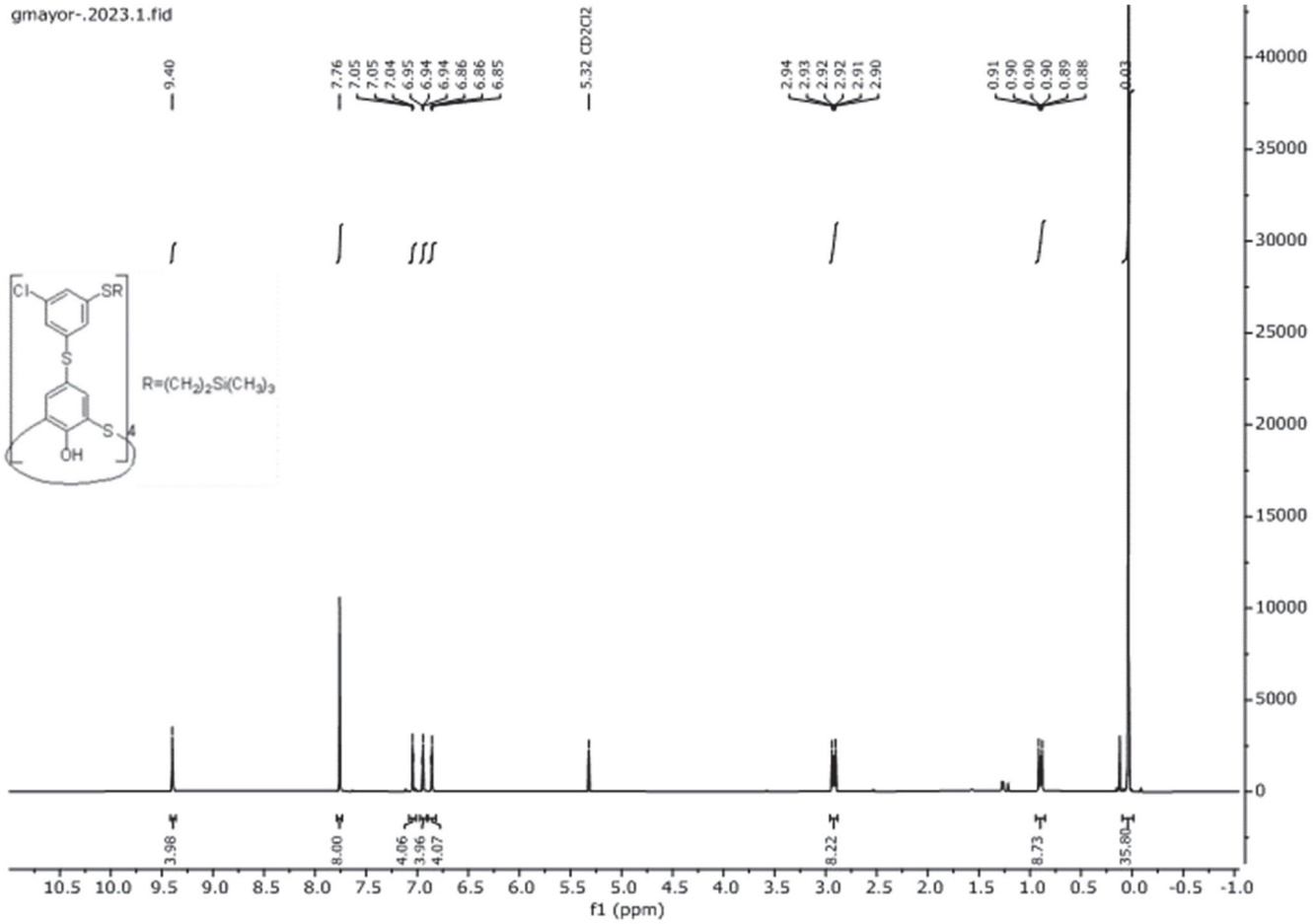

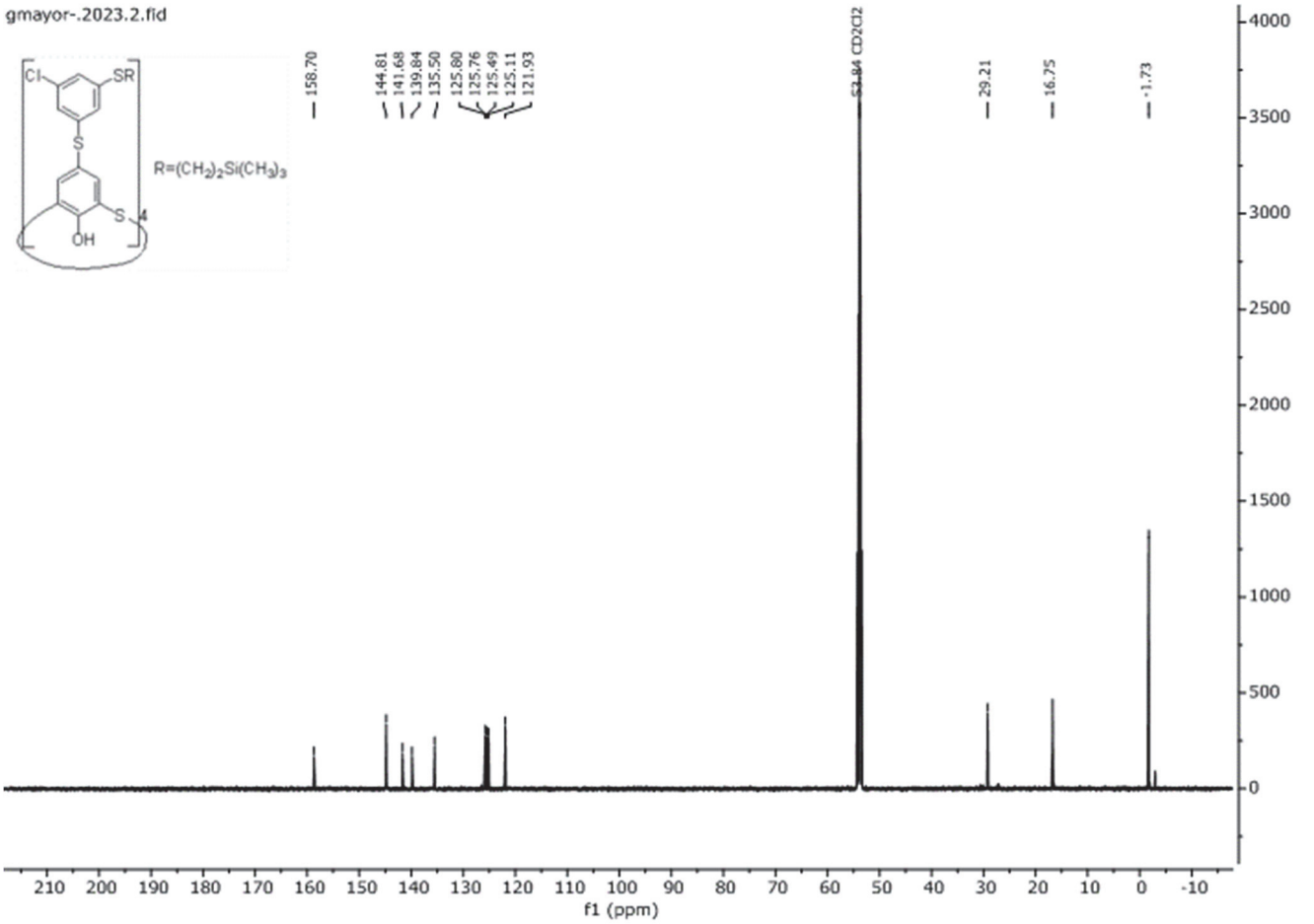

HR-ESI MS spectra of **115**

High Resolution Mass Spectrometry Report

Sample Name	**Lorenzo Bizzini / LDB204**	Instrument	maXis 4G
Comment	10 ug/mL in MeCN	Method	34 Direct_neg_high.m

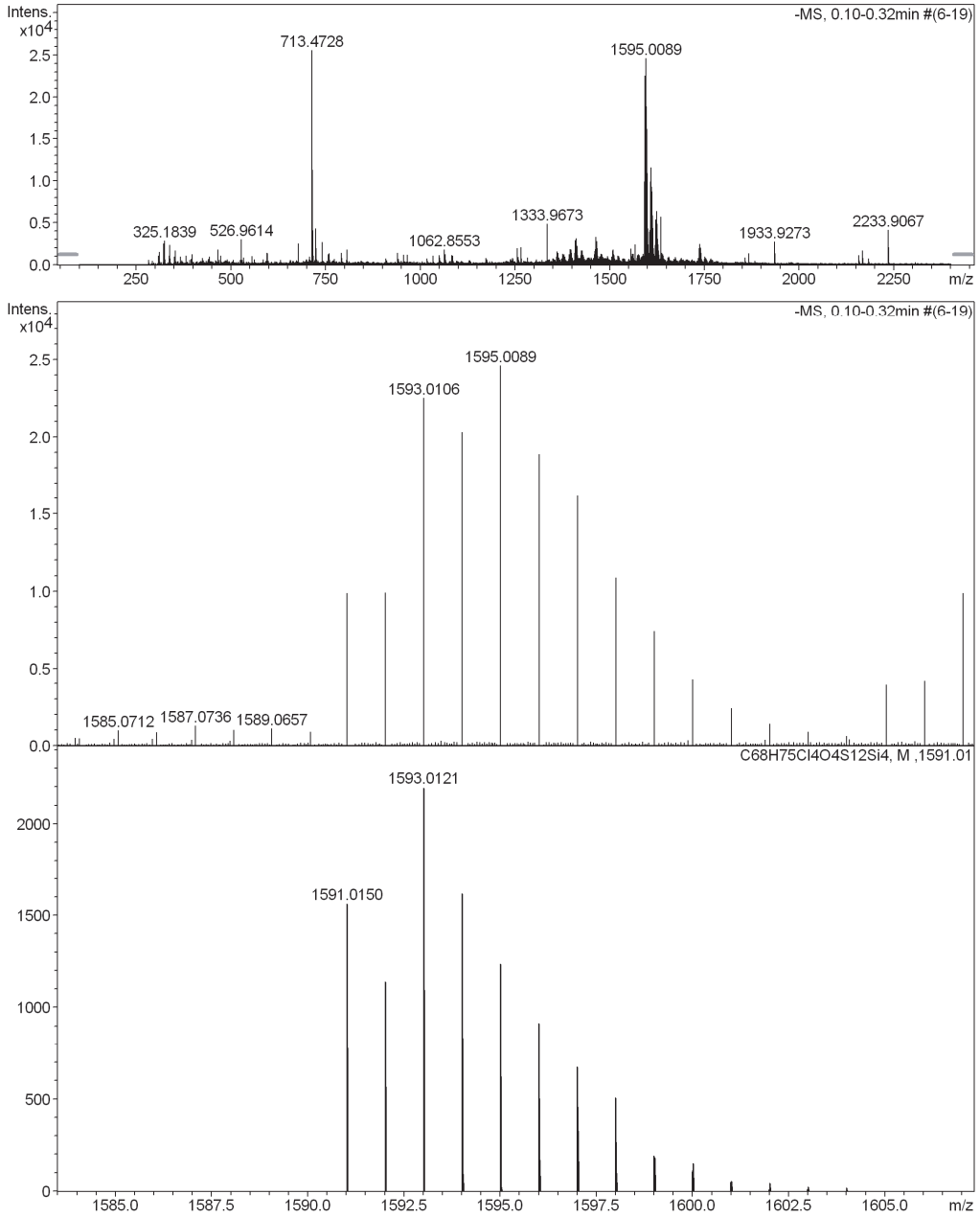

High Resolution Mass Spectrometry Report

Measured m/z vs. theoretical m/z

Meas. m/z	#	Formula	Score	m/z	err [mDa]	err [ppm]	mSigma	rdb	e^- Conf	z
1591.0125	1	C 68 H 75 Cl 4 O 4 S 12 Si 4	100.00	1591.0150	2.6	1.6	19.6	33.5	even	1-

Mass list

#	m/z	I %	I
1	311.1685	6.0	1526
2	323.0000	9.8	2503
3	325.1839	11.2	2859
4	339.1996	9.3	2360
5	353.2003	6.6	1670
6	465.3040	7.0	1784
7	526.9614	11.8	3003
8	594.8618	5.4	1385
9	677.4960	9.7	2482
10	713.4728	100.0	25499
11	714.4756	44.1	11255
12	715.4716	40.6	10357
13	716.4731	16.0	4092
14	723.5014	16.7	4265
15	724.5043	7.5	1923
16	740.4915	10.4	2663
17	791.4882	5.5	1402
18	805.9854	7.0	1794
19	939.6405	5.4	1372
20	1062.8553	7.0	1795
21	1255.9504	7.6	1944
22	1265.9798	8.2	2084
23	1333.9673	19.0	4839
24	1334.9712	6.2	1586
25	1360.9787	6.0	1539
26	1362.9785	5.5	1395
27	1394.9878	7.2	1832
28	1395.9886	5.6	1426
29	1396.9844	7.1	1804
30	1397.9830	5.4	1377
31	1398.9802	5.4	1373
32	1406.9985	5.5	1411
33	1408.9987	11.3	2883
34	1409.9991	9.0	2303
35	1410.9953	12.3	3143
36	1411.9957	8.8	2248
37	1412.9920	8.6	2199
38	1413.9907	5.8	1485
39	1425.0072	6.6	1674
40	1426.0061	5.3	1362
41	1427.0039	6.6	1673
42	1460.9704	6.4	1636
43	1461.0282	7.1	1823
44	1462.0298	6.5	1664
45	1463.0286	12.9	3286
46	1464.0291	10.4	2640
47	1465.0239	10.9	2780
48	1466.0263	7.7	1953
49	1467.0244	6.6	1688
50	1506.9568	6.6	1686
51	1508.9524	6.9	1768
52	1555.9313	7.4	1897
53	1565.9596	9.4	2389
54	1591.0125	38.7	9858
55	1592.0147	38.8	9900
56	1593.0106	88.2	22489
57	1594.0119	79.5	20277
58	1595.0089	96.4	24577
59	1596.0090	74.0	18879
60	1597.0066	63.6	16218
61	1598.0065	42.5	10838
62	1599.0044	29.1	7415

High Resolution Mass Spectrometry Report

#	m/z	I %	I
63	1600.0033	16.8	4278
64	1601.0013	9.4	2390
65	1602.0019	5.5	1402
66	1605.0266	15.3	3901
67	1606.0299	16.2	4139
68	1607.0240	38.7	9858
69	1608.0257	34.0	8660
70	1609.0212	45.3	11543
71	1610.0200	36.3	9254
72	1611.0165	34.0	8666
73	1612.0167	23.0	5869
74	1613.0119	17.0	4325
75	1614.0096	11.5	2921
76	1615.0044	7.7	1952
77	1619.0408	9.1	2330
78	1620.0448	9.1	2309
79	1621.0409	21.0	5362
80	1622.0417	18.8	4798
81	1623.0374	25.0	6364
82	1624.0374	19.1	4867
83	1625.0317	17.1	4352
84	1626.0309	12.0	3061
85	1627.0248	9.5	2420
86	1628.0247	6.5	1661
87	1633.9466	22.3	5693
88	1634.9504	8.4	2153
89	1637.0445	5.5	1406
90	1734.9771	7.6	1945
91	1735.9756	7.0	1774
92	1736.9730	9.7	2470
93	1737.9730	7.3	1864
94	1738.9732	7.8	1982
95	1739.9705	5.5	1413
96	1865.9407	5.3	1363
97	1933.9273	10.7	2740
98	2165.9218	6.6	1673
99	2233.9067	16.2	4118
100	2234.9121	8.2	2079

Acquisition Parameter

General	Fore Vacuum	2.69e+000 mBar	High Vacuum	9.94e-008 mBar	Source Type	ESI
	Scan Begin	100 m/z	Scan End	2400 m/z	Ion Polarity	Negative
Source	Set Nebulizer	0.4 Bar	Set Capillary	4500 V	Set Dry Gas	4.0 l/min
	Set Dry Heater	180 °C	Set End Plate Offset	-500 V		
Quadrupole	Set Ion Energy (MS only)	-10.0 eV				
Coll. Cell	Collision Energy	-20.0 eV	Set Collision Cell RF	500.0 Vpp		
Ion Cooler	Set Ion Cooler Transfer Time	140.0 µs	Set Ion Cooler Pre Pulse Storage Time	22.0 µs		

HR-ESI MS spectra of **100 and 114**

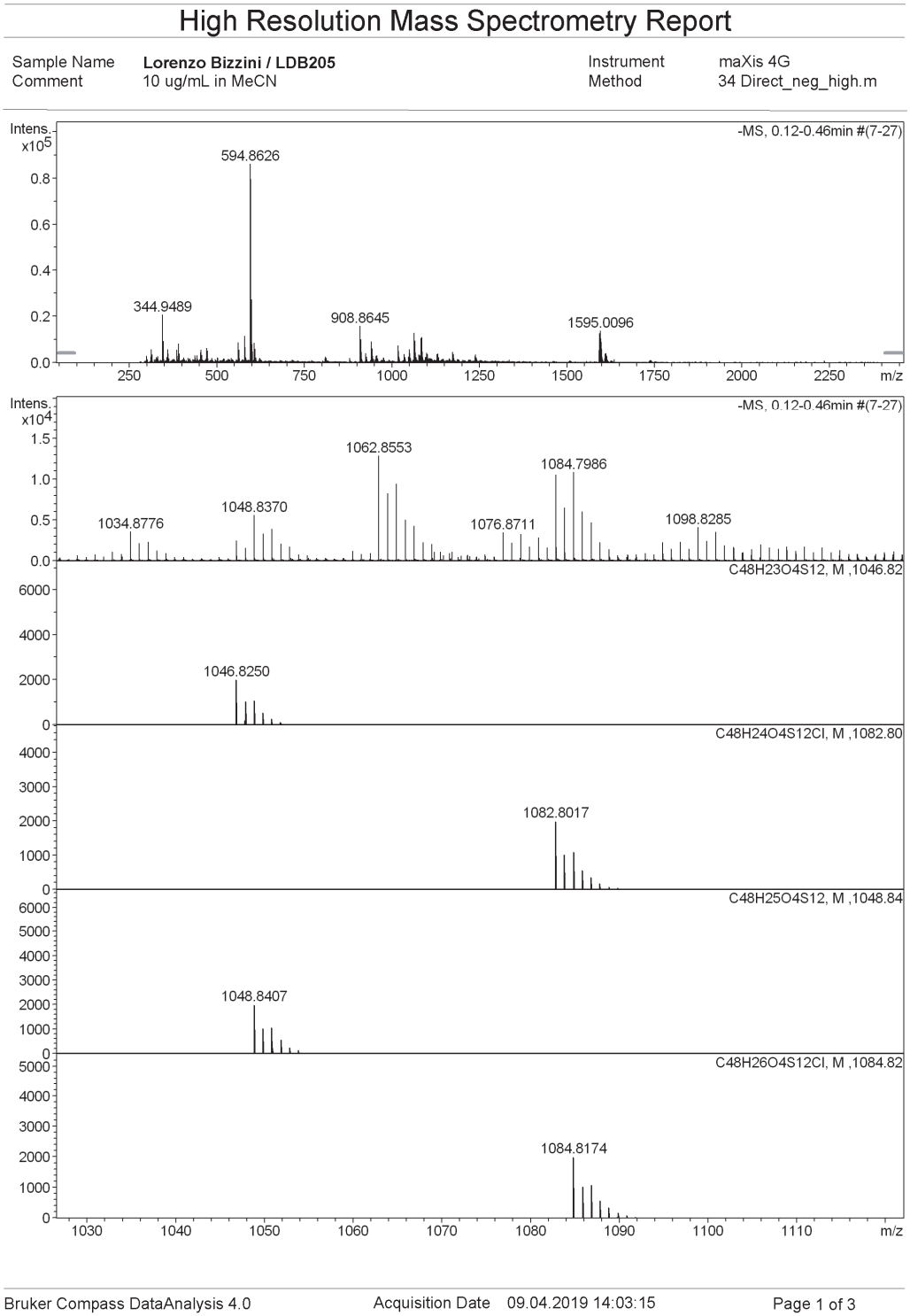

High Resolution Mass Spectrometry Report

Measured m/z vs. theoretical m/z

Meas. m/z	#	Formula	Score	m/z	err [mDa]	err [ppm]	mSigma	rdb	e⁻ Conf	z
1046.8243	1	C 48 H 23 O 4 S 12	100.00	1046.8250	0.8	0.7	277.9	37.5	even	1-
1082.8010	1	C 48 H 24 Cl O 4 S 12	100.00	1082.8017	0.7	0.7	15.6	36.5	even	

Mass list

#	m/z	I %	I
1	298.9613	3.3	2800
2	310.9877	2.9	2466
3	312.9589	6.5	5557
4	314.9557	4.0	3449
5	330.9331	3.0	2617
6	344.9489	23.9	20536
7	345.9517	3.8	3271
8	346.9457	10.6	9147
9	358.9648	6.5	5616
10	360.9441	4.4	3745
11	360.9608	3.1	2629
12	384.9803	6.3	5431
13	386.9773	3.2	2726
14	390.9694	9.4	8123
15	392.9664	4.3	3693
16	436.9573	3.4	2965
17	443.0585	3.6	3082
18	452.8980	5.1	4363
19	454.9299	6.4	5492
20	456.9254	3.7	3157
21	470.9269	2.8	2383
22	471.0898	7.2	6192
23	473.0864	3.3	2829
24	473.2829	5.8	5007
25	560.9013	10.0	8610
26	561.9043	3.2	2793
27	562.8983	6.3	5388
28	578.8918	13.4	11484
29	579.8949	4.0	3428
30	580.8888	7.7	6603
31	594.8626	100.0	85958
32	595.8652	29.3	25173
33	596.8595	92.4	79387
34	597.8619	26.9	23082
35	598.8562	31.5	27117
36	599.8585	9.1	7835
37	600.8529	5.6	4775
38	606.8890	9.9	8519
39	607.8917	3.4	2882
40	608.8856	6.8	5864
41	810.6232	2.9	2522
42	908.8645	18.3	15756
43	909.8674	9.9	8467
44	910.8652	11.6	9933
45	911.8672	5.3	4584
46	912.8668	3.8	3253
47	924.8951	4.7	4004
48	926.8889	2.9	2466
49	940.8362	10.6	9071
50	941.8392	5.8	5003
51	942.8336	7.0	6029
52	943.8345	3.3	2872
53	944.8347	3.3	2814
54	954.8518	3.3	2855
55	956.8599	3.6	3079
56	1016.8677	8.5	7347
57	1017.8706	5.5	4689
58	1018.8661	5.6	4831
59	1019.8676	2.9	2461
60	1034.8776	4.1	3550
61	1046.8243	2.8	2441

High Resolution Mass Spectrometry Report

#	m/z	I %	I
62	1048.8370	6.5	5571
63	1049.8398	3.8	3287
64	1050.8368	4.5	3901
65	1062.8553	14.9	12832
66	1063.8582	9.6	8222
67	1064.8531	10.9	9400
68	1065.8548	5.8	5007
69	1066.8466	5.0	4274
70	1076.8711	4.0	3444
71	1078.8652	3.7	3218
72	1080.8648	3.3	2827
73	1082.8010	12.2	10526
74	1083.8032	7.5	6459
75	1084.7986	12.6	10819
76	1085.7999	7.0	6004
77	1086.7967	5.5	4690
78	1098.8285	4.8	4109
79	1100.8270	4.1	3500
80	1128.7880	4.1	3488
81	1130.7864	4.3	3706
82	1172.8383	5.1	4409
83	1173.8406	3.4	2950
84	1174.8355	4.1	3540
85	1236.7917	3.0	2620
86	1238.7876	3.9	3315
87	1591.0131	6.0	5153
88	1592.0154	6.3	5451
89	1593.0113	14.6	12515
90	1594.0128	12.7	10928
91	1595.0096	15.9	13661
92	1596.0098	11.9	10259
93	1597.0076	10.3	8890
94	1598.0072	6.7	5801
95	1599.0049	4.6	3988
96	1609.0073	4.3	3679
97	1610.0086	3.7	3206
98	1611.0043	4.6	3929
99	1612.0061	3.5	3039
100	1613.0026	3.1	2640

Acquisition Parameter

General	Fore Vacuum	2.69e+000 mBar	High Vacuum	9.94e-008 mBar	Source Type	ESI
	Scan Begin	100 m/z	Scan End	2400 m/z	Ion Polarity	Negative
Source	Set Nebulizer	0.4 Bar	Set Capillary	4500 V	Set Dry Gas	4.0 l/min
	Set Dry Heater	180 °C	Set End Plate Offset	-500 V		
Quadrupole	Set Ion Energy (MS only)	-10.0 eV				
Coll. Cell	Collision Energy	-20.0 eV	Set Collision Cell RF	500.0 Vpp		
Ion Cooler	Set Ion Cooler Transfer Time	140.0 µs	Set Ion Cooler Pre Pulse Storage Time	22.0 µs		

^{1}H NMR (500 MHz, CD_2Cl_2) and ^{13}C NMR (126 MHz, CD_2Cl_2) of **116**

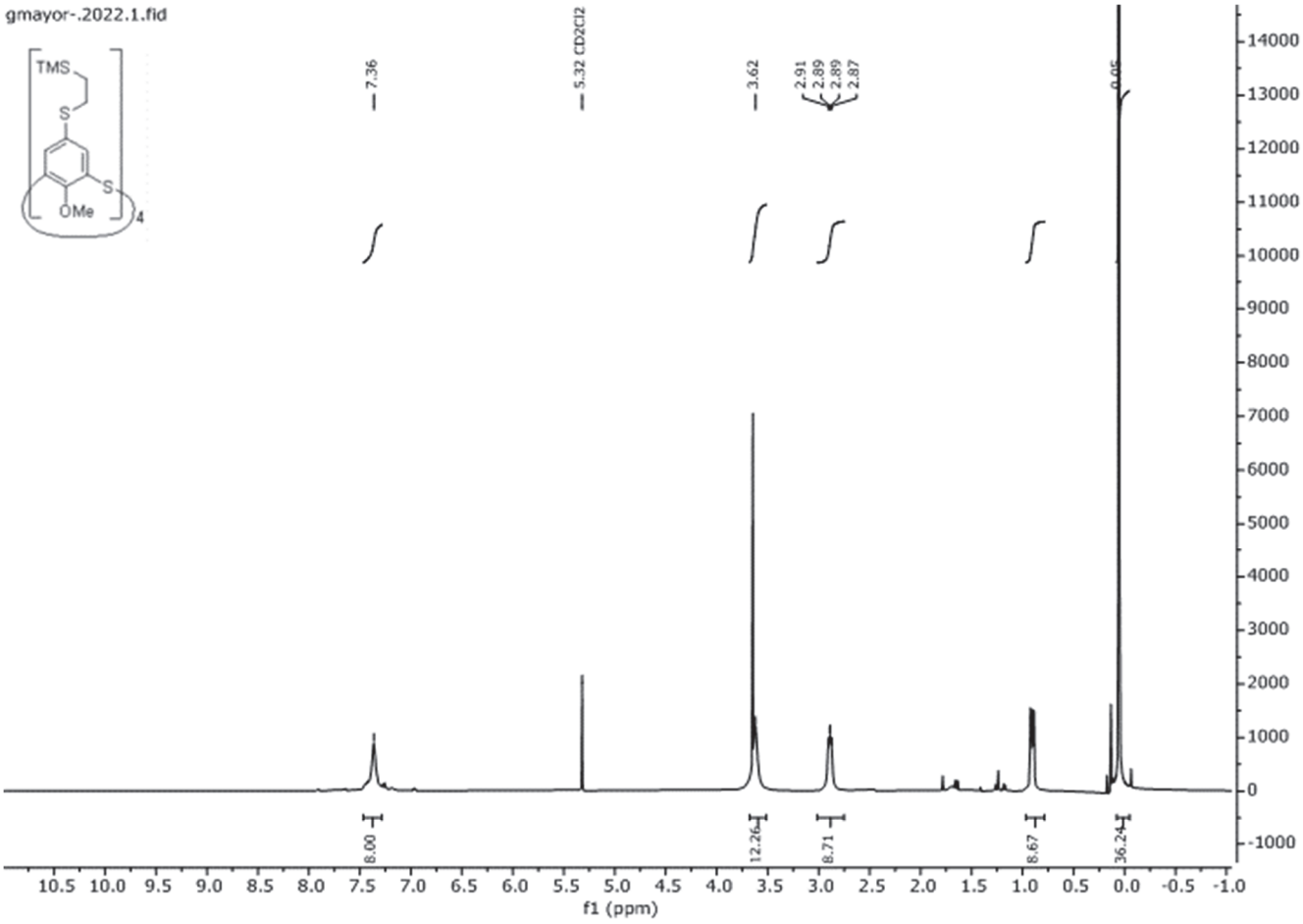

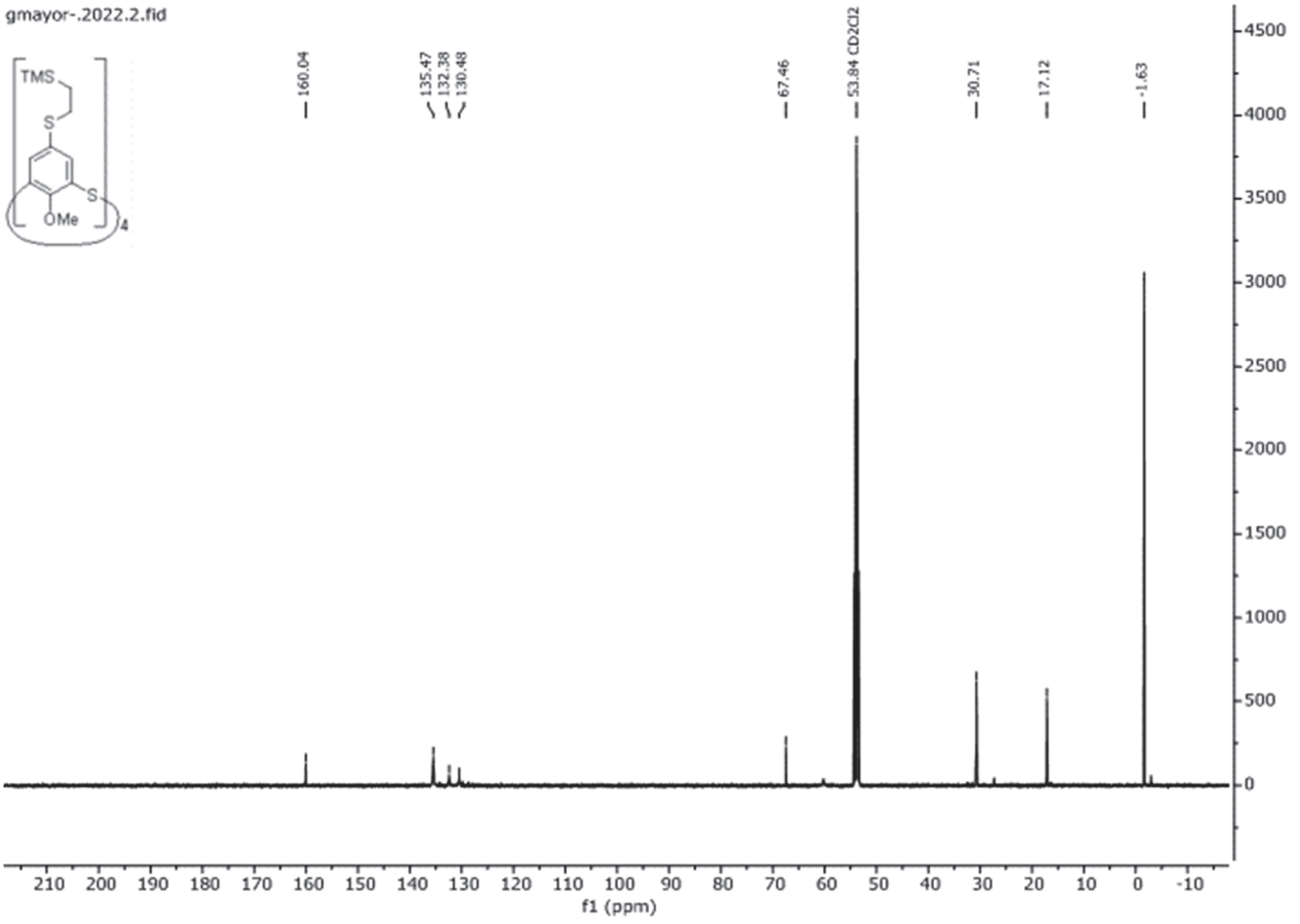

^{1}H NMR (500 MHz, CD_2Cl_2) and ^{13}C NMR (126 MHz, CD_2Cl_2) of **119**

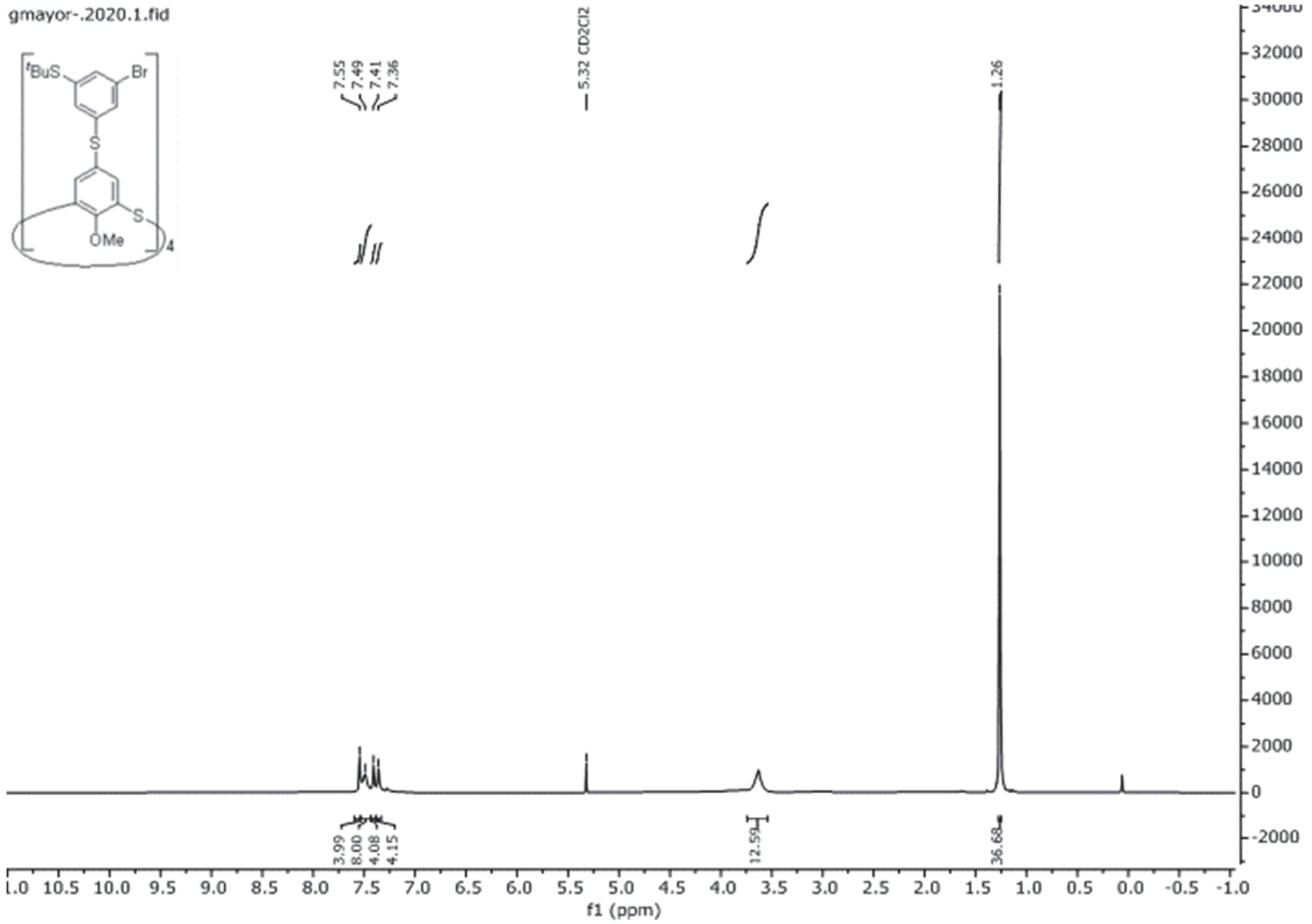

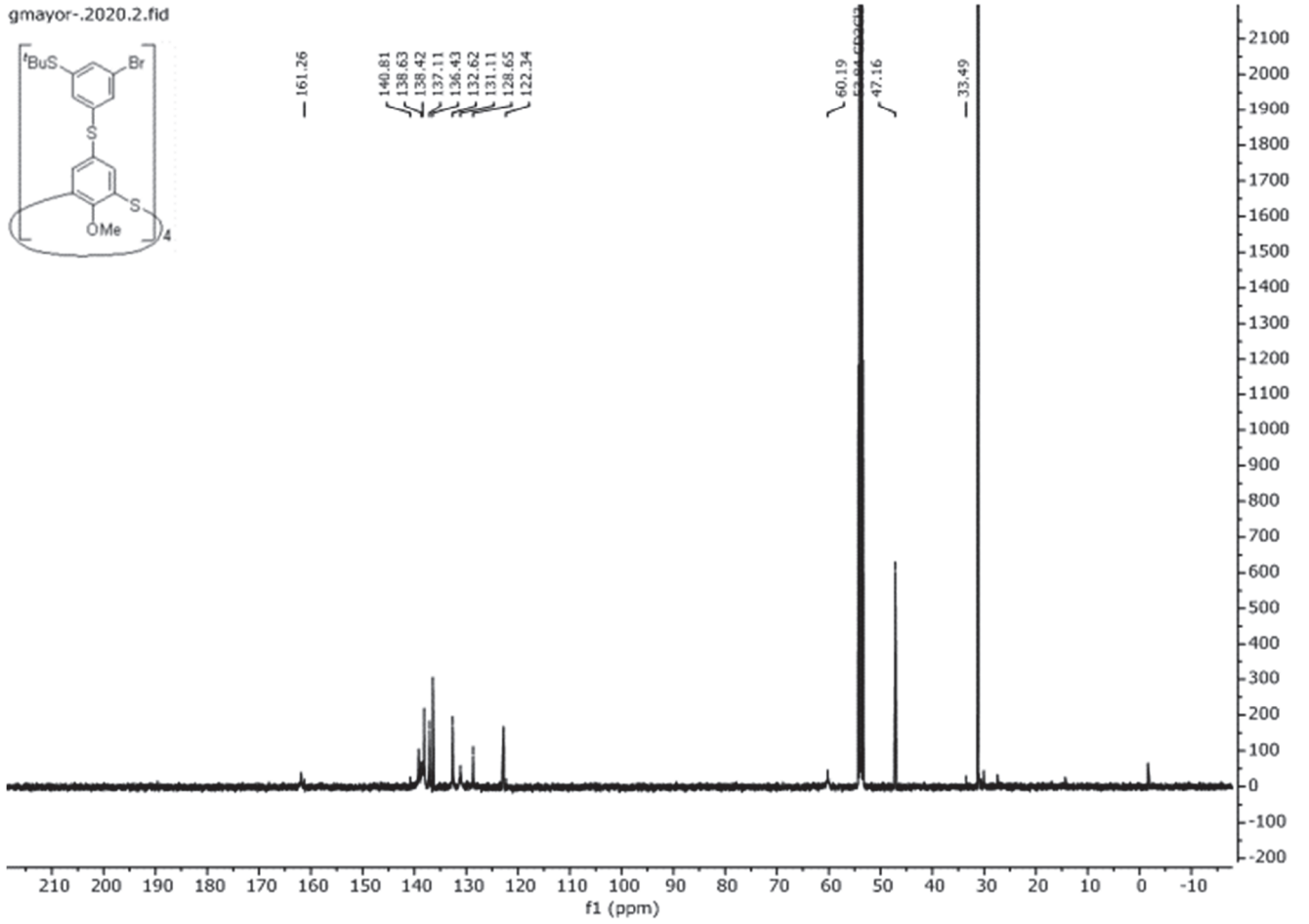

^{1}H

NMR (500 MHz, CD_2Cl_2) and ^{13}C NMR (126 MHz, CD_2Cl_2) of **121**

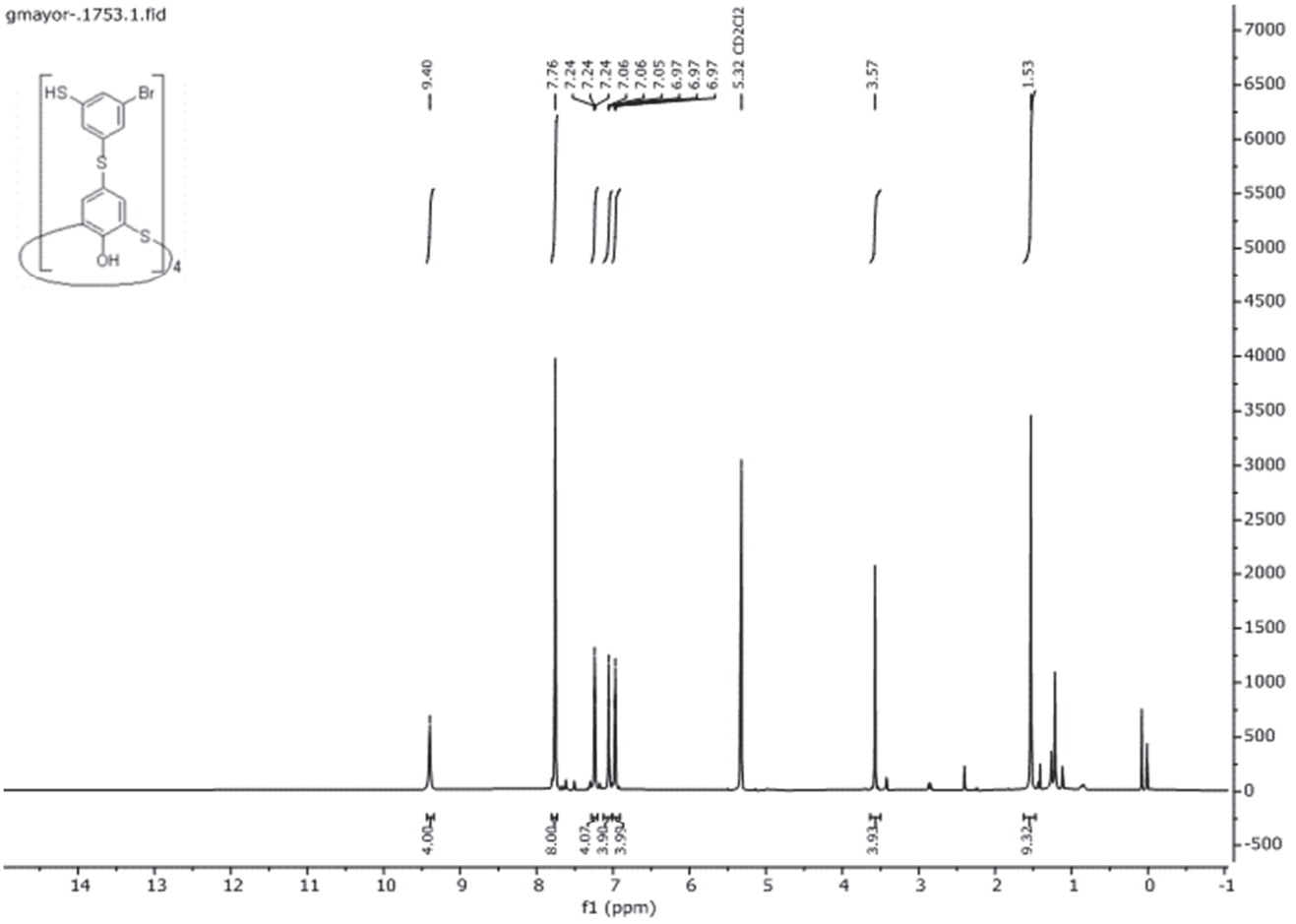

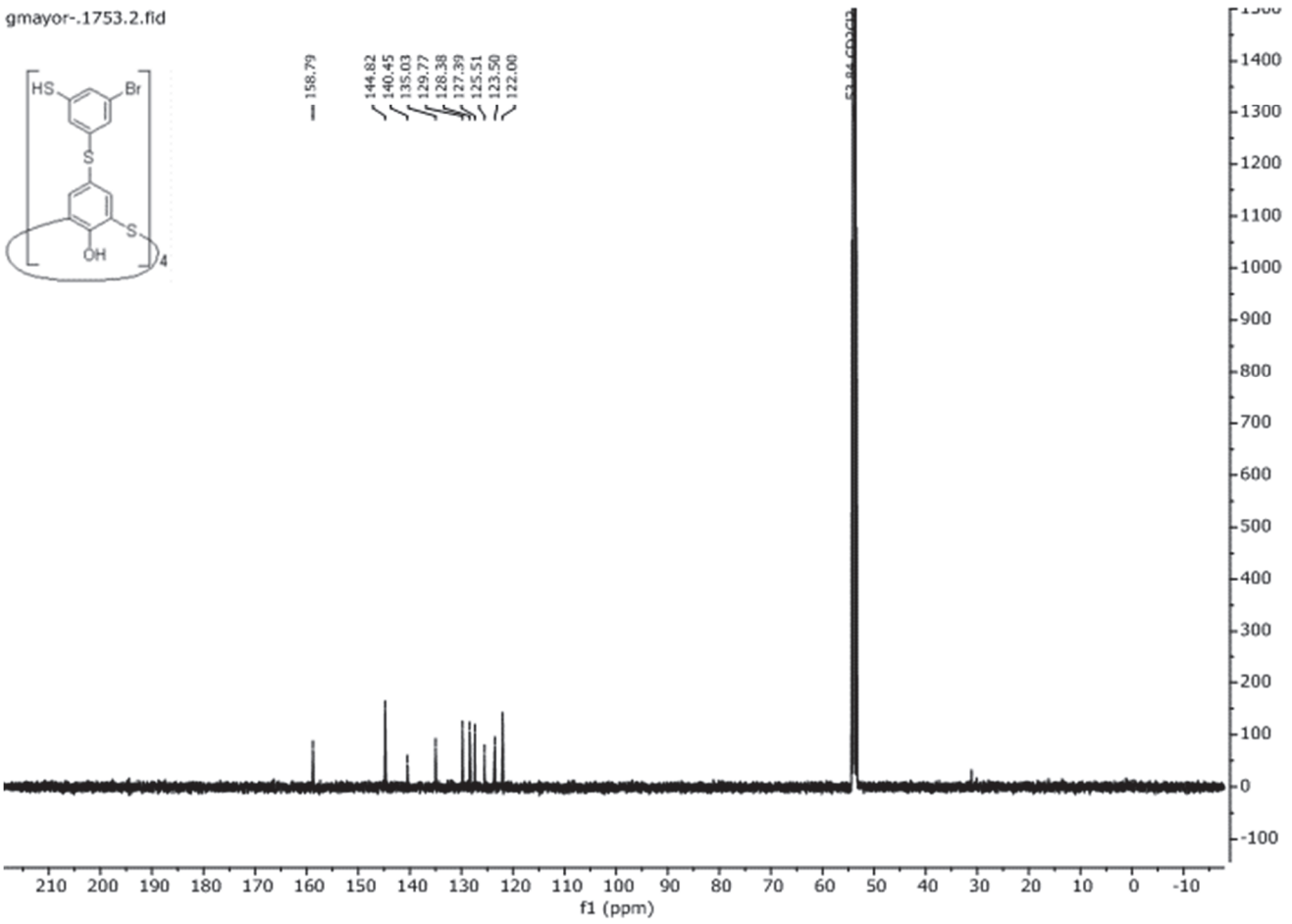

Disproportionation of *S*-*p*-methoxyphenyl bezenethiosulfonate followed by ^{1}H-NMR (CD_2Cl_2, 500 MHz, 298 K)

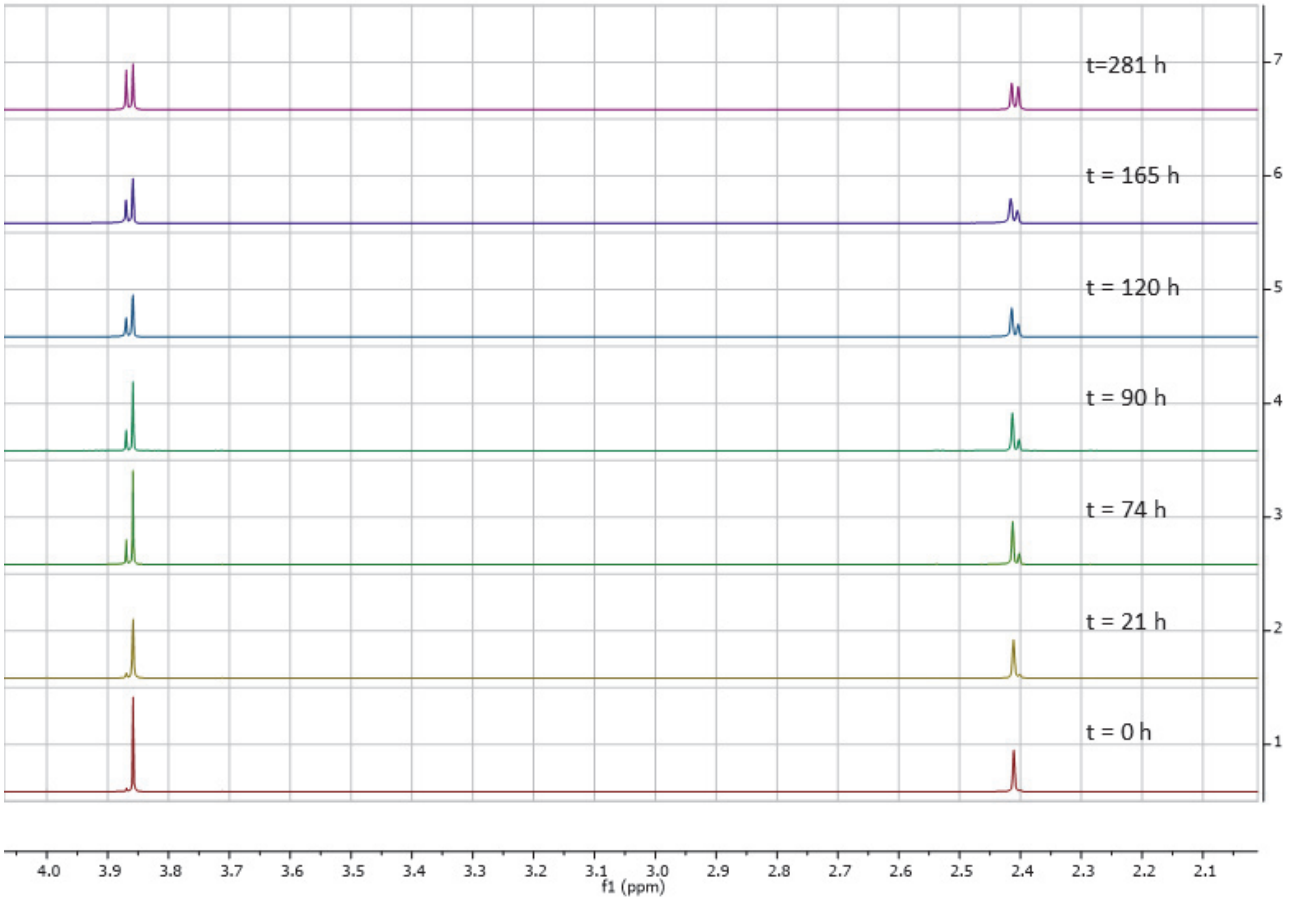

z

^{1}H-NMR (CD_2Cl_2, 500 MHz, 298 K) and ^{13}C-NMR (CD_2Cl_2, 126 MHz, 298 K) of S-1H,1H,2H,2H-perfluorodecyl bezenethiosulfonate.

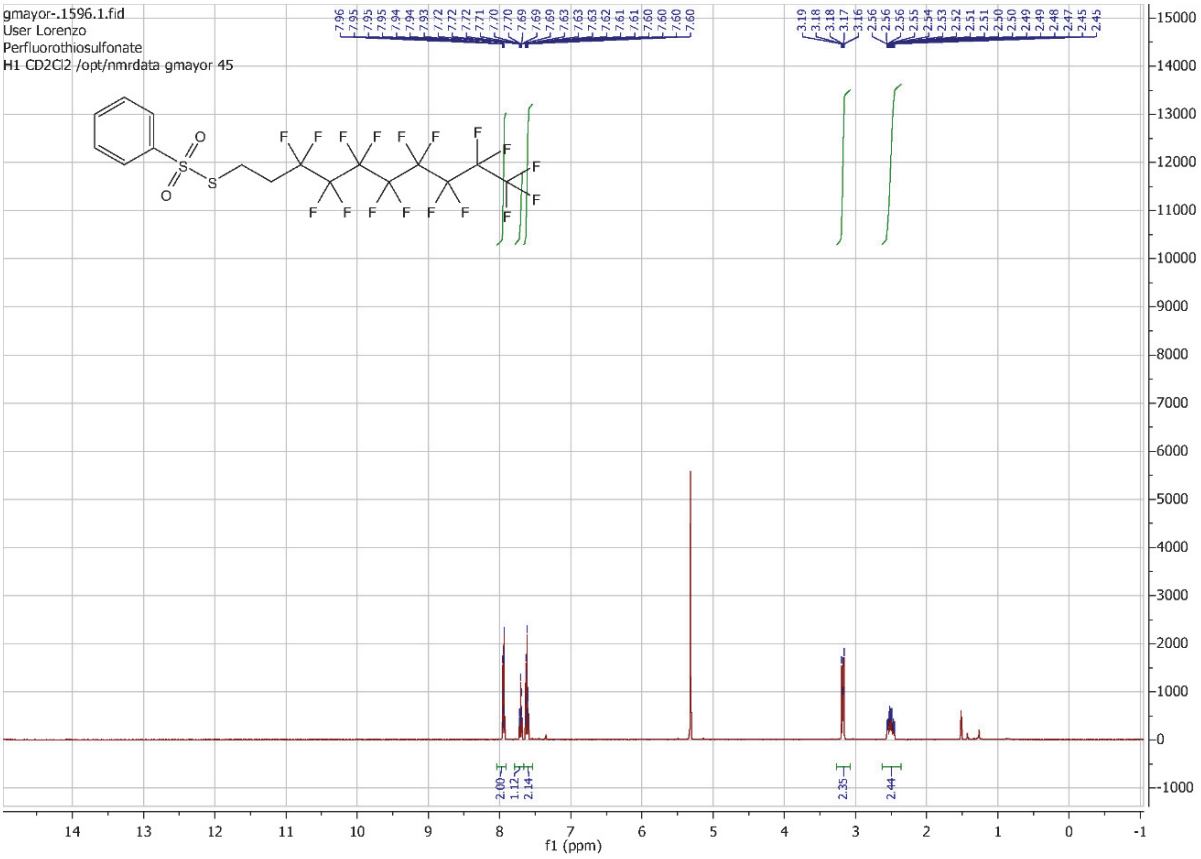

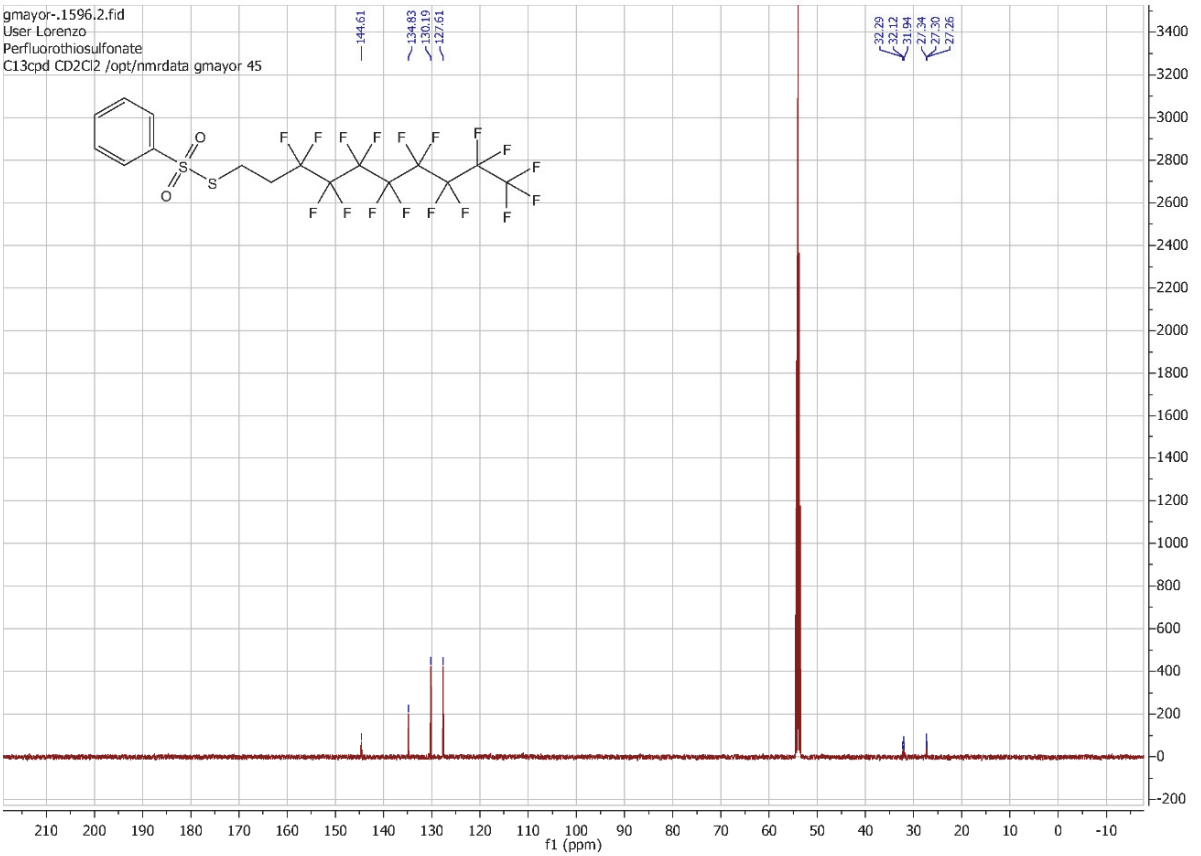

^{19}F-NMR (CD_2Cl_2, 471 MHz, 298 K) of *S*-1*H*,1*H*,2*H*,2*H*-perfluorodecyl bezenethiosulfonate.

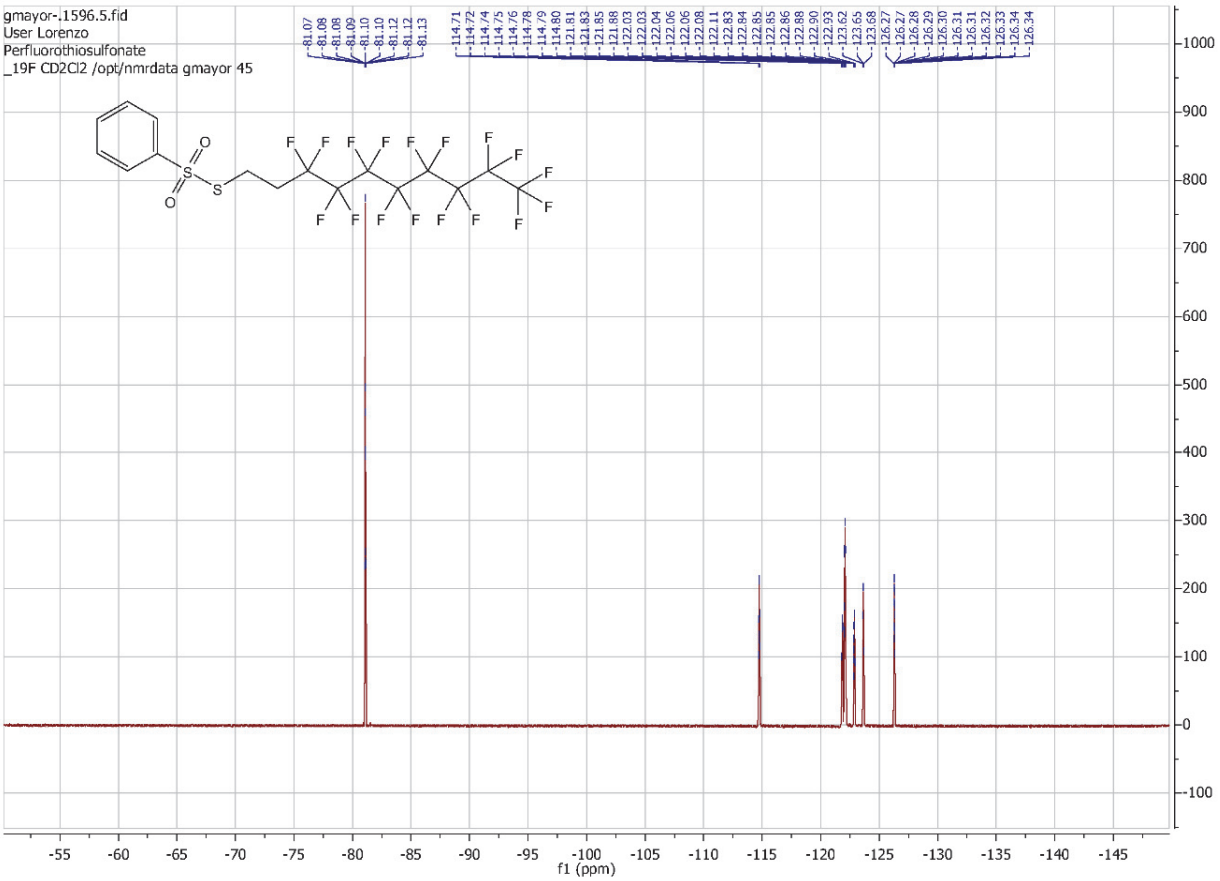

HR-ESI MS spectra of S-1H,1H,2H,2H-perfluorodecyl bezenethiosulfonate.

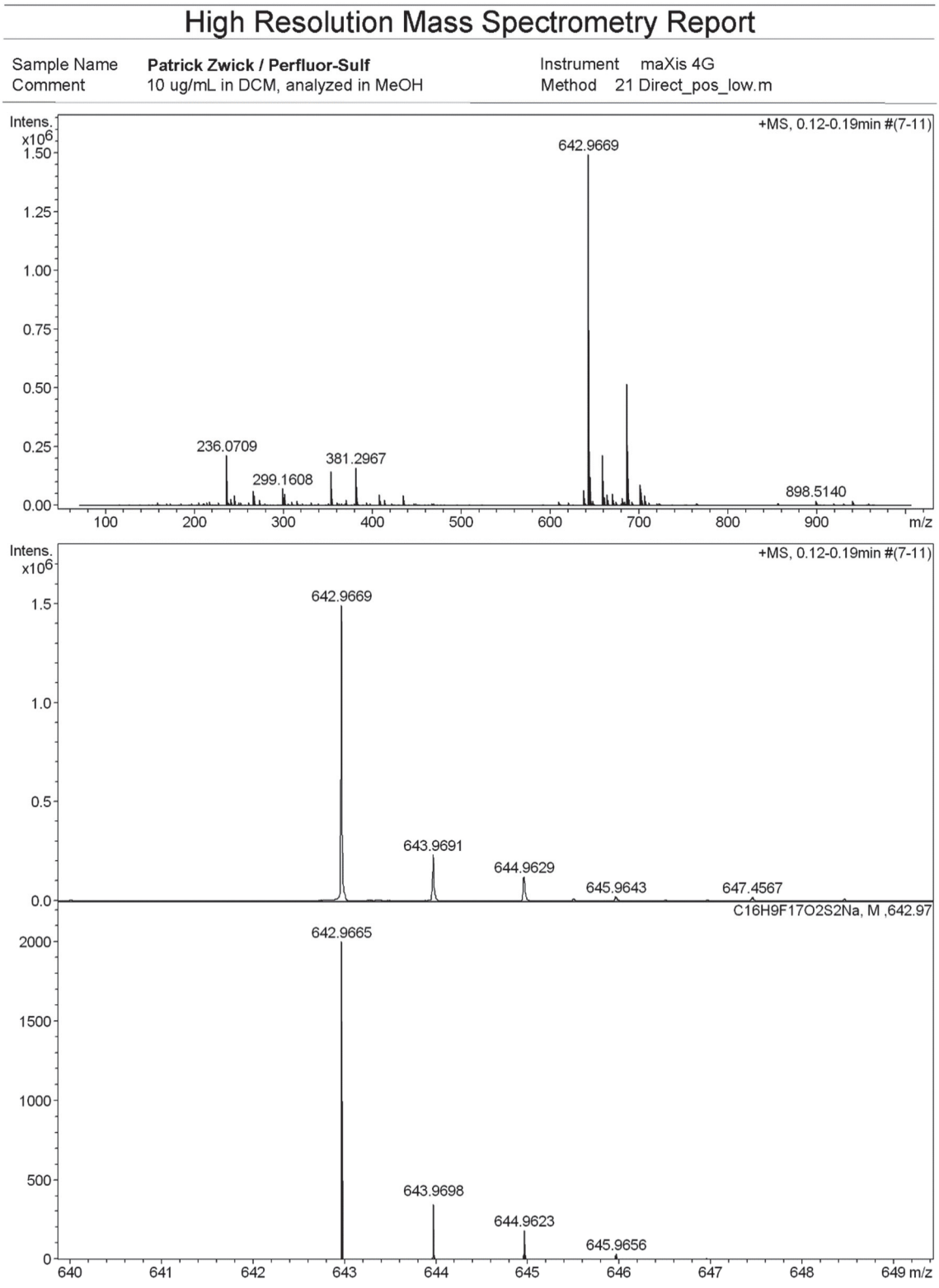

High Resolution Mass Spectrometry Report

Measured m/z vs. theoretical m/z

Meas. m/z	#	Formula	Score	m/z	err [mDa]	err [ppm]	mSigma	rdb	e⁻ Conf	z
642.9669	1	C 16 H 9 F 17 Na O 2 S 2	100.00	642.9665	-0.4	-0.6	21.9	3.5	even	1+

Mass list

#	m/z	I %	I
1	158.9637	0.8	12023
2	169.0465	0.6	9083
3	173.0779	0.6	9458
4	197.0775	0.6	9454
5	205.0595	0.8	11880
6	210.1092	0.7	10297
7	211.0931	0.7	9761
8	214.0885	0.7	10934
9	217.1039	1.1	17016
10	226.9505	0.7	10763
11	236.0709	14.3	214039
12	237.0738	1.7	25398
13	238.0668	0.7	10675
14	239.0879	0.7	10267
15	241.0285	1.8	26701
16	245.0776	2.8	41379
17	250.1769	1.0	14342
18	252.0444	1.0	14272
19	252.1561	0.6	9399
20	261.1295	0.7	11148
21	266.1717	4.0	60203
22	267.0475	1.4	20949
23	267.1741	2.8	42510
24	273.0004	1.7	25439
25	279.2281	0.6	9697
26	299.1608	4.8	72173
27	300.1638	0.9	12898
28	301.1400	3.3	48678
29	302.1432	0.6	9437
30	309.2028	1.0	15083
31	315.1345	0.6	8642
32	315.1917	1.2	18632
33	321.2389	0.6	9676
34	331.1867	0.7	11011
35	339.1767	0.6	9328
36	353.2653	9.8	147130
37	354.2683	2.0	29714
38	360.3224	0.7	11126
39	363.0069	0.6	9321
40	370.9953	1.6	23661
41	380.0003	0.6	9206
42	381.2967	10.8	161843
43	382.2998	2.4	36245
44	393.2967	0.9	13574
45	397.2703	0.6	9444
46	407.2757	3.2	47982
47	408.2792	0.9	12720
48	408.3072	1.4	20866
49	413.2651	1.5	22510
50	421.3280	0.6	9233
51	435.3069	2.8	42292
52	436.3105	0.8	11980
53	467.2426	0.7	10410
54	469.3275	0.6	8908
55	609.3243	1.1	17040
56	620.9825	0.7	10962
57	638.0101	4.5	66562
58	639.0125	0.9	13295
59	642.9669	100.0	1494549
60	643.9691	15.6	233119
61	644.9629	8.3	123855
62	645.5045	0.8	11292

High Resolution Mass Spectrometry Report

#	m/z	I %	I
63	645.9643	1.4	21045
64	647.4567	1.3	19416
65	648.4606	0.6	8907
66	658.9396	14.3	213390
67	659.9419	2.6	38968
68	660.9368	2.4	35515
69	663.4520	3.0	44863
70	663.5142	0.7	11106
71	664.4551	1.5	22728
72	669.4393	3.3	49653
73	670.4418	1.5	22971
74	673.5358	1.2	17218
75	679.4176	0.6	9227
76	680.4782	2.2	33346
77	681.4819	1.2	17431
78	683.9917	1.1	16212
79	685.4346	34.7	519081
80	686.4378	15.5	231983
81	687.4401	3.7	55723
82	688.4436	0.7	9723
83	691.5464	1.2	17701
84	701.4078	5.8	86773
85	702.4108	2.7	40271
86	703.4111	1.0	14865
87	705.5808	2.9	43063
88	706.5837	1.4	20320
89	710.9522	0.9	13140
90	721.5736	0.6	9347
91	722.5238	0.7	9727
92	764.5713	0.6	9535
93	856.0465	0.6	9547
94	898.5140	1.4	20551
95	899.5179	0.8	12686
96	919.1349	0.7	10601
97	929.7739	0.7	10284
98	939.5922	1.3	18922
99	940.5954	0.7	10615
100	957.8053	0.6	9193

Acquisition Parameter

General	Fore Vacuum	2.80e+000 mBar	High Vacuum	1.26e-007 mBar	Source Type	ESI
	Scan Begin	75 m/z	Scan End	1000 m/z	Ion Polarity	Positive
Source	Set Nebulizer	0.4 Bar	Set Capillary	3600 V	Set Dry Gas	3.0 l/min
	Set Dry Heater	180 °C	Set End Plate Offset	-500 V		
Quadrupole	Set Ion Energy (MS only)	4.0 eV				
Coll. Cell	Collision Energy	8.0 eV	Set Collision Cell RF	350.0 Vpp		
Ion Cooler	Set Ion Cooler Transfer Time	55.0 µs	Set Ion Cooler Pre Pulse Storage Time	7.0 µs		

^{1}H-NMR (CD_2Cl_2, 500 MHz, 298 K) of *S*-adamantyl benzenethiosulfonate.

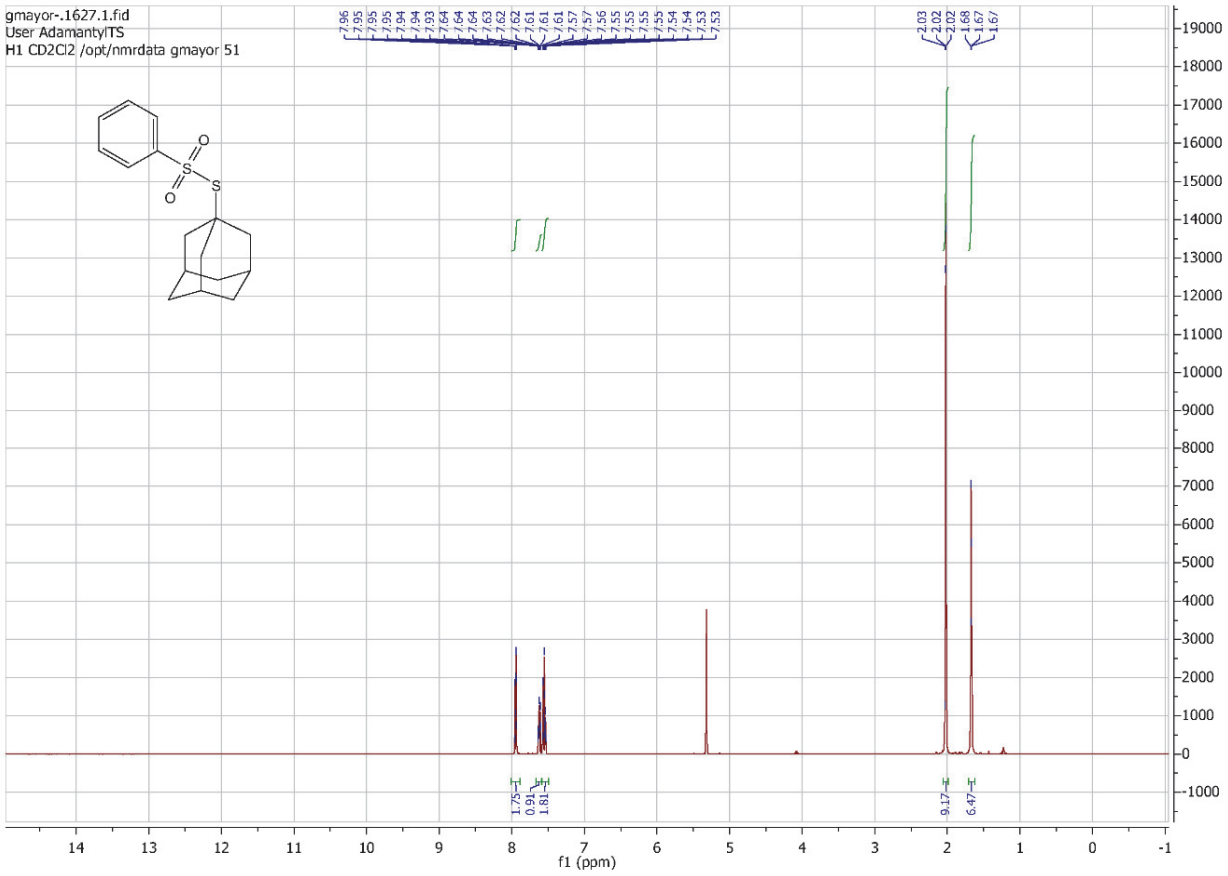

^{13}C-NMR (CD_2Cl_2, 126 MHz, 298 K) of S-adamantyl benzenethiosulfonate.

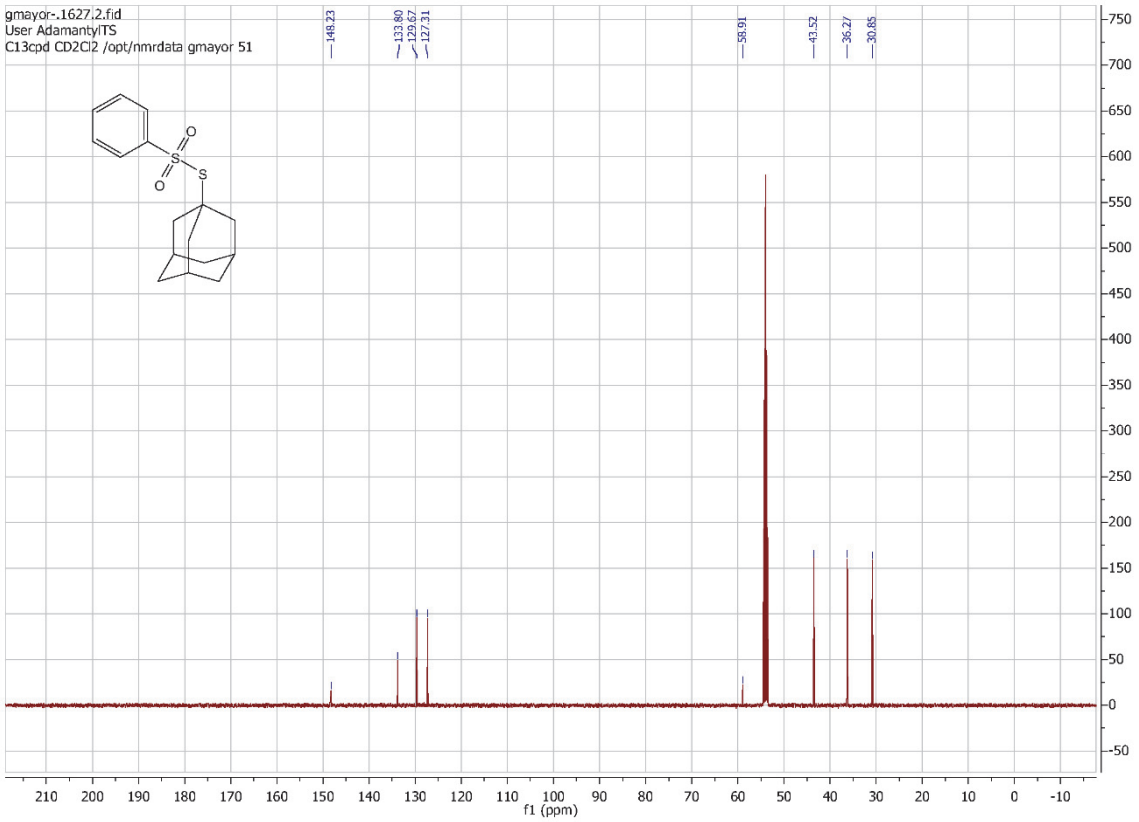

DEPT-NMR (CD_2Cl_2, 126 MHz, 298 K) of S-adamantyl benzenethiosulfonate.

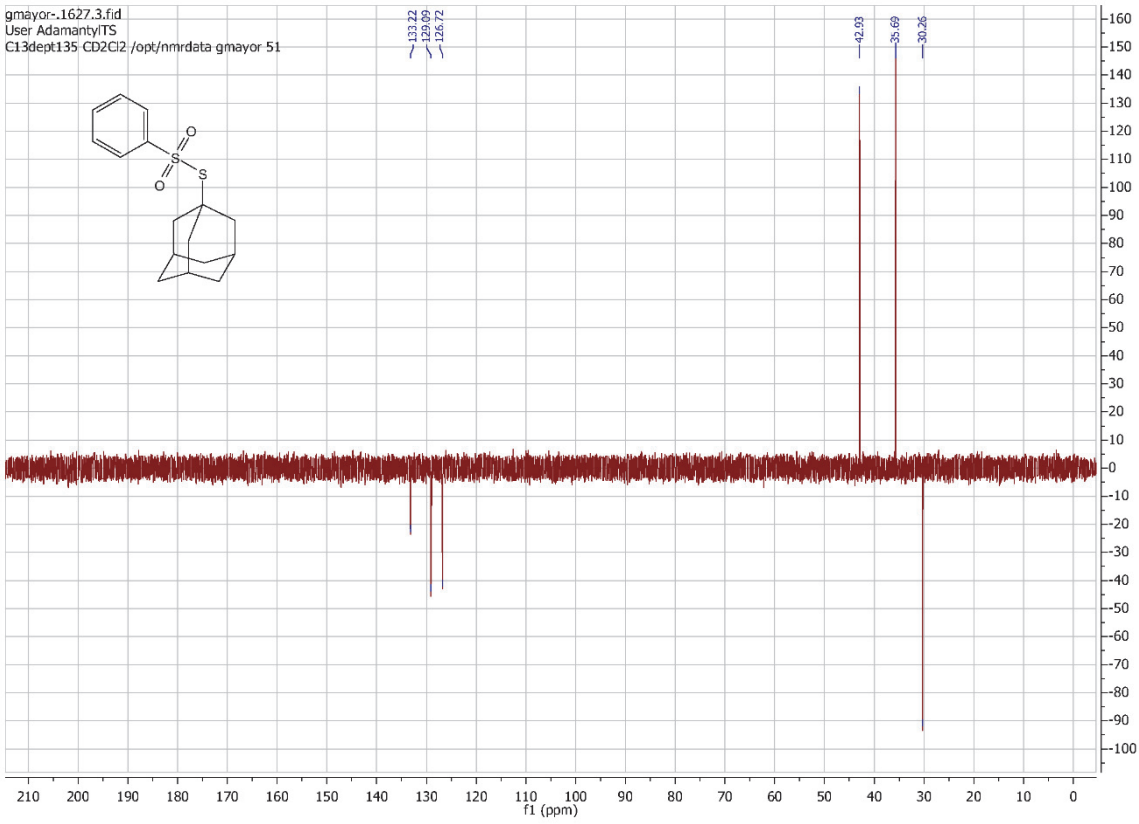

HR-ESI MS spectra of S-adamantyl bezenethiosulfonate.

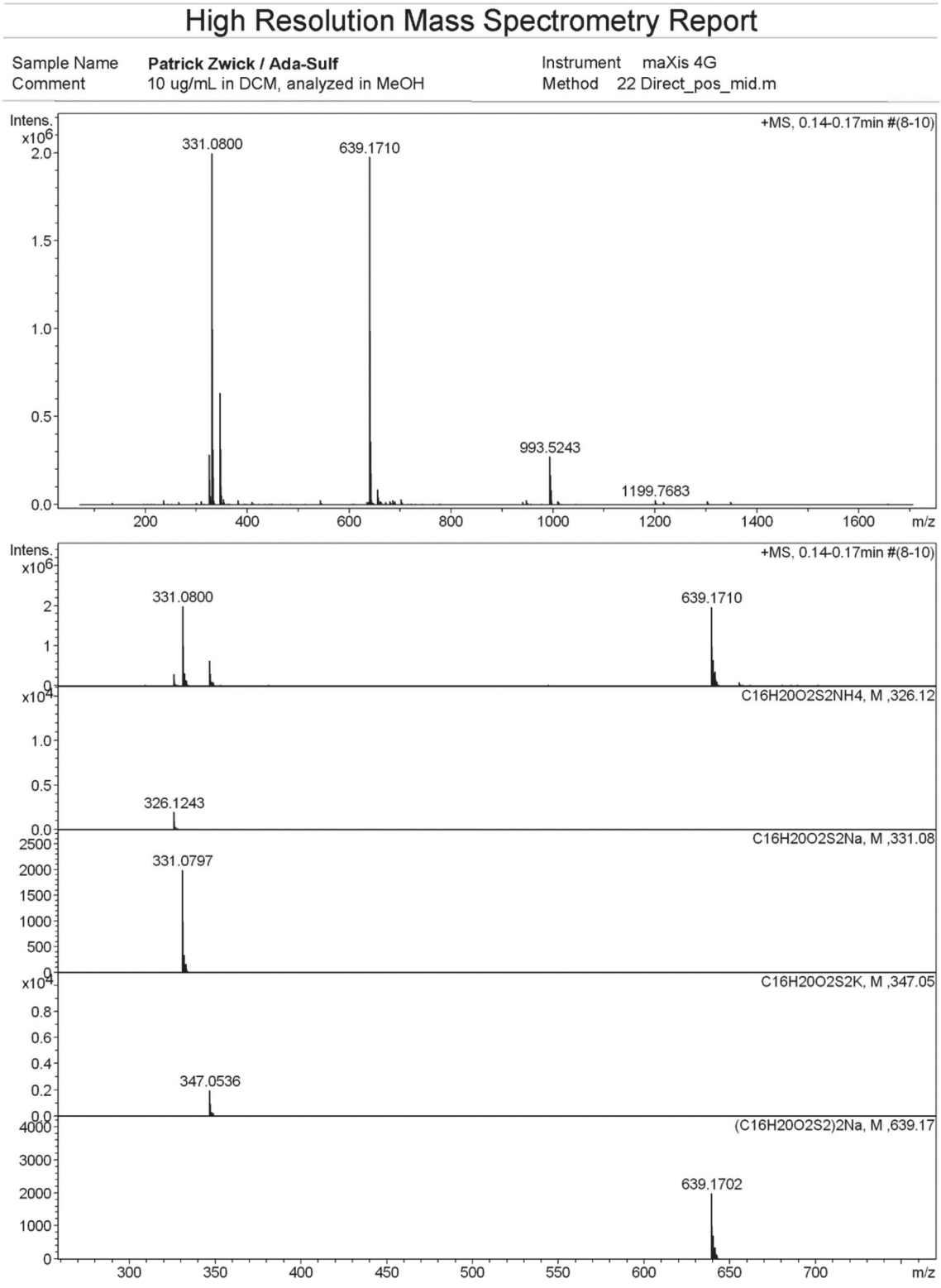

High Resolution Mass Spectrometry Report

Measured m/z vs. theoretical m/z

Meas. m/z	#	Formula	Score	m/z	err [mDa]	err [ppm]	mSigma	rdb	e⁻ Conf	z
326.1241	1	C 16 H 24 N O 2 S 2	100.00	326.1243	0.2	0.6	15.0	5.5	even	1+
331.0800	1	C 16 H 20 Na O 2 S 2	100.00	331.0797	-0.3	-1.0	26.4	6.5	even	
347.0536	1	C 16 H 20 K O 2 S 2	100.00	347.0536	-0.0	-0.1	20.9	6.5	even	
639.1710	1	C 32 H 40 Na O 4 S 4	100.00	639.1702	-0.8	-1.3	38.5	12.5	even	

Mass list

#	m/z	I %	I
1	135.1168	0.6	11858
2	205.0594	0.4	7789
3	236.0709	1.2	24943
4	245.0777	0.3	6863
5	266.1720	0.7	14762
6	299.1612	0.4	7836
7	301.1404	0.6	11774
8	309.0971	1.0	19929
9	326.1241	14.4	288260
10	327.1266	2.5	50423
11	328.1202	1.3	25384
12	331.0568	0.8	16691
13	331.0800	100.0	1998153
14	332.0827	15.9	316883
15	333.0761	6.8	136759
16	334.0784	1.3	26741
17	347.0536	31.9	638317
18	348.0563	5.4	108412
19	349.0506	4.5	90072
20	349.0895	0.6	12015
21	350.0530	0.8	16632
22	351.0485	0.3	5816
23	353.2654	1.5	30592
24	354.2687	0.3	6906
25	363.0510	0.4	7003
26	365.1049	0.4	7934
27	381.2965	1.3	25406
28	382.3002	0.3	6787
29	393.2970	0.3	5946
30	408.3079	0.4	8574
31	409.0926	0.8	15091
32	413.2651	0.4	8578
33	469.3275	0.4	8133
34	544.1614	1.4	28275
35	545.1638	0.5	9290
36	607.2513	0.3	5836
37	609.3260	0.3	5718
38	634.2136	0.9	17942
39	635.2160	0.3	6849
40	639.1354	1.1	22381
41	639.1710	98.9	1976644
42	640.1735	33.1	661882
43	641.1689	18.1	361640
44	642.1695	5.6	111862
45	643.1670	1.7	33338
46	644.1667	0.5	10051
47	647.4572	0.6	12036
48	648.4604	0.3	6789
49	655.1434	4.4	88171
50	656.1461	1.7	34475
51	657.1418	1.3	25811
52	658.1432	0.5	9330
53	661.3553	1.1	21080
54	662.3587	0.4	8708
55	663.4526	0.8	15452
56	664.4558	0.4	7194
57	671.1412	0.8	15876
58	672.1442	0.3	6146
59	680.4789	1.2	23247

High Resolution Mass Spectrometry Report

#	m/z	I %	I
60	681.4820	0.5	10816
61	685.4334	1.4	28567
62	686.4363	0.7	13237
63	689.3866	1.0	19749
64	690.3897	0.4	8522
65	701.4080	1.6	31113
66	702.4114	0.8	14987
67	703.4109	0.3	5704
68	715.3661	0.4	8624
69	721.3551	0.3	6521
70	743.3973	0.4	7252
71	777.4176	0.4	8777
72	939.5934	0.7	14428
73	940.5961	0.4	8782
74	947.2581	1.4	27333
75	948.2609	0.8	15778
76	949.2581	0.6	11659
77	955.5676	0.3	6431
78	993.5243	13.8	275047
79	994.5273	8.4	168833
80	995.5273	3.8	76341
81	996.5270	1.3	25022
82	997.5270	0.4	7960
83	1009.4968	1.2	23238
84	1010.5003	0.7	14403
85	1011.4994	0.4	8796
86	1194.8131	0.3	6814
87	1199.7683	1.5	29106
88	1200.7721	1.1	22499
89	1201.7747	0.5	10696
90	1215.7432	0.9	17377
91	1216.7467	0.7	13899
92	1217.7478	0.4	7310
93	1301.6118	1.1	22542
94	1302.6144	1.0	19661
95	1303.6147	0.6	12255
96	1347.8752	1.0	19027
97	1348.8794	0.9	18465
98	1349.8821	0.5	9106
99	1655.9633	0.3	6088
100	1656.9662	0.3	6035

Acquisition Parameter

General	Fore Vacuum	2.68e+000 mBar	High Vacuum	1.26e-007 mBar	Source Type	ESI
	Scan Begin	75 m/z	Scan End	1700 m/z	Ion Polarity	Positive
Source	Set Nebulizer	0.4 Bar	Set Capillary	3600 V	Set Dry Gas	4.0 l/min
	Set Dry Heater	180 °C	Set End Plate Offset	-500 V		
Quadrupole	Set Ion Energy (MS only)	4.0 eV				
Coll. Cell	Collision Energy	8.0 eV	Set Collision Cell RF	350.0 Vpp		
Ion Cooler	Set Ion Cooler Transfer Time	75.0 µs	Set Ion Cooler Pre Pulse Storage Time	10.0 µs		

^{1}H-NMR (CD_2Cl_2, 500 MHz, 298 K) and ^{13}C-NMR (CD_2Cl_2, 126 MHz, 298 K) of *S p* methoxyphenyl bezenethiosulfonate.

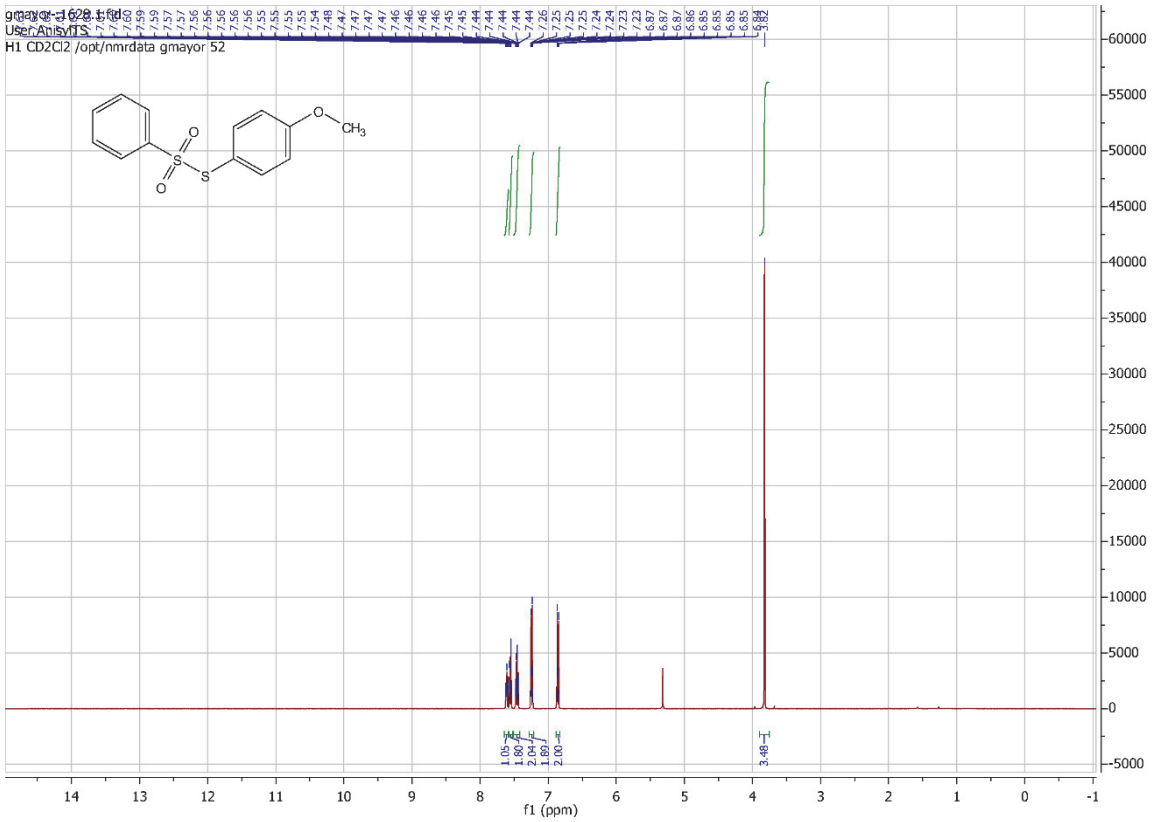

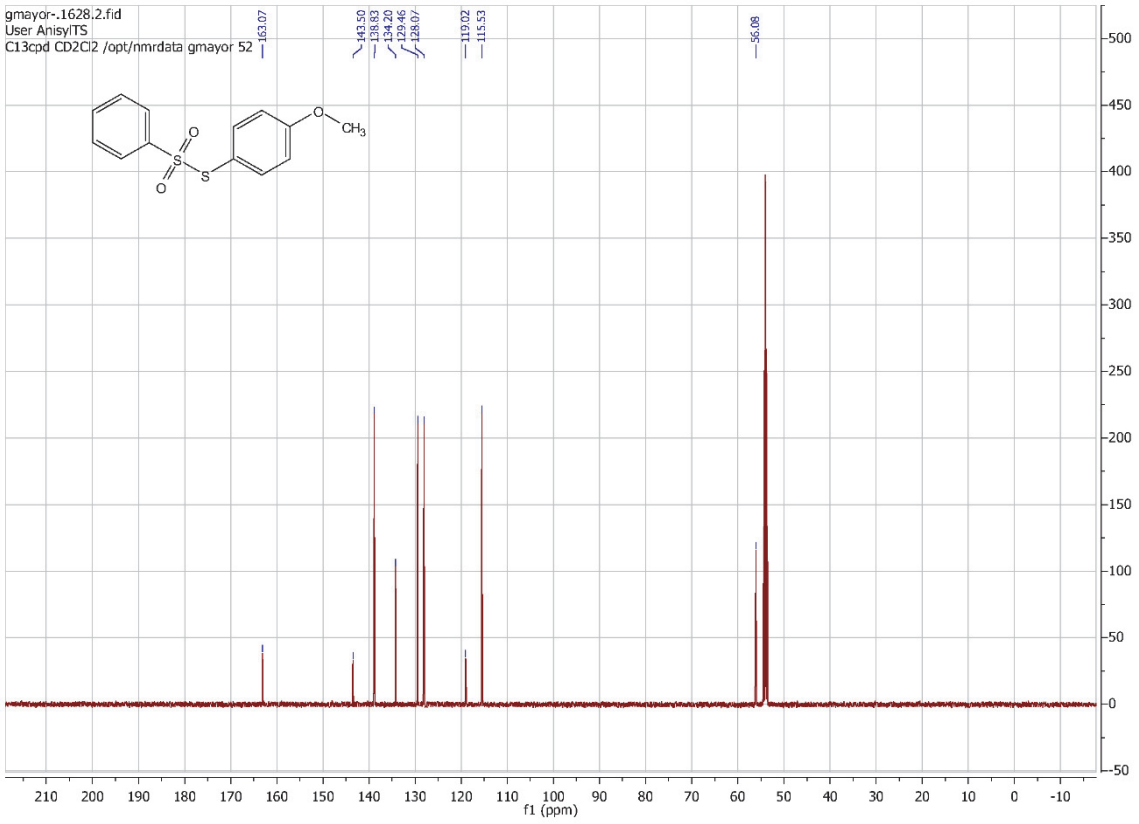

HR-ESI MS spectra of *S*-adamantyl bezenethiosulfonate.

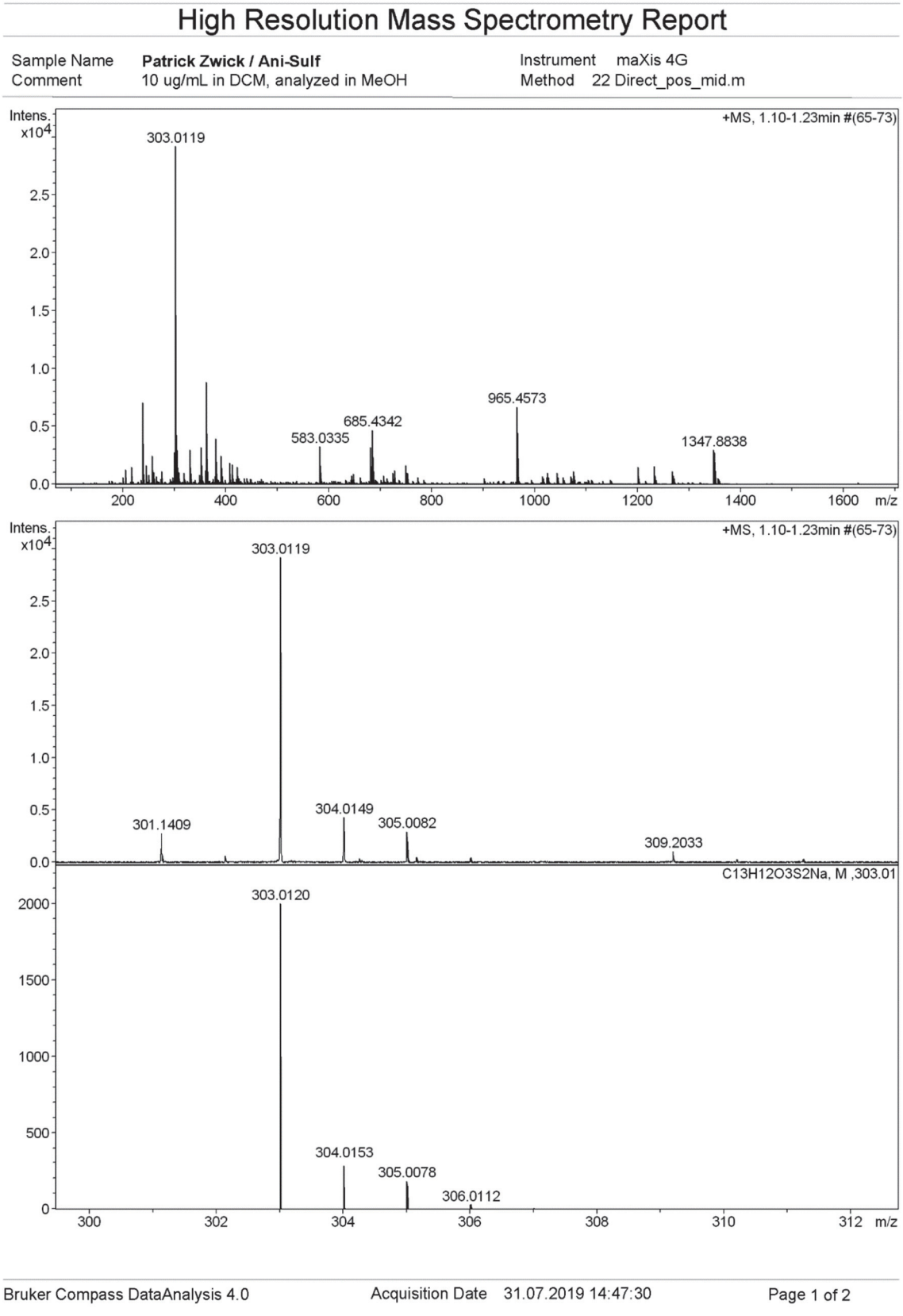

High Resolution Mass Spectrometry Report

Measured m/z vs. theoretical m/z

Meas. m/z	#	Formula	Score	m/z	err [mDa]	err [ppm]	mSigma	rdb	e⁻ Conf	z
303.0119	1	C 13 H 12 Na O 3 S 2	100.00	303.0120	0.1	0.4	9.0	7.5	even	1+

Mass list

#	m/z	I %	I
1	205.0600	4.3	1259
2	217.1042	5.3	1533
3	239.1251	24.2	7073
4	245.0785	5.7	1678
5	257.1359	8.4	2458
6	261.1310	3.5	1026
7	275.1467	3.9	1126
8	301.1409	9.5	2769
9	303.0119	100.0	29198
10	304.0149	14.7	4289
11	305.0082	10.2	2965
12	309.2033	3.6	1058
13	331.1280	10.3	2998
14	353.2660	10.9	3180
15	360.3230	4.2	1231
16	363.1564	30.3	8837
17	364.1596	7.7	2235
18	381.1669	8.0	2342
19	381.2973	13.6	3966
20	391.3105	8.5	2487
21	392.3134	3.5	1018
22	393.2970	4.9	1428
23	408.3084	6.4	1857
24	413.2659	5.8	1703
25	423.2141	5.2	1508
26	583.0335	11.2	3267
27	584.0365	3.6	1039
28	681.4186	11.1	3237
29	682.4215	4.5	1307
30	683.4169	4.5	1314
31	685.4342	16.2	4725
32	686.4373	7.9	2307
33	727.3664	4.1	1192
34	750.4050	5.6	1648
35	965.4573	23.0	6718
36	966.4604	15.4	4495
37	967.4595	6.5	1903
38	1075.7119	3.8	1099
39	1199.7732	5.1	1484
40	1231.7057	5.5	1614
41	1232.7089	4.4	1286
42	1267.8466	3.9	1149
43	1347.8838	10.2	2965
44	1348.8863	9.4	2749
45	1349.8895	4.2	1227

Acquisition Parameter

General	Fore Vacuum	2.68e+000 mBar	High Vacuum	1.26e-007 mBar	Source Type	ESI
	Scan Begin	75 m/z	Scan End	1700 m/z	Ion Polarity	Positive
Source	Set Nebulizer	0.4 Bar	Set Capillary	3600 V	Set Dry Gas	4.0 l/min
	Set Dry Heater	180 °C	Set End Plate Offset	-500 V		
Quadrupole	Set Ion Energy (MS only)	4.0 eV				
Coll. Cell	Collision Energy	8.0 eV	Set Collision Cell RF	350.0 Vpp		
Ion Cooler	Set Ion Cooler Transfer Time	75.0 µs	Set Ion Cooler Pre Pulse Storage Time	10.0 µs		

^{1}H-NMR ($CDCl_3$, 400 MHz, 298 K) and ^{13}C-NMR ($CDCl_3$, 101 MHz, 298 K) of S-pentyl bezenethiosulfonate.

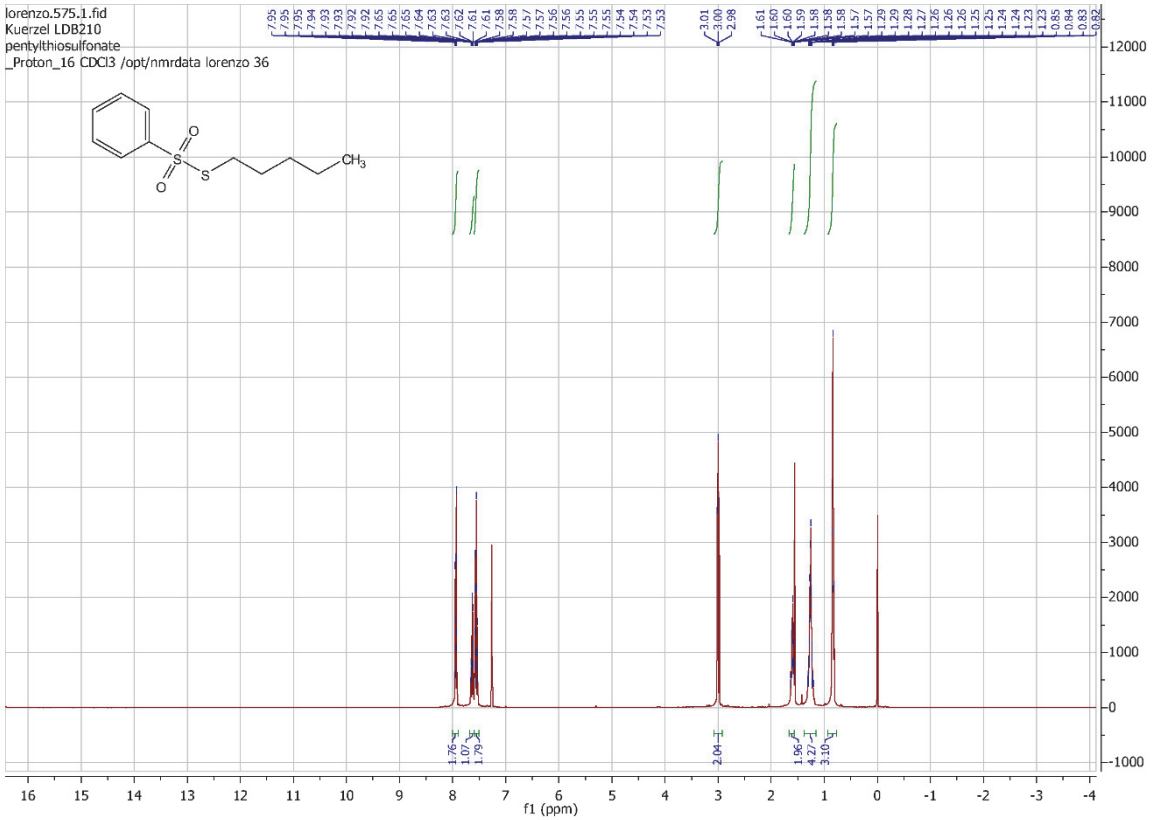

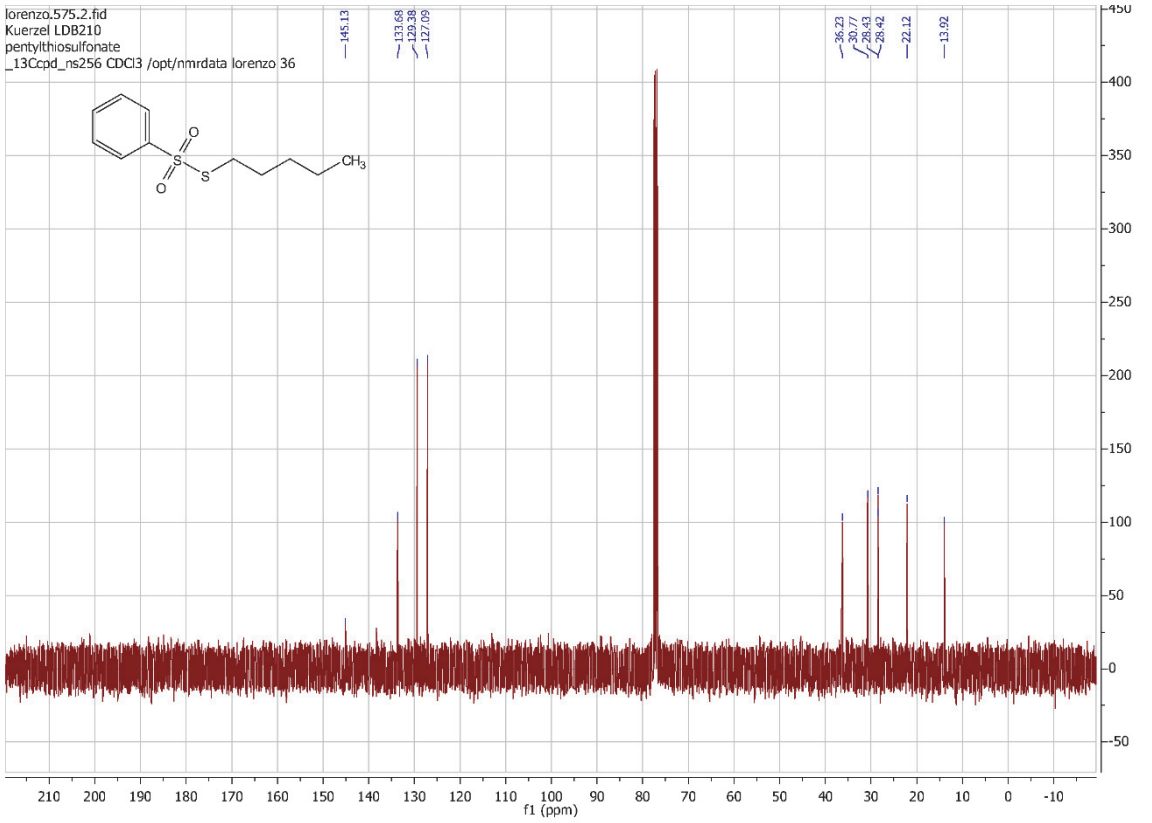

HR-ESI MS spectra of S-pentyl bezenethiosulfonate.

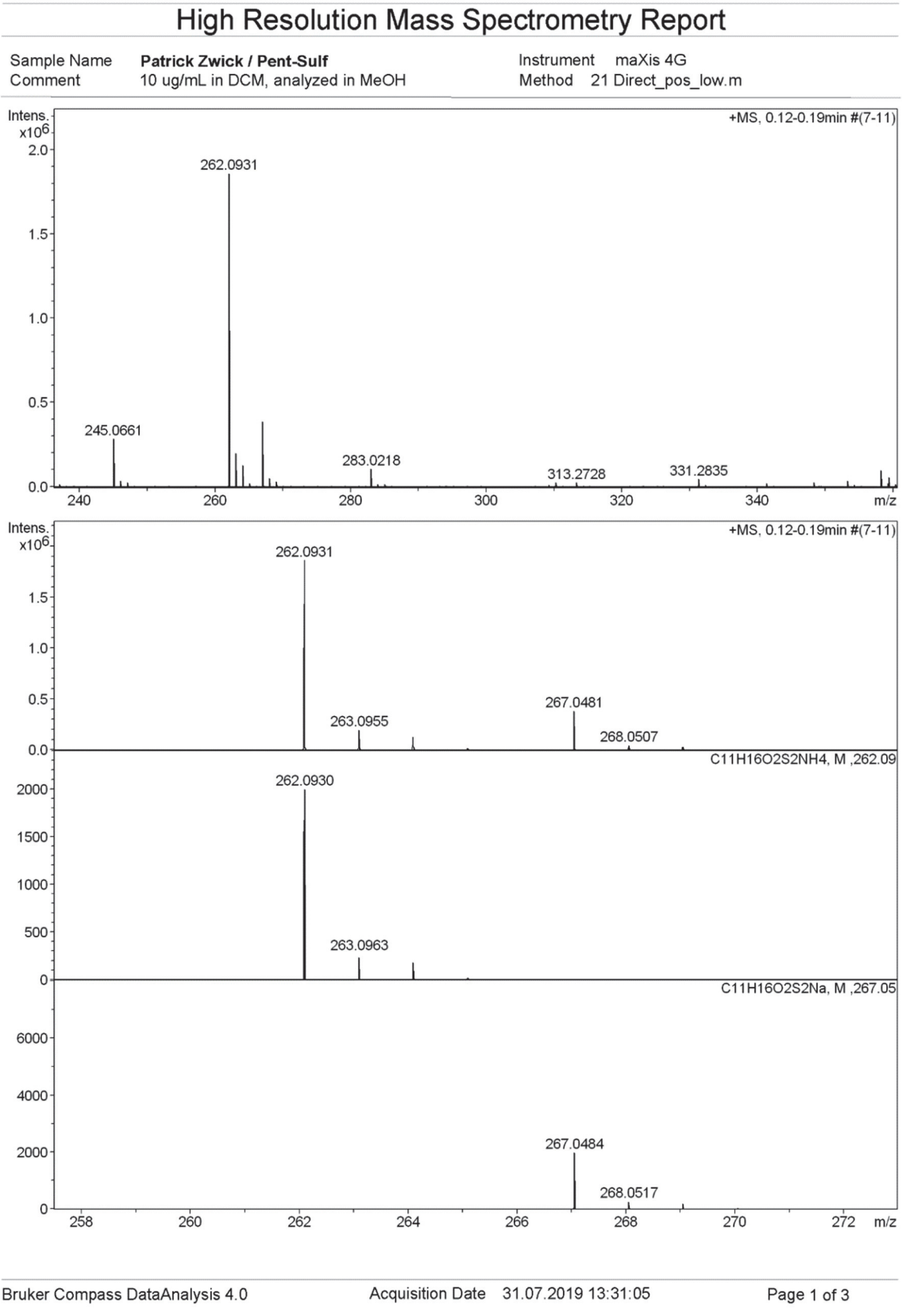

High Resolution Mass Spectrometry Report

Measured m/z vs. theoretical m/z

Meas. m/z	#	Formula	Score	m/z	err [mDa]	err [ppm]	mSigma	rdb	e⁻ Conf	z
262.0931	1	C 11 H 20 N O 2 S 2	100.00	262.0930	-0.1	-0.5	23.1	2.5	even	1+
267.0481	1	C 11 H 16 Na O 2 S 2	100.00	267.0484	0.3	1.1	10.1	3.5	even	

Mass list

#	m/z	I %	I
1	122.0968	1.3	24469
2	128.1071	0.4	7385
3	136.1122	3.8	70065
4	137.1153	0.4	7632
5	138.0914	0.4	7506
6	141.0006	7.4	137058
7	142.0036	0.5	9773
8	142.1226	0.6	11397
9	142.9963	0.4	7048
10	149.0232	0.7	12218
11	150.1126	0.6	10409
12	150.1276	3.9	72126
13	151.1309	0.5	8434
14	155.0465	0.3	5551
15	156.1382	0.7	12486
16	158.0269	0.6	10650
17	164.1431	2.0	36831
18	169.1443	0.5	9807
19	170.1534	0.5	8479
20	174.9879	6.3	117767
21	175.9907	0.5	8817
22	176.9838	0.6	10776
23	178.1585	0.6	11164
24	181.0853	0.5	9315
25	181.1333	0.7	13657
26	181.1432	0.5	8880
27	183.0776	0.5	10059
28	191.1062	0.5	10193
29	195.1486	0.9	16236
30	203.0698	0.3	5473
31	209.1163	0.3	6037
32	209.1639	0.6	11927
33	214.0891	1.7	31001
34	217.1047	0.3	6262
35	221.1167	0.3	5792
36	223.1800	0.4	6534
37	231.1161	0.3	5597
38	236.0711	0.3	5813
39	237.1478	0.8	14548
40	239.2360	0.3	6090
41	245.0661	15.3	284739
42	246.0689	1.9	35452
43	247.0619	1.3	23792
44	262.0931	100.0	1859324
45	263.0955	10.8	200049
46	264.0887	6.9	128847
47	265.0916	1.0	18099
48	267.0481	20.8	386132
49	267.2672	0.4	7339
50	268.0507	2.7	50111
51	269.0440	1.7	32252
52	282.2786	0.3	5958
53	283.0218	5.7	106325
54	284.0246	0.7	13759
55	285.0188	0.9	17002
56	309.2048	0.5	9504
57	310.2368	1.3	23924
58	311.2401	0.3	5450
59	313.2728	1.4	25222
60	325.1999	0.3	6335
61	331.2835	2.4	44651

High Resolution Mass Spectrometry Report

#	m/z	I %	I
62	332.2867	0.5	9558
63	338.3403	0.3	6038
64	341.3042	1.2	22403
65	348.3100	1.3	23499
66	353.2656	2.0	37181
67	354.2692	0.4	8055
68	358.2006	5.1	94922
69	359.2039	1.2	22306
70	359.3148	2.9	54380
71	360.3184	0.7	12982
72	363.1561	0.6	11781
73	369.2394	0.4	8019
74	376.2111	1.3	24299
75	376.3413	1.6	30416
76	377.2144	0.4	6593
77	377.3448	0.4	7861
78	379.1300	0.4	7526
79	381.1665	0.4	8193
80	381.2968	2.0	36285
81	382.3002	0.5	8420
82	391.2837	0.4	6999
83	394.2215	0.3	5615
84	397.2702	0.5	8807
85	511.1067	1.6	29379
86	512.1095	0.4	7610
87	561.3514	0.9	16098
88	562.3547	0.3	6186
89	642.3415	0.5	9802
90	647.4575	1.7	32335
91	648.4609	0.7	13846
92	663.4527	4.3	80853
93	664.4558	2.0	37036
94	665.4590	0.5	9002
95	680.4792	4.4	82210
96	681.4824	2.0	37657
97	682.4855	0.5	9317
98	685.4338	0.3	5627
99	700.6251	0.3	5738
100	701.4082	0.4	6995

Acquisition Parameter

General	Fore Vacuum	2.68e+000 mBar	High Vacuum	1.25e-007 mBar	Source Type	ESI
	Scan Begin	75 m/z	Scan End	1000 m/z	Ion Polarity	Positive
Source	Set Nebulizer	0.4 Bar	Set Capillary	3600 V	Set Dry Gas	3.0 l/min
	Set Dry Heater	180 °C	Set End Plate Offset	-500 V		
Quadrupole	Set Ion Energy (MS only)	4.0 eV				
Coll. Cell	Collision Energy	8.0 eV	Set Collision Cell RF	350.0 Vpp		
Ion Cooler	Set Ion Cooler Transfer Time	55.0 µs	Set Ion Cooler Pre Pulse Storage Time	7.0 µs		

^{1}H-NMR (CD_2Cl_2, 500 MHz, 298 K) and ^{13}C-NMR (CD_2Cl_2, 126 MHz, 298 K) of *S*-(2-(2-ethoxyethoxy)ethyl) benzenethiosulfonate.

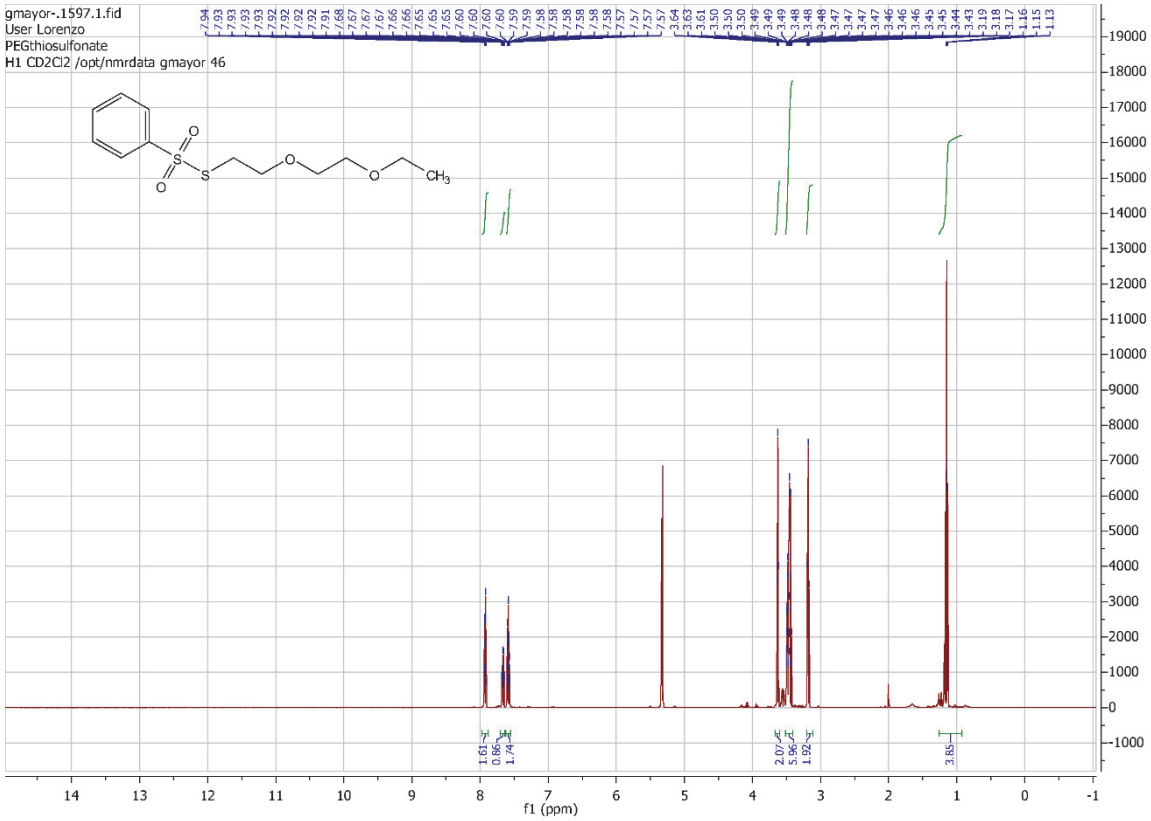

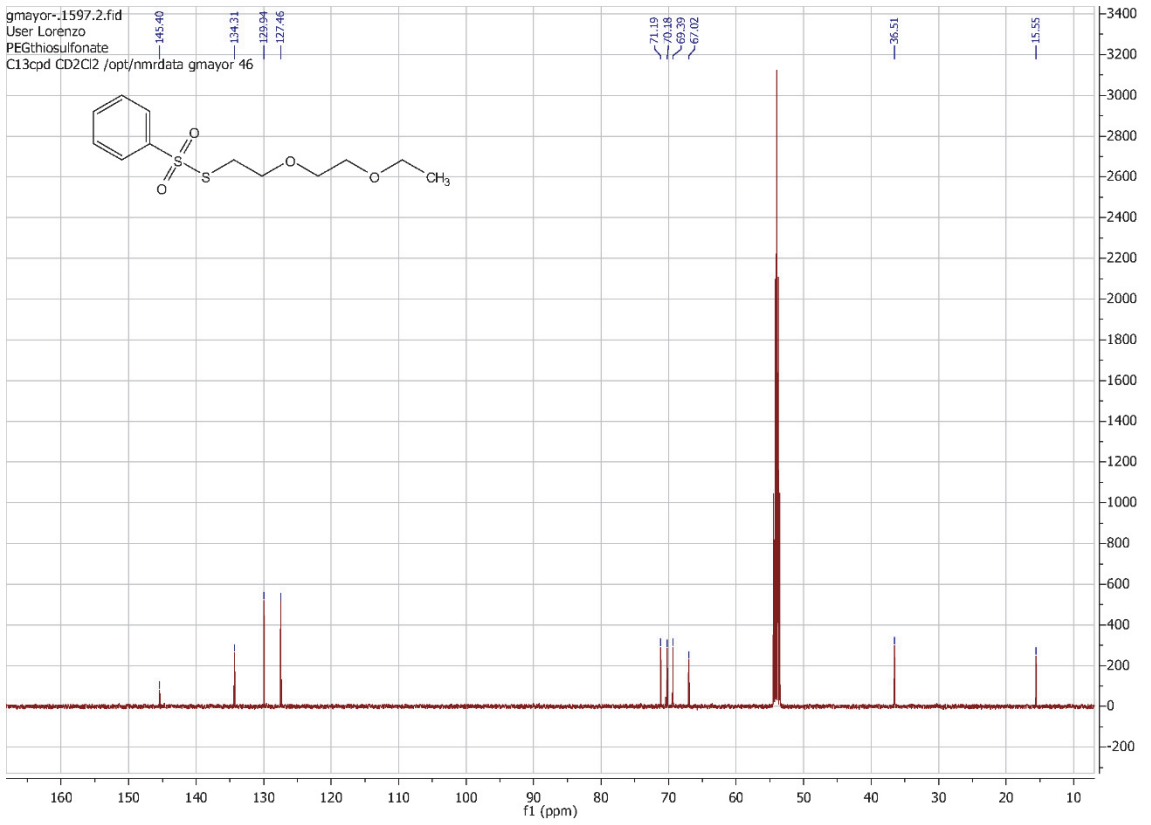

HR-ESI MS spectra of *S*-(2-(2-ethoxyethoxy)ethyl) benzenethiosulfonate.

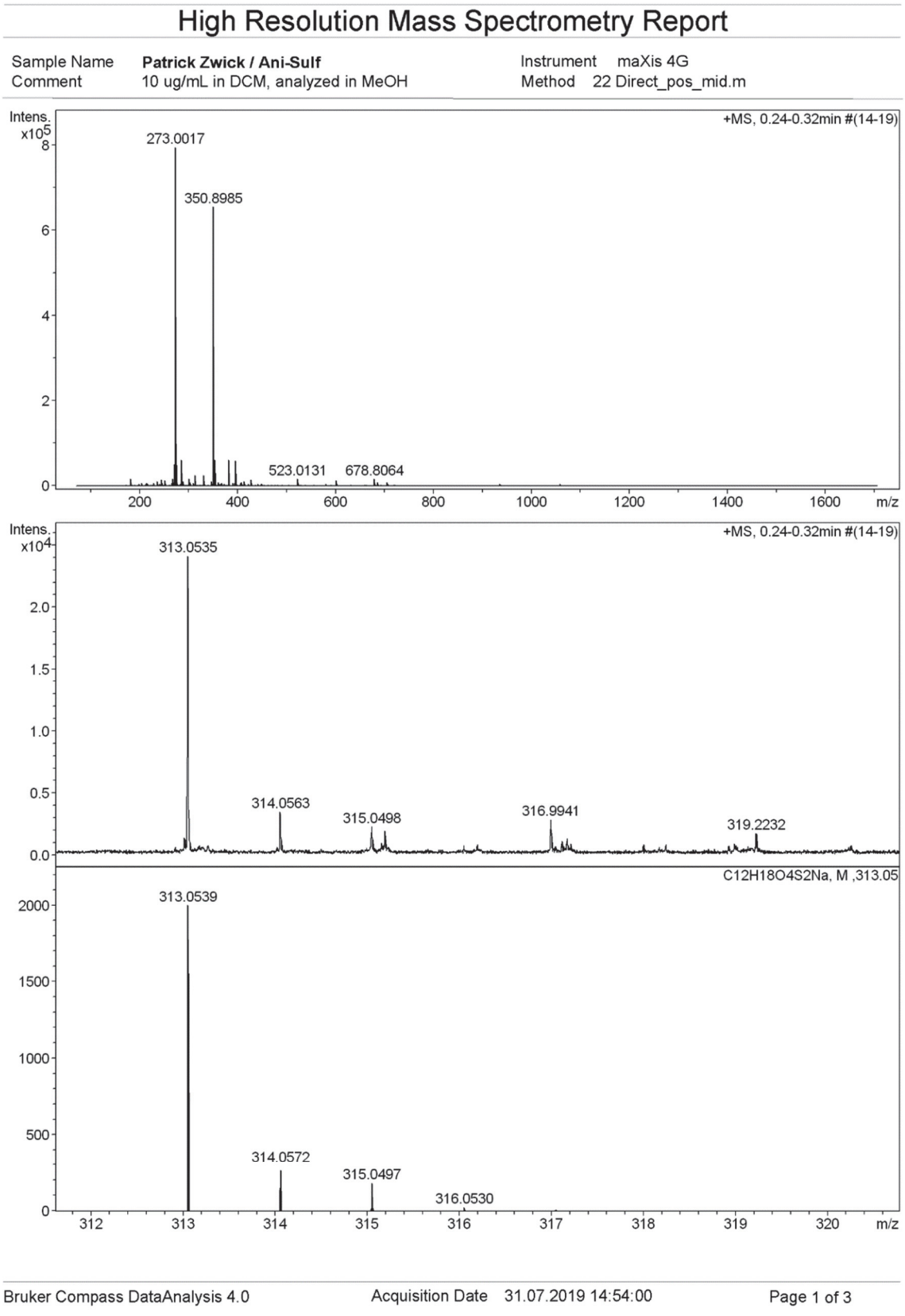

High Resolution Mass Spectrometry Report

Measured m/z vs. theoretical m/z

Meas. m/z	#	Formula	Score	m/z	err [mDa]	err [ppm]	mSigma	rdb	e⁻ Conf	z
313.0535	1	C 12 H 18 Na O 4 S 2	100.00	313.0539	0.3	1.1	9.3	3.5	even	1+

Mass list

#	m/z	I %	I
1	181.1445	2.0	15918
2	197.1394	0.4	3562
3	199.1551	0.7	5591
4	205.0599	0.8	6135
5	211.1548	0.4	3241
6	213.1706	0.7	5307
7	215.1250	0.7	5832
8	215.1498	0.7	5269
9	217.1044	0.7	5547
10	227.1497	0.4	3469
11	229.1657	0.8	6489
12	236.0713	1.3	10158
13	240.9959	0.4	3566
14	241.0289	0.6	4548
15	245.0779	1.7	13768
16	248.0709	0.4	3369
17	250.1771	0.4	3203
18	251.0190	1.5	12014
19	253.0498	0.4	3040
20	266.1721	0.8	6418
21	267.0458	1.0	8287
22	268.0459	2.0	16158
23	271.1877	6.5	51501
24	272.1909	1.1	8614
25	273.0017	100.0	794838
26	274.0042	12.5	99063
27	274.9973	7.6	60557
28	276.0004	1.1	8740
29	283.0608	0.7	5224
30	285.0552	7.7	61265
31	286.0584	1.3	10009
32	287.0522	0.4	2952
33	288.9749	1.4	11404
34	301.1405	2.1	17075
35	302.1439	0.4	3426
36	303.0115	1.1	8849
37	304.2608	0.5	3646
38	309.2032	0.9	7044
39	313.0535	3.0	24118
40	314.0563	0.4	3504
41	316.9941	0.4	2893
42	331.0790	3.2	25723
43	332.0822	0.7	5500
44	333.0758	0.4	2838
45	345.9421	1.3	10002
46	350.8985	82.4	655044
47	351.9007	7.1	56593
48	352.8941	6.6	52331
49	353.2658	7.7	61509
50	353.8967	0.6	5065
51	354.2691	1.7	13579
52	357.1852	0.4	3094
53	360.3229	1.2	9181
54	363.1567	0.6	4588
55	365.2664	0.5	3788
56	366.8715	0.8	6232
57	373.2034	0.6	4953
58	380.9891	2.1	16801
59	381.1667	0.6	4832
60	381.2971	7.7	61286
61	381.9918	0.4	3446
62	382.3001	1.8	14661

High Resolution Mass Spectrometry Report

#	m/z	I %	I
63	382.8700	0.4	3235
64	390.9500	0.8	5987
65	393.2976	0.8	6550
66	395.1859	7.3	58274
67	396.1892	1.6	12883
68	396.9647	0.5	3660
69	397.1848	0.4	3239
70	406.9237	0.9	7530
71	408.3081	1.0	8054
72	412.9942	1.4	11169
73	413.2653	1.2	9333
74	421.3287	0.5	4108
75	426.8961	1.8	14157
76	435.3442	0.4	3141
77	441.2965	0.5	3984
78	447.3440	0.4	3252
79	449.3615	0.5	4099
80	452.9117	0.4	3193
81	469.3282	0.5	3586
82	523.0131	2.1	16626
83	523.3237	0.4	2927
84	524.0158	0.6	4715
85	525.0111	0.4	3397
86	581.0917	0.5	4133
87	600.9100	1.7	13240
88	601.9121	0.4	3050
89	659.2651	0.4	3373
90	678.8064	2.0	15865
91	679.8087	0.4	3381
92	680.8025	0.5	3670
93	681.2462	0.6	4929
94	685.4351	1.0	8239
95	686.4384	0.5	4057
96	705.5814	1.0	8248
97	706.5841	0.5	4206
98	935.4459	0.5	3968
99	1057.6295	0.6	4574
100	1058.6322	0.4	3127

Acquisition Parameter

General	Fore Vacuum	2.68e+000 mBar	High Vacuum	1.26e-007 mBar	Source Type	ESI
	Scan Begin	75 m/z	Scan End	1700 m/z	Ion Polarity	Positive
Source	Set Nebulizer	0.4 Bar	Set Capillary	3600 V	Set Dry Gas	4.0 l/min
	Set Dry Heater	180 °C	Set End Plate Offset	-500 V		
Quadrupole	Set Ion Energy (MS only)	4.0 eV				
Coll. Cell	Collision Energy	8.0 eV	Set Collision Cell RF	350.0 Vpp		
Ion Cooler	Set Ion Cooler Transfer Time	75.0 µs	Set Ion Cooler Pre Pulse Storage Time	10.0 µs		

^{1}H-NMR ($CDCl_3$, 500 MHz, 298 K) and ^{13}C-NMR ($CDCl_3$, 126 MHz, 298 K) of *S*-*p*-nitrophenyl bezenethiosulfonate.

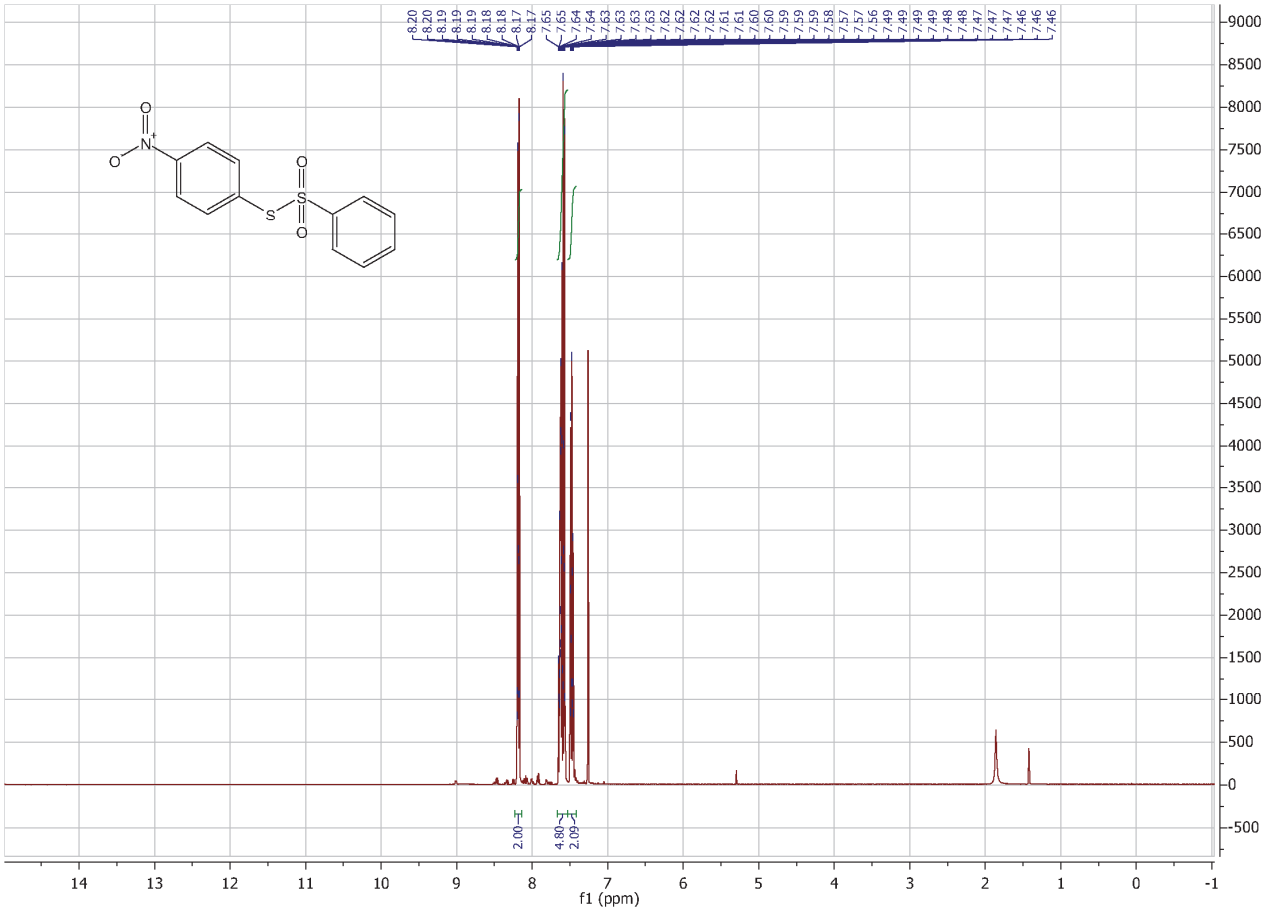

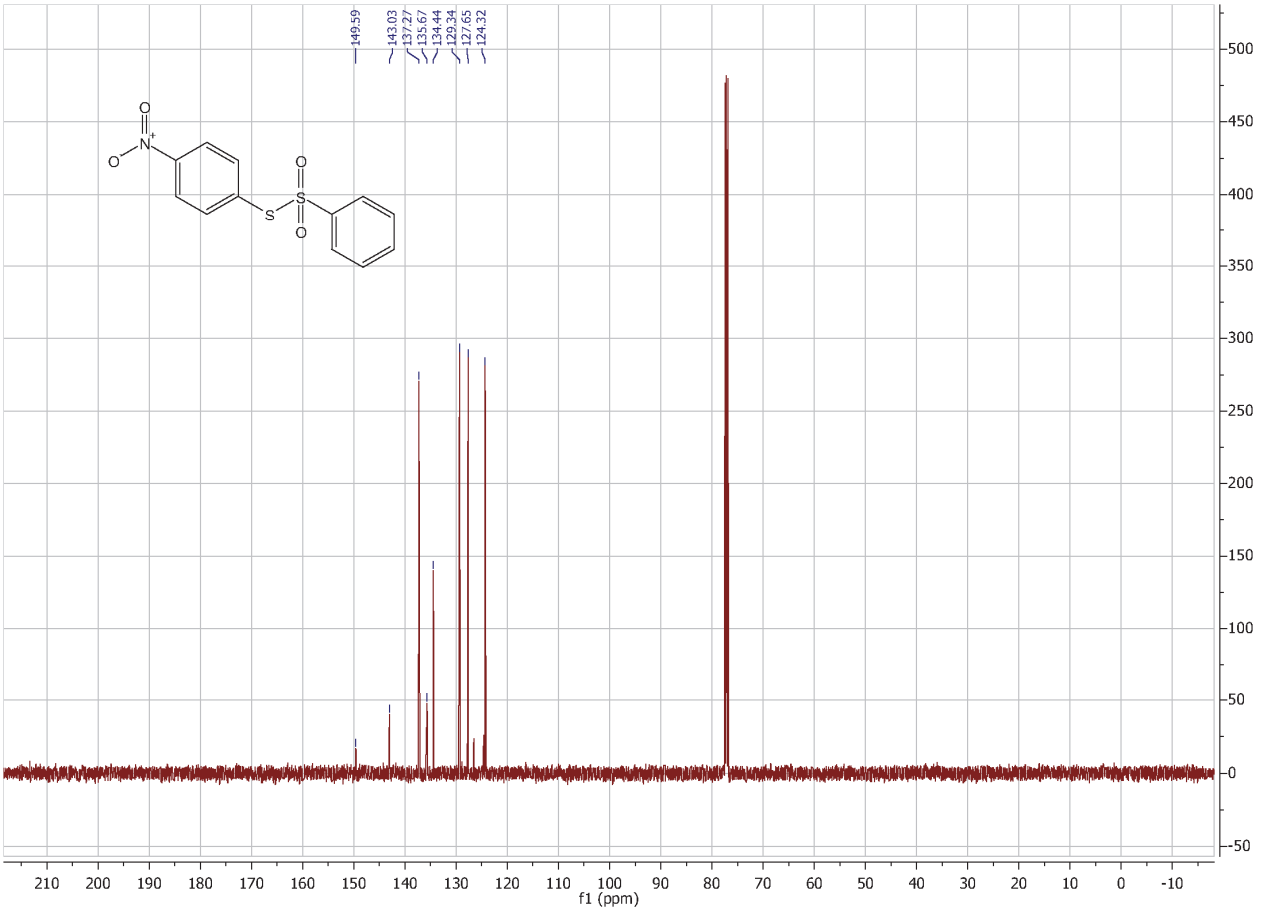

^{1}H-NMR ($CDCl_3$, 500 MHz, 298 K) and ^{13}C-NMR ($CDCl_3$, 126 MHz, 298 K) of *S*-*p*-aminophenyl bezenethiosulfonate.

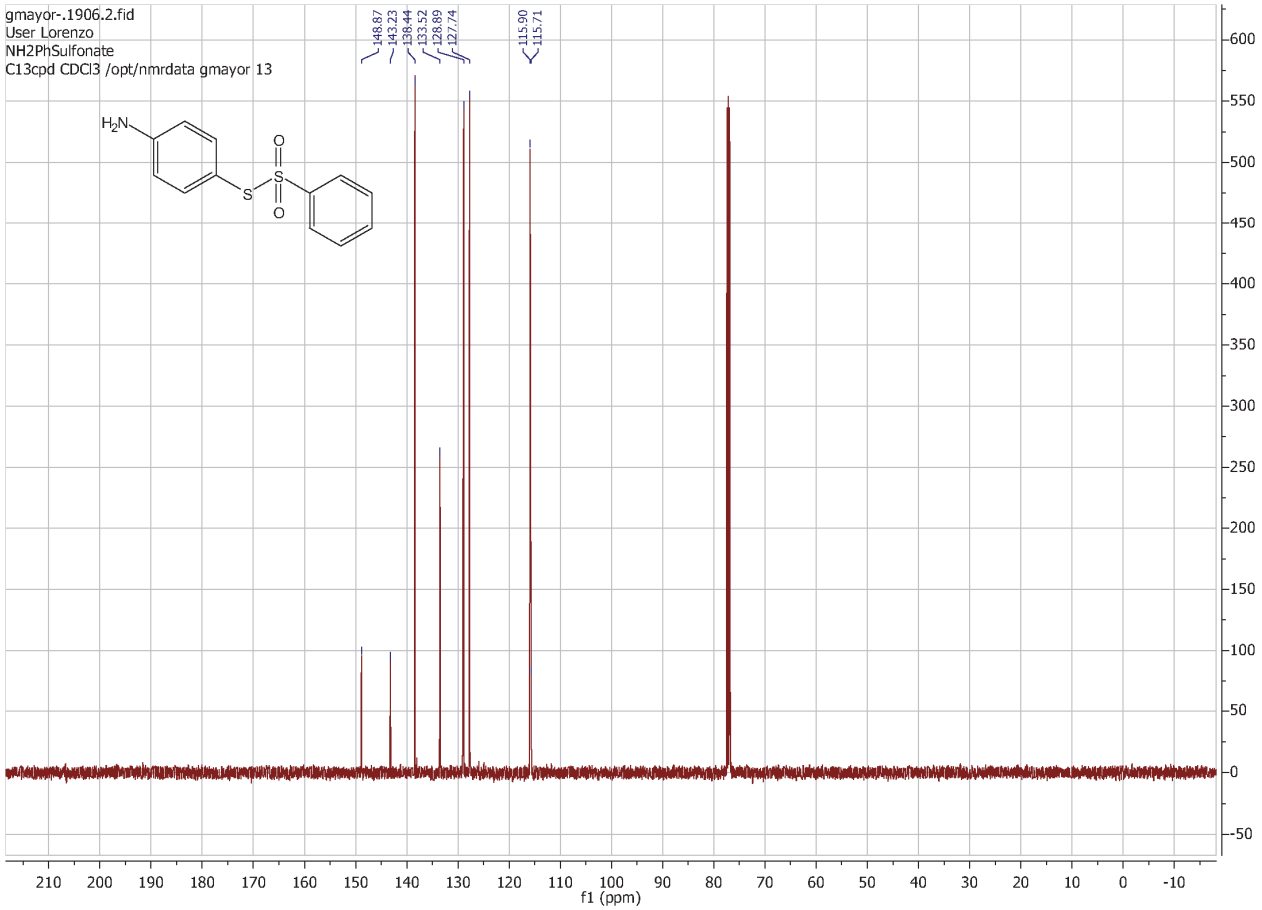

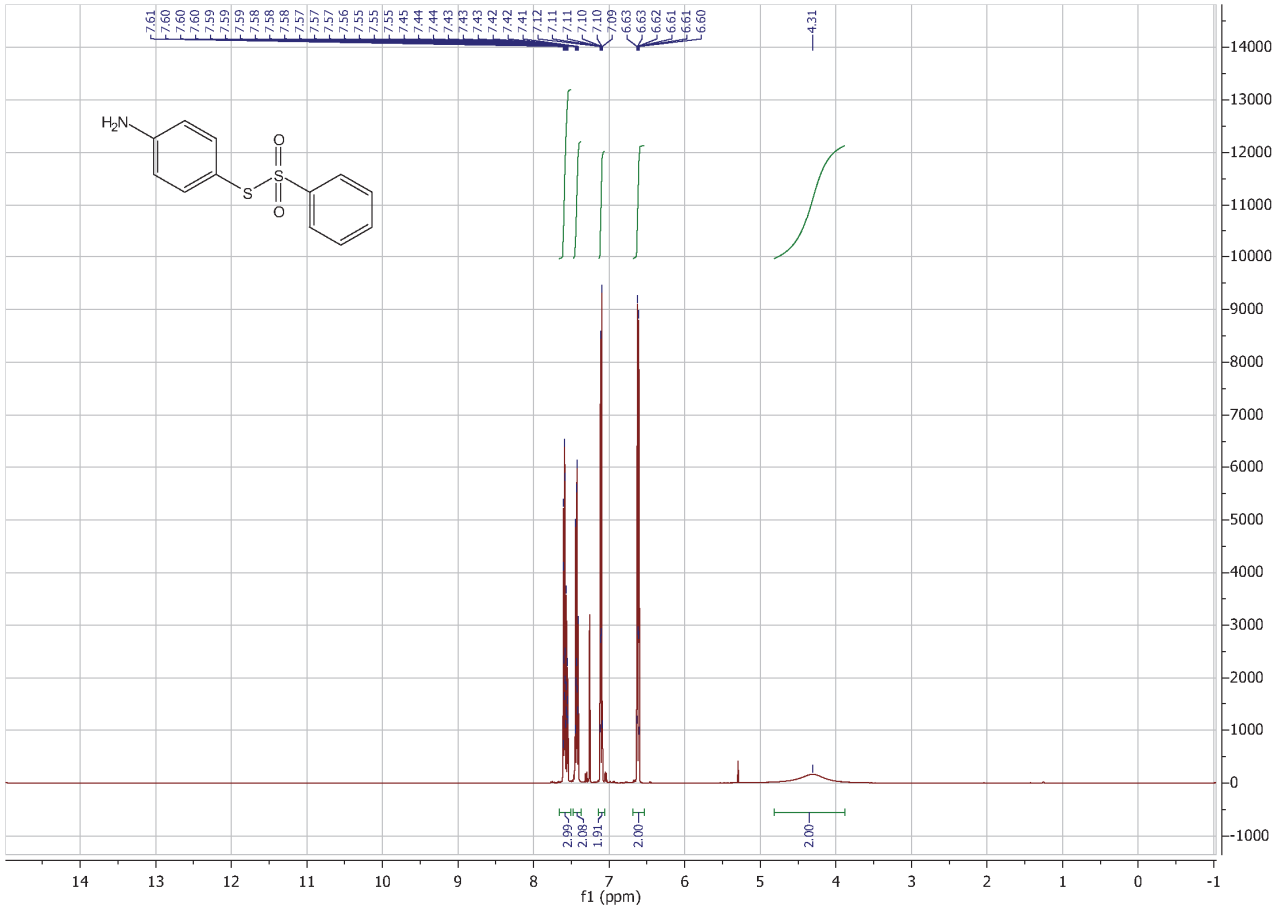

^{1}H-NMR ($CDCl_3$, 500 MHz, 298 K) and ^{13}C-NMR ($CDCl_3$, 126 MHz, 298 K) of Methyl 2-((phenylsulfonyl)thio)benzoate.

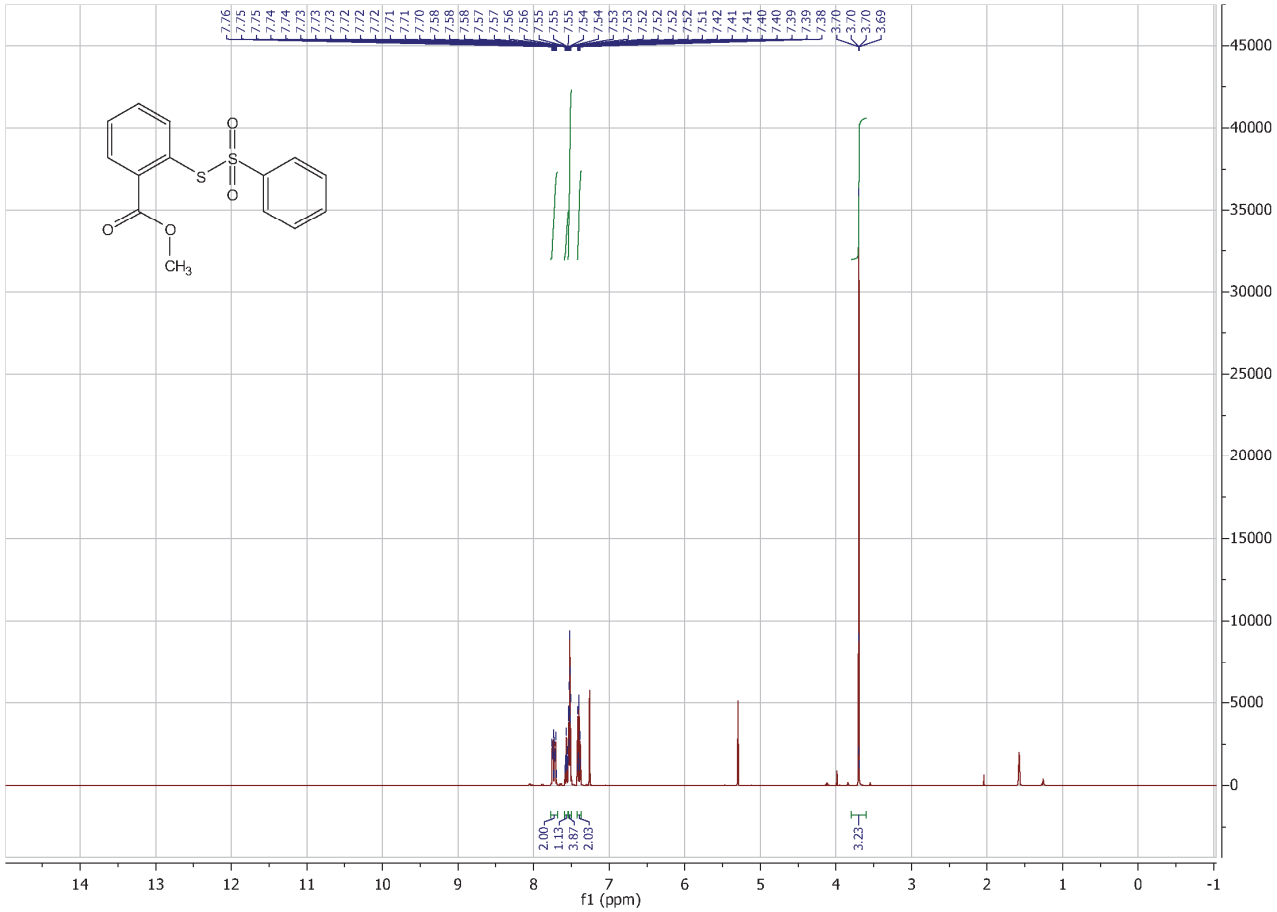

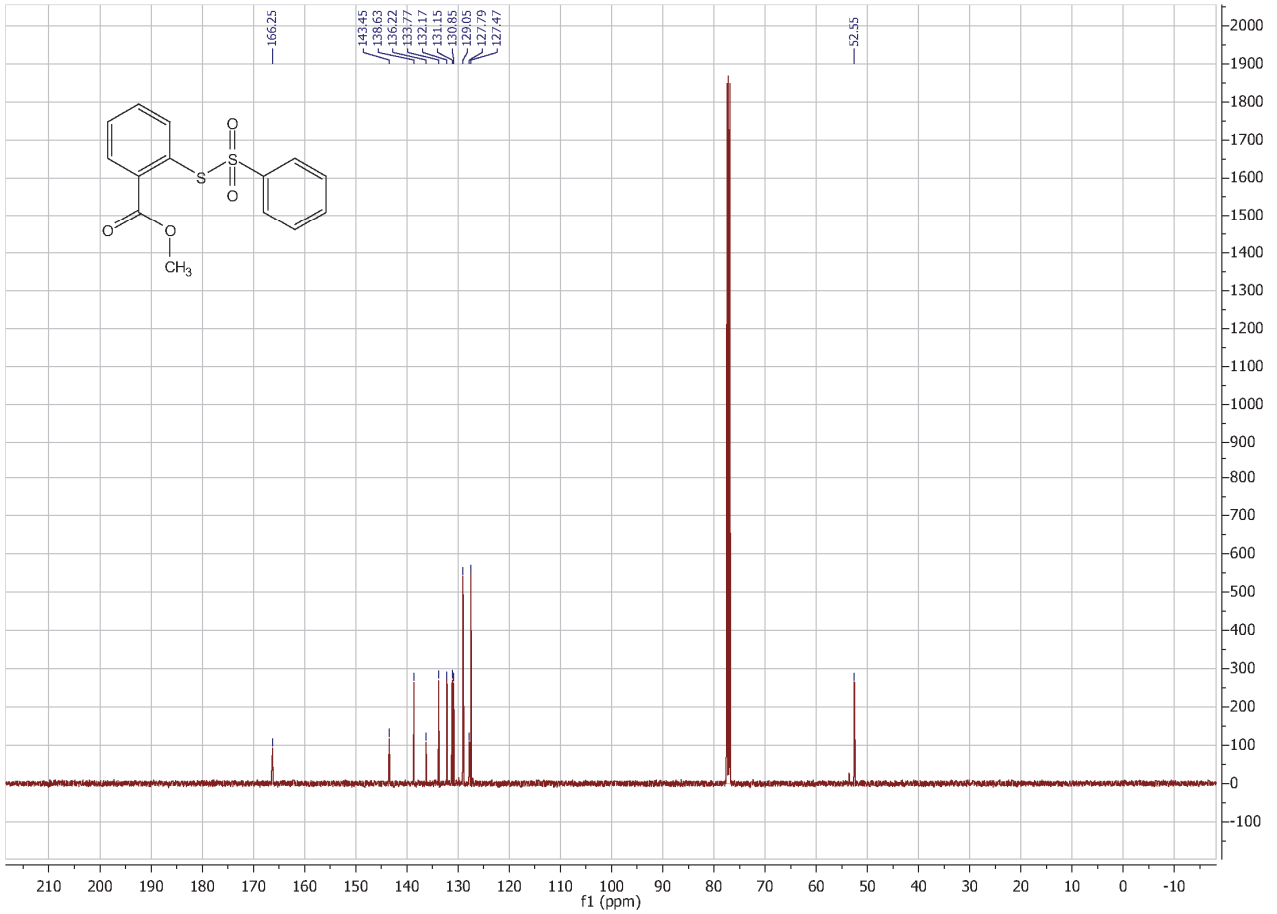

^{1}H-NMR ($CDCl_3$, 500 MHz, 298 K) and ^{13}C-NMR ($CDCl_3$, 126 MHz, 298 K) of 3,5-Difluorophenyl benzenethiosulfonate.

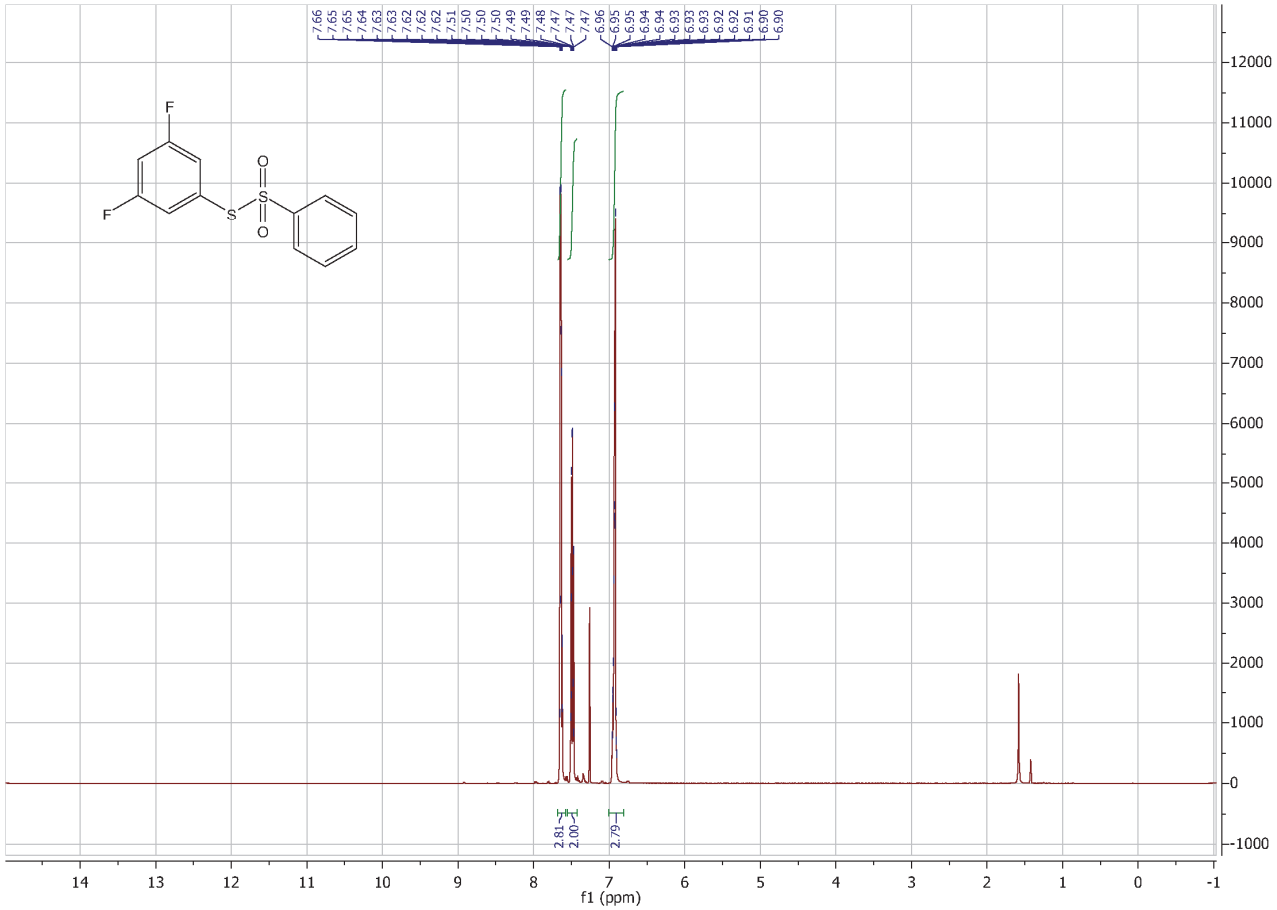

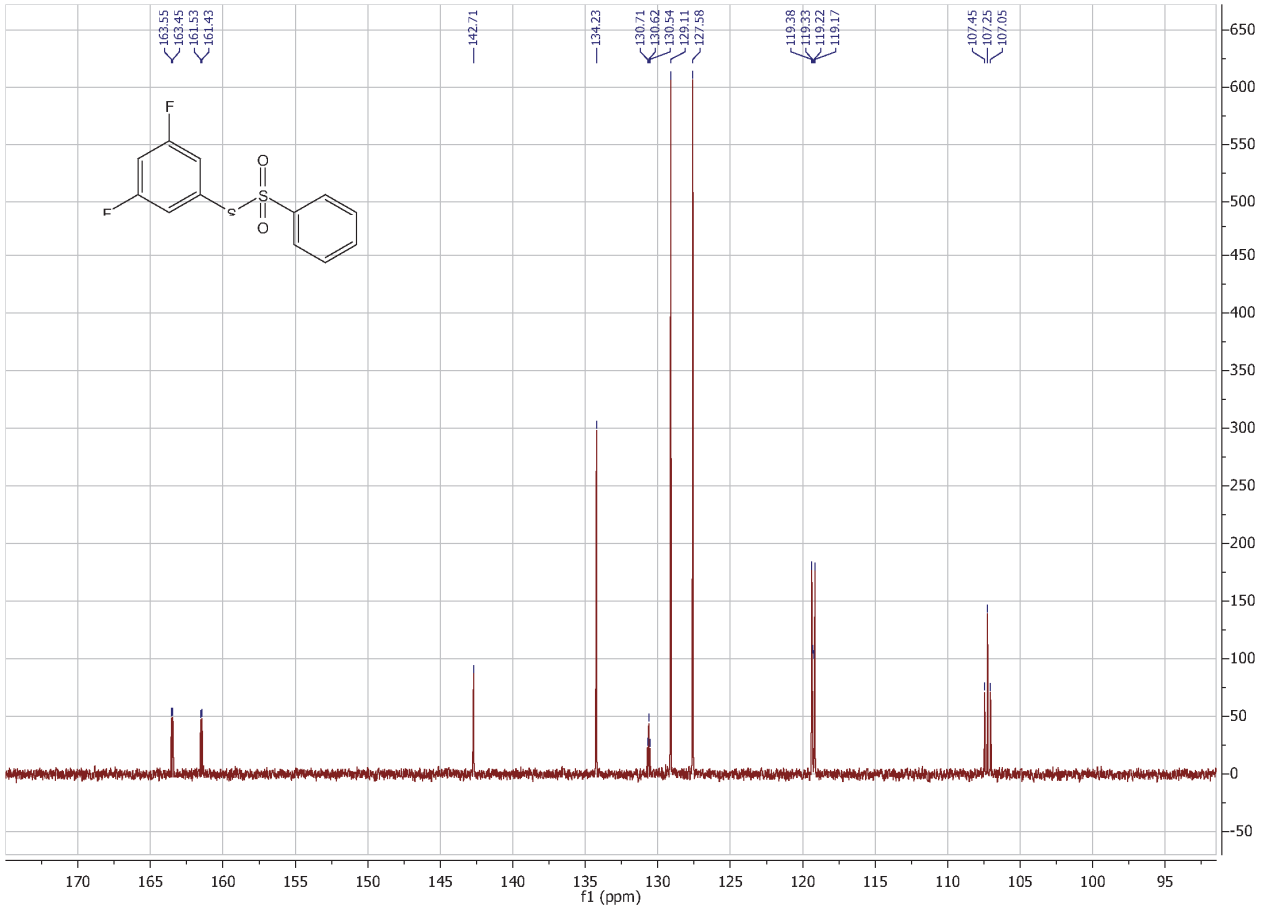

$^{19}F\{^{1}H\}$-NMR ($CDCl_3$, 471 MHz, 298 K) of 3,5-Difluorophenyl hexyl disulfide.

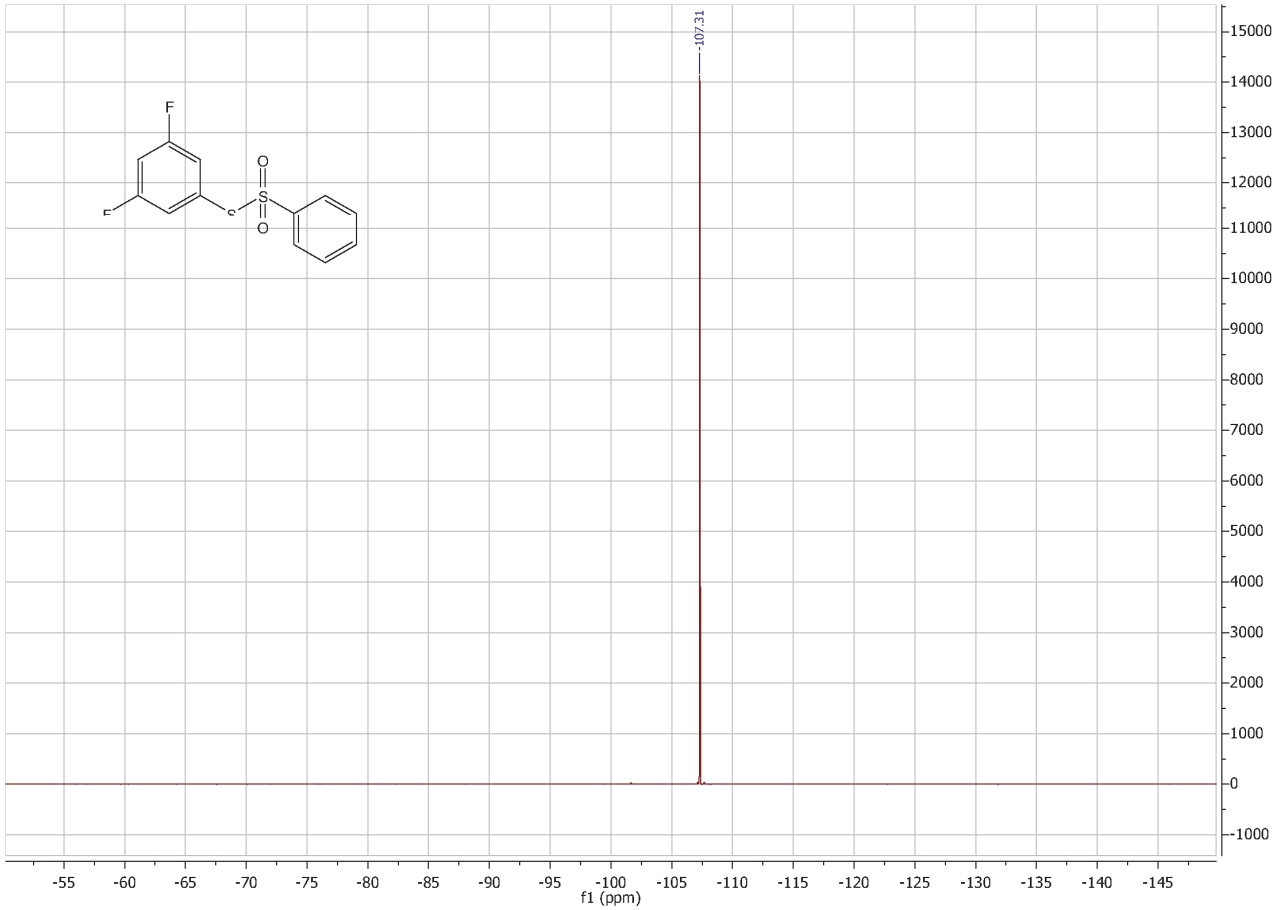

HR-ESI MS spectra of 3,5-Difluorophenyl benzenethiosulfonate.

High Resolution Mass Spectrometry Report

Sample Name **F2PhSSO2PhX**
Comment

Instrument maXis 4G
Method ms_nocolumn_300-600_pos.m

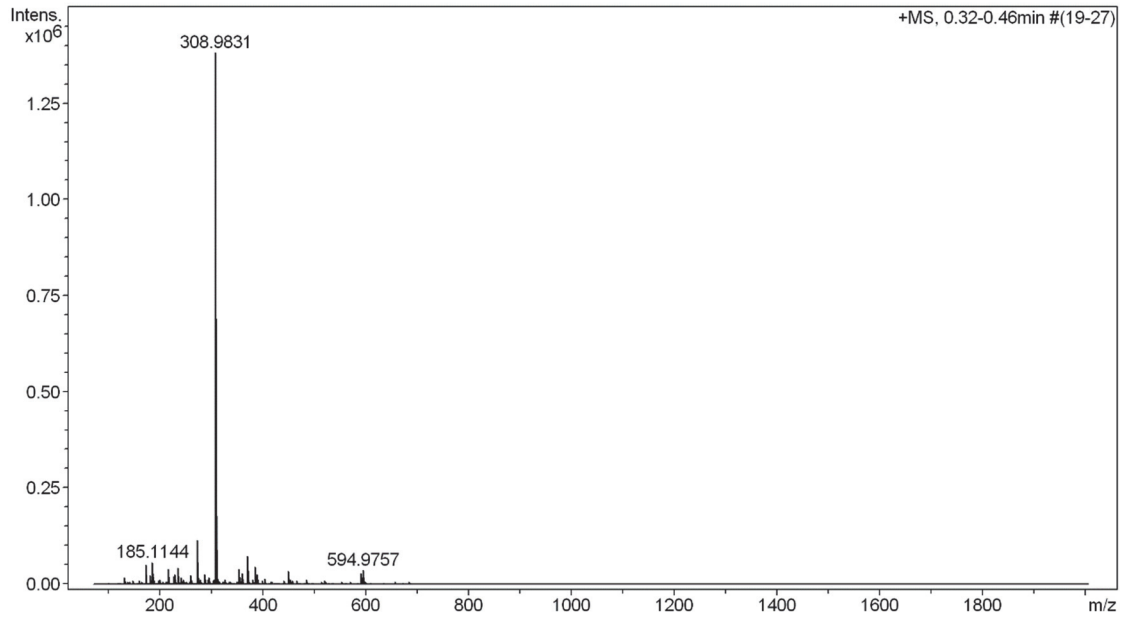

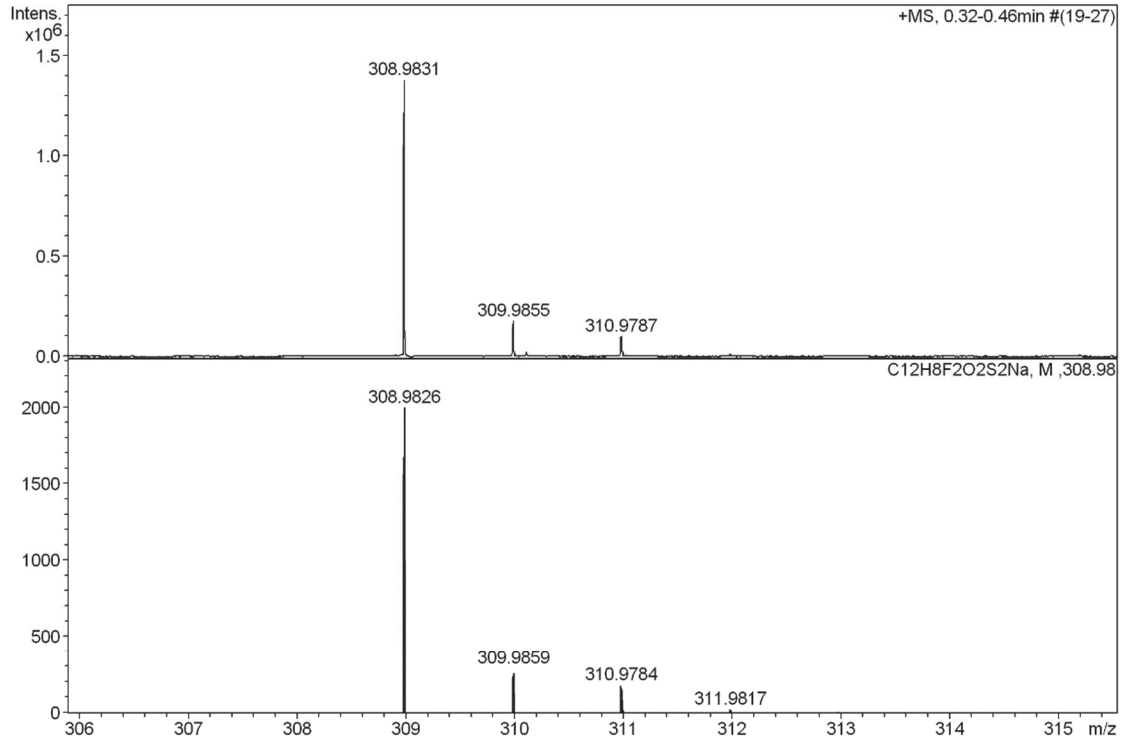

High Resolution Mass Spectrometry Report

Measured m/z vs. theoretical m/z

Meas. m/z	#	Formula	Score	m/z	err [mDa]	err [ppm]	mSigma	rdb	e⁻ Conf	z
308.9831	1	C 12 H 8 F 2 Na O 2 S 2	100.00	308.9826	-0.5	-1.6	17.6	7.5	even	1+

Mass list

#	m/z	I %	I
1	131.9612	1.3	18497
2	147.0914	0.7	9344
3	161.1070	0.7	9336
4	164.9980	0.5	6369
5	172.0942	3.7	51423
6	180.9626	1.7	22816
7	185.1144	4.1	56550
8	186.9795	1.4	19694
9	187.1223	0.5	7036
10	197.0109	0.7	9634
11	198.9732	0.9	13103
12	206.9603	0.4	5883
13	212.9884	0.5	7020
14	214.9170	0.4	5962
15	215.0217	0.5	7529
16	217.1042	2.9	39393
17	226.9513	0.5	6280
18	226.9679	0.9	11890
19	227.9643	1.4	19851
20	229.8928	1.9	25813
21	230.8897	0.5	6423
22	236.0711	3.1	43332
23	237.0740	0.4	5782
24	241.9435	0.5	6223
25	242.1026	1.3	17567
26	244.8682	0.9	12719
27	245.0991	0.5	7401
28	245.8653	0.4	5768
29	259.1299	0.4	5912
30	261.1304	1.6	22141
31	261.9081	0.5	7508
32	273.0013	8.2	113826
33	274.0040	1.2	16027
34	274.9973	0.8	11061
35	279.9454	0.9	12217
36	287.0002	1.8	25542
37	288.2891	0.9	12471
38	293.0083	0.9	13105
39	294.9195	1.2	16287
40	304.9909	0.7	9193
41	305.1565	0.8	11249
42	305.9740	0.6	8819
43	308.8997	0.5	7228
44	308.9617	0.8	11087
45	308.9831	100.0	1381489
46	309.9855	12.9	177638
47	310.1069	1.8	24500
48	310.9787	7.4	101879
49	311.0191	0.5	6243
50	311.9816	1.1	14510
51	315.1925	0.6	8217
52	325.8959	0.5	7571
53	326.9930	0.8	11251
54	349.1828	0.5	6583
55	350.9704	0.5	7068
56	351.9971	0.4	6097
57	353.1450	2.9	40738
58	353.2655	0.5	6613
59	354.1482	0.8	11570
60	354.9751	0.7	9538
61	355.2813	1.3	17732
62	360.3232	2.1	28862

High Resolution Mass Spectrometry Report

#	m/z	I %	I
63	361.3264	0.5	7018
64	370.9528	5.3	73796
65	371.9554	0.9	12316
66	372.9491	0.6	8305
67	372.9856	0.5	6831
68	381.2970	0.8	10479
69	385.9281	3.3	45158
70	386.9278	1.0	13916
71	387.0014	0.7	9480
72	387.9255	0.5	6597
73	388.9632	1.8	24614
74	399.3072	0.6	7807
75	403.9389	1.0	14391
76	441.2971	0.7	9849
77	448.9709	2.6	35267
78	449.4721	1.1	15170
79	449.9706	1.0	13604
80	452.9668	0.9	11899
81	453.7849	0.5	6239
82	456.4585	0.4	5990
83	457.9753	0.7	9839
84	466.9564	0.6	8582
85	485.8109	0.8	11205
86	513.9503	0.4	5974
87	519.9753	0.5	6860
88	521.4375	0.7	9108
89	521.9380	0.4	6202
90	553.4584	0.5	7451
91	569.4374	0.4	6157
92	591.9679	2.1	29324
93	592.4690	1.3	17475
94	592.9672	1.1	15732
95	593.4678	0.6	7878
96	594.9757	2.6	36269
97	595.9786	0.8	11075
98	596.9727	0.6	7769
99	599.4551	0.4	5832
100	685.4349	0.5	7260

Acquisition Parameter

General	Fore Vacuum	2.49e+000 mBar	High Vacuum	1.26e-007 mBar	Source Type	ESI
	Scan Begin	75 m/z	Scan End	2000 m/z	Ion Polarity	Positive
Source	Set Nebulizer	2.0 Bar	Set Capillary	4500 V	Set Dry Gas	8.0 l/min
	Set Dry Heater	200 °C	Set End Plate Offset	-500 V		
Quadrupole	Set Ion Energy (MS only)	4.0 eV				
Coll. Cell	Collision Energy	8.0 eV	Set Collision Cell RF	600.0 Vpp		
Ion Cooler	Set Ion Cooler Transfer Time	75.0 µs	Set Ion Cooler Pre Pulse Storage Time	10.0 µs		

^{1}H-NMR ($CDCl_3$, 500 MHz, 298 K) and ^{13}C-NMR ($CDCl_3$, 126 MHz, 298 K) of Methyl 2-((phenylsulfonyl)thio)benzoate.

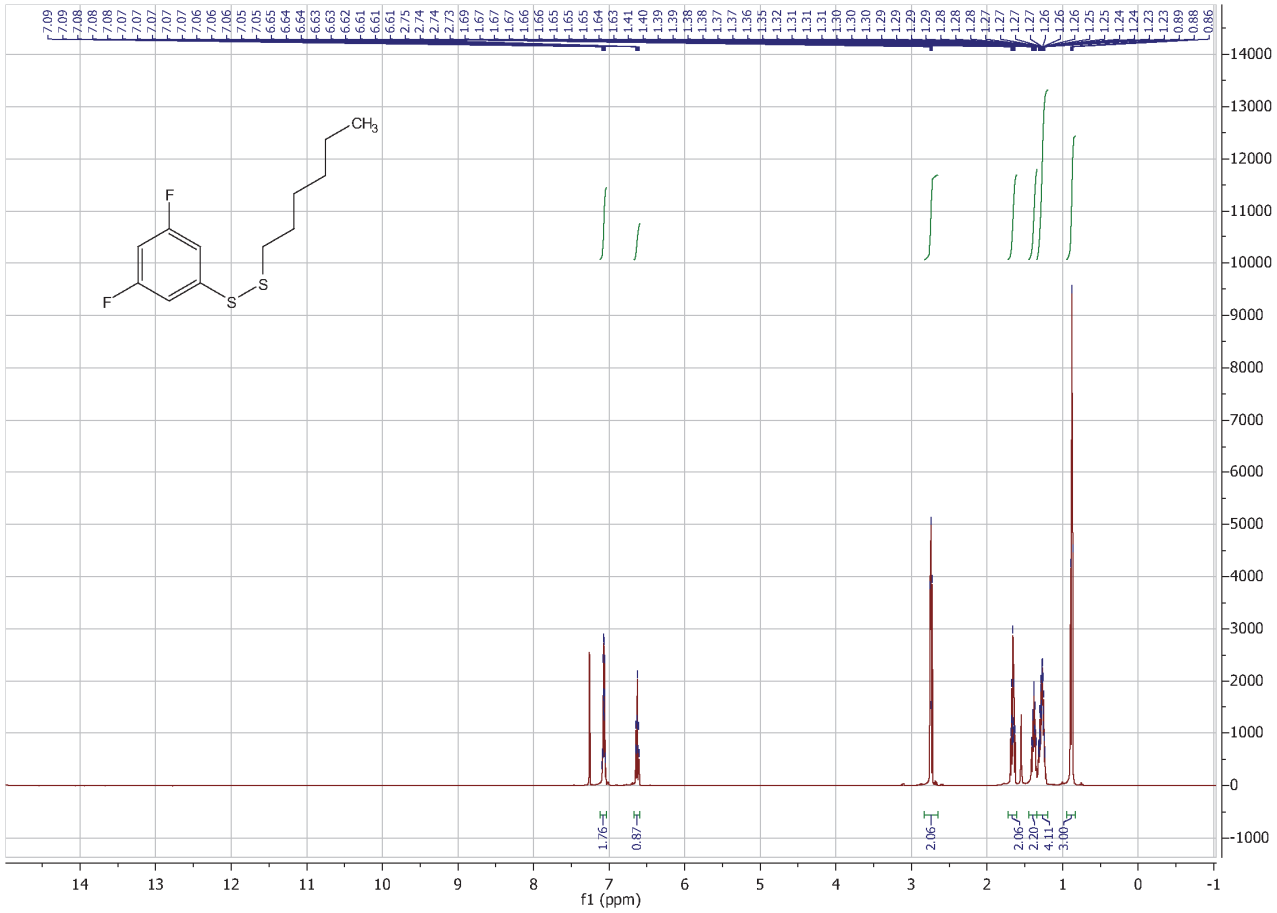

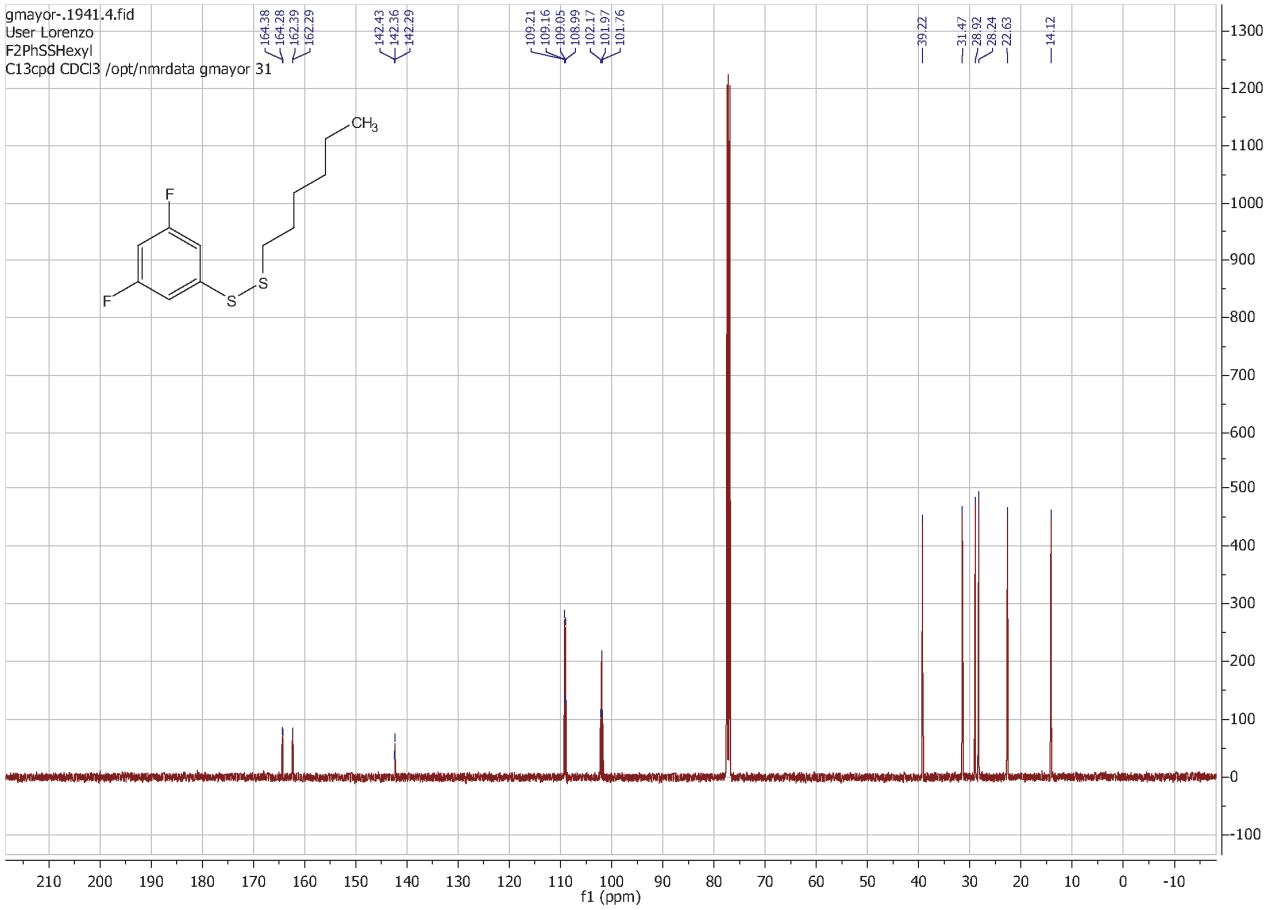

$^{19}F\{^{1}H\}$-NMR ($CDCl_3$, 471 MHz, 298 K) of 3,5-Difluorophenyl hexyl disulfide.

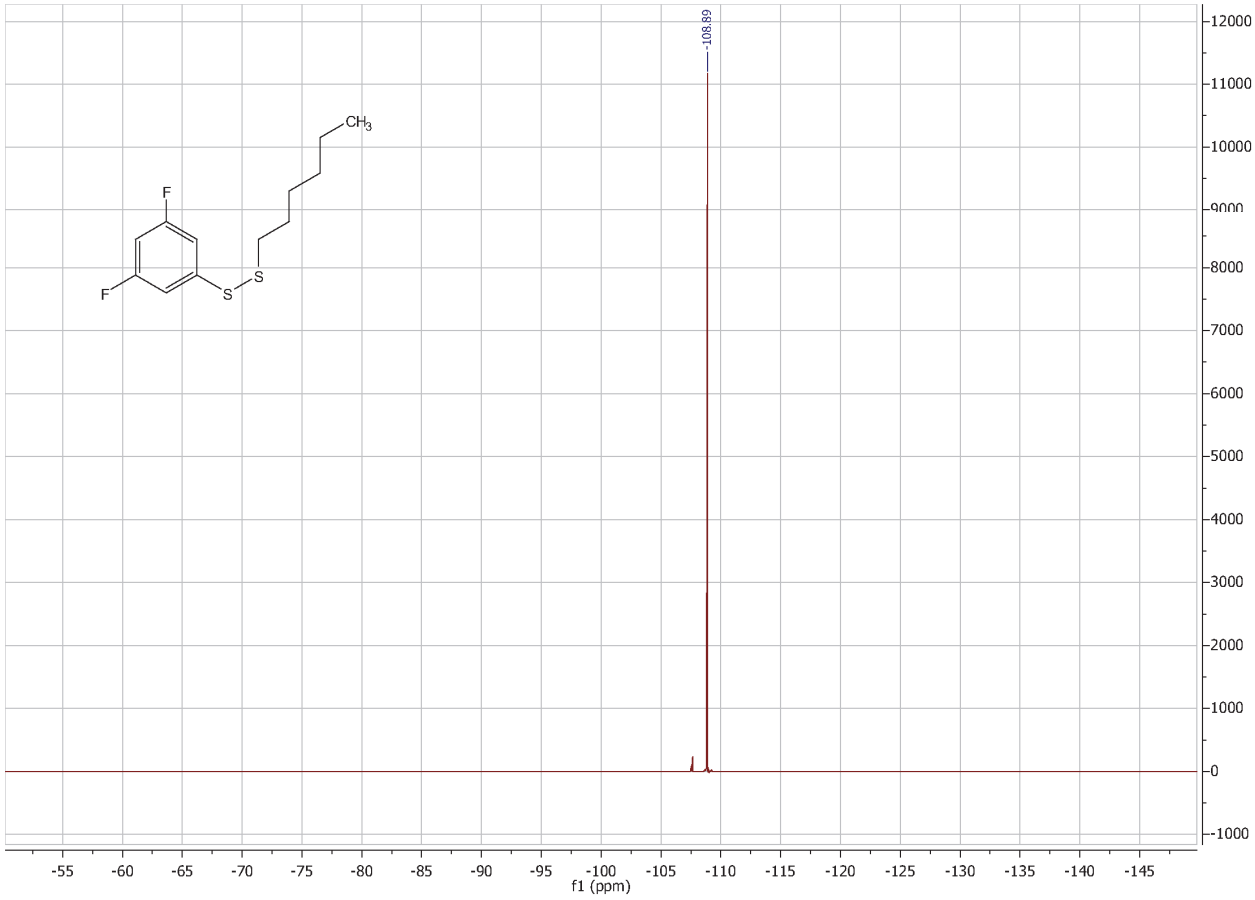

^{1}H-NMR ($CDCl_3$, 500 MHz, 298 K) and ^{13}C-NMR ($CDCl_3$, 126 MHz, 298 K) of 4-Nitrophenyl hexyl disulfide.

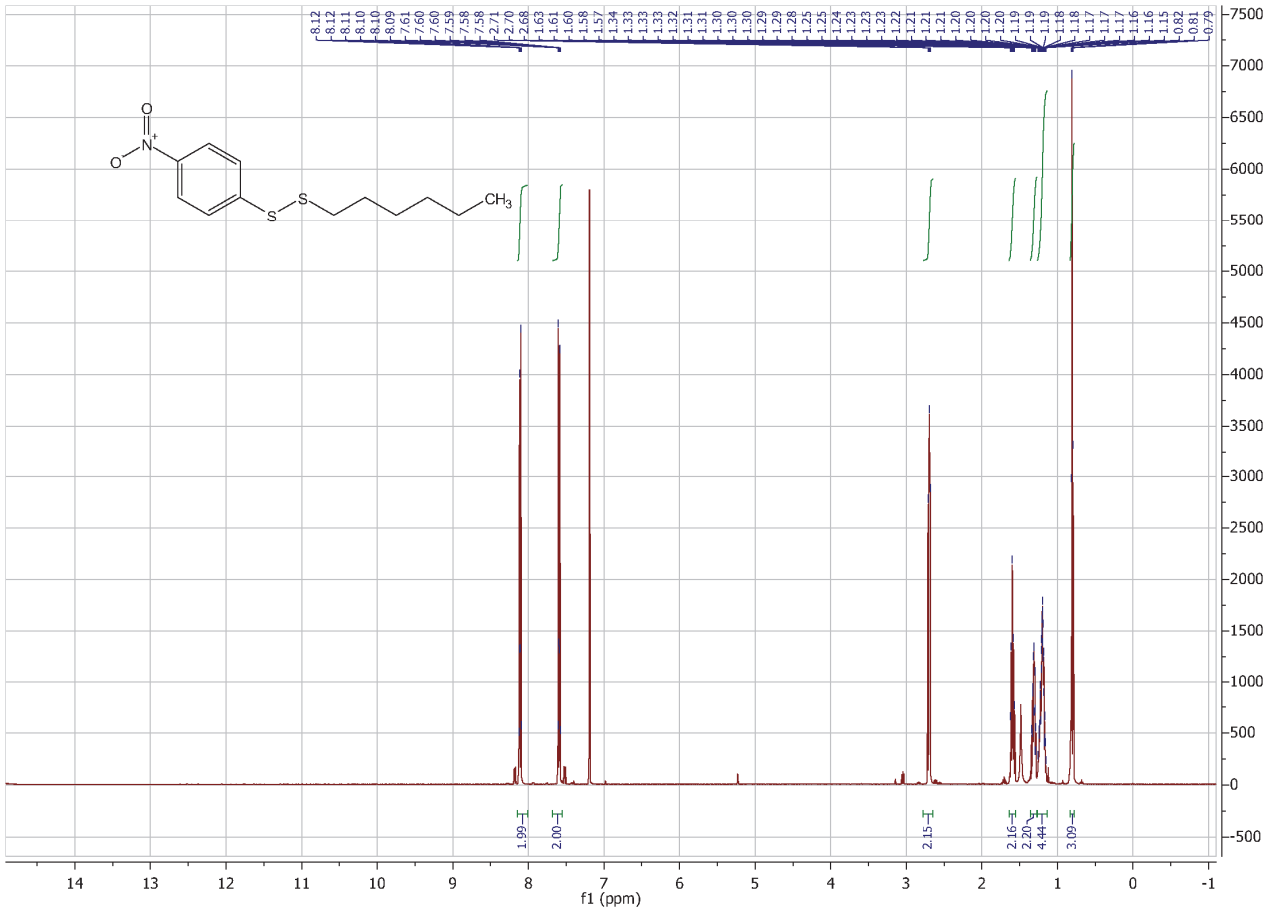

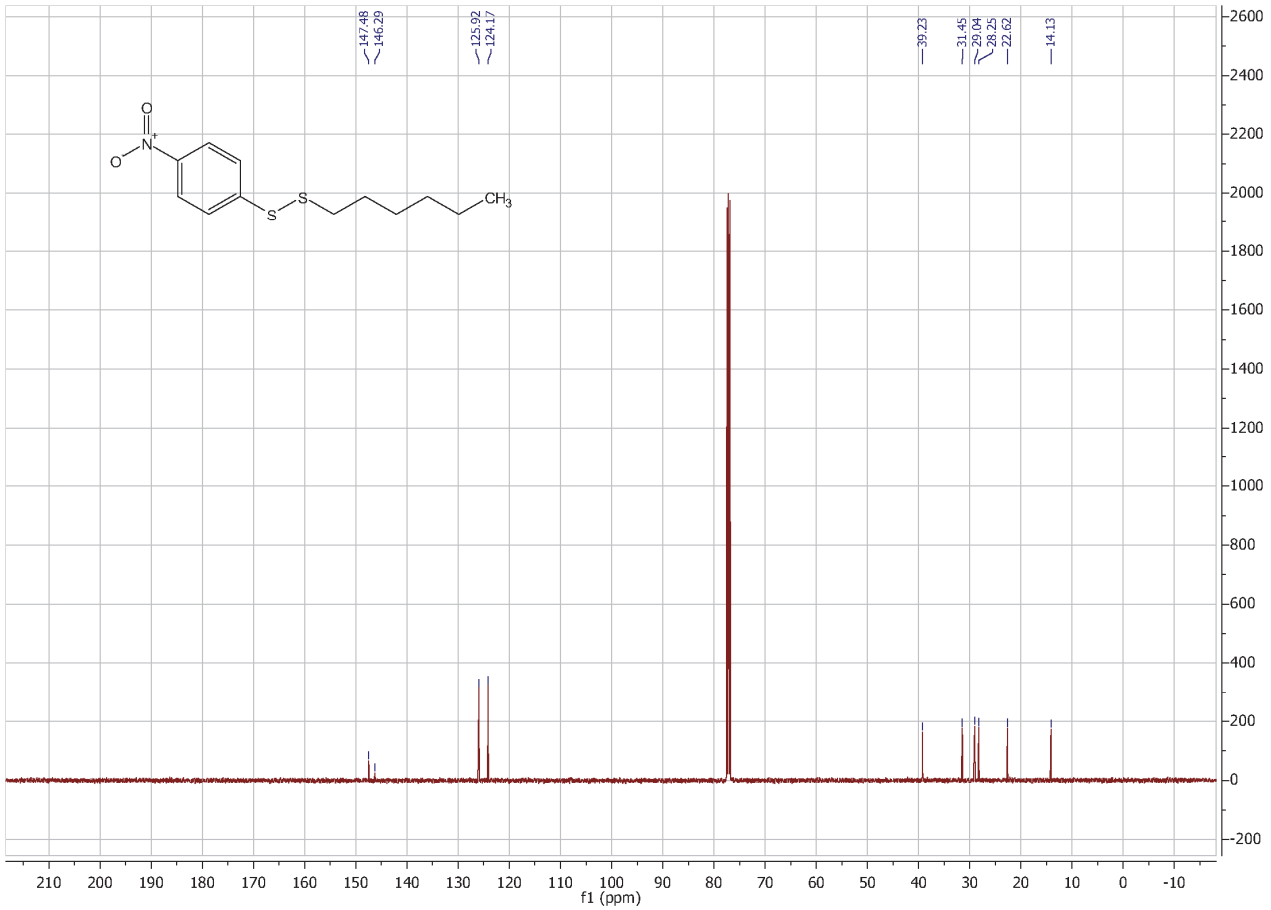

^{1}H-NMR spectrum of *p*-nitrophenyl pentyl disulfide in $CDCl_3$

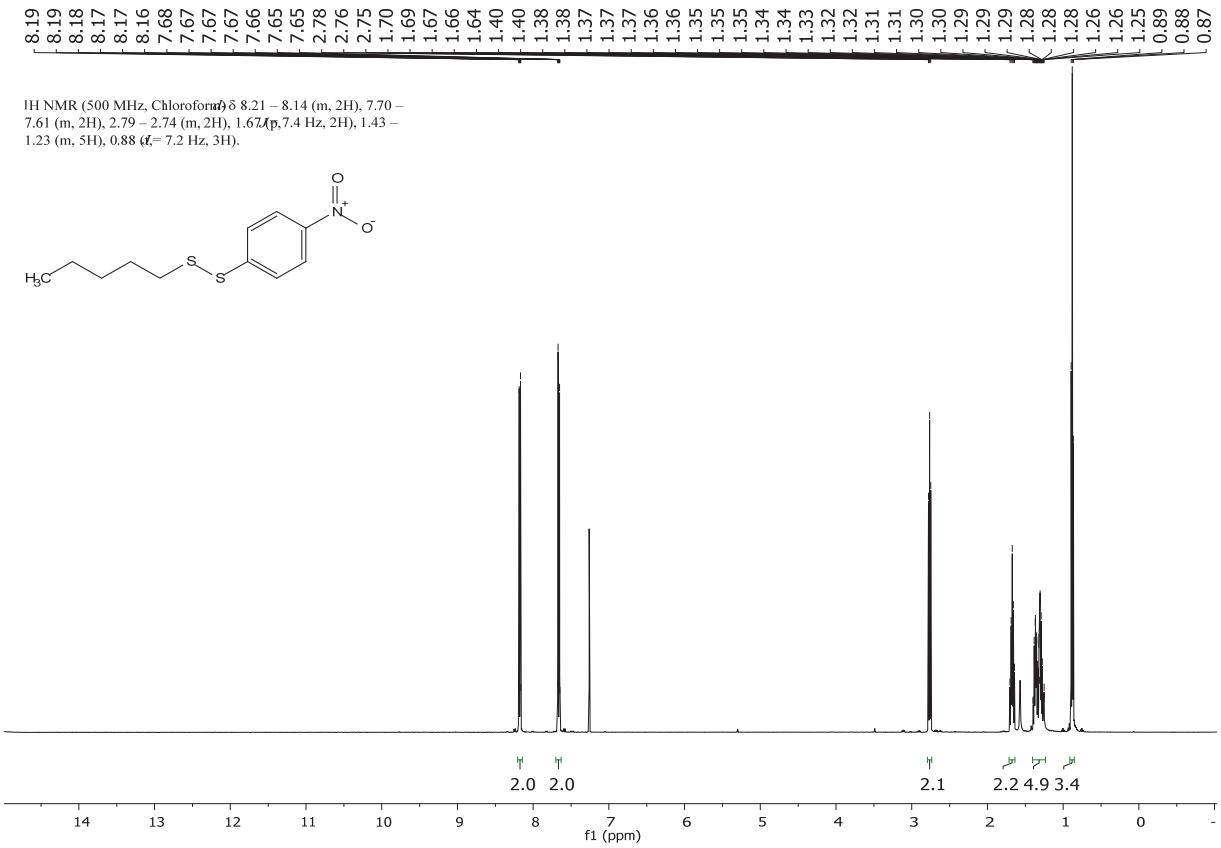

^{13}C{^{1}H}-NMR spectrum of *p*-nitrophenyl pentyl disulfide in $CDCl_3$.

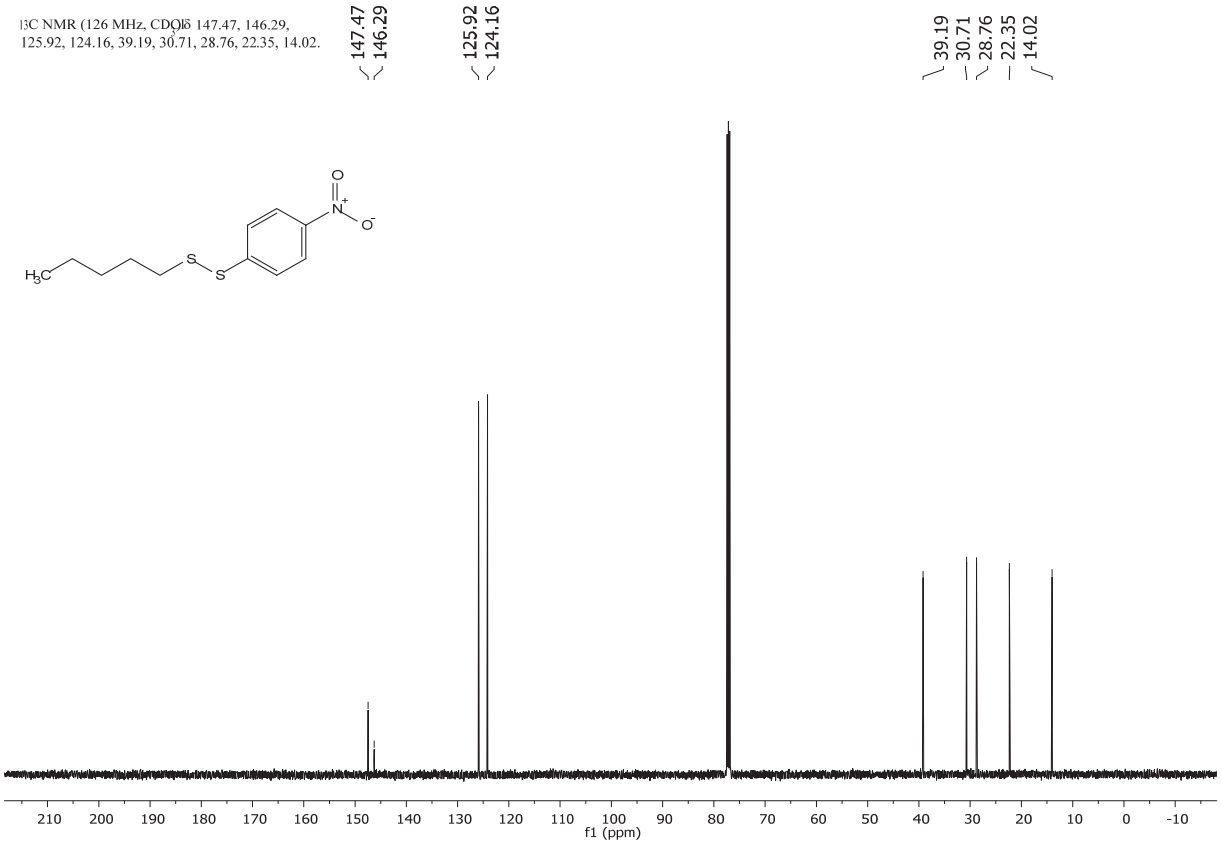

HR-ESI-MS spectrum of *p*-nitrophenyl pentyl disulfide.

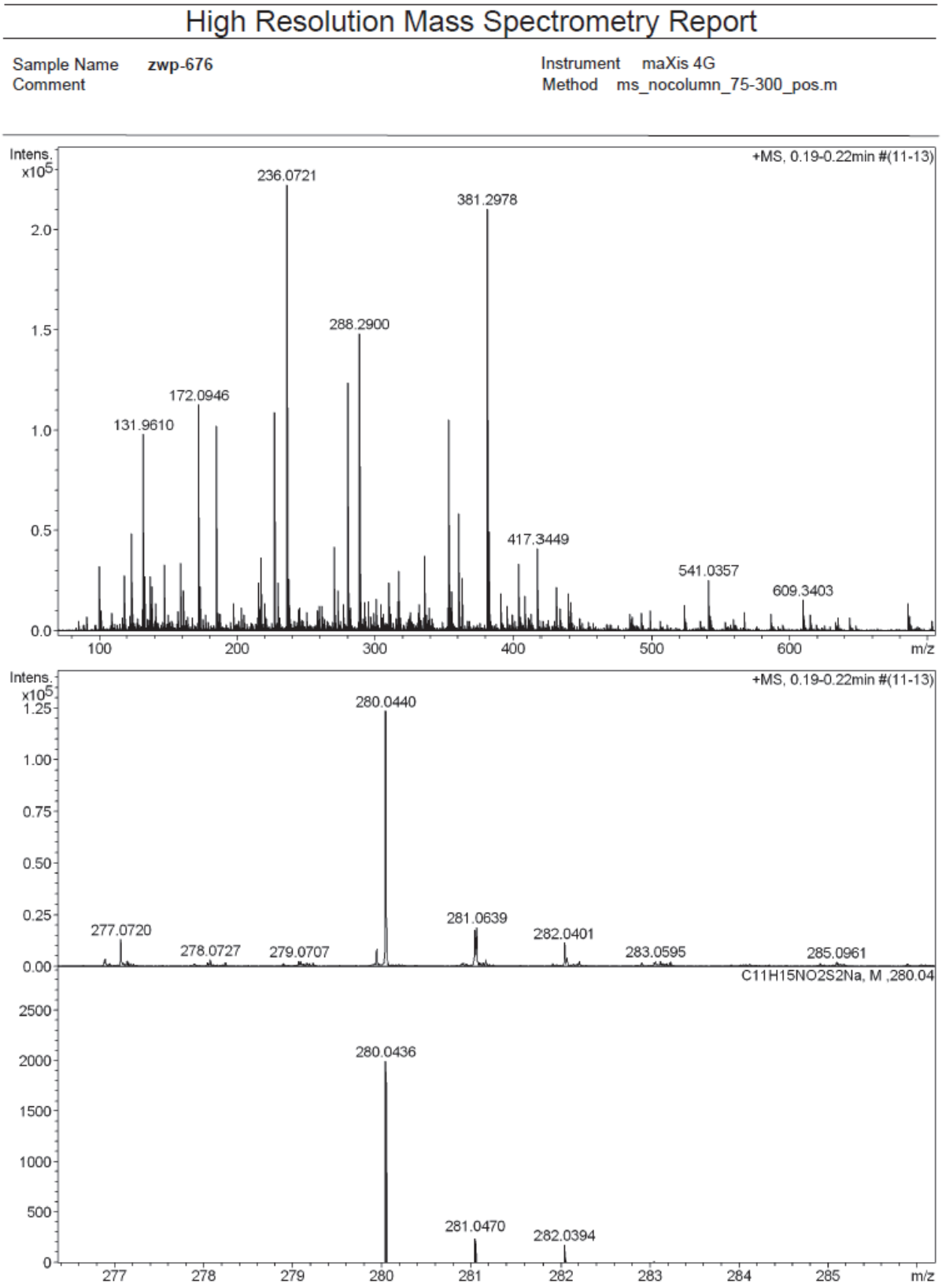

High Resolution Mass Spectrometry Report

Measured m/z vs. theoretical m/z

Meas. m/z	#	Formula	Score	m/z	err [mDa]	err [ppm]	mSigma	rdb	e⁻ Conf	z
280.0440	1	C 11 H 15 N Na O 2 S 2	100.00	280.0436	-0.4	-1.4	5.6	4.5	even	1+

Mass list

#	m/z	I %	I
1	99.9337	14.5	32344
2	101.0070	4.6	10193
3	109.0749	4.0	8881
4	117.9449	12.4	27691
5	123.0910	21.9	48759
6	124.0749	7.6	16863
7	130.9643	4.9	10965
8	131.9506	4.6	10158
9	131.9610	44.1	98204
10	132.9579	12.2	27223
11	133.0755	5.3	11762
12	137.1070	12.2	27159
13	138.0909	10.1	22390
14	140.9610	6.2	13817
15	141.0022	4.3	9468
16	147.0915	14.8	32950
17	157.0971	4.5	10035
18	158.9641	15.3	33950
19	161.1073	9.0	19999
20	172.0946	50.8	113130
21	173.0609	5.0	11167
22	173.0785	10.0	22232
23	185.1150	45.9	102238
24	186.1182	4.1	9212
25	187.1228	3.9	8655
26	197.0221	6.3	14085
27	203.1038	5.2	11547
28	215.1257	10.8	24030
29	216.9229	4.9	10828
30	217.1050	16.5	36792
31	220.1675	6.2	13768
32	226.9520	49.1	109332
33	227.1078	8.5	18885
34	229.8935	10.9	24273
35	236.0721	100.0	222590
36	237.0749	11.7	26076
37	238.0684	5.3	11766
38	244.2638	4.9	10854
39	244.8691	5.2	11522
40	245.1005	5.0	11154
41	250.1781	4.3	9522
42	258.0616	4.6	10307
43	259.1334	5.7	12755
44	261.1312	5.7	12606
45	270.2429	18.9	42128
46	273.1673	9.1	20361
47	277.0720	6.1	13486
48	279.9461	4.0	8964
49	280.0440	55.6	123807
50	281.0467	8.0	17758
51	281.0639	8.7	19344
52	282.0401	5.3	11715
53	288.2900	66.7	148487
54	288.9222	7.2	16050
55	289.2933	12.8	28545
56	292.2247	6.5	14398
57	294.9205	4.7	10503
58	294.9389	6.6	14740
59	299.1620	4.1	9215
60	301.1411	7.3	16175
61	303.8977	6.1	13467
62	304.2845	4.8	10594

High Resolution Mass Spectrometry Report

#	m/z	I %	I
63	310.2354	5.2	11673
64	310.2717	10.9	24165
65	311.2557	4.0	8823
66	316.3211	6.8	15044
67	317.1725	13.5	30114
68	325.2347	4.3	9477
69	331.1880	4.1	9095
70	332.2920	6.2	13703
71	336.2145	16.9	37572
72	339.1545	5.2	11653
73	353.1034	5.3	11795
74	353.1454	13.3	29583
75	353.2663	47.5	105711
76	354.2694	10.4	23257
77	355.2813	8.9	19890
78	360.3236	26.2	58423
79	361.3266	6.6	14676
80	362.9264	11.8	26280
81	381.2978	94.6	210664
82	382.0938	16.2	36054
83	382.3008	22.4	49913
84	391.2092	8.5	19023
85	395.3628	5.6	12538
86	404.0417	15.1	33716
87	408.3083	7.9	17637
88	417.3449	18.6	41379
89	418.3481	5.0	11185
90	430.9137	9.9	22027
91	433.0316	5.0	11118
92	438.9848	8.5	18894
93	441.2969	6.4	14229
94	492.4022	4.0	8879
95	498.9012	4.7	10472
96	523.3239	5.9	13154
97	541.0357	11.5	25674
98	566.8894	4.3	9580
99	609.3403	7.1	15695
100	685.4379	6.3	14060

Acquisition Parameter

General	Fore Vacuum	2.47e+000 mBar	High Vacuum	1.26e-007 mBar	Source Type	ESI
	Scan Begin	75 m/z	Scan End	700 m/z	Ion Polarity	Positive
Source	Set Nebulizer	2.0 Bar	Set Capillary	4500 V	Set Dry Gas	8.0 l/min
	Set Dry Heater	200 °C	Set End Plate Offset	-500 V		
Quadrupole	Set Ion Energy (MS only)	4.0 eV				
Coll. Cell	Collision Energy	8.0 eV	Set Collision Cell RF	350.0 Vpp		
Ion Cooler	Set Ion Cooler Transfer Time	55.0 µs	Set Ion Cooler Pre Pulse Storage Time	7.0 µs		

^{1}H-NMR spectrum of pentyl *p*-methoxyphenyl disulfide $CDCl_3$ immediately after column chromatography.

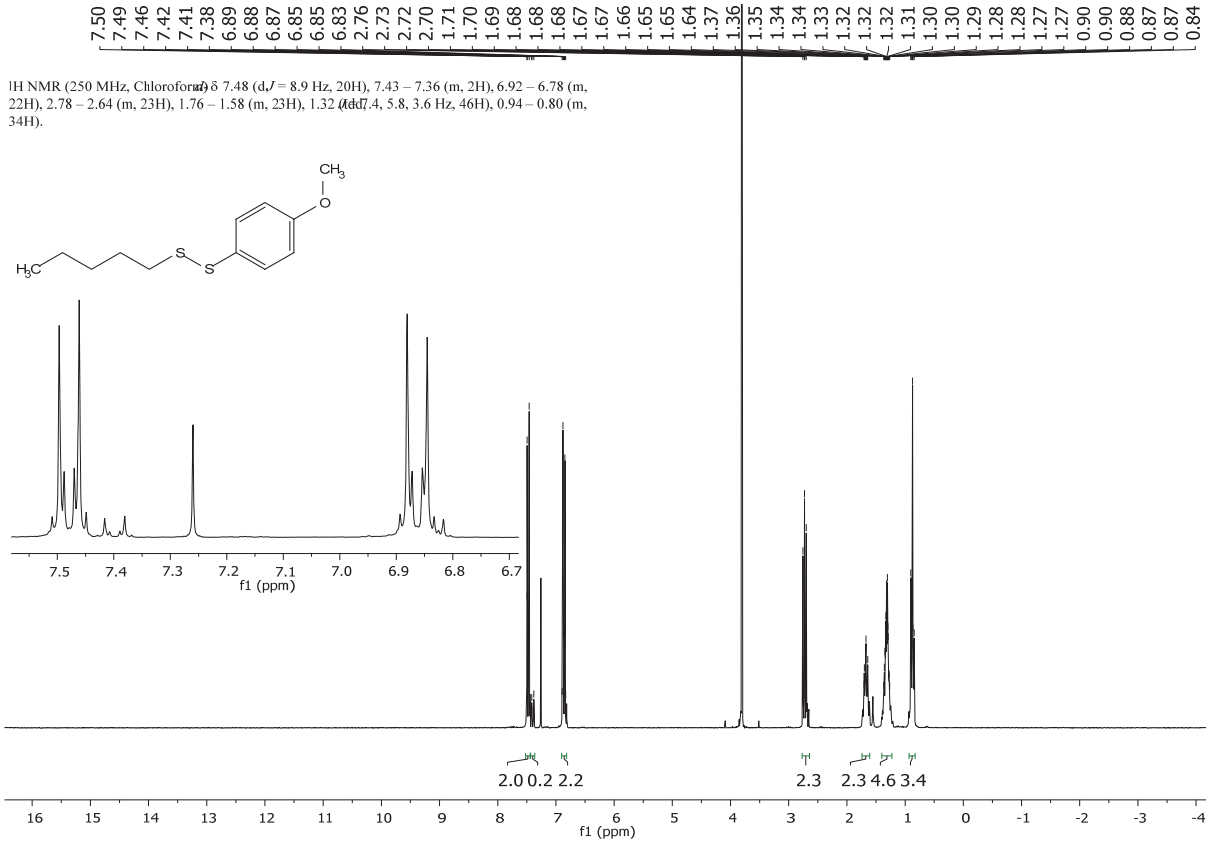

Stacked ^{1}H-NMR spectra of pentyl *p*-methoxyphenyl disulfide in $CDCl_3$ after 4 hours (middle spectrum) and 15 hours (lower spectrum) compared to the first measurement (upper spectrum).

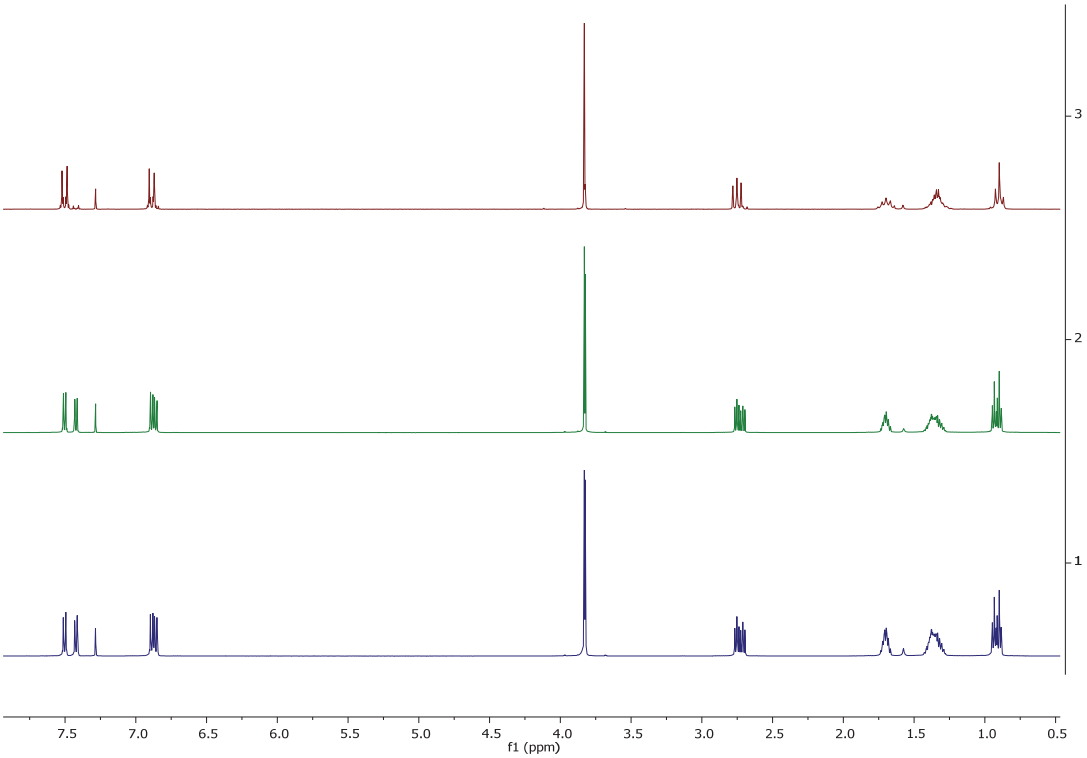

HR-ESI-MS spectrum of pentyl *p*-methoxyphenyl disulfide.

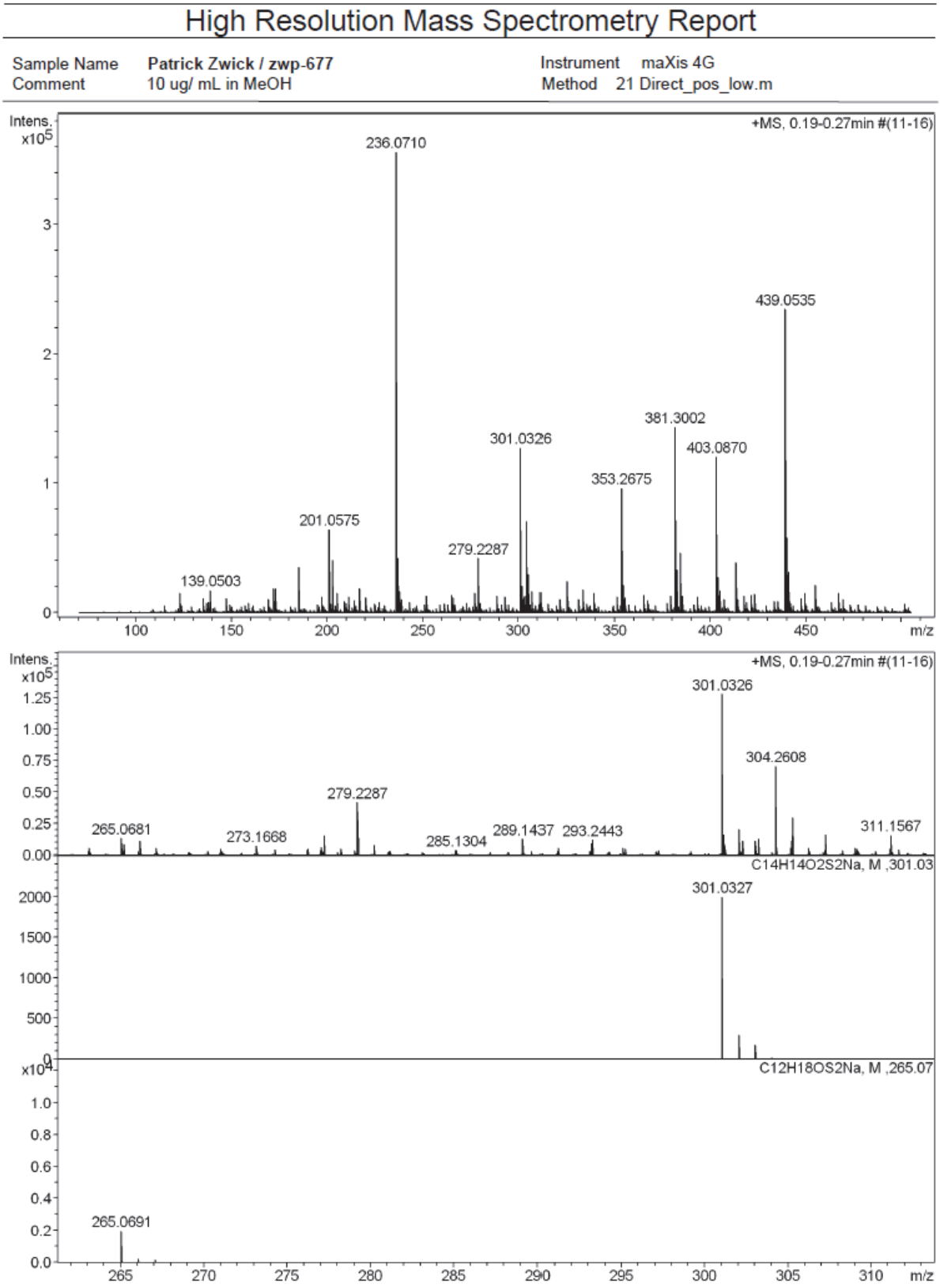

High Resolution Mass Spectrometry Report

Measured m/z vs. theoretical m/z

Meas. m/z	#	Formula	Score	m/z	err [mDa]	err [ppm]	mSigma	rdb	e⁻ Conf	z
265.0681	1	C 12 H 18 Na O S 2	100.00	265.0691	1.0	3.7	28.5	3.5	even	1+
301.0326	1	C 14 H 14 Na O 2 S 2	100.00	301.0327	0.2	0.5	8.1	7.5	even	

Mass list

#	m/z	I %	I
1	123.0919	4.2	15145
2	135.0029	3.2	11377
3	137.1073	2.1	7589
4	138.0914	2.4	8642
5	139.0213	4.2	14886
6	139.0503	5.0	17693
7	147.0916	3.1	10886
8	158.9638	2.1	7363
9	169.0469	3.0	10619
10	172.0941	5.2	18652
11	173.0782	5.2	18574
12	185.1143	10.0	35567
13	197.0778	3.6	12708
14	201.0575	18.2	64700
15	202.0606	2.0	7125
16	203.0524	3.8	13496
17	203.1036	11.4	40767
18	205.0604	4.1	14657
19	209.0236	2.6	9337
20	210.1095	2.1	7578
21	211.0934	3.4	12229
22	214.0886	2.7	9644
23	217.1040	5.2	18423
24	220.1665	3.4	12043
25	227.1246	2.4	8628
26	236.0710	100.0	356423
27	237.0738	11.8	42020
28	238.0671	4.6	16511
29	239.0883	2.9	10431
30	243.0833	2.3	8354
31	252.0444	3.7	13203
32	261.1293	2.1	7336
33	265.0681	3.8	13672
34	265.2133	2.6	9168
35	266.1719	3.4	11982
36	273.1668	2.1	7594
37	277.2131	4.4	15646
38	279.2287	11.8	41984
39	280.2319	2.2	7893
40	289.1437	3.6	12978
41	293.2081	2.7	9536
42	293.2443	3.4	12249
43	301.0326	35.8	127664
44	301.1407	4.7	16744
45	301.2111	2.0	7157
46	302.0355	5.8	20715
47	302.2450	3.2	11380
48	303.0289	3.3	11781
49	303.2292	3.8	13412
50	304.2608	19.8	70729
51	305.2449	8.4	29885
52	305.2630	4.3	15212
53	307.2605	4.6	16554
54	311.1567	4.6	16221
55	321.2399	2.8	10136
56	325.1083	6.8	24251
57	325.2350	2.8	10015
58	331.1881	3.0	10541
59	333.1705	5.0	17998
60	335.1368	2.0	7102
61	339.1784	4.3	15368

High Resolution Mass Spectrometry Report

#	m/z	I %	I
62	351.2515	3.5	12514
63	353.2312	2.1	7545
64	353.2675	27.1	96593
65	354.2707	6.1	21719
66	355.1854	3.3	11623
67	365.1072	4.0	14157
68	365.2725	3.1	11225
69	367.2109	2.8	10103
70	377.1990	2.1	7533
71	379.1965	2.9	10408
72	379.2841	3.7	13316
73	381.3002	40.2	143458
74	382.3035	9.4	33642
75	384.2461	13.1	46696
76	385.2495	3.8	13480
77	393.3015	3.6	12676
78	403.0870	33.9	120728
79	404.0900	7.7	27552
80	405.0839	4.8	17260
81	407.3174	3.0	10544
82	413.2707	11.0	39160
83	414.2740	2.9	10452
84	417.3500	3.7	13149
85	419.0619	2.3	8072
86	421.3342	3.8	13690
87	423.2253	4.1	14549
88	433.3860	2.5	8806
89	435.3505	2.5	9002
90	439.0535	65.9	234740
91	440.0565	16.4	58518
92	441.0506	9.0	31969
93	441.3040	2.7	9649
94	442.0527	2.1	7520
95	447.3515	3.0	10849
96	449.3787	4.3	15151
97	455.0284	6.0	21485
98	463.3840	2.3	8268
99	467.2552	4.2	15005
100	469.3375	2.9	10195

Acquisition Parameter

General	Fore Vacuum	2.69e+000 mBar	High Vacuum	1.27e-007 mBar	Source Type	ESI
	Scan Begin	75 m/z	Scan End	500 m/z	Ion Polarity	Positive
Source	Set Nebulizer	0.4 Bar	Set Capillary	3600 V	Set Dry Gas	3.0 l/min
	Set Dry Heater	180 °C	Set End Plate Offset	-500 V		
Quadrupole	Set Ion Energy (MS only)	4.0 eV				
Coll. Cell	Collision Energy	8.0 eV	Set Collision Cell RF	350.0 Vpp		
Ion Cooler	Set Ion Cooler Transfer Time	40.0 µs	Set Ion Cooler Pre Pulse Storage Time	5.0 µs		

^{1}H-NMR spectrum of *p*-aminophenyl hexyl disulfide in $CDCl_3$.

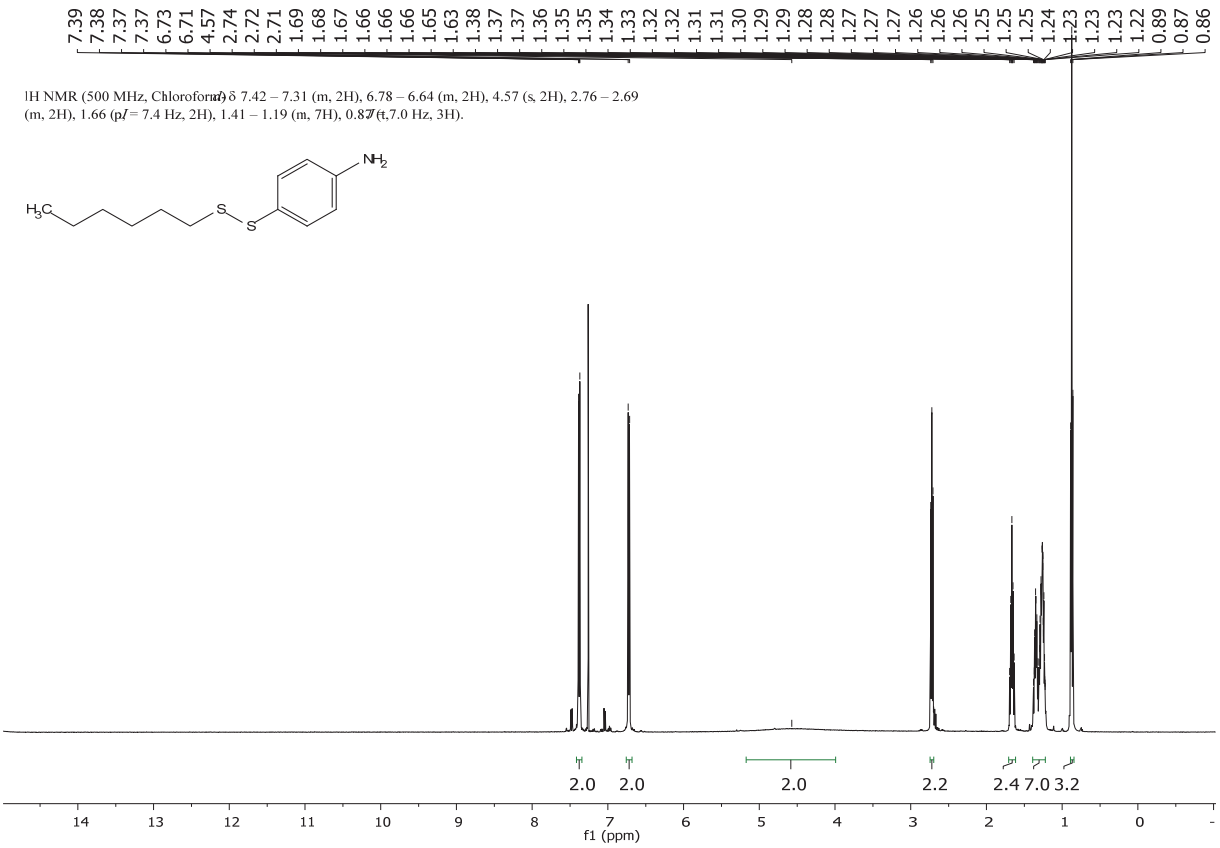

^{13}C{^{1}H}-NMR spectrum of *p*-aminophenyl hexyl disulfide in $CDCl_3$.

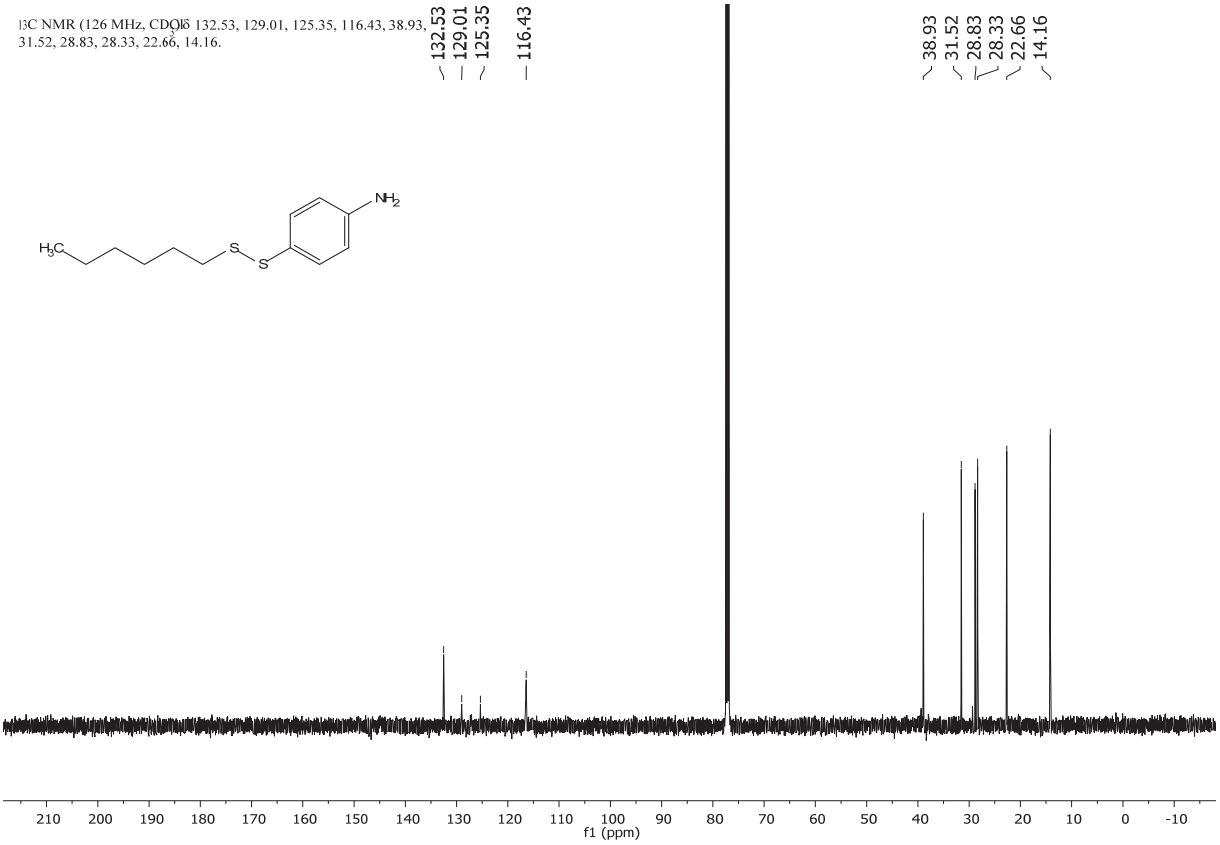

HR-ESI-MS spectrum of *p*-aminophenyl hexyl disulfide.

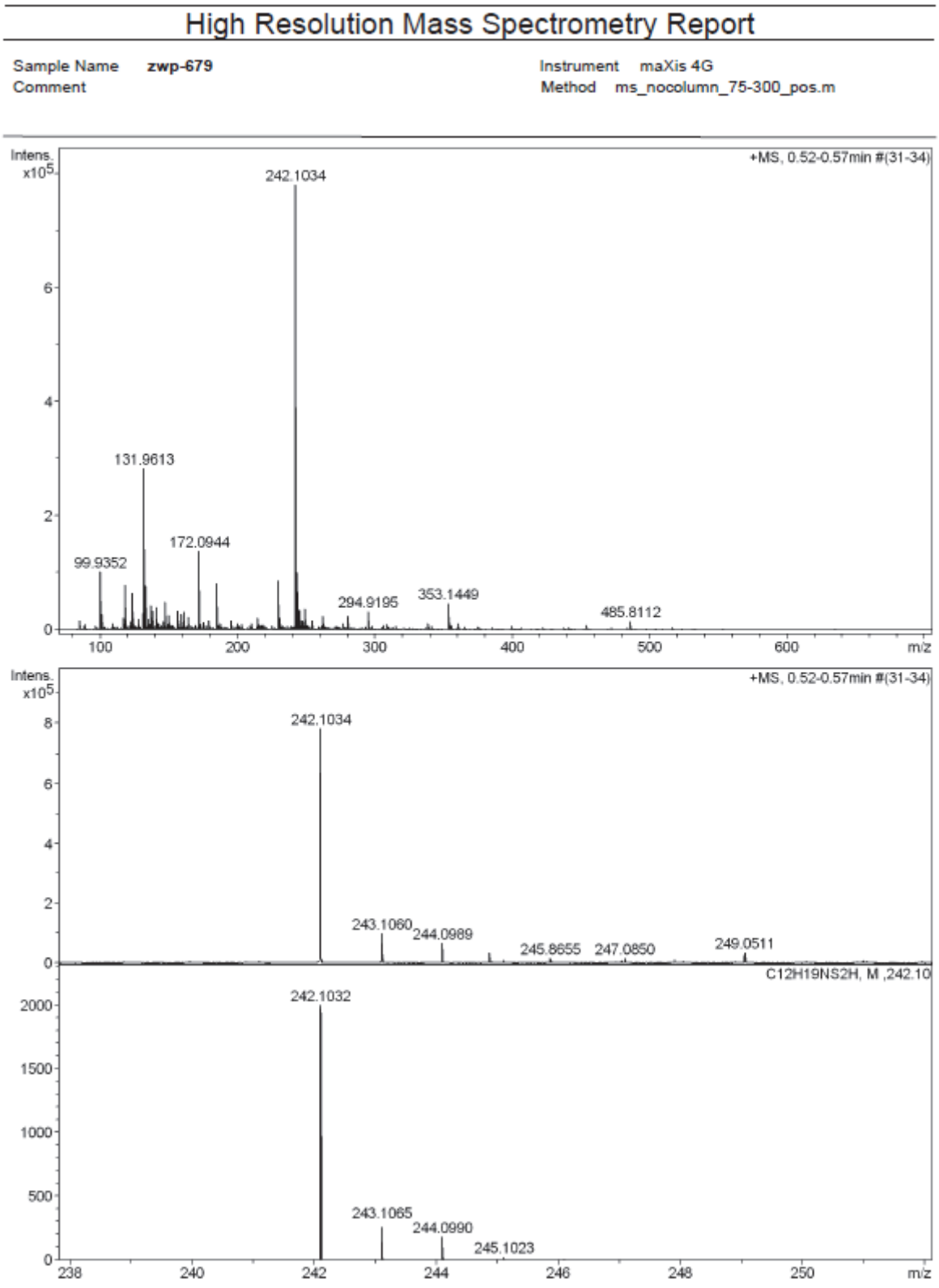

High Resolution Mass Spectrometry Report

Measured m/z vs. theoretical m/z

Meas. m/z	#	Formula	Score	m/z	err [mDa]	err [ppm]	mSigma	rdb	e¯ Conf	z
242.1034	1	C 12 H 20 N S 2	100.00	242.1032	-0.3	-1.2	13.3	3.5	even	1+

Mass list

#	m/z	I %	I
1	84.9598	2.0	15799
2	88.9687	1.2	9324
3	99.9352	13.0	101996
4	100.9321	1.0	7733
5	101.0084	3.5	27524
6	109.0760	1.4	11149
7	116.9857	2.6	20094
8	117.9457	10.1	78597
9	118.9427	1.4	11336
10	119.0189	2.3	18144
11	121.9325	1.9	14684
12	122.0963	1.4	11251
13	123.0032	2.2	17267
14	123.0916	8.3	65238
15	124.0756	2.7	20729
16	127.9415	2.4	19011
17	130.9648	3.7	29074
18	131.9508	4.0	31132
19	131.9613	36.2	283347
20	132.9026	1.0	7547
21	132.9583	9.8	76783
22	133.0343	1.0	7616
23	133.0758	2.2	16831
24	134.9584	2.5	19561
25	136.1120	1.2	9706
26	136.9539	1.1	8891
27	137.1073	5.4	42591
28	138.0912	4.2	32904
29	140.9613	5.1	39721
30	141.0024	3.7	29248
31	141.0119	1.0	7779
32	141.9585	1.4	10612
33	142.9493	1.4	10990
34	144.9481	1.0	7728
35	145.9405	1.8	14154
36	147.0915	6.3	49020
37	149.0026	1.3	9833
38	149.9609	2.0	15657
39	149.9717	3.2	25072
40	150.9687	0.9	7392
41	151.1228	1.0	7711
42	152.1066	1.0	7841
43	155.9934	4.3	33593
44	156.9999	1.0	7855
45	157.0969	1.4	11292
46	159.0130	3.5	27624
47	161.1072	4.0	31509
48	163.9765	2.8	21531
49	169.1405	1.0	7592
50	171.9922	1.0	7865
51	172.0944	17.6	137621
52	173.0980	1.3	9920
53	174.9912	1.7	13528
54	175.1223	1.2	9117
55	177.0068	1.0	7651
56	178.9956	2.0	15859
57	184.9737	1.1	8930
58	185.1146	10.5	82402
59	186.0078	1.1	8278
60	186.1177	1.1	8301
61	187.1226	1.5	12047
62	194.9727	2.0	15525

High Resolution Mass Spectrometry Report

#	m/z	I %	I
63	199.9485	1.5	11894
64	203.0588	1.2	9024
65	209.9482	1.5	11697
66	214.9172	2.7	21346
67	216.0712	1.0	8172
68	216.9792	0.9	7331
69	217.0781	1.0	7575
70	218.0344	1.0	7575
71	219.0538	1.1	8528
72	229.8929	11.1	86583
73	230.8902	2.7	21186
74	231.0538	1.0	8033
75	242.1034	100.0	781803
76	243.1060	12.8	100299
77	244.0989	8.5	66312
78	244.8683	4.5	35300
79	245.1016	1.3	10452
80	245.8655	2.0	15402
81	247.0353	1.1	8550
82	247.0850	2.1	16173
83	247.9037	1.8	14446
84	249.0511	4.6	35631
85	250.9920	1.1	8242
86	254.1029	2.1	16295
87	261.9083	3.0	23336
88	262.8787	1.5	11886
89	276.8928	1.5	11356
90	279.9454	3.1	24526
91	294.9195	4.1	31944
92	305.8980	1.1	8531
93	308.8989	1.2	9129
94	338.3410	1.4	11126
95	353.1449	5.9	46462
96	354.1482	1.7	13268
97	355.2811	1.1	8526
98	360.3231	1.5	11501
99	453.7848	1.0	8198
100	485.8112	1.9	14713

Acquisition Parameter

General	Fore Vacuum	2.60e+000 mBar	High Vacuum	1.26e-007 mBar	Source Type	ESI
	Scan Begin	75 m/z	Scan End	700 m/z	Ion Polarity	Positive
Source	Set Nebulizer	2.0 Bar	Set Capillary	4500 V	Set Dry Gas	8.0 l/min
	Set Dry Heater	200 °C	Set End Plate Offset	-500 V		
Quadrupole	Set Ion Energy (MS only)	4.0 eV				
Coll. Cell	Collision Energy	8.0 eV	Set Collision Cell RF	350.0 Vpp		
Ion Cooler	Set Ion Cooler Transfer Time	55.0 µs	Set Ion Cooler Pre Pulse Storage Time	7.0 µs		

^{1}H-NMR ($CDCl_3$, 500 MHz, 298 K) and ^{13}C-NMR ($CDCl_3$, 126 MHz, 298 K) of Methyl 2-(hexyldisulfaneyl)benzoate.

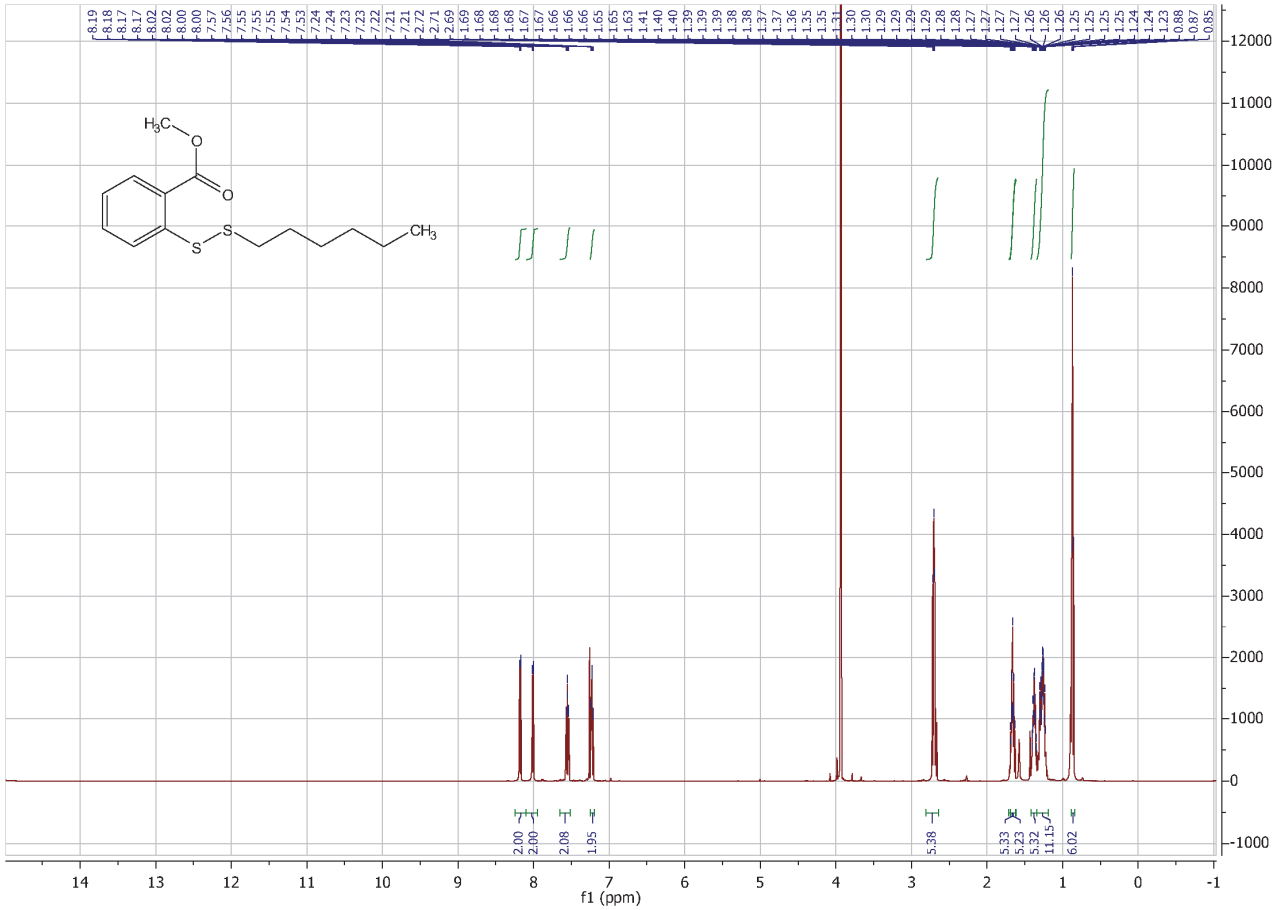

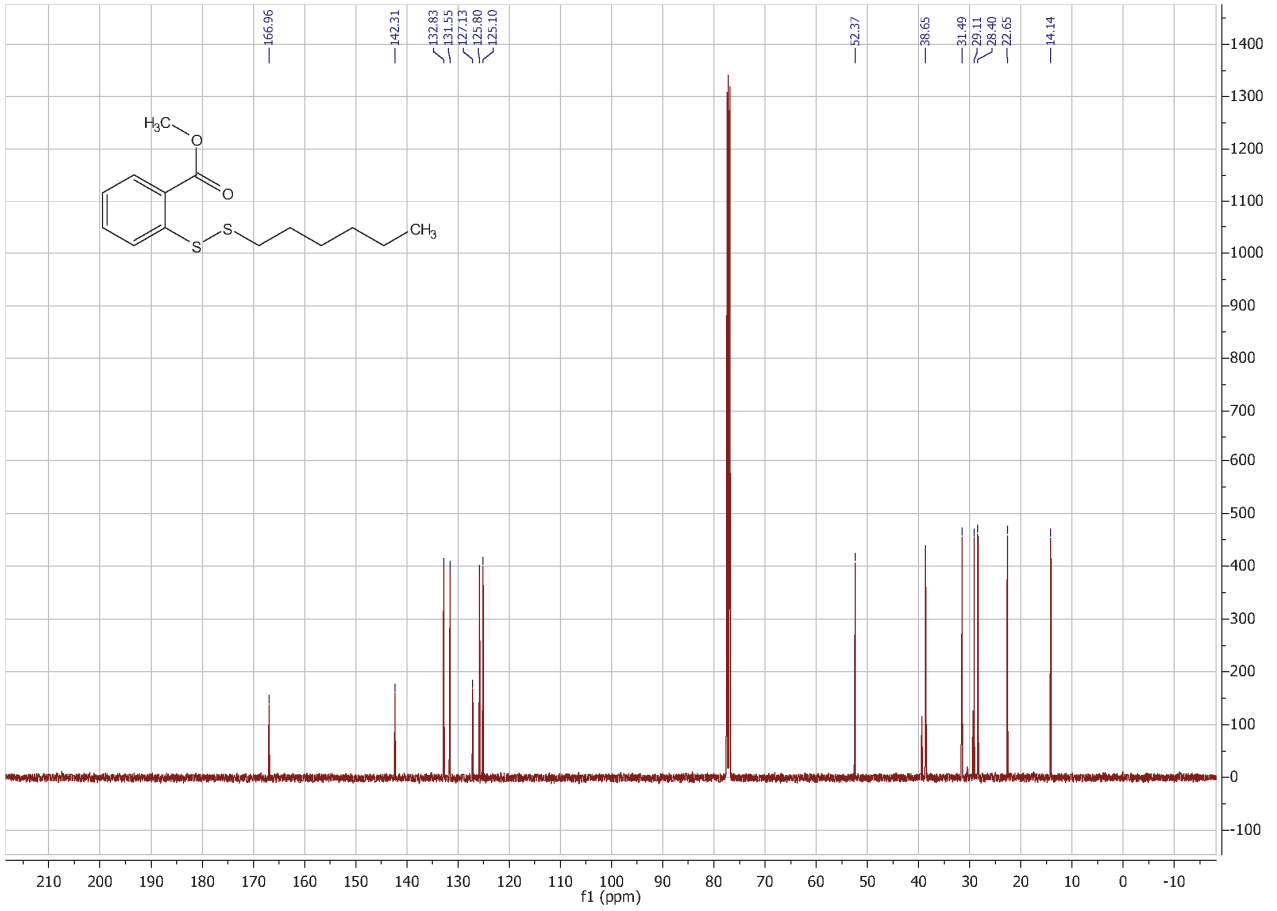

HR-ESI MS spectra of Methyl 2-(hexyldisulfaneyl)benzoate.

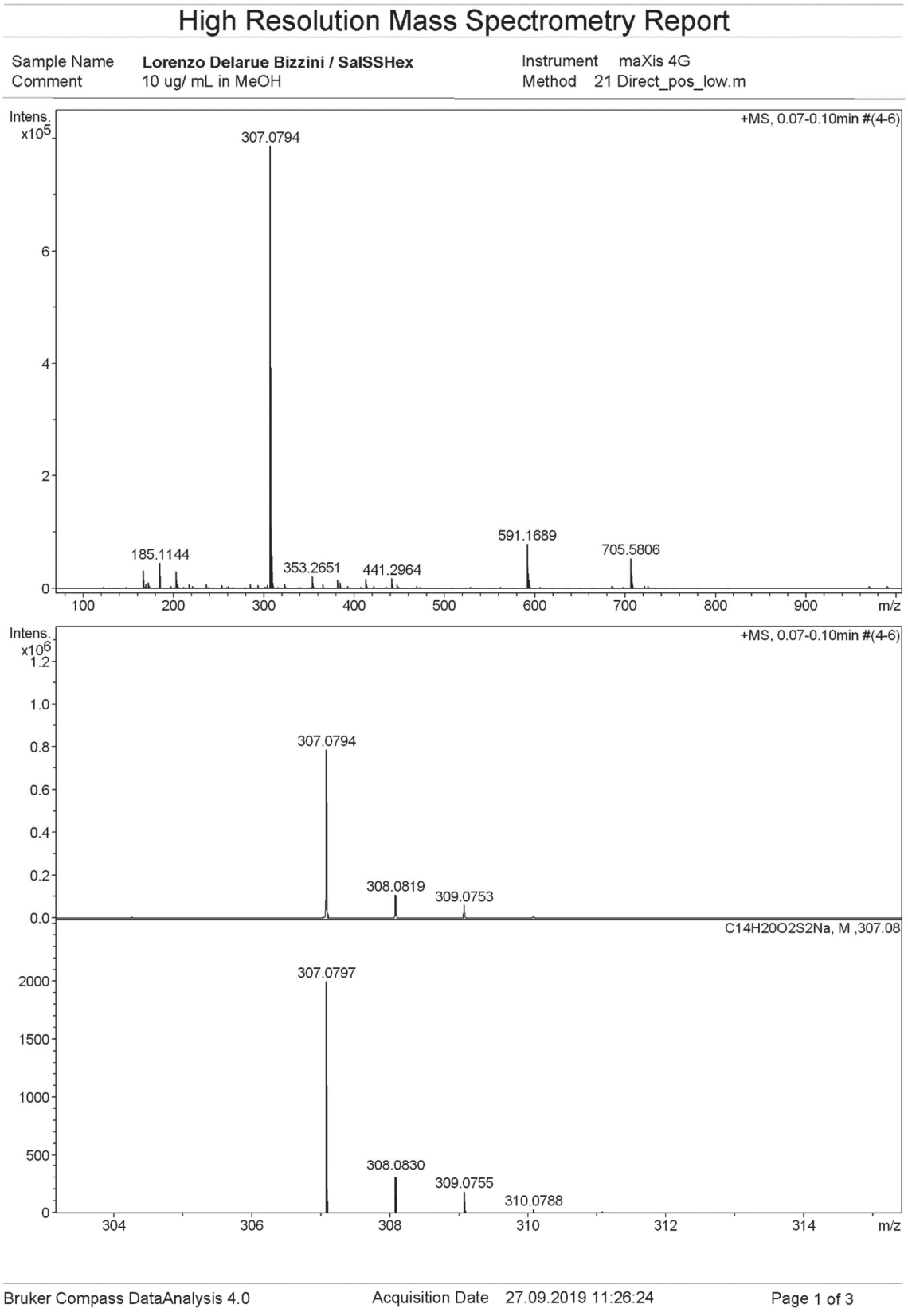

High Resolution Mass Spectrometry Report

Measured m/z vs. theoretical m/z

Meas. m/z	#	Formula	Score	m/z	err [mDa]	err [ppm]	mSigma	rdb	e⁻ Conf	z
307.0794	1	C 14 H 20 Na O 2 S 2	100.00	307.0797	0.3	1.0	21.3	4.5	even	1+

Mass list

#	m/z	I %	I
1	123.0924	0.5	3797
2	137.1070	0.3	2405
3	138.0915	0.3	2251
4	147.0916	0.4	2981
5	151.9924	0.3	2349
6	167.0159	4.1	32406
7	168.0191	0.4	3121
8	168.9772	1.1	8286
9	169.0468	0.5	4312
10	172.0941	1.4	10640
11	173.0779	0.7	5212
12	185.1144	5.8	45462
13	186.1178	0.5	3689
14	197.0778	0.6	4817
15	201.1019	0.4	3218
16	203.0520	3.9	30390
17	205.0622	0.7	5547
18	211.0933	0.4	3120
19	217.1037	1.0	7607
20	221.0238	0.6	4675
21	225.1087	0.3	2405
22	236.0708	1.0	8150
23	239.0880	0.4	3382
24	253.0704	0.7	5620
25	259.1293	0.4	3335
26	261.1296	0.5	4322
27	265.1763	0.3	2295
28	266.1726	0.3	2634
29	273.1666	0.3	2328
30	279.1918	0.3	2356
31	279.2291	0.5	3618
32	285.0964	0.9	7421
33	293.2075	0.7	5762
34	301.1404	0.5	3661
35	302.1234	0.5	3561
36	304.2599	0.9	6948
37	305.1557	0.3	2221
38	307.0794	100.0	787422
39	307.1862	0.3	2175
40	307.2234	0.4	2971
41	308.0819	13.9	109560
42	309.0753	7.6	59653
43	310.0779	1.3	10429
44	315.1911	0.4	3030
45	321.0943	0.3	2139
46	323.0527	0.9	7309
47	325.1612	0.3	2197
48	339.1769	0.4	3145
49	341.2658	0.3	2139
50	353.1440	0.4	2951
51	353.2651	2.7	21589
52	354.2685	0.6	4586
53	357.0210	0.3	2253
54	365.1046	1.1	8364
55	365.2666	0.3	2191
56	367.2081	0.3	2233
57	381.2966	2.0	15946
58	382.2998	0.5	3825
59	384.2422	1.4	10957
60	385.2455	0.5	3598
61	385.2912	0.3	2278
62	393.2966	0.6	4998

High Resolution Mass Spectrometry Report

#	m/z	I %	I
63	395.2752	0.3	2265
64	407.3120	0.3	2591
65	413.2651	2.1	16481
66	414.2682	0.7	5314
67	421.3279	0.5	4178
68	429.3181	0.3	2359
69	435.3434	0.3	2728
70	441.2964	2.3	18499
71	442.2998	0.7	5684
72	447.3436	1.0	7534
73	448.3466	0.3	2181
74	449.3605	0.4	3304
75	463.3734	0.3	2227
76	469.3278	0.6	4734
77	473.3441	0.4	2880
78	481.3119	0.3	2262
79	506.5274	0.3	2329
80	517.3701	0.3	2194
81	528.5100	0.4	3500
82	561.3953	0.3	2593
83	591.1689	10.1	79249
84	592.1721	3.5	27952
85	593.1662	2.0	15773
86	594.1689	0.7	5335
87	605.4218	0.3	2552
88	649.4483	0.3	2283
89	685.4336	0.5	4024
90	697.3553	0.4	2918
91	705.5806	6.8	53788
92	706.5839	3.2	24821
93	707.5844	0.9	7324
94	708.5837	0.3	2436
95	721.5746	0.5	4278
96	725.3861	0.5	4289
97	969.5218	0.5	4087
98	970.5264	0.3	2645
99	989.6695	0.6	4377
100	990.6713	0.4	2908

Acquisition Parameter

General	Fore Vacuum	2.69e+000 mBar	High Vacuum	1.26e-007 mBar	Source Type	ESI
	Scan Begin	75 m/z	Scan End	1000 m/z	Ion Polarity	Positive
Source	Set Nebulizer	0.4 Bar	Set Capillary	3600 V	Set Dry Gas	3.0 l/min
	Set Dry Heater	180 °C	Set End Plate Offset	-500 V		
Quadrupole	Set Ion Energy (MS only)	4.0 eV				
Coll. Cell	Collision Energy	8.0 eV	Set Collision Cell RF	350.0 Vpp		
Ion Cooler	Set Ion Cooler Transfer Time	55.0 µs	Set Ion Cooler Pre Pulse Storage Time	7.0 µs		

^{1}H-NMR ($CDCl_3$, 500 MHz, 298 K) and ^{13}C-NMR ($CDCl_3$, 126 MHz, 298 K) of 3,5 Difluorophenyl methyl sulfenate.

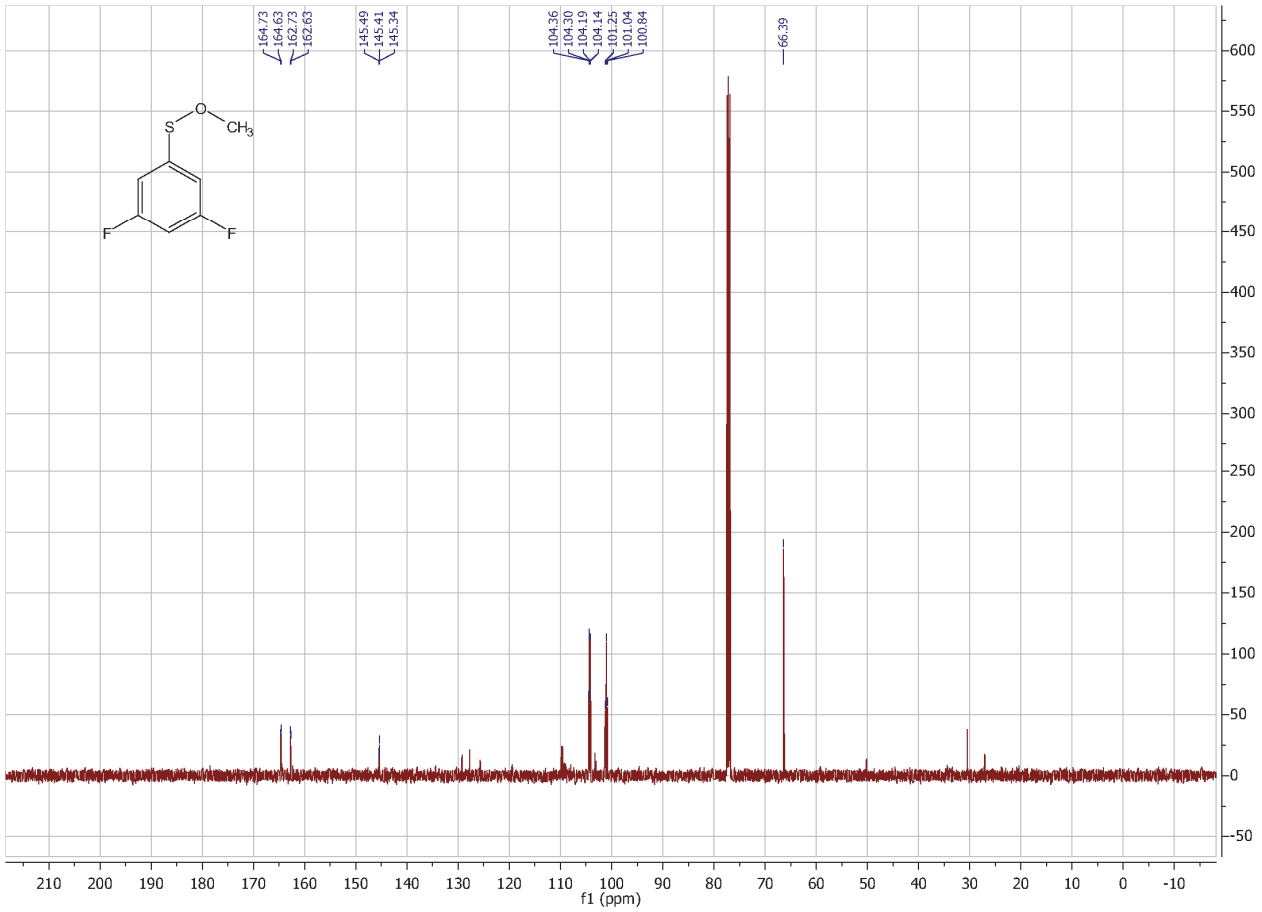

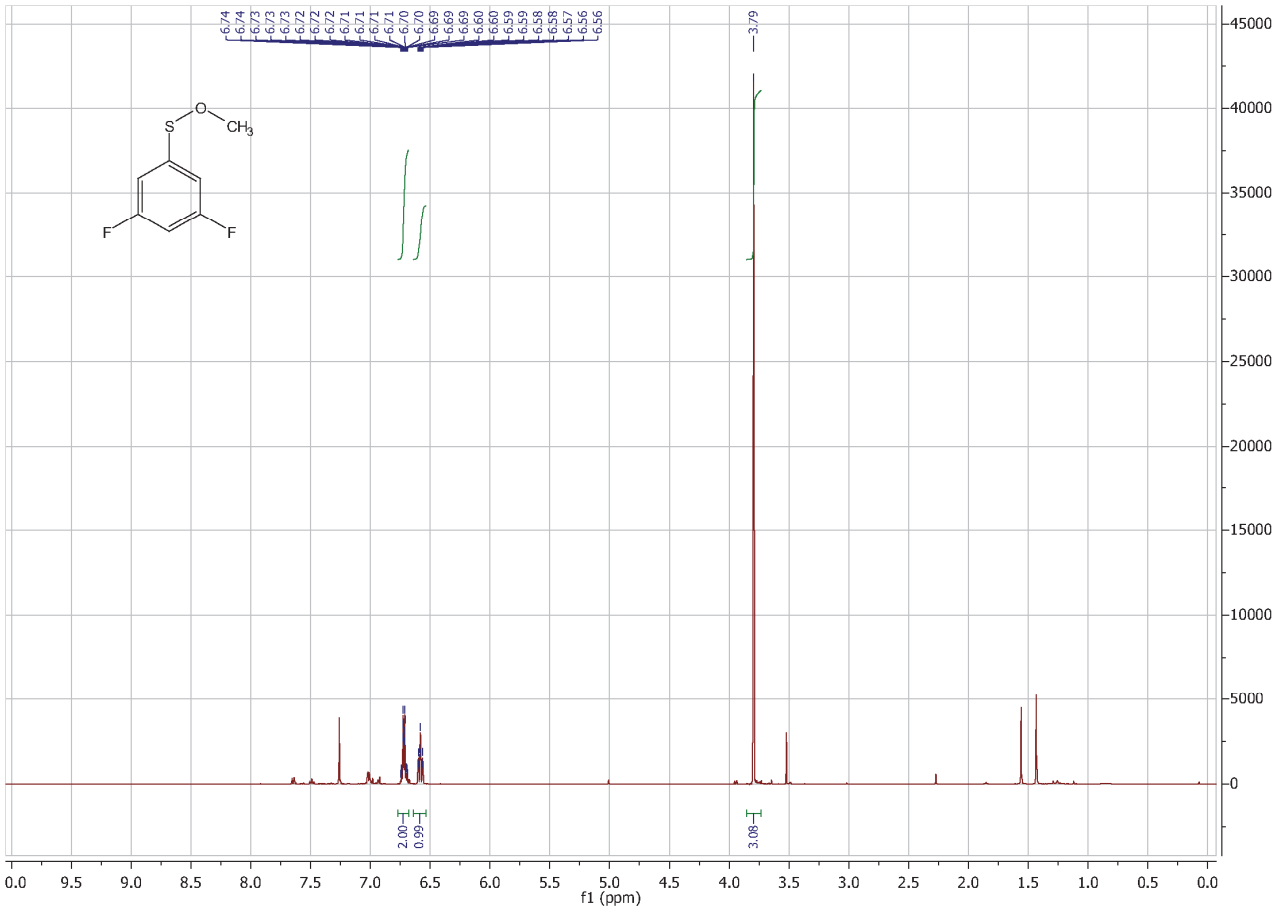

^{1}H-NMR (CD_2Cl_2, 500 MHz, 298 K) and ^{13}C-NMR (CD_2Cl_2, 126 MHz, 298 K) of 1*H*,1*H*,2*H,*2*H*-perfluorodecyl *p*-methylphenyl disulfide.

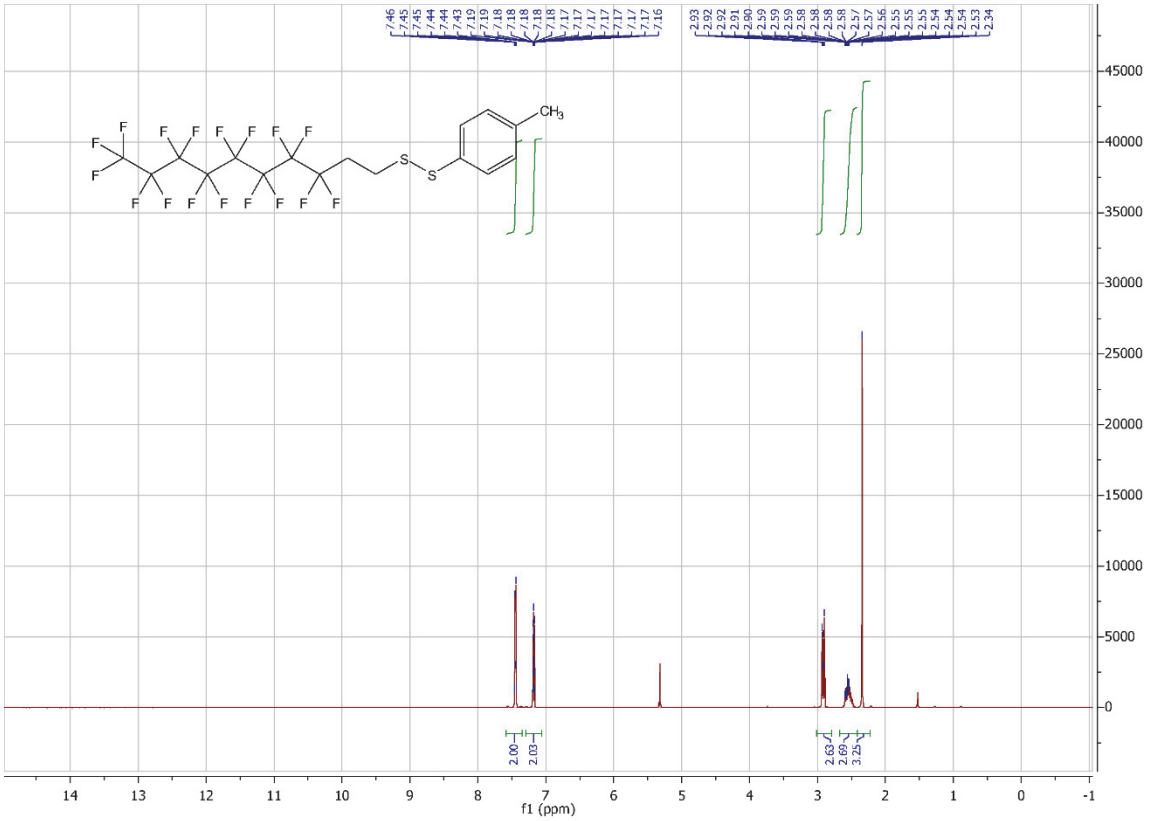

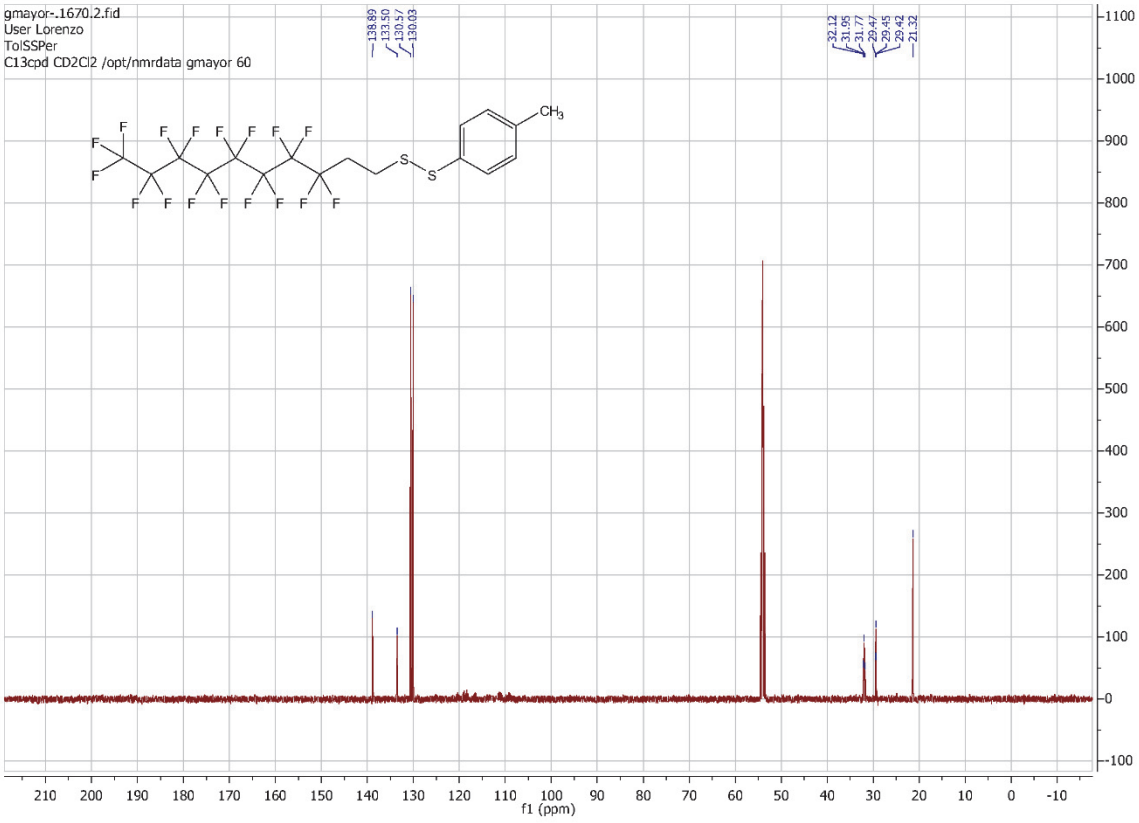

^{19}F-NMR (CD_2Cl_2, 471 MHz, 298 K) of 1*H*,1*H*,2*H*,2*H*-perfluorodecyl *p*-methylphenyl disulfide.

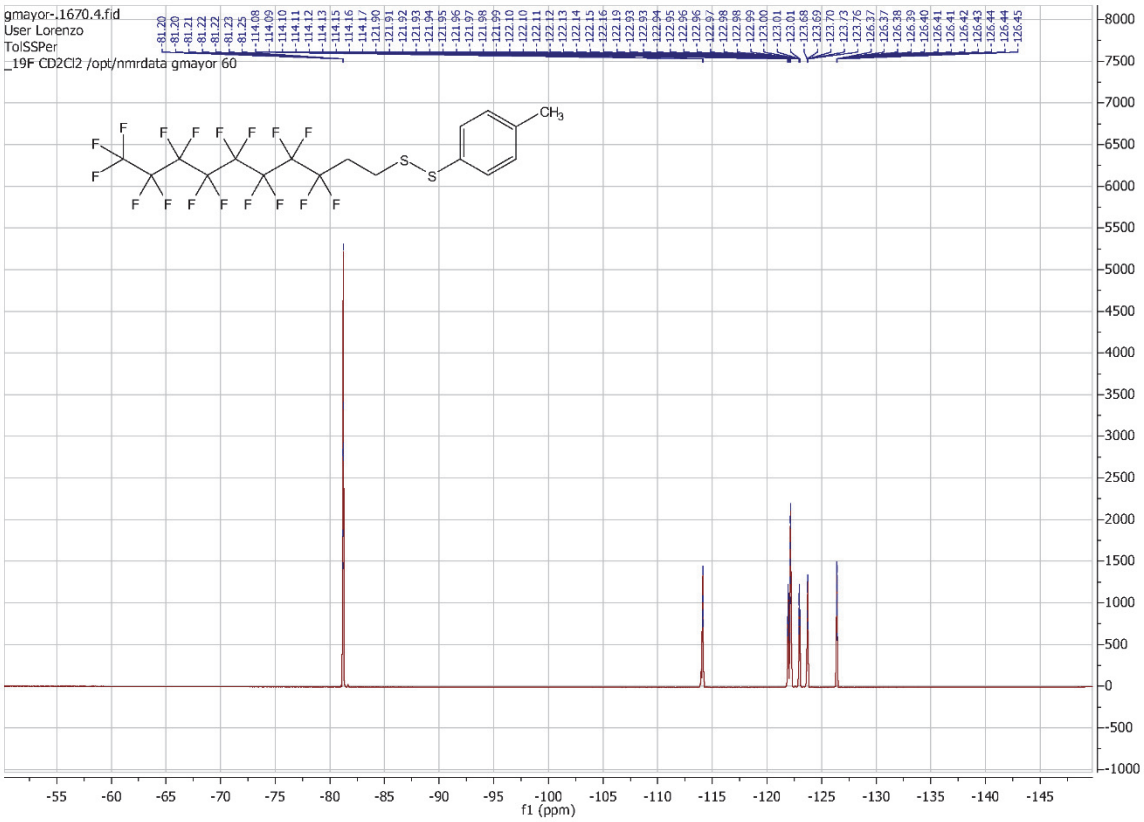

HR-MALDI-TOF MS spectra of 1H,1*H*,2*H*,2*H*-perfluorodecyl *p*-methylphenyl disulfide.

BSOL000570 Patrick Zwick/ - Perfluor-Tol-2 - Acetone - DCTB 1:10

ETH Eidgenössische Technische Hochschule Zürich Swiss Federal Institute of Technology Zurich

Acquisition Parameter

Method:	MALDI_MS_POS_100-1000_2M_16AvScans			Acquisition Date:	14.08.2019 13:15:47
File Name:	D:\ETH\Data\BSOL0005xx\BSOL000570 _0_F10_000002.d			Operator:	
Source	Dual (MALDI/ESI)	Polarity	Positive	Nebulizer Gas	1.0 bar
Broadband Low Mass	77.0 m/z	n/a	n/a	Drying Gas Flow Rate	3.7 L/min
Broadband High Mass	1050.0 m/z	Laser Power	36.4 lp	Capillary	3500.0 V
No. of Cell Fills	1	n/a	n/a	Drying Gas	200.0 °C
Apodization	Full-Sine	Time of Flight to Detector	0.000 sec	Temperature	

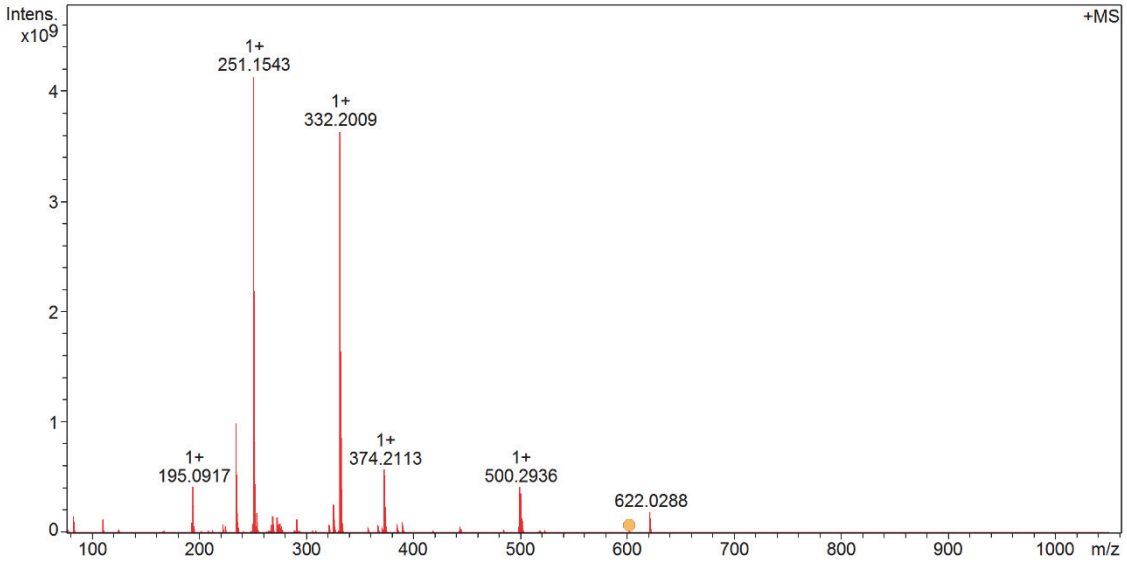

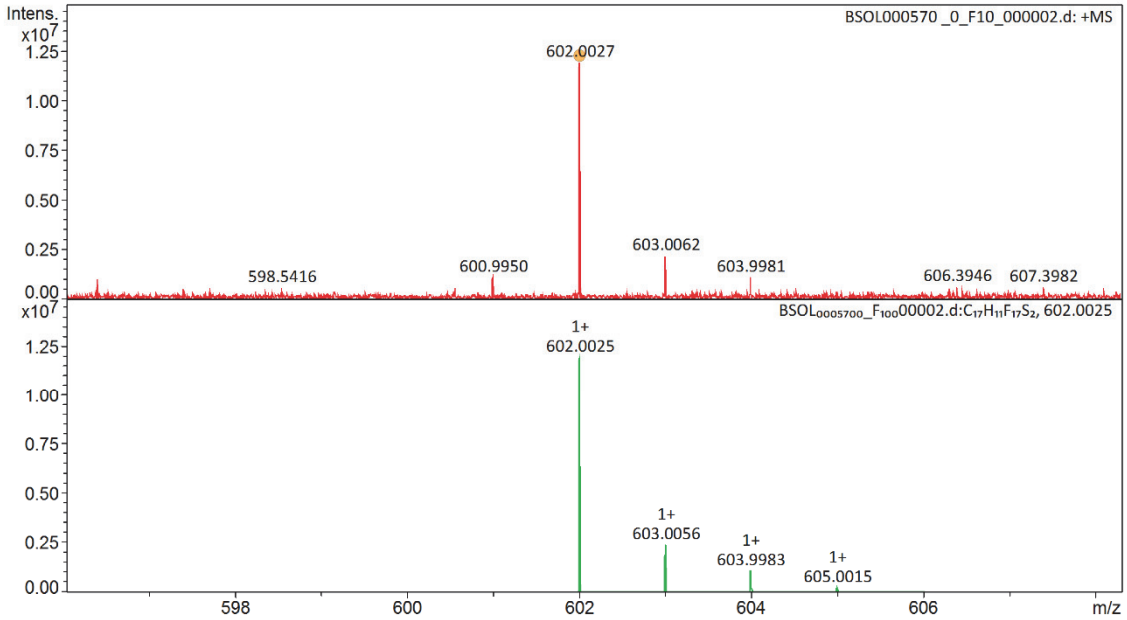

BSOL000570 Patrick Zwick/ - Perfluor-Tol-2 - Acetone - DCTB 1:10

ETH Eidgenössische Technische Hochschule Zürich Swiss Federal Institute of Technology Zurich

Evaluation Spectra / Validation Formula:

#	Ion Formula	Adduct	m/z	z	Meas. m/z	mSigma	N-Rule	err [mDa]	err [ppm]
1	C17H11F17S2	M	602.0025	1+	602.0027	13.9	ok	-0.2	-0.3

Calibration Info:

Date: 14.08.2019 13:16:39
Polarity: Positive
Calibration spectrum: +MS: Scan
Reference mass list: MALDI: DCTB Matrix + HP-Mix (pos)
Calibration mode: Quadratic

Reference m/z	Resulting m/z	Intensity	Error [ppm]
118.0863	118.0863	1200852	0.006
250.1464	250.1464	88443120	-0.133
251.1543	251.1543	4142229760	0.074
273.1362	273.1362	141627680	-0.085
322.0481	322.0482	75719464	0.118
332.2009	332.2009	3646785280	-0.115
500.2934	500.2936	421115712	0.210
501.3013	501.3015	359315296	0.414
523.2832	523.2832	23349624	-0.069
622.0290	622.0288	195417808	-0.252
750.4404	750.4407	3389882	0.393
751.4483	751.4484	7943192	0.202
773.4302			
922.0098	922.0089	5895994	-0.951
1000.5874			
1001.5953			
1023.5772			
1221.9906			
1521.9715			
1821.9523			
2121.9332			
2421.9140			
2721.8948			

Standard deviation: 0.388

Mass List:

#	m/z	Res.	S/N	I %	FWHM
1	194.0839	248208	2059.3	2.2	0.0008
2	195.0917	247940	9237.1	10.1	0.0008
3	196.0951	244327	1408.8	1.5	0.0008
4	223.2056	210875	1205.2	1.4	0.0011
5	225.1387	206533	1365.2	1.6	0.0011
6	235.1230	207469	20013.2	23.9	0.0011
7	236.1263	199474	3606.6	4.3	0.0012
8	236.1308	195274	1069.8	1.3	0.0012
9	237.2213	199953	901.8	1.1	0.0012
10	250.1464	188726	1737.0	2.1	0.0013
11	251.1543	195456	81434.4	100.0	0.0013
12	251.2369	189170	2978.4	3.7	0.0013
13	252.0880	190034	1353.0	1.7	0.0013
14	252.1576	191877	16306.5	20.0	0.0013
15	252.1620	183028	3609.6	4.4	0.0014
16	253.1610	184257	1221.0	1.5	0.0014
17	254.1903	189055	3498.4	4.4	0.0013
18	268.1570	177472	1329.1	1.7	0.0015
19	269.1648	176452	2919.1	3.8	0.0015
20	273.1362	169004	2655.6	3.4	0.0016
21	275.1794	171364	1583.5	2.0	0.0016
22	277.1700	167638	737.0	1.0	0.0017
23	292.2185	162416	2304.4	3.1	0.0018
24	322.0482	147328	1364.9	1.8	0.0022
25	326.3781	144456	4755.0	6.4	0.0023
26	327.3814	140568	1104.4	1.5	0.0023
27	332.2009	147266	65821.1	88.0	0.0023
28	332.2498	142970	1932.0	2.6	0.0023
29	333.2042	145018	16633.9	22.3	0.0023
30	334.2075	137218	1619.8	2.2	0.0024
31	367.1917	128744	1362.5	1.8	0.0029
32	374.2113	128440	10356.3	13.9	0.0029
33	375.2147	125509	2584.9	3.5	0.0030
34	386.2842	119826	747.0	1.0	0.0032
35	391.2843	120804	1036.0	1.4	0.0032
36	500.2936	98933	7122.2	10.2	0.0051
37	501.2965	103636	2514.0	3.6	0.0048
38	501.3015	99874	6076.7	8.7	0.0050
39	502.3048	99642	2324.9	3.3	0.0050
40	622.0288	78785	3177.0	4.7	0.0079

#	m/z	Res.	S/N	I %	FWHM
1	602.0025	82214		100.0	0.0073
2	603.0056	82351		20.1	0.0073
3	603.9983	82487		8.9	0.0073
4	604.0087	82488		1.9	0.0073
5	605.0015	82624		1.7	0.0073
6	605.0118	82625		0.1	0.0073
7	605.9944	82760		0.2	0.0073
8	606.0047	82761		0.2	0.0073

^{1}H-NMR (CD_2Cl_2, 500 MHz, 298 K) of 1-adamantyl p-methoxyphenyl disulfide.

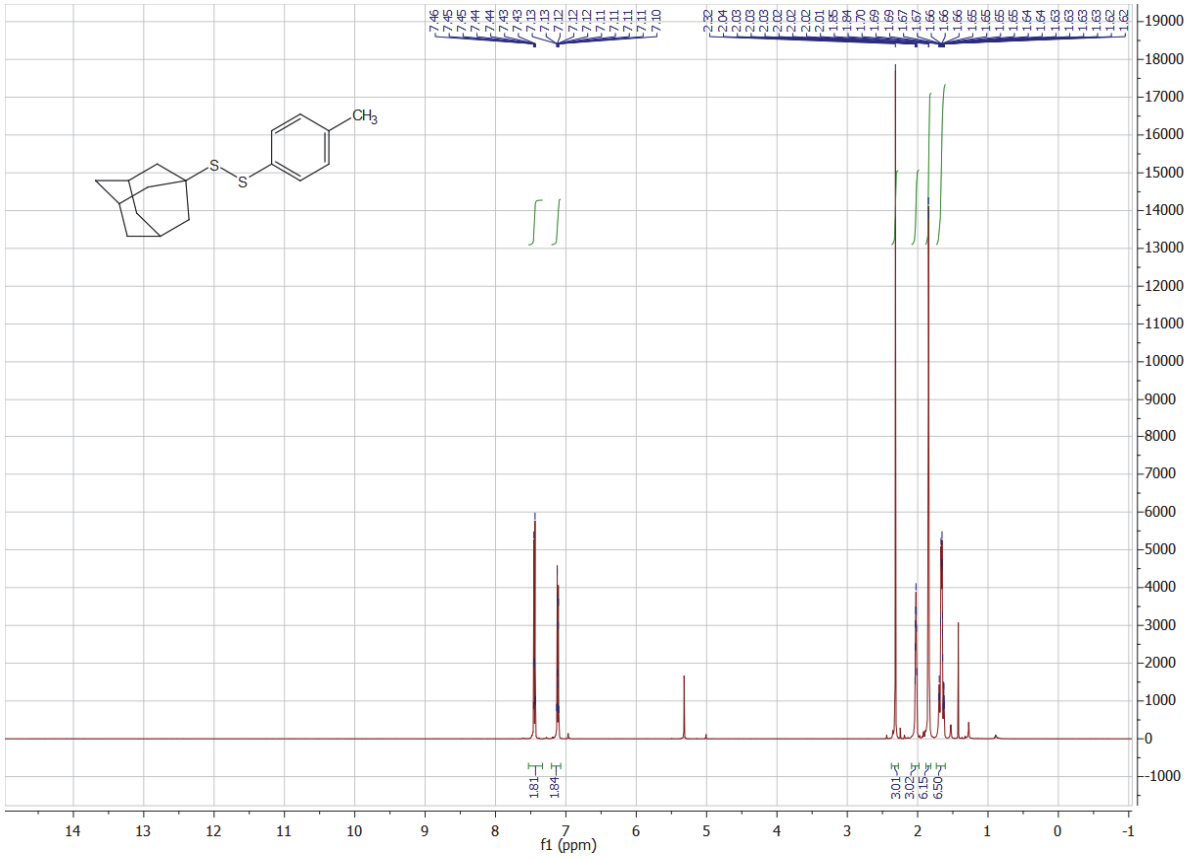

^{13}C-NMR (CD_2Cl_2, 126 MHz, 298 K) of 1-adamantyl p-methoxyphenyl disulfide.

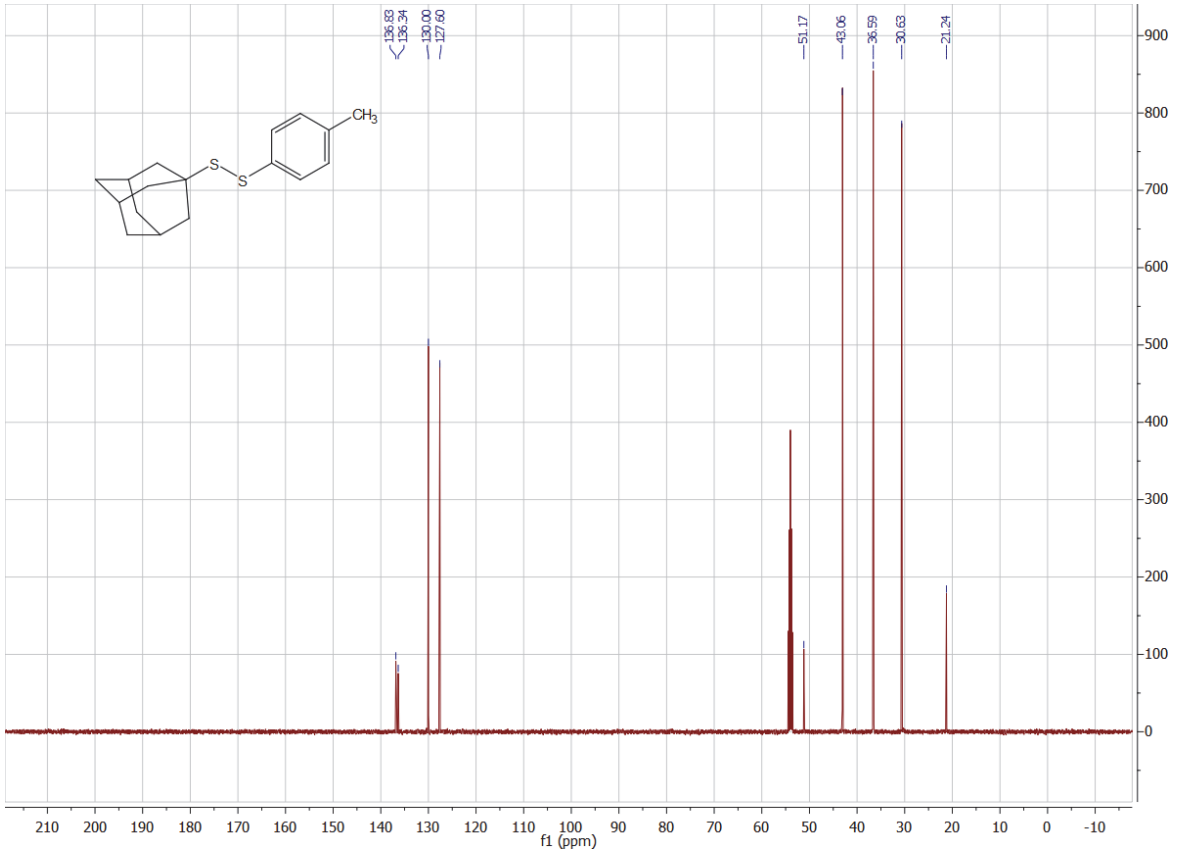

DEPT-NMR (CD_2Cl_2, 126 MHz, 298 K) of 1-adamantyl p-methoxyphenyl disulfide.

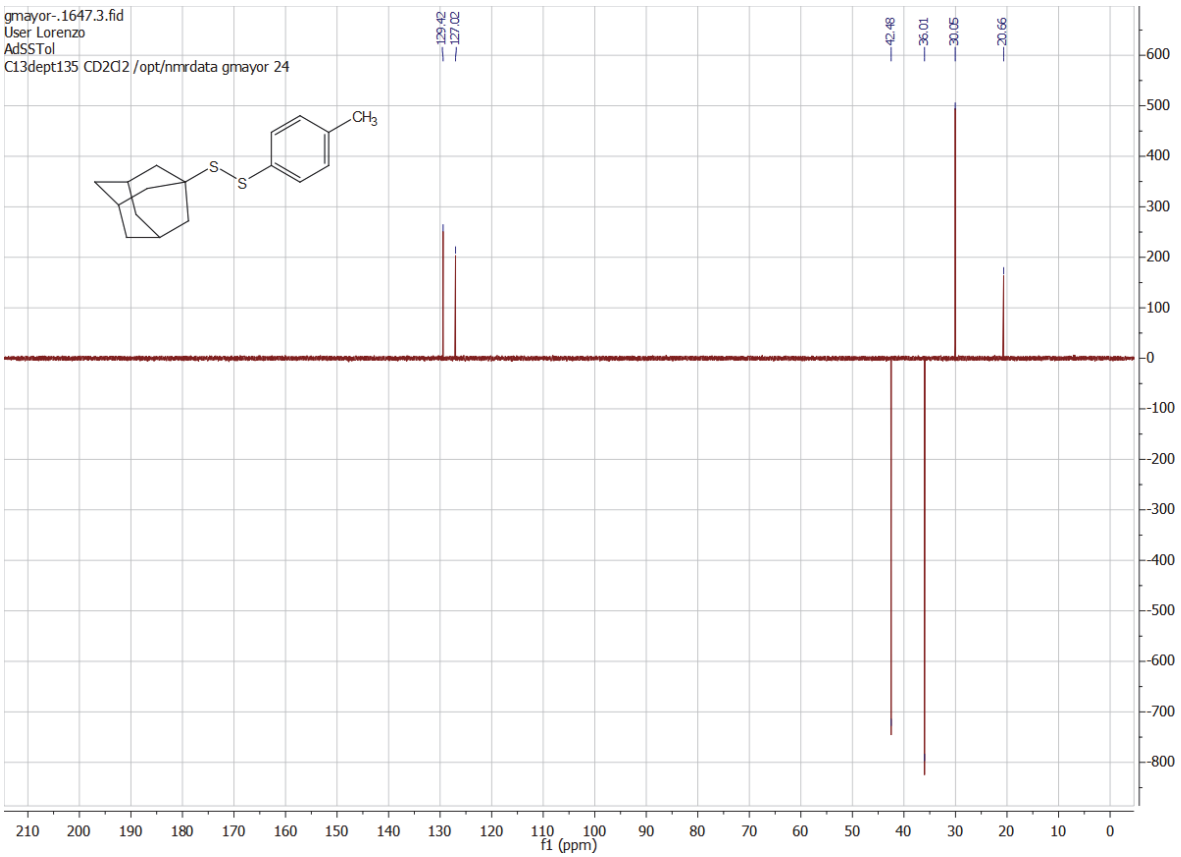

HR-ESI MS spectra of 1-adamantyl p-methoxyphenyl disulfide.

High Resolution Mass Spectrometry Report

Sample Name **Patrick Zwick / Ada-Tol**
Comment

Instrument maXis 4G
Method 22 Direct_pos_mid.m

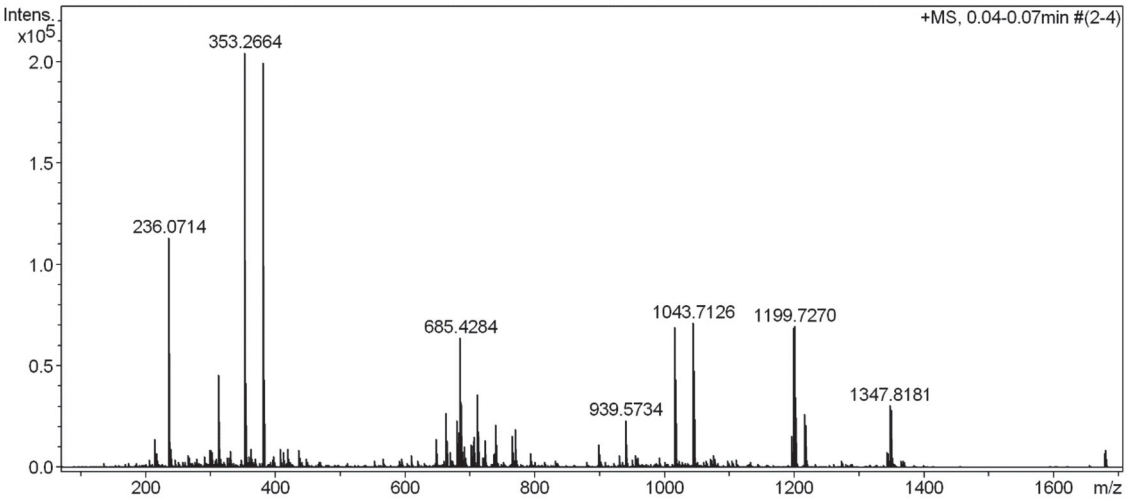

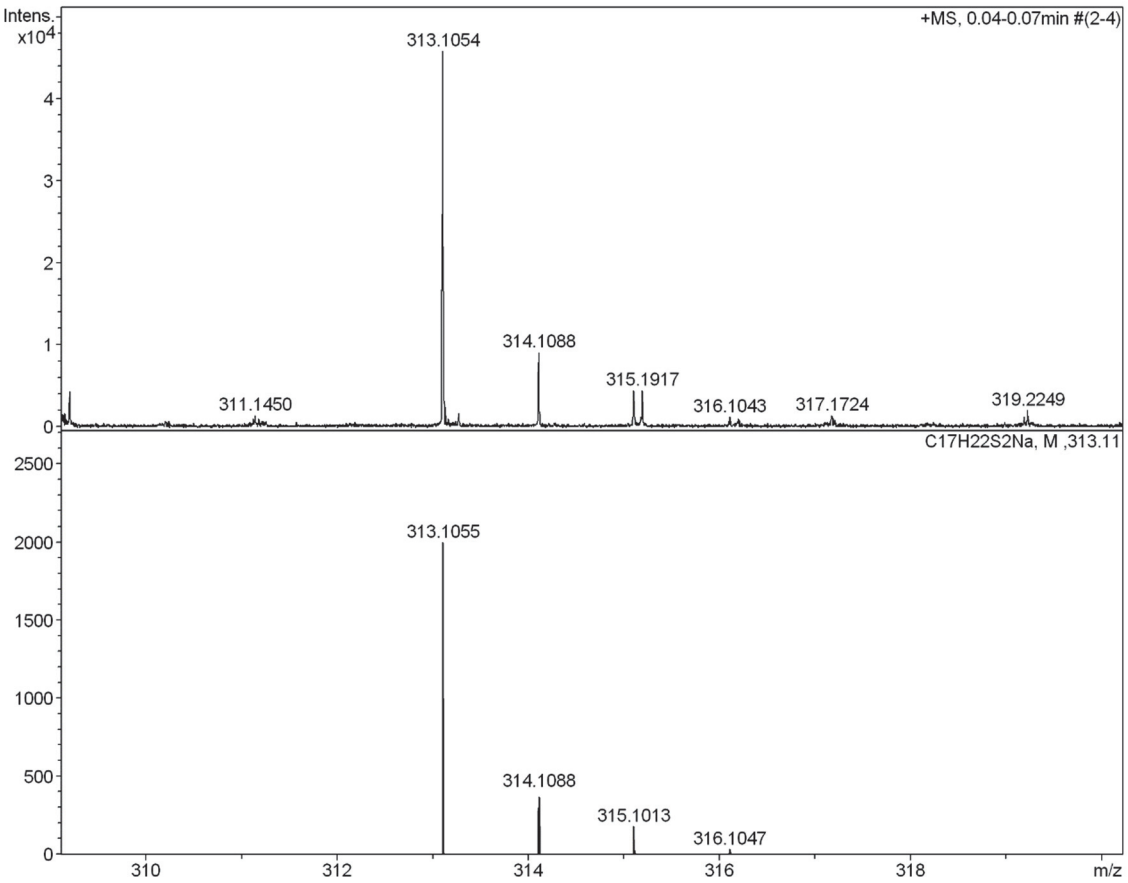

High Resolution Mass Spectrometry Report

Measured m/z vs. theoretical m/z

Meas. m/z	#	Formula	Score	m/z	err [mDa]	err [ppm]	mSigma	rdb	e⁻ Conf	z
313.1054	1	C 17 H 22 Na S 2	100.00	313.1055	0.1	0.3	9.3	6.5	even	1+

Mass list

#	m/z	I %	I
1	214.0894	7.0	14258
2	217.1047	3.6	7288
3	235.0401	2.5	5083
4	236.0714	55.5	113543
5	237.0746	6.3	12950
6	238.0673	2.6	5396
7	239.1252	4.6	9386
8	266.1724	3.0	6179
9	267.1755	2.5	5136
10	291.1232	2.7	5463
11	299.1618	4.3	8849
12	301.1406	4.2	8588
13	303.0118	3.8	7715
14	313.1054	22.4	45859
15	314.1088	4.5	9181
16	325.2345	2.5	5111
17	331.1880	4.1	8347
18	353.2664	100.0	204403
19	354.2695	20.5	41914
20	355.2717	2.6	5349
21	359.2185	2.7	5525
22	363.1563	4.6	9412
23	381.2975	97.7	199639
24	382.3006	21.2	43419
25	383.3030	2.9	5947
26	397.2712	2.9	5830
27	407.2765	4.6	9368
28	408.3079	3.7	7648
29	413.2652	3.7	7519
30	419.2400	4.6	9313
31	435.3071	4.3	8752
32	437.1925	2.6	5215
33	609.3278	3.0	6110
34	647.4526	7.0	14298
35	648.4551	3.7	7596
36	663.4470	13.3	27238
37	663.5098	2.9	5968
38	664.4502	6.3	12837
39	669.4340	3.7	7507
40	679.4112	7.2	14735
41	680.4140	3.3	6715
42	680.4729	11.3	23042
43	681.4762	5.8	11811
44	683.5360	8.4	17254
45	684.5386	4.0	8170
46	685.4284	31.4	64247
47	686.4318	15.3	31205
48	687.4351	4.1	8425
49	691.5398	5.1	10484
50	692.5447	2.4	4982
51	701.4014	5.6	11451
52	702.4046	2.6	5288
53	705.5731	7.4	15124
54	706.5771	4.2	8557
55	711.5661	17.6	36026
56	712.5696	7.8	15919
57	722.5174	6.6	13539
58	723.5204	3.3	6819
59	736.4973	3.3	6781
60	737.5426	3.5	7210
61	739.5960	10.5	21366
62	740.5987	5.4	11108

High Resolution Mass Spectrometry Report

#	m/z	I %	I
63	764.5626	5.6	11458
64	765.5709	7.7	15827
65	766.5757	3.7	7549
66	769.4665	9.4	19172
67	770.4690	5.5	11247
68	793.6025	3.6	7278
69	898.4977	5.5	11244
70	899.5003	3.2	6544
71	929.7562	3.0	6215
72	939.5734	11.5	23432
73	940.5768	7.1	14603
74	955.5484	3.1	6365
75	957.7851	2.5	5041
76	1015.6840	33.9	69191
77	1016.6867	21.4	43774
78	1017.6902	8.1	16510
79	1043.7126	34.9	71349
80	1044.7158	23.5	48085
81	1045.7188	8.7	17851
82	1046.7217	2.5	5151
83	1075.6784	3.0	6167
84	1194.7715	7.8	15856
85	1195.7738	5.9	11985
86	1196.7773	2.7	5511
87	1199.7270	34.1	69675
88	1200.7307	26.6	54350
89	1201.7333	12.2	24940
90	1202.7360	4.0	8142
91	1215.7020	13.0	26588
92	1216.7054	10.3	21135
93	1217.7069	5.6	11420
94	1342.8642	3.7	7487
95	1343.8655	3.5	7135
96	1347.8181	14.9	30510
97	1348.8215	14.0	28536
98	1349.8240	6.3	12942
99	1678.0454	3.5	7182
100	1679.0483	4.2	8655

Acquisition Parameter

General	Fore Vacuum	2.68e+000 mBar	High Vacuum	1.25e-007 mBar	Source Type	ESI
	Scan Begin	75 m/z	Scan End	1700 m/z	Ion Polarity	Positive
Source	Set Nebulizer	0.4 Bar	Set Capillary	3600 V	Set Dry Gas	4.0 l/min
	Set Dry Heater	180 °C	Set End Plate Offset	-500 V		
Quadrupole	Set Ion Energy (MS only)	4.0 eV				
Coll. Cell	Collision Energy	8.0 eV	Set Collision Cell RF	350.0 Vpp		
Ion Cooler	Set Ion Cooler Transfer Time	75.0 µs	Set Ion Cooler Pre Pulse Storage Time	10.0 µs		

^{1}H-NMR (CD_2Cl_2, 500 MHz, 298 K) and 13C-NMR (CD2Cl2, 126 MHz, 298 K) of *p*-methoxyphenyl *p*-methylphenyl disulfide.

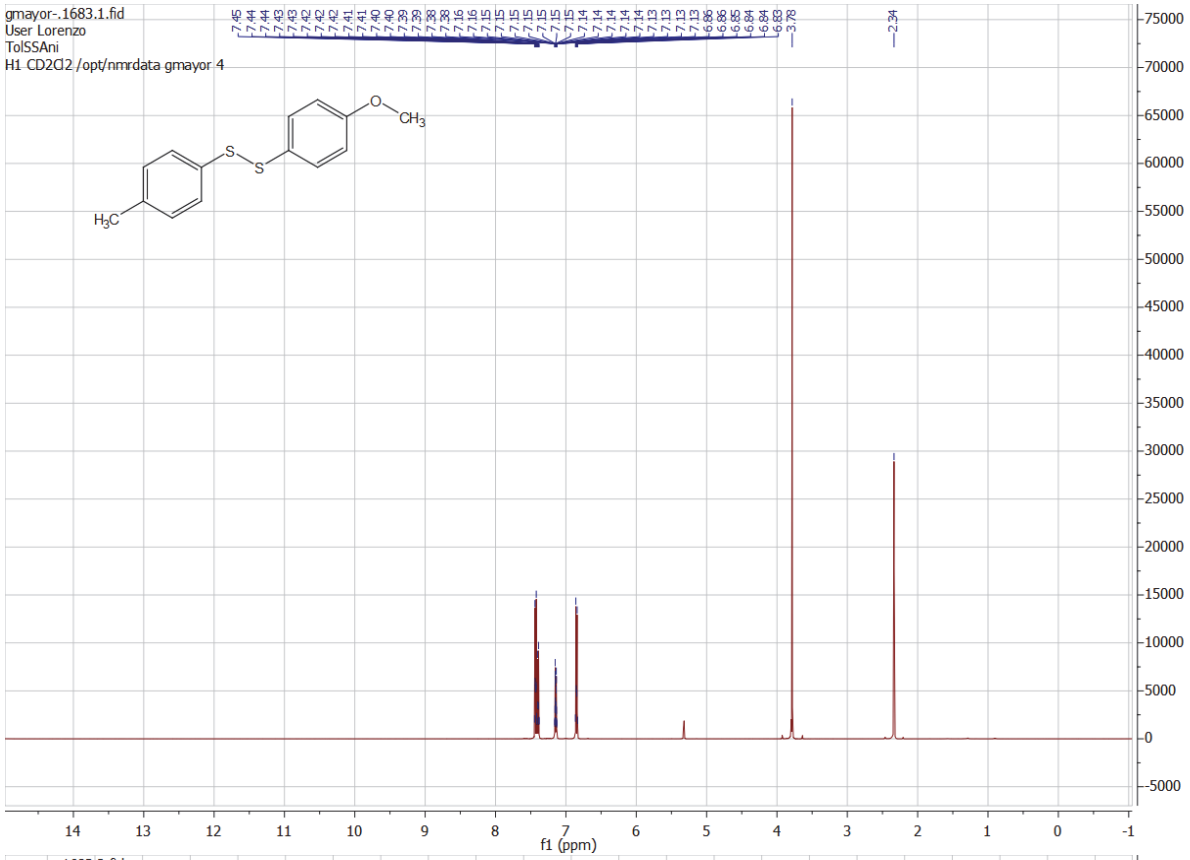

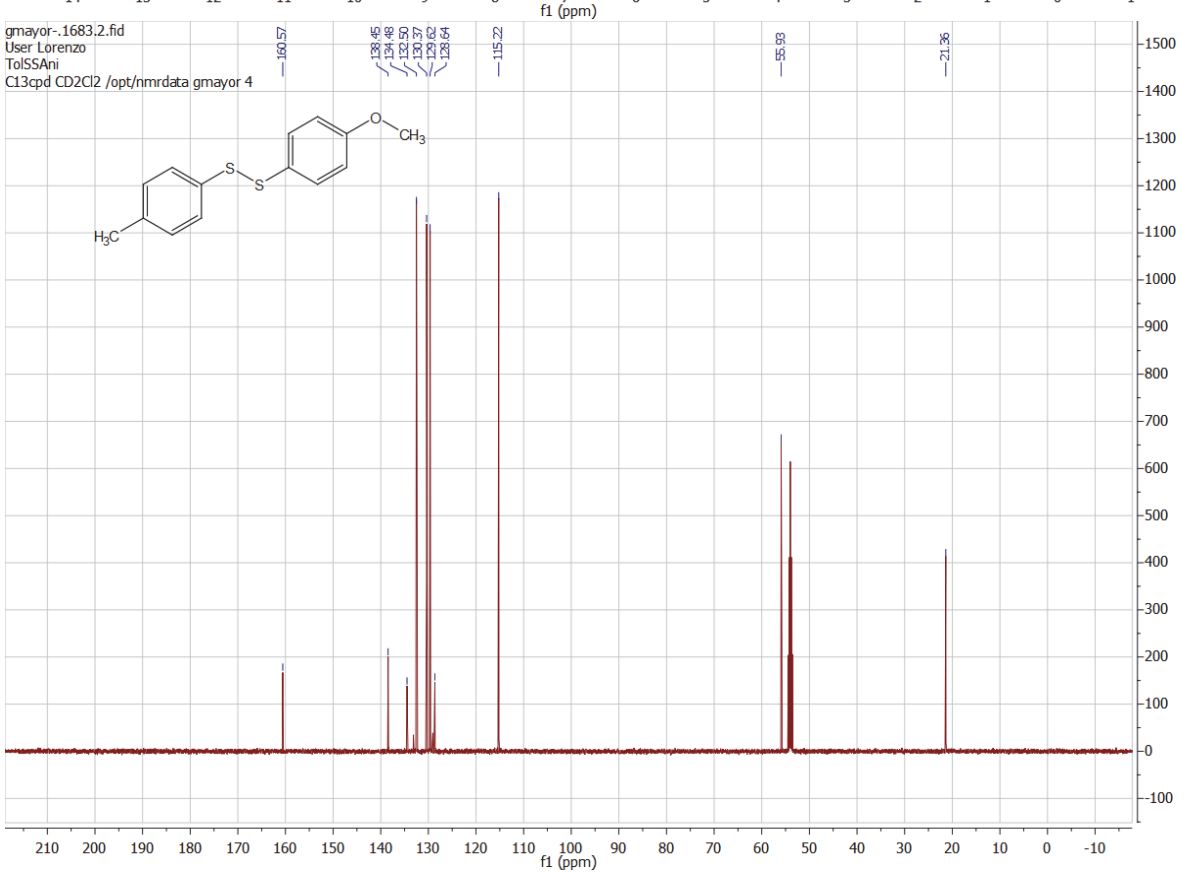

HR-ESI MS spectra of. *p*-methoxyphenyl *p*-methylphenyl disulfide.

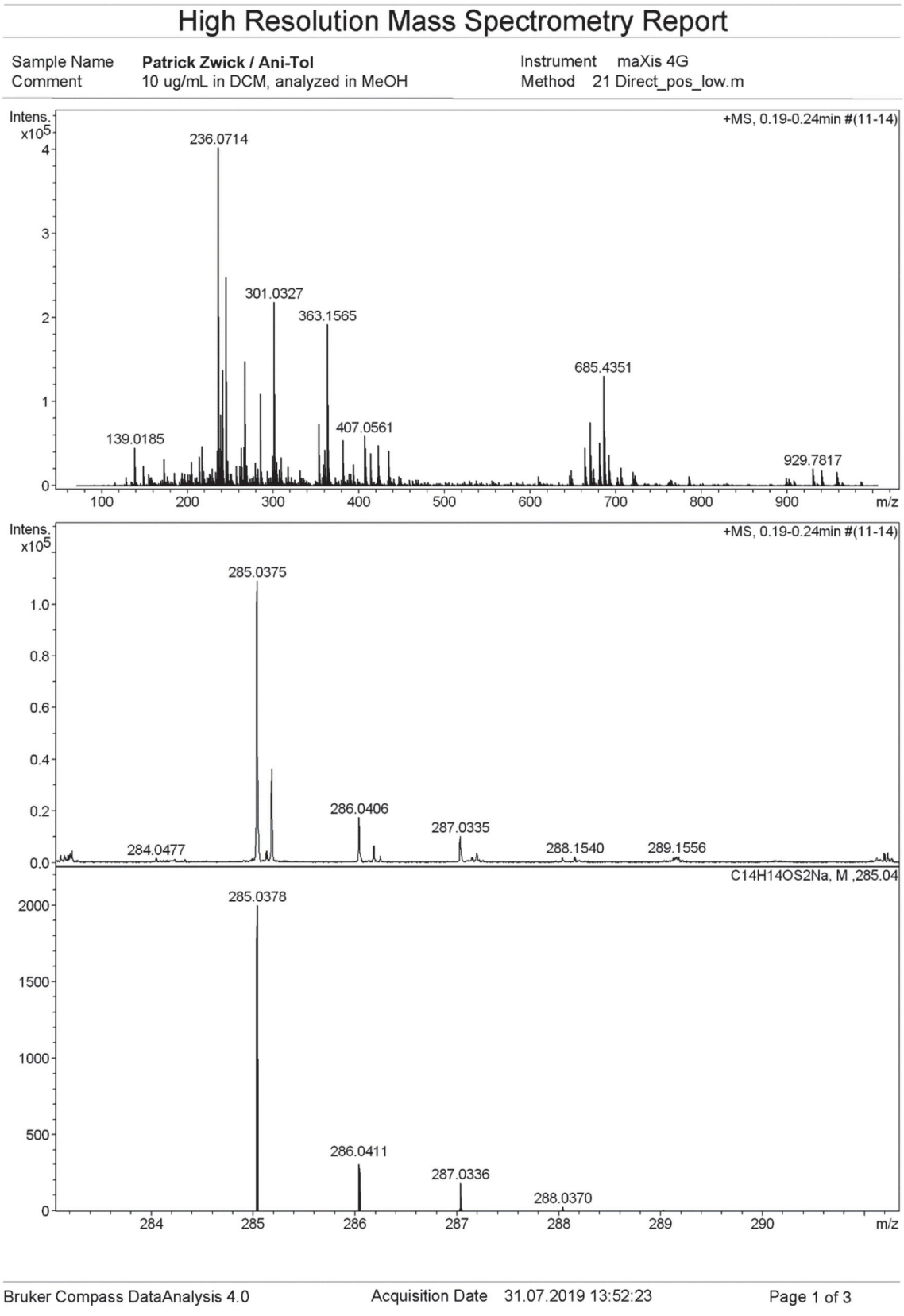

High Resolution Mass Spectrometry Report

Measured m/z vs. theoretical m/z

Meas. m/z	#	Formula	Score	m/z	err [mDa]	err [ppm]	mSigma	rdb	e⁻ Conf	z
285.0375	1	C 14 H 14 Na O S 2	100.00	285.0378	0.3	1.0	5.3	7.5	even	1+

Mass list

#	m/z	I %	I
1	139.0185	11.3	45523
2	149.0210	5.9	23562
3	155.0140	3.3	13319
4	173.0769	7.9	31605
5	185.1135	3.8	15437
6	194.1139	3.8	15204
7	197.0595	3.7	15011
8	201.0569	3.3	13122
9	203.0516	3.3	13334
10	205.0593	7.1	28627
11	214.0888	8.6	34602
12	217.1040	11.8	47554
13	219.0459	4.3	17205
14	226.1408	3.6	14406
15	227.1247	3.2	12996
16	229.0860	5.3	21224
17	233.0368	4.2	17098
18	235.0389	10.4	41869
19	236.0714	100.0	402354
20	237.0740	11.3	45541
21	238.0674	4.4	17590
22	239.0884	12.3	49507
23	239.1249	21.0	84641
24	241.0290	34.3	138095
25	242.0320	4.6	18516
26	245.0782	61.6	248040
27	246.0814	7.8	31373
28	247.1122	7.5	30082
29	250.1774	3.6	14450
30	251.0341	3.6	14584
31	257.1354	6.0	23998
32	261.1302	5.8	23353
33	263.0701	3.4	13657
34	263.1071	11.2	45265
35	266.1723	11.4	45738
36	267.0118	3.1	12544
37	267.0482	36.9	148632
38	267.1748	6.8	27367
39	268.0510	4.8	19226
40	269.0436	6.1	24633
41	279.0653	6.6	26386
42	279.2290	6.9	27721
43	282.2036	5.1	20361
44	285.0375	27.1	109158
45	285.1821	9.0	36192
46	286.0406	4.4	17746
47	293.2446	4.5	17933
48	299.1613	8.9	35849
49	301.0327	54.3	218606
50	301.1406	27.8	111909
51	302.0355	8.8	35372
52	302.1440	5.1	20660
53	303.0286	4.7	19079
54	304.2604	7.3	29343
55	307.2601	4.8	19203
56	309.2033	8.5	34374
57	317.0274	5.5	22311
58	331.1279	4.5	18170
59	353.2658	18.2	73295
60	354.2688	4.0	16024
61	358.2009	6.5	26161
62	360.3229	10.7	43219

High Resolution Mass Spectrometry Report

#	m/z	I %	I
63	363.1565	47.7	191730
64	364.1596	10.8	43593
65	365.1050	4.1	16597
66	381.1666	9.8	39509
67	381.2968	13.5	54314
68	389.0478	3.7	14802
69	391.0606	3.6	14440
70	393.2971	6.4	25861
71	407.0561	14.7	59106
72	407.2760	11.2	45173
73	408.0591	3.8	15101
74	413.2652	9.8	39576
75	423.0512	12.1	48630
76	423.2133	6.1	24624
77	424.0539	3.2	12797
78	435.3071	10.4	41995
79	647.2970	4.8	19145
80	647.4574	3.5	14164
81	663.4524	11.2	45188
82	663.5157	5.6	22495
83	664.4557	5.6	22367
84	669.4398	18.9	76084
85	670.4430	8.9	35696
86	673.5366	5.2	20761
87	680.4793	12.7	51045
88	681.4827	5.9	23691
89	685.4351	32.5	130585
90	686.4381	14.6	58802
91	687.4410	3.8	15094
92	691.5474	9.2	36967
93	692.5506	4.1	16670
94	705.5814	5.3	21288
95	719.5788	4.2	17033
96	721.5779	3.2	13057
97	929.7817	5.1	20326
98	930.7851	3.2	12686
99	939.5999	4.6	18541
100	957.8145	4.2	16742

Acquisition Parameter

General	Fore Vacuum	2.79e+000 mBar	High Vacuum	1.25e-007 mBar	Source Type	ESI
	Scan Begin	75 m/z	Scan End	1000 m/z	Ion Polarity	Positive
Source	Set Nebulizer	0.4 Bar	Set Capillary	3600 V	Set Dry Gas	3.0 l/min
	Set Dry Heater	180 °C	Set End Plate Offset	-500 V		
Quadrupole	Set Ion Energy (MS only)	4.0 eV				
Coll. Cell	Collision Energy	8.0 eV	Set Collision Cell RF	350.0 Vpp		
Ion Cooler	Set Ion Cooler Transfer Time	55.0 µs	Set Ion Cooler Pre Pulse Storage Time	7.0 µs		

^{1}H-NMR (CD_2Cl_2, 500 MHz, 298 K) and ^{13}C-NMR (CD_2Cl_2, 126 MHz, 298 K) of pentyl *p*-methylphenyl disulfide.

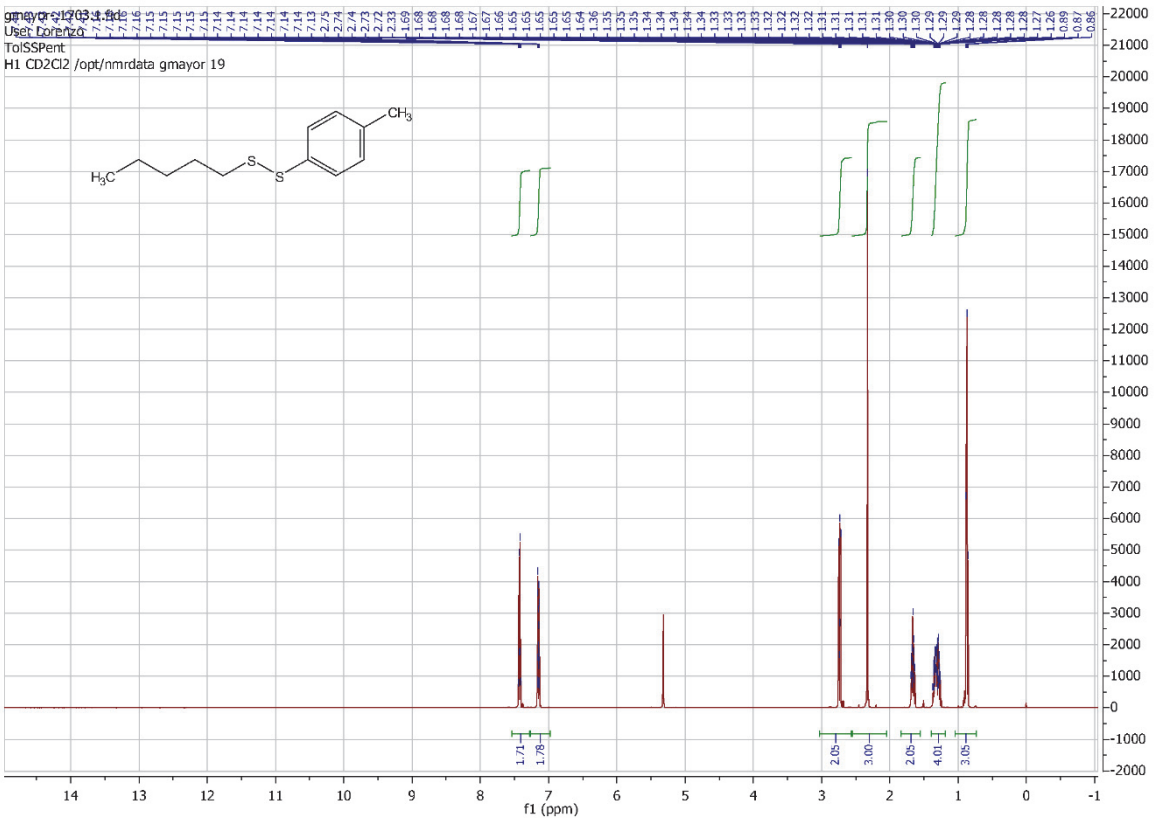

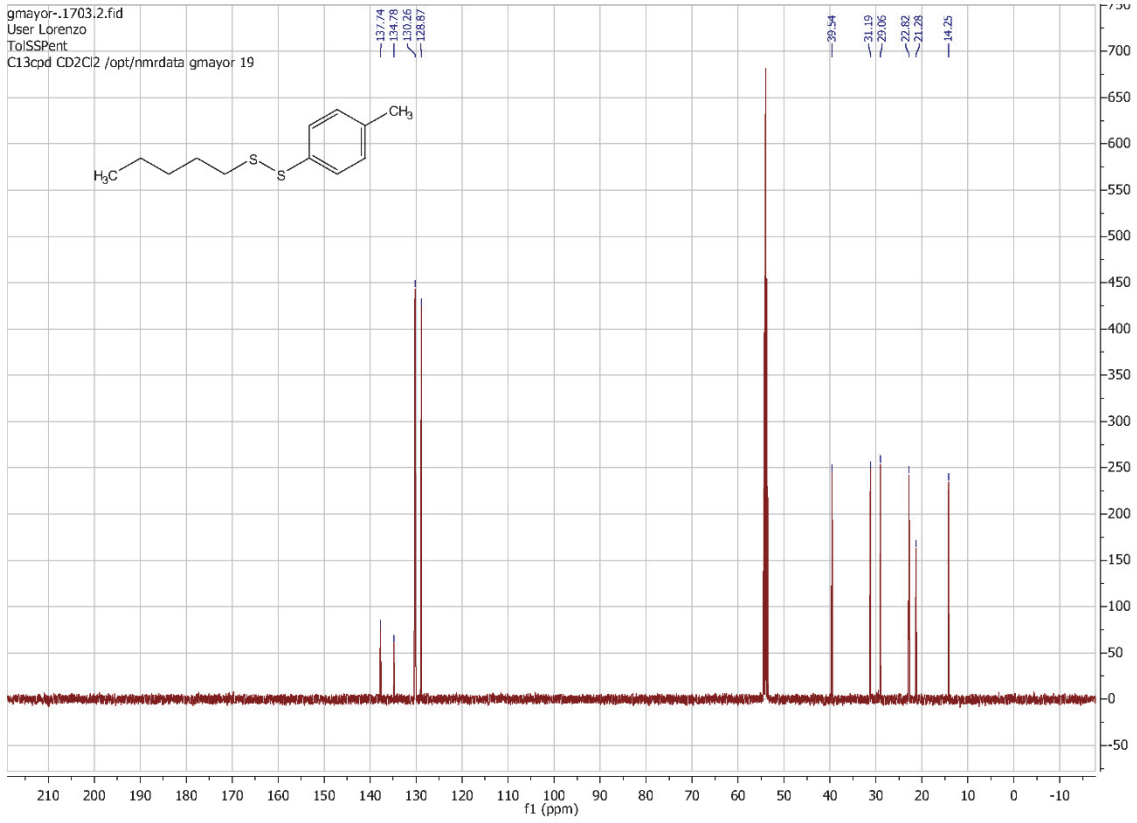

HR-ESI MS spectra of pentyl *p*-methylphenyl disulfide.

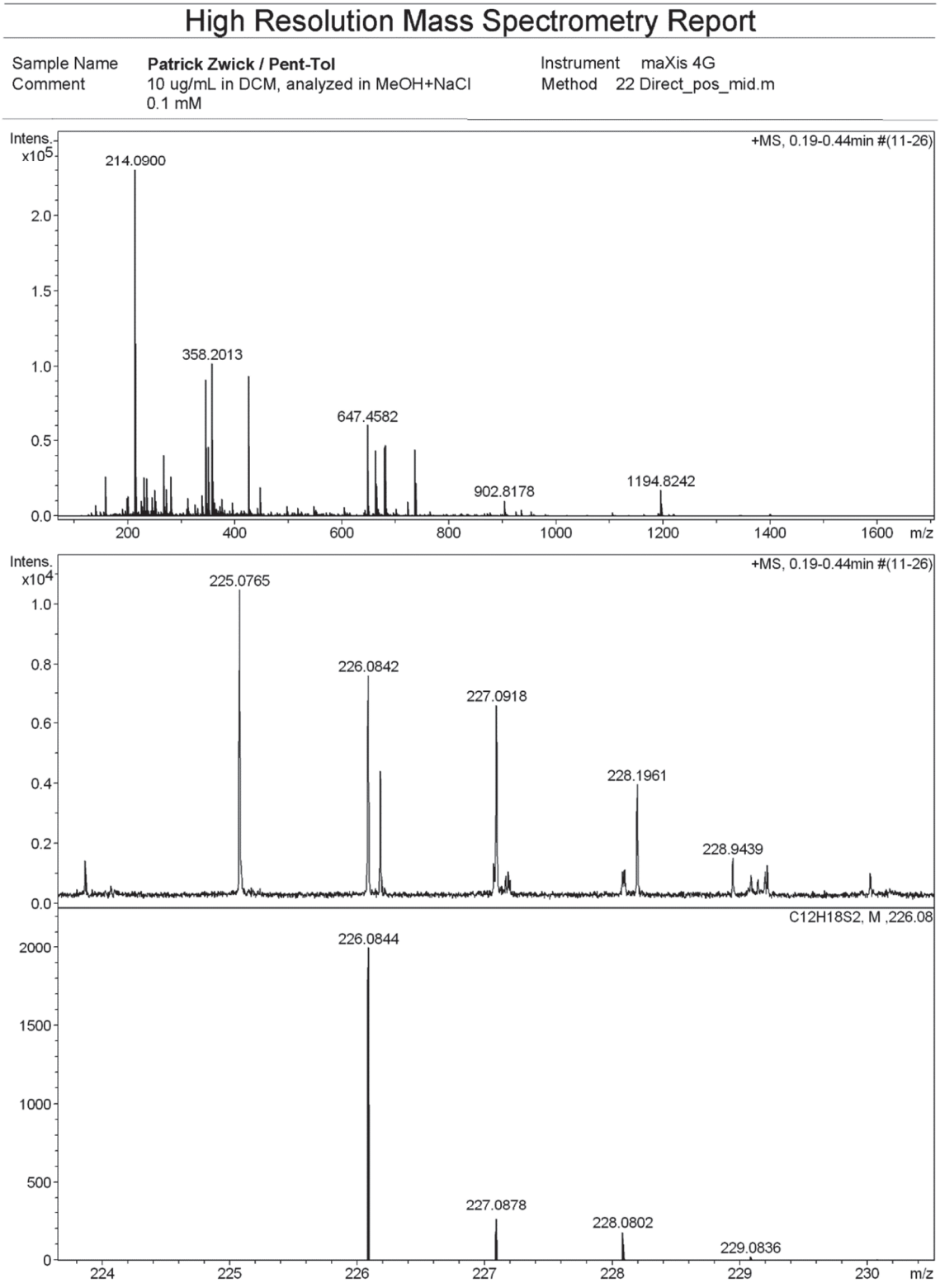

High Resolution Mass Spectrometry Report

Measured m/z vs. theoretical m/z

Meas. m/z	#	Formula	Score	m/z	err [mDa]	err [ppm]	mSigma	rdb	e⁻ Conf	z
226.0842	1	C 12 H 18 S 2	100.00	226.0844	0.2	1.0	88.7	4.0	odd	1+

Mass list

#	m/z	I %	I
1	141.0003	3.3	7560
2	149.0233	1.5	3484
3	158.0271	11.5	26579
4	191.1067	2.3	5208
5	196.1696	1.6	3707
6	198.1854	5.2	12020
7	201.0039	5.8	13373
8	214.0900	100.0	230733
9	215.0928	11.4	26365
10	216.0860	4.6	10668
11	225.0765	4.5	10467
12	226.0842	3.3	7619
13	226.1802	1.9	4432
14	227.0918	2.9	6606
15	228.1961	1.7	3976
16	231.1163	11.2	25792
17	234.1698	1.7	4028
18	236.0717	10.8	24965
19	237.9621	1.8	4221
20	239.1256	1.6	3658
21	244.1907	1.7	3904
22	245.0454	5.5	12644
23	249.2064	1.7	3966
24	251.0197	7.5	17399
25	251.9600	4.6	10574
26	252.9720	1.5	3448
27	268.0462	17.7	40894
28	269.0489	2.9	6729
29	269.9340	1.5	3457
30	270.0422	1.8	4081
31	273.0015	7.9	18329
32	281.2113	11.3	26116
33	282.2143	2.2	5058
34	310.2374	2.2	4978
35	313.1548	5.3	12247
36	313.2735	1.5	3525
37	326.1241	3.5	8049
38	326.1730	1.9	4393
39	331.2843	2.4	5595
40	338.3416	6.1	14034
41	339.3448	1.6	3689
42	345.9428	39.5	91136
43	346.9452	4.0	9193
44	347.9389	3.7	8555
45	349.1111	2.2	5060
46	350.8981	20.0	46121
47	351.9009	2.0	4611
48	352.8941	1.9	4280
49	353.2659	2.0	4660
50	358.2013	44.1	101801
51	359.2044	10.2	23549
52	359.3149	2.1	4889
53	363.1565	4.0	9137
54	365.1051	2.2	5011
55	369.3509	1.6	3786
56	373.2040	2.8	6503
57	376.2115	4.9	11292
58	381.1667	1.6	3669
59	381.2974	1.8	4225
60	391.2840	1.5	3510
61	395.1858	1.6	3774
62	395.3625	4.0	9182

High Resolution Mass Spectrometry Report

#	m/z	I %	I
63	412.9921	1.7	3851
64	418.2583	1.6	3578
65	425.3623	40.6	93750
66	426.3654	11.5	26570
67	427.3693	2.2	5092
68	428.4245	1.7	3854
69	442.3887	2.4	5557
70	447.3440	8.3	19097
71	448.3469	2.6	5957
72	498.4509	2.9	6620
73	518.3679	2.4	5576
74	548.5030	2.9	6609
75	550.5555	2.0	4552
76	604.3832	2.6	6062
77	642.3420	2.0	4668
78	647.4582	26.3	60798
79	648.4616	12.6	28998
80	649.4644	3.1	7117
81	663.4531	18.9	43685
82	664.4565	8.8	20357
83	665.4595	2.3	5238
84	668.5821	2.1	4760
85	680.4799	20.4	47135
86	681.4830	9.6	22204
87	682.4863	2.5	5750
88	700.6261	2.0	4714
89	722.5266	4.2	9764
90	723.5307	2.2	5064
91	736.5426	19.1	44026
92	737.5460	9.7	22484
93	738.5491	2.7	6157
94	902.8178	4.5	10492
95	903.8215	2.8	6525
96	924.8232	1.5	3458
97	934.6417	1.9	4492
98	1194.8242	7.6	17421
99	1195.8277	6.1	14143
100	1196.8306	2.7	6237

Acquisition Parameter

General	Fore Vacuum	2.68e+000 mBar	High Vacuum	1.26e-007 mBar	Source Type	ESI
	Scan Begin	75 m/z	Scan End	1700 m/z	Ion Polarity	Positive
Source	Set Nebulizer	0.4 Bar	Set Capillary	3600 V	Set Dry Gas	4.0 l/min
	Set Dry Heater	180 °C	Set End Plate Offset	-500 V		
Quadrupole	Set Ion Energy (MS only)	4.0 eV				
Coll. Cell	Collision Energy	8.0 eV	Set Collision Cell RF	350.0 Vpp		
Ion Cooler	Set Ion Cooler Transfer Time	75.0 µs	Set Ion Cooler Pre Pulse Storage Time	10.0 µs		

^{1}H-NMR (CD_2Cl_2, 500 MHz, 298 K) and ^{13}C-NMR (CD_2Cl_2, 126 MHz, 298 K) of tetrakis(4-(pentyldisulfanyl)phenyl)methane (**140**)

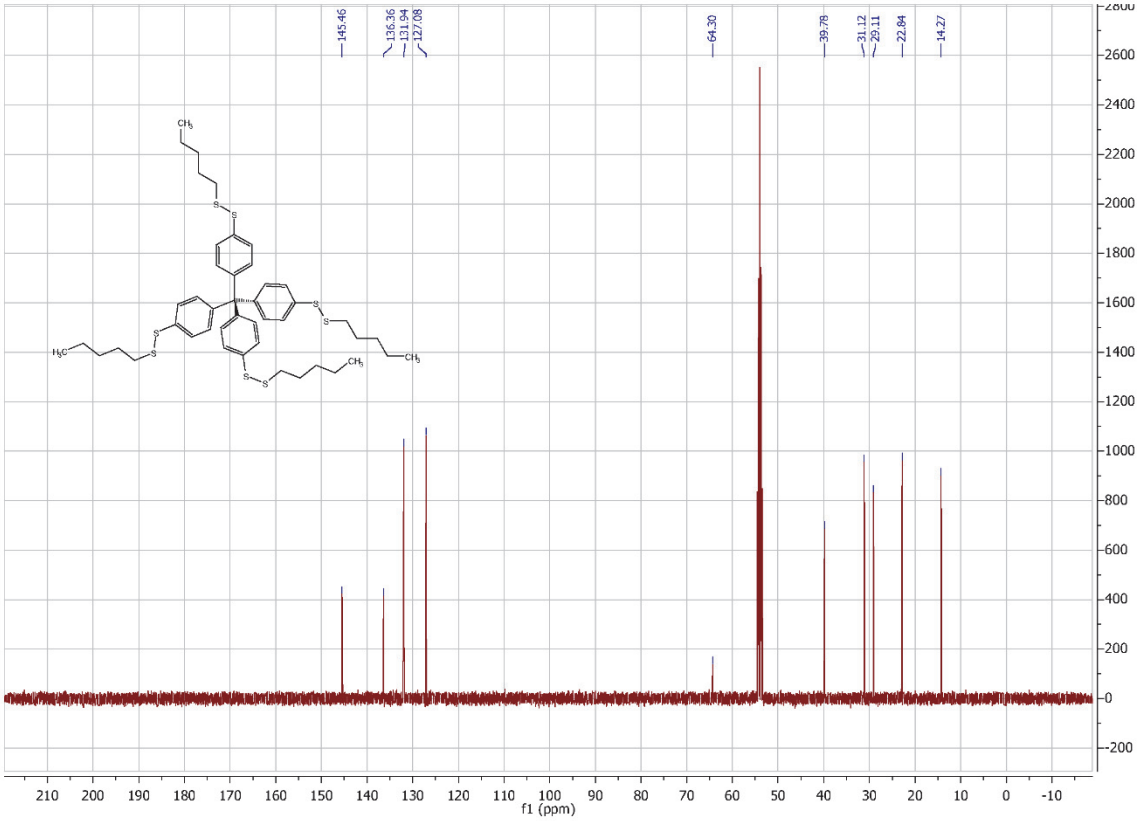

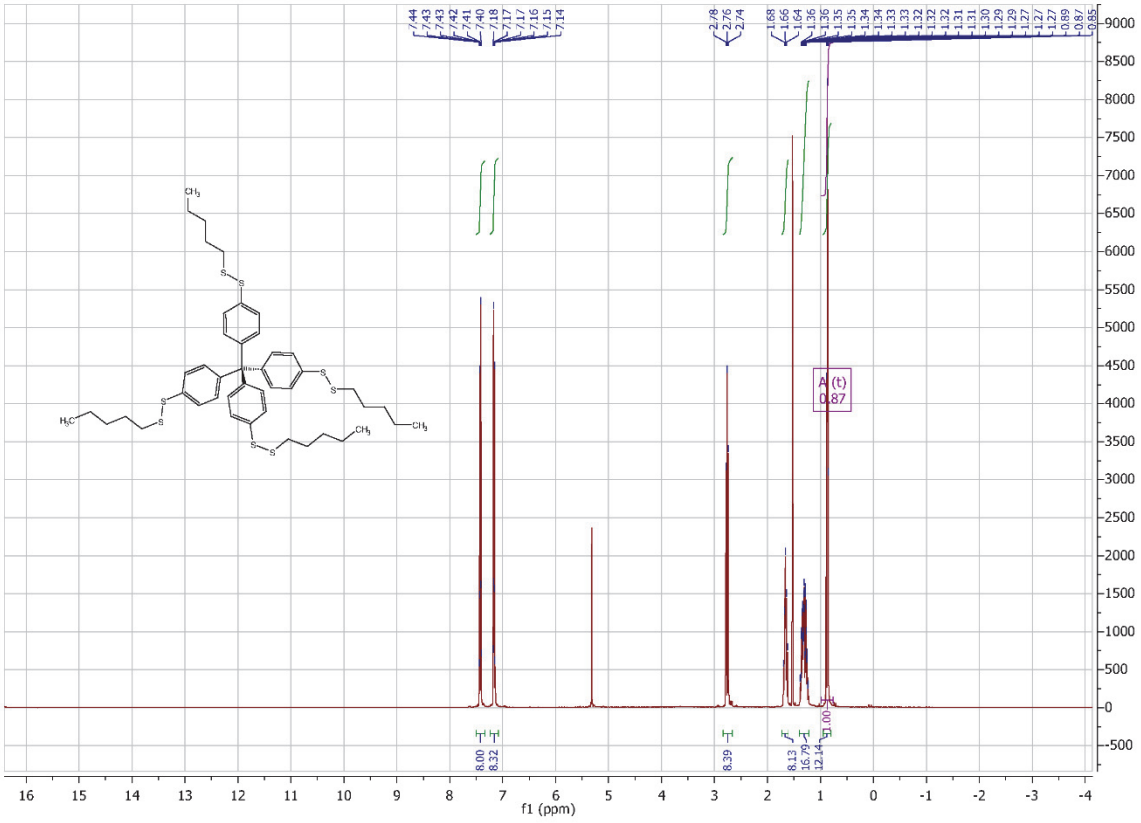

HR-ESI MS spectra of tetrakis(4-(pentyldisulfanyl)phenyl)methane (**143**.

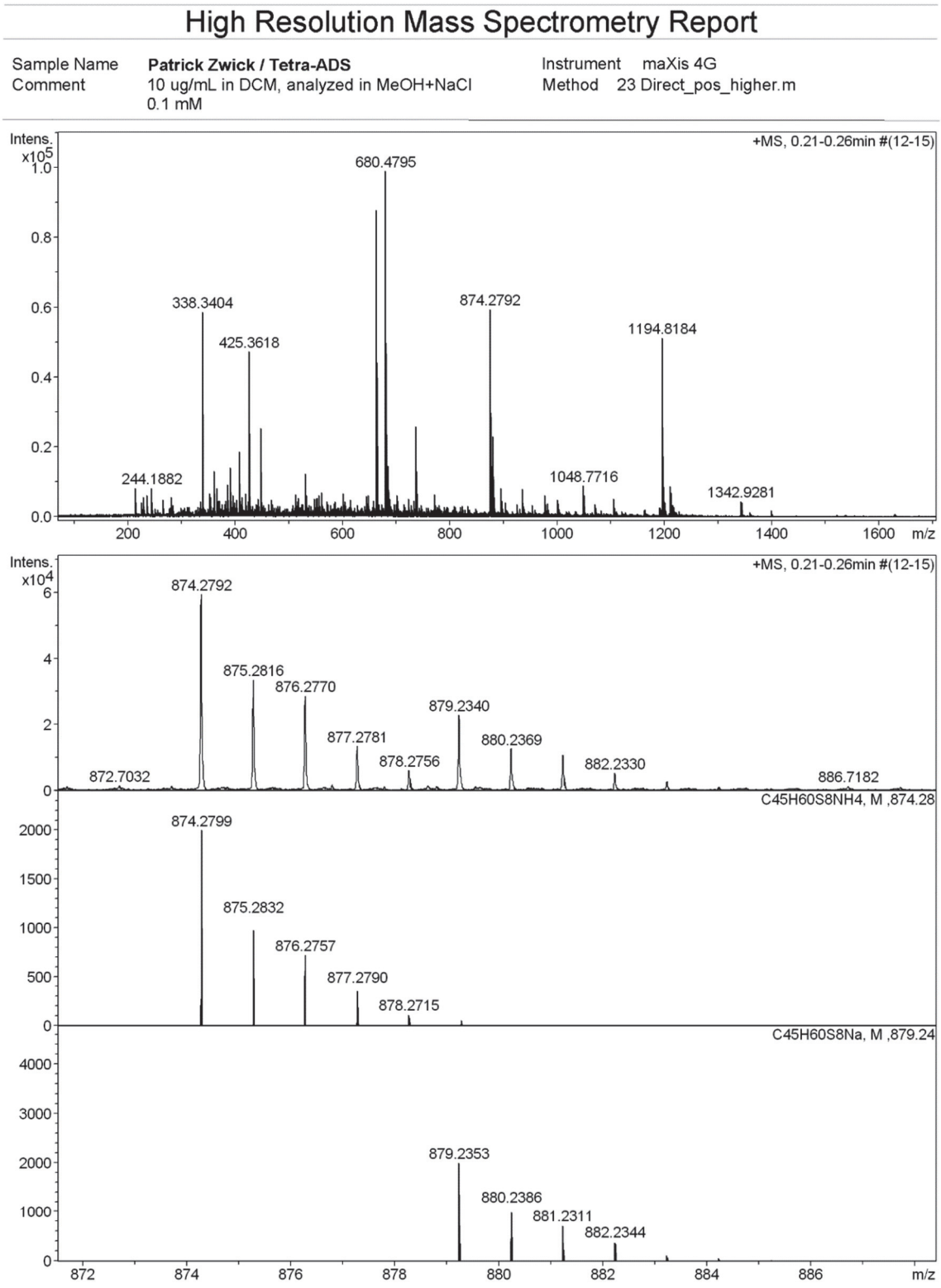

High Resolution Mass Spectrometry Report

Measured m/z vs. theoretical m/z

Meas. m/z	#	Formula	Score	m/z	err [mDa]	err [ppm]	mSigma	rdb	e⁻ Conf	z
874.2792	1	C 45 H 64 N S 8	100.00	874.2799	0.6	0.7	20.5	14.5	even	1+
879.2340	1	C 45 H 60 Na S 8	100.00	879.2353	1.3	1.4	22.5	15.5	even	

Mass list

#	m/z	I %	I
1	214.0859	8.3	8195
2	228.1933	5.8	5725
3	236.0702	6.3	6236
4	244.1882	8.5	8397
5	266.1704	4.9	4874
6	281.2089	5.9	5832
7	338.3404	59.3	58730
8	339.3435	14.9	14776
9	352.3194	6.9	6796
10	354.3349	5.8	5697
11	360.3223	13.2	13102
12	365.1044	8.3	8175
13	367.3343	4.6	4505
14	369.3502	4.8	4780
15	371.3151	4.8	4726
16	383.1394	4.6	4589
17	386.3257	9.5	9404
18	391.2832	14.3	14124
19	392.2869	4.8	4737
20	395.3610	6.4	6297
21	402.3716	5.0	4903
22	408.3076	18.9	18664
23	409.3107	4.6	4588
24	413.2654	5.7	5640
25	419.3145	6.9	6850
26	424.2818	4.6	4552
27	425.3618	47.9	47377
28	426.3652	14.3	14111
29	427.3752	5.4	5337
30	428.4238	6.1	6065
31	442.3893	5.4	5314
32	447.3447	25.7	25471
33	448.3476	7.5	7448
34	468.3885	4.8	4739
35	512.4145	6.5	6462
36	515.4119	4.5	4499
37	518.3686	5.6	5581
38	531.4069	12.4	12287
39	532.4118	4.7	4673
40	532.4385	6.2	6122
41	548.5027	5.2	5145
42	550.5557	5.4	5327
43	553.3885	5.4	5382
44	556.4407	6.4	6311
45	561.3514	7.1	7039
46	570.4561	4.6	4563
47	586.5394	4.5	4494
48	600.4672	6.8	6738
49	604.3832	4.6	4561
50	614.4827	5.0	4929
51	644.4930	6.0	5910
52	647.4574	6.2	6183
53	658.5105	4.7	4678
54	663.4530	88.7	87830
55	664.4563	40.3	39927
56	665.4596	10.5	10429
57	679.4299	42.2	41767
58	680.4335	22.4	22200
59	680.4795	100.0	99011
60	681.4349	7.6	7535
61	681.4828	47.5	47002

High Resolution Mass Spectrometry Report

#	m/z	I %	I
62	682.4859	12.1	12014
63	685.4345	14.7	14567
64	686.4379	7.4	7357
65	688.5186	5.1	5091
66	700.6248	5.1	5072
67	701.4103	6.4	6315
68	702.5348	4.7	4638
69	722.5247	5.2	5123
70	732.5451	4.8	4780
71	736.5418	26.2	25900
72	737.5452	13.3	13149
73	738.5487	4.6	4530
74	771.6444	6.5	6482
75	874.2792	60.0	59448
76	875.2816	34.0	33685
77	876.2770	29.1	28788
78	877.2781	13.6	13473
79	878.2756	6.1	6044
80	879.2340	23.2	23003
81	880.2369	12.9	12767
82	881.2327	11.0	10858
83	882.2330	5.5	5409
84	895.2080	8.2	8157
85	896.2112	4.8	4790
86	934.6399	8.1	8058
87	935.6428	5.3	5227
88	976.3291	6.4	6357
89	1000.7864	5.0	4918
90	1048.7716	9.1	8972
91	1049.7751	6.3	6230
92	1104.8357	5.4	5308
93	1194.8184	51.9	51362
94	1195.8215	41.4	40963
95	1196.8249	17.8	17604
96	1197.8270	5.5	5397
97	1199.7732	4.7	4686
98	1210.8125	8.8	8691
99	1211.8165	7.2	7119
100	1342.9281	4.6	4522

Acquisition Parameter

General	Fore Vacuum	2.68e+000 mBar	High Vacuum	1.26e-007 mBar	Source Type	ESI
	Scan Begin	75 m/z	Scan End	1700 m/z	Ion Polarity	Positive
Source	Set Nebulizer	0.4 Bar	Set Capillary	3600 V	Set Dry Gas	4.0 l/min
	Set Dry Heater	180 °C	Set End Plate Offset	-500 V		
Quadrupole	Set Ion Energy (MS only)	4.0 eV				
Coll. Cell	Collision Energy	8.0 eV	Set Collision Cell RF	500.0 Vpp		
Ion Cooler	Set Ion Cooler Transfer Time	80.0 µs	Set Ion Cooler Pre Pulse Storage Time	18.0 µs		

^{1}H-NMR (CD_2Cl_2, 500 MHz, 298 K) and ^{13}C-NMR (CD_2Cl_2, 126 MHz, 298 K) of 2-(2-ethoxyethoxy)ethan-1-thiol.

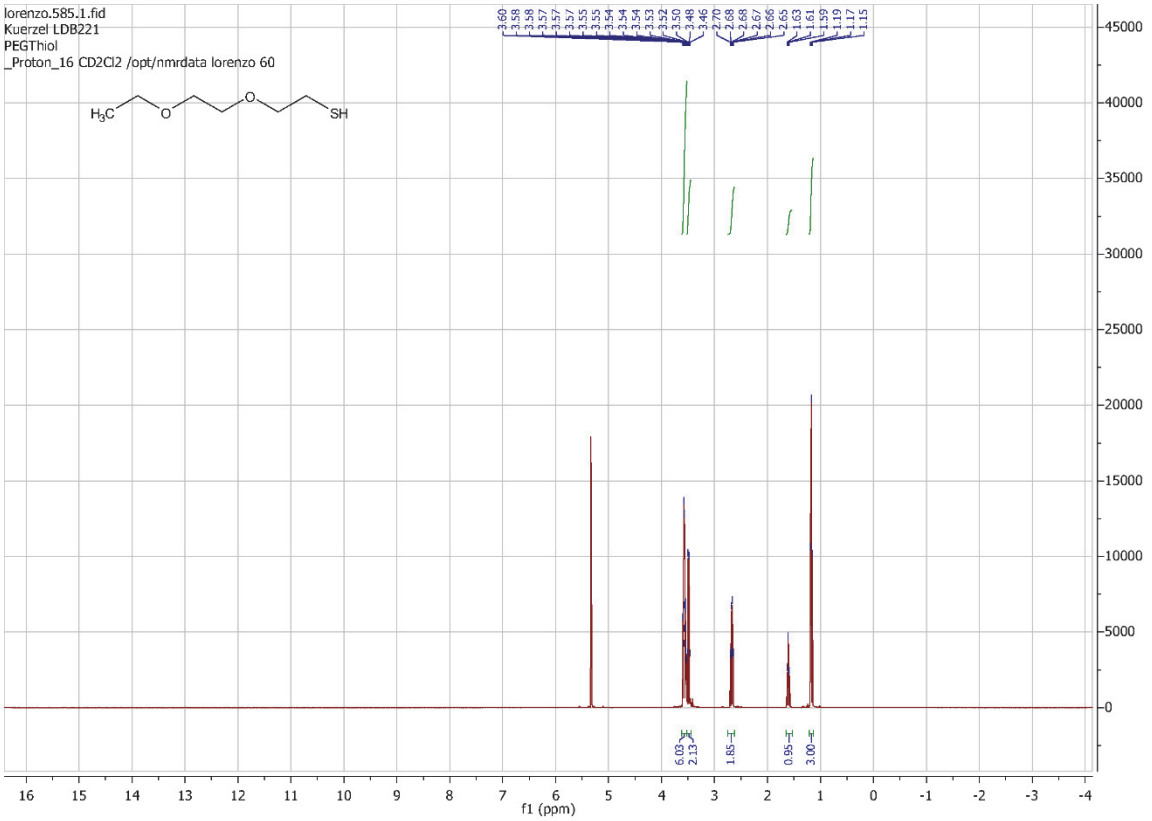
lorenzo.585.1.fid
Kuerzel LDB221
PEGThiol
_Proton_16 CD2Cl2 /opt/nmrdata lorenzo 60
H3C
O
O
SH
6.03
2.13
1.85
0.95
3.00
f1 (ppm)

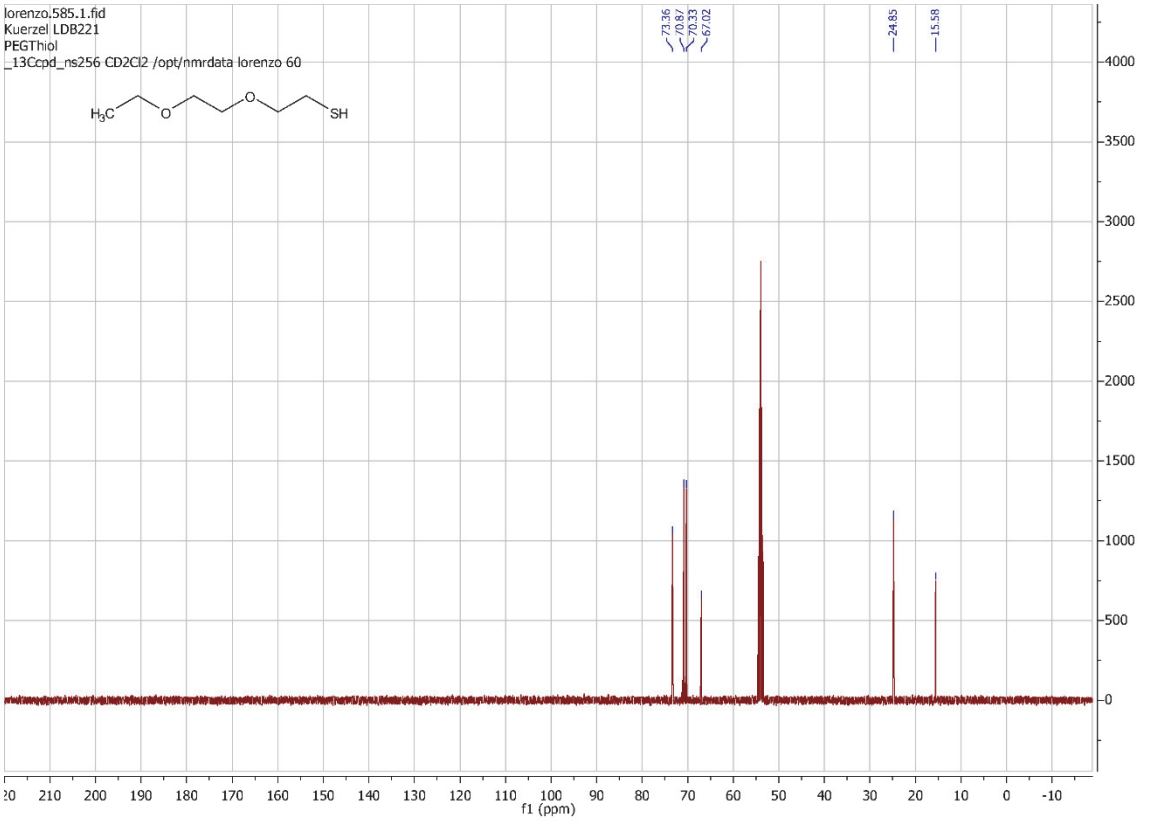
lorenzo.585.1.fid
Kuerzel LDB221
PEGThiol
_13Ccpd_ns256 CD2Cl2 /opt/nmrdata lorenzo 60
H3C
O
O
SH
73.36
70.87
70.33
67.02
24.85
15.58
f1 (ppm)

^{1}H-NMR (CD_2Cl_2, 400 MHz, 298 K) and ^{13}C-NMR (CD_2Cl_2, 101 MHz, 298 K) of 1,4-Bis((4-(pentyldisulfaneyl)phenyl)ethynyl)benzene (OPE-3-ADS, **142**).

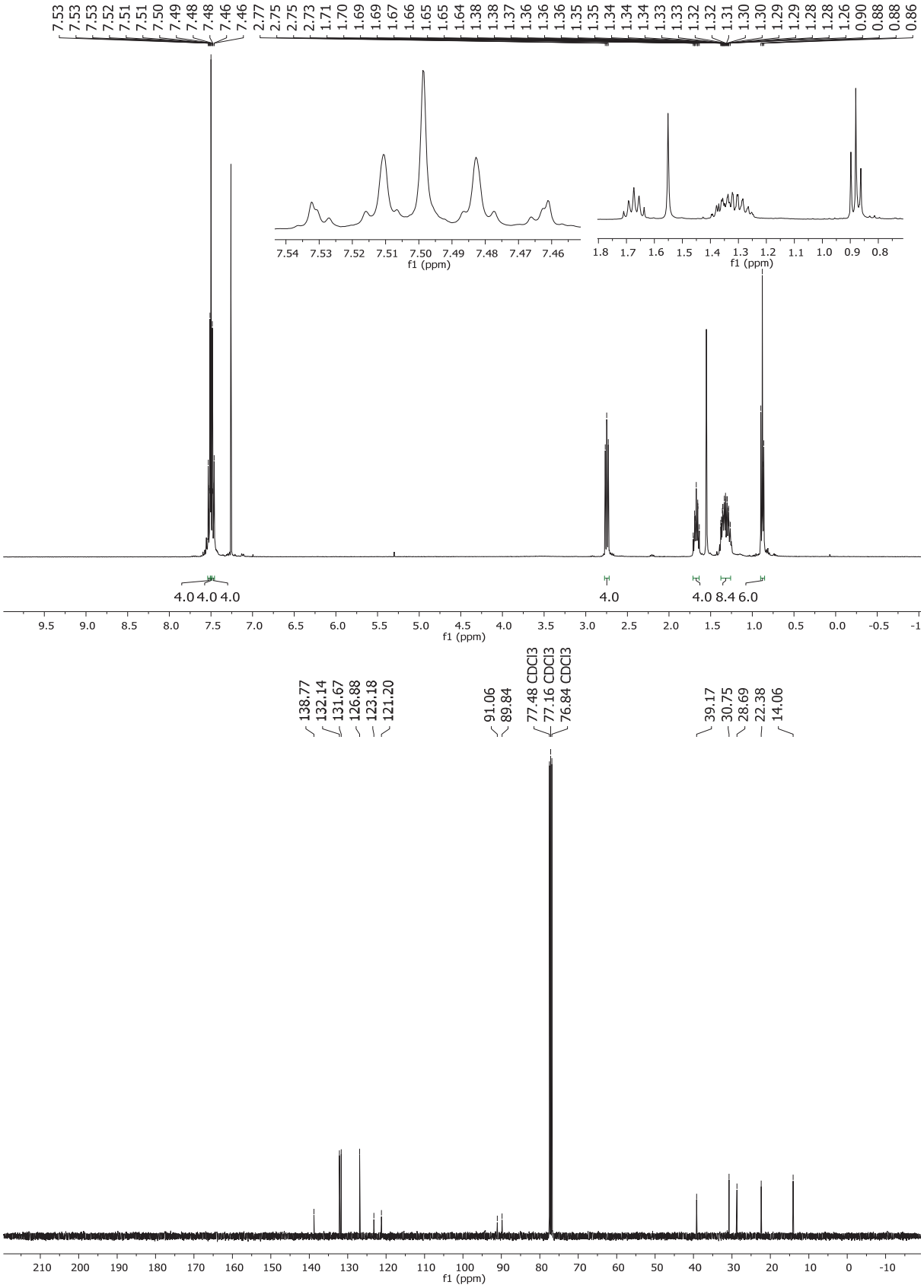

HR-ESI MS spectra of 1,4-Bis((4-(pentyldisulfaneyl)phenyl)ethynyl)benzene (OPE-3-ADS, **142**).

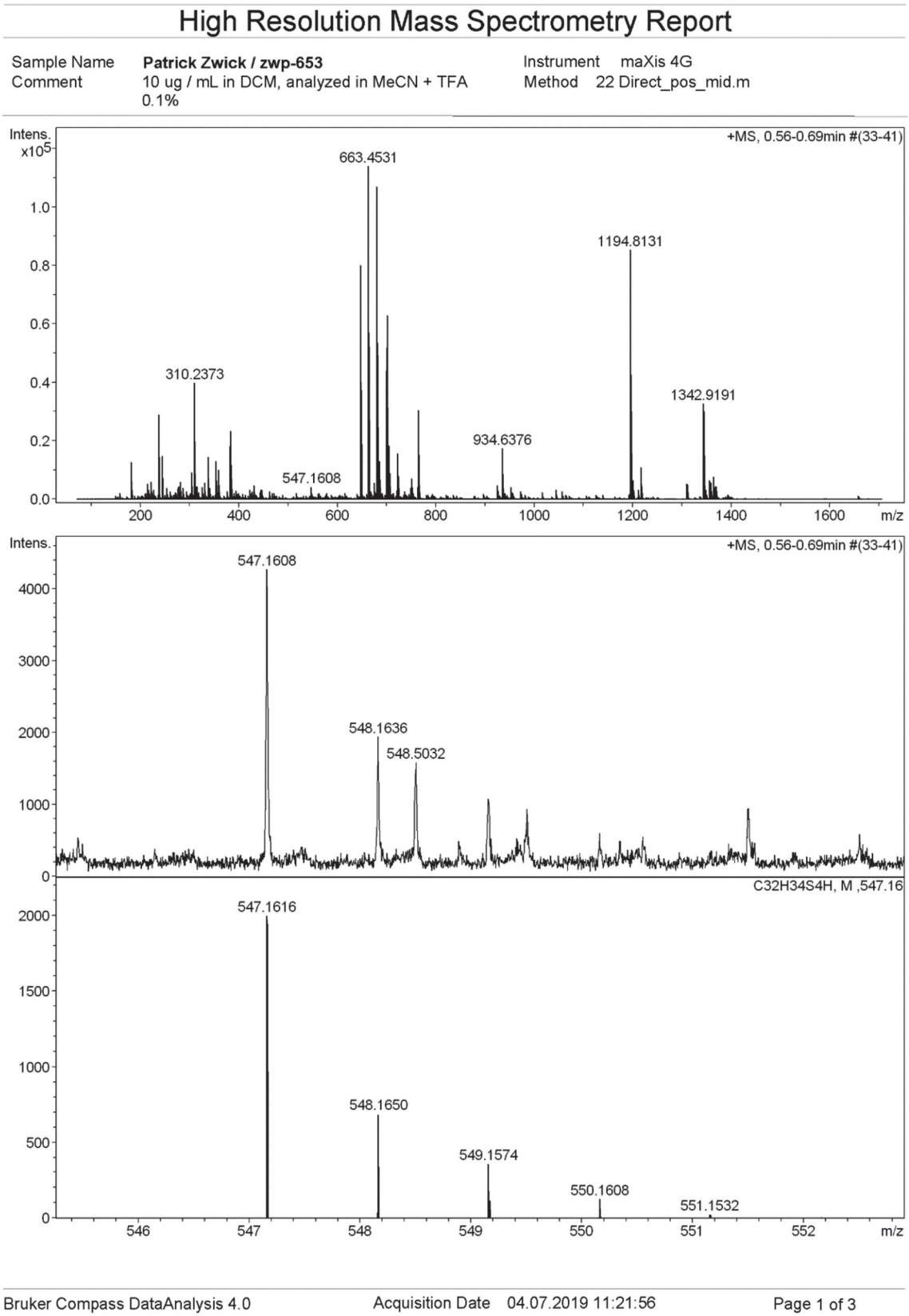

High Resolution Mass Spectrometry Report

Measured m/z vs. theoretical m/z

Meas. m/z	#	Formula	Score	m/z	err [mDa]	err [ppm]	mSigma	rdb	e⁻ Conf	z
547.1608	1	C 32 H 35 S 4	100.00	547.1616	0.8	1.5	112.0	15.5	even	1+

Mass list

#	m/z	I %	I
1	181.0854	11.3	12912
2	214.0892	4.7	5332
3	217.1045	3.1	3495
4	221.1168	5.3	6004
5	226.9592	3.0	3461
6	237.1481	25.4	28962
7	238.1514	4.2	4752
8	244.9940	13.1	14894
9	252.9730	3.4	3925
10	253.1426	3.0	3427
11	277.1793	4.0	4518
12	282.2786	5.3	5990
13	285.9957	3.5	3952
14	304.0314	8.0	9140
15	309.2056	25.7	29336
16	310.2093	6.1	6958
17	310.2373	35.0	39942
18	311.2405	7.8	8946
19	313.2728	2.9	3333
20	315.1921	4.0	4558
21	325.2001	3.7	4201
22	331.1875	3.4	3879
23	331.2838	5.0	5724
24	337.0413	12.8	14568
25	337.0674	4.1	4639
26	341.3044	3.5	3993
27	353.2655	11.6	13230
28	355.0914	4.4	4970
29	359.3151	9.0	10214
30	380.9690	3.1	3506
31	381.2970	16.0	18190
32	382.3001	4.0	4504
33	384.2429	20.6	23447
34	385.2460	6.4	7249
35	422.3412	3.0	3390
36	430.9135	4.2	4796
37	547.1608	3.8	4274
38	647.4581	70.2	80010
39	648.4614	33.0	37583
40	649.4644	8.5	9659
41	663.4531	100.0	113965
42	664.4562	46.0	52447
43	665.4590	11.8	13431
44	674.4619	5.1	5765
45	680.4795	93.8	106945
46	681.4828	43.4	49452
47	682.4858	10.6	12044
48	683.5990	10.2	11641
49	684.6034	5.2	5961
50	685.4344	11.6	13236
51	686.4380	5.7	6473
52	686.5922	3.7	4179
53	699.5945	3.9	4417
54	700.6261	55.4	63151
55	701.1821	2.9	3343
56	701.6295	26.9	30713
57	702.6299	8.4	9625
58	705.5813	16.1	18370
59	706.5846	7.9	8984
60	722.4903	13.9	15839
61	723.4928	6.8	7792
62	749.5075	3.4	3904

High Resolution Mass Spectrometry Report

#	m/z	I %	I
63	750.4059	6.3	7213
64	751.4092	3.2	3690
65	752.4060	3.8	4346
66	763.5156	3.7	4178
67	764.5726	26.7	30452
68	765.5761	14.7	16701
69	766.5789	4.4	5002
70	924.8194	4.3	4892
71	934.6376	15.3	17472
72	935.6408	9.8	11152
73	936.6436	3.4	3893
74	952.8508	3.8	4291
75	1194.8131	74.9	85348
76	1195.8163	61.8	70444
77	1196.8190	26.6	30335
78	1197.8216	8.5	9704
79	1199.7675	5.7	6501
80	1200.7720	4.8	5486
81	1210.8068	3.1	3484
82	1215.7421	9.7	11032
83	1216.7450	7.9	9047
84	1217.7480	3.9	4466
85	1309.8978	4.7	5361
86	1310.9012	4.6	5243
87	1342.9191	28.8	32778
88	1343.9229	26.6	30264
89	1344.9256	13.0	14799
90	1345.9288	4.3	4911
91	1347.8718	3.0	3385
92	1355.8246	5.9	6697
93	1356.8276	5.2	5892
94	1357.8265	5.0	5720
95	1358.8269	3.1	3489
96	1363.0665	6.9	7827
97	1364.0690	6.5	7357
98	1365.0715	3.3	3744
99	1368.0221	4.0	4521
100	1369.0248	3.9	4490

Acquisition Parameter

General	Fore Vacuum	2.69e+000 mBar	High Vacuum	1.26e-007 mBar	Source Type	ESI
	Scan Begin	75 m/z	Scan End	1700 m/z	Ion Polarity	Positive
Source	Set Nebulizer	0.4 Bar	Set Capillary	3600 V	Set Dry Gas	4.0 l/min
	Set Dry Heater	180 °C	Set End Plate Offset	-500 V		
Quadrupole	Set Ion Energy (MS only)	4.0 eV				
Coll. Cell	Collision Energy	8.0 eV	Set Collision Cell RF	350.0 Vpp		
Ion Cooler	Set Ion Cooler Transfer Time	75.0 µs	Set Ion Cooler Pre Pulse Storage Time	10.0 µs		

^{1}H-NMR (CD_2Cl_2, 400 MHz, 298 K) of 5,15-bis(4-(tert-butyl)phenyl)-10,20-bis((4-(pentyldisulfaneyl)phenyl)ethynyl)porphyrin (P-1-ADS, **141**).

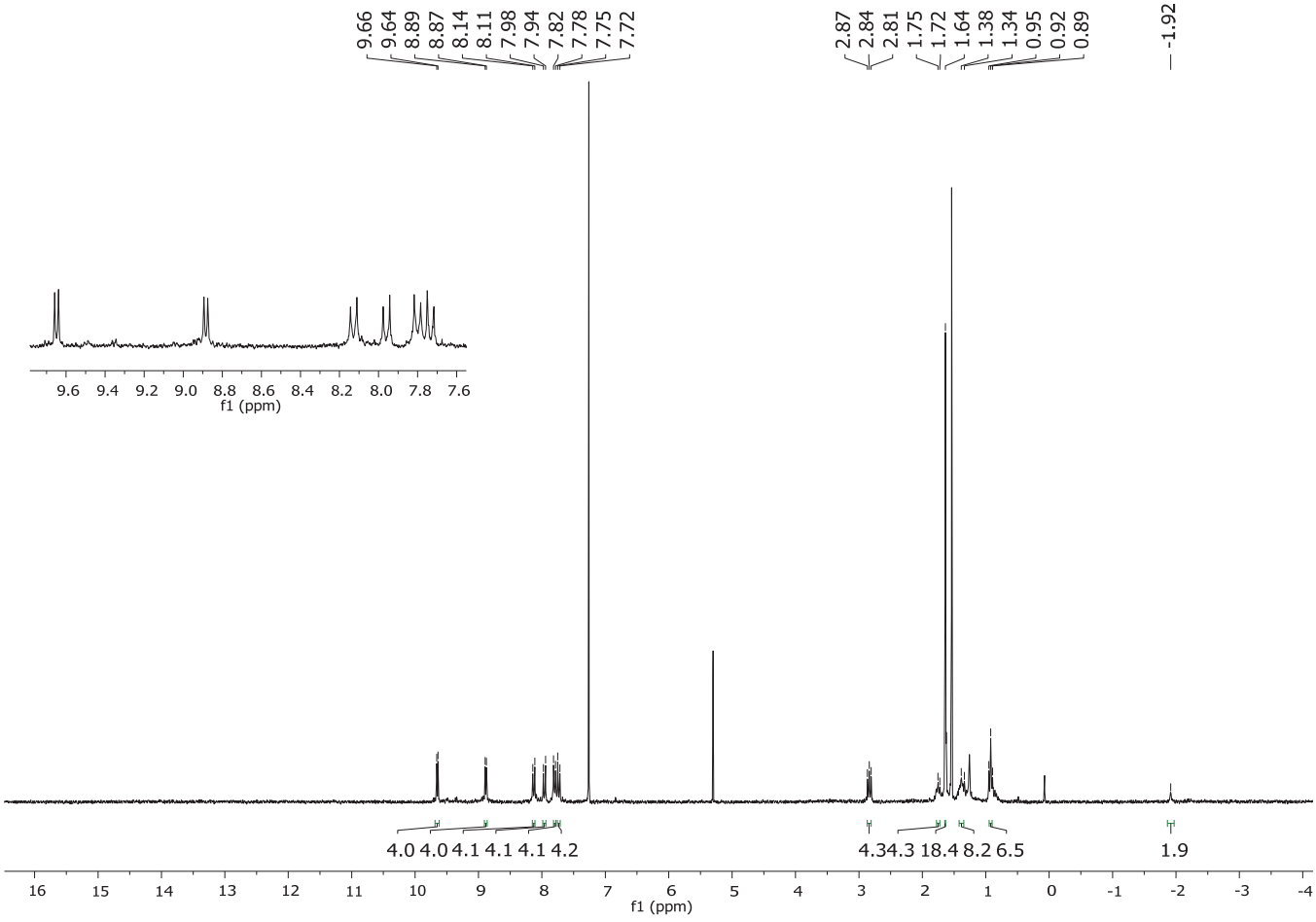

HR-ESI MS spectra of 5,15-bis(4-(tert-butyl)phenyl)-10,20-bis((4-(pentyldisulfaneyl)phenyl)ethynyl)porphyrin (P-1-ADS, **141**)

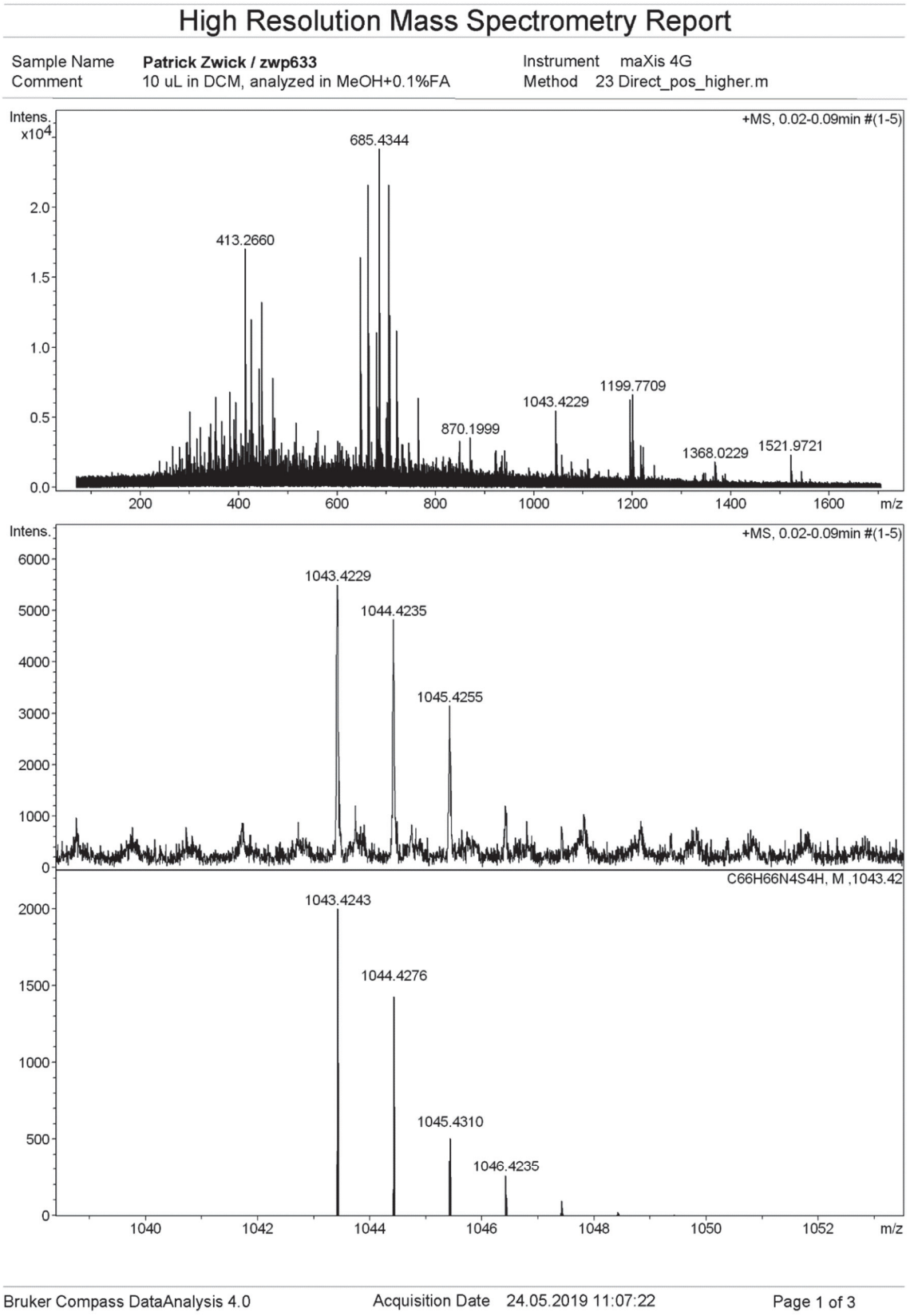

High Resolution Mass Spectrometry Report

Measured m/z vs. theoretical m/z

Meas. m/z	#	Formula	Score	m/z	err [mDa]	err [ppm]	mSigma	rdb	e⁻ Conf	z
1043.4229	1	C 66 H 67 N 4 S 4	100.00	1043.4243	1.4	1.3	110.0	35.5	even	1+

Mass list

#	m/z	I %	I
1	266.1723	12.3	2989
2	279.2284	12.0	2897
3	293.2441	13.2	3198
4	295.1921	13.6	3285
5	301.1407	22.4	5410
6	315.1924	14.6	3544
7	321.2753	17.9	4330
8	339.1783	15.2	3679
9	341.1995	14.7	3557
10	343.2948	19.0	4597
11	351.1962	16.6	4022
12	353.1448	13.8	3351
13	353.2656	26.8	6482
14	365.1051	19.6	4734
15	367.2088	12.7	3073
16	371.3260	15.3	3711
17	371.3630	11.9	2874
18	381.2970	28.2	6835
19	383.1408	11.9	2886
20	385.2919	11.4	2761
21	391.2833	20.2	4899
22	392.2288	14.2	3442
23	393.2969	19.8	4793
24	394.3470	25.2	6098
25	405.1212	16.0	3882
26	407.3128	12.6	3046
27	409.2931	12.2	2962
28	413.2660	70.4	17045
29	414.2691	20.2	4886
30	419.3139	13.4	3239
31	421.3285	17.0	4116
32	425.2144	49.8	12049
33	425.3617	21.3	5144
34	426.2183	13.9	3365
35	429.3186	16.2	3925
36	435.3444	12.5	3022
37	441.2965	35.2	8522
38	442.3013	13.6	3300
39	447.3441	54.8	13260
40	448.3488	18.7	4538
41	449.3606	14.8	3589
42	465.3702	11.4	2761
43	469.3278	32.4	7838
44	469.3868	11.9	2887
45	470.3319	15.7	3799
46	473.3446	20.6	4981
47	481.3132	11.6	2818
48	487.3587	13.2	3204
49	513.4133	13.5	3263
50	517.3704	19.1	4611
51	531.3875	12.4	3001
52	555.5097	11.8	2860
53	557.4400	13.2	3201
54	561.3968	17.0	4104
55	575.4131	12.5	3029
56	601.4653	13.9	3372
57	605.4231	13.3	3210
58	609.3602	12.2	2946
59	637.3919	12.0	2914
60	647.4581	68.1	16478
61	648.4604	33.5	8118
62	649.4563	13.5	3256

High Resolution Mass Spectrometry Report

#	m/z	I %	I
63	663.4530	89.2	21597
64	664.4559	42.0	10176
65	665.4606	13.4	3254
66	669.4391	13.6	3294
67	680.4786	45.9	11100
68	681.4813	23.5	5679
69	683.6001	14.3	3459
70	685.4344	100.0	24201
71	686.4377	49.5	11977
72	687.4412	12.8	3094
73	689.5195	11.9	2871
74	699.5931	20.5	4959
75	700.6257	25.3	6112
76	701.4076	13.7	3322
77	701.6275	15.4	3725
78	705.5247	12.3	2974
79	705.5814	89.5	21651
80	706.5842	50.9	12312
81	707.5836	15.8	3814
82	721.5748	46.5	11243
83	722.5785	25.6	6185
84	731.4908	12.8	3108
85	733.5558	12.7	3065
86	745.5059	13.3	3222
87	764.5714	26.6	6434
88	765.5760	20.9	5059
89	848.2180	13.7	3318
90	870.1999	14.8	3583
91	1043.4229	22.7	5504
92	1044.4235	19.9	4826
93	1045.4255	13.0	3153
94	1194.8160	24.7	5983
95	1195.8194	21.2	5142
96	1199.7709	27.5	6653
97	1200.7766	23.4	5654
98	1215.7488	12.6	3052
99	1216.7506	11.7	2841
100	1221.9909	12.0	2905

Acquisition Parameter

General	Fore Vacuum	2.69e+000 mBar	High Vacuum	1.17e-007 mBar	Source Type	ESI
	Scan Begin	75 m/z	Scan End	1700 m/z	Ion Polarity	Positive
Source	Set Nebulizer	0.4 Bar	Set Capillary	3600 V	Set Dry Gas	4.0 l/min
	Set Dry Heater	180 °C	Set End Plate Offset	-500 V		
Quadrupole	Set Ion Energy (MS only)	4.0 eV				
Coll. Cell	Collision Energy	8.0 eV	Set Collision Cell RF	500.0 Vpp		
Ion Cooler	Set Ion Cooler Transfer Time	80.0 µs	Set Ion Cooler Pre Pulse Storage Time	18.0 µs		

7.1 Contributions

All compounds were synthesized and characterized by Lorenzo Delarue Bizzini except:
136, 137, 139, 141 Patrick Zwick; **17, 18, 21-23** Zlatko Jovov; **65** Yves Aeschi, **7, 53, 56-58** Simon Studer.

The MCBJ measurements in section 1.2.3 were performed by Dr. Pascal Gehring (in the group of Prof. Dr. Herre van der Zant).